

**SYNTHESIS, CHARACTERIZATION AND BIOLOGICAL
APPLICATIONS OF SELENOSEMICARBAZONES AND THEIR
COMPLEXES WITH Fe, Co, Ni, Cu AND Zn**

Thesis Submitted for the Award of the Degree of

DOCTOR OF PHILOSOPHY

in

Chemistry

By

Rinku Malhi

Registration Number: 11720079

Supervised By

Dr. Rekha (14537)

Department of Chemistry (Professor)

Lovely Professional University



**LOVELY PROFESSIONAL UNIVERSITY, PUNJAB
2023**

DECLARATION

I, hereby declared that the presented work in the thesis entitled, "**Synthesis, Characterization and Biological Applications of Selenosemicarbazones and their Complexes with Fe, Co, Ni, Cu and Zn**" in fulfillment of **degree of Doctor of Philosophy (Ph. D.)** is outcome of research work carried out by me under the supervision of **Dr. Rekha Sharma**, working as **Associate Professor in Chemistry**, in the **School of Chemical Engineering and Physical Sciences** of Lovely Professional University, Punjab, India. In keeping with general practice of reporting scientific observations, due acknowledgements have been made whenever work described here has been based on findings of other investigator. This work has not been submitted in part or full to any other University or Institute for the award of any degree.

(Signature of Scholar)

Name of the scholar: **Rinku Malhi**

Registration No.: **11720079**

Department/school: **School of Chemical Engineering and Physical Sciences**

Lovely Professional University

Punjab, India

CERTIFICATE

This is to certify that the work reported in the Ph. D. thesis entitled, "**Synthesis, Characterization and Biological Applications of Selenosemicarbazones and their Complexes with Fe, Co, Ni, Cu and Zn**" submitted in fulfillment of the requirement for the award of degree of **Doctor of Philosophy (Ph.D.)** in the **School of Chemical Engineering and Physical Sciences**, is a research work carried out by **Rinku Malhi, Registration No. 11720079**, is bonafide record of her original work carried out under my supervision and that no part of thesis has been submitted for any other degree, diploma or equivalent course.

(Signature of Supervisor)

Dr. Rekha Sharma

Professor in Chemistry

Department/school: School of Chemical Engineering and Physical Sciences

University: Lovely Professional University, Phagwara, Punjab-14400

ACKNOWLEDGEMENT

With the Divine Grace of Almighty God, I must say, it is the moment when my ship comes home as I am submitting my thesis. This thesis is the culmination of five years of work (2017-2022) at School of Chemical Engineering and Physical Sciences, **Lovely Professional University**.

There are numerous people I wish to thank for contributing to this work and probably words will fall short. First of all my warmest thanks go to **Dr. Rekha**, Associate Professor, Department of Chemistry, Lovely Professional University, who has been a most reliable supervisor, who gave me freedom to do things in my own order and supported and guided me to see important things of research. I also want to sincerely thank her for innumerable opportunities she offered beyond the domain of my PhD work, which enriched me both personally and professionally. I shall be forever obliged for her care for me.

I wish to express my warm and sincere thanks to **Dr. Ashok Kumar Mittal**, Chancellor, **Dr. Preeti Bajaj**, Vice-Chancellor, **Mrs. Rashmi Mittal**, Pro-Chancellor, **Dr. Lovi Raj Gupta**, Pro-Vice Chancellor, Lovely Professional University for providing me with infrastructure and other necessary facilities to execute the present study in the well-equipped laboratory of LPU.

I sincerely express my gratitude to all other faculty members of LPU during pre-PhD course work for their unstinting help & cooperation, for their periodic assessments and valuable suggestions. Timely help and cooperation from science faculty members of Baring Union Christian College during the pre-PhD course work is gratefully acknowledged. I want to thank all former and present students of LPU for motivating me throughout this endeavor.

Next, my thanks to these wonderful people -**Raanan Carmieli, Ahmet Savci, Charan Singh, Vijay Kumbar, Dr. Jay Singh Meena, Preeti, Brad Dodrill** - who have supported me in completing the research work.

My thesis work is dedicated to my loving father. My journey during PhD course work was not so smooth. During this period, my father Late **Sh. Surinder Malhi**, passed away. He was a deeply intellectual person with a humble personality. I firmly believe that my parents shaped not just my career but my life as well. Especially my father, who had complete faith in me and supported me in every possible way all my life. The lessons that my father taught me are very valuable to me. He was the pillar of support I needed whenever I was down. He was my guiding star who had always taught me to take the right path even though the right path is generally not the easy path. He was the one who taught me and prepared me for the hardships of life. He was my hero and will always be.

Also, I am grateful to my mother and my entire family for their support. Thanks for your understanding, your never-ending encouragement, and for always being there for me.

Finally, I would like to thank the Lord for providing me with the ability and perseverance that was needed to complete this work.

Thank you

Rinku Malhi

LIST OF CONTENTS

	Page No.
Chapter 1	
1.1 Introduction of Selenium	16-19
1.2 Applications of Selenium	20
1.3 Biological Properties of Selenium	20
Chapter 2	
2. 1 Introduction of Selenosemicarbazones	21-23
2.2 Literature Survey	23-30
2.3 Complexes of Selenosemicarbazones	31-36
2.4 Biological Applications of Selenosemicarbazones and their Complexes	36-40
2.5 Aims and Objectives	40-41
Chapter 3	
GENERAL EXPERIMENTAL	
3.1 Materials and Instrumentation	42, 43
3.1.1 Materials	
3.1.2 Instrumentation	
3.1.2.1 Melting Point	
3.1.2.2 Infrared Spectroscopy	
3.1.2.3 Nuclear Magnetic Resonance (NMR) Spectroscopy	
3.1.2.4 Mass Spectrometry	
3.1.2.5 Electron Spin Resonance	
3.1.2.6 CHN Analysis	
3.1.2.7 Vibrating Sample Magnatometer (VSM)	

3.1.2.8 Powder X-Ray Diffractometer (XRD)

3.1.2.9 Mössbauer Spectroscopy

3.2 Synthesis of Selenosemicarbazone Ligands **44-51**

3.2.1 Synthesis of cyclohexanoneselenosemicarbazone (Hcysesc, H¹L)

3.2.2 Synthesis of 2-furfural selenosemicarbazone (2-Hfursesc, H²L)

3.2.3 Synthesis of 2-thiophene selenosemicarbazone (2-Hthiosesc, H³L)

3.2.4 Synthesis of N-methyl-2-pyrrole selenosemicarbazone (N-MeHPysesc, H⁴L)

3.2.5 Synthesis of 3-methyl-2-oxindole selenosemicarbazone (3-MeHOxsesc, H⁵L)

3.2.6 Synthesis of 2-oxindole selenosemicarbazone (2-HOxsesc, H⁶L)

3.2.7 Synthesis of 6-chloro-2-oxindole selenosemicarbazone (6-ClHOxsesc, H⁷L)

3.2.8 Synthesis of 5-chloro isatin selenosemicarbazone (5-ClHIstsesc, H⁸L)

3.2.9 Synthesis of 1-methyl isatin selenosemicarbazone (1-meHIstsesc, H⁹L)

3.2.10 Synthesis of indole-3-selenosemicarbazone (3-HIndsesc, H¹⁰L)

3.2.11 Synthesis of 3-acetyl indole selenosemicarbazone (3-AcHIndsesc, H¹¹L)

3.2.12 Synthesis of 9-anthrальdehyde selenosemicarbazone (9-HAnsesc, H¹²L)

3.2.13 Synthesis of 1-naphthaldehyde selenosemicarbazone (1-HNapsesc, H¹³L)

3.1.14 Synthesis of 2-naphthaldehyde selenosemicarbazone (2-HNapsesc, H¹⁴L)

3.2 Complexes of Iron (III)

3.2.1-3.2.14 Synthesis of iron complexes **1-14** **51-59**

3.3 Complexes of Cobalt(II)

3.3.1-3.3.14 Synthesis of cobalt complexes 15-28	60-68
3.4 Complexes of Nickel(II)	
3.4.1-3.4.14 Synthesis of nickel complexes 29-42	68-76
3.5 Complexes of Copper(II)	
3.5.1-3.5.14 Synthesis of copper complexes 43-56	76-83
3.6 Complexes of Zinc(II)	
3.6.1-3.6.14 Synthesis of zinc complexes 57-70	83-90

Chapter 4

RESULT AND DISCUSSION

(SELENOSEMICARBAZONES)	91-94
4.1 Discussion on Synthesis of Ligands	
4.2 IR Spectroscopy	94, 95
4.3 NMR Spectroscopy	96-98
4.3.1 ¹ H NMR Spectroscopy	
4.3.2 ¹³ C NMR Spectroscopy	99-100

Chapter 5

IRON(III) COMPLEXES

5. Complexes of Iron(III)

5.1 Discussion on Synthesis of iron metal complexes	137-139
5.2 IR Spectroscopy	140-142
5.3 Vibrating Sample Magnetometer Spectroscopy	143-150
5.4 Mössbauer Spectroscopy	151-153
5.5 ESR Spectroscopy	153-154

5.6	Mass Spectrometry	154
5.7	XRD Studies	154-156
Chapter 6		
COBALT(II) COMPLEXES		
6	Complexes of Cobalt(II)	
6.1	Discussion on Synthesis of copper metal complexes	171-173
6.2	IR Spectroscopy	173-176
6.3	Mass Spectrometry	176-177
6.4	CHN Analysis	177-178
6.5	ESR Spectroscopy	178-179
Chapter 7		
NICKEL(II) COMPLEXES		
7	Complexes of Nickel(II)	
7.1	Discussion on Synthesis of nickel metal complexes	195-197
7.2	IR Spectroscopy	198-200
7.3	NMR Spectroscopy	
7.3.1	^1H NMR Spectroscopy	200-204
7.3.2	^{13}C NMR Spectroscopy	204-207
7.4	Mass Spectrometry	207
Chapter 8		
COPPER(II) COMPLEXES		
8	Complexes of Copper(II)	
8.1	Discussion on Synthesis of copper metal complexes	240-242
8.2	IR Spectroscopy	242-244
8.3	ESR Spectroscopy	245-252

8.4 Mass Spectrometry	253
Chapter 9	
ZINC(II) COMPLEXES	
9. Complexes of Zinc(II)	
9.1 Discussion on Synthesis of zinc metal complexes	264-266
9.2 IR Spectroscopy	266-268
9.3 NMR Spectroscopy	
9.3.1 ^1H NMR Spectroscopy	269-272
9.3.2 ^{13}C NMR Spectroscopy	272-273
9.4 Mass Spectrometry	274
Chapter 10	
BIOLOGICAL ACTIVITIES	
10.1 Anti-M. Tuberculosis Activity	301-304
10.1.1 AntiM. Tuberculosis Activity of Selenosemicarbazones ($\text{H}^1\text{L-H}^{14}\text{L}$)	
10.2 Anticancer Activity	305-311
10.2.1 Cell Culture	
10.2.2 MTT Assay	
Annexure I	
Conclusion	312-326
References	327-329
List of Publications, National and International Conferences, Short-Term Courses and Workshops	330-338
Annexure II	339-340
	341-360

GLOSSARY OF ABBREVIATIONS

Hcysesc	Cyclohexanone selenosemicarbazone
2-Hfursesc	2-furfural selenosemicarbazone
2-Hthiosesc	2-thiophene selenosemicarbazone
N-MeHPysesc	N-methyl-2-pyrrole selenosemicarbazone
3-MeHOxsesc	3-methyl-2-oxindole selenosemicarbazone
2-HOxsesc	2-oxindole selenosemicarbazone
6-ClHOxsesc	6-chloro-2-oxindole selenosemicarbazone
5-ClHIstsesc	5-chloro isatin selenosemicarbazone
1-MeHIstsesc	1-methyl isatin selenosemicarbazone
3-HIndsesc	Indole-3-selenosemicarbazone
3-AcHIndsesc	3-acetyl indole selenosemicarbazone
9-HAnsesc	9-anthrальdehyde selenosemicarbazone
1-HNapsesc	1-naphthaldehyde selenosemicarbazone
2-HNapsesc	2-naphthaldehyde selenosemicarbazone
Hqasesc	2-quinolinecarboxaldehyde selenosemicarbazone
Hqasesc	8-quinolinecarboxaldehyde selenosemicarbazone
Hfpsesc	2-formypyridine selenosemicarbazone
H₂dapsesc	2,6-diacetylpyridinebisselenosemicarbazone
Se-3-Ap	Aminopyridine-2-carboxaldehydeselenosemicarbazone(selenotriapine)
Ap44mSe	2-acetylpyridine 4,4-dimethyl-3-selenosemicarbazone
Hdapsesc	2-acetylpyridine-N,N-dimethylselenosemicarbazone
5-HP	5-hydroxy-2-formylpyridin
M.P.	Melting point
IR	Infrared
NMR	Nuclear magnetic resonance
MS	Mass spectrometry
ESR	Electron spin resonance
CHN	Carbon, hydrogen and nitrogen
VSM	Vibrating sample magnetometer
XRD	X-ray diffractometer
MS	Mössbauer spectroscopy
ppm	Parts per million
amu	Atomic mass unit
m	Medium
s	Sharp
w	Weak
t	Triplet
d	Doublet
s	Singlet
Ms	Saturation magnetization
Mr	Remanence magnetization
Hc	Coercivity magnetization
emu	Electromagnetic unit
m/z	Mass/charge
nm	Nanometre

RT	Room temperature
µg/ml	Microgram per milliliter
KSeCN	Potassium selenocyanate
Fe(OAc)₃	Iron acetate
Ni(OAc)₂	Nickel acetate
Cu(OAc)₂	Copper acetate
Co(OAc)₂	Cobalt acetate
Zn(OAc)₂	Zinc acetate
CDCl₃	Deuterated chloroform
KBr	Potassium bromide
DMSO-<i>d</i>₆	Deuterated dimethyl sulfoxide
H₂Se	Hydrogen selenide
Na₂SeO₃	Sodium selenite
K₂SeO₄	Potassium selenate
MIC	Minimal inhibitory concentration
PA-1	Human ovarian cancer
DU145	Human prostate cancer
Anti-TB activity	Anti-tuberculous activity
B16	Murine melanoma
FemX	Human melanoma cells
MDA-361	Breast cancer cells
AsPC-1	Pancreatic adenocarcinoma cell lines
H460	Lung carcinoma cell lines
U251	Glioma cell lines
EMT	Epithelial-mesenchymal transition
Ea.hy 926	Human endothelial cell lines
MS1	Murine endothelial cell lines
THP-1	Monocytic leukemia cell lines
CSC	Cancer cell line
CDDP	Cisplatin
DNA	Deoxyribonucleic acid
RNA	Ribonucleic acid
ATCC	The american type culture
MMP-2	Matrix metalloproteinase 2
MABA	Microplate alamar blue assay
S	Sensitive
R	Resistant
DMEM	Dulbecco's modified eagle media
MTT	3-(4, 5-dimethylthiazol-2-yl)-2,5-diphenyl tetrazolium bromide (E,Z)-5-(4,5-dimethylthiazol-2-yl)-1,3-diphenylformazan
IC₅₀	Half-maximal inhibitory concentration

Abstract

In the present thesis 14 new selenosemicarbazones and their complexes with iron(III), cobalt(II), nickel(II), copper(II) and zinc(II) are synthesized and characterized using various spectroscopic techniques. Reaction of cyclohexanone with KSeCN and hydrazine hydrate in acidic medium results in the formation of cyclohexanone selenosemicarbazone, which was then reacted to various aldehydes or ketones to form respective selenosemicarbazones. These selenosemicarbazones are: Cyclohexanone selenosemicarbazone (**H_{eyesc}, H¹L**); 2-furfural selenosemicarbazone (**2-H_{fursesc}, H²L**); 2-thiophene selenosemicarbazone (**2-H_{thiosesc}, H³L**); N-methyl-2-pyrrole selenosemicarbazone (**N-MeH_{Pysesc}, H⁴L**); 3-methyl-2-oxindole selenosemicarbazone (**3-MeH_{Oxsesc}, H⁵L**); 2-oxindole selenosemicarbazone (**2-H_{Oxsesc}, H⁶L**); 6-chloro-2-oxindole selenosemicarbazone (**6-ClH_{Oxsesc}, H⁷L**); 5-chloro isatin selenosemicarbazone (**5-ClH_{Istsesc}, H⁸L**); 1-methyl isatin selenosemicarbazone (**1-MeH_{Istsesc}, H⁹L**); indole-3-selenosemicarbazone (**3-H_{Indsesc}, H¹⁰L**); 3-acetyl indole selenosemicarbazone (**3-AcH_{Indsesc}, H¹¹L**); 9-anthraldehyde selenosemicarbazone (**9-H_{Ansesc}, H¹²L**); 1-Naphthaldehyde selenosemicarbazone (**1-H_{Napsesc}, H¹³L**) and 2-Naphthaldehyde selenosemicarbazone (**2-H_{Napsesc}, H¹⁴L**). All these ligands are characterized using M.P., IR and NMR (¹H and ¹³C NMR).

Reaction of iron acetate with selenosemicarbazones (HL) in 1: 3 (M : L) molar ratio in methanol has formed complexes of stoichiometry, [Fe(L)₃] (L = ¹L **1**; ²L **2**; ³L **3**; ⁴L **4**; ⁵L **5**; ⁶L **6**; ⁷L **7**; ⁸L **8**; ⁹L **9**; ¹⁰L **10**; ¹¹L **11**; ¹²L **12**; ¹³L **13**; ¹⁴L **14**). Complexes are characterized via IR and VSM studies. Representative complexes are also studied using ESR, Mössbauer spectroscopy and XRD studies to establish their geometry. From the VSM graphs, three parameters have been calculated: i) Saturation magnetization (M_s): A point where no further increase in magnetization is possible with increase in external magnetic field; ii) remanence (M_r): magnetization left behind after removal of external magnetic field; iii) coercivity (H_c): it is the measure of reverse field required to bring the magnetization to zero after saturation. The remanence magnetization of **1-14** lie in the range, -0.37866 to -0.29117 emu/g, indicates that the iron metal in these complexes is magnetically soft. To establish the oxidation state and spin state, complex **2** was studied for Mössbauer spectroscopy. Isomer shift value of 0.393 mm/s in complex **2** indicates the formation of iron(III) high spin octahedral complex. Quadrupolar splitting indicates the asymmetric charge distribution around the iron(III) nuclei. ESR spectrum of complex **12** give a broad signal with g value approximately equal to 2.

supports formation X-ray diffraction analysis was employed for complex **7**, **10** and **12** respectively and peaks obtained confirmed the formation of complexes.

Reaction of synthesized selenosemicarbazones ligands (**H¹L-H¹⁴L**) with cobalt acetate in 2: 1 formed complexes of stoichiometry, [Co(L)₂] (L = ¹L **15**; ²L **16**; ³L **17**; ⁴L **18**; ⁵L **19**; ⁶L **20**; ⁷L **21**; ⁸L **22**; ⁹L **23**; ¹⁰L **24**; ¹¹L **25**; ¹²L **26**; ¹³L **27**; ¹⁴L **28**). Complexes are characterized by IR spectroscopy, Mass spectrometry and elemental analysis. Parent ion peak in mass spectrum and % age carbon, hydrogen and nitrogen in elemental analysis are in well agreement with the proposed stoichiometry. Electron Spin Resonance spectroscopy has been used as a powerful technique to determine the spin state of cobalt(II) complexes. From ESR spectrum, the structure of complex **28** is found to be square planar as measured with respect to given g values (g_{||}= 2.0 and g_⊥= 2.2).

Reaction of nickel acetate with selenosemicarbazones (**H¹L-H¹⁴L**) in 1 : 2 molar ratio has yielded complexes of stoichiometry, [Ni(L)₂] (L = ¹L **29**; ²L **30**; ³L **31**; ⁴L **32**; ⁵L **33**; ⁶L **34**; ⁷L **35**; ⁸L **36**; ⁹L **37**; ¹⁰L **38**; ¹¹L **39**; ¹²L **40**; ¹³L **41**; ¹⁴L **42**). All the complexes are characterized using IR, NMR (¹H and ¹³NMR) spectroscopy and Mass spectrometry. Similarly reaction of synthesized selenosemicarbazones ligands (**H¹L-H¹⁴L**) with copper acetate in 2: 1 may form complexes of stoichiometry, [Cu(L)₂] (L = ¹L **43**; ²L **44**; ³L **45**; ⁴L **46**; ⁵L **47**; ⁶L **48**; ⁷L **49**; ⁸L **50**; ⁹L **51**; ¹⁰L **52**; ¹¹L **53**; ¹²L **54**; ¹³L **55**; ¹⁴L **56**). All the complexes are characterized using IR, Electron Spin Resonance spectroscopy and Mass spectrometry (few complexes). Parent ion peak obtained in the mass spectrum of complexes is in accordance to the proposed stoichiometry. The two well-defined g values i.e. g_{||} and g_⊥ in these complexes (except **53**), represents axially symmetrical system. In these complexes g value follows the trend, g_{||}>g_⊥>g_e, suggesting the d_{x²-y²} ground term in square planar geometry. The ESR spectrum of complex **53** gave three g values (g₁, 2.095; g₂, 2.15; g₃, 2.26) indicate rhombic distortion in its geometry. Reaction of synthesized selenosemicarbazones ligands (**H¹L-H¹⁴L**) with zinc acetate in 2: 1(L : M) molar ratio has formed complexes of stoichiometry, [Zn(L)₃] (L = ¹L **57**; ²L **58**; ³L **59**; ⁴L **60**; ⁵L **61**; ⁶L **62**; ⁷L **63**; ⁸L **64**; ⁹L **65**; ¹⁰L **66**; ¹¹L **67**; ¹²L **68**; ¹³L **69**; ¹⁴L **70**). The complexes are characterized using IR, NMR spectroscopy and mass spectrometry.

Selenosemicarbazones (**H¹L-H¹⁴L**) and their complexes **1-70** are tested for their antimycobacterial against *M. tuberculosis*. Hcysesc (**H¹L**), 2-Hthiosesc (**H³L**), 1-MeHIsctsesc (**H⁹L**), 9-HAnsesc (**H¹²L**), 1-HNapsesc (**H¹³L**) and 2-HNapsesc (**H¹⁴L**) are found to be most active (MIC = 1.6 μ g /mL). The antiTB activity of **H²L**, **H⁴L**, **H⁸L**, **H¹⁰L** and **H¹¹L** get

enhanced on complexation. Enhancement in antiTB activity is more in case of **H¹¹L** (MIC = 25 µg/mL) and its nickel(II) complex (**39**) is found to be most active (MIC = 0.8 µg/mL). Its activity is even better than the standard drugs used Pyrazinamide (MIC = 3.125 µg/mL), Ethambutol (MIC = 1.6 µg/mL) and Isoniazid (MIC = 1.6 µg/mL). Amongst the various metals, copper(II) and nickel(II) complexes have shown better result. Fused ring selenosemicarbazones (**H⁵L-H¹⁴L**), cyclohexanone selenosemicarbazone (**H¹L**) and their complexes with nickel(II) and zinc(II) has been tested for their anticancer activity against PA-1 (human ovarian cancer) and DU145 (human prostate cancer) cell lines. All the ligands exhibit very good anticancer activity against PA-1 as compare to DU145. In case of anticancer activity against PA-1, amongst the various selenosemicarbazones, 2-oxindole selenosemicarbazone (**H⁶L**, IC₅₀, 1.76 µg/ml) and 3-acetyl indoleselenosemicarbazoe (**H¹¹L**, IC₅₀ 1.63 µg/ml) are most active compounds. Their activity is almost similar or close to the Doxorubicin (control, IC₅₀, 1.60 µg/ml). On complexation with zinc(II) or nickel(II) metals, anticancer activity of most of the selenosemicarbazones get enhanced against both the cell lines PA-1 and DU145. Selenosemicarbazone complexes of zinc(II) metal have shown better results than nickel(II). Complexes [Zn(⁹L)₂]**65** and [Zn(¹³L)₂]**69** have shown highest anticancer activity against PA-1 with IC₅₀ value of 1.30 µg/ml and 1.26 µg/ml respectively.

CHAPTER 1

1.1 Introduction of Selenium

Discovery of selenium was done in 1817 by the scientist Jones Jacob Berzelius, a Swedish Chemist. The name is derived from ‘selene’ Greek word meaning ‘moon’. Selenium belongs to p-block and has atomic number 34. The electronic configuration of selenium is ([Ar] 3d¹⁰ 4s² 4p⁴). It is a member of chalcogen family (oxygen, sulfur, tellurium and polonium). Selenium is widely distributed in the earth’s crust and it occurs mainly in iron, copper, nickel and lead ores in the form of metallic selenides and it is obtained from the anode muds during electrolytic refining of copper. The various properties of selenium are listed in the Table 1.1.1

Table 1.1.1 Various Properties of Selenium

Atomic Mass	78.971
Atomic Number	34
Density	4.809
Melting Point	494K, 220.8°C
Boiling Point	958K, 685°C
Isotopes	⁷⁴ Se, ⁷⁶ Se, ⁷⁷ Se, ⁷⁸ Se, ⁷⁹ Se, ⁸⁰ Se, ⁸² Se
Electronegativity (Pauling Scale)	2.55
Electron Affinity	-4.21ev
Ionization Potential	1 st 941.0 Kj/mol 2 nd 2045.0 Kj/mol 3 rd 2973.7 Kj/mol
Covalent Radius	116 pm
Atomic Radius	103 pm
Electronic Configuration	[Ar] 3d ¹⁰ 4s ² 4p ⁴
Van Der Waals Radius	190 pm
Oxidation States	-2, 0, +4, +6

Selenium exists in amorphous as well as crystalline forms. The crystalline allotropes have monoclinic selenium ranging in color from red to brown to gray or black [1]. Grey form of selenium is the most stable and dense form. Gray selenium is formed by mild heating of other allotropes and gray selenium is a semiconductors showing photoconductivity. Selenium

shows five stable ^{74}Se , ^{76}Se , ^{77}Se , ^{78}Se , ^{80}Se isotopes and twenty-four radioactive isotopes [2-4]. Half-life range of radioactive isotopes is from 20 minutes to 295000 years. Selenium radioactive isotopes are used for the production of medical and industrial bromine radioisotopes. Selenium can form organic and inorganic compounds. Inorganic selenium compounds can be divided into three categories:

- i) Selenide (Se^{2-}): The oxidation state of selenium in selenide is -2. Example: Lead selenide (PbSe), Zinc selenide (ZnSe) and Hydrogen selenide (H_2Se).
- ii) Selenite (SeO_3^{2-}): The oxidation state of selenium in selenite is +4. Example: Silver selenite (Ag_2SeO_3) and Sodium selenite (Na_2SeO_3).
- iii) Selenate (SeO_4^{2-}): The oxidation state of selenium in selenate is +6. Example: Anhydrous potassium selenate (K_2SeO_4).

Bioavailability of organoselenium compounds is more than its inorganic forms [5, 6]. Organoselenium compounds play the main role in certain biochemical processes such as anticancer, antioxidants and antiviral agent [7-9]. Organoselenium compounds include selenols (RSeH analogues of thiols), diselenides (R_2Se_2 analogues of disulfides), selenoxides, selenones, selenium acids, selenides (R_2Se analogues of thioethers), selenium halides and selenaheterocyclic compounds. Structured of organoselenium compounds are listed in Table 1.1.2.

Table 1.1.2 List of Organoselenium Compounds

Compound	General formula	Examples
Selenols	R-Se-H	 Selenocysteine
Selenides	R-S e-R	 Dimethylselenide
Diselenides	R-Se-Se-R	 Diphenyldiselenide
Selenoxides	R-Se(O)R	 Phenylselenoxide
Selenones	R-Se(O)₂R	 Ethylselenoyl benzene
Selenium acids		
Seleninic acid	R—Se—(O)OH	
Selenenic acid	R-Se-OH	Methyl seleninic acid
Selenonic acid	R-Se(O)₃H	

Selenium is also present in plants and animals in the form of selenoprotein and selenopeptides [10]. Selenium containing amino acids present in plant and animals are listed in Table 1.1.3.

Table 1.1.3 List of selenium containing amino acids present in plants and animals

Name	Molecular structure	Distribution
Selenohomocysteine		Plants and Mammals
Selenomethionine		Plants and Mammals
Methyl selenocysteine		Plants
Selenocysteine		Plants
Se-cystathione		Plants
Se-containing protein		Plants and Mammals: Amino acid Selenomethionine

Main class of organoselenium contains selenols, which is present in the amino acid selenocysteine. It is also present in the active sites of various enzymes such as glutathione peroxidase, iodothyronine deiodinase and thioredoxin reductase [11]. Selenides can be generated from alkyl halides using selenol as nucleophiles [12]. Diselenides also acts as antioxidant [13]. Selenocyanates also exhibits antioxidative, antimutagenic and anticarcinogenic properties [14, 15]. Selenaheterocyclic compounds also acts as antioxidants, enzyme inhibitors and antiinfective agents [16-23].

1.2. Applications of Selenium

The chemical, physical and the biological interest in this element have been growing along the years [24-26]. Selenium plays an important role in each field. Due to its semiconductor nature, it is used in photocells and solar cells. It is also used in manufacturing of transistors, lithium selenium batteries, electronic games and photocopy machines. As some of the selenium compound decolorize glass and some can give red color, these compounds are used in paints, rubber, pigments and enamels [27-34].

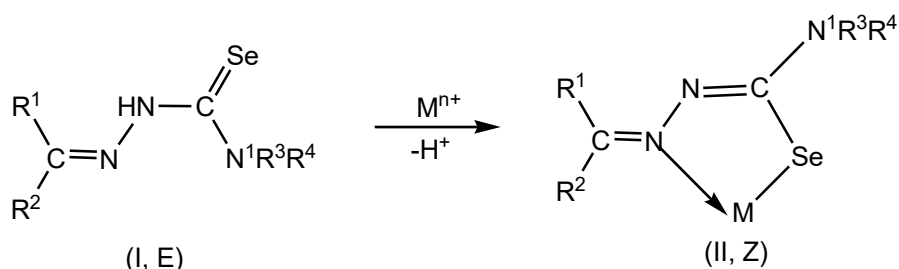
1.3. Biological properties of Selenium

Biological importance of selenium for microorganism was discovered in 1954, whereas it is an essential element for mammals was identified in 1957 [35-38]. Selenium is an essential trace element and its deficiency leads to the serious diseases such as cancer, diabetes, HIV/AIDS and tuberculosis [39-52]. Caspase 3 gets activated by selenium dioxide, which stop apoptosis thus can act as anticancer agent. Glutathione peroxidase (GPX), protects against oxidative damage against cells is also activated by selenium [53-59]. Selenium and Vitamin E Cancer Prevention Trial are in process as for examining the role of selenium in cancer prevention. Apart from that selenium containing compound shows a wide of biological activities like, antimalaria, antiproliferative, anticancer, antimicrobial, antiinflammatory, antitumor, antioxidant and antiviral activity etc.

CHAPTER 2

2. 1 Introduction of selenosemicarbazones

Selenosemicarbazones contains selenium and nitrogen donors available for binding to the coordination site of the metal due to the presence of a lone pair of electrons on these atoms. They are the selenium analogue of thiosemicarbazones [60]. In neutral form, binding to metal centre takes place through selenosemicarbazone atom (E-mode, I), whereas on deprotonation of hydrazine N²H hydrogen, it form a chelate ring (Z mode, II).



The various methods to prepare selenosemicarbazones are mentioned:

Method I. Semicarbazide can be directly condensed with aldehyde or ketone to give respective selenosemicarbazone (Chart I) [61, 62].

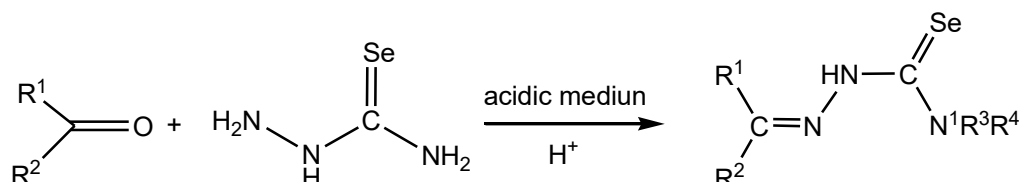


Chart 1

Method II. Aldehyde / ketone can be reacted cyclohexanone selenosemicarbazone, which was prepared by reaction of hydrazine hydrate, cyclohexanone and KSeCN and in acidic medium to form respective selenosemicarbazone (Chart 2) [63, 64].

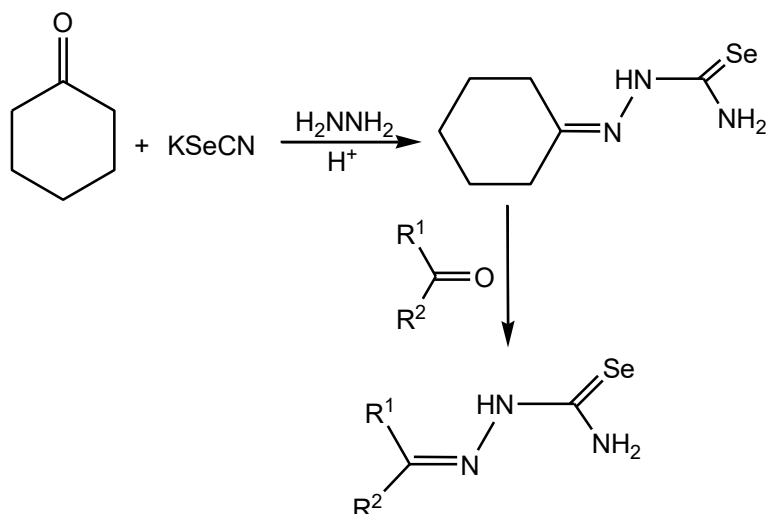


Chart 2

Method III. Selensemicarbazones can also be prepared by replacement of sulfur by selenium in thiosemicarbazones. Thiosemicarbazone was first methylated by reacting it with methyl iodide (CH_3I) and then treated with sodium hydride selenide and NaBH_4 under inert atmosphere to give corresponding selenosemicarbazone (Chart 3) [65].

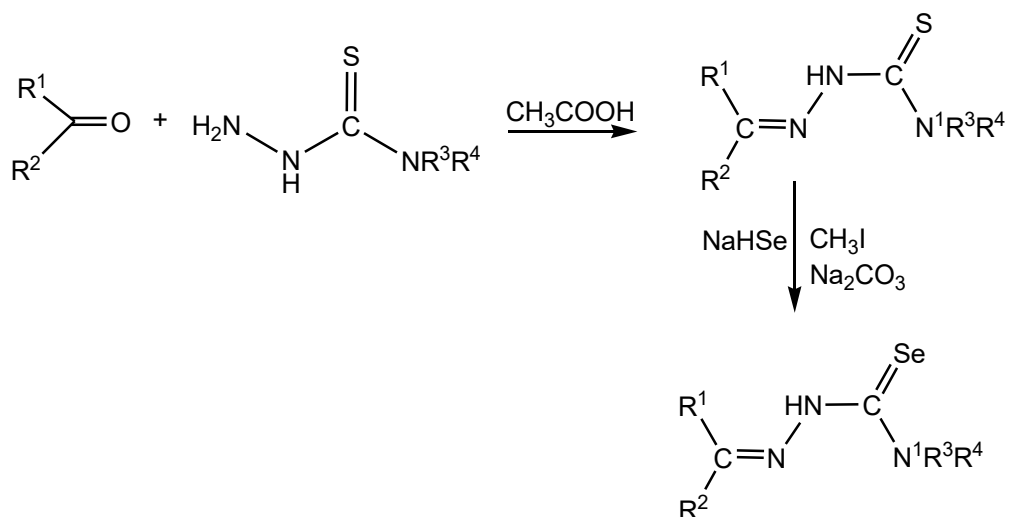


Chart 3

Method IV. Not only sulfur, oxygen of semicarbazone can also be replaced by selenium to form selenosemicarbazone. In this method, PCl_5 was added to a solution of semicarbazide in dry CH_2Cl_2 at 0°C and then reacted with a freshly prepared THF solution of LiAlHSeH (Chart 4) [66].

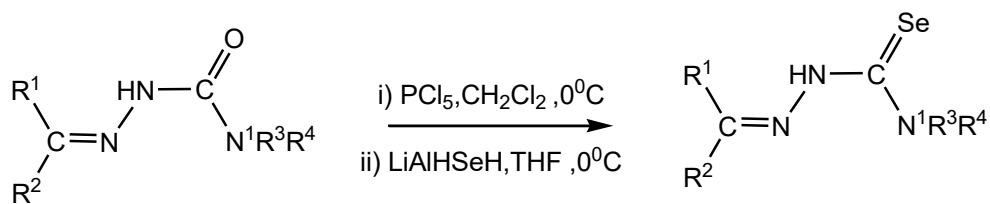
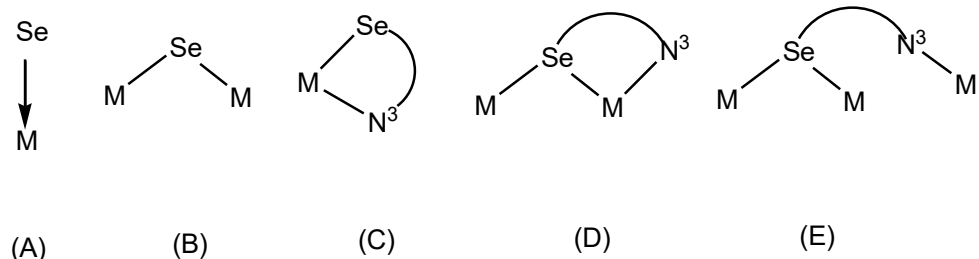


Chart 4

Selenosemicarbazone can coordinate with metal centre in different ways like: i) bind terminally through selenium only, $\eta^1\text{-Se}$ (mode A) [67]; ii) bridging of two central centres by selenium atom, $\mu\text{-Se}$ (mode B) [68]; iii) N, Se- chelation (mode C) [69]; iv) N, Se- chelation-cum-Se-bridging (mode D) [70]; v) Se-bridging-cum-Se, N- bridging (mode E) [71].



Coordination of selenosemicarbazone with metal centre also affects their biological properties, as in many cases biological activities of selenosemicarbazones get enhanced on complexation. Selenosemicarbazone and their complexes showed various biological activity such as antifungal [72, 73], antiparasitic [74], antibacterial [75-77], antimarial [78-81], anticancer [64, 65, 82-92], antioxidant, antiproliferative [93], antiangiogenic [94] and antidiabetic activity [84]. Some of the complexes of selenosemicarbazones displayed better biological activities as compare to their sulfur analogues than the corresponding thiosemicarbazones and their complexes [64, 74, 76, 84, 92, 95-97] while oxygen analogues showed the lower activity [64, 72, 77, 83, 97, 98].

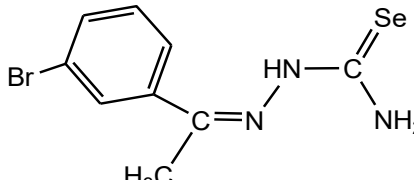
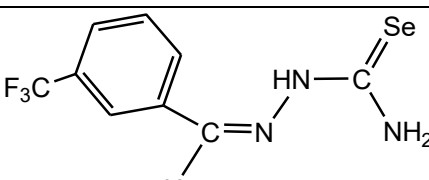
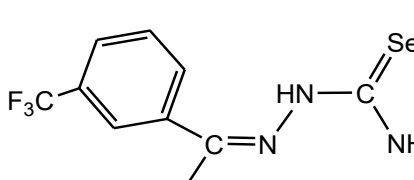
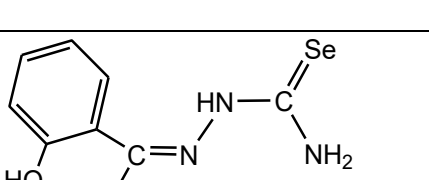
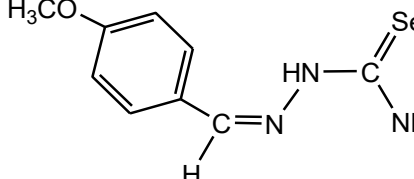
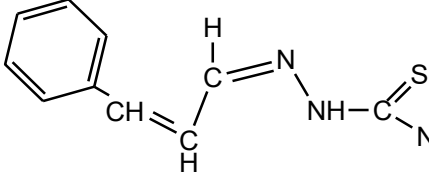
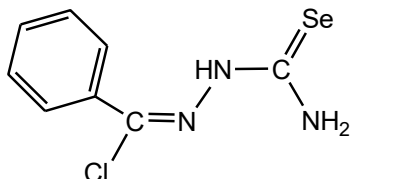
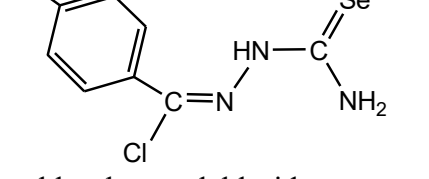
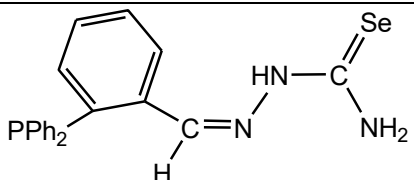
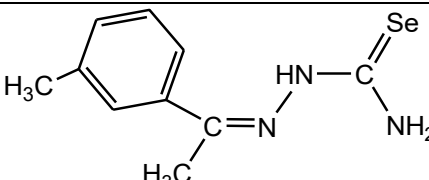
2.2 Literature survey: A number of selenosemicarbazones has been reported in literature. Depending on the substituent at C^2 carbon and number of selenosemicarbazone moiety, these ligands are divided into following categories:

I. Selenosemicarbazones with un-substituted and substituted aromatic ring at C^2 carbon: Selenosemicarbazones with mono-substituted, di-substituted and tri-substituted benzene rings are known. Halogens, methyl group, hydroxyl, diphosphines etc. are presented

at ortho- or meta- or para- positions of benzene ring [63, 65, 83, 99-102]. The various ligands with un-substituted and substituted aromatic ring at C² carbon are listed in Table 2.2.1.

Table 2.2.1 List of selenosemicarbazones with un-substituted and substituted aromatic ring at C² carbon

S.No.	Ligand	S.No.	Ligand
1.		2.	
3.		4.	
5.		6.	
7.		8.	

9.	 m-bromobenzaldehyde selenosemicarbazone	10.	 m-trifluorocarbaldehyde selenosemicarbazone
11.	 m-trifluoromethylphenylpropanone selenosemicarbazone	12.	 salicylaldehyde selenosemicarbazone
13.	 p-methoxybenzaldehyde selenosemicarbazone	14.	 cinnamicaldehyde selenosemicarbazone
15.	 benzoylchloride selenosemicarbazone	16.	 p-chlorobenzoylchloride selenosemicarbazone
17.	 2(diphenylphosphino)benzaldehyde selenosemicarbazone	18.	 m-methylphenylethanone selenosemicarbazone

<p>19.</p> <p>p-dimethylamino benzaldehyde selenosemicarbazone</p>	<p>20.</p> <p>3-hydroxy Ar = Ph, C10H7</p> <p>3, 4-dihydroxy</p> <p>3, 4, 5-trihydroxy</p>
--	---

II. Selenosemicarbazones with aliphatic chain at C² carbon:

Selenosemicarbazones with aliphatic chains having carbon atom ranging from 3 to 10 at C² carbon are also known and listed in Table 2.2.2 [102, 66].

Table 2.2.2 List of selenosemicarbazones with aliphatic chain at C² carbon

S.No.	Ligand	S.No.	Ligand
1.		2.	
	isopropylethanone selenosemicarbazone		n-heptanal selenosemicarbazone
3.		4.	
	n-octanal selenosemicarbazone		n-nonanal selenosemicarbazone
5.		6.	
	n-decanal selenosemicarbazone		n-undecanal selenosemicarbazone

7.	<p>n-dodecanal selenosemicarbazone</p>
----	--

III. Selenosemicarbazones with heterocyclic ring at C² carbon: Selenosemicarbazones with un-substituted and substituted pyridine ring at C² carbon are well known. With five membered heterocyclic ring, a few selenosemicarbazones are formed for example thiophen-2-carbaldehyde selenosemicarbazone, thiazol-4-carbaldehyde selenosemicarbazone, where two heteroatoms are present in the ring is also known [61-63, 65, 75, 87, 89, 101, 103-107]. These ligands are listed in Table 2.2.3.

Table 2.2.3 List of selenosemicarbazones with heterocyclic ring at C² carbon

S.No.	Ligand	S.No.	Ligand
1.	<p>formylpyridine selenosemicarbazone</p>	2.	<p>picolinaldehyde selenosemicarbazone</p>
3.	<p>(Se-3-Ap)</p>	4.	<p>5-hydroxy-2-formylpyridine selenosemicarbazone</p>
5.	<p>2,acetylpyridine 4,4-dimethyl-3-</p>	6.	<p>1-azabicyclo[3.2.7] nonane-3-</p>

	selenosemicarbazone		thiocarboxylic acid 2-[1-(2-pyridine)ethylidene] hydrazide
7.	<p>N₄,N₄-azacycloheptane 2-acylpyridine, 1-acetylisoquinoline, and 2-acetylquinoline selenosemicarbazones</p>	8.	<p>2-thiophencarboxaldehyde selenosemicarbazone</p>
9.	<p>di-2-pyridyl ketone 4,4-dimethyl-3-selenosemicarbazide(2-24a)</p>	10.	<p>cyclohexanone selenosemicarbazone</p>
11.	<p>2-phenyl- thiazol-4- carbaldehyde selenosemicarbazone</p>	12.	<p>N_{sub}-substituted 2-acetylpyridine selenosemicarbazone</p> <p>NR¹R² = NH Ph , H₃C-cyclopentyl , H₃C-cyclohexyl</p>

IV. Selenosemicarbazones with fused ring at C² carbon:

Few selenosemicarbazones with fused ring at C² carbon are also known [63, 75, 90, 107-111]. Fused ring in these ligands is either aromatic or one aromatic and one heterocyclic. Such types of ligands are listed in Table 2.2.4.

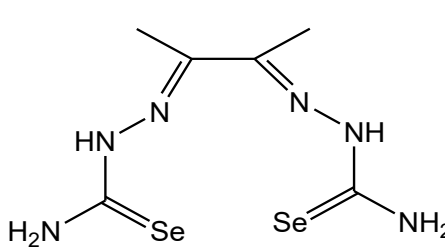
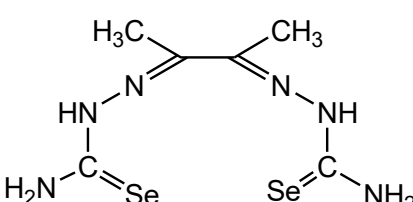
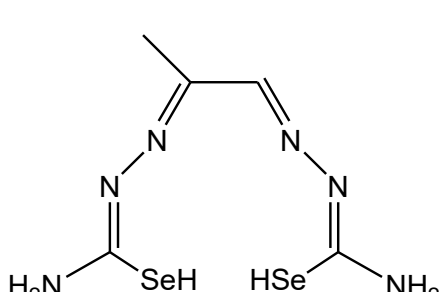
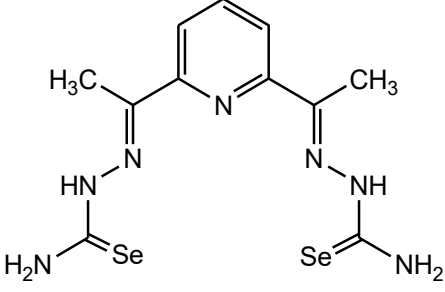
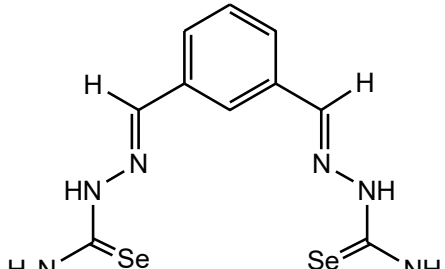
Table 2.2.4 List of selenosemicarbazones with fused ring at C² carbon

S.No.	Ligand	S.No.	Ligand
1.	<p>2-quinolinecarboxaldehyde selenosemicarbazone</p>	2.	<p>8-quinolinecarboxaldehyde selenosemicarbazone</p>
3.	<p>2-hydroxynaphthaldehyde selenosemicarbazone</p>		

V. Bis-Selenosemicarbazones at C² carbon:

Selenosemicarbazones, where two arms are connected via a ring or a C–C bond are reported [75, 88, 112-115]. These are called bis-ligands and are listed in Table 2.2.5.

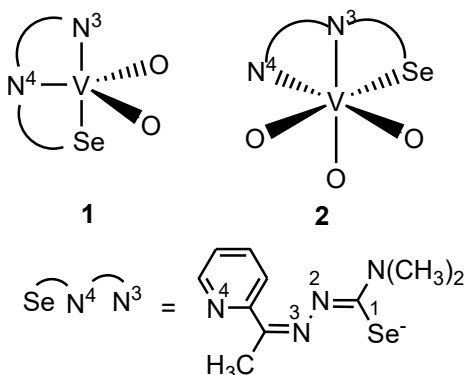
Table 2.2.5 List of bis-selenosemicarbazones at C² carbon

S.No.	Ligand	S.No.	Ligand
1.	 glyoxal bis(selenosemicarbazone)	2.	 2,3-butanedione bis(selenosemicarbazone)
3.	 pyruvaldehyde bis(selenosemicarbazone)	4.	 2,6-diacetylpyridine-bis selenosemicarbazone
5.	 iso-phthaloyldicarboxaldehyde selenosemicarbazone		

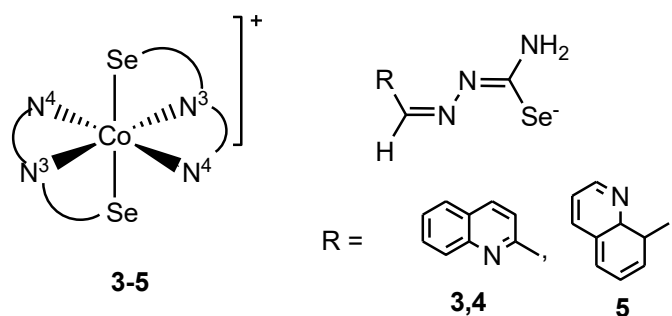
2.3. Complexes of selenosemicarbazones:

A large number of complexes of thiosemicarbazones with d-block elements are known [60, 116-139], but only few complexes of selenosemicarbazones are reported till date. A brief description of coordination chemistry of complexes of selenosemicarbazones is given below:

Vanadium and Cobalt: Vanadium(II) reacted with 2-acetylpyridine N,N- dimethyl selenosemicarbazone (HLSe) to form complexes of stoichiometry, $[V(O)_2(LSe)]\mathbf{1}$ and $[VO(acac)(LSe)]\mathbf{2}$ [131]. Complex **1** has distorted trigonal bipyramidal geometry, whereas complex **2** is octahedral. In complex **1**, axial positions are taken up by pyridine nitrogen atom and selenium atom. Two oxygen atoms from oxo ligands and imine nitrogen atom were present in the triangular base. In these complexes, selenosemicarbazone bind via N, N, Se-donor atoms and act as monanionic tridentate ligand.

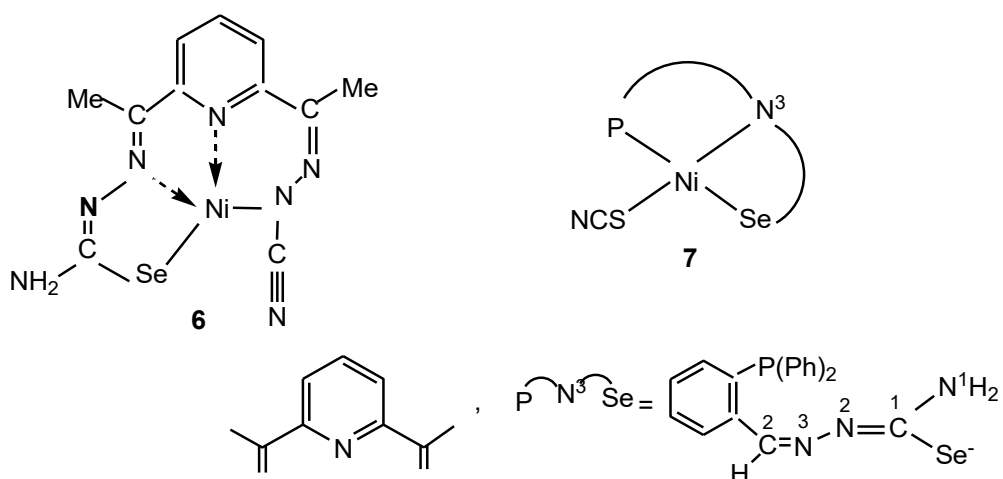


2-quinolinecarboxaldehyde selenosemicarbazone ($Hqasesc$) and 8-quinolinecarboxaldehyde selenosemicarbazone ($Hqasesc$) reacted with cobalt(II) to complexes of stoichiometry, $[Co(2qasesc)_2]X \cdot H_2O$ ($X = ClO_4 \mathbf{3}$; $BF_4^- \mathbf{4}$) and $[Co(8qasesc)_2]ClO_4 \mathbf{5}$ respectively [75, 109, 111]. Geometry around cobalt is octahedral in all these complexes.

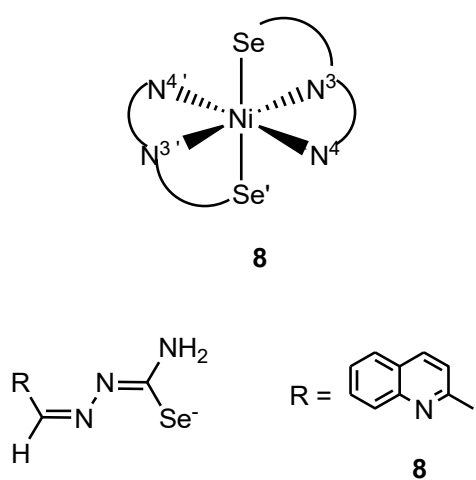


Nickel, Platinum and Palladium:

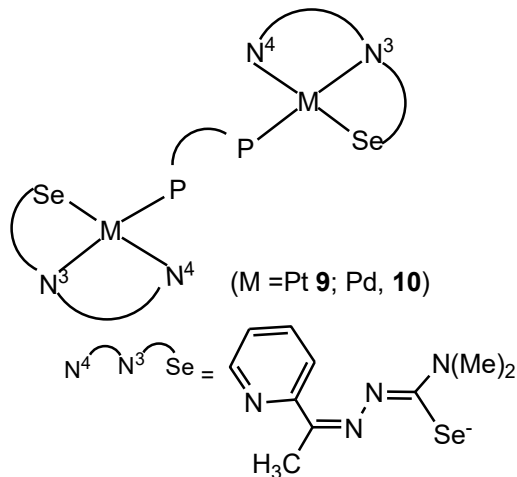
Reaction of $\text{Ni}(\text{OAc})\cdot 4\text{H}_2\text{O}$ with 2,6-diacetylpyridine-bis(selenosemicarbazone) (H_2L) formed complex, $[\text{Ni}(\text{L})]\mathbf{6}$, where one arm of the ligand bind to metal through N^3 , Se but the second arm gets modified hydrazine carbonitrile with evolution of hydrogen selenide resulting. A diamagnetic complex of formula $[\text{Ni}(\text{L})(\text{NCS})]\mathbf{7}$ is obtained with 2-(diphenylphosphino) benzaldehyde selenosemicarbazone (HL) [99, 112]. Both the complexes exhibited square planer geometry with ligand binding via hydrazinic nitrogen, selenium and heteroatom of the ring.



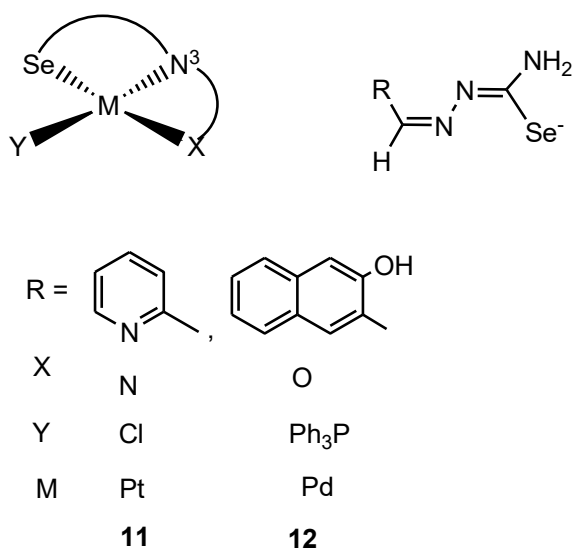
Nickel(II) reacted also with 2-quinolinecarboxaldehyde selenosemicarbazones (Hqasesc) to form complex of stoichiometry, $[\text{Ni}(\text{qasesc})_2]\mathbf{8}$ [107]. Geometry around nickel is octahedral in complex **8**.



Platinum(II) and Palladium(II) reacted with 2-acetylpyridine-N,N-dimethyl selenosemicarbazone (HL) and bis(diphenylphosphine) ethane to form dimeric complexes, $[M_2(L)_2(\mu\text{-dppe})](BPh_4)_2$ ($M = Pt$, **9**; Pd , **10**) [132]. The geometry around each metal is square planar and dppe acts as bridging ligand between two metal centers.

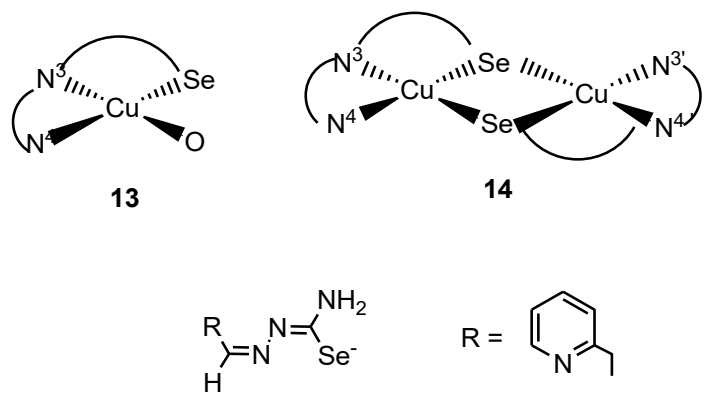


Pyridine-2-carboxaldehyde selenosemicarbazone also formed a four coordinated complex, $[Pt(L)Cl]11$ [67]. Palladium(II) also reacted with 2-hydroxynaphthaldehyde selenosemicarbazone (H_2L) and triphenylphosphine to form, $[Pd(L)(Ph_3P)]12$ [63, 75]. Geometry around palladium in complex **12** is square planar with selenosemicarbazone ligand binding via selenium atom, the imine N and O of hydroxyl group.

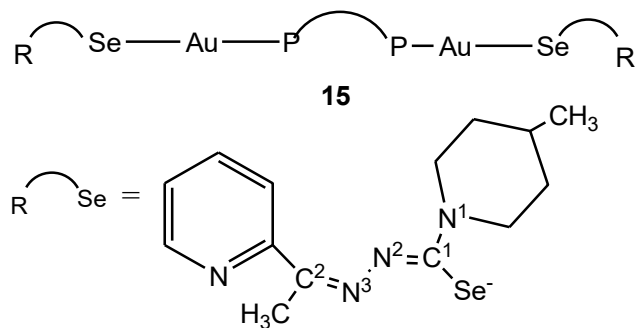


Copper and Gold: Copper(II) reacted with 2-acetylpyridine 4,4-dimethyl selenosemicarbazone (Ap44mSe) to form complex of formula, $[Cu(Ap44mSe)(OAc)]13$ and

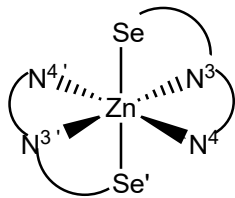
$[\text{Cu}_2(\text{AP}44\text{mSe})_3](\text{ClO}_4)_2 \cdot 3\text{H}_2\text{O}$ **14** [61]. The complex **13** have distorted square planar geometry. Selenosemicarbazine bind via hydrazinic nitrogen, selenium and pyridine nitrogen to act as tridentate ligand and also co-ordinate through a monodentate acetate ligand. The dinuclear-square planar complex **14** is also showing the connectivity of copper ions via Cu-Se-Cu bridges.



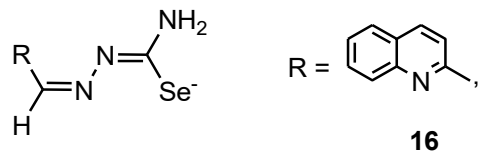
A dinuclear complex of gold(I) phosphine with acetylpyridyl based selenosemicarbazines (HL), $[\text{Au}_2(\text{L})_2(\mu\text{-dppf})]$ **15** [133] has been formed. Geometry around gold in this complex **15** is linear. The linear co-ordination about gold atoms is completed by phosphine ligand. The nitrogen atom of the pyridyl ring is directed towards the azomethine nitrogen atom.



Zinc and Cadmium: Zinc(II) reacted with 2-quinoliniccarboxaldehyde selenosemicarbazines (Hqasesc) to form complex of formula, $[\text{Zn}(\text{Hqasesc})_2](\text{ClO}_4)_2 \cdot \text{EtOH}$ **16** [110]. The geometry of this complex **16** is octahedral.

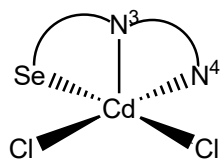


16

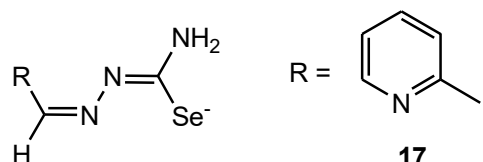


16

Cadmium(II) also reacted with 2-formypyridine selenosemicarbazone (Hfpsesc) to form the complex $[\text{CdCl}_2(\text{Hfpsesc})]$ **17** [89]. Selenosemicarbazone chelates with the cadmium cation by tridentate (NNSe) system having the involvement of the pyridinic and iminic nitrogen as well as selenium donor atoms. The cadmium ion completes its five-coordination by other two chloride ligands. The square pyramid geometry is in distorted form in which one chloride ligand occupies the base and other in apical position.



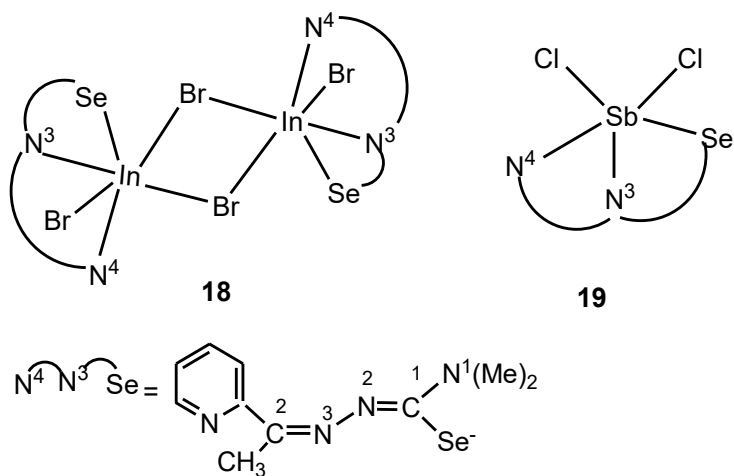
17



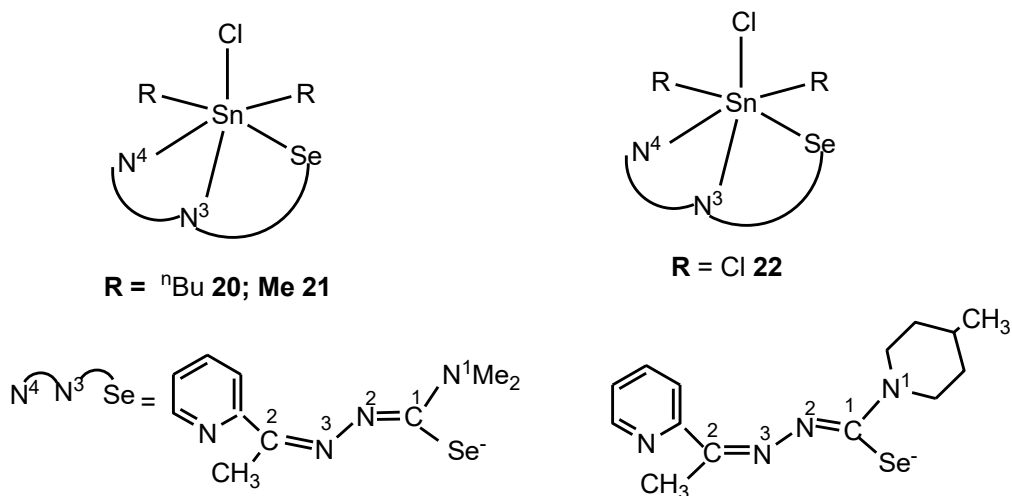
17

Indium, Tin, Antimony and Bismuth:

Indium(III) and antimony(III) reacted with pyridine based selenosemicarbazone to form complexes $[\text{In}(\text{L})\text{Br}_2]$ **18** and $[\text{Sb}(\text{L})\text{Cl}_2]$ **19** respectively [134]. Coordination number of indium is six in complex **18**. Sixth coordination site was taken by bromide ligand of next molecule takes through weak interaction. Chloride ligands attached on axial site of complex **19** are slightly bent slightly towards the selenosemicarbazone ligands.



Similar complexes of pyridine based selenosemicarbazone with tin(IV) of type, [SnLClR₂] (R = ⁿBu **20**, Me **21**, Cl **22**) are also known [105].



2.4. Biological applications of selenosemicarbazones and their complexes: Importance of selenosemicarbazones and their complexes lies in their vide range of biological activities. These activities include Anticancer, Antiproliferative, Antibacterial, Antioxidant, Antitumor, Antituberculosis, Antidiabetic, Antiproapoptotic, Antineoplastic, Antimicrobial, Antimetastatic, Antimalarial, Antiangiogenic, Antifungal and Antichagasic etc. A brief description of biological activities of selenosemicarbazones and their complexes are given below:

i) Anticancer activity: 2-formylpyridine selenosemicarbazone (Hfpsesc) and its complexes $[CdCl_2(Hfpsesc)] \cdot DMSO$ and $[ZnCl_2(Hfpsesc)] \cdot H_2O$ showed anticancer activity against eight tumor cell lines- MDA-453, MDA-361, HeLa cells, human melanoma (FemX), murine melanoma (B16), human colorectal adenocarcinoma (LS-174), EA.hy 926, human osteosarcoma U2OS and MS 1. It has been observed that anticancer activity of complexes is more as compare to free ligand [75, 86, 87, 89].

2, 6-diacetylpyridinebis (selenosemicarbazone) ($H_2dapsesc$) and its metal complexes $[Cd(dapsesc)]$ and $[Zn(dapsesc)]$ showed anticancer activity [75, 88, 112, 113]. Aminopyridine-2-carboxaldehyde selenosemicarbazone (selenotriapine) (Se-3-Ap) has shown better apoptosis inducer property than 3-aminopyridine-2-carboxaldehyde thiosemicarbazone (S-3-Ap) [103].

2-quinolinecarboxaldehyde selenosemicarbazone ($Hqasesc$) was evaluated against human cervix carcinoma cells (HeLa), human melanoma cells (FemX) and breast cancer cells (MDA-361). Its palladium(II) complex, $[PdCl(qasesc)]$ showed a strong dose-dependent cytotoxicity activity than platinum(II) complex, $[PtCl(qasesc)]$ due to higher reactivity or lower stability of palladium complex. $[Cd(AcO)(L)] \cdot H_2O$ and $[Ni(L)_2]DMSO$ metal complexes also showed cytotoxicity activity and this activity was tested against lung carcinoma (H460) and glioma (U251). Cell cycle analysis of H460 cells after treatment with the complexes, explained that $[Cd(AcO)(L)] \cdot H_2O$ and $[Ni(L)_2]DMSO$ complexes exhibit cell cycle disturbance. Only complex $[Cd(AcO)(L)] \cdot H_2O$ showed the most efficient effects regarding cytotoxicity activity and also some effects on cell cycle [75, 90, 108-110].

8-quinolinecarboxaldehyde selenosemicarbazone ($Hqasesc$) and its complex, $[Co(8qasesc)_2]ClO_4 \cdot DMSO$ complex showed anticancer activity and pancreatic adenocarcinoma cell line (AsPC-1) that is expressing epithelial-mesenchymal transition (EMT)- connected genes which promote tumor progression and also label that cell line as a good cancer stem cell line. Evaluation of anticancer potency of ligand and cobalt(III) complex was managed in order to determine pro-apoptotic activity on two malignant cell lines with pro-differentiation activity on cancer stem cells . The complex $[PtCl(L)]$ with this same ligand showed cytotoxicity activity and this activity was tested against lung carcinoma (H460) cell lines and glioma (U251) cell lines. Cell cycle analysis of H460 cells after treatment with the complex, explained that $[PtCl(L)]$ complex exhibit cell cycle disturbance [108, 111].

2-acetylpyridine 4, 4-dimethyl-3-selenosemicarbazone (Ap44mSe) has ability to form redox active copper complexes [Cu(Ap44mSe)(OAc)], that mediate intracellular reactive oxygen species generation and target the lysosome to induce lysosomal membrane permeabilization. Ap44mSe acts as an anti-cancer agent that limits metHb formation and significantly plays a very high therapeutic and pharmacological feature [61].

ii) Antiproliferative activity: Phenolic selenosemicarbazones developed multi- target drugs in the treatment of cancer like diseases. In vitro, the isosteric phenolic selenosemicarbazone compounds showed antiproliferative activity against A549 (non-small cell lung), HBL-100 (breast), SW1573 (non-small cell lung) and T-47D (breast). N-naphthyl selenosemicarbazones exhibited a better antiproliferative activity against HBL-100, HeLa, SW1573, T-47D and WiDr cell lines than cisplatin and 5-fluorouracil [84].

2-formylpyridine selenosemicarbazone (Hfpsesc) with corresponding cadmium(II), zinc(II) and nickel(II) complex showed antiproliferative activity [87, 89]. 2, 6-diacetylpyridine-bis(selenosemicarbazone) (H₂dapsesc) with [Cd(dapsesc)], [Zn(dapsesc)] and [Ni(hcn)] complexes showed antiproliferative characteristics [88].

iii) Antioxidant activity: 2- quinolinecarboxaldehydeselenosemicarbazone (Hqasesc) showed that the free selenosemicarbazone ligand (Hqasesc) is more active than cobalt(II) complex [108, 109].

2, 6-diacetylpyridine-bis (selenosemicarbazone) (H₂dapsesc) with [Cd(dapsesc)], [Zn(dapsesc)] and [Ni(hcn)] selenosemicarbazone complexes showed high in vitro antioxidant potential. The IC₅₀ values indicated that ligand 2, 6-diacetylpyridine-bis (selenosemicarbazone) (H₂dapsesc) and the complexes showed antioxidant activity. It has observed that the antioxidative capacity of ligand is lowest as compare to the complexes and the complex [Cd(dapsesc)] shows the highest antioxidative activity [113].

iv) Antitumor activity: 2-quinolinecarboxaldehyde selenosemicarbazone (Hqasesc) The antitumor activity of the ligand and as well as metal complex [Zn(Hqasesc)₂](ClO₄)₂.EtOH, AsPC-1 and THP-1 cells. Both the compounds are strong apoptosis inducers in THP-1 cells and activity is dependent on the concentraration [110].

v) Antituberculosis and antidiabetic activity(insulin-mimetic activity) : 2-acetylpyridine-N,N-dimethylselenosemicarbazone (Hdapsesc) revealed as insulin-mimetic activity which is mainly for the treatment of diabetes and this activity showed in complexes [VO(acac)(LSe)] and [V(O)₂(LSe)] [131].

vi) Antiproapoptotic and antineoplastic activity: 8-quinolinecarboxaldehyde selenosemicarbazone (Hqasesc) and $[\text{Co}(\text{qasesc})_2]\text{ClO}_4\cdot\text{DMSO}$ complex showed antineoplastic activity which was tested on THP-1 and AsPC-1 cancer cell line [111].

vii) Antineoplastic activity: 5-hydroxy-2-formylpyridin thiosemicarbazone (5-HP) and its seleno analog (5-HPSe) both revealed inhibition of DNA synthesis in vitro. 5-HP and its selenosemicarbazone depressed the subsequent progression of radioactivity traces into the DNA of Sarcoma 180 ascites cells [64].

viii) Antimicrobial activity: The ligand 8-quinolinecarboxaldehyde selenosemicarbazone (L^1) shows modest activity against the Gram-positive strains and ligand 2-quinolinecarboxaldehyde selenosemicarbazones (L^2) has activity against gram-positive strains. The complexes $[\text{PdCl}(\text{L}^1)]$, $[\text{PdCl}(\text{L}^2)]$, $[\text{PtCl}(\text{L}^1)]$, $[\text{PtCl}(\text{L}^2)]$, $[\text{Ni}(\text{L}^2)_2]$ and $[\text{Cd}(\text{AcO}(\text{L}^2)]$ are more active as comparsion to the ligands. 2-quinolineselenosemicarbazone (Hqasesc) has greater antibacterial activity against *Bacillus cereus* and this ligand also shows selectivity to *E.coli* [75, 108].

2-formylpyridineselenosemicarbazone (Hfpsesc) and synthesized complexes $[\text{PtCl}(\text{fpsesc})]$, $[\text{PdCl}(\text{fpsesc})]$ and $[\text{Co}(\text{fpsesc})]\text{BF}_4\cdot 2\text{H}_2\text{O}$ screened antibacterial activity against three Gram-positive bacteria, *Staphylococcus aureus* ATCC 25923, *Micrococcus lysodeikticus* ATCC 4698 and *Escherichia coli* ATCC 35218. It has been determined that the ligands and complexes are active [75].

ix) Antimalarial activity: 2-acetylpyridine selenosemicarbazone (Hdepsesc) with gold(I) phosphine complex significantly represents antimalaria activity. The IC_{50} data shows that selenium derivatives $[\text{Au}(\text{Se}_1)(\text{PPh}_3)]$ and $[\text{Au}(\text{Se}_2)(\text{PPh}_3)]$ display moderate antimalaria activity [133].

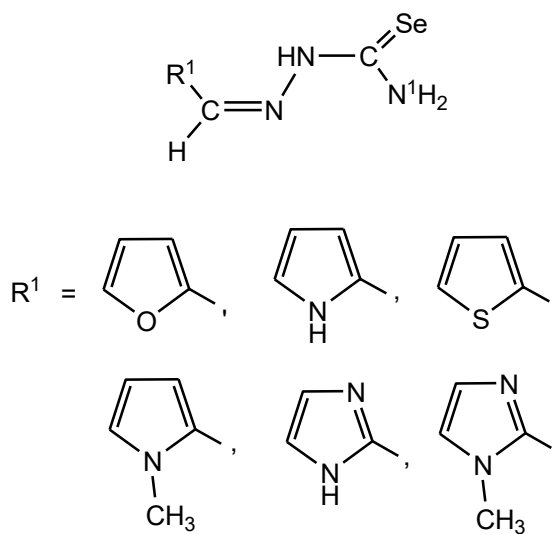
x) Antifungal activity: 2-formylpyridineselenosemicarbazone (Hfpsesc) with all the synthesized complexes $[\text{PtCl}(\text{fpsesc})]$, $[\text{PdCl}(\text{fpsesc})]$ and $[\text{Co}(\text{fpsesc})_2]\text{BF}_4\cdot \text{H}_2\text{O}$ were showing antifungal activity. One fungus was also observed by using *Candida albicans* strain ATCC 244433 on different medium. It has been observed that both the ligand and complexes are active [75].

xi) Antichagasic activity: A series of selenosemicarbazone compounds which are act as Cruzipain inhibitors and anti *Trypanosoma cruzi* agents against non-infective and infective form of the parasite. In vitro, selenosemicarazone compounds showed anti-chagasic activity at low μM concentration [66].

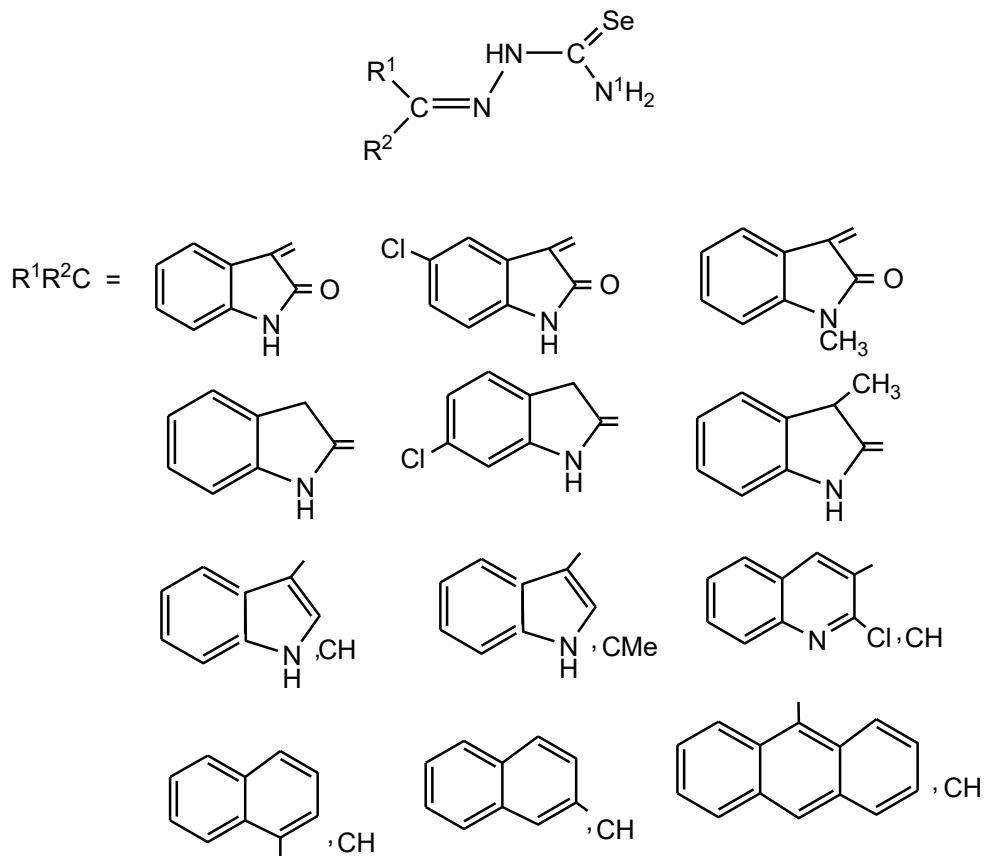
2.5. Aims and objectives: From the above literature survey, it has been observed that selenosemicarbazones already known mainly contain aromatic ring or pyridine ring or

aliphatic chain at C² carbon. Selenosemicarbazones with five membered heterocyclic rings containing or more than one hetero atoms at C² carbon are not known till date. Moreover selenosemicarbazone with fused ring at C² are also very limited in number. Heterocyclic rings either alone or fused are very important, as these rings are important part of biological system. Also only few x-ray characterized complexes of selenosemicarbazones are known till date. Keeping in mind the biological importance of heterocyclic ring / fused rings and a huge gap in the complexes synthesized, current research is aimed to have following objectives:

1. Synthesis and characterization (IR, NMR) of selenosemicarbazones given in Scheme 1 and Scheme 2
2. Synthesis and characterization (Elemental analysis, UV-Vis, IR, magnetic susceptibility, single crystal X-ray crystallography (wherever possible)) of complexes of selenosemicarbazones (Scheme 1 and 2) with Fe, Co, Ni, Cu and Zn.
3. Evaluation of biological activities (antitubercular and anticancer) of synthesized ligands.
4. Evaluation of biological activities (antitubercular and anticancer) of complexes and their comparison vis-à-vis free ligand.



Scheme 1



Scheme 2

CHAPTER 3

GENERAL EXPERIMENTAL

3.1 Materials and Instrumentation:

3.1.1 Materials

Cyclohexanone, hydrazine hydrate, HCl, methanol, ethanol are purchased from LobaChem, whereas KSeCN, furfural-2-carbaldehyde, N-methyl-2-pyrrole carbaldehyde, 2-naphthaldehyde, 3-acetyl indole carbaldehyde, 6-chloro-2-oxindole, isatin, 5-chloro isatin, i-methyl isatin, 3-indole, 2-oxindole, 1-naphthaldehyde, 9-anthrinaldehyde, 2-thiophene carboxaldehyde, 3-methyl-2-oxindole, iron acetate, cobalt acetate, nickel acetate, copper acetate and zinc acetate are procured from Sigma-Aldrich.

3.1.2 Instrumentation:

3.1.2.1 Melting Point: With the lab fit electrically heated apparatus, the melting point of synthesized selenosemicarbazones ligands and their complexes were determined.

3.1.2.2 Infrared Spectroscopy: Infra-red (IR) spectra were recorded using KBr pellets by SHIMADZUFTIR 8400S, Fourier Transform, Infrared spectrophotometer.

3.1.2.3 Nuclear Magnetic Resonance (NMR) Spectroscopy: A BRUCKER ADVANCE III NMR Spectrophotometer at 500 MHz in DMSO and CDCl₃ with TMS (trimethyl silane) as the internal reference used for recording ¹H and ¹³C NMR spectra.

3.1.2.4 Mass Spectrometry: Model Q-ToF with electrospray ionization (ESI) and atmospheric pressure chemical ionization (APCI) sources having mass Range of 4000 amu in quadrupole and 20000 amu in ToF used for recording Mass spectra on LC-MS Spectrometer.

3.1.2.5 Electron Spin Resonance Spectroscopy (ESR): JEOL, JES - FA200 ESR Spectrometer with X band used for recording ESR spectra at room temperature. The standard frequency for X- band used is 8.75-9.65 GHz. ESR spectra were recorded at 295K on JEOL, JES - FA200 ESR Spectrometer. Simulation studies are done using a MATLAB program based on Easy Spin sub routines.

3.1.2.6 CHN Analysis: Elemental analysis for C, H and N were carried out using a thermo scientific FLASH2000 analyzer.

3.1.2.7 Vibrating Sample Magnatometer (VSM): VSM studies of iron(III)-selenosemicarbazone complexes was done on Lakeshore VSM7410 at room temperature.

3.1.2.8 Powder X-Ray Diffractometer (XRD):

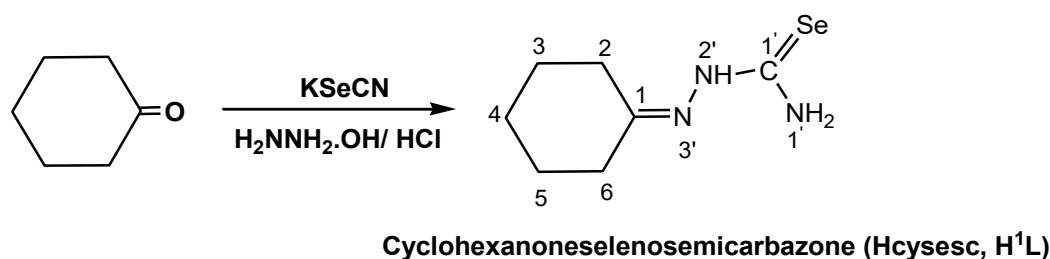
The powder XRD spectrum of some representative complexes was obtained from BRUKER D8 X-ray diffractometer using Cu K α radiation with $\lambda = 1.5405\text{\AA}$.

3.1.2.9 Mössbauer Spectroscopy: Mossbauer spectra of complex were obtained from MS-1104E rapid spectrometer and analyzed using UNIVEM computer program.

3.2 Synthesis of Selenosemicarbazone ligands

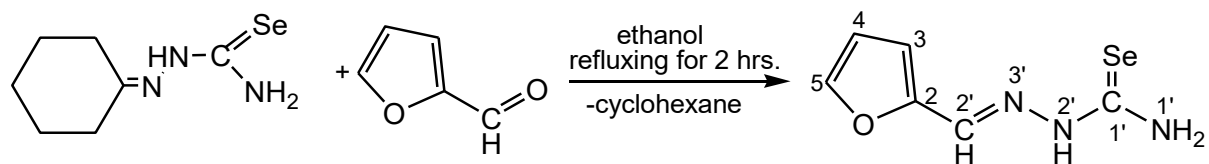
3.2.1 Synthesis of cyclohexanoneselenosemicarbazone (**Hcysesc, H¹L**):

Cyclohexanone selenosemicarbazone was prepared by the similar methods used in literature [63, 64] Yield, 70%, m. p., 180-182°C. Important IR peaks (KBr, cm⁻¹): $\nu(\text{NH}_2)$ 3362s, 3225s; $\nu(-\text{NH}-)$ 3157s; $\nu(\text{C}-\text{H}_{\text{cyclo}})$, 2986s, 2854s; $\nu(\text{C}=\text{N})$ 1591s; $\nu(\text{C}=\text{C})$ 1489s; $\delta(\text{NH}_2)$ 1454s; $\nu(\text{C}=\text{Se})$ 856s (selenoamidemoiety). ¹H NMR (CDCl₃, δppm): 9.23 s (1H, N^{2'}H), 7.65 s (1H, N^{1'}H₂), 7.15 s (1H, N^{1'}H₂), 2.32-1.54 m (10H, cyclic ring proton). ¹³C NMR (CDCl₃, δppm): 175.6 (C^{1'}), 35.4-25.3 (cyclic ring carbon) respectively.



3.2.2 Synthesis of 2-furfural selenosemicarbazone (**2-Hfursesc, H²L**):

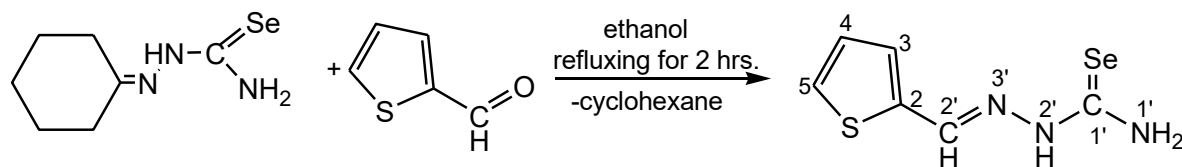
Cyclohexanoneselenosemicarbazone, (0.5g, 2.29mmol) was dissolved in 20 ml of ethanol with heating. To it was added 2-furfural (0.22g, 2.29mmol) and the mixture was refluxed for 2 hours. 1ml of glacial acetic acid was added during refluxing. Light reddish solution formed was then filtered and at room temperature reddish solution kept for crystallization. Yield, 62%, m. p., 140-143°C. Important IR data (KBr, cm⁻¹): $\nu(\text{NH}_2)$ 3379m, 3240m; $\nu(-\text{NH}-)$ 3142w; $\nu(\text{C}=\text{N})$ 1600s; $\nu(\text{C}=\text{C})$ 1579s; $\delta(\text{NH}_2)$ 1464s; $\nu(\text{C}=\text{Se})$ 812s (selenoamidemoiety). ¹H NMR (CDCl₃, δppm): 10.95 s (1H, N^{2'}H), 10.00 s (1H, C^{2'}H), 7.87 d (1H, C⁵H), 7.74 d (1H, C³H), 7.58 t (1H, C⁴H), 6.60 s (1H, N^{1'}H₂), 6.54 s (1H, N^{1'}H₂). ¹³C NMR (CDCl₃, δppm): 145.2 (C^{2'}), 133.9 (C⁵), 127.5 (C⁴), 117.3 (C³), 112.3 (C²).



2-furfural selenosemicarbazone (2-Hfursesc, H²L)

3.2.3 Synthesis of 2-thiophene selenosemicarbazone (2-Hthiosesc, H³L):

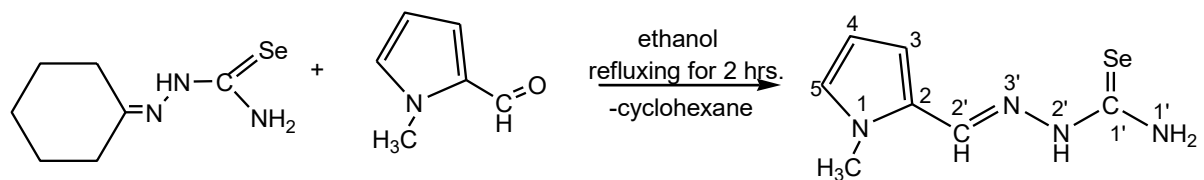
Cyclohexanoneselenosemicarbazone, (0.5g, 2.29mmol) was dissolved in 20 ml of ethanol with heating. To it was added 2-thiophene (0.25g, 2.29mmol) and the mixture was refluxed for 2 hours. 1ml of glacial acetic acid was added during refluxing. Light brownish solution formed was then filtered and at room temperature brownish solution kept for crystallization. Yield, 60%, m. p., 140-142°C. Important IR peaks (KBr, cm⁻¹): $\nu(\text{NH}_2)$ 3389m, 3221m; $\nu(-\text{NH}-)$ 3095w; $\nu(\text{C}=\text{N})$ 1599s; $\nu(\text{C}=\text{C})$ 1527m; $\delta(\text{NH}_2)$ 1415s; $\nu(\text{C}=\text{Se})$ 844s (selenoamidemoiety). ¹H NMR (CDCl₃, δppm): 9.64 s (1H, N^{2'}H), 8.10 s (1H, C^{2'}H), 7.47m (1H, C⁴H), 7.37 d (1H, C³H), 7.12 d (1H, C⁵H), 7.58 s (1H, N^{1'}H₂), 6.71 s (1H, N^{1'}H₂). ¹³C NMR (CDCl₃, δppm): 155.8 (C^{2'}), 132.4 (C⁵), 130.0 (C⁴), 127.8 (C³), 127.3 (C²).



2-thiophene selenosemicarbazone (2-Hthiosesc, H³L)

3.2.4 Synthesis of N-methyl-2-pyrrole selenosemicarbazone (N-MeHPysesc, H⁴L):

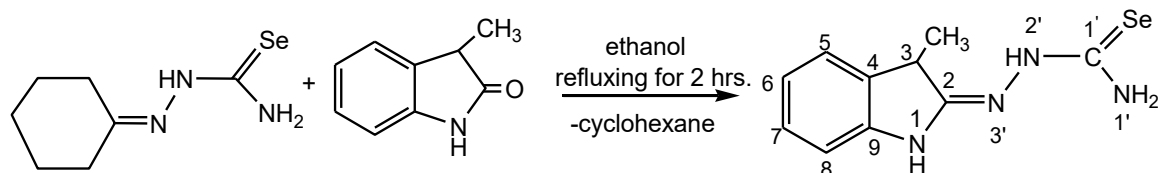
Cyclohexanoneselenosemicarbazone, (0.5g, 2.29mmol) was dissolved in 20 ml of ethanol with heating. To it was added N-methyl-2-pyrrole (0.25g, 2.29mmol) and the mixture was refluxed for 2 hours. 1ml of glacial acetic acid was added during refluxing. Bright reddish solution formed was then filtered and at room temperature reddish solution kept for crystallization. Yield, 60%, m. p., 150-152°C. Important IR peaks (KBr, cm⁻¹): $\nu(\text{NH}_2)$ 3412m, 3223m; $\nu(-\text{NH}-)$ 3110w; $\nu(\text{C}=\text{N})$ 1633s; $\nu(\text{C}=\text{C})$ 1562m; $\delta(\text{NH}_2)$ 1496s; $\nu(\text{C}=\text{Se})$ 854s (selenoamidemoiety). ¹H NMR (CDCl₃, δppm): 10.05 s (1H, N^{2'}H), 7.98 d (1H, C⁵H), 6.82 t (1H, C⁴H), 6.62 d (1H, C³H), 3.84 (CH₃), 6.21s, 6.20s (2H, N^{1'}H₂), 3.87 (CH₃). ¹³C NMR (CDCl₃, δppm): 173.4 (C^{1'}), 138.3 (C^{2'}), 129.2 (C⁴), 125.8 (C⁵), 117.9 (C³), 109.3(C²), 36.8 (CH₃).



N-methyl-2-pyrrole selenosemicarbazone (N-MeHPyseSc, H⁴L)

3.2.5 Synthesis of 3-methyl-2-oxindole selenosemicarbazone (3-MeHOxsesc, H⁵L):

Cyclohexanone selenosemicarbazone, (0.5g, 2.29mmol) was dissolved in 20 ml of ethanol with heating. To it was added 3-methyl-2-oxindole (0.33g, 2.29mmol) and the mixture was refluxed for 2 hours. 1ml of glacial acetic acid was added during refluxing. Light reddish solution formed was then filtered and at room temperature reddish solution kept for crystallization. Yield, 60%, m. p., 160-162°C. Important IR peaks (KBr, cm⁻¹): $\nu(\text{NH}_2)$ 3358m, 3248m; $\nu(-\text{NH}-)$ 3157w; $\nu(\text{C}=\text{N})$ 1591s; $\nu(\text{C}=\text{C})$ 1425m; $\delta(\text{NH}_2)$ 1450s; $\nu(\text{C}=\text{Se})$ 854s (selenoamidemoiety). ¹H NMR (CDCl₃, δppm): 9.16 s (1H, N^{2'}H), 7.24-6.95m(4 H, C^{5,6,7,8}H), 1.54 s (cyclic proton ring), 3.51 s (3H, CH₃). ¹³C NMR (CDCl₃, δppm): 181.6 (C^{1'}), 141.3 (C⁵), 131.2 (C⁶), 127.8 (C⁷), 123.7 (C⁸), 109.8 (C⁹), 41.1 (CH₃), 15.2 (cyclic carbon ring).

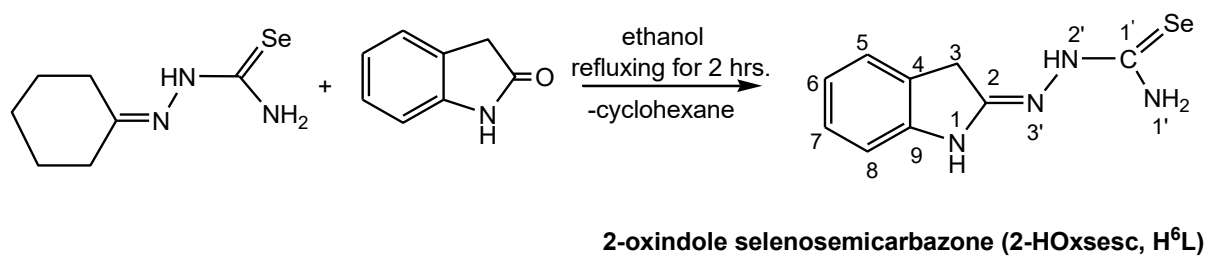


3-methyl-2-oxindole selenosemicarbazone (3-MeHOxsesc, H⁵L)

3.2.6 Synthesis of 2-oxindole selenosemicarbazone (2-HOxsesc, H⁶L):

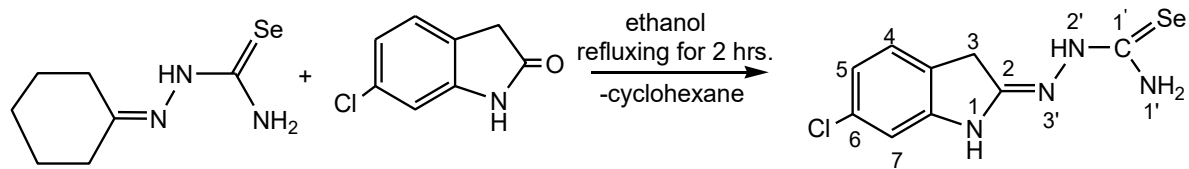
Cyclohexanone selenosemicarbazone, (0.5g, 2.29mmol) was dissolved in 20 ml of ethanol with heating. To it was added 2-oxindole (0.30g, 2.29mmol) and the mixture was refluxed for 2 hours. 1ml of glacial acetic acid was added during refluxing. Light reddish solution formed was then filtered and at room temperature reddish solution kept for crystallization. Yield, 60%, m. p., 180-183°C. Important IR peaks (KBr, cm⁻¹): $\nu(\text{NH}_2)$ 3362m, 3225m; $\nu(-\text{NH}-)$ 3157w; $\nu(\text{C}=\text{N})$ 1591s; $\nu(\text{C}=\text{C})$ 1489m; $\delta(\text{NH}_2)$ 1454s; $\nu(\text{C}=\text{Se})$ 856s (selenoamidemoiety). ¹H NMR (CDCl₃, δppm): 9.03 s(1H, N^{2'}H), 5.54 s (1H, N^{1'}H₂), 5.46 s (1H, N^{1'}H₂), 8.34-6.90

m(4H, C^{5,6,7,8}H), 3.56 (cyclic proton ring). ¹³C NMR (CDCl₃, δppm): 177.4 (C^{1'}), 142.3 (C⁵), 127.9 (C⁶), 124.6 (C⁷), 122.3 (C⁸), 109.7 (C⁹), 36.1 (cyclic carbon ring).



3.2.7 Synthesis of 6-chloro-2-oxindole selenosemicarbazone (6-ClHOxsesc, H⁷L):

Cyclohexanone selenosemicarbazone, (0.5g, 2.29mmol) was dissolved in 20 ml of ethanol with heating. To it was added 6-chloro-2-oxindole(0.38g, 2.29mmol) and the mixture was refluxed for 2 hours. 1ml of glacial acetic acid was added during refluxing. Light brownish solution formed was then filtered and at room temperature brownish solution kept for crystallization. Yield, 65%, m. p., 187-189°C. Important IR peaks (KBr, cm⁻¹): ν(NH₂) 3417m, 3255m; ν(-NH-) 3142w; ν(C=N) 1589s; ν(C=C) 1512m; δ(NH₂) 1499s; ν(C=Se) 879s (selenoamidemoiety). ¹H NMR (CDCl₃, δppm): 9.51 s (1H, N^{2'}H), 7.13 d (1H, C⁵H), 6.99 d (1H, C⁴H), 6.92s (1H, C⁷H), 4.89s (1H, N^{1'}H₂), 4.26 s (1H, N^{1'}H₂). ¹³C NMR (CDCl₃, δppm): 177.9 (C^{1'}), 143.6 (C⁵), 133.1 (C⁶), 125.3 (C⁷), 110.7 (C⁸), 58.2 (C⁴), 35.3 (C³).

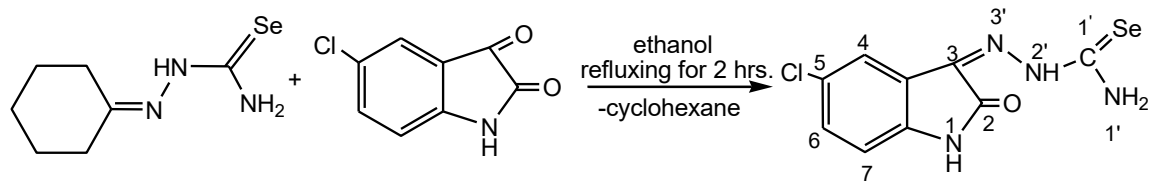


6-chloro-2-oxindole selenosemicarbazone (6-ClHOxsesc, H⁷L)

3.2.8 Synthesis of 5-chloro isatin selenosemicarbazone (5-ClHIstsesc, H⁸L):

Cyclohexanone selenosemicarbazone, (0.5g, 2.29mmol) was dissolved in 20 ml of ethanol with heating. To it was added 5-chloroisatin (0.41g, 2.29mmol) and the mixture was refluxed for 2 hours. 1ml of glacial acetic acid was added during refluxing. Light reddish solution formed was then filtered and at room temperature reddish solution kept for crystallization. Yield, 60%, m. p., 150-152°C. Important IR peaks (KBr, cm⁻¹): ν(NH₂) 3219m; ν(-NH-) 3110w; ν(C=O) 1694s; ν(C=N) 1618s; ν(C=C) 1559m; δ(NH₂) 1447s; ν(C=Se) 885s

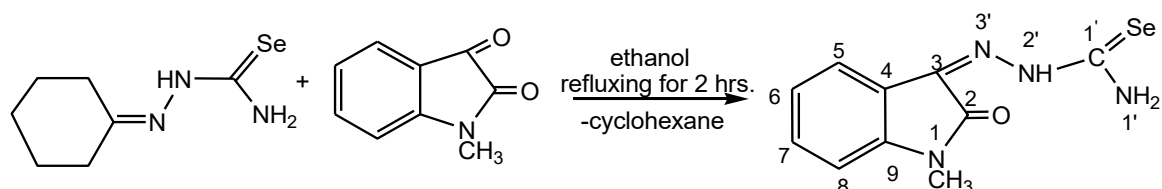
(selenoamidemoiety). ^1H NMR (CDCl_3 , δ ppm): 11.21 s (1H, $\text{N}^2\text{-H}$), 8.80 s (1H, $\text{N}^1\text{-H}_2$), 8.56 s (1H, $\text{N}^1\text{-H}_2$), 7.49 d (1H, C^4H), 7.21 d (1H, C^7H), 6.83 m (2H, $\text{C}^{5,6}\text{H}$). ^{13}C NMR (CDCl_3 , δ ppm): 163.1 ($\text{C}^{1'}$), 131.0 (C^5), 129.8 (C^6), 125.2 (C^7), 119.5 (C^4), 42.1 (C^3), 34.9 (C^2).



5-chloro isatin selenosemicarbazone (5-ClH1stsesc, H⁸L)

3.2.9 Synthesis of 1-methyl isatin selenosemicarbazone (1-MeH1stsesc, H⁹L):

Cyclohexanone selenosemicarbazone, (0.5g, 2.29mmol) was dissolved in 20 ml of ethanol with heating. To it was added 1-methylisatin (0.41g, 2.29mmol) and the mixture was refluxed for 2 hours. 1ml of glacial acetic acid was added during refluxing. Bright reddish solution formed was then filtered and at room temperature reddish solution kept for crystallization. Yield, 60%, m. p., 120-122°C. Important IR peaks (KBr, cm^{-1}): $\nu(\text{NH}_2)$ 3408m, 3228m; $\nu(-\text{NH}-)$ 3134w; $\nu(\text{C=O})$ 1676s; $\nu(\text{C=N})$ 1604s; $\nu(\text{C=C})$ 1492m; $\delta(\text{NH}_2)$ 1415s; $\nu(\text{C=Se})$ 889s (selenoamidemoiety). ^1H NMR (CDCl_3 , δ ppm): 13.1 s (1H, $\text{N}^2\text{-H}$), 7.61-6.90 m (4H, $\text{C}^{5,6,7,8}\text{H}$), 8.01 s (1H, $\text{N}^1\text{-H}_2$), 7.60 s (1H, $\text{N}^1\text{-H}_2$), 3.29 (CH_3). ^{13}C NMR (CDCl_3 , δ ppm): 178.7 ($\text{C}^{1'}$), 161.0 (C^5), 144.1 (C^6), 132.0 (C^8), 129.2 (C^7), 123.5 (C^9), 121.1 (C^3), 119.2 (C^2), 109.3 (C^4), 25.6 (CH_3), 20.4(cyclic ring).

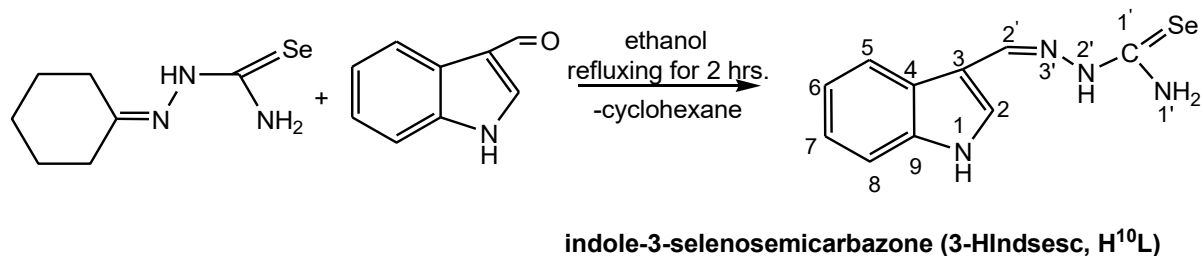


1-methyl isatin selenosemicarbazone (1-MeH1stsesc, (H⁹L)

3.2.10 Synthesis of indole-3-selenosemicarbazone (3-H1ndsesc, H¹⁰L):

Cyclohexanone selenosemicarbazone, (0.5g, 2.29mmol) was dissolved in 20 ml of ethanol with heating. To it was added indole-3-carboxaldehyde (0.33g, 2.29mmol) and the mixture was refluxed for 2 hours. 1ml of glacial acetic acid was added during refluxing. Bright brownish solution formed was then filtered and at room temperature brownish solution kept for crystallization. Yield, 60%, m. p., 110-113°C. Important IR peaks (KBr, cm^{-1}): $\nu(\text{NH}_2)$

3356m, 3246m; ν (-NH-) 3153w; ν (C=N) 1591s; ν (C=C) 1487m; δ (NH₂) 1450s; ν (C=Se) 898s (selenoamidemoiety). ¹H NMR (CDCl₃, δ ppm): 10.0 s (1H, N^{2'}H), 7.85 s (1H, C^{2'}H), 7.76 s (1H, N^{1'}H₂), 7.56 s (1H, N^{1'}H₂), 8.30-7.28 (5H, Cyclic ring proton). ¹³C NMR (CDCl₃, δ ppm): 145.2 (C^{2'}), 133.9 (C⁶), 127.5 (C⁵), 117.3 (C⁴), 112.3 (C³).

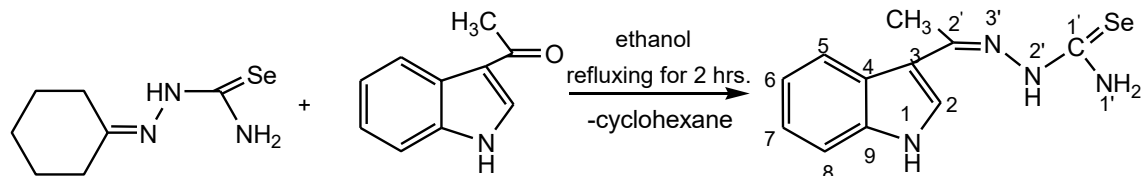


indole-3-selenosemicarbazone (3-H1ndsesc, H¹⁰L)

3.2.11 Synthesis of 3-acetyl indole selenosemicarbazone (3-AcHIndsesc, H¹¹L):

Cyclohexanone selenoamidemoiety, (0.5g, 2.29mmol) was dissolved in 20 ml of ethanol with heating. To it was added 3-acetylindole (0.36g, 2.29mmol) and the mixture was refluxed for 2 hours. 1ml of glacial acetic acid was added during refluxing. Light reddish solution formed was then filtered and at room temperature reddish solution kept for crystallization.

Yield, 60%, m. p., 100-103°C. Important IR peaks (KBr, cm⁻¹): ν (NH₂) 3290m; ν (-NH-) 3142w; ν (C=N) 1624s; ν (C=C) 1502m; δ (NH₂) 1406s; ν (C=Se) 877s (selenoamidemoiety). ¹H NMR (CDCl₃, δ ppm): 8.42 d (1H, C⁷H), 7.90 d (1H, C⁶H), 7.65 s (1H, N^{1'}H₂), 7.46-7.32 m (2H, C^{5,8}H), 7.29 s (1H, C²H), 6.63 s (1H, N^{1'}H₂), 2.58 s (3H, CH₃). ¹³C NMR (CDCl₃, δ ppm): 193.6 (C^{1'}), 158.2 (C^{2'}), 131.5 (C⁶), 123.7 (C⁵), 122.6 (C⁷), 118.6 (C⁸), 111.3 (C⁴), 35.4 (CH₃), 26.9 (C³).

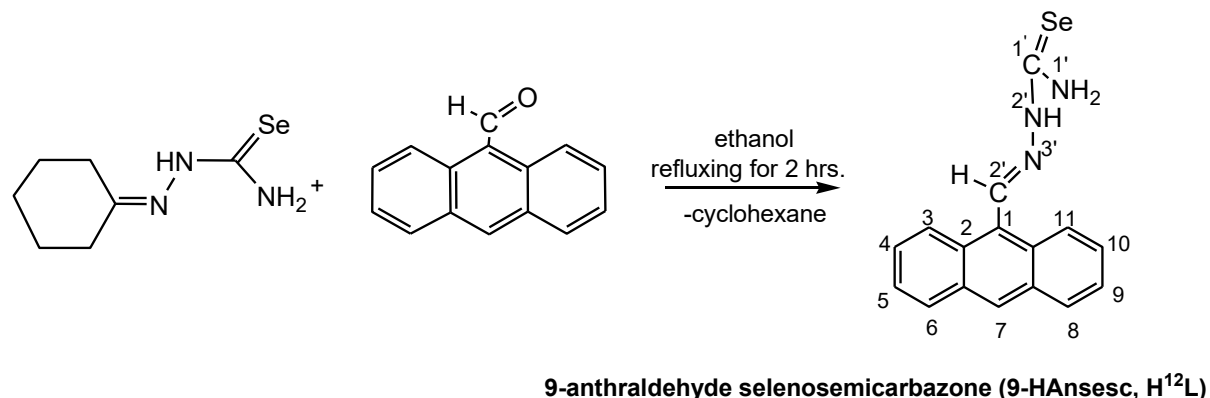


3-acetyl indole selenosemicarbazone (3-AcHIndsesc, H¹¹L)

9-anthraldehyde selenosemicarbazone (9-HAnsesc, H¹²L), 1-Naphthaldehyde selenosemicarbazone(1-HNapsesc, H¹³L) and 2-Naphthaldehyde selenosemicarbazone(2-HNapsesc, H¹⁴L) are synthesized using method similar to that of H²L.

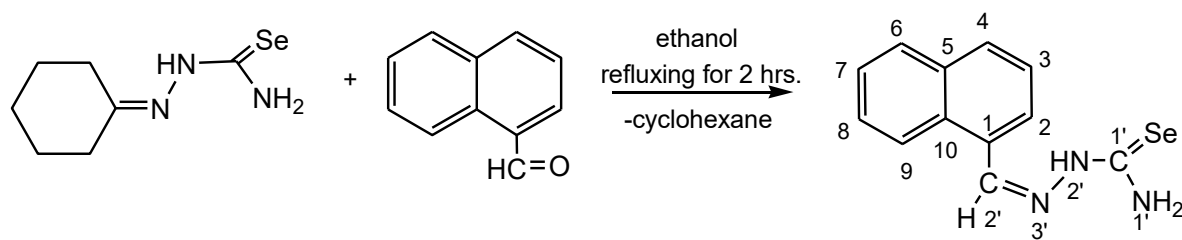
3.2.12 Synthesis of 9-anthraldehyde selenosemicarbazone (9-HAnsesc, H¹²L):

Yield, 60%, m. p., 210-213°C. Important IR peaks (KBr, cm⁻¹): $\nu(\text{NH}_2)$ 3385m, 3248m; $\nu(-\text{NH}-)$ 3151w; $\nu(\text{C}=\text{N})$ 1639s; $\nu(\text{C}=\text{C})$ 1587m; $\delta(\text{NH}_2)$ 1402s; $\nu(\text{C}=\text{Se})$ 887s (selenoamidemoiety). ¹H NMR (CDCl₃, δppm): 11.5 s (1H, N²H), 9.02 s (1H, C^{2'}H), 8.73 d (2H, C^{3,11}H), 8.08 d (2H, C^{6,8}H), 7.73 t (2H, C^{5,9}H), 7.60 t (2H, C^{4,10}H), 7.29 s (1H, C⁷H). ¹³C NMR (CDCl₃, δppm): 193.0 (C^{1'}), 135.0 (C^{2'}), 132.4-122.7 (aromatic ring carbon), 114.0 (C⁸).



3.2.13 Synthesis of 1-Naphthaldehyde selenosemicarbazones (1-HNapsesc, H¹³L):

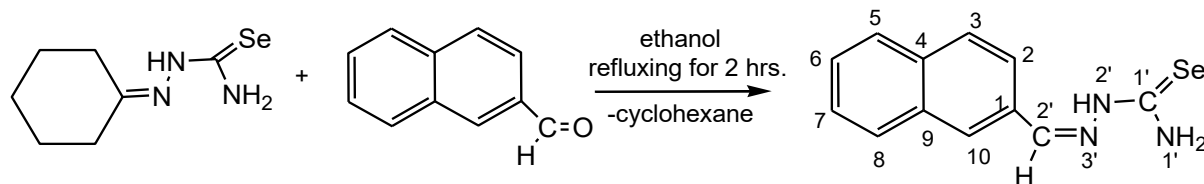
Yield, 50%, m. p., 175-179°C. Important IR peaks (KBr, cm⁻¹): $\nu(\text{NH}_2)$ 3400s, $\nu(-\text{NH}-)$ 3147w; $\nu(\text{C}=\text{N})$ 1599s; $\nu(\text{C}=\text{C})$ 1516m; $\delta(\text{NH}_2)$ 1452s; $\nu(\text{C}=\text{Se})$ 871s (selenoamidemoiety). ¹H NMR (CDCl₃, δppm): 9.51 s (1H, N²H), 9.00 s (1H, C^{2'}H), 8.17 d (1H, C⁹H), 8.02 d (1H, C⁴H), 7.95 d (1H, C⁶H), 7.97 s (1H, N¹H₂), 7.62 m (2H, C^{3,7}H), 7.29 s (1H, C⁸H). ¹³C NMR (CDCl₃, δppm): 162.1 (C^{1'}), 134.1 (C^{2'}), 131.8-124.9 (Aromatic ring carbon), 115.0 (C⁵).



1-naphthaldehyde selenosemicarbazone (1-HNapsesc, H¹³L)

3.1.14 Synthesis of 2-Naphthaldehyde selenosemicarbazones (2-HNapsesc, H¹⁴L):

Yield, 50%, m. p., 178-180°C. Important IR peaks (KBr, cm⁻¹): $\nu(\text{NH}_2)$ 3352m; $\nu(-\text{NH}-)$ 3124w; $\nu(\text{C}=\text{N})$ 1597s; $\nu(\text{C}=\text{C})$ 1533m; $\delta(\text{NH}_2)$ 1446s; $\nu(\text{C}=\text{Se})$ 856s (selenoamidemoiety). ¹H NMR (CDCl₃, δppm): 10.1 s (1H, N^{2'}H), 8.38 s (1H, C^{2'}H), 7.70 s (1H, N^{1'}H₂), 8.05-7.29 m (ring proton). ¹³C NMR (CDCl₃, δppm): 192.2 (C^{1'}), 136.4 (C^{2'}), 134.5-122.8 (ring carbon), 115.0 (C^{5'}).

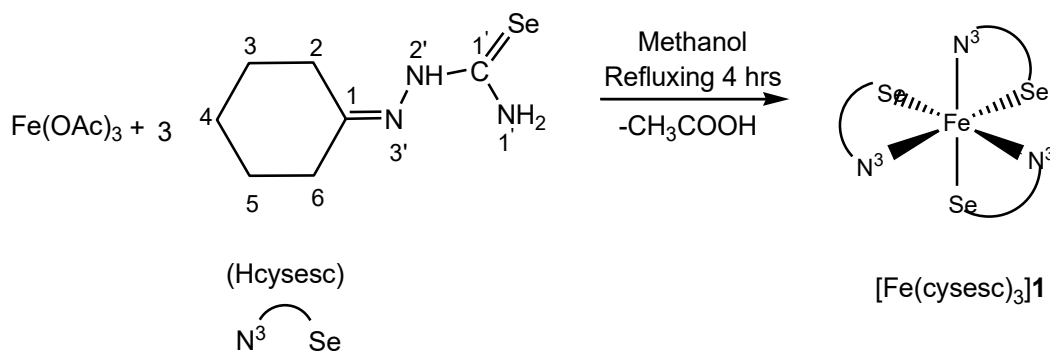


2-naphthaldehyde selenosemicarbazone (2-HNapsesc, H¹⁴L)

3.2 Complexes of Iron (III)

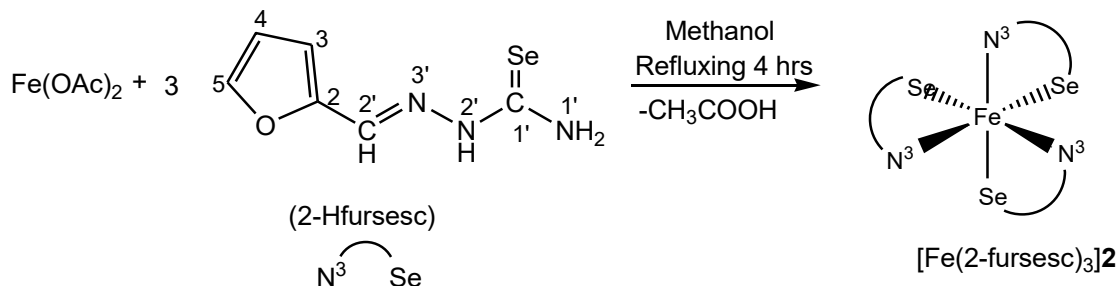
3.2.1 Synthesis of [Fe(cysesc)₃]1:

Iron acetate (0.025g, 0.103mmol) was dissolved in 30 ml of methanol with heating. To it was added cyclohexanoneselenosemicarbazone, (0.070g, 0.32mmol) and the mixture was refluxed for 4 hours. Light red solution formed was then filtered and at room temperature red solution kept for crystallization. Yield, 60%, m. p., 210-213°C. Important IR peaks (KBr, cm⁻¹): $\nu(\text{NH}_2)$ 3354m; $\nu(\text{C}=\text{N})$ 1635s; $\nu(\text{C}=\text{C})$ 1504m; $\delta(\text{NH}_2)$ 1438s; $\nu(\text{C}=\text{Se})$ 748s (selenoamidemoiety). The Saturation magnetization, Coercivity magnetization and Remanence magnetization parameters obtained from the VSM analysis are Ms = 0.00520emu/g, Mr = 0.00268emu/g and Hc = -0.34888emu/g respectively. Mass spectra (m/z): [Fe(C₇H₁₄N₃Se)₃]⁺: 709amu (parent ion peak).



3.2.2 Synthesis of [Fe(2-fursesc)3]2:

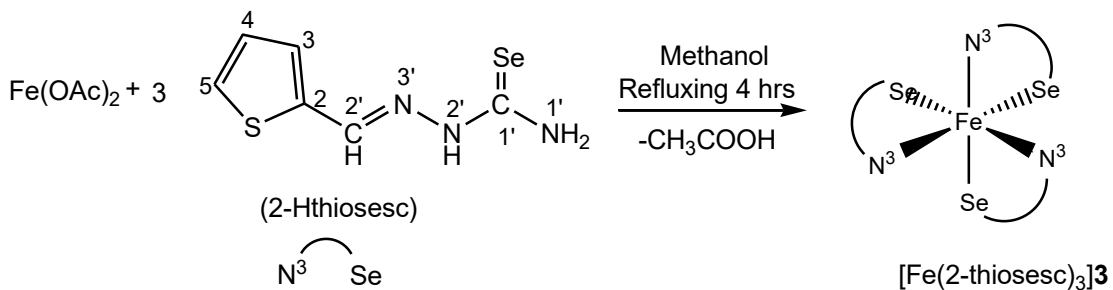
Iron acetate (0.025g, 0.10mmol) was dissolved in 20 ml of methanol with heating. To it was added 2-furfural selenosemicarbazone (0.069g, 0.32mmol) and the mixture was refluxed for 4 hours. Light reddish solution formed was then filtered and at room temperature reddish solution kept for crystallization. Yield, 60%, m. p., 210-213°C. Important IR peaks (KBr, cm⁻¹): $\nu(\text{NH}_2)$ 3366m; $\nu(\text{C}=\text{N})$ 1617s; $\nu(\text{C}=\text{C})$ 1537m; $\delta(\text{NH}_2)$ 1439s; $\nu(\text{C}=\text{Se})$ 738s (selenoamidemoiety). The Saturation magnetization, Coercivity magnetization and Remanence magnetization parameters obtained from the VSM analysis are Ms = 0.03626emu/g, Mr = 0.02722emu/g and Hc= -0.35224emu/g respectively. Mass spectra (m/z): Na-[Fe(C₆H₆N₃OSe)₃]⁺: 675amu (parent ion peak).



3.2.3 Synthesis of [Fe(2-thiosesc)3]3:

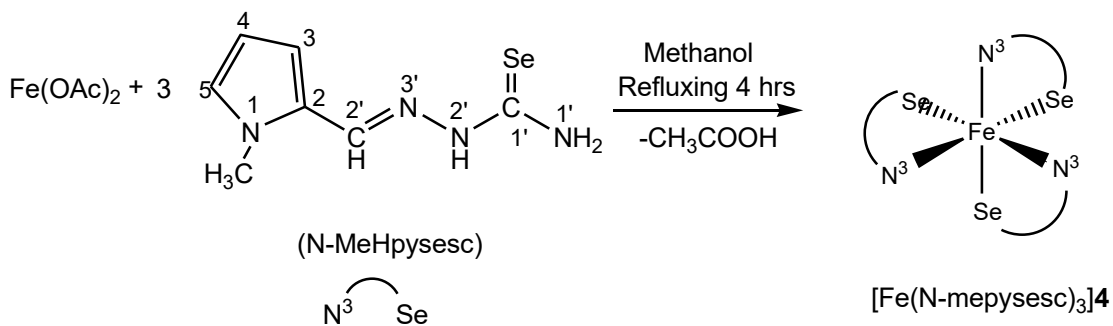
Iron acetate (0.025g, 0.10mmol) was dissolved in 20 ml of methanol with heating. To it was added 2-thiophene selenosemicarbazone (0.074g, 0.31mmol) and the mixture was refluxed for 4 hours. Light reddish solution formed was filtered and kept for crystallization at room temperature. Yield, 60%, m. p., 210-213°C. Important IR peaks (KBr, cm⁻¹): $\nu(\text{NH}_2)$ 3219m; $\nu(\text{C}=\text{N})$ 1671s; $\nu(\text{C}=\text{C})$ 1605m; $\delta(\text{NH}_2)$ 1419s; $\nu(\text{C}=\text{Se})$ 715s (selenoamidemoiety). The Saturation magnetization, Coercivity magnetization and Remanence magnetization parameters obtained from the VSM analysis are Ms = 0.07771emu/g, Mr = 0.03224emu/g

and $H_c = -0.35406$ emu/g respectively. Mass spectra (m/z): $[Fe(C_6H_8N_3SSe)_3]^+$: 751 amu (parent ion peak).



3.2.4 Synthesis of $[Fe(N\text{-mepysesc})_3]4$:

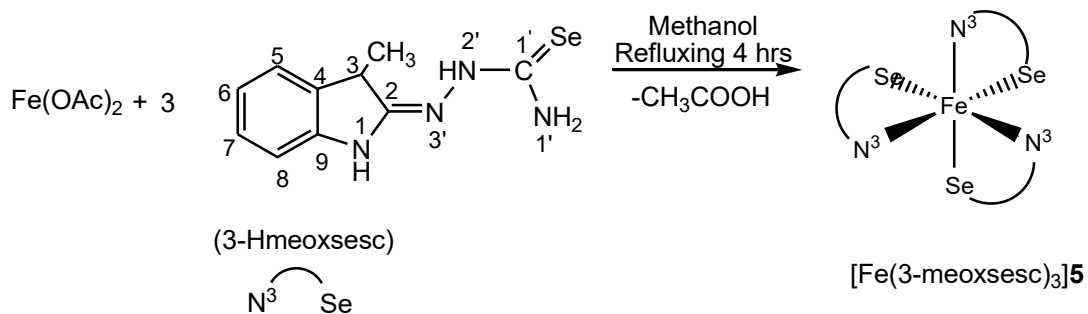
Iron acetate (0.025g, 0.10mmol) was dissolved in 20 ml of methanol with heating. To it was added N-methyl-2-pyrrole selenosemicarbazone (0.073g, 0.30mmol) and the mixture was refluxed for 4 hours. Light reddish solution formed was then filtered and at room temperature reddish solution kept for crystallization. Yield, 60%, m. p., 215-218°C. Important IR peaks (KBr, cm^{-1}): $\nu(\text{NH}_2)$ 3399m, 3244m; $\nu(\text{C}=\text{N})$ 1599s; $\nu(\text{C}=\text{C})$ 1504m; $\delta(\text{NH}_2)$ 1465s; $\nu(\text{C}=\text{Se})$ 767s (selenoamidemoiety). The Saturation magnetization, Coercivity magnetization and Remanence magnetization parameters obtained from the VSM analysis are $M_s = 0.00565$ emu/g, $M_r = 0.00267$ emu/g and $H_c = -0.32375$ emu/g respectively. Mass spectra (m/z): $[Fe(C_7H_{13}N_4Se)_3]^+$: 731 amu (parent ion peak).



3.2.5 Synthesis of $[Fe(3\text{-meoxsesc})_3]5$:

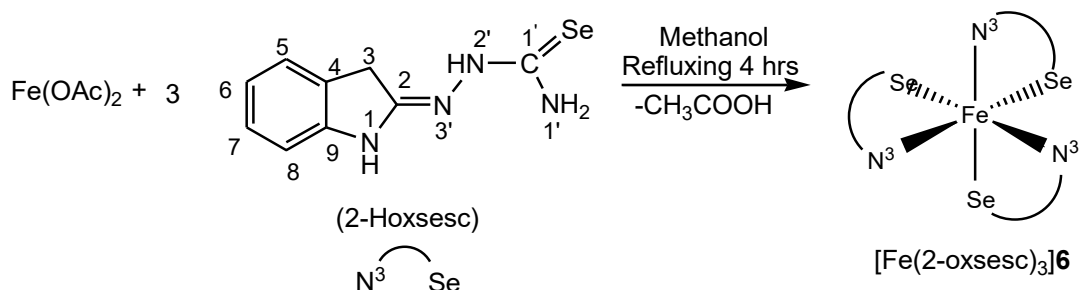
Iron acetate (0.025g, 0.10mmol) was dissolved in 30 ml of methanol with heating. To it was added 3-methyl-2-oxindole selenosemicarbazone, (0.085g, 0.31mmol) and the mixture was refluxed for 4 hours. Light reddish solution formed was then filtered and at room temperature reddish solution kept for crystallization. Yield, 62%, m. p., 210-213°C. Important IR peaks

(KBr, cm^{-1}): $\nu(\text{NH}_2)$ 3226m; $\nu(\text{C=O})$ 1695s; $\nu(\text{C=N})$ 1617s; $\nu(\text{C=C})$ 1559m; $\delta(\text{NH}_2)$ 1447s; $\nu(\text{C=Se})$ 747s (selenoamidemoiety). The Saturation magnetization, Coercivity magnetization and Remanence magnetization parameters obtained from the VSM analysis are $M_s = 0.0745\text{emu/g}$, $M_r = 0.02590\text{emu/g}$, and $H_c = -0.37635\text{emu/g}$ respectively. Mass spectra (m/z): $[\text{Fe}(\text{C}_{10}\text{H}_{11}\text{N}_4\text{Se})_3]^+$: 851amu (parent ion peak).



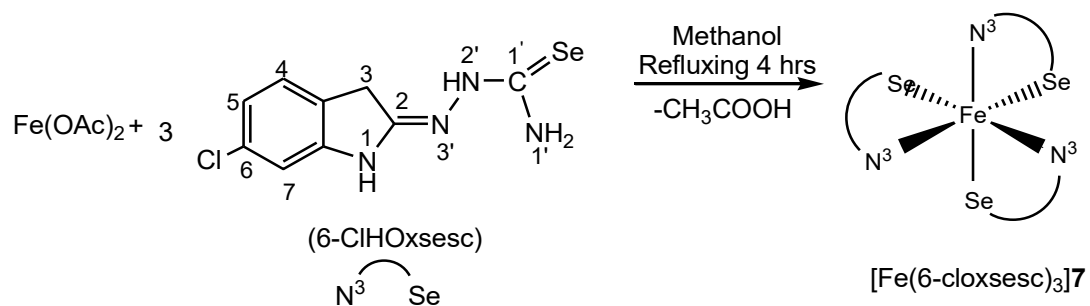
3.2.6 Synthesis of $[\text{Fe}(2\text{-oxsesc})_3]6$:

Iron acetate (0.025g, 0.10mmol) was dissolved in 30 ml of methanol with heating. To it was added 2-oxindole selenosemicarbazone, (0.082g, 0.30mmol) and the mixture was refluxed for 4 hours. Light reddish solution formed was then filtered and at room temperature reddish solution kept for crystallization. Yield, 62%, m. p., 205-208°C. Important IR peaks (KBr, cm^{-1}): $\nu(\text{NH}_2)$ 3267m; $\nu(\text{NH})_{\text{ox}}$ 3147m; $\nu(\text{C=N})$ 1656s; $\nu(\text{C=C})$ 1570m; $\delta(\text{NH}_2)$ 1411s; $\nu(\text{C=Se})$ 740s (selenoamidemoiety). The Saturation magnetization, Coercivity magnetization and Remanence magnetization parameters obtained from the VSM analysis are $M_s = 0.0531\text{emu/g}$, $M_r = 0.01702\text{emu/g}$, and $H_c = -0.31422\text{emu/g}$ respectively. Mass spectra (m/z): $[\text{Fe}(\text{C}_9\text{H}_9\text{N}_4\text{Se})_3]^+$: 809amu (parent ion peak).



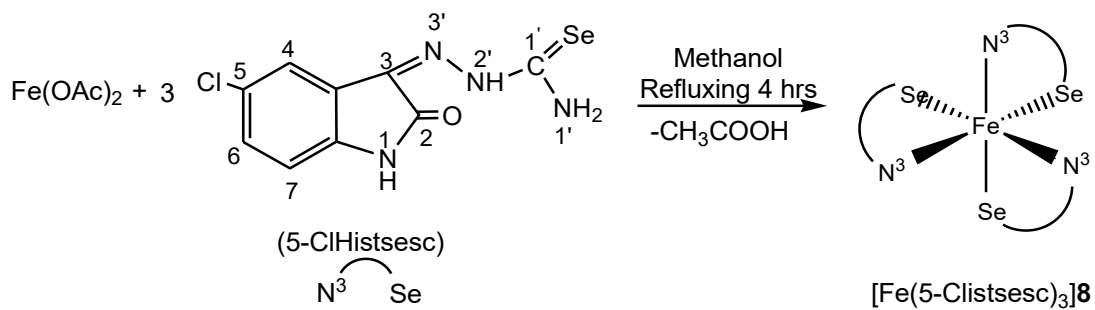
3.2.7 Synthesis of $[\text{Fe}(6\text{-cloxsesc})_3]7$:

Iron acetate (0.025g, 0.10mmol) was dissolved in 30 ml of methanol with heating. To it was added 6-chloro-2-oxindole selenosemicarbazone, (0.092g, 0.30mmol) and the mixture was refluxed for 4 hours. Light reddish solution formed was then filtered and at room temperature reddish solution kept for crystallization. Yield, 62%, m. p., 220-225°C. Important IR peaks (KBr, cm^{-1}): $\nu(\text{NH}_2)$ 3267m; $\nu(\text{NH})_{\text{clox}}$ 3192m; $\nu(\text{C}=\text{N})$ 1646s; $\nu(\text{C}=\text{C})$ 1517m; $\delta(\text{NH}_2)$ 1427s; $\nu(\text{C=Se})$ 739s (selenoamidemoiety). The Saturation magnetization, Coercivity magnetization and Remanence magnetization parameters obtained from the VSM analysis are $M_s = 0.0957 \text{ emu/g}$, $M_r = 0.03276 \text{ emu/g}$, and $H_c = -0.37866 \text{ emu/g}$ respectively. Mass spectra (m/z): $[\text{Fe}(\text{C}_8\text{H}_6\text{N}_4\text{ClSe})_3]^+$: 905amu (parent ion peak).



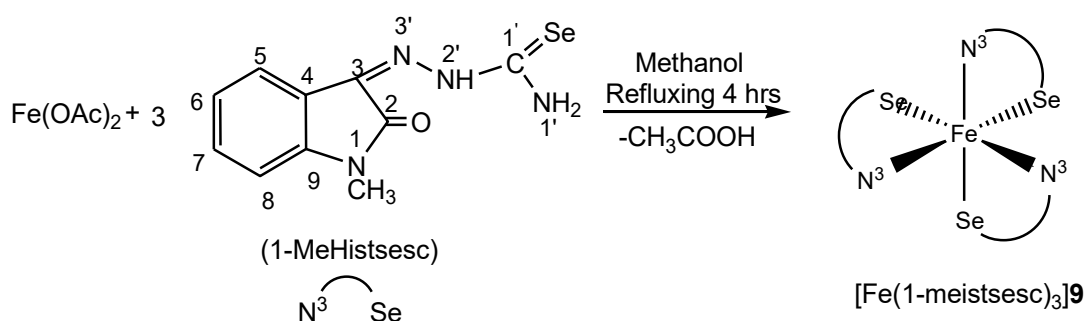
3.2.8 Synthesis of $[\text{Fe}(5\text{-clistsesc})_3]8$:

Iron acetate (0.025g, 0.10mmol) was dissolved in 30 ml of methanol with heating. To it was added 5-chloro isatin selenosemicarbazone, (0.085g, 0.30mmol) and the mixture was refluxed for 4 hours. Light reddish solution formed was then filtered and at room temperature reddish solution kept for crystallization. Yield, 62%, m. p., 225-228°C. Important IR peaks (KBr, cm^{-1}): $\nu(\text{NH}_2)$ 3217m; $\nu(\text{C=O})$ 1703s; $\nu(\text{C}=\text{N})$ 1614s; $\nu(\text{C}=\text{C})$ 1511m; $\delta(\text{NH}_2)$ 1460s; $\nu(\text{C=Se})$ 747s (selenoamidemoiety). The Saturation magnetization, Coercivity magnetization and Remanence magnetization parameters obtained from the VSM analysis are $M_s = 0.0711 \text{ emu/g}$, $M_r = 0.02738 \text{ emu/g}$, and $H_c = -0.35183 \text{ emu/g}$ respectively. Mass spectra (m/z): $[\text{Fe}(\text{C}_9\text{H}_5\text{N}_4\text{ClOSe})_3]^+$: 950amu (parent ion peak).



3.2.9 Synthesis of $[\text{Fe}(1\text{-meistsesc})_3]\text{9}$:

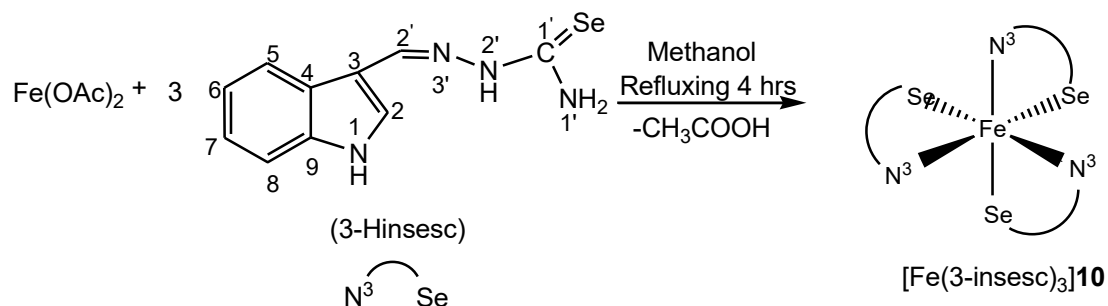
Iron acetate (0.025g, 0.10mmol) was dissolved in 30 ml of methanol with heating. To it was added 1-methyl isatin selenosemicarbazone, (0.090g, 0.30mmol) and the mixture was refluxed for 4 hours. Light reddish solution formed was then filtered and at room temperature reddish solution kept for crystallization. Yield, 62%, m. p., 230-233°C. Important IR peaks (KBr, cm^{-1}): $\nu(\text{NH}_2)$ 3219m; $\nu(\text{C=O})$ 1701; $\nu(\text{C=N})$ 1607m; $\nu(\text{C=C})$ $\delta(\text{NH}_2)$ 1466s; $\nu(\text{C=Se})$ 750s (selenoamidemoiety). The Saturation magnetization, Coercivity magnetization and Remanence magnetization parameters obtained from the VSM analysis are $M_s = 0.00490\text{emu/g}$, $M_r = 0.00204\text{emu/g}$, and $H_c = -0.29117\text{emu/g}$ respectively. Mass spectra (m/z): $[\text{Fe}(\text{C}_{10}\text{H}_5\text{N}_4\text{OSe})_3]^+$: 895amu (parent ion peak).



3.2.10 Synthesis of $[\text{Fe}(3\text{-insesc})_3]\text{10}$:

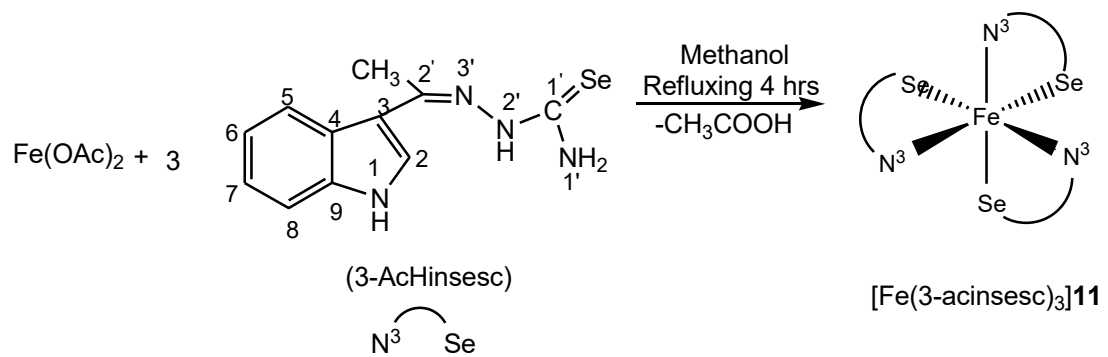
Iron acetate (0.025g, 0.10mmol) was dissolved in 30 ml of methanol with heating. To it was added 3-indole selenosemicarbazone, (0.085g, 0.32mmol) and the mixture was refluxed for 4 hours. Dark reddish solution formed was then filtered and at room temperature reddish solution kept for crystallization. Yield, 62%, m. p., 213-215°C. Important IR peaks (KBr, cm^{-1}): $\nu(\text{NH}_2)$ 3394m, 3240m; $\nu(\text{NH})_{\text{ind}}$ 3146m; $\nu(\text{C=N})$ 1643s; $\nu(\text{C=C})$ 1576m; $\delta(\text{NH}_2)$ 1464s; $\nu(\text{C=Se})$ 764s (selenoamidemoiety). The Saturation magnetization, Coercivity magnetization and Remanence magnetization parameters obtained from the VSM analysis are $M_s =$

0.00929emu/g, Mr = 0.00253emu/g and Hc = -0.33698emu/g respectively. Mass spectra (m/z): [Fe(C₁₀H₁₃N₄Se)₃]⁺: 850amu (parent ion peak).



3.2.11 Synthesis of [Fe(3-acinsesc)₃]11:

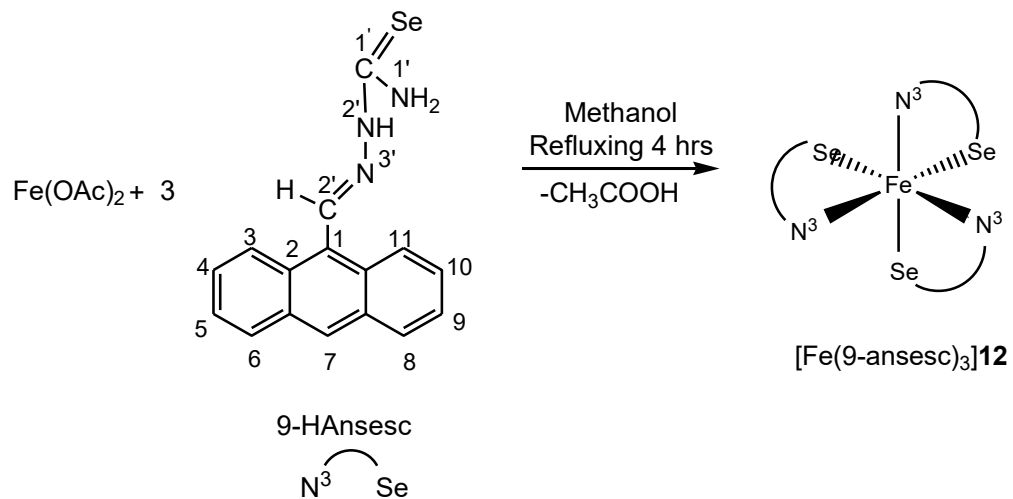
Iron acetate (0.025g, 0.10mmol) was dissolved in 30 ml of methanol with heating. To it was added 3-acetyl indole selenosemicarbazone, (0.089g, 0.31mmol) and the mixture was refluxed for 4 hours. Light reddish solution formed was then filtered and at room temperature reddish solution kept for crystallization. Yield, 62%, m. p., 218-220°C. Important IR peaks (KBr, cm⁻¹): $\nu(\text{NH})_{\text{acind}}$ 3172m; $\nu(\text{C}=\text{N})$ 1613s; $\nu(\text{C}=\text{C})$ 1572m; $\delta(\text{NH}_2)$ 1432s; $\nu(\text{C}=\text{Se})$ 744s (selenoamidemoiety). The Saturation magnetization, Coercivity magnetization and Remanence magnetization parameters obtained from the VSM analysis are Ms = 0.00513emu/g, Mr = 0.00198emu/g, and Hc= -0.31079emu/g respectively. Mass spectra (m/z): [Fe(C₁₁H₁₁N₄Se)₃]⁺: 930amu (parent ion peak).



3.2.12 Synthesis of [Fe(9-ansesc)₃]12:

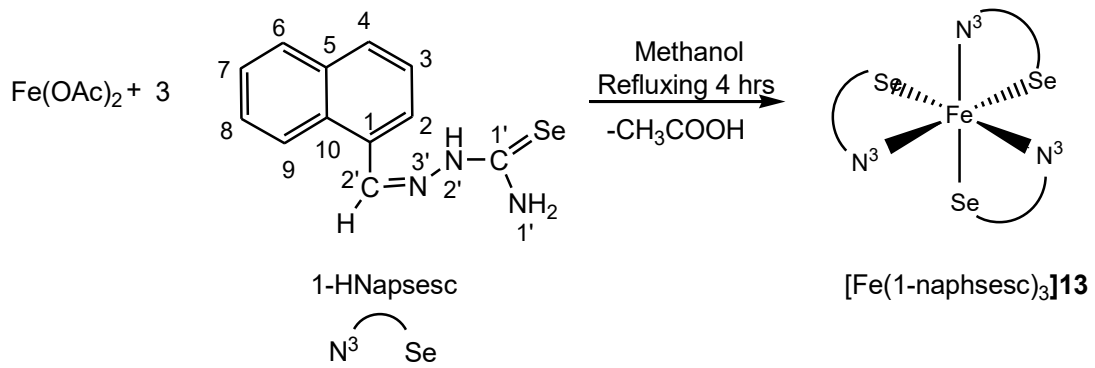
Iron acetate (0.025g, 0.10mmol) was dissolved in 30 ml of methanol with heating. To it was added 9-anthracene selenosemicarbazone, (0.015g, 0.32mmol) and the mixture was refluxed for 4 hours. Light brownish red solution formed was then filtered and at room temperature brownish red solution kept for crystallization. Yield, 62%, m. p., 220-225°C. Important IR

peaks (KBr, cm^{-1}): $\nu(\text{NH}_2)$ 3257m; $\nu(\text{C}=\text{N})$ 1665s; $\nu(\text{C}=\text{C})$ 1552m; $\delta(\text{NH}_2)$ 1437s; $\nu(\text{C}=\text{Se})$ 780s (selenoamidemoiety). The Saturation magnetization, Coercivity magnetization and Remanence magnetization parameters obtained from the VSM analysis are $M_s = 0.00665\text{emu/g}$, $M_r = 0.00298\text{emu/g}$, and $H_c = -0.37337\text{emu/g}$ respectively. ESR data (g, tensor, A, gauss): $g_{\parallel}, 2.1$; $g_{\perp}, 2.65$; Hyperfine values, 40 gauss. Mass spectra (m/z): $\text{Na}_2[\text{Fe}(\text{C}_{17}\text{H}_{16}\text{N}_3\text{Se})_3]^+$: 1076amu (parent ion peak).



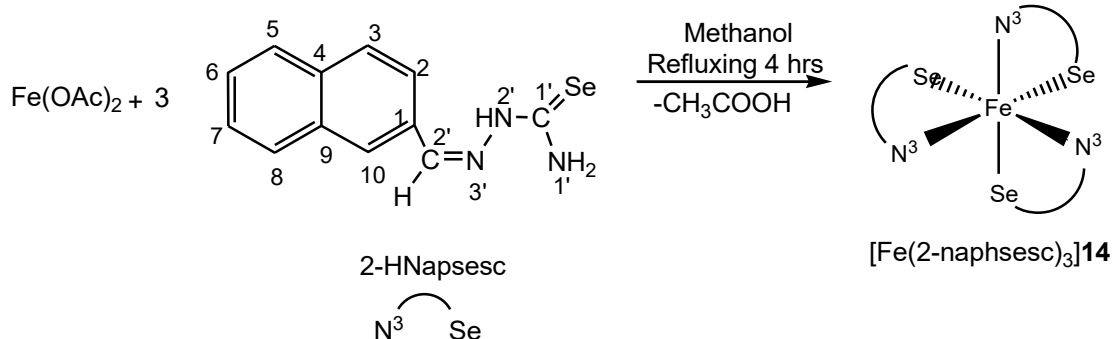
3.2.13 Synthesis of $[\text{Fe}(1\text{-naphsesc})_3]\textbf{13}$:

Iron acetate (0.025g, 0.10mmol) was dissolved in 30 ml of methanol with heating. To it was added 1-naphthaldehyde selenosemicarbazone, (0.088g, 0.37mmol) and the mixture was refluxed for 4 hours. Light brownish solution formed was then filtered and at room temperature brownish solution kept for crystallization. Yield, 60%, m. p., 210-213°C. Important IR peaks (KBr, cm^{-1}): $\nu(\text{NH}_2)$ 3358m; $\nu(\text{C}=\text{N})$ 1631s; $\nu(\text{C}=\text{C})$ 1597s; $\delta(\text{NH}_2)1446\text{s}$; $\nu(\text{C}=\text{Se})$ 744s (selenoamidemoiety). The Saturation magnetization, Coercivity magnetization and Remanence magnetization parameters obtained from the VSM analysis are $M_s = 0.00898\text{emu/g}$, $M_r = 0.00383\text{emu/g}$, and $H_c = -0.36404\text{emu/g}$ respectively. Mass spectra (m/z): $[\text{Fe}(\text{C}_{12}\text{H}_{12}\text{N}_3\text{Se})_3]^+$: 884amu (parent ion peak).



3.2.14 Synthesis of $[\text{Fe}(2\text{-naphsesc})_3]\mathbf{14}$:

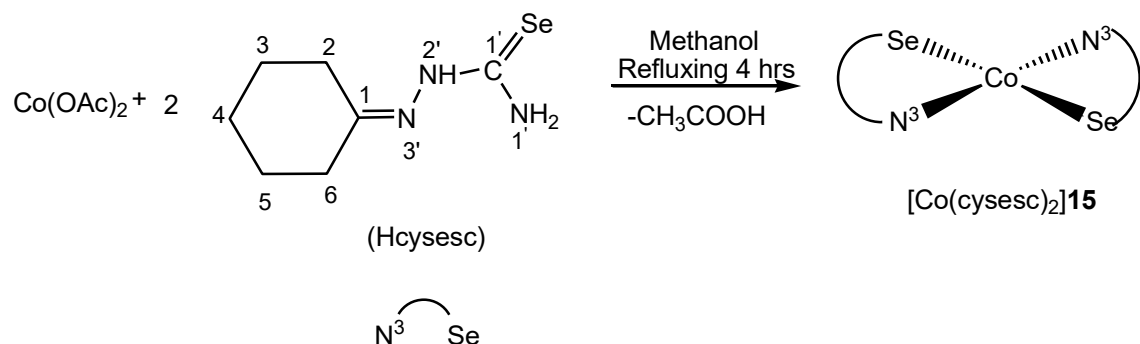
Iron acetate (0.025g, 0.10mmol) was dissolved in 30 ml of ethanol with heating. To it was added 2-naphthaldehyde selenoimine (0.088g, 0.37mmol) and the mixture was refluxed for 4 hours. Light brownish solution formed was then filtered and at room temperature brownish solution kept for crystallization. Yield, 60%, m. p., 230-233°C. Important IR peaks (KBr, cm^{-1}): $\nu(\text{NH}_2)$ 3219m; $\nu(\text{C}=\text{N})$ 1618s; $\nu(\text{C}=\text{C})$ 1539m; $\delta(\text{NH}_2)1442\text{s}$; $\nu(\text{C=Se})$ 745s (selenoamidemoiety). The Saturation magnetization, Coercivity magnetization and Remanence magnetization parameters obtained from the VSM analysis are $M_s = 0.01652\text{emu/g}$, $M_r = 0.00768\text{emu/g}$, and $H_c = -0.35653\text{emu/g}$ respectively. Mass spectra (m/z): $[\text{Fe}(\text{C}_{12}\text{H}_9\text{N}_3\text{Se})_3]^+$: 875amu (parent ion peak).



3.3Complexes of Cobalt(II)

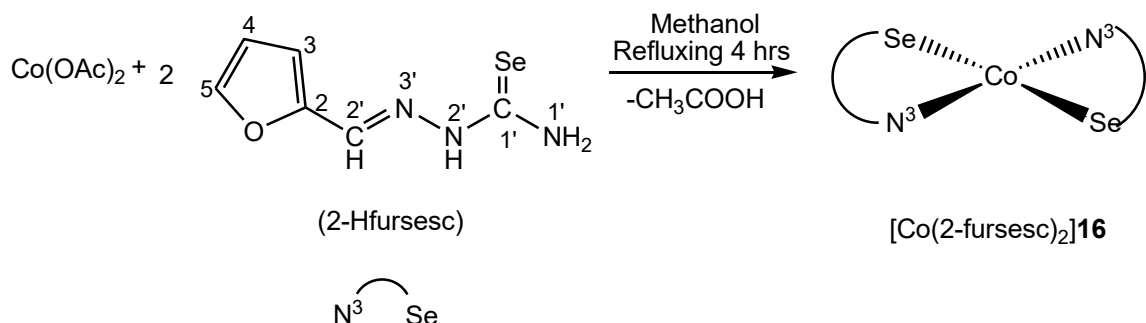
3.3.1 Synthesis of $[\text{Co}(\text{cysesc})_2]15$:

Cobalt acetate (0.025g, 0.103mmol) was dissolved in 30 ml of methanol with heating. To it was added cyclohexanoneselenosemicarbazone, (0.061g, 0.27mmol) and the mixture was refluxed for 4 hours. Light red solution formed was then filtered and at room temperature red solution kept for crystallization. Yield, 60%, m. p., 210-213°C. Important IR peaks (KBr, cm^{-1}): $\nu(\text{NH}_2)$ 3301m; $\nu(\text{C}=\text{N})$ 1627s; $\nu(\text{C}=\text{C})$ 1556m; $\delta(\text{NH}_2)$ 1422s; $\nu(\text{C}=\text{Se})$ 752s (selenoamidemoiety). Mass spectra (m/z): $[\text{Co}(\text{C}_7\text{H}_{13}\text{N}_3\text{Se})_2]^+$: 492amu (parent ion peak). CHN analysis (% age) of $[\text{Co}(\text{C}_7\text{H}_{13}\text{N}_3\text{Se})_2]^+$: Calculated values, C, 33.9, H, 5.2, N, 16.9; Found values, C, 33.7, H, 5.0, N, 16.6; respectively.



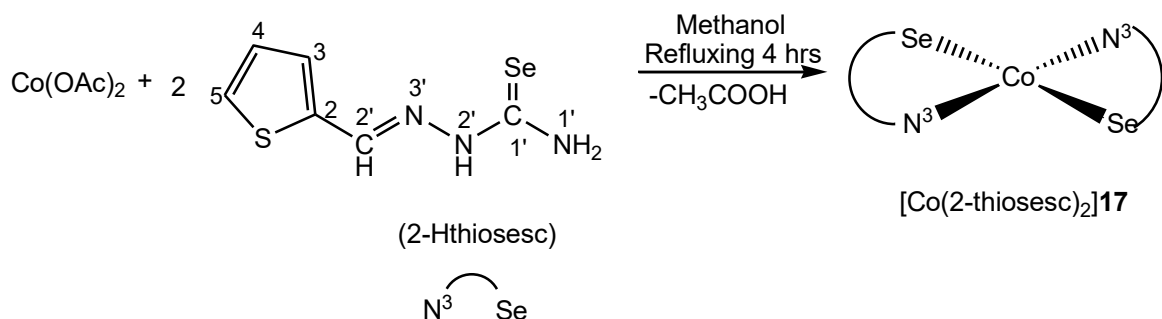
3.3.2 Synthesis of $[\text{Co}(2\text{-fursesc})_2]16$:

Cobalt acetate (0.025g, 0.10mmol) was dissolved in 20 ml of methanol with heating. To it was added 2-furfural selenosemicarbazone (0.060g, 0.27mmol) and the mixture was refluxed for 4 hours. Light reddish solution formed was then filtered and at room temperature reddish solution kept for crystallization. Yield, 60%, m. p., 210-213°C. Important IR peaks (KBr, cm^{-1}): $\nu(\text{NH}_2)$ 3303m; $\nu(\text{C}=\text{N})$ 1582s; $\nu(\text{C}=\text{C})$ 1499m; $\delta(\text{NH}_2)$ 1466s; $\nu(\text{C}=\text{Se})$ 744s (selenoamidemoiety). Mass spectra m/z: $[\text{Co}(\text{C}_6\text{H}_5\text{N}_3\text{OSe})_2]^+$: 484amu (parent ion peak). CHN analysis (% age) of $[\text{Co}(\text{C}_6\text{H}_7\text{N}_3\text{OSe})_2]^+$: Calculated values, C, 25.7, H, 2.9, N, 17.9; Found values, C, 25.4, H, 2.7, N, 17.6; respectively.



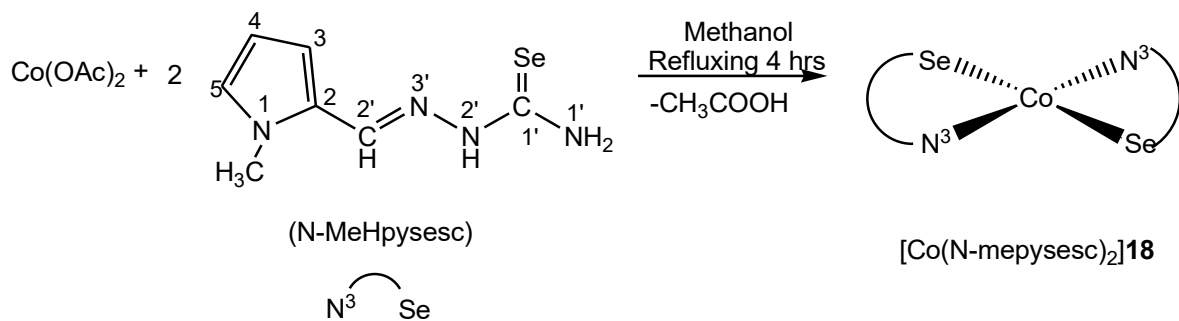
3.3.3 Synthesis of [Co(2-thiosesc)₂]17:

Cobalt acetate (0.025g, 0.10mmol) was dissolved in 20 ml of methanol with heating. To it was added 2-thiophene selenosemicarbazone (0.065g, 0.28mmol) and the mixture was refluxed for 4 hours. Light reddish solution formed was then filtered and at room temperature reddish solution kept for crystallization. Yield, 60%, m. p., 210-213°C. Important IR peaks (KBr, cm⁻¹): $\nu(\text{NH}_2)$ 3304m; $\nu(\text{C}=\text{N})$ 1605s; $\nu(\text{C}=\text{C})$ 1564m; $\delta(\text{NH}_2)$ 1416s; $\nu(\text{C}=\text{Se})$ 703s (selenoamidemoiety). Mass spectra m/z: $[\text{Co}(\text{C}_6\text{H}_3\text{N}_3\text{SSe})_2]^+$: 513amu (parent ion peak). CHN analysis (% age) of $[\text{Co}(\text{C}_6\text{H}_3\text{N}_3\text{SSe})_2]^+$: Calculated values, C, 24.0, H, 2.8, N, 16.9; Found values, C, 23.8, H, 2.6, N, 16.5; respectively.



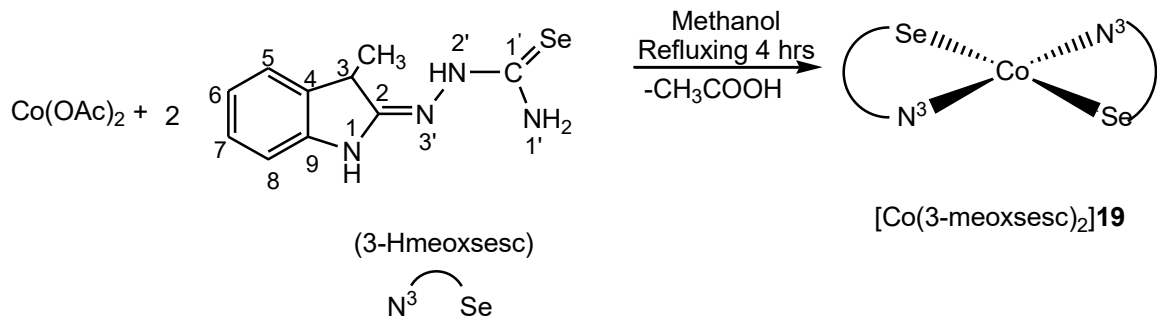
3.3.4 Synthesis of [Co(N-mepysesc)2]18:

Cobalt acetate (0.025g, 0.10mmol) was dissolved in 20 ml of methanol with heating. To it was added N-methyl-2-pyrrole selenosemicarbazone (0.064g, 0.27mmol) and the mixture was refluxed for 4 hours. Light reddish solution formed was then filtered and at room temperature reddish solution kept for crystallization. Yield, 60%, m. p., 215-218°C. Important IR peaks (KBr, cm⁻¹): $\nu(\text{NH}_2)$ 3344m; $\nu(\text{C}=\text{N})$ 1603s; $\nu(\text{C}=\text{C})$ 1567m; $\delta(\text{NH}_2)$ 1417s; $\nu(\text{C}=\text{Se})$ 728s (selenoamidemoiety). Mass spectra m/z: $[\text{Co}(\text{C}_7\text{H}_8\text{N}_4\text{Se})_2]^+$: 511amu (parent ion peak). CHN analysis (% age) of $[\text{Co}(\text{C}_7\text{H}_{10}\text{N}_4\text{Se})_2]^+$: Calculated values, C, 34.3, H, 4.0, N, 17.1; Found values, C, 34.0, H, 3.8, N, 16.8; respectively.



3.3.5 Synthesis of $[\text{Co}(3\text{-meoxsesc})_2]19$:

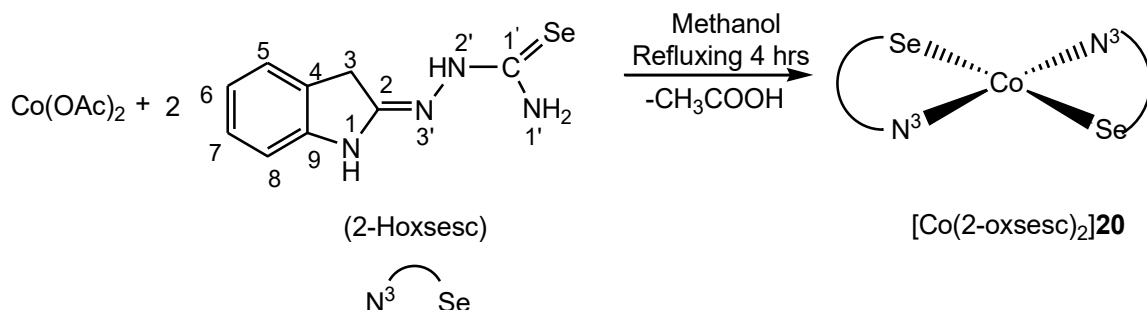
Cobalt acetate (0.25g, 0.10mmol) was dissolved in 30 ml of methanol with heating. To it was added 3-methyl-2-oxindole selenosemicarbazone, (0.075g, 0.28mmol) and the mixture was refluxed for 4 hours. Light reddish solution formed was then filtered and at room temperature reddish solution kept for crystallization. Yield, 62%, m. p., 210-213°C. Important IR peaks (KBr, cm^{-1}): $\nu(\text{NH}_2)$ 3208m; $\nu(\text{C}=\text{N})$ 1613s; $\nu(\text{C}=\text{C})$ 1572m; $\delta(\text{NH}_2)$ 1427s; $\nu(\text{C}=\text{Se})$ 742s (selenoamidemoiety). Mass spectra m/z: $[\text{Co}(\text{C}_{10}\text{H}_{13}\text{N}_4\text{Se})_2]^+$: 593amu (parent ion peak). CHN analysis (% age) of $[\text{Co}(\text{C}_{10}\text{H}_{12}\text{N}_4\text{Se})_2]^+$: Calculated values, C, 40.4, H, 4.0, N, 18.8; Found values, C, 40.1, H, 3.8, N, 18.5; respectively.



3.3.6 Synthesis of $[\text{Co}(2\text{-oxsesc})_2]20$:

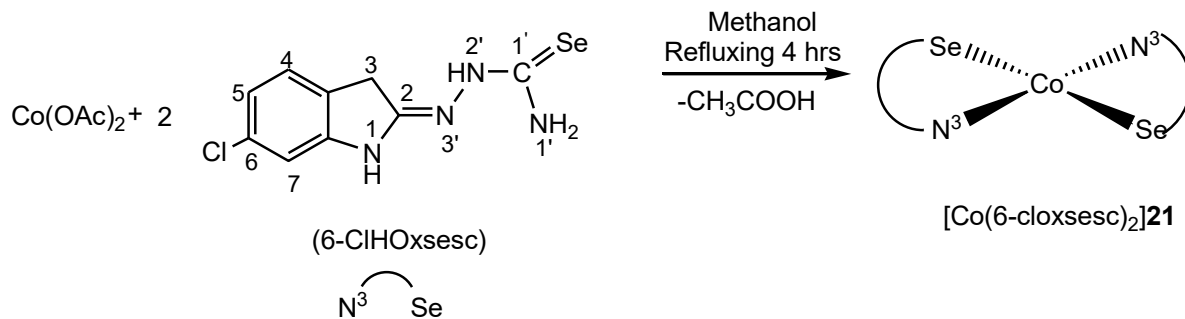
Cobalt acetate (0.25g, 0.10mmol) was dissolved in 30 ml of methanol with heating. To it was added 2-oxindole selenosemicarbazone, (0.071g, 0.28mmol) and the mixture was refluxed for 4 hours. Light reddish solution formed was then filtered and at room temperature reddish solution kept for crystallization. Yield, 62%, m. p., 205-208°C. Important IR peaks (KBr, cm^{-1}): $\nu(\text{NH}_2)$ 3249m; $\nu(\text{C}=\text{N})$ 1616s; $\nu(\text{C}=\text{C})$ 1554m; $\delta(\text{NH}_2)$ 1436s; $\nu(\text{C}=\text{Se})$ 814s (selenoamidemoiety). Mass spectra m/z: $[\text{Co}(\text{C}_9\text{H}_{10}\text{N}_4\text{Se})_2]^+$: 563amu (parent ion peak). CHN

analysis (% age) of $[\text{Co}(\text{C}_9\text{H}_{10}\text{N}_4\text{Se})_2]^+$: Calculated values, C, 33.9, H, 5.2, N, 16.9; Found values, C, 33.6, H, 5.0, N, 16.7; respectively.



3.3.7 Synthesis of $[\text{Co}(6\text{-cloxsesc})_2]21$:

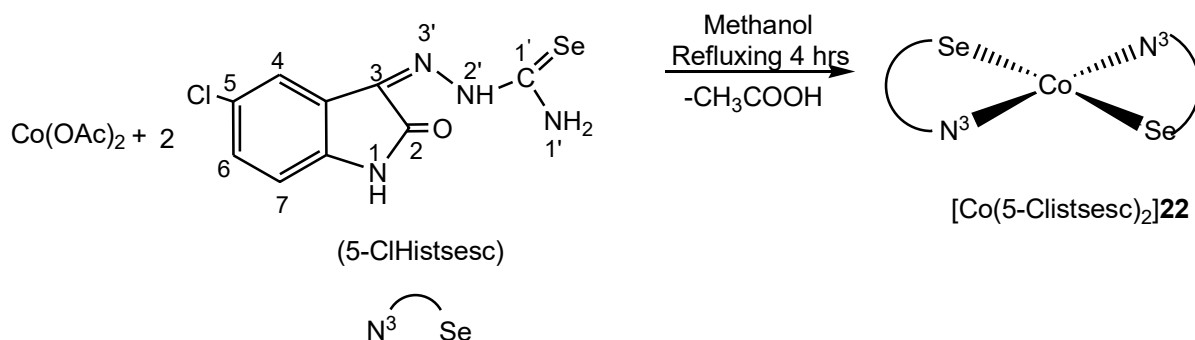
Cobalt acetate (0.25g, 0.10mmol) was dissolved in 30 ml of methanol with heating. To it was added 6-chloro-2-oxindole selenosemicarbazone, (0.081g, 0.28mmol) and the mixture was refluxed for 4 hours. Light reddish solution formed was then filtered and at room temperature reddish solution kept for crystallization. Yield, 62%, m. p., 220-225°C. Important IR peaks (KBr, cm^{-1}): $\nu(\text{NH}_2)$ 3339m; $\nu(\text{C}=\text{N})$ 1606s; $\nu(\text{C}=\text{C})$ 1598m; $\delta(\text{NH}_2)$ 1418s; $\nu(\text{C}=\text{Se})$ 717s (selenoamidemoiety). Mass spectra m/z: $[\text{Co}(\text{C}_9\text{H}_9\text{N}_4\text{ClSe})_2]^+$: 631amu (parent ion peak). CHN analysis (% age) of $[\text{Co}(\text{C}_9\text{H}_9\text{N}_4\text{ClSe})_2]^+$: Calculated values, C, 33.9, H, 5.2, N, 16.9; Found values, C, 33.7, H, 5.1, N, 16.4; respectively.



3.3.8 Synthesis of $[\text{Co}(5\text{-clistsesc})_2]22$:

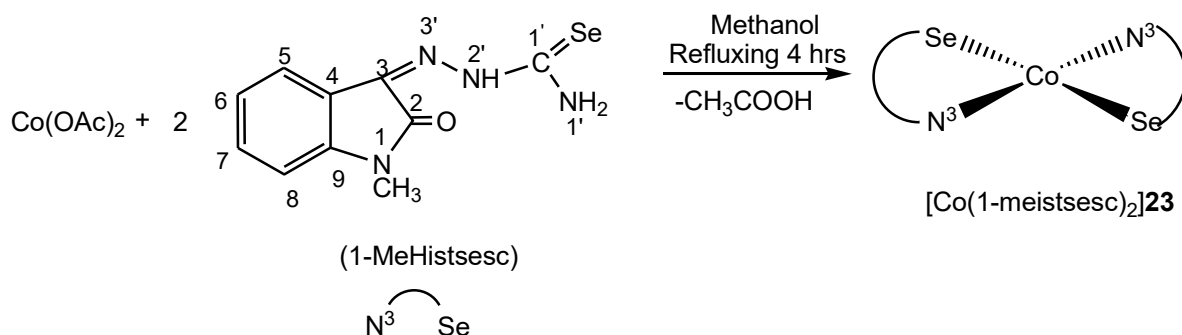
Cobalt acetate (0.25g, 0.10mmol) was dissolved in 30 ml of methanol with heating. To it was added 5-chloro isatin selenosemicarbazone, (0.075g, 0.28mmol) and the mixture was refluxed for 4 hours. Light reddish solution formed was then filtered and at room temperature reddish solution kept for crystallization. Yield, 62%, m. p., 225-228°C. Important IR peaks (KBr, cm^{-1}):

¹): $\nu(\text{NH}_2)$ 3256m; $\nu(\text{C=O})$ 1697s; $\nu(\text{C=O})$ 1610s; $\nu(\text{C=C})$ 1575m; $\delta(\text{NH}_2)$ 1481s; $\nu(\text{C=Se})$ 767s (selenoamidemoiety). Mass spectra m/z: $[\text{Co}(\text{C}_9\text{H}_7\text{N}_4\text{OClSe})_2]^+$: 658amu (parent ion peak). CHN analysis (% age) of $[\text{Co}(\text{C}_9\text{H}_7\text{N}_4\text{OClSe})_2]^+$: Calculated values, C, 33.9, H, 5.2, N, 16.9; Found values, C, 33.8, H, 5.3, N, 16.6; respectively.



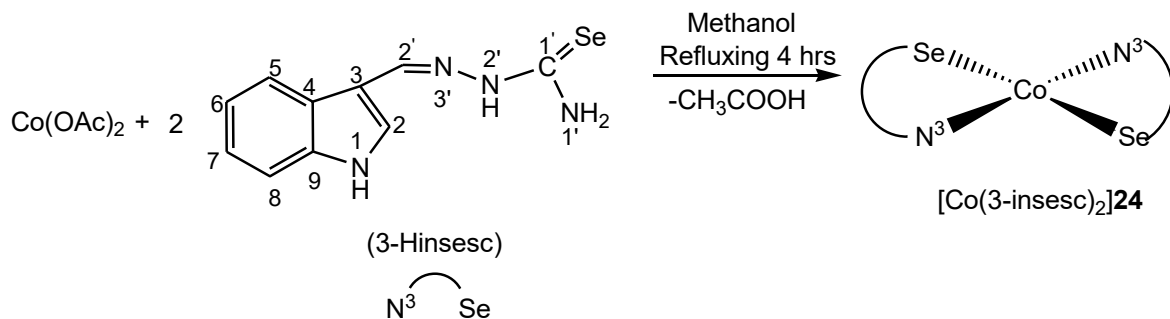
3.3.9 Synthesis of $[\text{Co}(1\text{-meistsesc})_2]23$:

Cobalt acetate (0.025g, 0.136mmol) was dissolved in 30 ml of methanol with heating. To it was added 1-methyl isatin selenosemicarbazone, (0.079g, 0.28mmol) and the mixture was refluxed for 4 hours. Light reddish solution formed was then filtered and at room temperature reddish solution kept for crystallization. Yield, 62%, m. p., 230-233°C. Important IR peaks (KBr, cm^{-1}): $\nu(\text{NH}_2)$ 3248m; $\nu(\text{C=O})$ 1693s; $\nu(\text{C=N})$ 1505m; $\nu(\text{C=C})$ 1505m; $\delta(\text{NH}_2)$ 1464s; $\nu(\text{C=Se})$ 749s (selenoamidemoiety). Mass spectra m/z: $[\text{Co}(\text{C}_{10}\text{H}_8\text{N}_4\text{OSe})_2]^+$: 614amu (parent ion peak). CHN analysis (% age) of $[\text{Co}(\text{C}_{10}\text{H}_{10}\text{N}_4\text{OSe})_2]^+$: Calculated values, C, 33.9, H, 5.2, N, 16.9; Found values, C, 33.7, H, 5.0, N, 16.7; respectively.



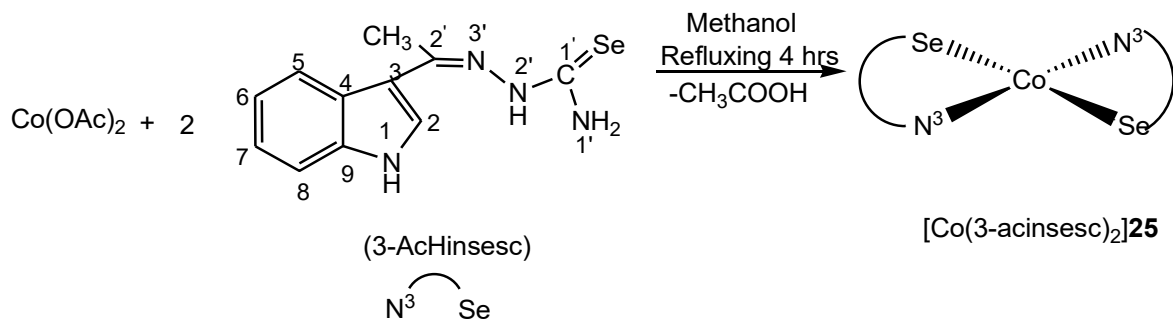
3.3.10 Synthesis of $[\text{Co}(\text{3-insesc})_2]24$:

Cobalt acetate (0.025g, 0.136mmol) was dissolved in 30 ml of methanol with heating. To it was added 3-indole selenosemicarbazone, (0.074g, 0.27mmol) and the mixture was refluxed for 4 hours. Dark reddish solution formed was then filtered and at room temperature reddish solution kept for crystallization. Yield, 62%, m. p., 213-215°C. Important IR peaks (KBr, cm^{-1}): $\nu(\text{NH}_2)$ 3361m; $\nu(\text{C}=\text{N})$ 1615s; $\nu(\text{C}=\text{C})$ 1567m; $\delta(\text{NH}_2)$ 1441s; $\nu(\text{C}=\text{Se})$ 784s (selenoamidemoiety). Mass spectra m/z: $[\text{Co}(\text{C}_{10}\text{H}_9\text{N}_4\text{Se})_2]^+$: 587amu (parent ion peak). CHN analysis (% age) of $[\text{Co}(\text{C}_{10}\text{H}_9\text{N}_4\text{Se})_2]^+$: Calculated values, C, 40.8, H, 3.4, N, 19.0; Found values, C, 40.5, H, 3.2, N, 18.8; respectively.



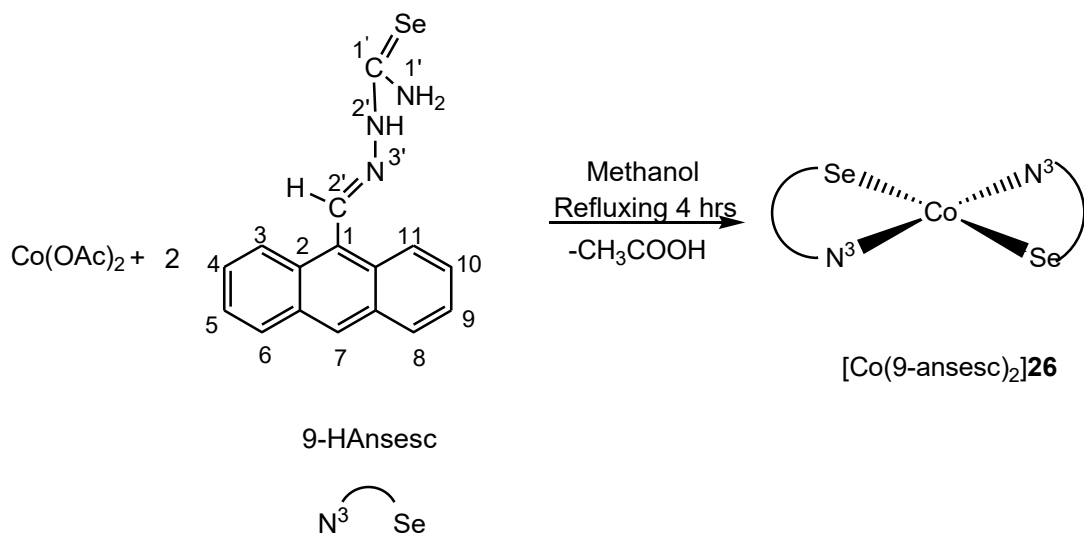
3.3.11 Synthesis of $[\text{Co}(\text{3-acinsesc})_2]25$:

Cobalt acetate (0.025g, 0.10mmol) was dissolved in 30 ml of methanol with heating. To it was added 3-acetyl indole selenosemicarbazone, (0.078g, 0.27mmol) and the mixture was refluxed for 4 hours. Light reddish solution formed was then filtered and at room temperature reddish solution kept for crystallization. Yield, 62%, m. p., 218-220°C. Important IR peaks (KBr, cm^{-1}): $\nu(\text{NH})_{\text{acind}}$ 3156w; $\nu(\text{C}=\text{N})$ 1610s; $\nu(\text{C}=\text{C})$ 1573m; $\delta(\text{NH}_2)$ 1426s; $\nu(\text{C}=\text{Se})$ 749s (selenoamidemoiety). Mass spectra m/z: $[\text{Co}(\text{C}_{11}\text{H}_{12}\text{N}_4\text{Se})_2]^+$: 615amu (parent ion peak). CHN analysis (% age) of $[\text{Co}(\text{C}_{11}\text{H}_{12}\text{N}_4\text{Se})_2]^+$: Calculated values, C, 42.8, H, 3.8, N, 18.1; Found values, C, 42.7, H, 3.6, N, 18.0; respectively.



3.3.12 Synthesis of $[\text{Co}(9\text{-ansesc})_2]26$:

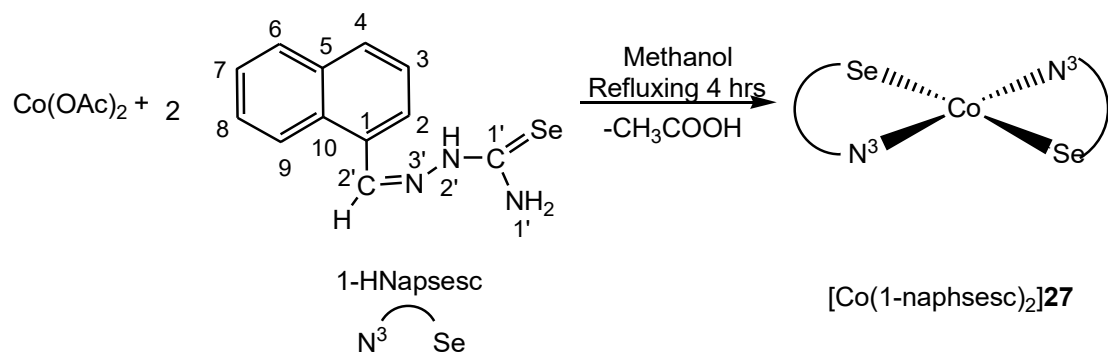
Cobalt acetate (0.025g, 0.100mmol) was dissolved in 30 ml of methanol with heating. To it was added 9-anthracene selenosemicarbazone, (0.092g, 0.28mmol) and the mixture was refluxed for 4 hours. Light brownish red solution formed was then filtered and at room temperature brownish red solution kept for crystallization. Yield, 62%, m. p., 220-225°C. Important IR peaks (KBr, cm^{-1}): $\nu(\text{NH}_2)$ 3243m; $\nu(\text{C}=\text{N})$ 1635s; $\nu(\text{C}=\text{C})$ 1547m; $\delta(\text{NH}_2)$ 1485s; $\nu(\text{C}=\text{Se})$ 752s (selenoamidemoiety). Mass spectra m/z: $[\text{Co}(\text{C}_{16}\text{H}_{13}\text{N}_3\text{Se})_2]^+$: 709amu (parent ion peak). CHN analysis (% age) of $[\text{Co}(\text{C}_{16}\text{H}_{13}\text{N}_3\text{Se})_2]^+$: Calculated values, C, 54.0, H, 3.6, N, 11.8; Found values, C, 53.8, H, 3.4, N, 11.6; respectively.



3.3.13 Synthesis of $[\text{Co}(1\text{-naphsesc})_2]27$:

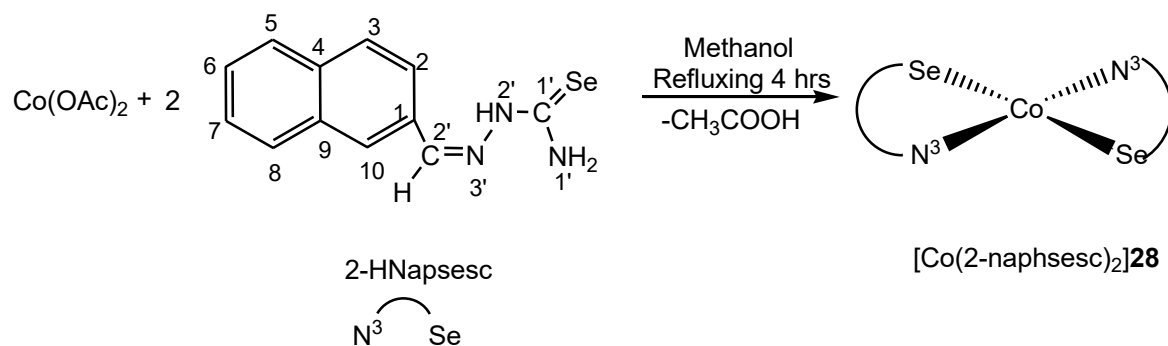
Cobalt acetate (0.025g, 0.10mmol) was dissolved in 30 ml of methanol with heating. To it was added 1-naphthaldehyde selenosemicarbazone, (0.077g, 0.28mmol) and the mixture was refluxed for 4 hours. Light brownish solution formed was then filtered and at room

temperature brownish solution kept for crystallization. Yield, 60%, m. p., 210-213°C. Important IR peaks (KBr, cm^{-1}): $\nu(\text{NH}_2)$ 3358m; $\nu(\text{C}=\text{N})$ 1604s; $\nu(\text{C}=\text{C})$ 1545s; $\delta(\text{NH}_2)$ 1456s; $\nu(\text{C}=\text{Se})$ 765s (selenoamidemoiety). Mass spectra m/z: $[\text{Co}(\text{C}_{12}\text{H}_{10}\text{N}_3\text{Se})_2]^+$: 608amu (parent ion peak). CHN analysis (% age) of $[\text{Co}(\text{C}_{12}\text{H}_{11}\text{N}_3\text{Se})_2]^+$: Calculated values, C, 47.1, H, 3.6, N, 13.7; Found values, C, 46.9, H, 3.4, N, 13.6; respectively.



3.3.14 Synthesis of $[\text{Co}(2\text{-naphsesc})_2]28$:

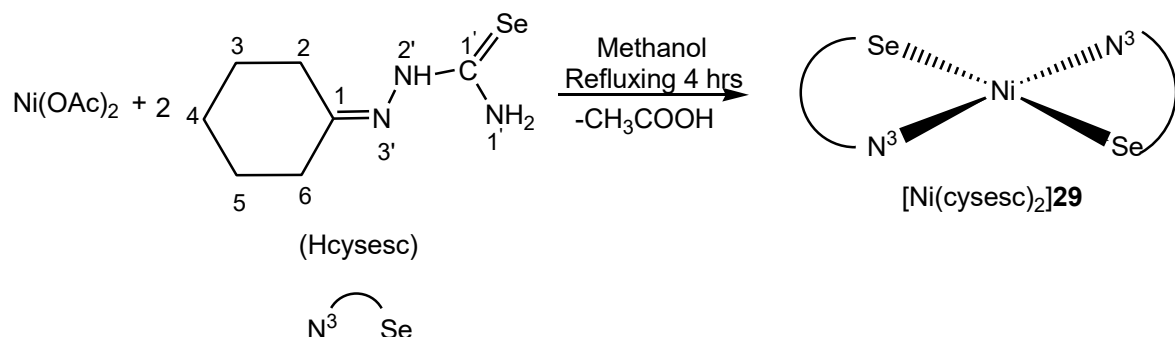
Cobalt acetate (0.25g, 0.10mmol) was dissolved in 30 ml of ethanol with heating. To it was added 2-naphthaldehyde selenosemicarbazone, (0.077g, 0.28mmol) and the mixture was refluxed for 4 hours. Light brownish solution formed was then filtered and at room temperature brownish solution kept for crystallization. Yield, 60%, m. p., 230-233°C. Important IR peaks (KBr, cm^{-1}): $\nu(\text{NH}_2)$ 3331m; $\nu(\text{C}=\text{N})$ 1614s; $\nu(\text{C}=\text{C})$ 1543m; $\delta(\text{NH}_2)$ 1460s; $\nu(\text{C}=\text{Se})$ 765s (selenoamidemoiety). Mass spectra (m/z): $[\text{Co}(\text{C}_{12}\text{H}_{12}\text{N}_3\text{Se})_2]^+$: 610amu (parent ion peak). CHN analysis (% age) of $[\text{Co}(\text{C}_{12}\text{H}_{11}\text{N}_3\text{Se})_2]^+$: Calculated values, C, 47.1, H, 3.6, N, 13.7; Found values, C, 46.9, H, 3.4, N, 13.5; respectively. ESR data (g, tensor, A, guass): $g_{\parallel}, 2.2$; $g_{\perp}, 2.0$; $A_{\parallel}, 20$; $A_{\perp}, 165$.



3.4 Complexes of Nickel(II)

3.4.1 Synthesis of $[\text{Ni}(\text{cysesc})_2]29$:

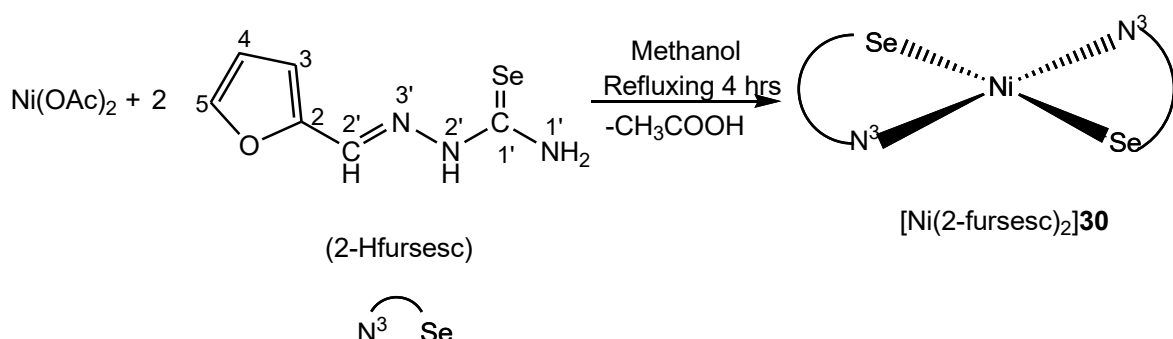
Nickel acetate (0.025g, 0.10mmol) was dissolved in 30 ml of methanol with heating. To it was added cyclohexanoneselenosemicarbazone, (0.061g, 0.27mmol) and the mixture was refluxed for 4 hours. Green solution formed was then filtered and at room temperature green solution kept for crystallization. Yield, 62%, m. p., 216-219°C. Important IR peaks (KBr, cm^{-1}): $\nu(\text{NH}_2)$ 3492m, 3372m, 3320m; $\nu(\text{C}=\text{N})$ 1630s; $\nu(\text{C}=\text{C})$ 1584m; $\delta(\text{NH}_2)$ 1423s; $\nu(\text{C}=\text{Se})$ 781s (selenoamidemoiety). Mass spectra (m/z): $[\text{Ni}(\text{C}_7\text{H}_{13}\text{N}_3\text{Se})_2]^+$: 492 amu (parent ion peak).



3.4.2 Synthesis of $[\text{Ni}(2\text{-fursesc})_2]30$:

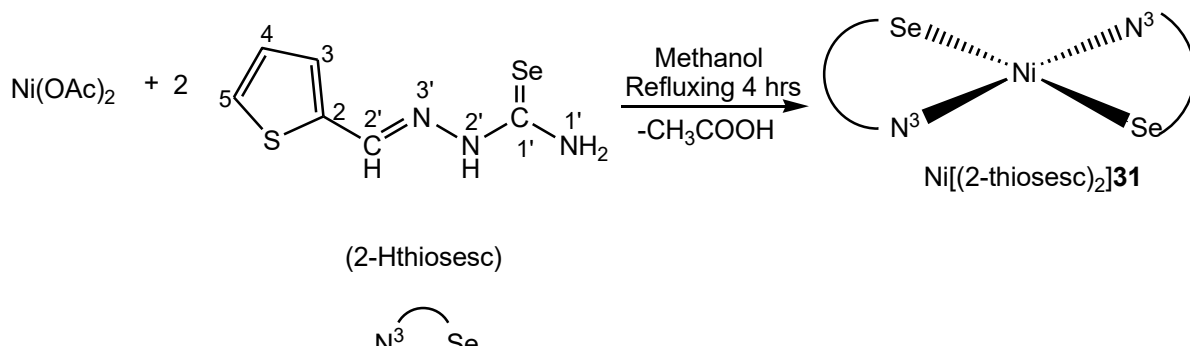
Nickel acetate (0.025g, 0.10mmol) was dissolved in 20 ml of methanol with heating. To it was added 2-furfural selenosemicarbazone (0.060g, 0.27mmol) and the mixture was refluxed for 4 hours. Light reddish solution formed was then filtered and at room temperature reddish solution kept for crystallization. Yield, 62%, m. p., 208-210°C. Important IR peaks (KBr, cm^{-1}): $\nu(\text{NH}_2)$ 3410m, 3300m; $\nu(\text{C}=\text{N})$ 1649s; $\nu(\text{C}=\text{C})$ 1597s; $\delta(\text{NH}_2)$ 1454s; $\nu(\text{C}=\text{Se})$ 738s (selenoamidemoiety). ^1H NMR (δ , ppm; $d^6\text{-dms}\text{o}$ and CDCl_3): 8.80 s (1H, C^2H), 7.51 d (1H,

C^5H), 7.45 d (1H, C^3H), 7.29 s (1H, $N^{1'}H_2$) and 7.14 t (1H, C^4H). ^{13}C NMR (δ , ppm): 155.8 (C^2), 139.3 (C^4), 132.3 (C^3), 130.0 (C^5) and 127.9 (C^2) respectively.



3.4.3 Synthesis of $[\text{Ni}(2\text{-thiosesc})_2]\textbf{31}$:

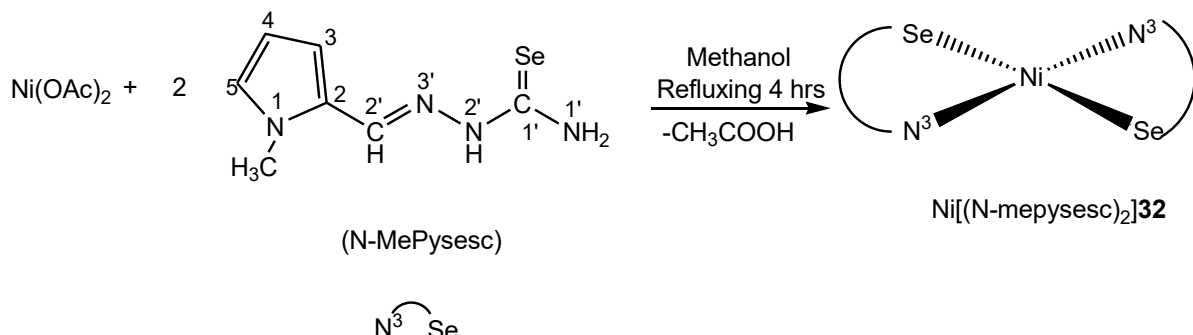
Nickel acetate (0.025g, 0.10mmol) was dissolved in 20 ml of methanol with heating. To it was added 2-thiophene selenosemicarbazone (0.065g, 0.28mmol) and the mixture was refluxed for 4 hours. Light reddish solution formed was then filtered and at room temperature reddish solution kept for crystallization. Yield, 60%, m. p., 210-213°C. Important IR peaks (KBr, cm^{-1}): $\nu(\text{NH}_2)$ 3291m; $\nu(\text{C}=\text{N})$ 1607s; $\nu(\text{C}=\text{C})$ 1563s; $\delta(\text{NH}_2)$ 1417s; $\nu(\text{C}=\text{Se})$ 798s (selenoamidemoiety). ^1H NMR (δ , ppm; d^6 -dmso and CDCl_3): 8.80 s (1H, C^2H), 7.51 d (1H, C^5H), 7.45 d (1H, C^3H), 7.29 s (1H, $N^{1'}H_2$) and 7.14 t (1H, C^4H). ^{13}C NMR (δ , ppm): 155.7 (C^2), 139.0 (C^4), 132.3 (C^3) 129.9 (C^5) and 127.7 (C^2) respectively.



3.4.4 Synthesis of $[\text{Ni}(\text{N-mepysesc})_2]\textbf{32}$:

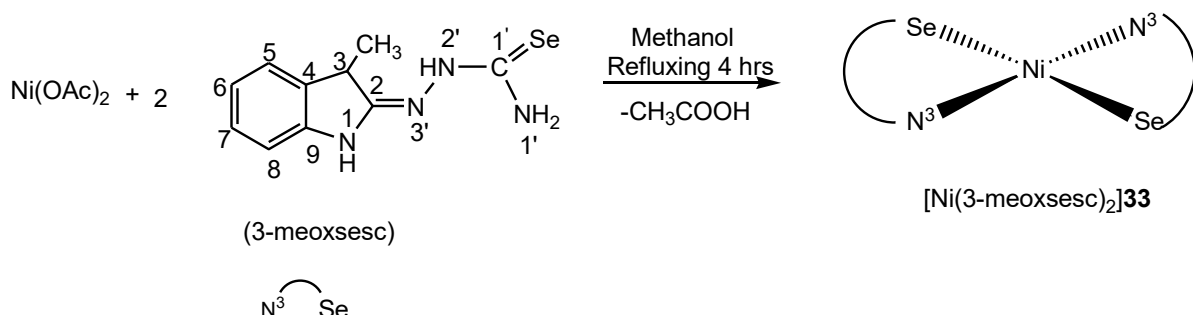
Nickel acetate (0.025g, 0.10mmol) was dissolved in 20 ml of methanol with heating. To it was added N-methyl-2-pyrrole selenosemicarbazone (0.064g, 0.27mmol) and the mixture was refluxed for 4 hours. Light reddish solution formed was then filtered and at room temperature reddish solution kept for crystallization. Yield, 60%, m. p., 215-218°C. Important IR peaks (KBr, cm^{-1}): $\nu(\text{NH}_2)$ 3443m, 3390m, 3242m; $\nu(\text{C}=\text{N})$ 1548s; $\nu(\text{C}=\text{C})$

1467s; $\delta(\text{NH}_2)$ 1410s; $\nu(\text{C}=\text{Se})$ 731s (selenoamidemoiety). ^1H NMR (δ , ppm; d⁶-dmso and CDCl₃): 7.94 s (1H, C²'H), 7.32 d (1H, C⁵H), 6.61 d (1H, C³H) and 6.20 m (1H, C⁴H) and 3.87 s (CH₃). ^{13}C NMR (δ , ppm): 138.2 (C²'), 129.3 (C⁴) 125.8 (C⁵), 118.0 (C³), 109.4 (C²) and 36.8 (CH₃) respectively.



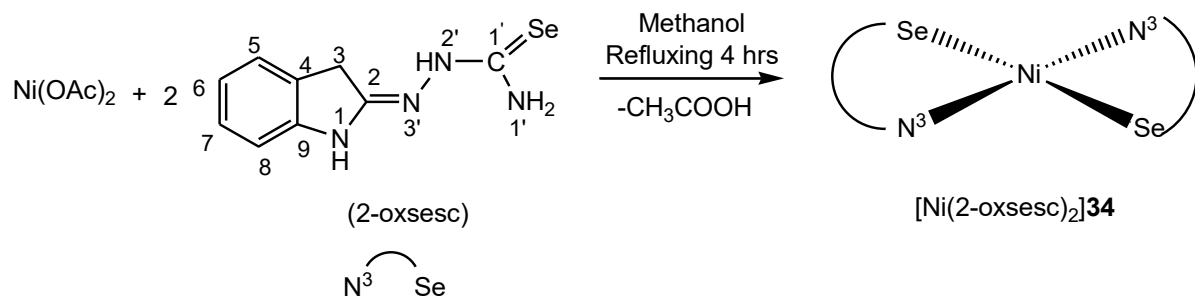
3.4.5 Synthesis of [Ni(3-meoxsesc)₂]33:

Nickel acetate (0.025g, 0.10mmol) was dissolved in 30 ml of methanol with heating. To it was added 3-methyl-2-oxindole selenosemicarbazone, (0.075g, 0.28mmol) and the mixture was refluxed for 4 hours. Light reddish solution formed was then filtered and at room temperature reddish solution kept for crystallization. Yield, 62%, m. p., 200-202°C. Important IR peaks (KBr, cm⁻¹): $\nu(\text{NH}_2)$ 3377m, 3327m, 3273m; $\nu(\text{NH})_{\text{meox}}$ 3123w; $\nu(\text{C}=\text{N})$ 1626s; $\nu(\text{C}=\text{C})$ 1595m; $\delta(\text{NH}_2)$ 1473s; $\nu(\text{C}=\text{Se})$ 792s (selenoamidemoiety). ^1H NMR (δ , ppm; d⁶-dmso and CDCl₃): 8.50 s (1H, N¹'H₂), 7.29 m (2H, C^{6,7}H), 7.04 d (1H, C⁵H), 6.92 d (1H, C⁸H), 3.57 (CH₃) and 1.69 s (1H, N¹H). ^{13}C NMR (δ , ppm): 181.3 (C¹'), 141.1 (C⁵), 131.2 (C⁶) 127.8 (C⁷), 123.7 (C⁸), 122.4 (C⁴), 109.6 (C⁹) and 41.0 (CH₃) respectively. Mass spectra m/z: [Ni(C₁₀H₁₄N₄Se)₂]⁺ : 594 amu (parent ion peak).



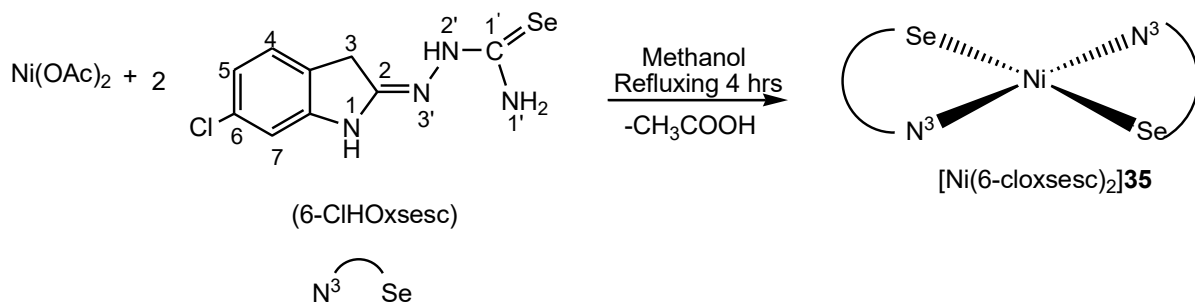
3.4.6 Synthesis of [Ni(2-oxsesc)₂]34:

Nickel acetate (0.025g, 0.10mmol) was dissolved in 30 ml of methanol with heating. To it was added 2-oxindole selenosemicarbazone, (0.071g, 0.28mmol) and the mixture was refluxed for 4 hours. Light reddish solution formed was then filtered and at room temperature reddish solution kept for crystallization. Yield, 62%, m. p., 210-213°C. Important IR peaks (KBr, cm^{-1}): $\nu(\text{NH}_2)$ 3269m; $\nu(\text{NH})_{\text{ox}}$ 3134w; $\nu(\text{C}=\text{N})$ 1643s; $\nu(\text{C}=\text{C})$ 1602m; $\delta(\text{NH}_2)$ 1448s; $\nu(\text{C}=\text{Se})$ 742s (selenoamidemoiety). ^1H NMR (δ , ppm; d^6 -dmso and CDCl_3): 8.50 s (1H, N^1H_2), 7.25 m (2H, $\text{C}^6, \text{C}^7\text{H}$), 7.04 d (1H, C^5H), 6.92 d (1H, C^8H), 3.56 (cyclic proton ring) and 1.68 s (1H, N^1H). ^{13}C NMR (δ , ppm): 142.4 (C^5), 127.9 (C^7) 125.2 (C^6), 124.6 (C^7), 122.3 (C^8), 109.6 (C^4) and 36.2 (C^3) respectively.



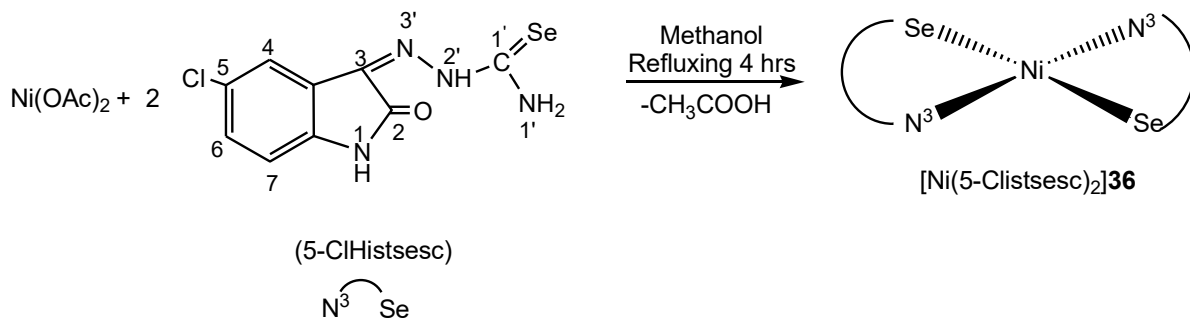
3.4.7 Synthesis of $[\text{Ni}(6\text{-cloxsesc})_2]35$:

Nickel acetate (0.025g, 0.10mmol) was dissolved in 30 ml of methanol with heating. To it was added 6-chloro-2-oxindole selenosemicarbazone, (0.081g, 0.028mmol) and the mixture was refluxed for 4 hours. Light reddish solution formed was then filtered and at room temperature reddish solution kept for crystallization. Yield, 62%, m. p., 215-217°C. Important IR peaks (KBr, cm^{-1}): $\nu(\text{NH}_2)$ 3429m, 3267m; $\nu(\text{NH})_{\text{clox}}$ 3147w; $\nu(\text{C}=\text{N})$ 1656s; $\nu(\text{C}=\text{C})$ 1507m; $\delta(\text{NH}_2)$ 1411s; $\nu(\text{C}=\text{Se})$ 740s (selenoamidemoiety). ^1H NMR (δ , ppm; d^6 -dmso and CDCl_3): 8.64 s (1H, N^1H_2), 7.28 d (1H, C^7H), 7.01 d (1H, C^4H), 6.93 s (1H, C^5H) and 3.45 (cyclic ring). ^{13}C NMR (δ , ppm): 143.4 (C^5), 133.6 (C^6), 125.5 (C^7), 123.3 (C^8), 110.3 (C^9) and 35.7 (C^3) respectively.



3.4.8 Synthesis of $[\text{Ni}(5\text{-clistsesc})_2]\textbf{36}$:

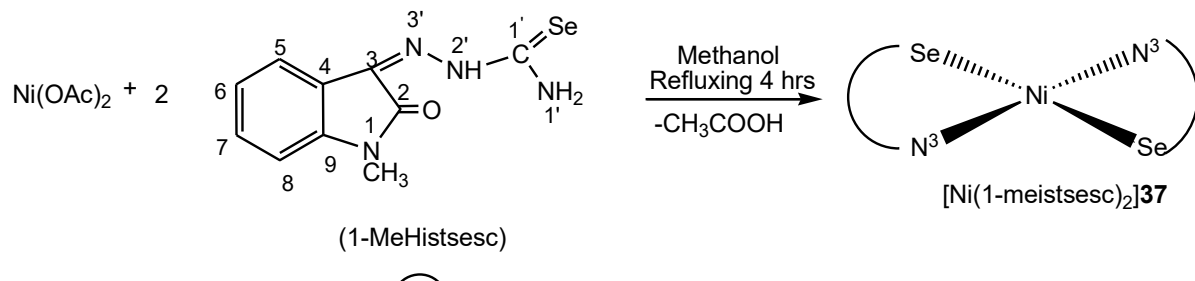
Nickel acetate (0.025g, 0.10mmol) was dissolved in 30 ml of methanol with heating. To it was added 5-chloro isatin selenosemicarbazone, (0.075g, 0.28mmol) and the mixture was refluxed for 4 hours. Light reddish solution formed was then filtered and at room temperature reddish solution kept for crystallization. Yield, 62%, m. p., 218-220°C. Important IR peaks (KBr, cm^{-1}): $\nu(\text{NH}_2)$ 3464m, 3257m; $\nu(\text{NH})_{\text{clist}}$ 3147w; $\nu(\text{C=O})$ 1681s; $\nu(\text{C=N})$ 1612s; $\nu(\text{C=C})$ 1575m; $\delta(\text{NH}_2)$ 1448s; $\nu(\text{C=Se})$ 779s (selenoamidemoiety). Mass spectra m/z: $[\text{Ni}(\text{C}_9\text{H}_4\text{N}_4\text{OClSe})_2]^+$: 593amu (parent ion peak).



3.4.9 Synthesis of $[\text{Ni}(1\text{-meistsesc})_2]\textbf{37}$:

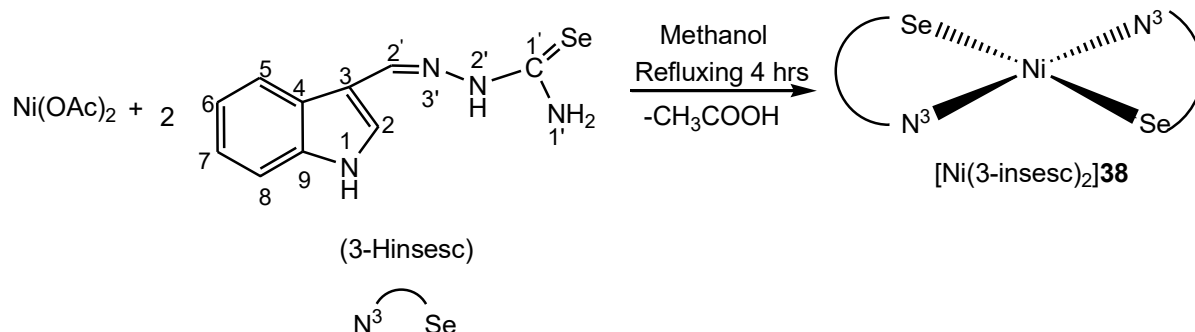
Nickel acetate (0.025g, 0.10mmol) was dissolved in 30 ml of methanol with heating. To it was added 1-methyl isatin selenosemicarbazone, (0.079g, 0.28mmol) and the mixture was refluxed for 4 hours. Light reddish solution formed was then filtered and at room temperature reddish solution kept for crystallization. Yield, 62%, m. p., 210-213°C. Important IR peaks (KBr, cm^{-1}): $\nu(\text{NH}_2)$ 3410m, 3300m; $\nu(\text{C=N})$ 1649s; $\nu(\text{C=C})$ 1597m; $\delta(\text{NH}_2)$ 1454s; $\nu(\text{C=Se})$ 738s (selenoamidemoiety). ^1H NMR (δ , ppm; $d^6\text{-dms}\text{o}$ and CDCl_3): 8.71 s (1H, N^1H_2), 7.24 m (2H, $\text{C}^5, \text{C}^8\text{H}$), 7.06 d (1H, C^6H), 6.93 d (1H, C^7H), 3.49 (CH_3). ^{13}C NMR (δ ,

ppm): 181.4 (C^1), 141.1 (C^6), 131.2 (C^8) 127.8 (C^7), 123.8 (C^9), 122.4 (C^3), 109.6 (C^4) and 41.0 (CH_3) respectively. Mass spectra m/z: $[Ni(C_{10}H_{10}N_4OSe)_2]^+$: 619amu (parent ion peak).



3.4.10 Synthesis of $[Ni(3\text{-insesc})_2]38$:

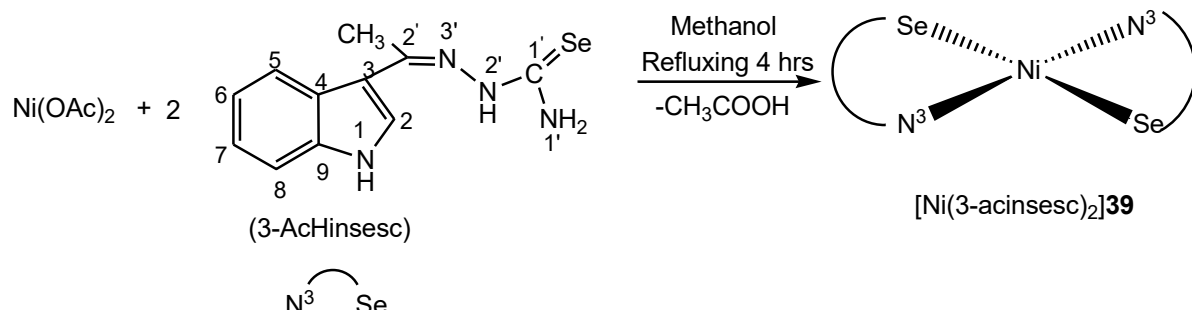
Nickel acetate (0.025g, 0.136mmol) was dissolved in 30 ml of methanol with heating. To it was added 3-indole selenosemicarbazone, (0.075g, 0.28mmol) and the mixture was refluxed for 4 hours. Light reddish solution formed was then filtered and at room temperature reddish solution kept for crystallization. Yield, 62%, m. p., 210-215°C. Important IR peaks (KBr, cm^{-1}): $\nu(NH_2)$ 3461m; $\nu(NH)_{ind}$ 3050w; $\nu(C=N)$ 1533s; $\nu(C=C)$ 1495m; $\delta(NH_2)$ 1413s; $\nu(C=Se)$ 739s (selenoamidemoiety). Mass spectra m/z: $[Ni(C_{10}H_{12}N_4Se)_2]^+$: 587amu (parent ion peak).



3.4.11 Synthesis of $[Ni(3\text{-acinsesc})_2]39$:

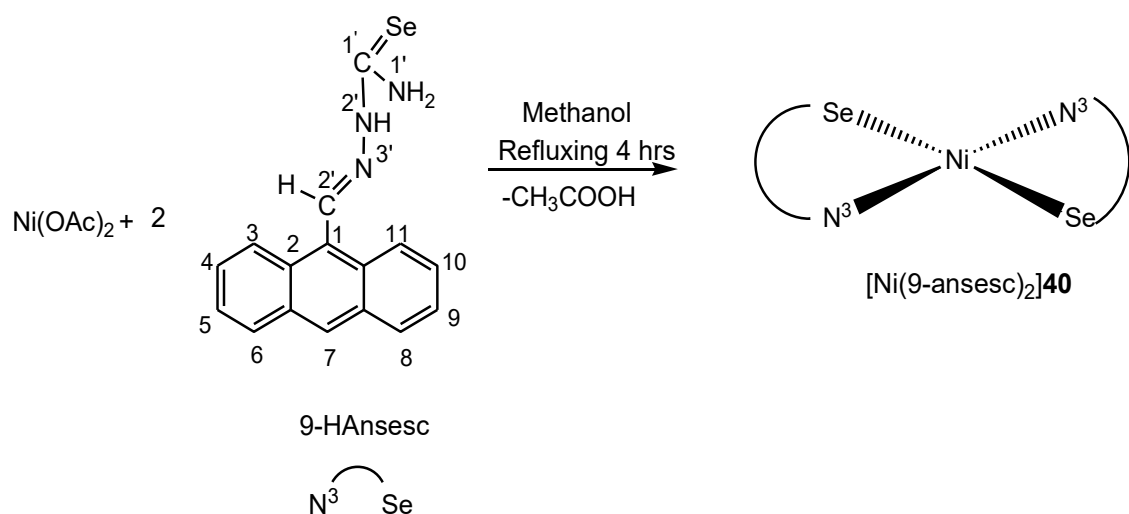
Nickel acetate (0.025g, 0.10mmol) was dissolved in 30 ml of methanol with heating. To it was added 3-acetyl indole selenosemicarbazone, (0.079g, 0.28mmol) and the mixture was refluxed for 4 hours. Light reddish solution formed was then filtered and at room temperature reddish solution kept for crystallization. Yield, 62%, m. p., 230-233°C. Important IR peaks (KBr, cm^{-1}): $\nu(NH)_{acind}$ 3153w; $\nu(C=N)$ 1608s; $\nu(C=C)$ 1564m; $\delta(NH_2)$ 1421s; $\nu(C=Se)$ 798s (selenoamidemoiety). 1H NMR (δ , ppm; d^6 -dmso and $CDCl_3$): 8.81 s (1H, N^1H_2), 8.43 d (1H, C^5H), 7.89 s (1H, C^2H), 7.45 d (1H, C^8H), 7.32 m (2H, $C^6, ^7H$) and 2.58 (CH_3)

respectively. ^{13}C NMR (δ , ppm): 136.3 (C^{2'}), 131.4 (C⁶) 125.4 (C⁵), 122.4 (C⁷), 118.6 (C⁸), 111.3 (C⁴) and 27.6 (CH₃) respectively.



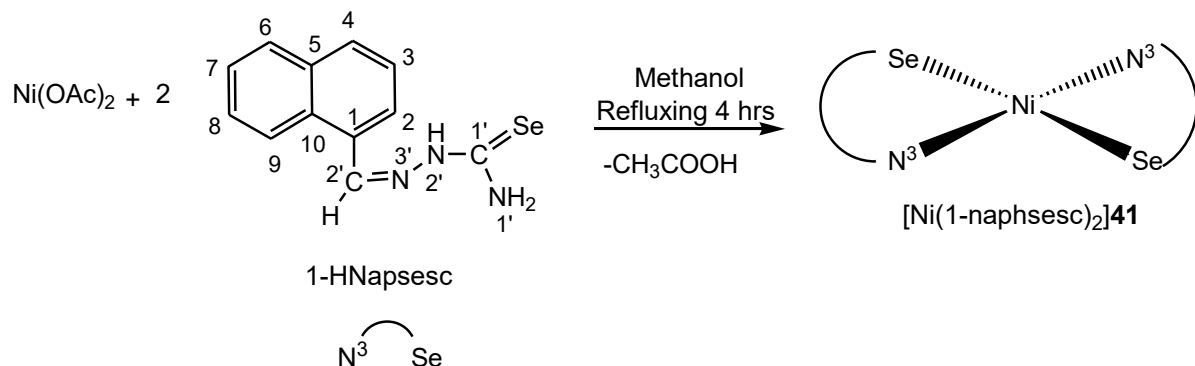
3.4.12 Synthesis of [Ni(9-ansesc)₂]40:

Nickel acetate (0.025g, 0.10mmol) was dissolved in 30 ml of methanol with heating. To it was added 9-anthracene selenosemicarbazone, (0.092g, 0.28mmol) and the mixture was refluxed for 4 hours. Light reddish solution formed was then filtered and at room temperature reddish solution kept for crystallization. Yield, 65%, m. p., 220-223°C. Important IR peaks (KBr, cm⁻¹): $\nu(\text{NH}_2)$ 3458m, 3262m; $\nu(\text{C}=\text{N})$ 1616s; $\nu(\text{C}=\text{C})$ 1523m; $\delta(\text{NH}_2)$ 1440s; $\nu(\text{C}=\text{Se})$ 728s (selenoamidemoiety). ^1H NMR (δ , ppm; d⁶-dmso and CDCl₃): 9.50 s (1H, C^{2'}H), 9.00 d (1H, C³H), 8.56 s (1H, N^{1'}H₂), 8.18 d (1H, C⁸H), 8.01 d (1H, C¹¹H), 7.96 d (1H, C⁶H), 7.70-7.62 m (4H, C^{4, 5, 9, 10}H). ^{13}C NMR (CDCl₃, δ ppm): 162.0 (C^{1'}), 131.8 (C^{2'}), 131.5-124.6 (ring carbon) respectively.



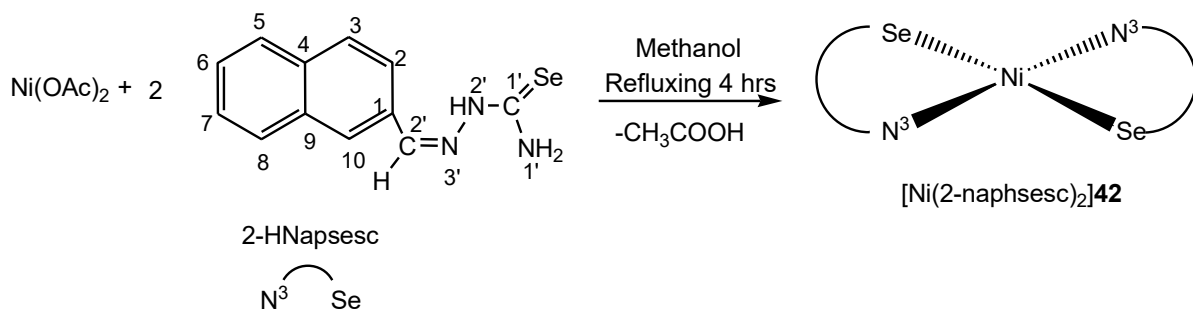
3.4.13 Synthesis of $[\text{Ni}(1\text{-naphsesc})_2]41$:

Nickel acetate (0.025g, 0.10mmol) was dissolved in 30 ml of ethanol with heating. To it was added 1-naphthaldehyde selenosemicarbazone, (0.077g, 0.28mmol) and the mixture was refluxed for 4 hours. Light reddish solution formed was then filtered and at room temperature reddish solution kept for crystallization. Yield, 62%, m. p., 220-225°C. Important IR peaks (KBr, cm^{-1}): $\nu(\text{NH}_2)$ 3396m; $\nu(\text{C}=\text{N})$ 1602s; $\nu(\text{C}=\text{C})$ 1519m; $\delta(\text{NH}_2)$ 1465s; $\nu(\text{C}=\text{Se})$ 759s (selenoamidemoiety). ^1H NMR (δ , ppm; d⁶-dms and CDCl_3): 9.04 d (2H, $\text{C}^6, ^9\text{H}$), 8.75 s (1H, N^1H_2), 8.12 d (2H, $\text{C}^4, ^2\text{H}$), 7.71 - 7.59 m (4H, $\text{C}^3, ^7\text{H}$). ^{13}C NMR (CDCl_3 , δ ppm): 193.0 (C^1), 135.2 (C^2), 132.1(C^7), 131.1(C^6), 129.3(C^8), 129.1(C^4), 125.7(C^3) and 123.5(C^3) respectively.



3.4.14 Synthesis of $[\text{Ni}(2\text{-naphsesc})_2]42$:

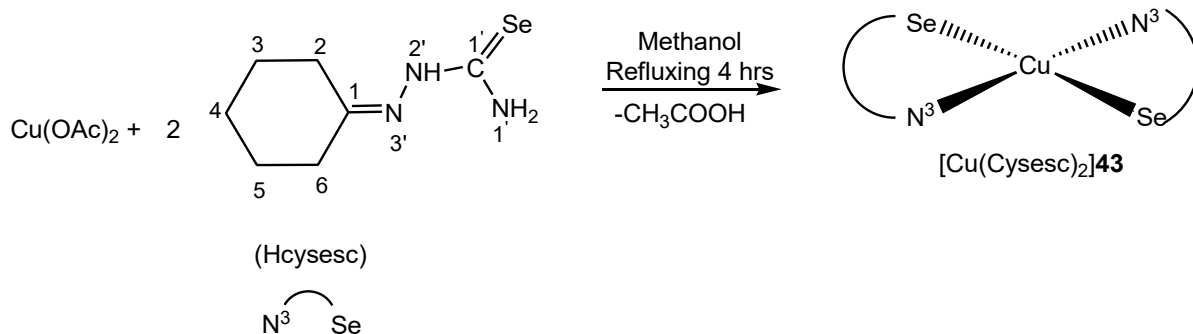
Nickel acetate (0.025g, 0.10mmol) was dissolved in 30 ml of ethanol with heating. To it was added 2-naphthaldehyde selenosemicarbazone, (0.077g, 0.28mmol) and the mixture was refluxed for 4 hours. Light brownish solution formed was then filtered and at room temperature brownish solution kept for crystallization. Yield, 60%, m. p., 240-242°C. Important IR peaks (KBr, cm^{-1}): $\nu(\text{NH}_2)$ 3269m; $\nu(\text{C}=\text{N})$ 1662s; $\nu(\text{C}=\text{C})$ 1593m; $\delta(\text{NH}_2)$ 1448s; $\nu(\text{C}=\text{Se})$ 744s (selenoamidemoiety). ^1H NMR (δ , ppm; d⁶-dms and CDCl_3): 8.89 s(1H, N^1H_2), 7.16 d(1H, C^5H), 7.01 d(1H, C^3H), 5.12 s (1H, C^7H), 2.97-2.38 m(4H, $\text{C}^{2,6}\text{H}$) respectively. Mass spectra m/z: $[\text{Ni}(\text{C}_{12}\text{H}_{10}\text{N}_3\text{Se})_2]^+$: 606amu (parent ion peak).



3.5 Complexes of Copper(II)

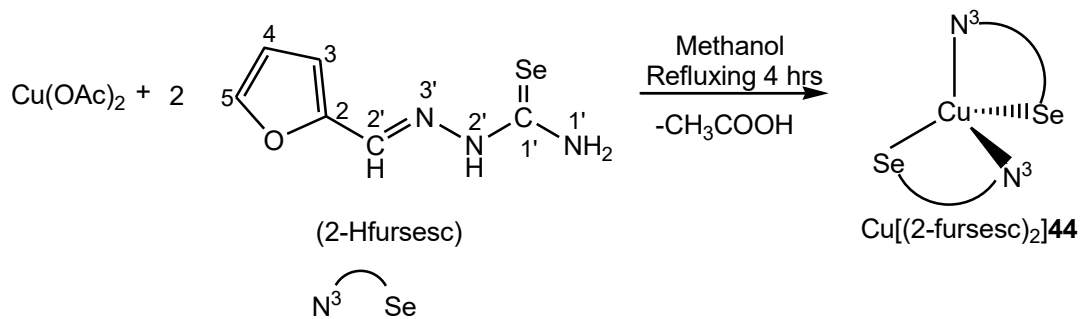
3.5.1 Synthesis of [Cu(cysesc)2]43:

Copper acetate(0.025g, 0.137mmol) was dissolved in 30 ml of methanol with heating. To it was added cyclohexanoneselenosemicarbazone, (0.060g, 0.27mmol) and the mixture was refluxed for 4 hours. Light red solution formed was then filtered and at room temperature red solution kept for crystallization. Yield, 60%, m. p., 215-220°C. Important IR peaks (KBr, cm⁻¹): $\nu(\text{NH}_2)$ 3274m; $\nu(\text{C}=\text{N})$ 1647s; $\nu(\text{C}=\text{C})$ 1547s; $\delta(\text{NH}_2)$ 1413s; $\nu(\text{C}=\text{Se})$ 717s (selenoamidemoiety). ESR data (g, tensor, A, gauss): g_{\parallel} , 2.24; g_{\perp} , 2.07; A_{\parallel} , 20; A_{\perp} , 250. Mass spectra m/z: $[\text{Cu}(\text{C}_7\text{H}_{11}\text{N}_3\text{Se})_2]^+$: 496amu (parent ion peak).



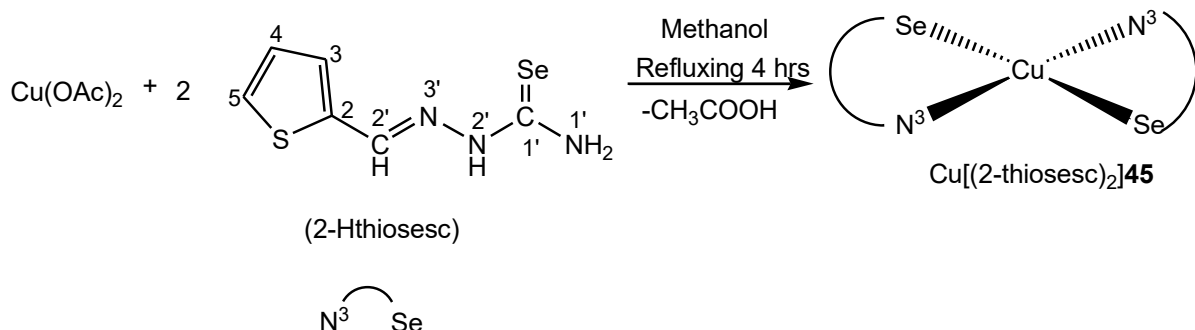
3.5.2 Synthesis of [Cu(2-fursesc)2]44:

Copper acetate (0.025g, 0.13mmol) was dissolved in 20 ml of methanol with heating. To it was added 2-furfural selenosemicarbazone (0.026g, 0.27mmol) and the mixture was refluxed for 4 hours. Light reddish solution formed was then filtered and at room temperature reddish solution kept for crystallization. Yield, 60%, m. p., 210-213°C. Important IR peaks (KBr, cm⁻¹): $\nu(\text{NH}_2)$ 3333m; $\nu(\text{C}=\text{N})$ 1648s; $\nu(\text{C}=\text{C})$ 1546s; $\delta(\text{NH}_2)$ 1461s; $\nu(\text{C}=\text{Se})$ 736s (selenoamidemoiety). ESR data (g, tensor, A, gauss): g_{\parallel} , 2.28; g_{\perp} , 2.07; A_{\parallel} , 15; A_{\perp} , 125.



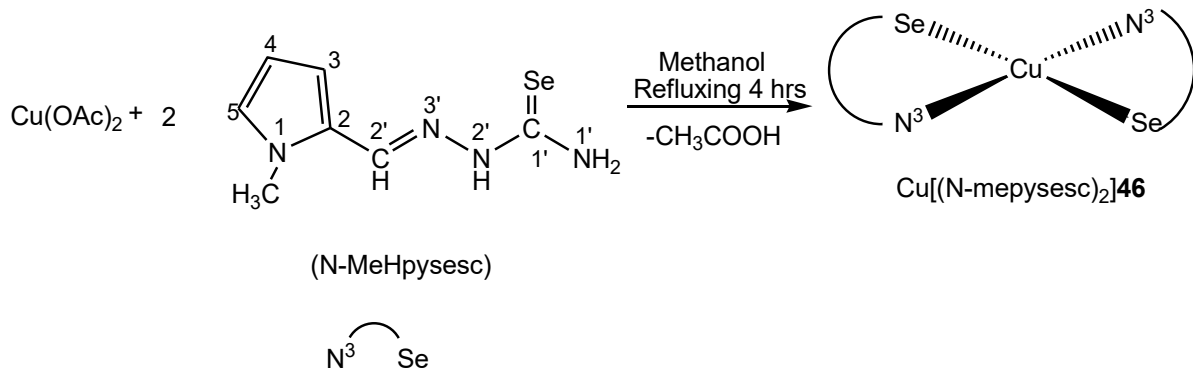
3.5.3 Synthesis of $[\text{Cu}(2\text{-thiosesc})_2]\textbf{45}$:

Copper acetate (0.025g, 0.13mmol) was dissolved in 20 ml of methanol with heating. To it was added 2-thiophene selenosemicarbazone (0.063g, 0.27mmol) and the mixture was refluxed for 4 hours. Light reddish solution formed was then filtered and at room temperature reddish solution kept for crystallization. Yield, 60%, m. p., 210-213°C. Important IR peaks (KBr, cm^{-1}): $\nu(\text{NH}_2)$ 3361m; $\nu(\text{C}=\text{N})$ 1606s; $\nu(\text{C}=\text{C})$ 1548m; $\delta(\text{NH}_2)$ 1418s; $\nu(\text{C}=\text{Se})$ 717s (selenoamidemoiety). ESR data (g, tensor, A, gauss): $g_{||}, 2.19$; $g_{\perp}, 2.075$; $A_{||}, 20$; $A_{\perp}, 210$.



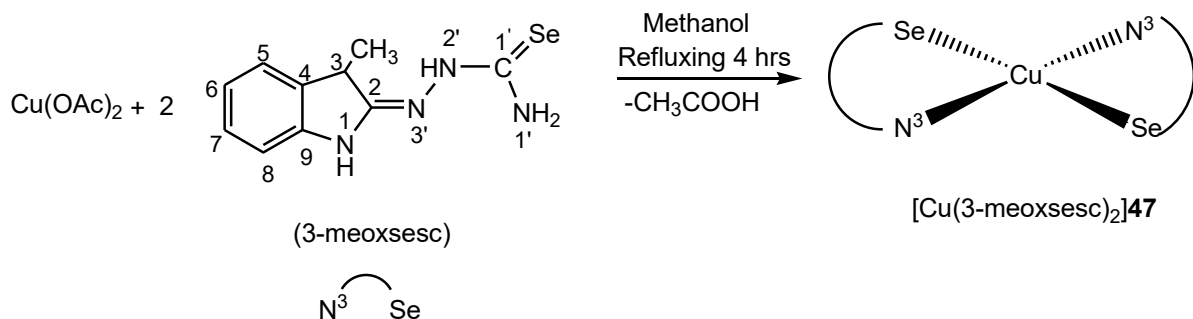
3.5.4 Synthesis of $[\text{Cu}(\text{N-mepysesc})_2]\textbf{46}$:

Copper acetate (0.025g, 0.13mmol) was dissolved in 20 ml of methanol with heating. To it was added N-methyl-2-pyrrole selenosemicarbazone (0.063g, 0.27mmol) and the mixture was refluxed for 4 hours. Light reddish solution formed was then filtered and at room temperature reddish solution kept for crystallization. Yield, 60%, m. p., 215-218°C. Important IR peaks (KBr, cm^{-1}): $\nu(\text{NH}_2)$ 3215m; $\nu(\text{C}=\text{N})$ 1619s; $\nu(\text{C}=\text{C})$ 1542m; $\delta(\text{NH}_2)$ 1464s; $\nu(\text{C}=\text{Se})$ 721s (selenoamidemoiety). ESR data (g, tensor, A, gauss): $g_{||}, 2.30$; $g_{\perp}, 2.08$; $A_{||}, 20$; $A_{\perp}, 110$.



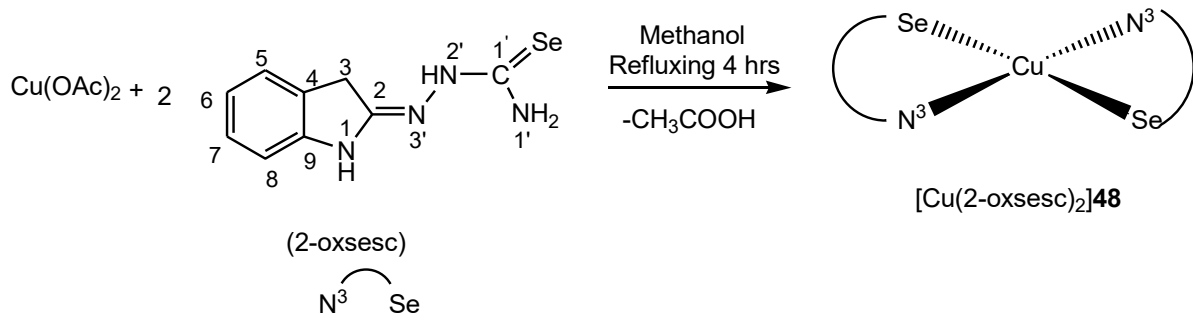
3.5.5 Synthesis of $[\text{Cu}(3\text{-meoxsesc})_2]\text{47}$:

Copper acetate (0.025g, 0.13mmol) was dissolved in 30 ml of methanol with heating. To it was added 3-methyl-2-oxindole selenosemicarbazone, (0.073g, 0.27mmol) and the mixture was refluxed for 4 hours. Light reddish solution formed was then filtered and at room temperature reddish solution kept for crystallization. Yield, 62%, m. p., 205-210°C. Important IR peaks (KBr, cm^{-1}): $\nu(\text{NH}_2)$ 3373m; $\nu(\text{C}=\text{N})$ 1608s; $\nu(\text{C}=\text{C})$ 1527m; $\delta(\text{NH}_2)$ 1421s; $\nu(\text{C}=\text{Se})$ 754s (selenoamidemoiety). ESR data (g, tensor, A, gauss): $g_{||}, 2.25$; $g_{\perp}, 2.0$; $A_{||}, 20$; $A_{\perp}, 160$.



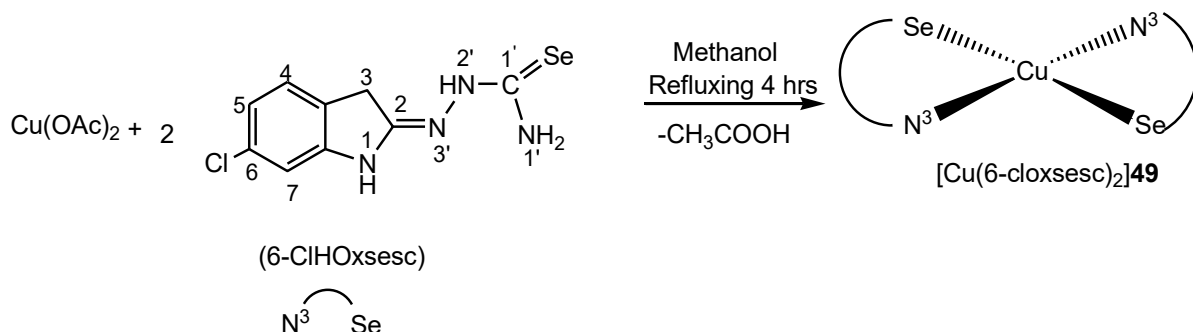
3.5.6 Synthesis of $[\text{Cu}(2\text{-oxsesc})_2]\text{48}$:

Copper acetate(0.025g, 0.13mmol) was dissolved in 30 ml of methanol with heating. To it was added 2-oxindole selenosemicarbazone, (0.069g, 0.27mmol) and the mixture was refluxed for 4 hours. Light reddish solution formed was then filtered and at room temperature reddish solution kept for crystallization. Yield, 62%, m. p., 205-210°C. Important IR peaks (KBr, cm^{-1}): $\nu(\text{NH}_2)$ 3342m; $\nu(\text{C}=\text{N})$ 1601s; $\nu(\text{C}=\text{C})$ 1547m; $\delta(\text{NH}_2)$ 1413s; $\nu(\text{C}=\text{Se})$ 730s (selenoamidemoiety). ESR data (g, tensor, A, gauss): $g_{||}, 2.31$; $g_{\perp}, 2.05$; $A_{||}, 30$; $A_{\perp}, 150$.



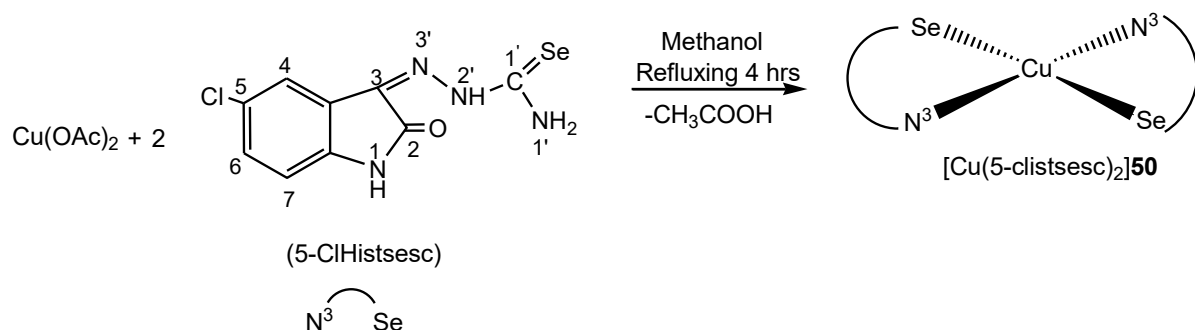
3.5.7 Synthesis of $[\text{Cu}(6\text{-cloxsesc})_2]49$:

Copper acetate(0.025g, 0.13mmol) was dissolved in 30 ml of methanol with heating. To it was added 6-chloro-2-oxindole selenosemicarbazone, (0.079g, 0.27mmol) and the mixture was refluxed for 4 hours. Light reddish solution formed was then filtered and at room temperature reddish solution kept for crystallization. Yield, 62%, m. p., 210-215°C. Important IR peaks (KBr, cm^{-1}): $\nu(\text{NH}_2)$ 3453; $\nu(\text{C}=\text{N})$ 1610s; $\nu(\text{C}=\text{C})$ 1483m; $\delta(\text{NH}_2)$ 1435s; $\nu(\text{C}=\text{Se})$ 723s (selenoamidemoiety). ESR data (g, tensor, A, gauss): $g_{\parallel}, 2.21$; $g_{\perp}, 2.0$; $A_{\parallel}, 20$; $A_{\perp}, 210$.



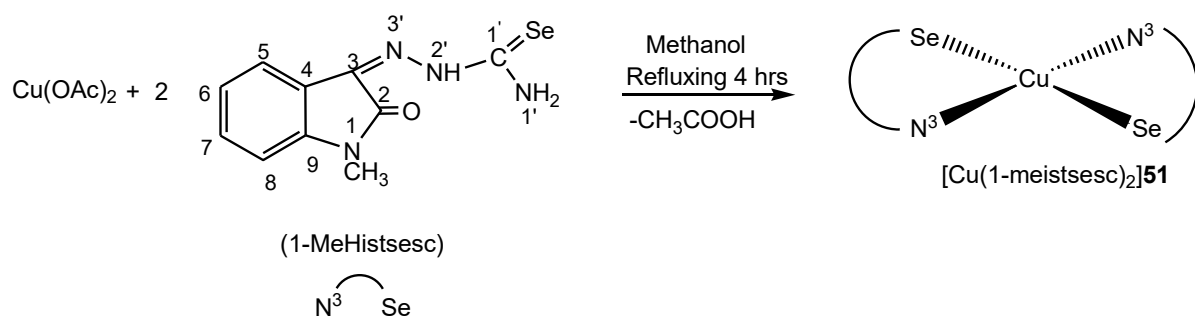
3.5.8 Synthesis of $[\text{Cu}(5\text{-clistsesc})_2]50$:

Copper acetate (0.025g, 0.137mmol) was dissolved in 30 ml of methanol with heating. To it was added 5-chloro isatin selenosemicarbazone, (0.073g, 0.27mmol) and the mixture was refluxed for 4 hours. Light reddish solution formed was then filtered and at room temperature reddish solution kept for crystallization. Yield, 62%, m. p., 210-215°C. Important IR peaks (KBr, cm^{-1}): $\nu(\text{NH}_2)$ 3249m; $\nu(\text{C}=\text{O})$ 1694s; $\nu(\text{C}=\text{N})$ 1648s; $\nu(\text{C}=\text{C})$ 1470m; $\delta(\text{NH}_2)$ 1443s; $\nu(\text{C}=\text{Se})$ 742s (selenoamidemoiety). ESR data (g, tensor, A, gauss): $g_{\parallel}, 2.24$; $g_{\perp}, 2.05$; $A_{\parallel}, 20$; $A_{\perp}, 165$. Mass spectra m/z: $[\text{Cu}(\text{C}_9\text{H}_8\text{N}_4\text{OClSe})_2]^+$: 666amu (parent ion peak).



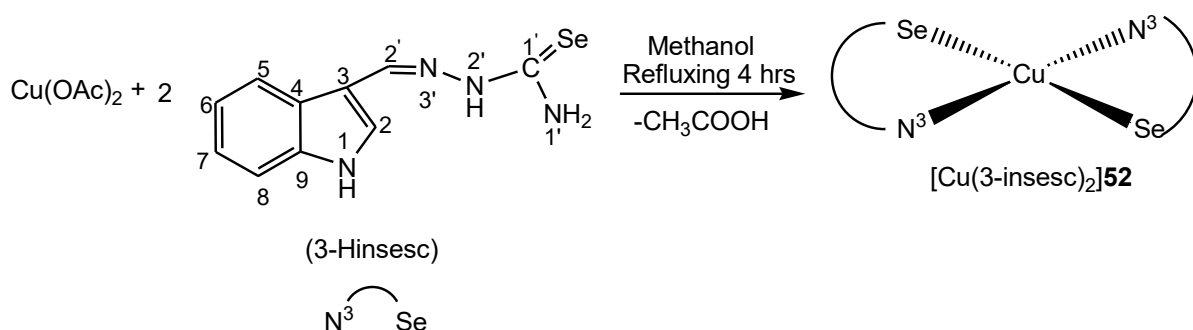
3.5.9 Synthesis of [Cu(1-meistsesc)2]51:

Cobalt acetate (0.025g, 0.136mmol) was dissolved in 30 ml of methanol with heating. To it was added 1-methyl isatin selenosemicarbazone, (0.076g, 0.27mmol) and the mixture was refluxed for 4 hours. Light reddish solution formed was then filtered and at room temperature reddish solution kept for crystallization. Yield, 62%, m. p., 210-215°C. Important IR peaks (KBr, cm⁻¹): $\nu(\text{NH}_2)$ 3380m; $\nu(\text{C}=\text{O})$ 1695s; $\nu(\text{C}=\text{N})$ 1607s; $\nu(\text{C}=\text{C})$ $\delta(\text{NH}_2)$ 1465s; $\nu(\text{C}=\text{Se})$ 749s (selenoamidemoiety). ESR data (g, tensor, A, gauss): g_{\parallel} , 2.19; g_{\perp} , 2.07; A_{\parallel} , 20; A_{\perp} , 202. Mass spectra m/z: [Cu(C₁₀H₁₀N₄OSe)₂]⁺: 624amu (parent ion peak).



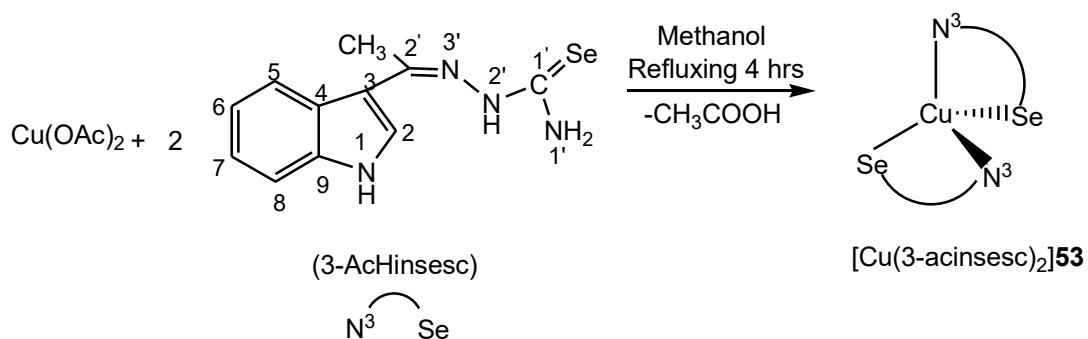
3.5.10 Synthesis of [Cu(3-insesc)2]52:

Copper acetate (0.025g, 0.136mmol) was dissolved in 30 ml of methanol with heating. To it was added 3-indole selenosemicarbazone, (0.072g, 0.27mmol) and the mixture was refluxed for 4 hours. Light reddish solution formed was then filtered and at room temperature reddish solution kept for crystallization. Yield, 62%, m. p., 213-215°C. Important IR peaks (KBr, cm⁻¹): $\nu(\text{NH}_2)$ 3452m; $\nu(\text{C}=\text{N})$ 1602s; $\nu(\text{C}=\text{C})$ 1546s; $\delta(\text{NH}_2)$ 1417s; $\nu(\text{C}=\text{Se})$ 759s (selenoamidemoiety). ESR data (g, tensor, A, gauss): g_{\parallel} , 2.24; g_{\perp} , 2.13; A_{\parallel} , 35; A_{\perp} , 220. Mass spectra m/z: [Cu(C₁₀H₁₁N₄Se)₂]⁺: 594amu (parent ion peak).



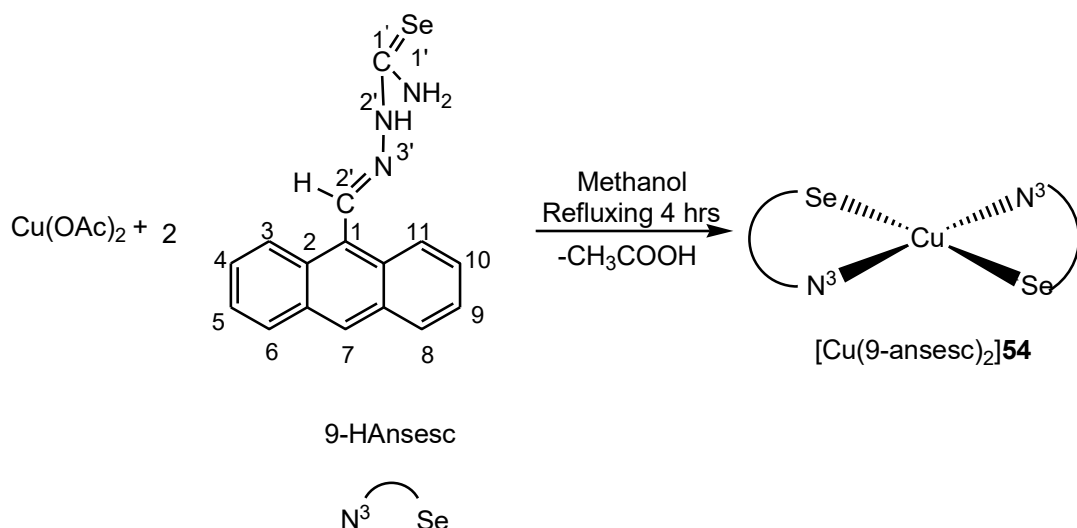
3.5.11 Synthesis of $[\text{Cu}(3\text{-acinsesc})_2]\mathbf{53}$:

Copper acetate (0.025g, 0.13mmol) was dissolved in 30 ml of methanol with heating. To it was added 3-acetyl indole selenosemicarbazone, (0.076g, 0.27mmol) and the mixture was refluxed for 4 hours. Light reddish solution formed was then filtered and at room temperature reddish solution kept for crystallization. Yield, 62%, m. p., 210-215°C. Important IR peaks (KBr, cm^{-1}): $\nu(\text{NH}_2)$ 3220m; $\nu(\text{C}=\text{N})$ 1609s; $\nu(\text{C}=\text{C})$ 1572s; $\delta(\text{NH}_2)$ 1430s; $\nu(\text{C}=\text{Se})$ 748s (selenoamidemoiety). ESR data (g, tensor, A, gauss): g_x , 2.04; g_y , 2.15; g_z , 2.26; A_{\parallel} , 35; A_{\perp} , 155. Mass spectra m/z: $[\text{Cu}(\text{C}_{11}\text{H}_{11}\text{N}_4\text{Se})_2]^+$: 617amu (parent ion peak).



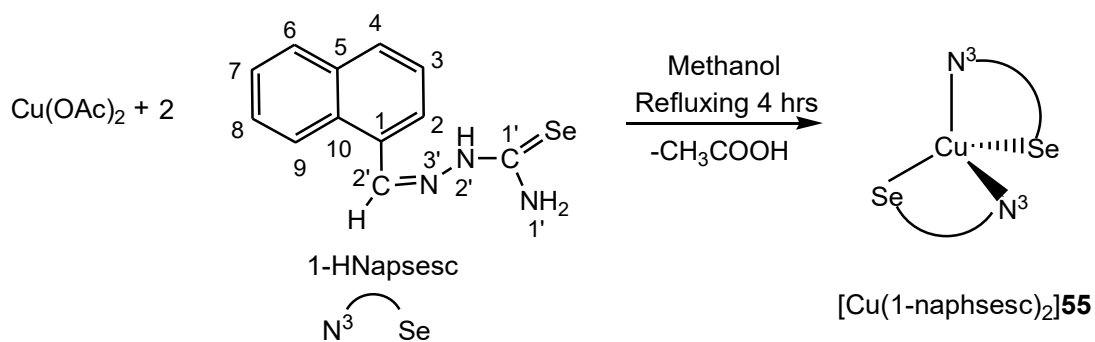
3.5.12 Synthesis of $[\text{Cu}(9\text{-ansesc})_2]\mathbf{54}$:

Copper acetate (0.025g, 0.137mmol) was dissolved in 30 ml of methanol with heating. To it was added 9-anthracene selenosemicarbazone, (0.056g, 0.27mmol) and the mixture was refluxed for 4 hours. Light reddish solution formed was then filtered and at room temperature reddish solution kept for crystallization. Yield, 62%, m. p., 220-225°C. Important IR peaks (KBr, cm^{-1}): $\nu(\text{NH}_2)$ 3481m, 362m; $\nu(\text{C}=\text{N})$ 1569s; $\nu(\text{C}=\text{C})$ 1499m; $\delta(\text{NH}_2)$ 1406s; $\nu(\text{C}=\text{Se})$ 732s (selenoamidemoiety). ESR data (g, tensor, A, gauss): g_{\parallel} , 2.24; g_{\perp} , 2.07; A_{\parallel} , 20; A_{\perp} , 250.



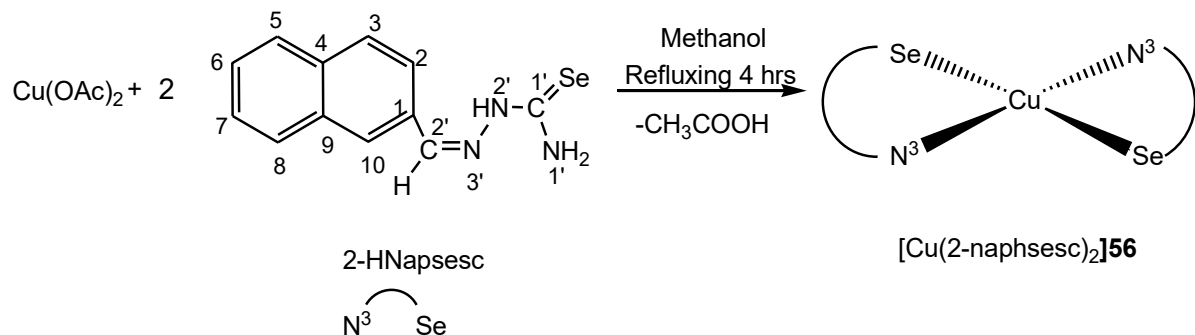
3.5.13 Synthesis of $[\text{Cu}(1\text{-naphsesc})_2]55$:

Copper acetate (0.025g, 0.137mmol) was dissolved in 30 ml of methanol with heating. To it was added 1-naphthaldehydeselenoimine (0.075g, 0.275mmol) and the mixture was refluxed for 4 hours. Light brownish solution formed was then filtered and at room temperature brownish solution kept for crystallization. Yield, 60%, m. p., 210-215°C. Important IR peaks (KBr, cm^{-1}): $\nu(\text{NH}_2)$ 3331m; $\nu(\text{C}=\text{N})$ 1614s; $\nu(\text{C}=\text{C})$ 1543m; $\delta(\text{NH}_2)$ 1460s; $\nu(\text{C}=\text{Se})$ 765s (selenoamidemoiety). ESR data (g, tensor, A, gauss): $g_{\parallel}, 2.3$; $g_{\perp}, 2.08$; $A_{\parallel}, 15$; $A_{\perp}, 145$.



3.5.14 Synthesis of $[\text{Cu}(2\text{-naphsesc})_2]56$:

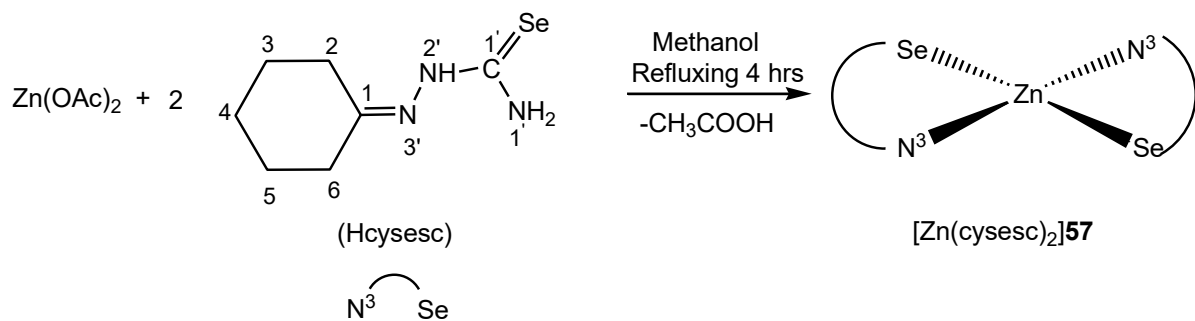
Copper acetate (0.025g, 0.137mmol) was dissolved in 30 ml of ethanol with heating. To it was added 2-naphthaldehyde selenosemicarbazone, (0.075g, 0.27mmol) and the mixture was refluxed for 4 hours. Light brownish solution formed was then filtered and at room temperature brownish solution kept for crystallization. Yield, 60%, m. p., 230-235°C. Important IR peaks (KBr, cm^{-1}): $\nu(\text{NH}_2)$ 3218m; $\nu(\text{C}=\text{N})$ 1607s; $\nu(\text{C}=\text{C})$ 1546s; $\delta(\text{NH}_2)$ 1466s; $\nu(\text{C}=\text{Se})$ 758s (selenoamidemoiety). ESR data (g, tensor, A, gauss): $g_{\parallel}, 2.23$; $g_{\perp}, 2.04$; $A_{\parallel}, 20$; $A_{\perp}, 170$. Mass spectra m/z: $[\text{Cu}(\text{C}_{12}\text{H}_{10}\text{N}_3\text{Se})_2]^+$: 612amu (parent ion peak).



3.6 Complexes of Zinc(II)

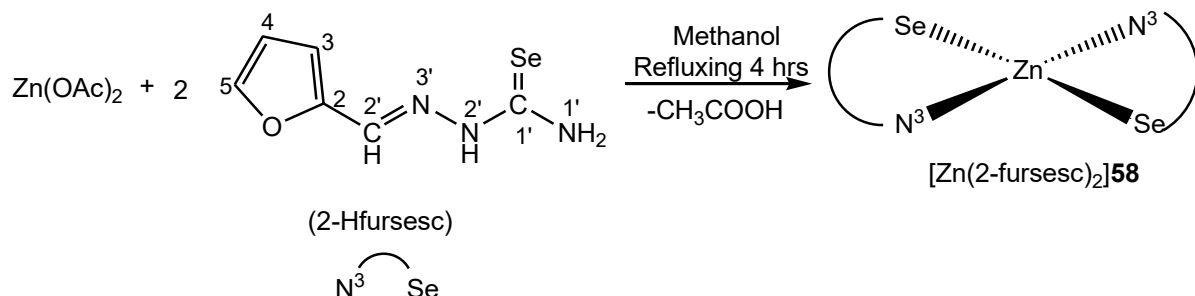
3.6.1 Synthesis of $[\text{Zn}(\text{cysesc})_2]57$:

Zinc acetate (0.025g, 0.136mmol) was dissolved in 30 ml of methanol with heating. To it was added cyclohexanoneselenosemicarbazone, (0.059g, 0.270mmol) and the mixture was refluxed for 4 hours. Whitish solution formed was then filtered and at room temperature whitish solution kept for crystallization. Yield, 60%, m. p., 200-203°C. Important IR peaks (KBr, cm^{-1}): $\nu(\text{NH}_2)$ 3364m, 3293m; $\nu(\text{C}=\text{N})$ 1606s; $\nu(\text{C}=\text{C})$ 1580m; $\delta(\text{NH}_2)$ 1432s; $\nu(\text{C}=\text{Se})$ 710s (selenoamidemoiety). ^1H NMR (δ , ppm; $d^6\text{-dmsO}$ and CDCl_3): 5.08 s (1H, N^1H_2), 3.52-1.73 m (10H, Cy ring proton). ^{13}C NMR (δ , ppm): 172.6 ($\text{C}^{1'}$), 36.1-25.5 (cyclic ring carbon) respectively. Mass spectra m/z: $[\text{Zn}(\text{C}_7\text{H}_{12}\text{N}_3\text{Se})_2]^+$: 497 amu (parent ion peak).



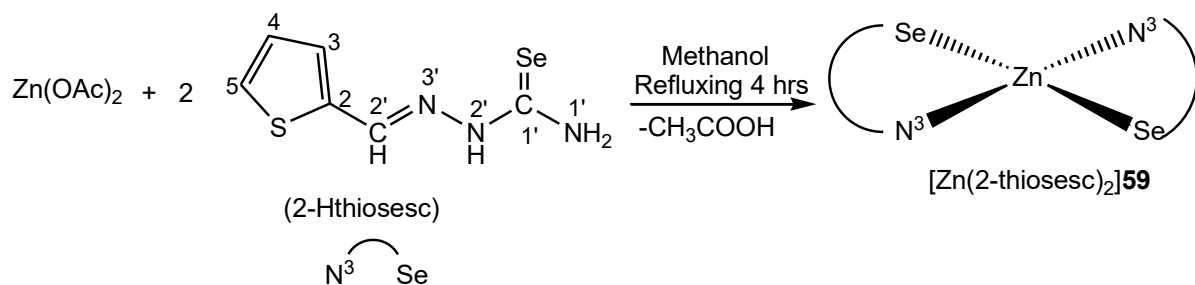
3.6.2 Synthesis of $[Zn(2\text{-fursesc})_2]58$:

Zinc acetate (0.025g, 0.13mmol) was dissolved in 20 ml of methanol with heating. To it was added 2-furfural selenosemicarbazone (0.026g, 0.27mmol) and the mixture was refluxed for 4 hours. Light reddish solution formed was then filtered and at room temperature reddish solution kept for crystallization. Yield, 60%, m. p., 218-220°C. Important IR peaks (KBr, cm^{-1}): $\nu(\text{NH}_2)$ 3350m, 3230m; $\nu(\text{C}=\text{N})$ 1595s; $\nu(\text{C}=\text{C})$ 1531m; $\delta(\text{NH}_2)$ 1479s; $\nu(\text{C}=\text{Se})$ 744s (selenoamidemoiety). Mass spectra m/z: $[\text{Zn}(\text{C}_6\text{H}_6\text{N}_3\text{OSe})_2]^+$: 494 amu (parent ion peak).



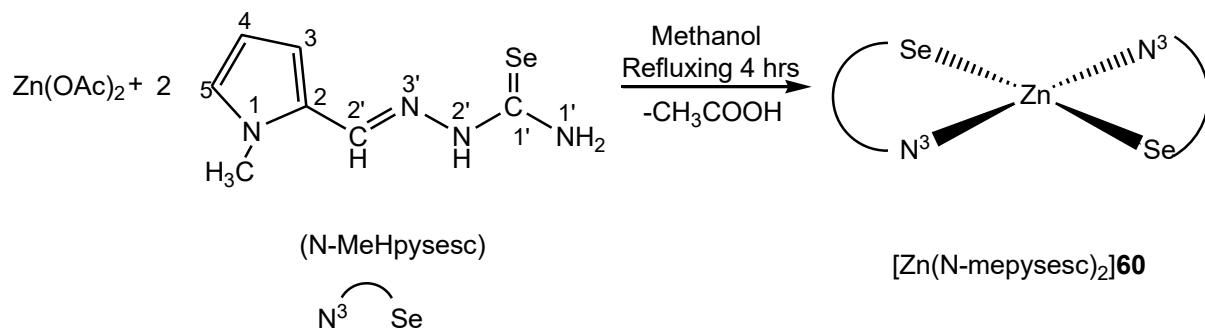
3.6.3 Synthesis of $[Zn(2\text{-thiosesc})_2]59$:

Zinc acetate (0.025g, 0.13mmol) was dissolved in 20 ml of methanol with heating. To it was added 2-thiophene selenosemicarbazone (0.063g, 0.27mmol) and the mixture was refluxed for 4 hours. Light reddish solution formed was then filtered and at room temperature reddish solution kept for crystallization. Yield, 60%, m. p., 220-223°C. Important IR peaks (KBr, cm^{-1}): $\nu(\text{NH}_2)$ 3451m; $\nu(\text{C}=\text{N})$ 1645s; $\nu(\text{C}=\text{C})$ 1542s; $\delta(\text{NH}_2)$ 1420s; $\nu(\text{C}=\text{Se})$ 702s (selenoamidemoiety). ^1H NMR (CDCl_3 , δ ppm): 8.80 s (1H, C^2H), 7.50 d (1H, C^4H), 7.44 d (1H, C^3H), 7.37 s (1H, N^1H_2), 7.22 s (1H, N^1H_2), 7.15 t (1H, C^5H). ^{13}C NMR (CDCl_3 , δ ppm): 155.7 (C^2), 132.3 (C^5), 130.0 (C^4), 127.8 (C^3), 115.0 (C^2) respectively. Mass spectra m/z: $[\text{Zn}(\text{C}_6\text{H}_7\text{N}_3\text{SSe})_2]^+$: 528 amu (parent ion peak).



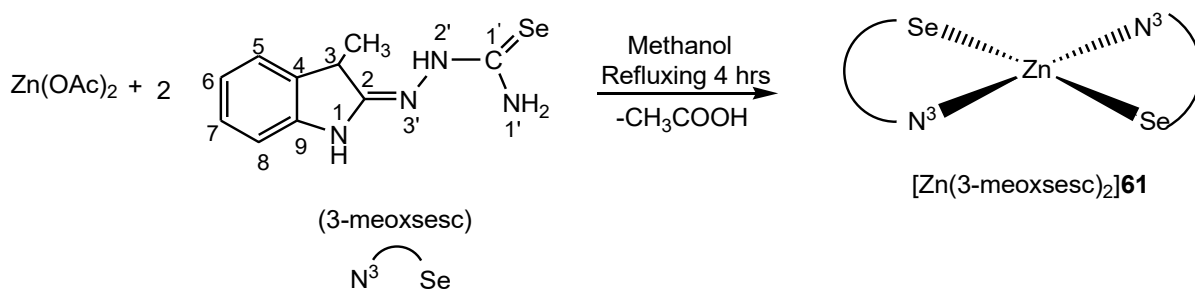
3.6.4 Synthesis of $[\text{Zn}(\text{N-mepysesc})_2]\text{60}$:

Zinc acetate (0.025g, 0.13mmol) was dissolved in 20 ml of methanol with heating. To it was added N-methyl-2-pyrrole selenosemicarbazone (0.062g, 0.27mmol) and the mixture was refluxed for 4 hours. Light reddish solution formed was then filtered and at room temperature reddish solution kept for crystallization. Yield, 60%, m. p., 225-228°C. Important IR peaks (KBr, cm^{-1}): $\nu(\text{NH}_2)$ 3397m, 3248m; $\nu(\text{C}=\text{N})$ 1586s; $\nu(\text{C}=\text{C})$ 1560s; $\delta(\text{NH}_2)$ 1477s; $\nu(\text{C}=\text{Se})$ 734s (selenoamidemoiety). Mass spectra m/z: $[\text{Zn}(\text{C}_7\text{H}_7\text{N}_4\text{Se})_2]^+$: 514 amu (parent ion peak).



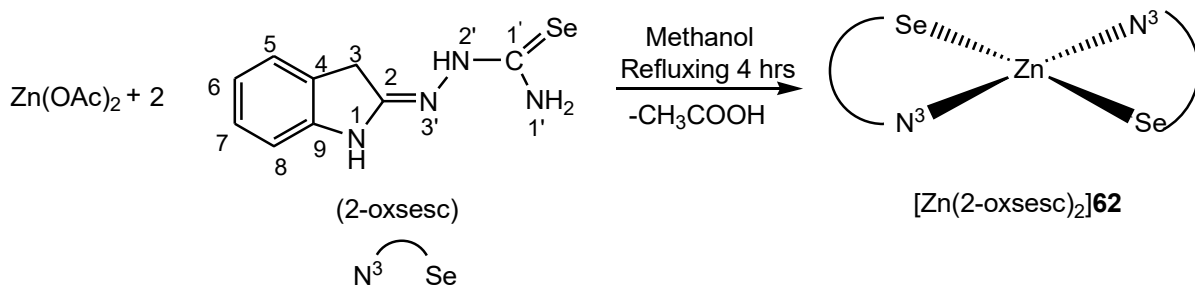
3.6.5 Synthesis of $[\text{Zn}(3\text{-meoxsesc})_2]\text{61}$:

Zinc acetate(0.025g, 0.13mmol) was dissolved in 30 ml of methanol with heating. To it was added 3-methyl-2-oxindole selenosemicarbazone, (0.072g, 0.26mmol) and the mixture was refluxed for 4 hours. Light reddish solution formed was then filtered and at room temperature reddish solution kept for crystallization. Yield, 62%, m. p., 220-223°C. Important IR peaks (KBr, cm^{-1}): $\nu(\text{NH}_2)$ 3417m, 3255m; $\nu(\text{NH})_{\text{ox}}$ 3142w; $\nu(\text{C}=\text{N})$ 1589s; $\nu(\text{C}=\text{C})$ 1512s; $\delta(\text{NH}_2)$ 1499s; $\nu(\text{C}=\text{Se})$ 723s (selenoamidemoiety). Mass spectra m/z: $[\text{Zn}(\text{C}_{10}\text{H}_{11}\text{N}_4\text{Se})_2]^+$: 596 amu (parent ion peak).



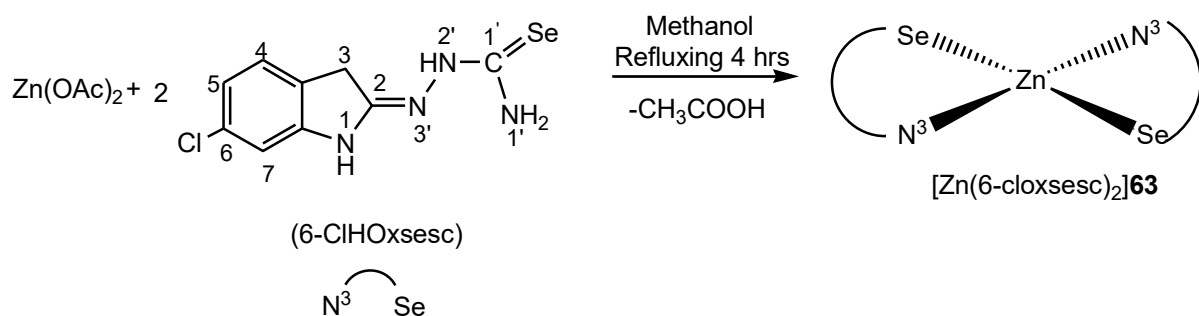
3.6.6 Synthesis of $[\text{Zn}(2\text{-oxsesc})_2]\textbf{62}$:

Zinc acetate (0.025g, 0.13mmol) was dissolved in 30 ml of methanol with heating. To it was added 2-oxindole selenosemicarbazone, (0.068g, 0.27mmol) and the mixture was refluxed for 4 hours. Light reddish solution formed was then filtered and at room temperature reddish solution kept for crystallization. Yield, 62%, m. p., 230-233°C. Important IR peaks (KBr, cm^{-1}): $\nu(\text{NH}_2)$ 3398m, 3242m; $\nu(\text{NH})_{\text{ox}}$ 3147w; $\nu(\text{C}=\text{N})$ 1599s; $\nu(\text{C}=\text{C})$ 1516s; $\delta(\text{NH}_2)$ 1452s; $\nu(\text{C}=\text{Se})$ 761s (selenoamidemoiety). Mass spectra m/z : $[\text{Zn}(\text{C}_9\text{H}_9\text{N}_4\text{Se})_2]^+$: 574 amu (parent ion peak).



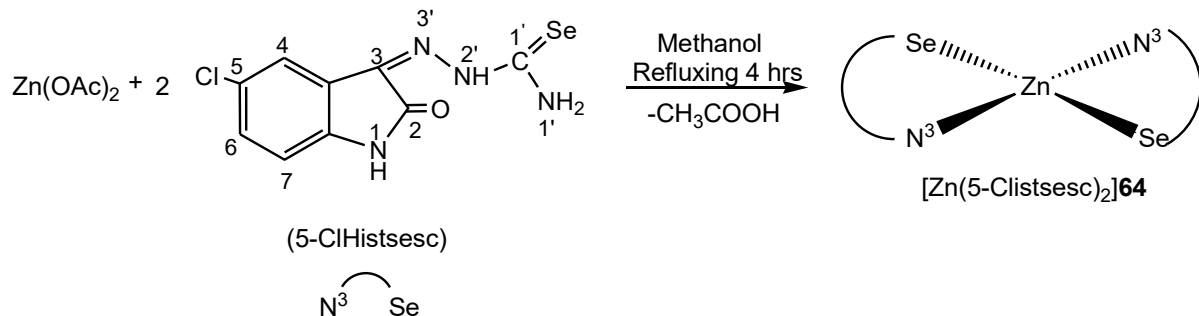
3.6.7 Synthesis of $[\text{Zn}(6\text{-cloxsesc})_2]\textbf{63}$:

Zinc acetate (0.025g, 0.136mmol) was dissolved in 30 ml of methanol with heating. To it was added 6-chloro-2-oxindole selenosemicarbazone, (0.078g, 0.27mmol) and the mixture was refluxed for 4 hours. Light reddish solution formed was then filtered and at room temperature reddish solution kept for crystallization. Yield, 62%, m. p., 228-230°C. Important IR peaks (KBr, cm^{-1}): $\nu(\text{NH}_2)$ 3396m; $\nu(\text{NH})_{\text{ox}}$ 3146w; $\nu(\text{C}=\text{N})$ 1599s; $\nu(\text{C}=\text{C})$ 1514m; $\delta(\text{NH}_2)$ 1498s; $\nu(\text{C}=\text{Se})$ 763s (selenoamidemoiety). ^1H NMR (CDCl_3 , δ ppm): 8.48 s (1H, N^1H_2), 7.15 d (1H, C^7H), 7.03 d (1H, C^4H), 6.92 s (1H, C^5H), 3.54 (cyclic proton ring). ^{13}C NMR (CDCl_3 , δ ppm): 177.1 (C^1), 143.4 (C^5), 133.6 (C^6), 125.5 (C^7), 110.2 (C^8), 35.3 (C^3) respectively.



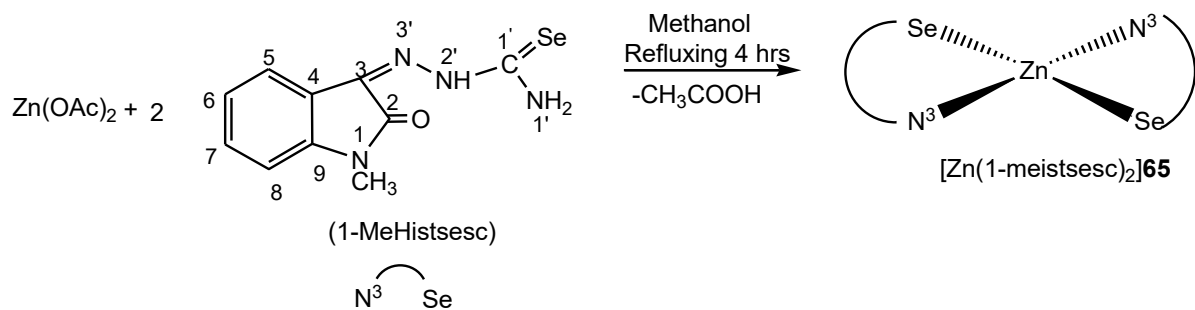
3.6.8 Synthesis of $[\text{Zn}(5\text{-clistsesc})_2]\textbf{64}$:

Zinc acetate (0.025g, 0.13mmol) was dissolved in 30 ml of methanol with heating. To it was added 5-chloro isatin selenosemicarbazone, (0.072g, 0.27mmol) and the mixture was refluxed for 4 hours. Light reddish solution formed was then filtered and at room temperature reddish solution kept for crystallization. Yield, 62%, m. p., 225-228°C. Important IR peaks (KBr, cm^{-1}): $\nu(\text{NH}_2)$ 3417m, 3254m; $\nu(\text{NH})_{\text{ist}}$ 3144w; $\nu(\text{C=O})$ 1668s; $\nu(\text{C=N})$ 1589s; $\nu(\text{C=C})$ 1516m; $\delta(\text{NH}_2)$ 1448s; $\nu(\text{C=Se})$ 725s (selenoamidemoiety). Mass spectra m/z: $[\text{Zn}(\text{C}_9\text{H}_5\text{N}_4\text{OClSe})_2]^+$: 662 amu (parent ion peak).



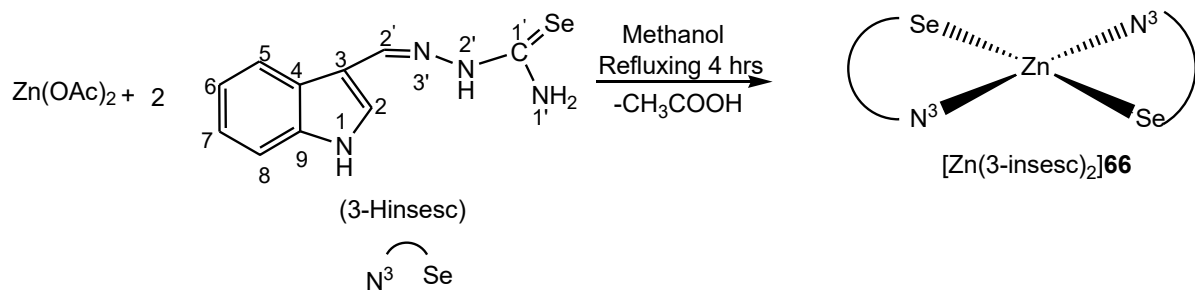
3.6.9 Synthesis of $[\text{Zn}(1\text{-meistsesc})_2]\textbf{65}$:

Zinc acetate (0.025g, 0.136mmol) was dissolved in 30 ml of methanol with heating. To it was added 1-methyl isatin selenosemicarbazone, (0.076g, 0.27mmol) and the mixture was refluxed for 4 hours. Light reddish solution formed was then filtered and at room temperature reddish solution kept for crystallization. Yield, 60%, m. p., 230-235°C. Important IR peaks (KBr, cm^{-1}): $\nu(\text{NH}_2)$ 3281; $\nu(\text{NH})_{\text{ist}}$ 3161w; $\nu(\text{C=N})$ 1683s; $\nu(\text{C=C})$ 1566m; $\delta(\text{NH}_2)$ 1404s; $\nu(\text{C=Se})$ 740s (selenoamidemoiety). Mass spectra m/z: $[\text{Zn}(\text{C}_{10}\text{H}_9\text{N}_4\text{OSe})_2]^+$: 624 amu (parent ion peak).



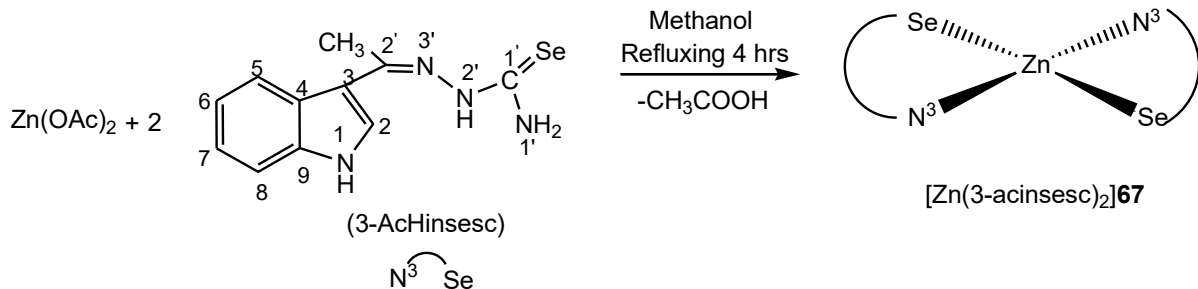
3.6.10 Synthesis of $[\text{Zn}(3\text{-insesc})_2]66$:

Zinc acetate (0.025g, 0.136mmol) was dissolved in 30 ml of methanol with heating. To it was added 3-indole selenosemicarbazone, (0.072g, 0.27mmol) and the mixture was refluxed for 4 hours. Light reddish solution formed was then filtered and at room temperature reddish solution kept for crystallization. Yield, 62%, m. p., 228-230°C. Important IR peaks (KBr, cm^{-1}): $\nu(\text{NH}_2)$ 3352m, 3234m; $\nu(\text{NH})_{\text{ind}}$ 3126w; $\nu(\text{C}=\text{N})$ 1595s; $\nu(\text{C}=\text{C})$ 1533m; $\delta(\text{NH}_2)$ 1498s; $\nu(\text{C}=\text{Se})$ 742s (selenoamidemoiety). ^1H NMR (CDCl_3 , δ ppm): 8.86 s (1H, C^2H), 8.51 d (1H, C^5H), 8.35 d (1H, C^8H), 7.45-7.36 m (2H, $\text{C}^{6,7}\text{H}$), 7.86 s (1H, N^1H_2). Mass spectra m/z: $[\text{Zn}(\text{C}_{10}\text{H}_9\text{N}_4\text{Se})_2]^+$: 591 amu (parent ion peak).



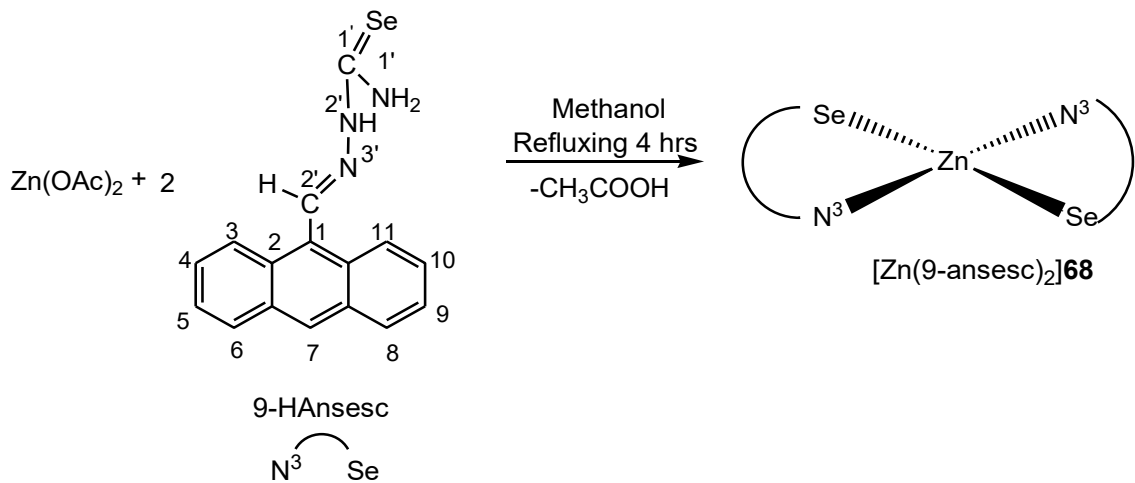
3.6.11 Synthesis of $[\text{Zn}(3\text{-acinsesc})_2]67$:

Zinc acetate (0.025g, 0.13mmol) was dissolved in 30 ml of methanol with heating. To it was added 3-acetyl indole selenosemicarbazone, (0.076g, 0.27mmol) and the mixture was refluxed for 4 hours. Light reddish solution formed was then filtered and at room temperature reddish solution kept for crystallization. Yield, 62%, m. p., 230-232°C. Important IR peaks (KBr, cm^{-1}): $\nu(\text{NH})_{\text{ind}}$ 3155; $\nu(\text{C}=\text{N})$ 1608s; $\nu(\text{C}=\text{C})$ 1572m; $\delta(\text{NH}_2)$ 1418s; $\nu(\text{C}=\text{Se})$ 750s (selenoamidemoiety). Mass spectra m/z: $[\text{Zn}(\text{C}_{11}\text{H}_{12}\text{N}_4\text{Se})_2]^+$: 621 amu (parent ion peak).



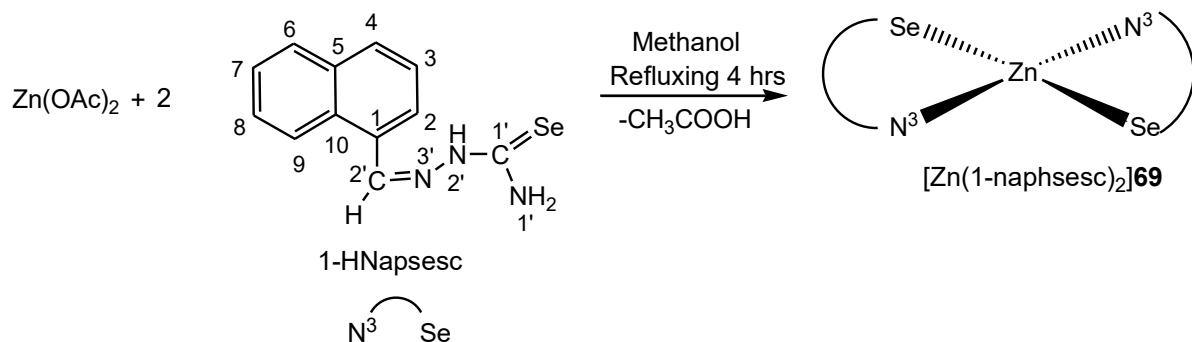
3.6.12 Synthesis of [Zn(9-ansesc)2]68:

Zinc acetate(0.025g, 0.136mmol) was dissolved in 30 ml of methanol with heating. To it was added 9-anthracene selenosemicarbazone, (0.056g, 0.27mmol) and the mixture was refluxed for 4 hours. Light reddish solution formed was then filtered and at room temperature reddish solution kept for crystallization. Yield, 64%, m. p., 230-233°C. Important IR peaks (KBr, cm⁻¹): $\nu(\text{NH}_2)$ 3317m; $\nu(\text{C}=\text{N})$ 1566s; $\nu(\text{C}=\text{C})$ 1496m; $\delta(\text{NH}_2)$ 1400s; $\nu(\text{C}=\text{Se})$ 796s (selenoamidemoiety). ¹H NMR (CDCl_3 , δ ppm): 9.84 s (1H, N^1H_2), 9.26 s (1H, N^1H_2), 9.10 s (1H, $\text{C}^{2'}\text{H}$), 8.10 m (2H, $\text{C}^{3,11}\text{H}$), 8.01m (2H, $\text{C}^{6,8}\text{H}$), 7.86 t (2H, $\text{C}^{5,9}\text{H}$), 7.67 t (2H, $\text{C}^{4,10}\text{H}$). Mass spectra m/z: $[\text{Zn}(\text{C}_{16}\text{H}_{9}\text{N}_3\text{Se})_2]^+$: 707 amu (parent ion peak).



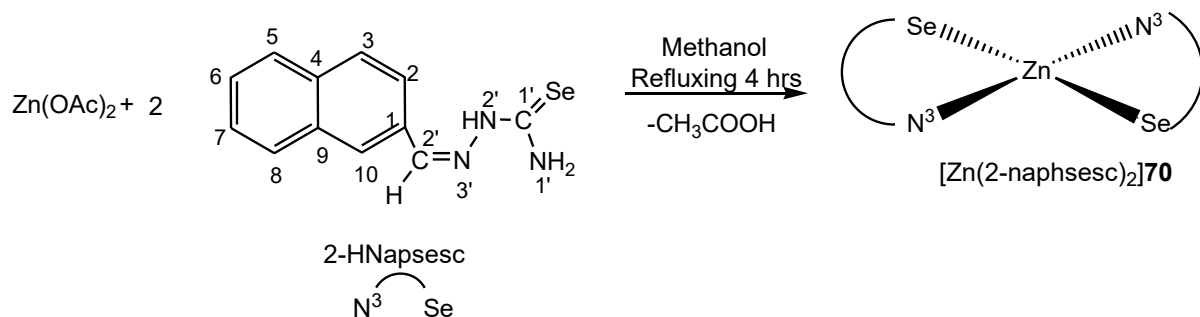
3.6.13 Synthesis of [Zn(1-naphsesc)2]69: Zinc acetate(0.025g, 0.136mmol) was dissolved in 30 ml of methanol with heating. To it was added 1-naphthaldehydeselenosemicarbazone, (0.074g, 0.269mmol) and the mixture was refluxed for 4 hours. Light brownish solution formed was then filtered and at room temperature brownish solution kept for crystallization. Yield, 62%, m. p., 215-219°C. Important IR peaks (KBr, cm⁻¹): $\nu(\text{NH}_2)$ 3346m, 3228m; $\nu(\text{C}=\text{N})$ 1593s; $\nu(\text{C}=\text{C})$ 1527m; $\delta(\text{NH}_2)$ 1440s; $\nu(\text{C}=\text{Se})$ 736s (selenoamidemoiety). ¹H NMR (CDCl_3 , δ ppm): 9.51 s (1H, $\text{C}^{2'}\text{H}$), 8.98 d (1H, C^4H), 8.16 d (1H, C^9H), 8.01 d (1H, C^4H),

7.97 d (1H, C⁶H), 7.70 m (1H, C³H), 7.62 m (1H, C⁸H). ¹³C NMR (CDCl₃, δppm): 162.0 (C^{1'}), 133.9 (C^{2'}), 131.6-124.2 (ring carbon). Mass spectra m/z: [Zn(C₁₂H₈N₃Se)₂]⁺: 610 amu (parent ion peak).



3.6.14 Synthesis of [Zn(2-naphsesc)2]70:

Zinc acetate(0.025g, 0.136mmol) was dissolved in 30 ml of ethanol with heating. To it was added 2-naphthaldehyde selenosemicarbazone, (0.074g, 0.26mmol) and the mixture was refluxed for 4 hours. Light reddish solution formed was then filtered and at room temperature reddish solution kept for crystallization. Yield, 63%, m. p., 240-242°C. Important IR peaks (KBr, cm⁻¹): ν(NH₂) 3348m, 3230m; ν(C=N) 1568s; ν(C=C) 1535m; δ(NH₂) 1400s; ν(C=Se) 742s (selenoamidemoiety). ¹H NMR (δ, ppm; d⁶-dmso and CDCl₃): 10.1 s (1H, C^{2'}H), 8.91 s (1H, N^{1'}H₂), 8.18-7.29 (ring proton). Mass spectra m/z:[Zn(C₁₂H₉N₃Se)₂]⁺: 611 amu (parent ion peak).

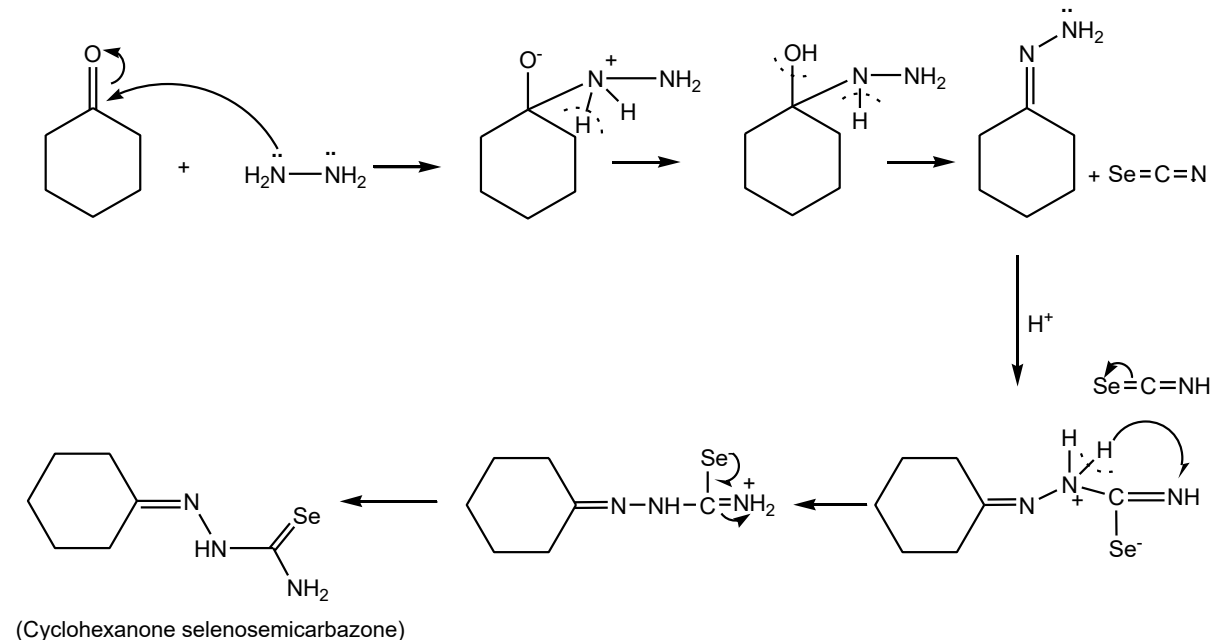


CHAPTER 4
RESULT AND DISCUSSION
(SELENOSEMICARBAZONES)

4.1 Discussion on Synthesis of Ligands

Reaction of cyclohexanone with KSeCN and hydrazine hydrate in acidic medium results in the formation of cyclohexanone selenosemicarbazone.

The mechanism of formation of cyclohexanone selenosemicarbazone is given in Scheme 4.1



Scheme 4.1

Cyclohexanone selenosemicarbazone is reacted with aldehyde or ketones to for other selenosemicarbazones. The synthesized selenosemicarbazones along with their structures and numbering scheme are listed in table 4.1

Table 4.1 List of synthesized selenosemicarbazones ($\mathbf{H^1L - H^{14}L}$)

Sr. No.	Name of Synthesized Selenosemicarbazone Compound and Ligands	Structure of Synthesized Selenosemicarbazone Compound and Ligands
1.	Cyclohexanone selenosemicarbazone (Hcysesc, $\mathbf{H^1L}$)	
2.	2-furfural selenosemicarbazone (2-Hfursesc, $\mathbf{H^2L}$)	
3.	2-thiophene selenosemicarbazone (2-Hthiosesc, $\mathbf{H^3L}$)	
4.	N-methyl-2-pyrrole selenosemicarbazone (N-MeHPysesc, $\mathbf{H^4L}$)	
5.	3-methyl-2-oxindole selenosemicarbazone (3-MeHOxsesc, $\mathbf{H^5L}$)	
6.	2-oxindole selenosemicarbazone (2-HOxsesc, $\mathbf{H^6L}$)	

7.	6-chloro-2-oxindole selenosemicarbazone (6-ClHOxsesc, H⁷L)	
8.	5-chloro isatin selenosemicarbazone (5-ClHIstsesc, H⁸L)	
9.	1-methyl isatin selenosemicarbazone (1-MeHIstsesc, H⁹L)	
10.	indole-3-selenosemicarbazone (3-HIndsesesc, H¹⁰L)	
11.	3-acetyl indole selenosemicarbazone (3-AcHIndsesesc, H¹¹L)	
12.	9-anthraldehyde selenosemicarbazone (9-HAnsesc, H¹²L)	

13.	1-Naphthaldehyde selenosemicarbazone (1-HNapsesc, H¹³L)	
14.	2-Naphthaldehyde selenosemicarbazone (2-HNapsesc, H¹⁴L)	

4.2 IR Spectroscopy:

Important IR peaks of selenosemicarbazones are given in table 4.2 and IR spectra are given in figures 4.2.1-4.2.14. The $\nu(-\text{NH}-)$ band can be divided broadly in two categories (i) bands in the range 3417-3219cm⁻¹ for symmetric and asymmetric stretching, (ii) bands due to amide group $\nu(-\text{NH}-)$ of selenosemicarbazone in the range 3157-3095 cm⁻¹. The stretching bond of NH group of isatin ring and indole ring gets merged with amide group. The characteristic C=Se in ligands **H¹L - H¹⁴L** appeared in the range, 898-812 cm⁻¹. Apperence of $\nu(\text{C}=\text{N})$ band in the range, 1639-1591cm⁻¹ supports formation of condensation product (selenosemicarbazones). The results are in line with the previous reported results in literature [61-80].

Table 4.2 Important IR peaks of selenosemicarbazones (**H¹L - H¹⁴L**)

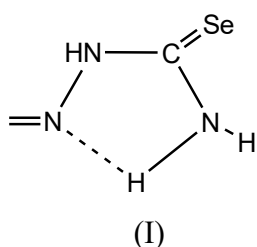
Synthesized Selenosemicarbazones Ligands	$\nu(\text{N}^1\text{H}_2)$	$\nu(-\text{N}^2\text{H}-)$	$\nu(\text{C}=\text{N}), \nu(\text{C}=\text{C}), \delta (\text{NH}_2)$	$\nu(\text{C}=\text{Se})$
Cyclohexanone selenosemicarbazone(Hcysescc, H¹L)	3362m, 3225m	3157w	1591s, 1489m, 1454s	856s
2-furfural selenosemicarbazone (2-Hfurasesc, H²L)	3379m, 3340m	3142w	1600s, 1579m, 1464s	812s
2-thiophene selenosemicarbazone (2-Hthiosesc, H³L)	3389m, 3221m	3095w	1599s, 1527m, 1415s	844s
N-methyl-2-pyrrole selenosemicarbazone	3412m, 3223m	3110w	1633s, 1562m, 1496s	854s

(N-MeHPysesc, H⁴L)				
3-methyl-2-oxindole selenosemicarbazone (3-MeHOxsesc, H⁵L)	3358m, 3248m	3157w	1591s, 1489m, 1425s	854s
2-oxindole selenosemicarbazone (2-HOxsesc, H⁶L)	3362m, 3225m	3157w	1591s, 1489m, 1454s	856s
6-chloro-2-oxindole selenosemicarbazone (6-ClHOxsesc, H⁷L)	3417m, 3255m	3142w	1589s, 1512m, 1499s	879s
5-chloroisatin selenosemicarbazone (5-ClHIstsesc, H⁸L)	3219m	3110w	1618s, 1559m, 1447s	885s
1-methylisatin selenosemicarbazone (1-MeHIstsesc, H⁹L)	3408m, 3228m	3128w	1604s, 1492m, 1415s	889s
3-indole selenosemicarbazone (3-HIndsesc, H¹⁰L)	3356m, 3246m	3153w	1591s, 1487m, 1450s	898s
3-acetylindole selenosemicarbazone (3-AcHIndsesc, H¹¹L)	3290m	3142w	1624s, 1502m, 1406s	877s
9-anthracene selenosemicarbazone (9-HAnsesc, H¹²L)	3385m, 3248m	3151w	1639s, 1518m, 1402s	887s
1-naphthaldehyde selenosemicarbazone (1-HNapsesc, H¹³L)	3400m	3147w	1599s, 1516m, 1452s	871s
2-naphthaldehyde selenosemicarbazone (2-HNapsesc, H¹⁴L)	3352m	3124w	1597s, 1533m, 1446s	856s

4.3 NMR Spectroscopy:

4.3.1 ^1H NMR Spectroscopy:

For establishing the structure of ligands using spectroscopic techniques, these selenosemicarbazones are divided into the following three types. Important NMR signals of selenosemicarbazones are given in Table 4.3 and ^1H NMR spectra of synthesized ligands are given in figures 4.3.1.1-4.3.1.14. For the discussion on ^1H NMR signal, selenosemiracbazones are splitup into three types: i) Cyclohexanone Selenosemicarbazone (H^1L); ii) Heterocyclic Selenosemicarbazones ($\text{H}^2\text{L}-\text{H}^4\text{L}$); iii) Fused ring Selenosemicarbazones ($\text{H}^5\text{L}-\text{H}^{14}\text{L}$). Signal due to $\text{N}^2\text{'H}$ proton signal of cyclohexanone selenosemicarbazone (H^1L) appeared at δ 9.23 ppm. The amino protons ($\text{N}^1\text{'H}_2$) gave two broad singlet at δ 7.65 ppm and δ 7.15 ppm indicating that two protons are non-equivalent probably due to the H-bonding between one at the amino hydrogen and azomethine nitrogen (I). Cyclic ring protons signal of cyclohexanone selenosemicarbazone (H^1L) appeared in the range δ 2.32- δ 1.54 ppm.



In selenosemicarbazone, containing five membered heterocyclic ($\text{H}^2\text{L}-\text{H}^4\text{L}$), $\text{N}^2\text{'H}$ proton signal appeared at the range δ 10.95- δ 9.64 ppm. The amino protons appeared as two broad singlets (Table 4.3.1). The $\text{C}^2\text{'H}$ proton signal in these ligand appeared in the range δ 10.00- δ 8.10 ppm. This signal cannot be obtained for N-methyl-2-pyrrole selenosemicarbazone (H^4L) probably due to its poor solubility. The amino protons ($\text{N}^1\text{'H}_2$) gave two broad singlet at the range δ 7.58- δ 6.20 ppm indicating that two protons are non-equivalent probably due to the H-bonding between one at the amino hydrogen and azomethine nitrogen (I). Other ring protons appeared in the range, δ 7.89- δ 6.62 ppm. The methyl protons of N-methyl 2- pyrrole ring appeared as singlet at δ 3.87 ppm.

In case of fused ring selenosemicarbazones ligands $\text{H}^{10}\text{L}-\text{H}^{14}\text{L}$, $\text{N}^2\text{'H}$ proton signal appeared at the range δ 11.6- δ 9.51 ppm. The $\text{C}^2\text{'H}$ proton signal in these ligand appeared in the range δ 9.02- δ 7.85 ppm. The amino protons ($\text{N}^1\text{'H}_2$) gave two broad singlet at δ 7.97- δ 6.63 ppm indicating that two protons are non-equivalent probably due to the H-bonding

between one at the amino hydrogen and azomethine nitrogen (I) (Table 4.3.1). Due to low solubility, two broad singlet of the amino protons (N^1H_2) not appeared in case of selenosemicarbazones ligand H^{11}L . Other ring protons signal appeared in the range, δ 8.73- δ 7.28 ppm. The methyl protons of 3-acetyl indole ring appeared as singlet at δ 2.58 ppm. The ^1H NMR data of selenosemicarbazones is in well agreement with literature [65-80].

Table 4.3.1 ^1H NMR signals of synthesized selenosemicarbazones ligands

Synthesized Compound and Selenosemicarbazones Ligands	(1H, N^2H)	(1H, C^2H)	(1H, N^1H_2)	(Ring protons)
Cyclohexanone selenosemicarbazone (Hcysesc, H¹L)	9.23 s	-	7.65 s, 7.15 s	2.32-1.54 m (10H, cyclic proton ring)
2-furfural selenosemicarbazone (2-Hfurdesc, H²L)	10.95 s	10.00 s	6.60 s, 6.54 s	7.87 d (1H, C^5H), 7.74 d (1H, C^3H), 7.58 t (1H, C^4H)
2-thiophene selenosemicarbazone (2-Hthiosesc, H³L)	9.64 s	8.10 s	7.58 s, 6.71 s	7.47 m (1H, C^4H), 7.37 d (1H, C^3H), 7.12 d (1H, C^5H)
N-methyl-2-pyrrole selenosemicarbazone (N-MeHPysesc, H⁴L)	10.05 s	-	6.21 s, 6.20 s	7.98 d (1H, C^5H), 6.82 t (1H, C^4H), 6.62 d (1H, C^3H), 3.87 (CH_3)
3-methyl-2-oxindole selenosemicarbazone (3-MeHOxsesc, H⁵L)	9.16 s	-	-	7.24-6.95 m (4 H, $\text{C}^{5,6,7,8}\text{H}$), 3.51 (3H, CH_3), 1.54 s (cyclic proton ring)
2-oxindole selenosemicarbazone (2-HOxsesc, H⁶L)	9.03 s	-	5.54 s, 5.46 s	8.34-6.90 m (4H, $\text{C}^{5,6,7,8}\text{H}$), 3.56 (cyclic proton ring)
6-chloro-2-oxindole selenosemicarbazone (6-ClHOxsesc, H⁷L)	9.51 s	-	4.89 s, 4.26 s	7.13 d (1H, C^5H), 6.99 d (1H, C^4H), 6.92 s (1H, C^7H)

5-chloroisatin selenosemicarbazone (5-ClHIsesc, H⁸L)	11.21 s	-	8.80 s, 8.56 s	7.49 d (1H, C ⁴ H), 7.21 d (1H, C ⁷ H), 6.86 m (2H, C ^{5,6} H)
1-methylisatin selenosemicarbazone (1-MeHIsesc, H⁹L)	13.1 s	-	8.01 s, 7.60s	7.61-6.90 m (4H, C ^{5,6,7,8} H), 3.29 (CH ₃)
3-indole selenosemicarbazone (3-HIndesc, H¹⁰L)	10.0 s	7.85 s	7.76 s, 7.56 s	8.30-7.28 (5H, Cyclic ring proton)
3-acetylindole selenosemicarbazone (3-AcHIndesc, H¹¹L)	-	-	7.65 s, 6.63 s	8.42 d (1H, C ⁷ H), 7.90 d (1H, C ⁶ H), 7.46-7.32 m (2H, C ^{5,8} H), 7.29 s (1H, C ² H), 2.58 s (3H, CH ₃)
9-anthracene selenosemicarbazone (9-HAnsesc, H¹²L)	11.5 s	9.02 s	-	8.73 d (2H, C ^{3,11} H), 8.08 d (2H, C ^{6,8} H), 7.73 t (2H, C ^{5,9} H), 7.60 t (2H, C ^{4,10} H), 7.29 s (1H, C ⁷ H)
1-naphthaldehyde selenosemicarbazone (1-HNapsesc, H¹³L)	9.51 s	9.00 s	7.97 s	8.17 d (1H, C ⁹ H), 8.02 d (1H, C ⁴ H), 7.95 d (1H, C ⁶ H), 7.62 m (2H, C ^{3,7} H), 7.29 s (1H, C ⁸ H)
2-naphthaldehyde selenosemicarbazone (2-HNapsesc, H¹⁴L)	10.1 s	8.38 s	7.70 s	8.05-7.29 m (ring proton)

In ketone based selenosemicarbazones **H⁵L-H⁹L**, N²H proton signal appeared at the range δ 13.1-δ 9.16 ppm. Two broad singlets for amino protons appeared at δ 8.80-δ 4.26 ppm indicating that two protons are non-equivalent probably due to the H-bonding between one at the amino hydrogen and azomethine nitrogen (I) (Table 4.3.1). Due to low solubility, two broad singlet of the amino protons (N¹H₂) not appeared in case of selenosemicarbazones ligand **H⁵L**. Ring protons signal appeared in the range, δ 8.34-δ 6.83 ppm. The methyl protons of 3-methyl-2-oxindole and 1-methyl isatin selenosemicarbazone ring appeared as singlet at δ 3.51 ppm and δ 3.29 ppm respectively. Appearance of all the protons present in selenosemicarbazones confirmed their formation.

4.3.2 ^{13}C NMR Spectroscopy

Important signals in ^{13}C NMR spectra of selenosemicarbazones are given in Table 4.3.2 and spectra are given in figure 4.3.2.1-4.3.2.14. C^1 ' carbon signal of H^1L appeared at δ 175.6 ppm, whereas the cyclic carbons signal appeared in the range, δ 35.4- δ 25.3 ppm. The C^1 ' signal of N-methyl-2-pyrrole selenosemicarbazone (H^4L) appeared at δ 173.4 ppm whereas same signal could not be detected in H^2L – H^3L due to low solubility of these ligands. The C^2 ' signal of heterocyclic selenosemicarbazones appeared in the range, δ 155.8- δ 138.3 ppm. The ring carbons signal appeared in the range, δ 133.9- δ 109.3 ppm. Methyl carbon of N-methyl-2-pyrrole selenosemicarbazone appeared as singlet at δ 36.8 ppm.

In case of fused ring selenosemicarbazones ligands H^{10}L - H^{14}L , C^1 ' and C^2 ' signal appeared in the range, δ 193.6- δ 162.1 ppm and δ 158.2- δ 134.1 ppm respectively. Other ring carbons signal appeared at the range between δ 134.5- δ 112.3 ppm and methyl group showed a signal at δ 35.4 ppm in case of 3-acetylindole selenosemicarbazone (3-AcHIndesc, H^{11}L). In ketone based selenosemicarbazones H^5L – H^9L , C^1 ' carbon signal appeared in the range δ 181.6- δ 163.1 ppm. Other ring carbons signal appeared in the range, δ 161.0- δ 109.3 ppm. The methyl carbons of 3-methyl-2-oxindole and 1-methyl isatin selenosemicarbazone ring appeared as singlet at δ 41.1 ppm and δ 25.8 ppm respectively. Appearance of ^{13}C signal due to all the carbon atoms present in the selenosemicrabaones confirms its formation.

Table 4.3.2 Important ^{13}C signal of selenosemicarbazones (H^1L - H^{14}L)

Synthesised Ligands	(C^1)	(C^2)	(Ring carbons)
Cyclohexanone selenosemicarbazone (Hcysesc, H¹L)	175.6	-	35.4-25.3(cyclic carbon ring)
2-furfural selenosemicarbazone (2-Hfursesc, H²L)	-	145.2	133.9 (C^5), 127.5 (C^4), 117.3 (C^3), 112.3 (C^2).
2-thiophene selenosemicarbazone (2-Hthiosesc, H³L)	-	155.8	132.4 (C^5), 130.0 (C^4), 127.8 (C^3), 127.3 (C^2)
N-methyl-2-pyrrole selenosemicarbazone	173.4	138.3	129.2 (C^4), 125.8 (C^5), 117.9 (C^3), 109.8 (C^2), 36.8 (CH_3)

(N-MeHPysesc, H⁴L)			
3-methyl-2-oxindole selenosemicarbazone (3-MeHOxsesc, H⁵L)	181.6	-	141.3 (C ⁵), 131.2 (C ⁶), 127.8 (C ⁷), 123.7 (C ⁸), 109.3 (C ⁹), 41.1 (CH ₃), 15.2 (cyclic carbon ring).
2-oxindole selenosemicarbazone (2-HOxsesc, H⁶L)	177.4	-	142.3 (C ⁵), 127.9 (C ⁶), 124.6 (C ⁷), 122.3 (C ⁸), 109.7 (C ⁹), 36.1 (cyclic carbon ring).
6-chloro-2-oxindole selenosemicarbazone (6-ClHOxsesc, H⁷L)	177.9	-	143.6 (C ⁵), 133.1 (C ⁶), 125.3 (C ⁷), 123.4 (C ⁸), 110.7 (C ⁹), 58.2 (C ⁴), 35.3 (C ³)
5-chloroisatin selenosemicarbazone (5-ClHIstsesc, H⁸L)	163.1	-	131.0 (C ⁵), 129.8 (C ⁶), 125.2 (C ⁷), 119.5 (C ⁴), 42.1(C ³), 34.9 (C ²).
1-methylisatin selenosemicarbazone (1-MeHIstsesc, H⁹L)	178.7	-	161.0 (C ⁵), 144.1 (C ⁶), 132.0 (C ⁸), 129.2 (C ⁷), 123.5 (C ⁹), 121.1 (C ³), 119.1 (C ²), 109.3 (C ⁴), 25.8(CH ₃), 20.4(cyclic ring).
3-indole selenosemicarbazone (3-HIndsesc, H¹⁰L)	-	145.2	133.9 (C ⁶), 127.5 (C ⁵), 117.3 (C ⁴), 112.3 (C ³).
3-acetylindole selenosemicarbazone (3-AcHIndsesc, H¹¹L)	193.6	158.2	131.5 (C ⁶), 123.7 (C ⁵), 122.6 (C ⁷), 118.6 (C ⁸), 111.3 (C ⁴), 35.4 (CH ₃), 26.9 (C ³)
9-anthracene selenosemicarbazone (9-HAnsesc, H¹²L)	193.0	135.0	132.4-122.7 (ring carbon), 114.0 (C ⁸)
1-naphthaldehyde selenosemicarbazone (1-HNapsesc, H¹³L)	162.1	134.1	131.8-124.9 (ring carbon), 115.0 (C ⁵)
2-naphthaldehyde selenosemicarbazone (2-HNapsesc, H¹⁴L)	192.2	136.4	134.5-122.8 (ring carbon), 115.0 (C ⁵)

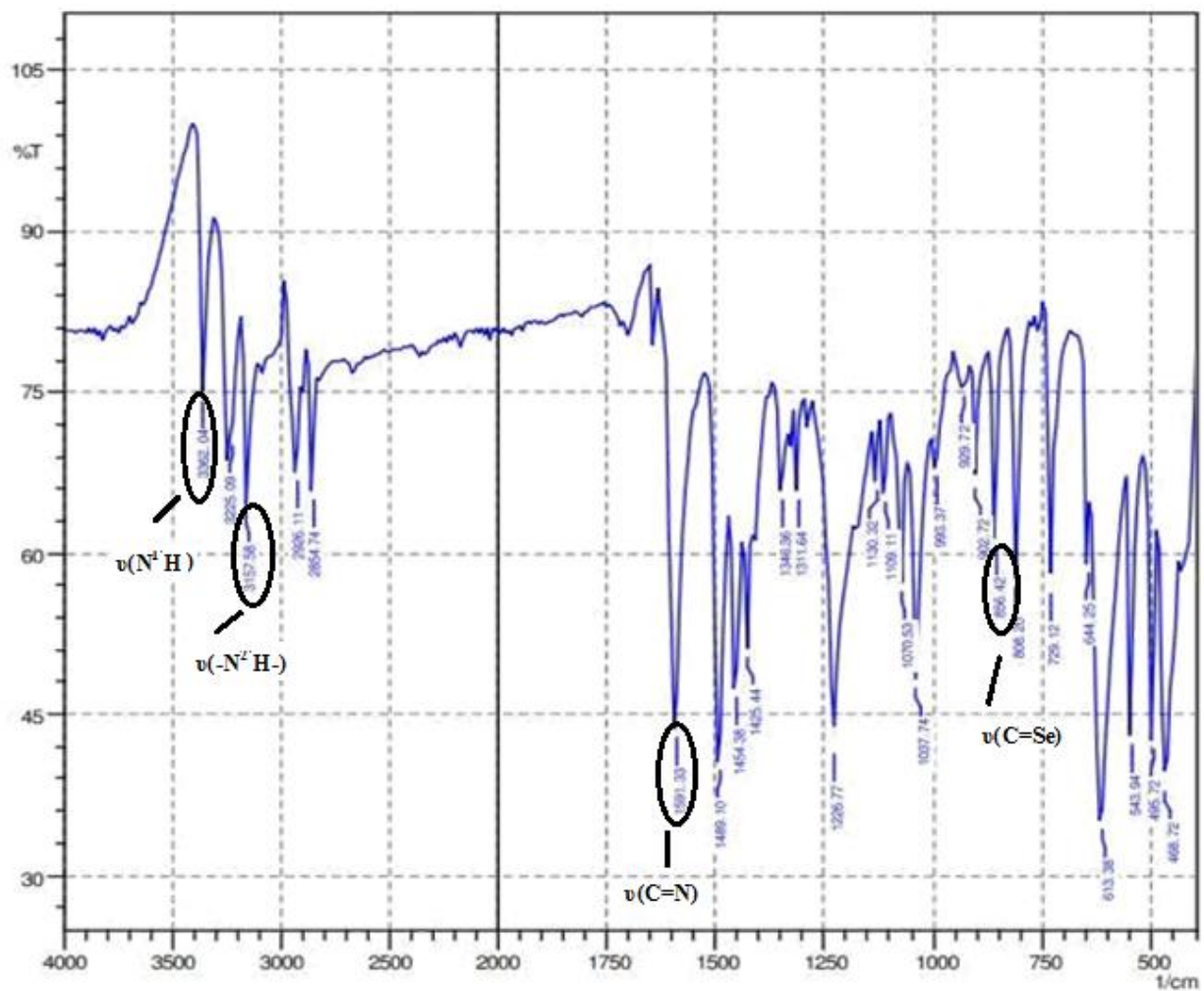


Figure 4.2.1 IR spectrum of cyclohexanone selenosemicarbazone(H^1L)

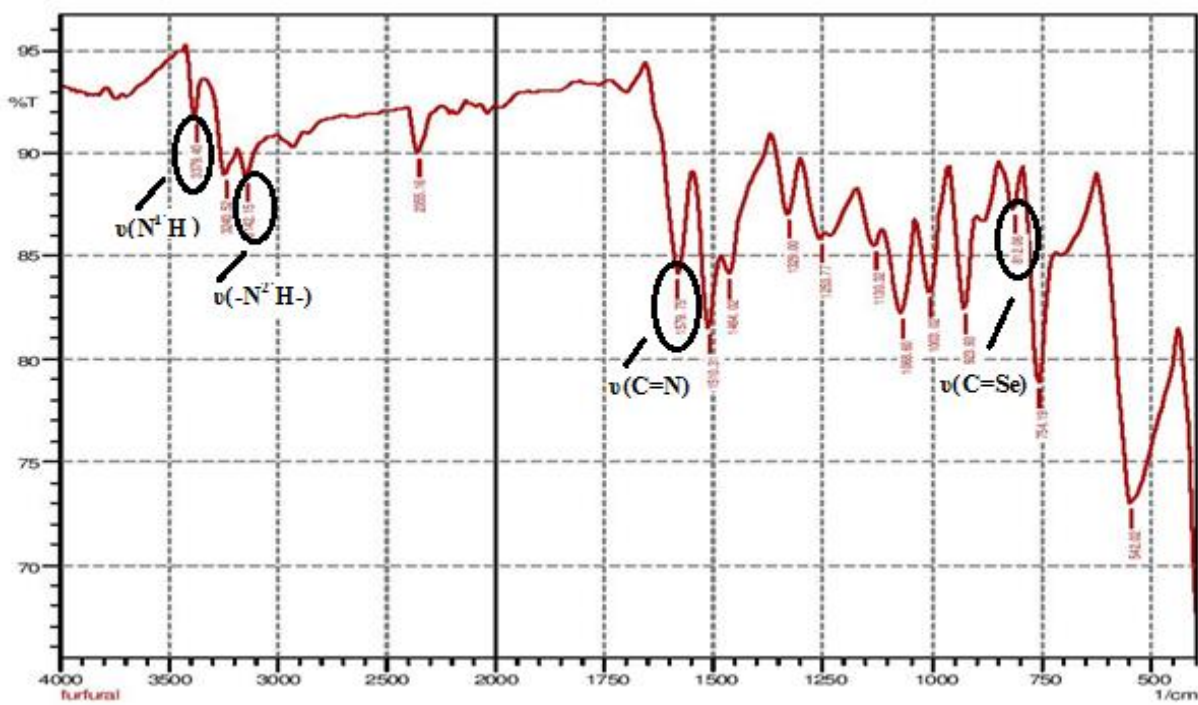


Figure 4.2.2 IR spectrum of 2-furfural selenosemicarbazone(H^2L)

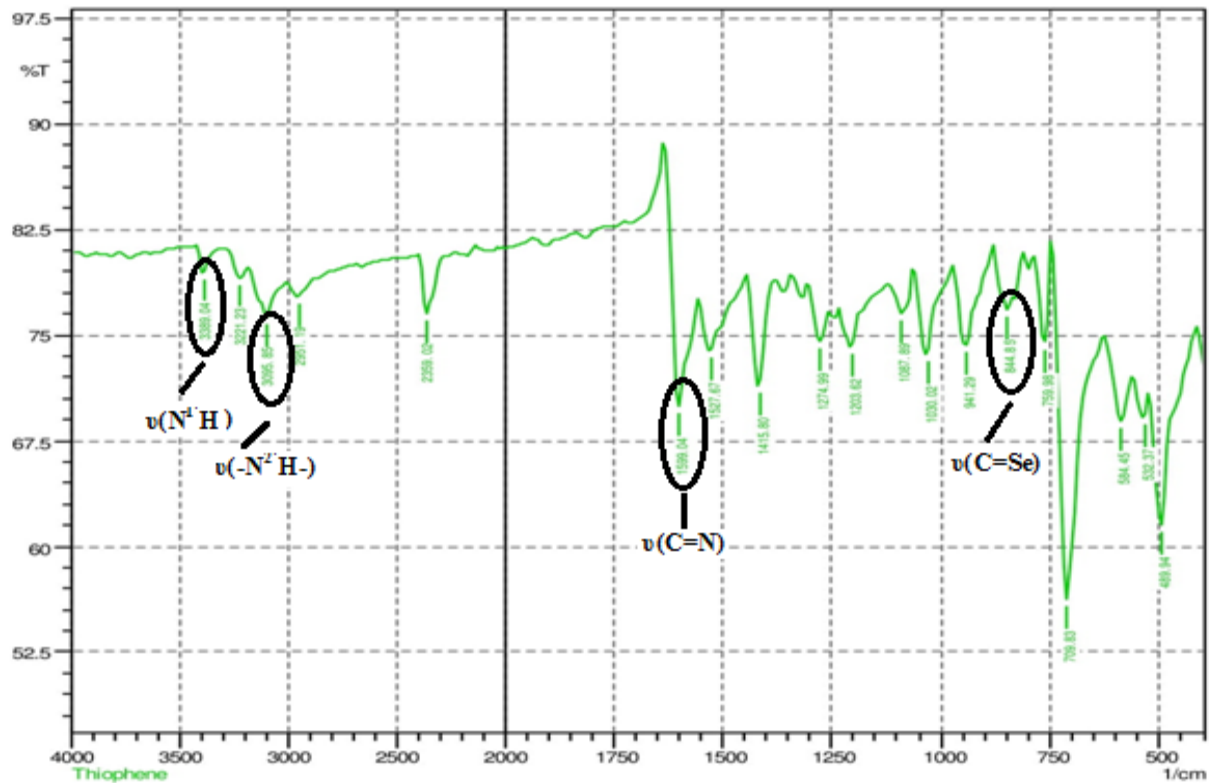


Figure 4.2.3 IR spectrum of 2-thiophene selenosemicarbazone(H^3L)

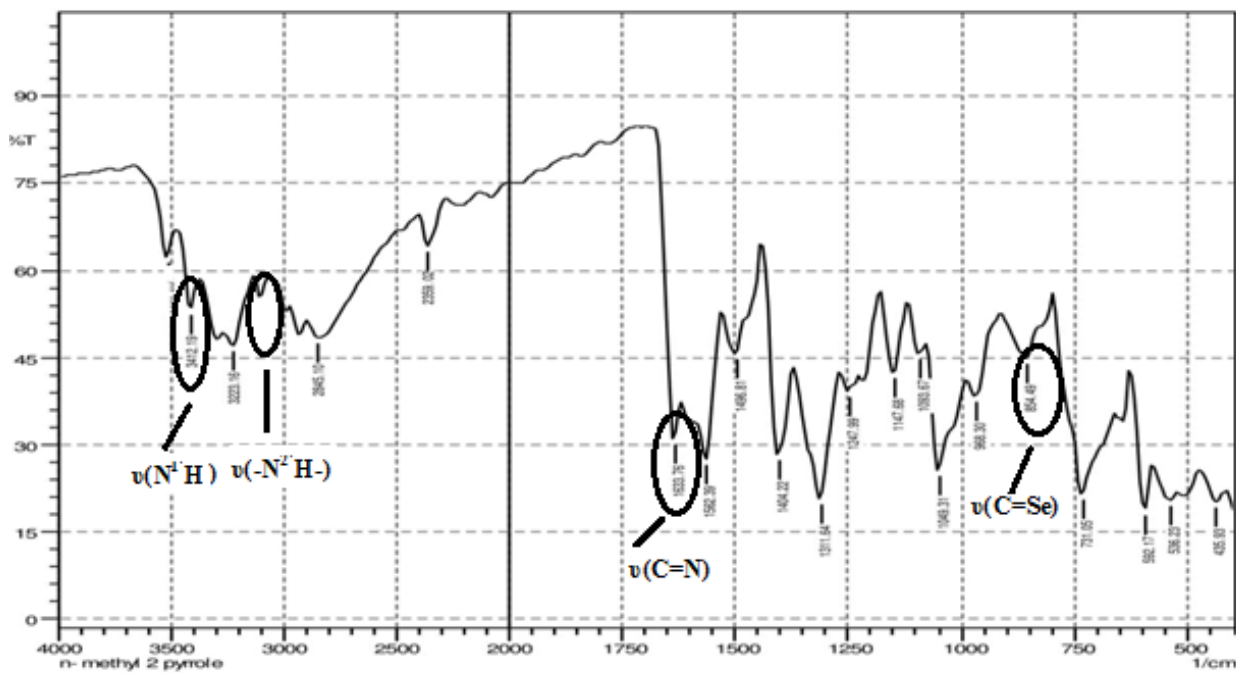


Figure 4.2.4 IR spectrum of N-methyl-2-pyrrole selenosemicarbazone(**H⁴L**)

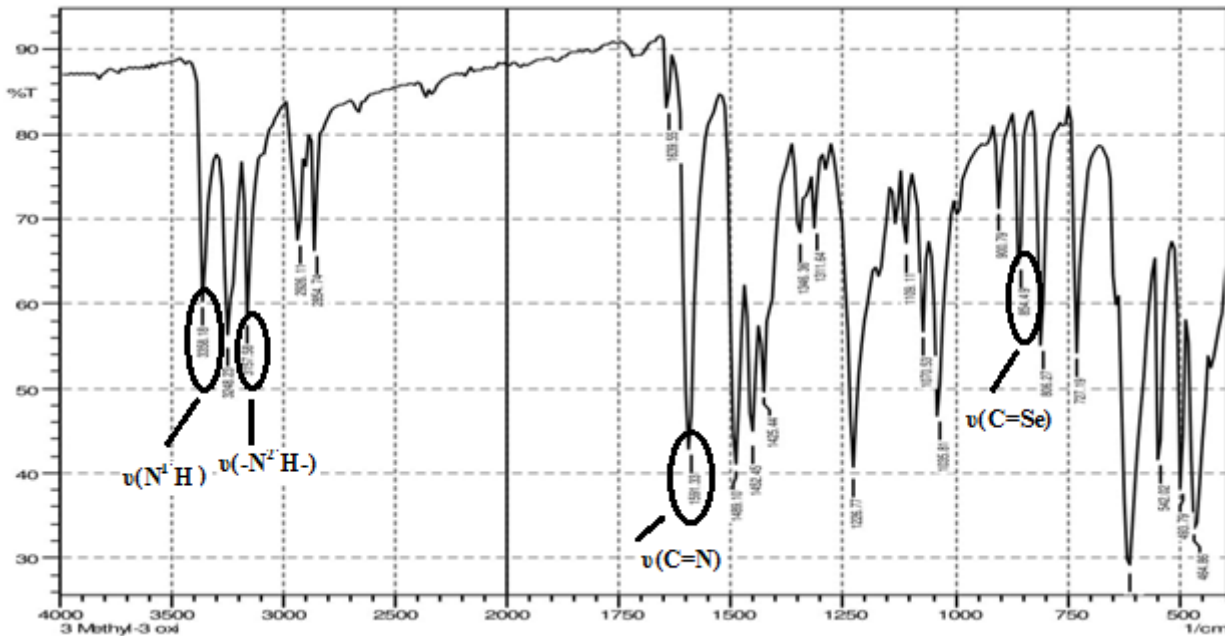


Figure 4.2.5 IR spectrum of 3-methyl-2-oxindole selenosemicarbazone(**H⁵L**)

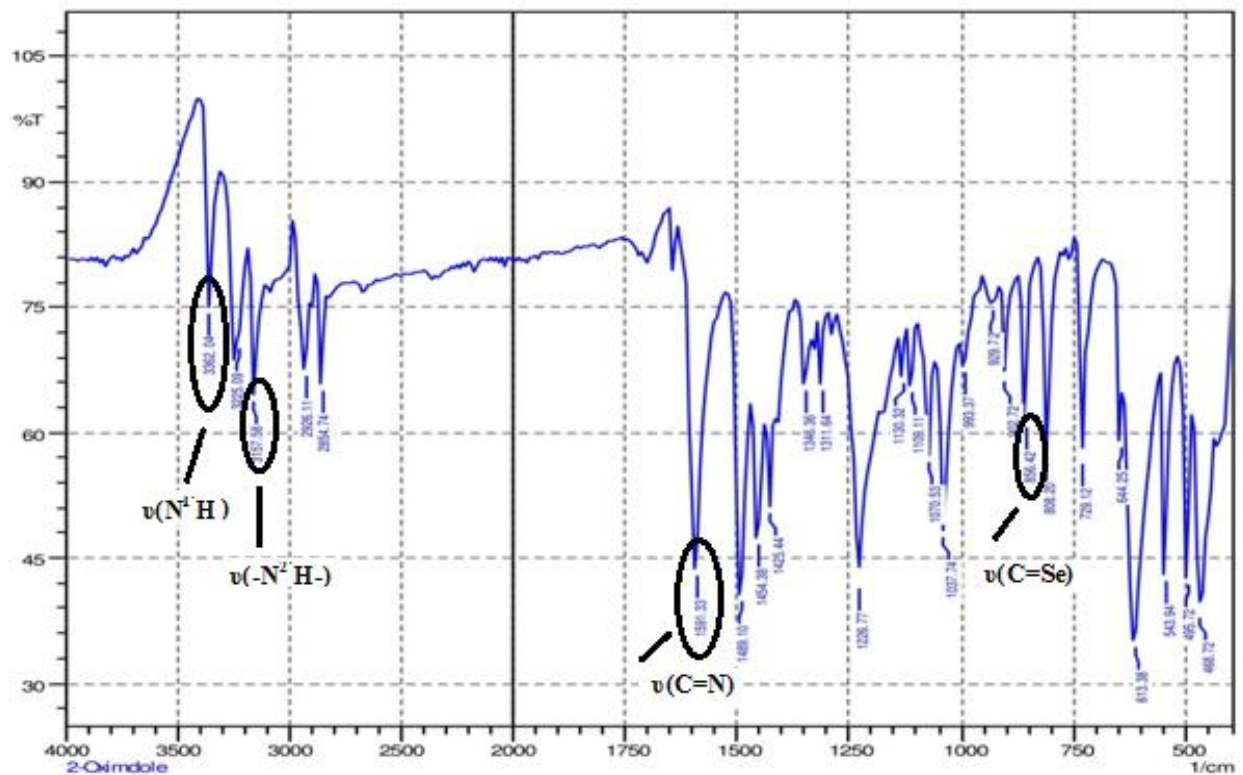


Figure 4.2.6 IR spectrum of 2-oxindole selenosemicarbazone(H^6L)

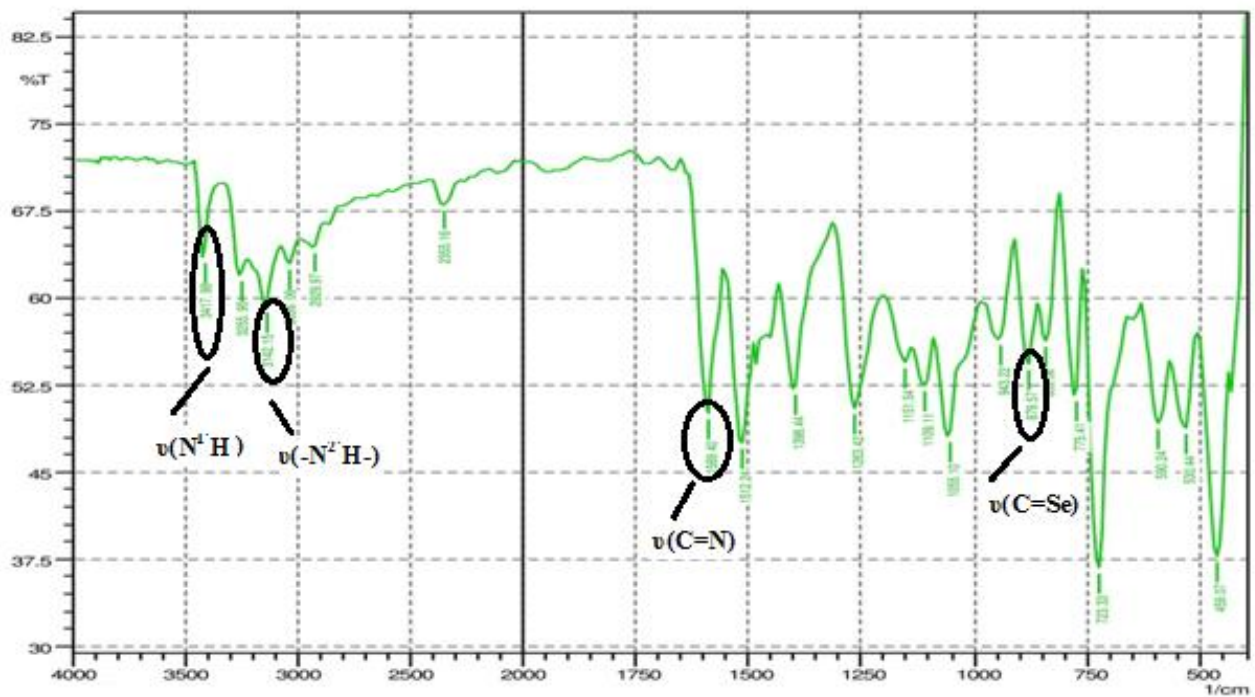


Figure 4.2.7 IR spectrum of 6-chloro-2-oxindole selenosemicarbazone(H^7L)

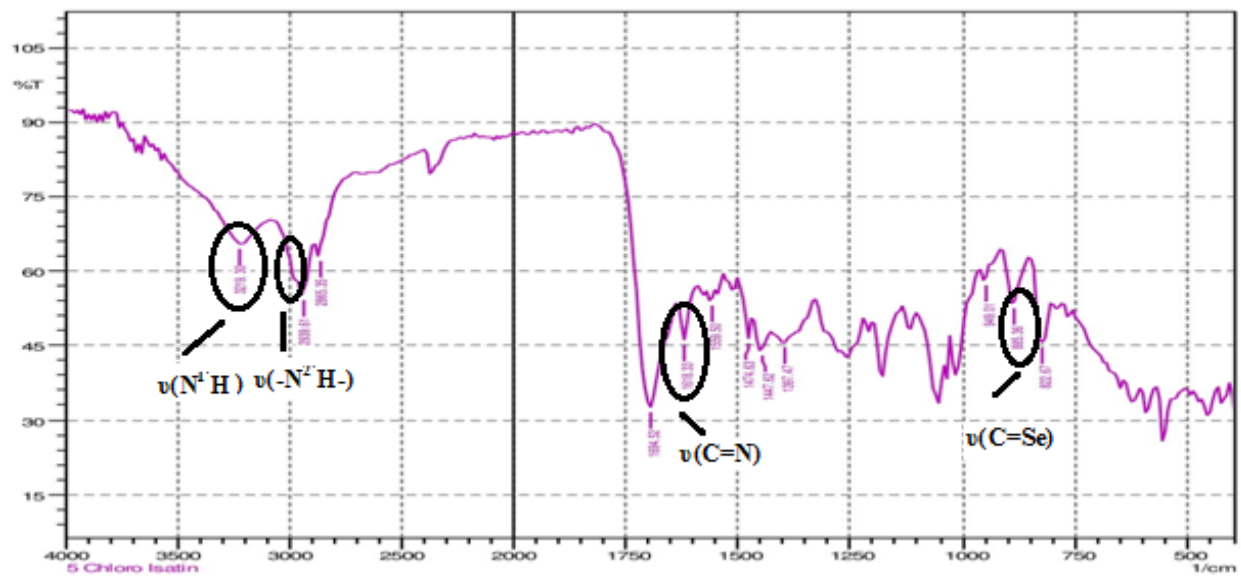


Figure 4.2.8 IR spectrum of 5-chloro isatin selenosemicarbazone(H^8L)

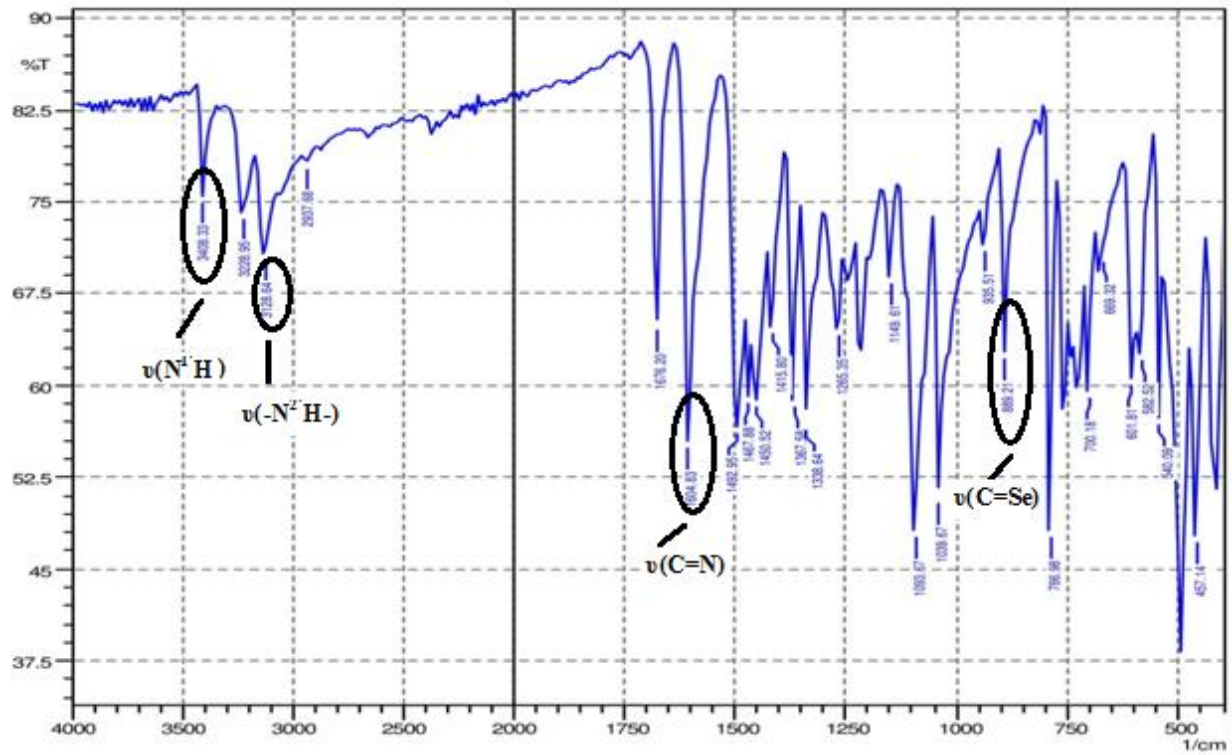


Figure 4.2.9 IR spectrum of 1-methyl isatin selenosemicarbazone(H^9L)

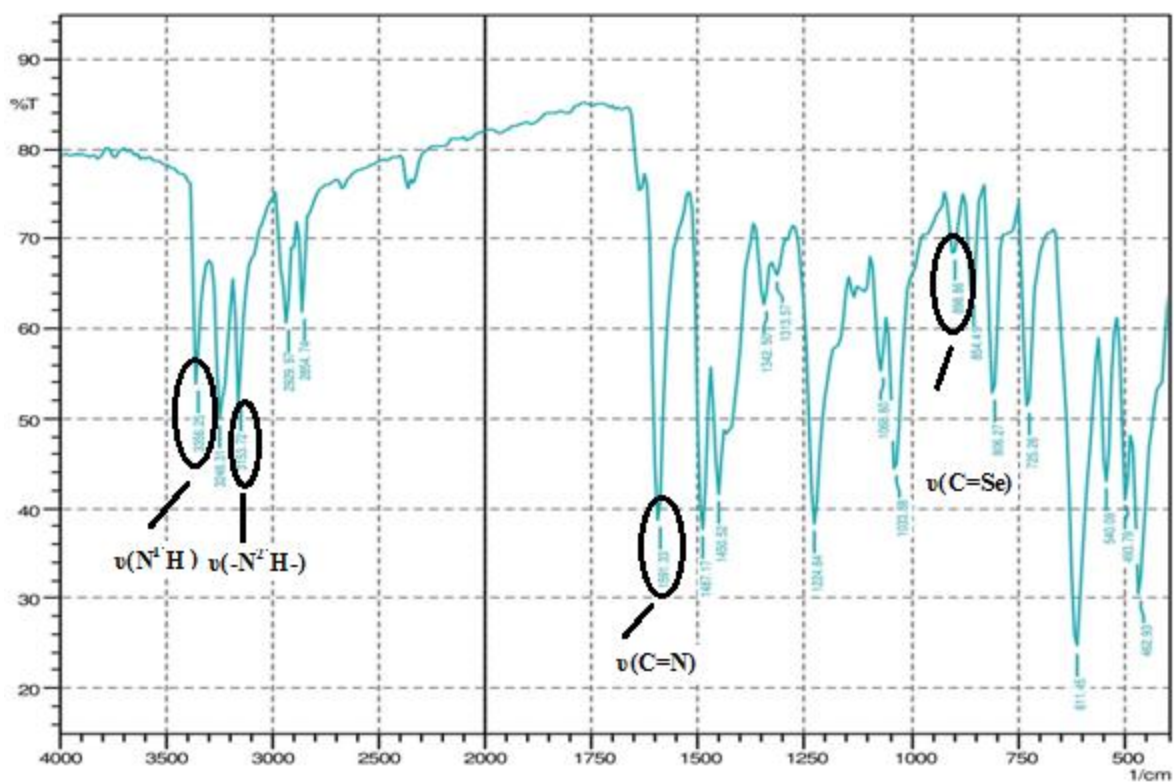


Figure 4.2.10 IR spectrum of 3-indole selenosemicarbazone(H^{10}L)

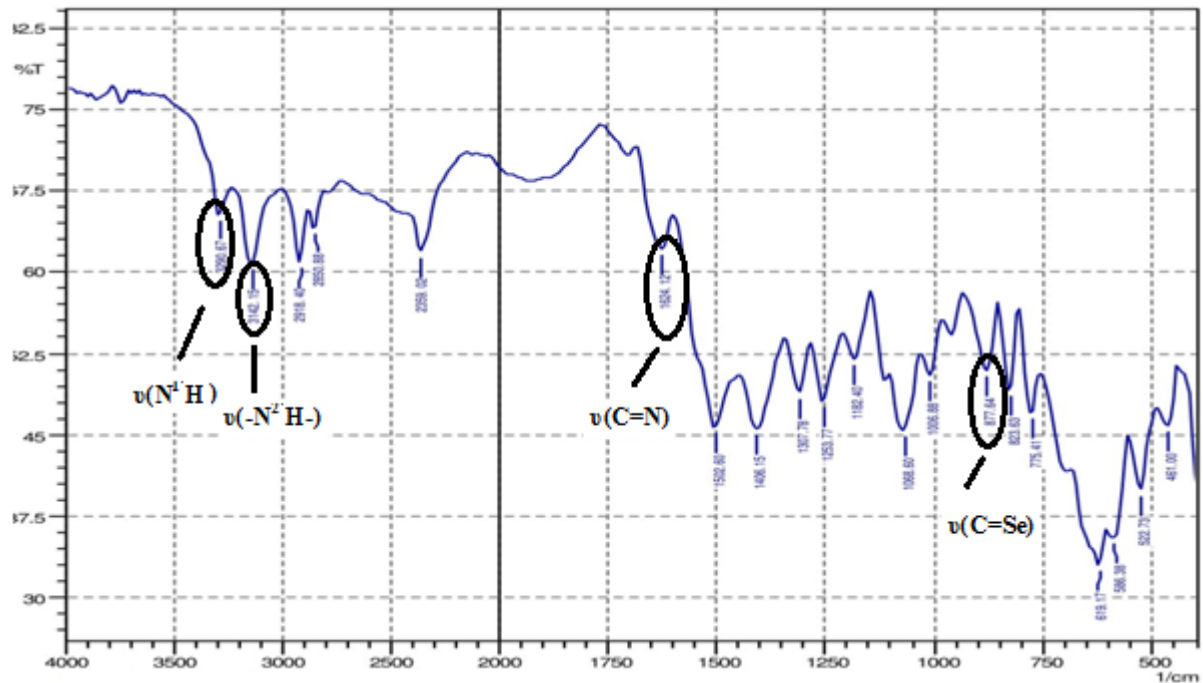


Figure 4.2.11 IR spectrum of 3-acetyl indole selenosemicarbazone(H^{11}L)

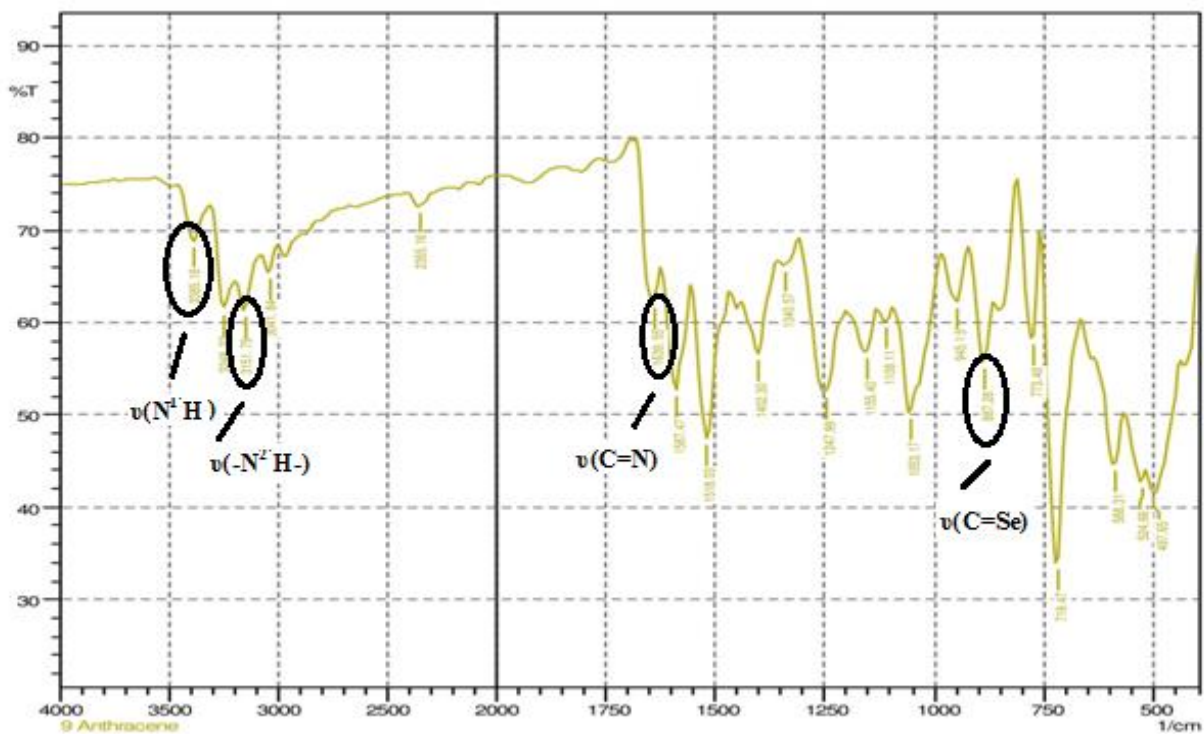


Figure 4.2.12 IR spectrum of 9-anthracene selenosemicarbazone($\mathbf{H}^{12}\mathbf{L}$)

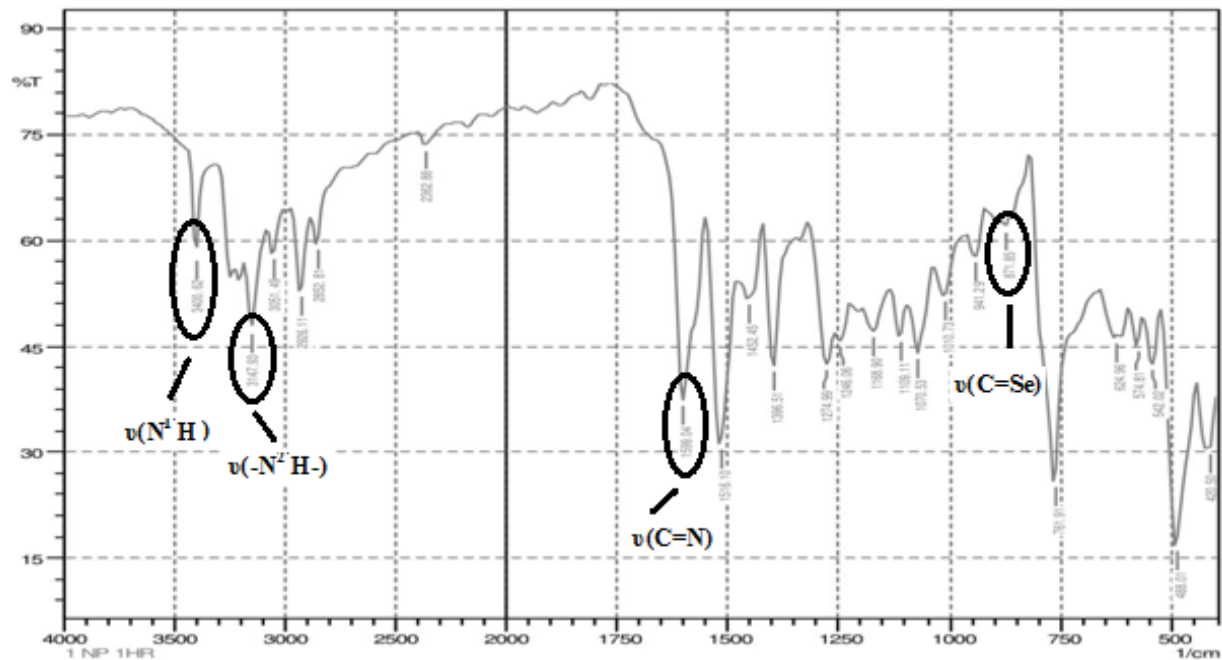


Figure 4.2.13 IR spectrum of 1-naphthaldehyde selenosemicarbazone($\mathbf{H}^{13}\mathbf{L}$)

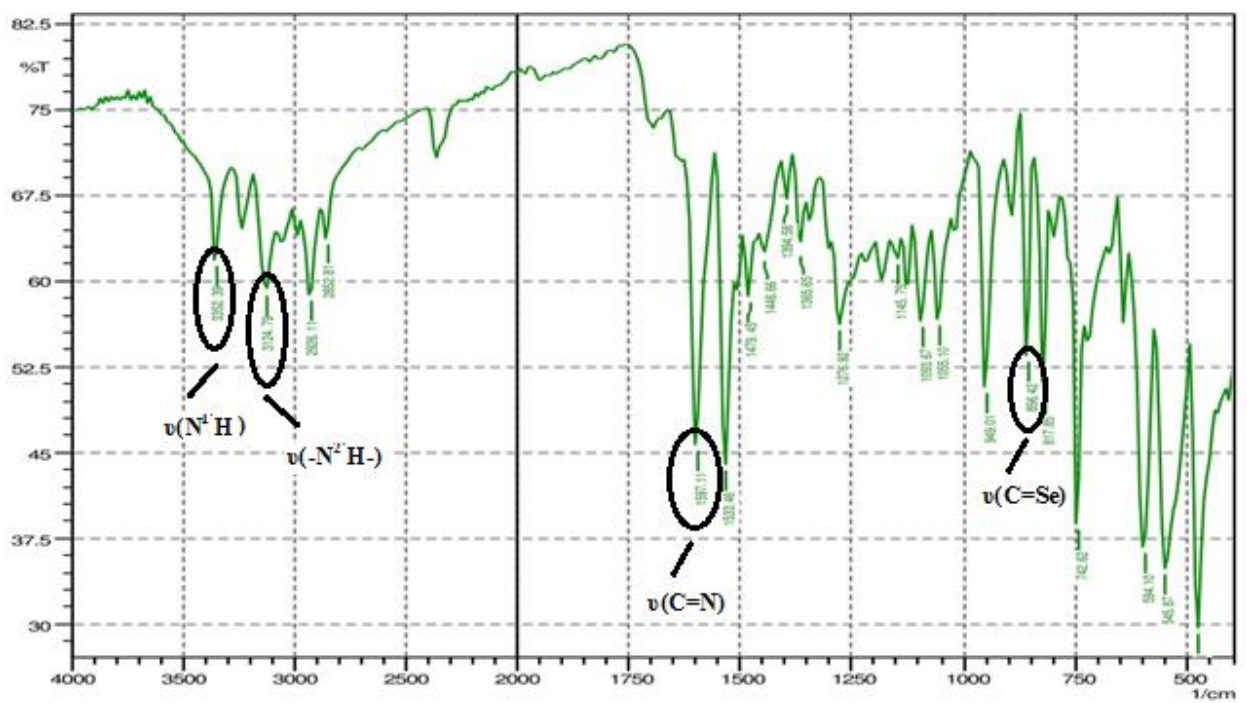


Figure 4.2.14 IR spectrum of 2-naphthaldehyde selenosemicarbazone(H¹⁴L)

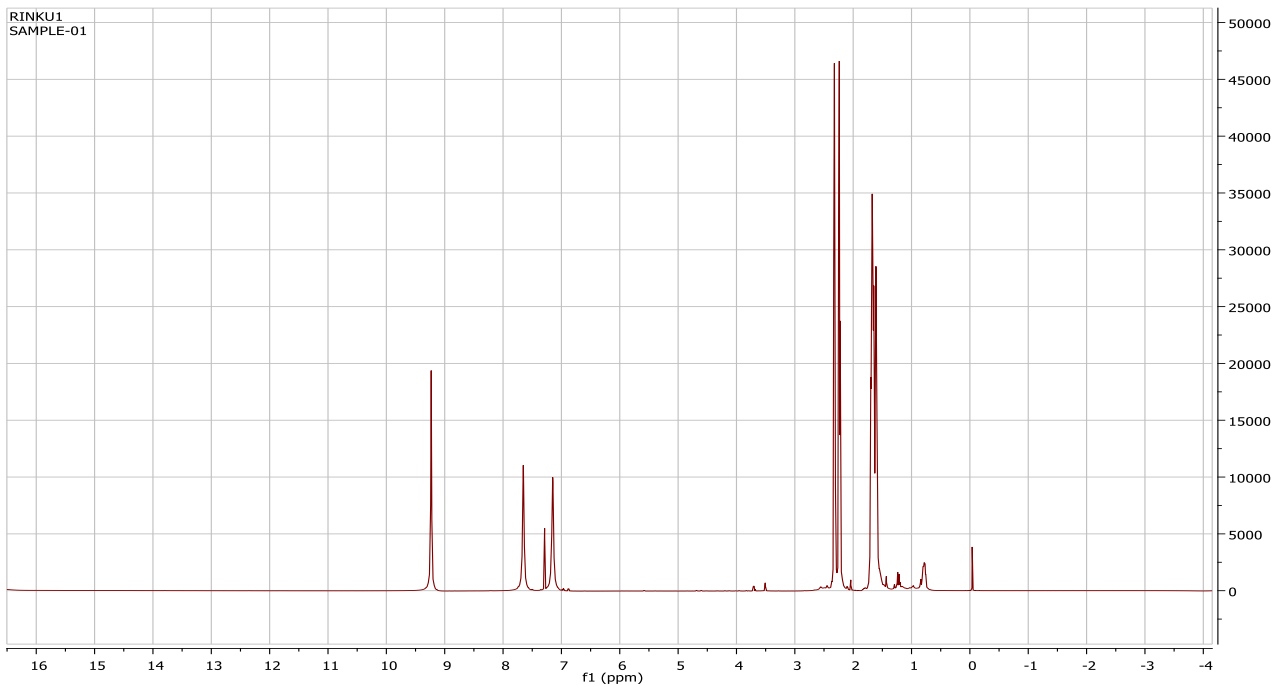


Figure 4.3.1.1a) ^1H NMR spectrum of cyclohexanoneselenosemicarbazone(H^1L)

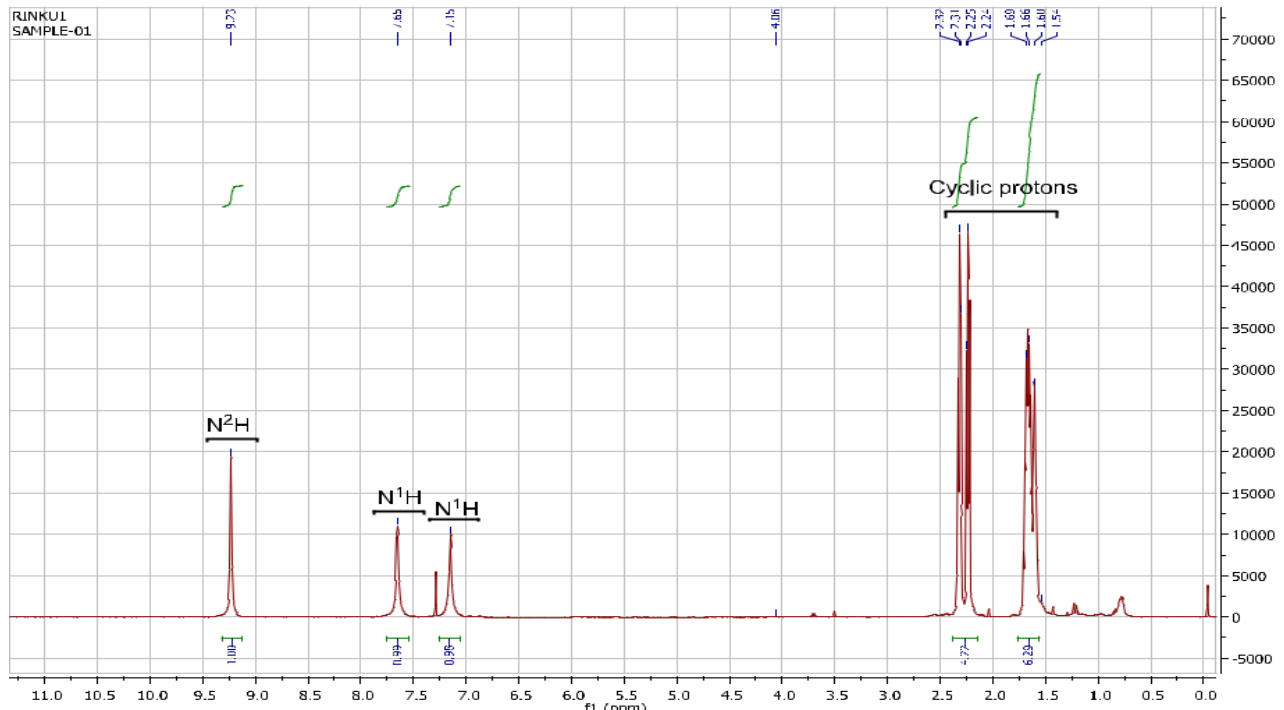


Figure 4.3.1.1b) ^1H NMR spectrum of cyclohexanoneselenosemicarbazone(H^1L)(expanded form)

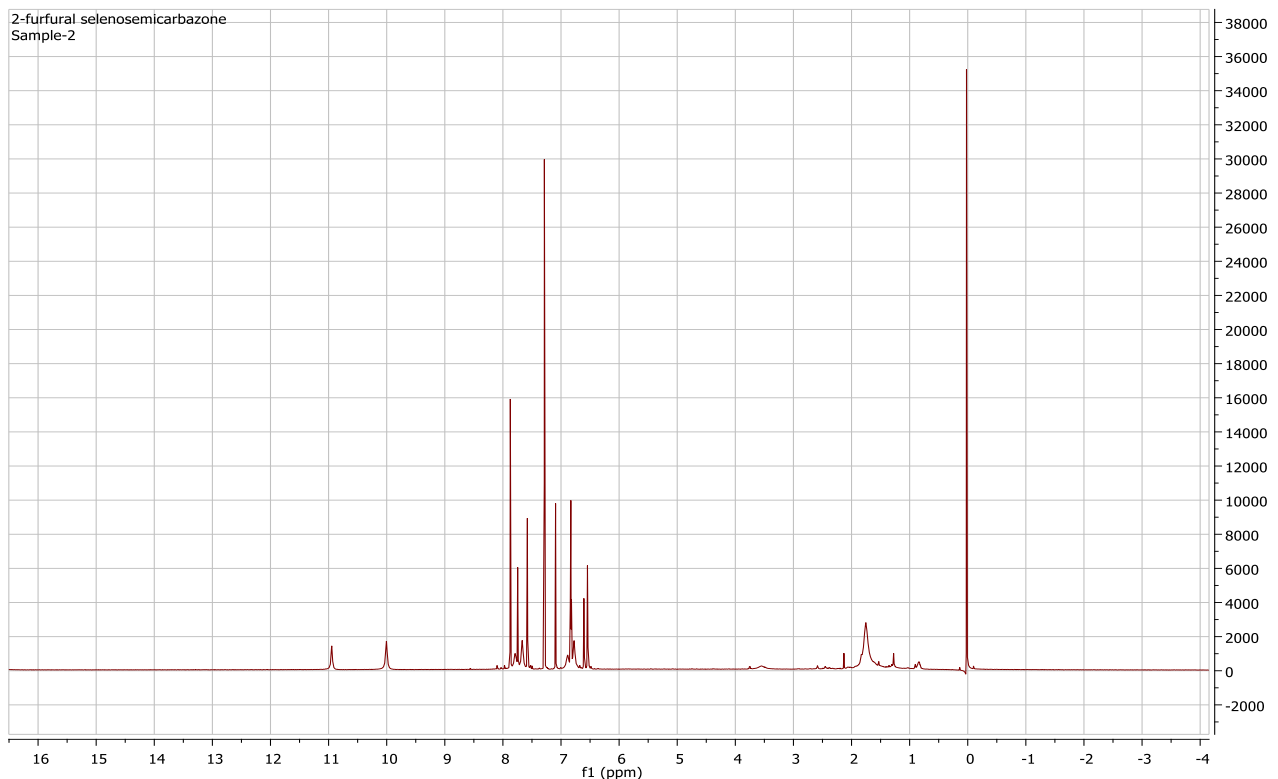


Figure 4.3.1.2a) ^1H NMR spectrum of 2-furfural selenosemicarbazone(H^2L)

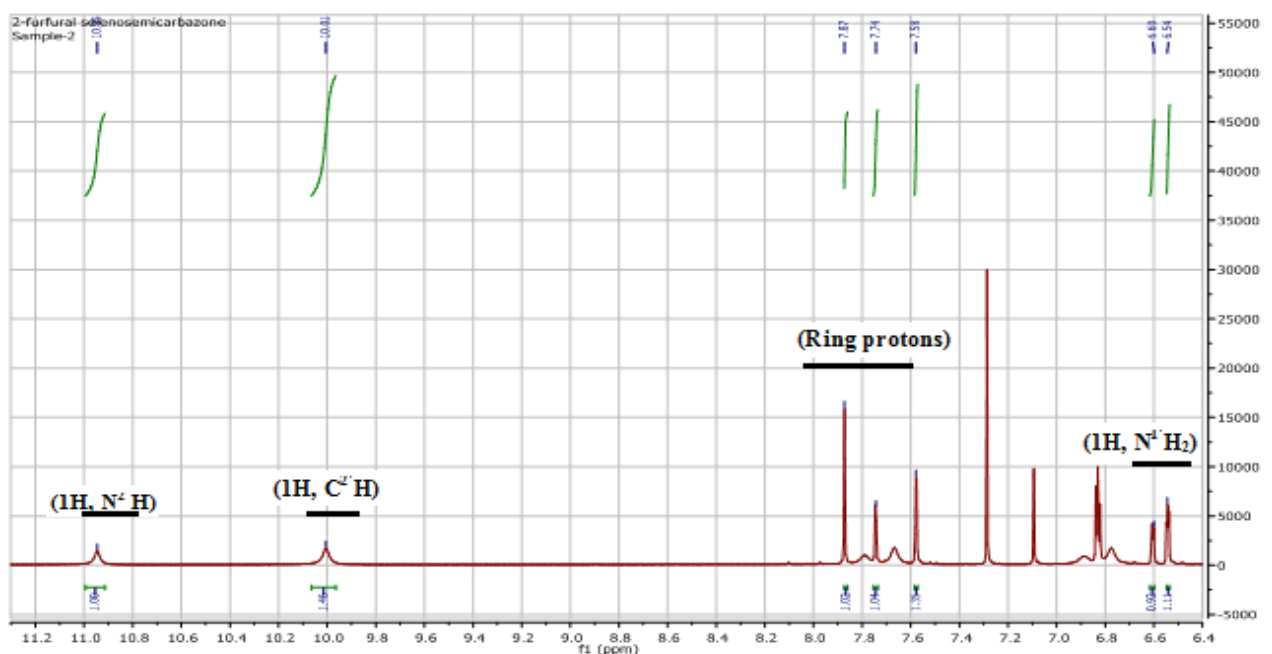


Figure 4.3.1.2b) ^1H NMR spectrum of 2-furfural selenosemicarbazone(H^2L)(expanded form)

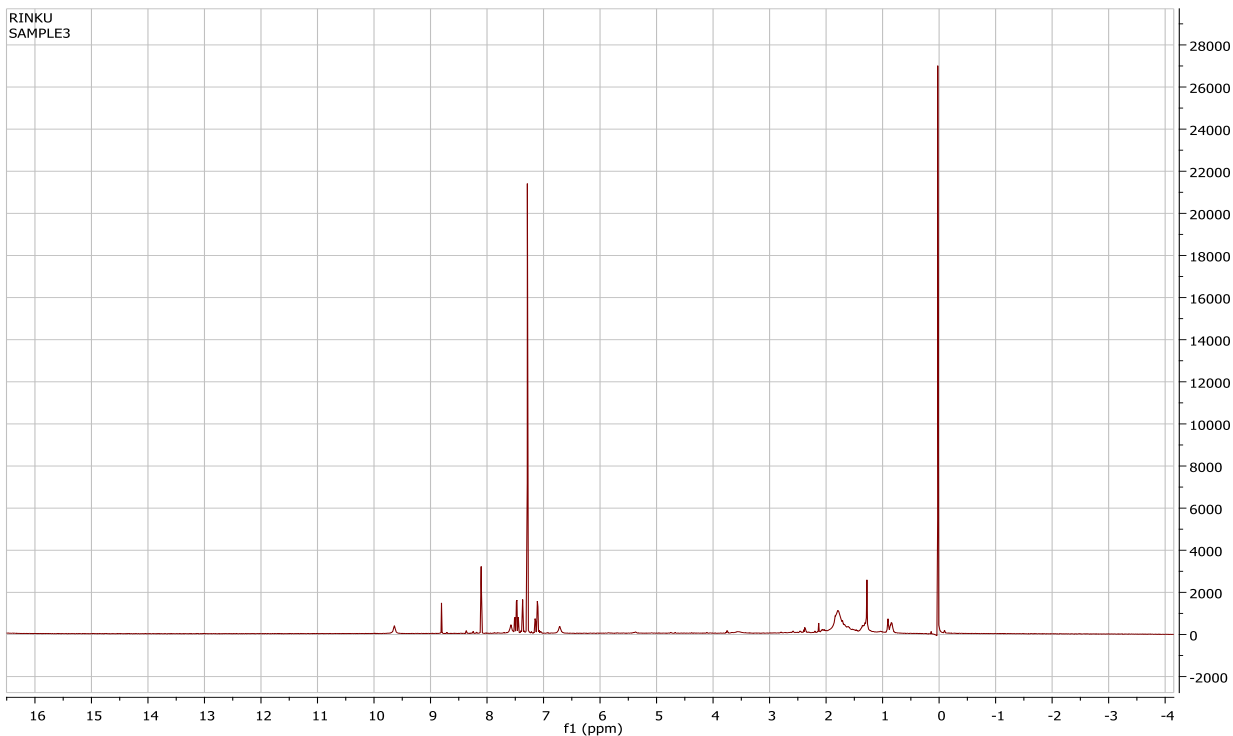


Figure 4.3.1.3a) ^1H NMR spectrum of 2-thiophene selenosemicarbazone(H^3L)

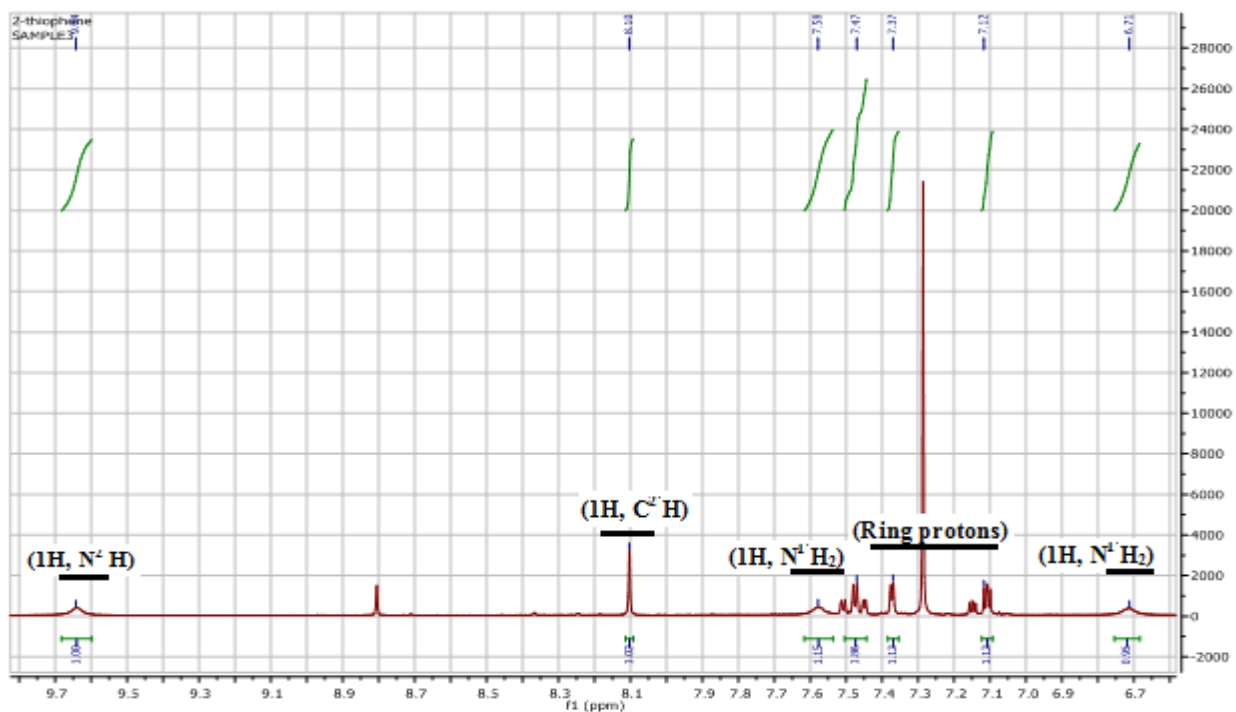


Figure 4.3.1.3b) ^1H NMR spectrum of 2-thiophene selenosemicarbazone(H^3L) (expanded view)

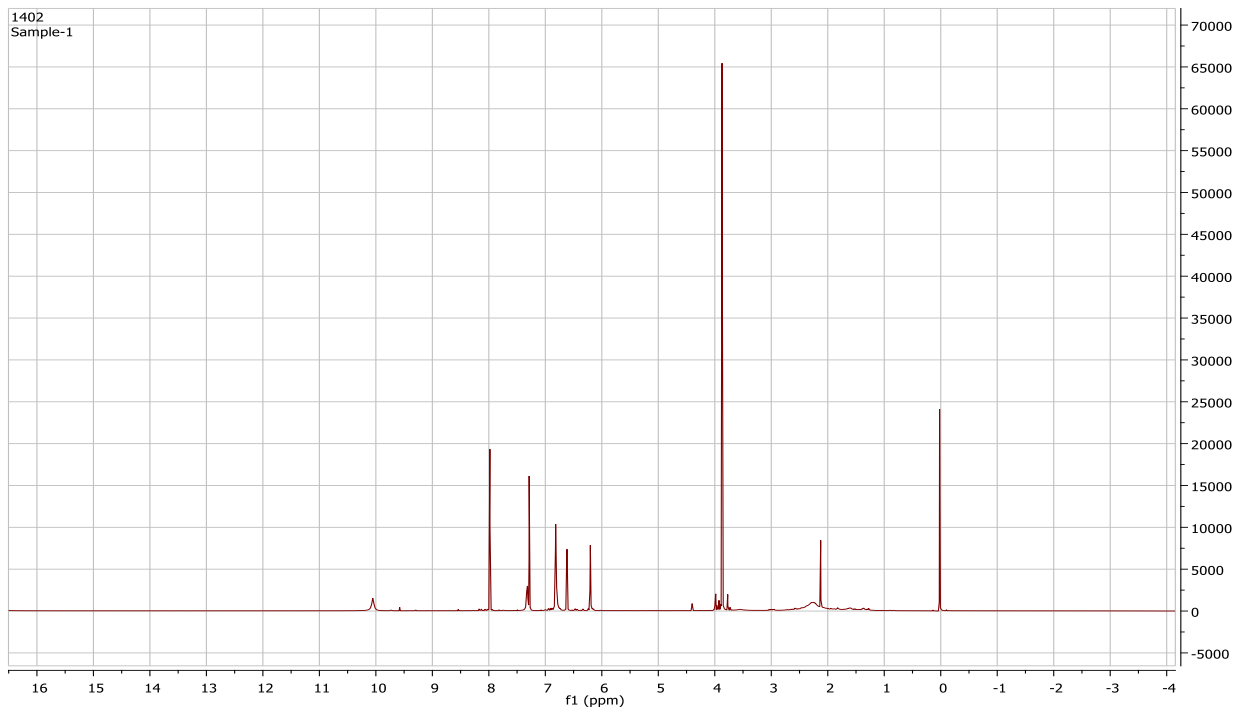


Figure 4.3.1.4a) ^1H NMR spectrum of N-methyl-2-pyrrole selenosemicarbazone(H^4L)

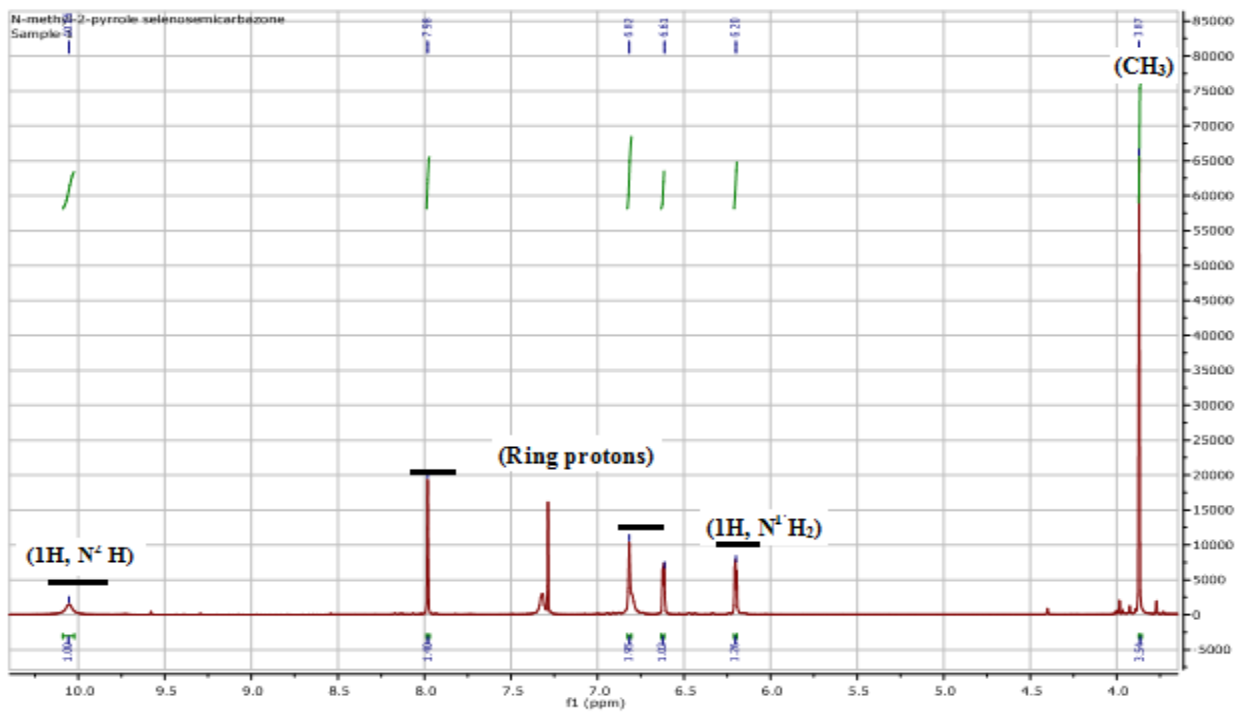


Figure 4.3.1.4b) ^1H NMR spectrum of N-methyl-2-pyrroleselenosemicarbazone(H^4L)(expanded view)

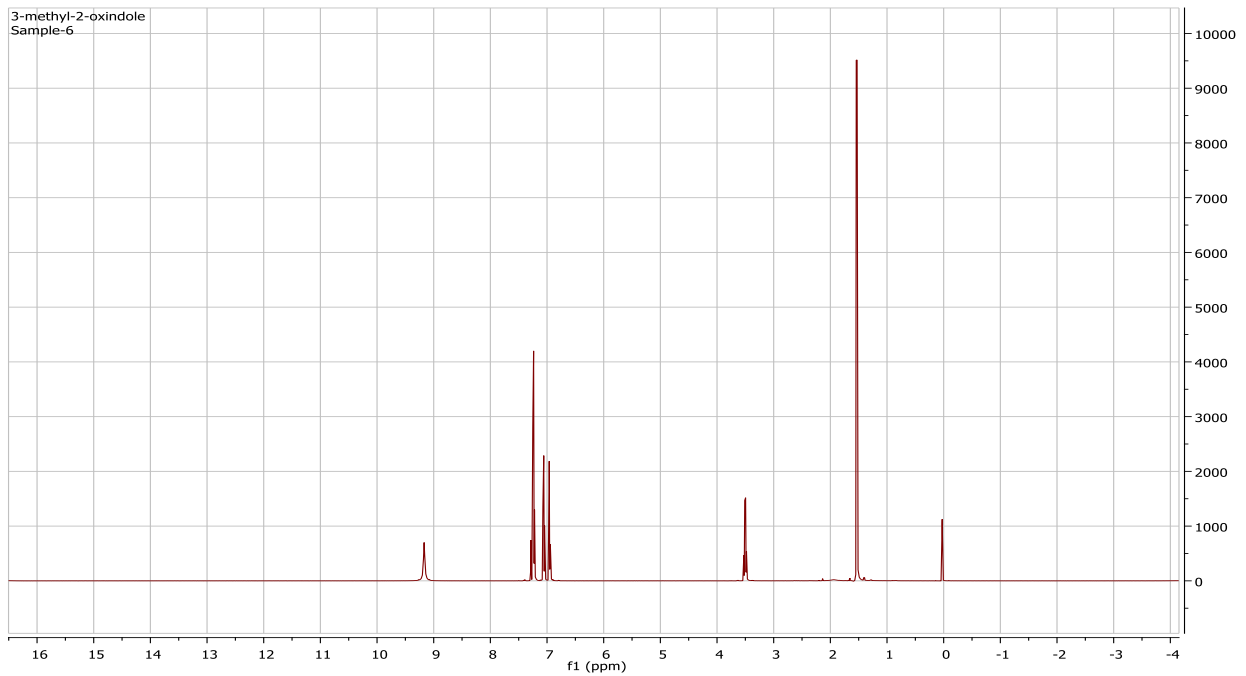


Figure 4.3.1.5a) ^1H NMR spectrum of 3-methyl-2-oxindole selenosemicarbazone(H^5L)

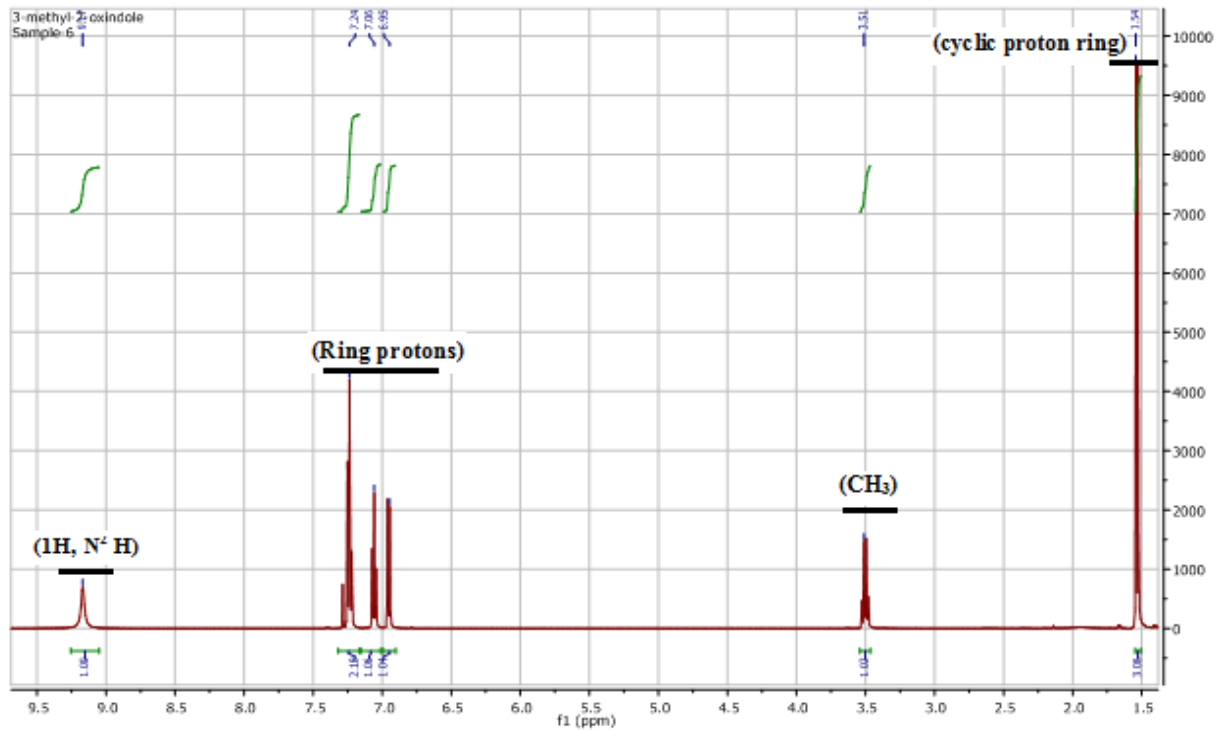


Figure 4.3.1.5b) ^1H NMR spectrum of 3-methyl-2-oxindole selenosemicarbazone(H^5L)(expanded form)

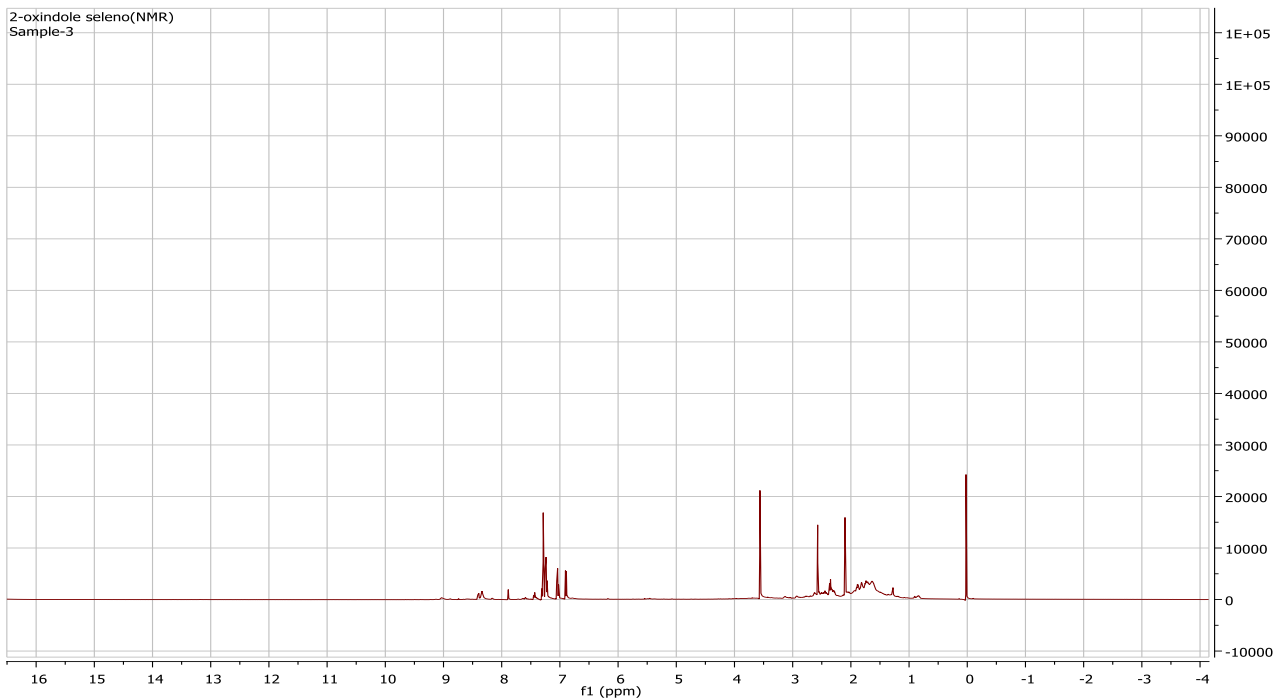


Figure 4.3.1.6a) ^1H NMR spectrum of 2-oxindole selenosemicarbazone(H^6L)

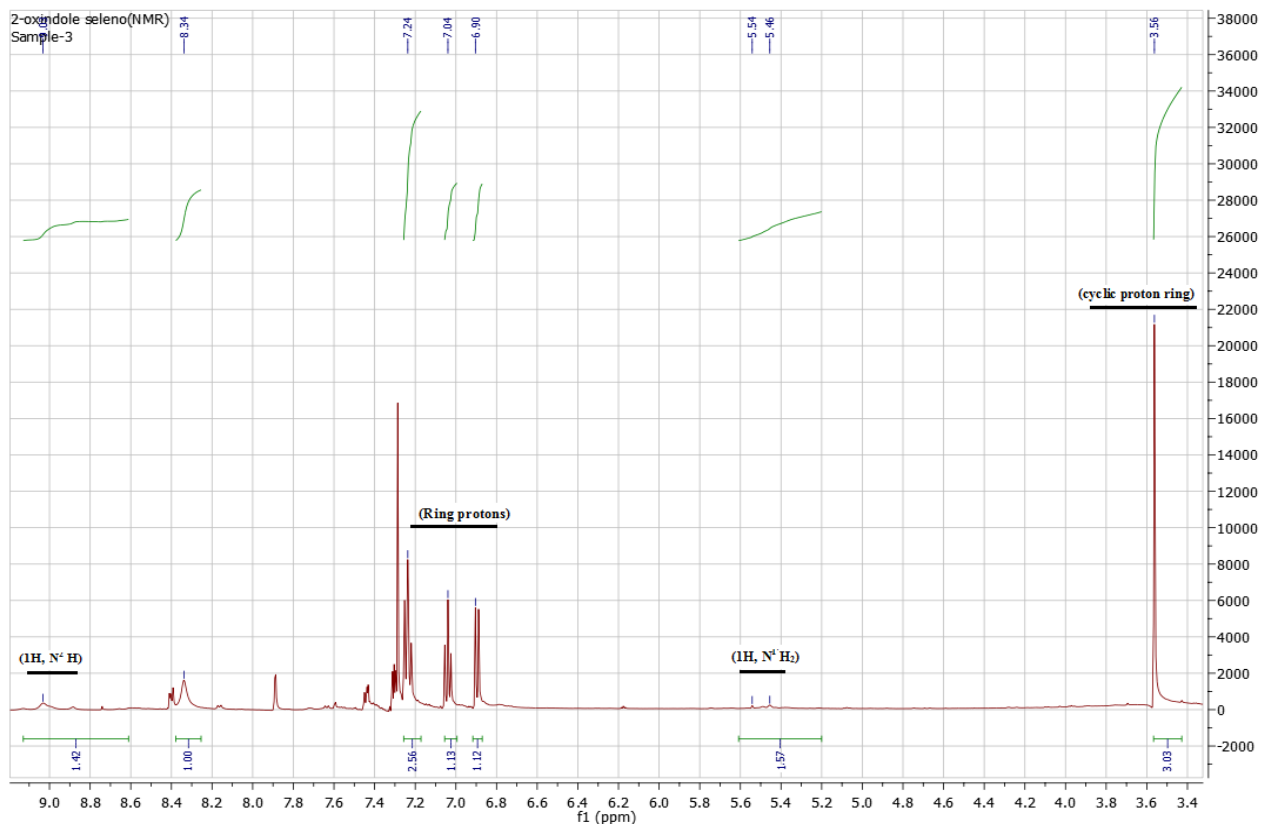


Figure 4.3.1.6b) ^1H NMR spectrum of 2-oxindole selenosemicarbazone(H^6L)(expanded form)

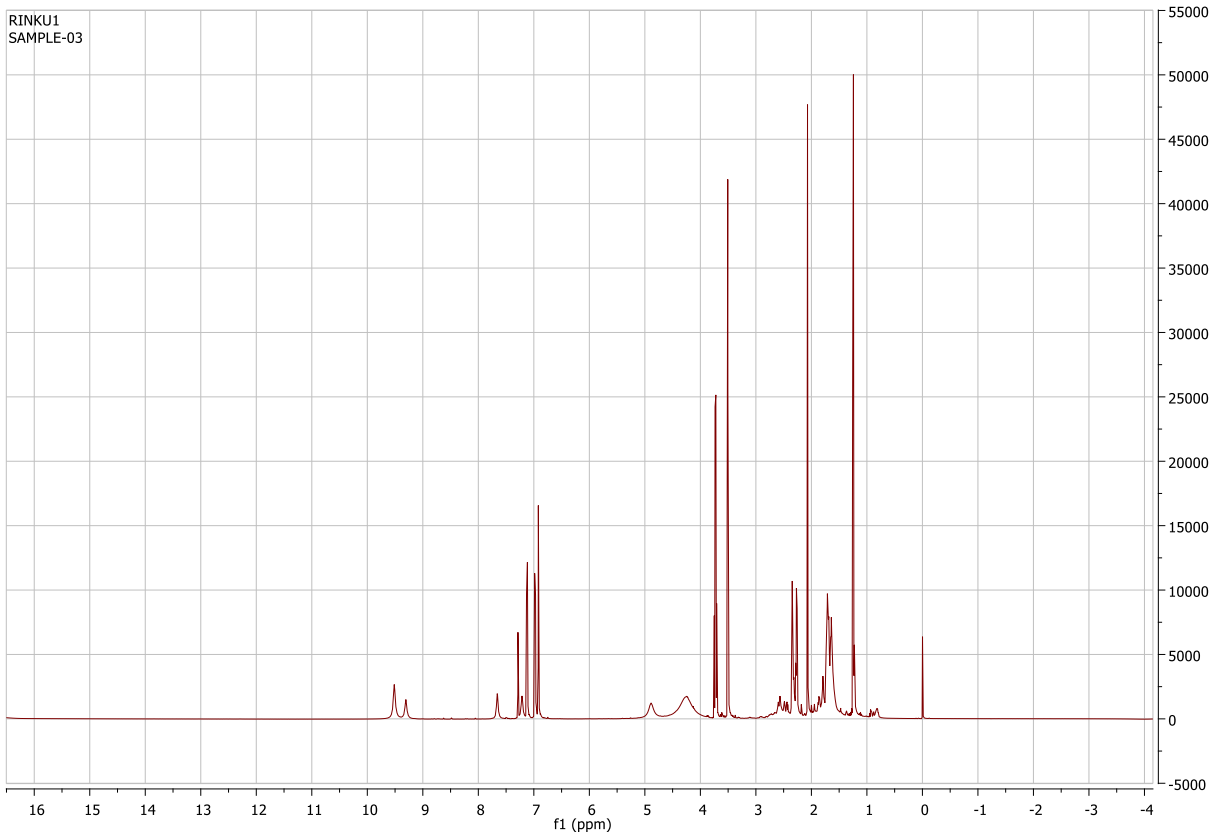


Figure 4.3.1.7a) ^1H NMR spectrum of 6- chloro-2-oxindole selenosemicarbazone(H^7L)

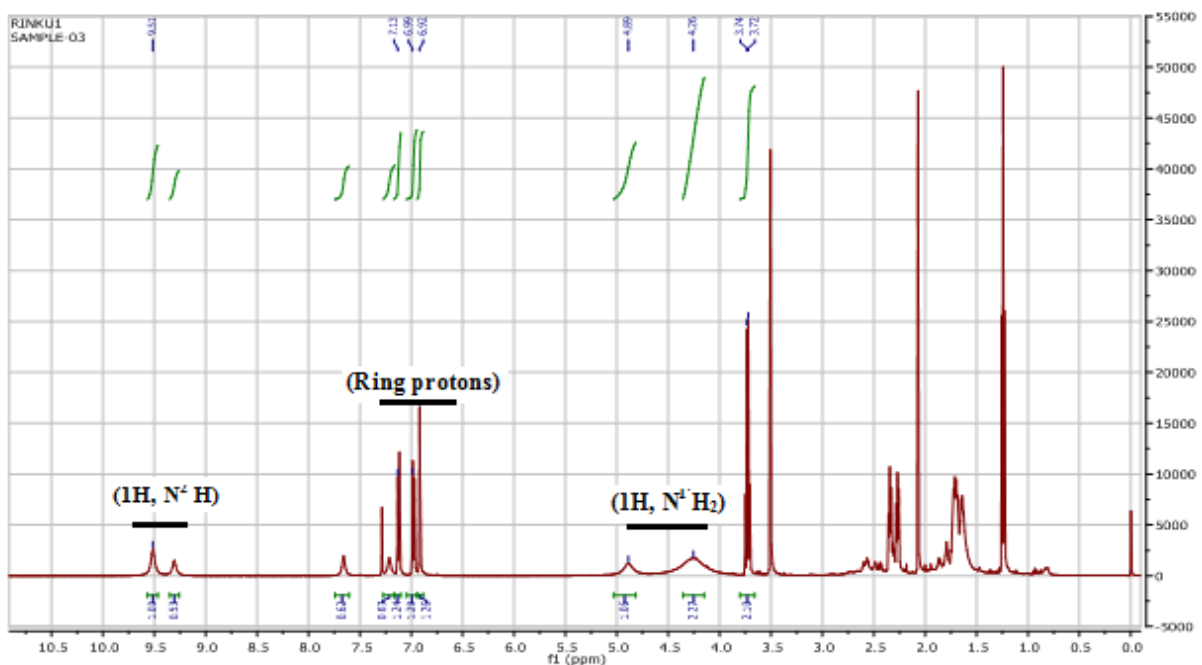


Figure 4.3.1.7a') ^1H NMR spectrum of 6-chloro-2-oxindole selenosemicarbazone(H^7L)

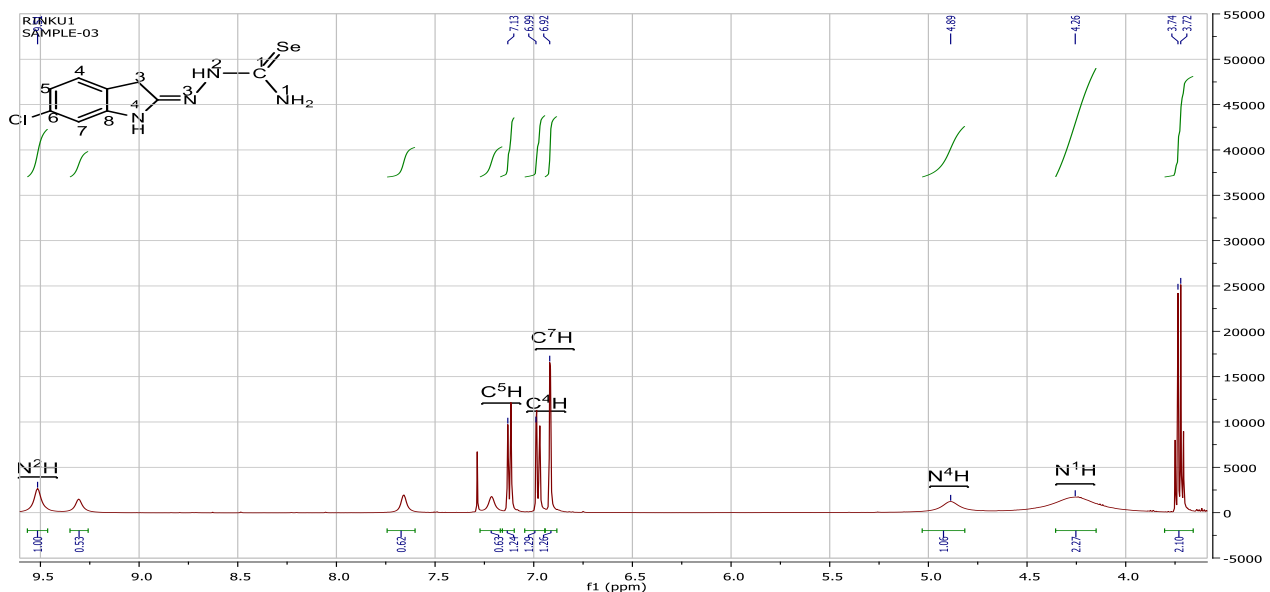


Figure 4.3.1.7b) ^1H NMR spectrum of 6-chloro-2-oxindole selenosemicarbazone(H^7L) (expanded form)

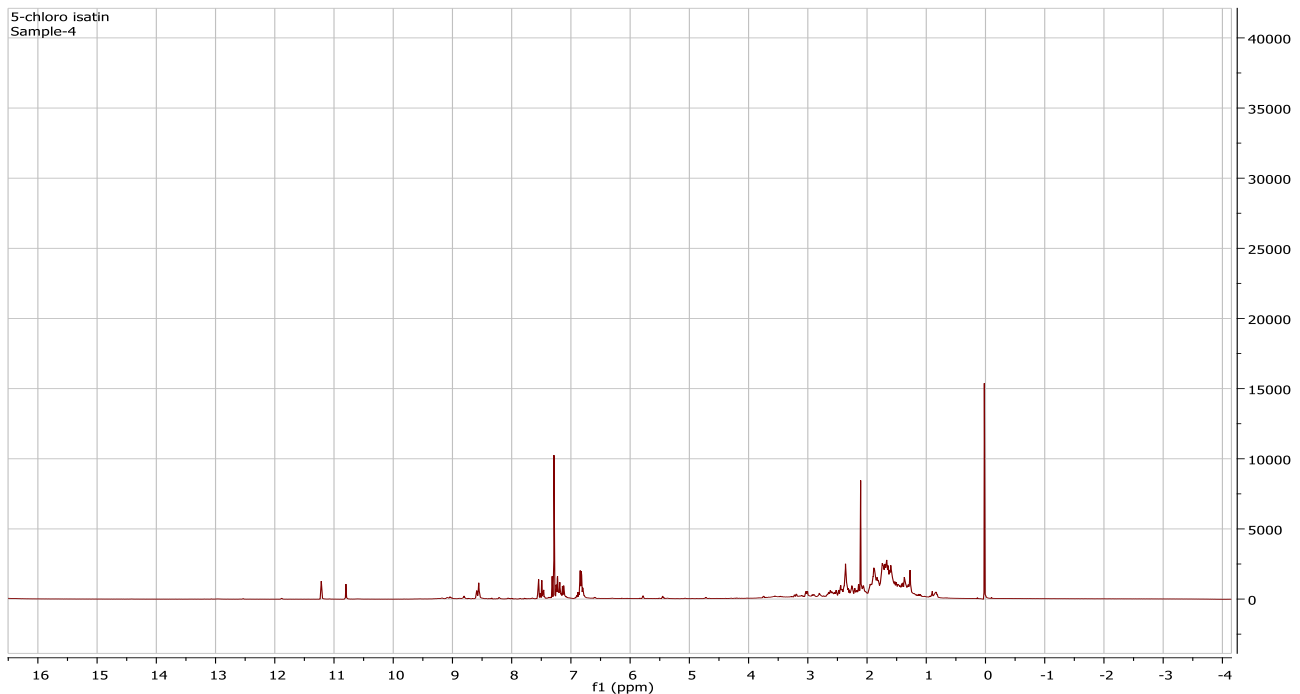


Figure 4.3.1.8a) ^1H NMR spectrum of 5- chloroisatin selenosemicarbazone(H^8L)

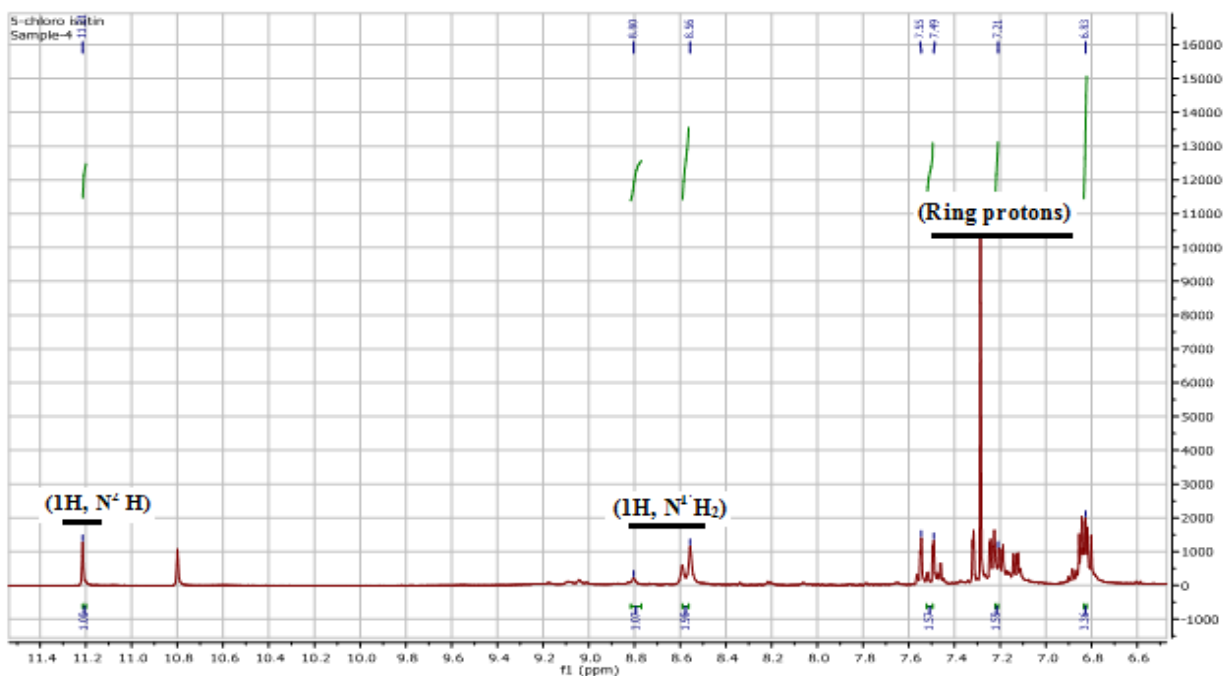


Figure 4.3.1.8b) ^1H NMR spectrum of 5-chloroisatin selenosemicarbazone(H^8L)(expanded view)

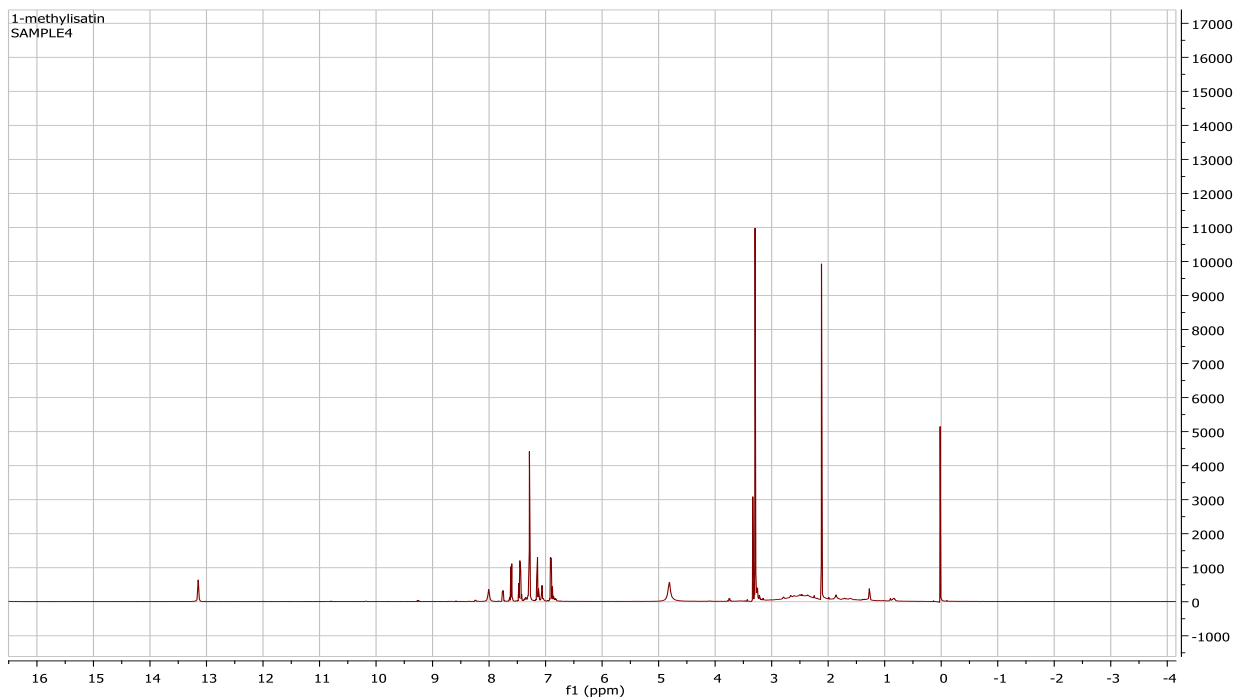


Figure 4.3.1.9 a) ^1H NMR spectrum of 1-methyl isatin selenosemicarbazone(H^9L)

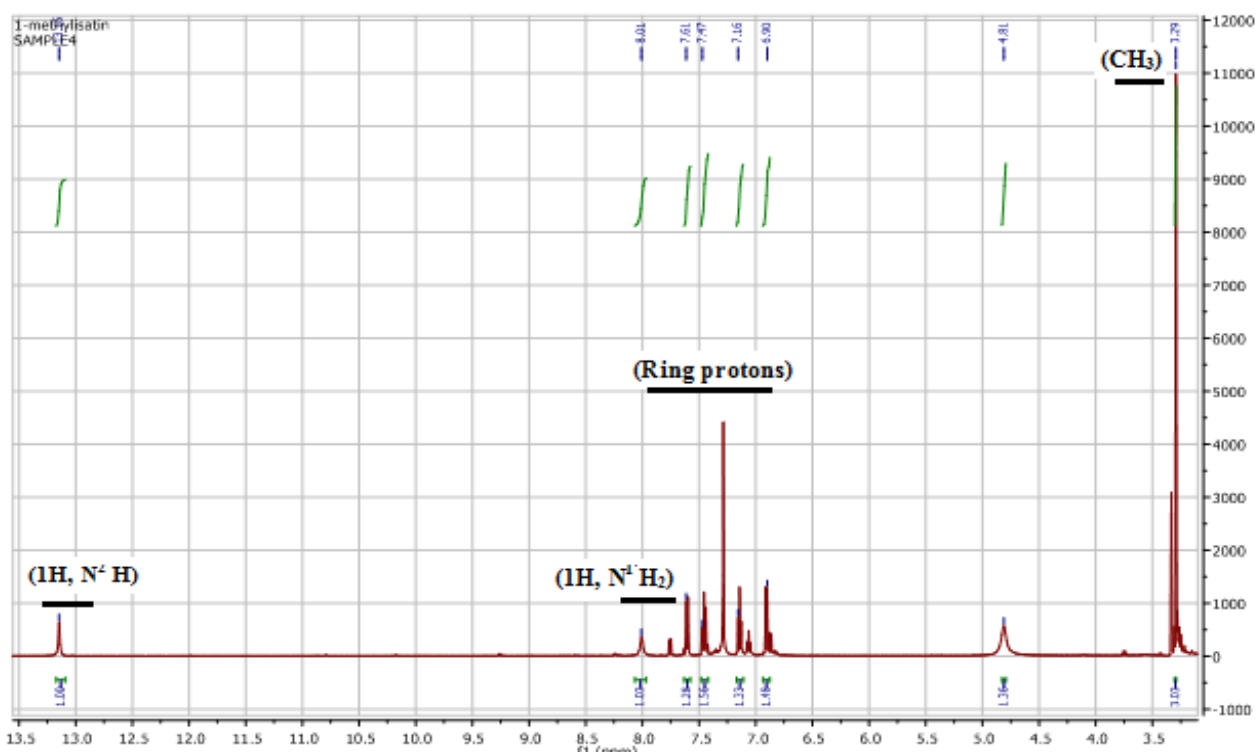


Figure 4.3.1.9b) ^1H NMR spectrum of 1-methylisatin selenosemicarbazone(**H⁹L**)(expanded form)

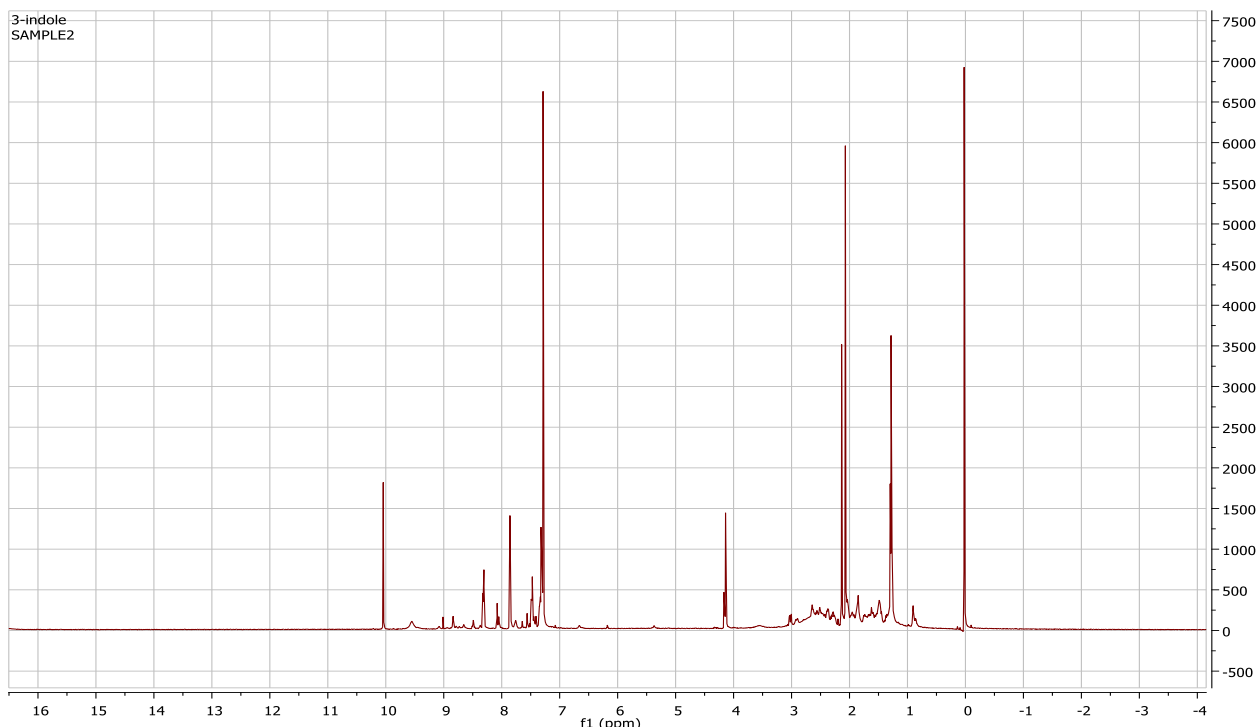


Figure 4.3.1.10 a) ^1H NMR spectrum of 3-indole selenosemicarbazone(**H¹⁰L**)

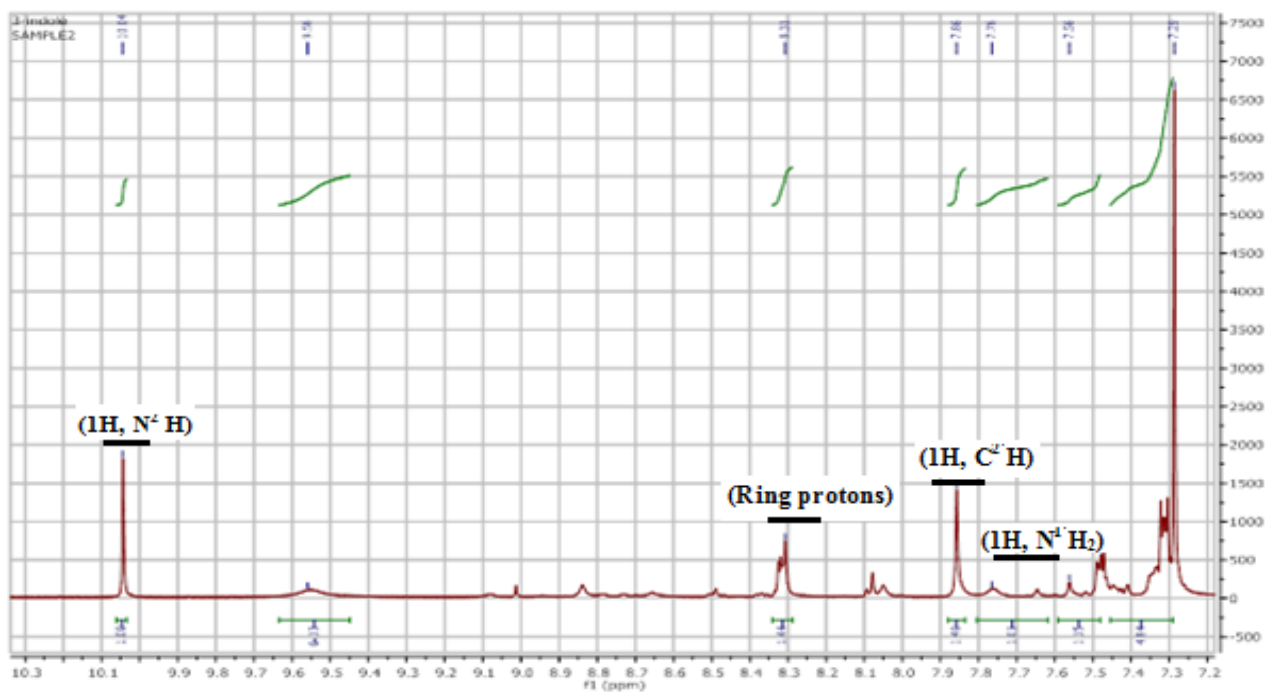


Figure 4.3.1.10b) ^1H NMR spectrum of 3-indole selenosemicarbazone(H^{10}L)(expanded form)

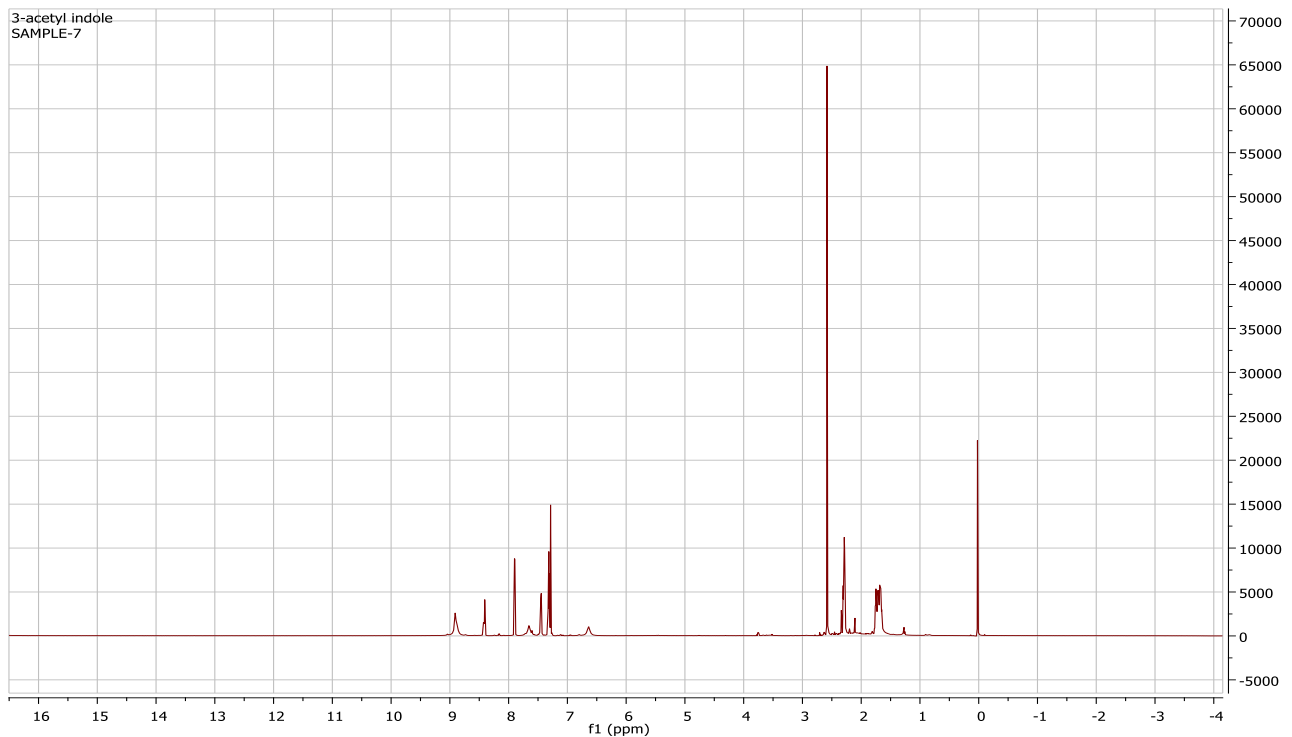


Figure 4.3.1.11a) ^1H NMR spectrum of 3-acetyl indole selenosemicarbazone(H^{11}L)

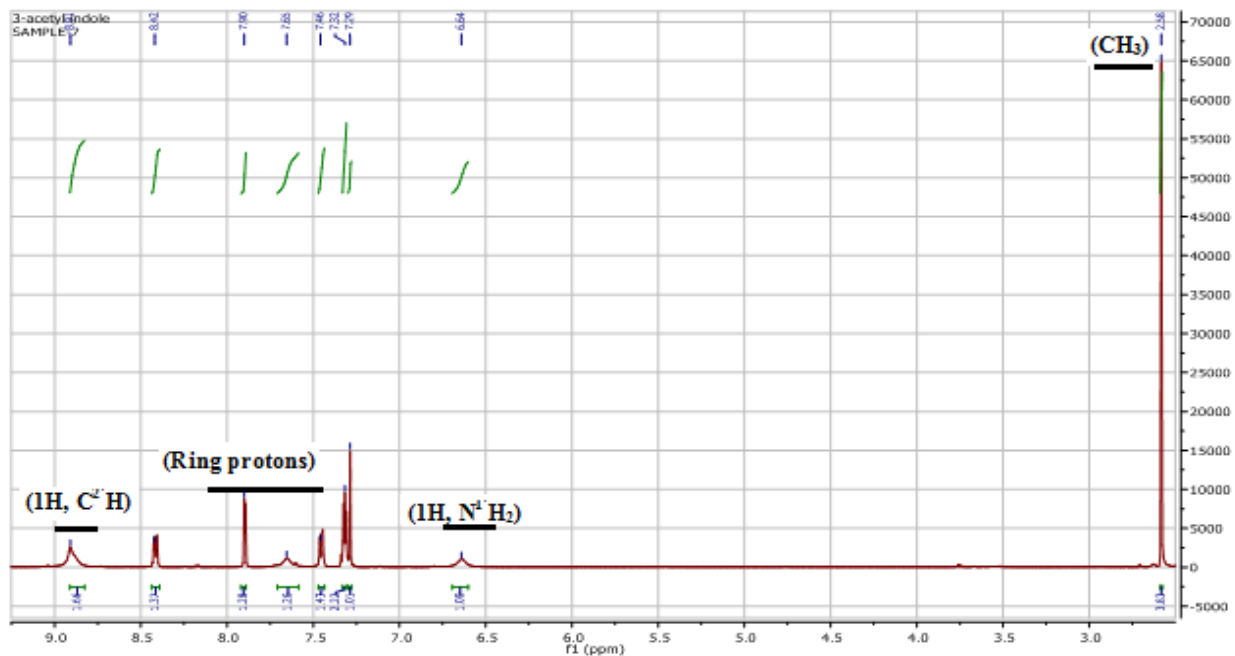


Figure 4.3.11b) ^1H NMR spectrum of 3-acetyl indole selenosemicarbazone (H^{11}L) (expanded form)

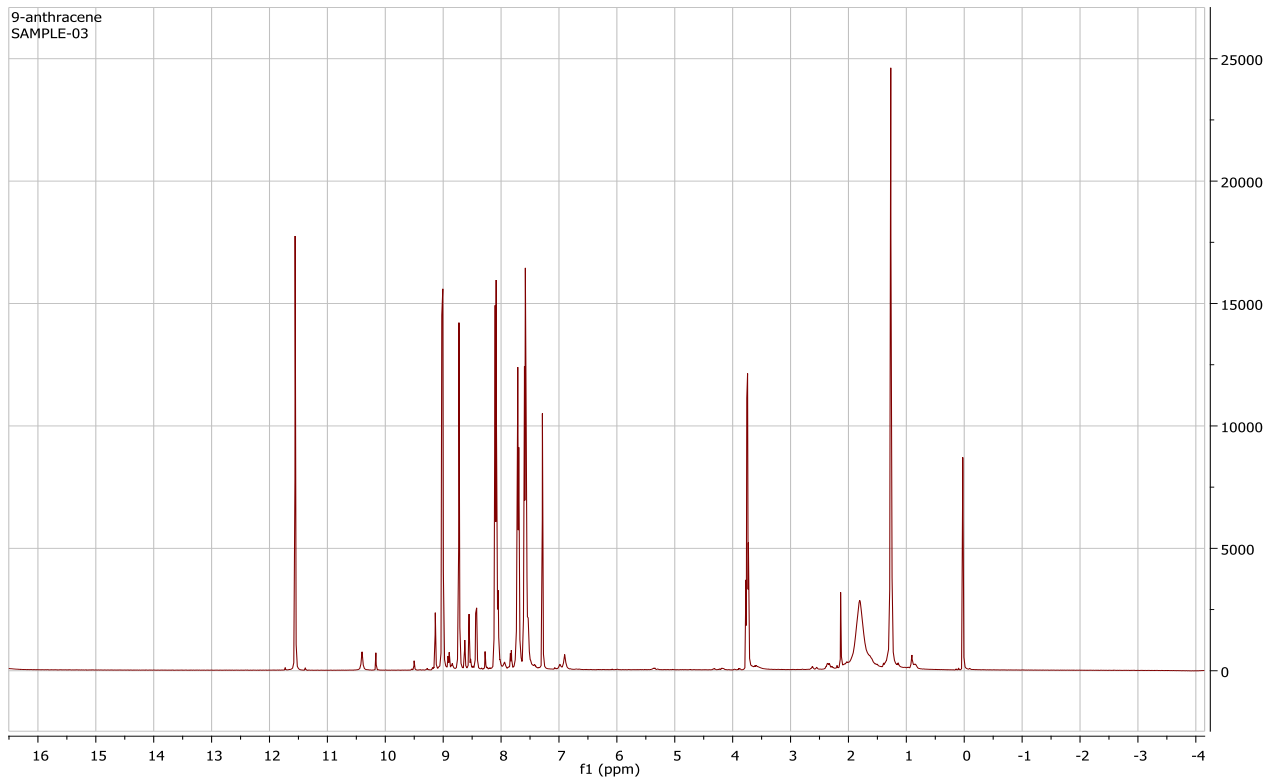


Figure 4.3.12a) ^1H NMR spectrum of 9-anthracene selenosemicarbazone(H^{12}L)

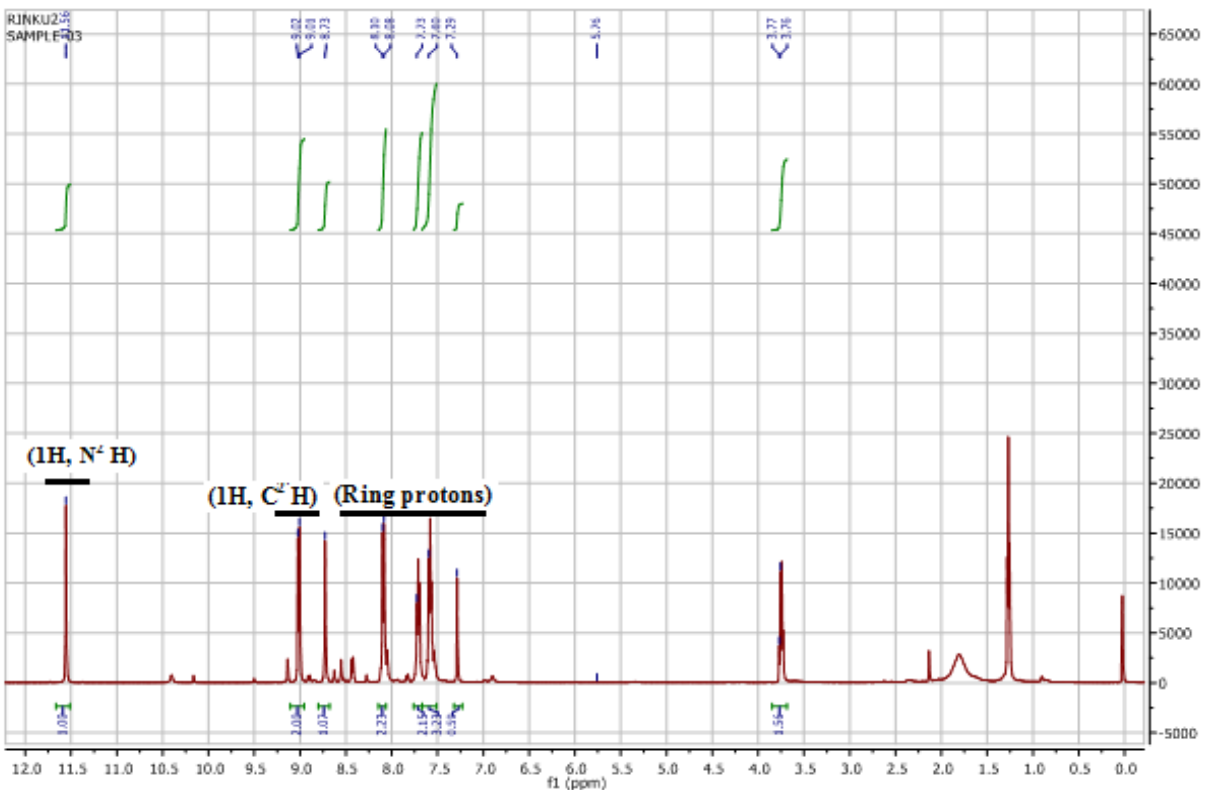


Figure 4.3.1.12a') ^1H NMR spectrum with full view of 9-anthraldehyde selenosemicarbazone(H^{12}L)

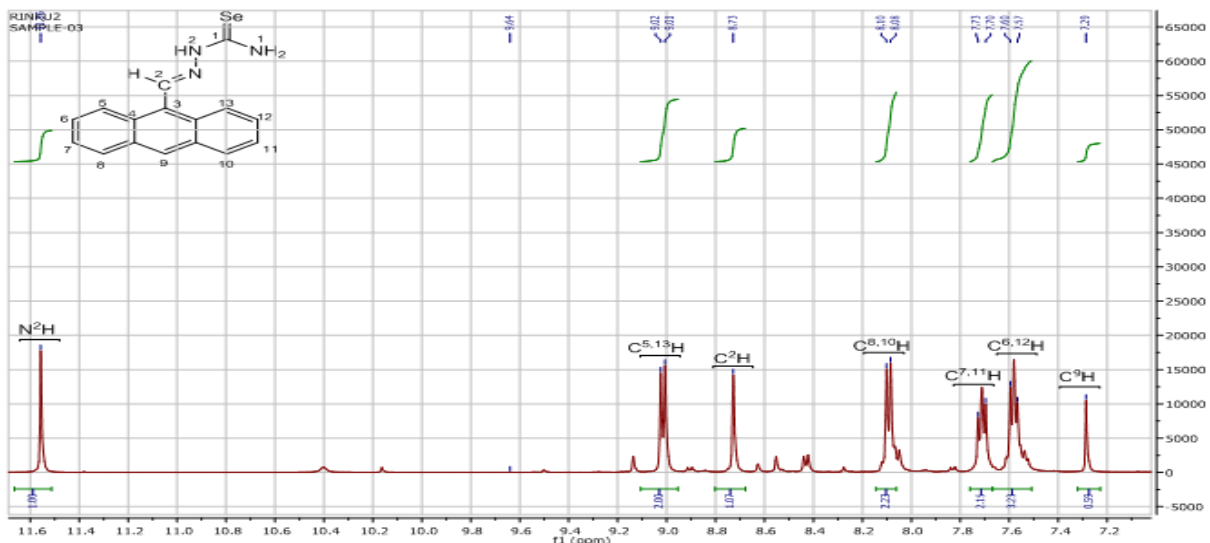


Figure 4.3.1.12b) ^1H NMR spectrum of 9-anthraldehyde selenosemicarbazone(H^{12}L) (expanded form)

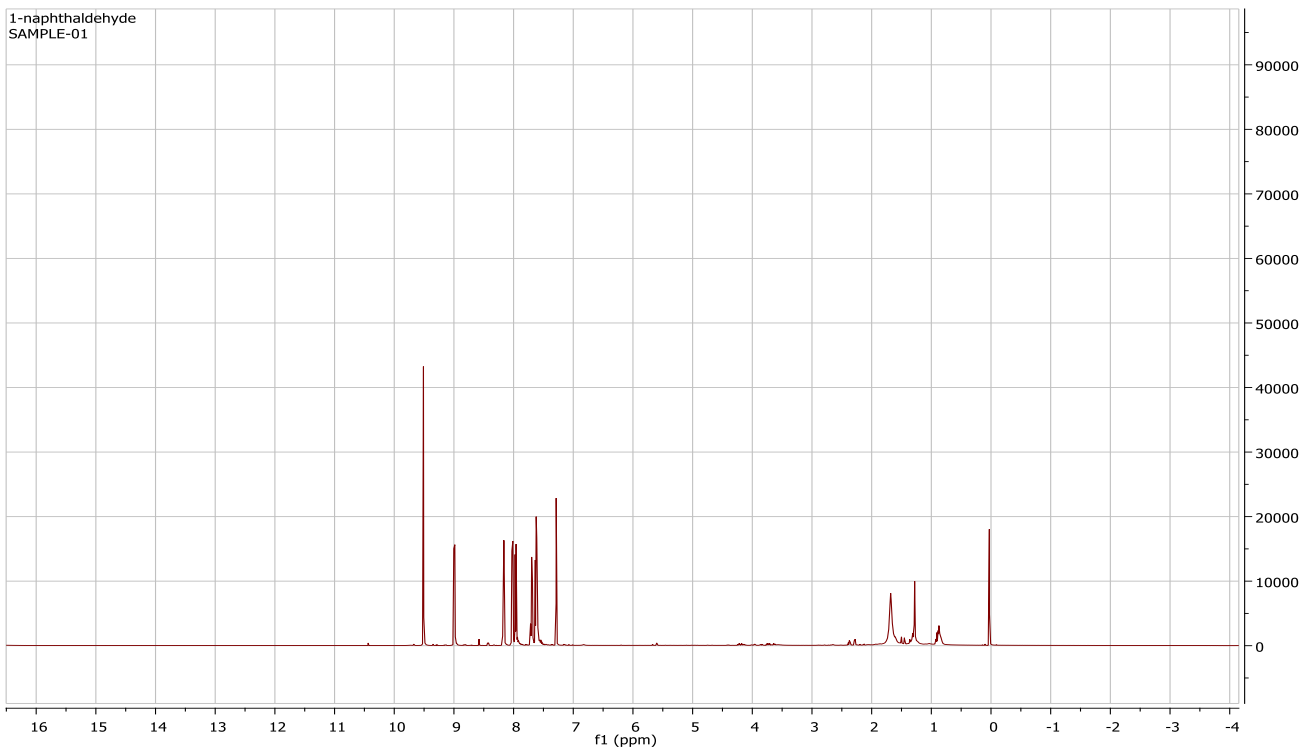


Figure 4.3.1.13a) ^1H NMR spectrum of 1-naphthaldehyde selenosemicarbazone(H^{13}L)

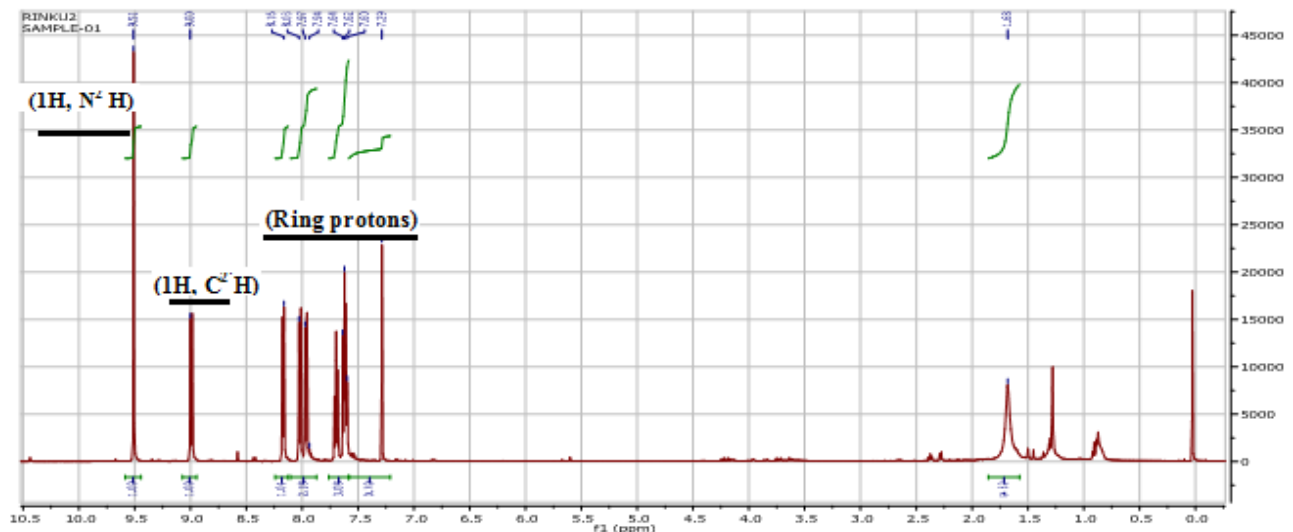


Figure 4.3.1.13b) ^1H NMR spectrum of 1-naphthaldehydeselenosemicarbazone (H^{13}L)(expanded form)

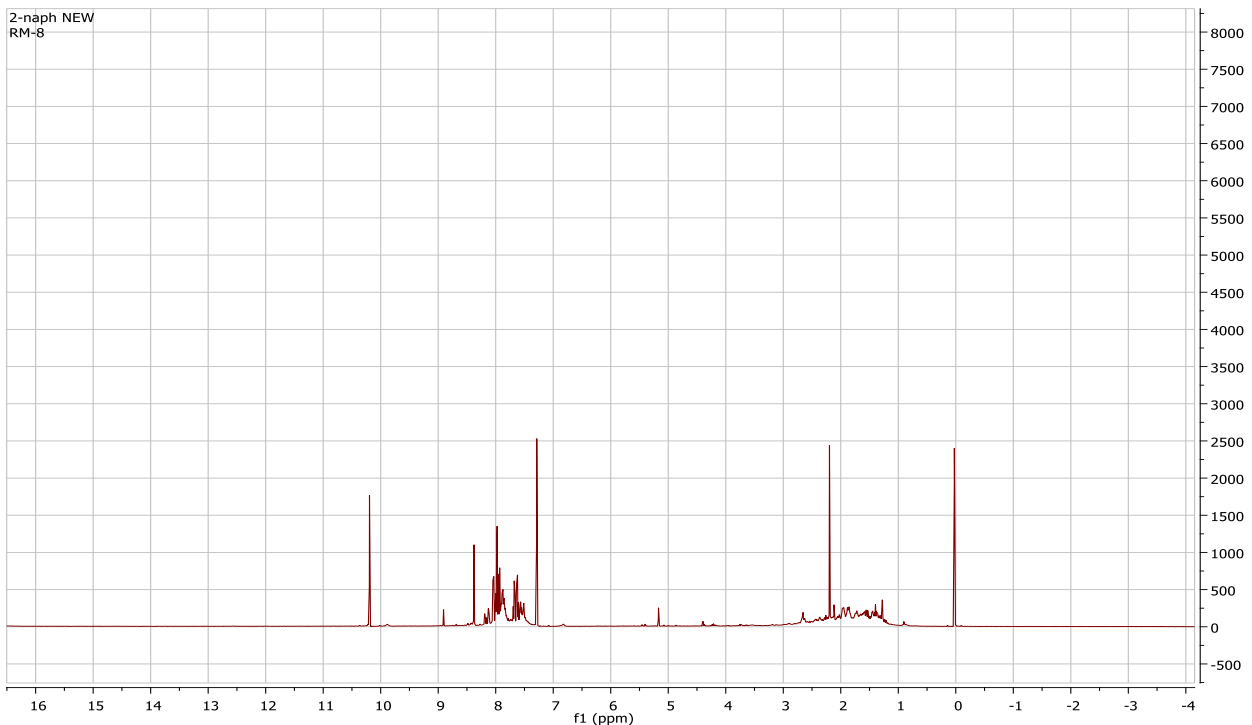


Figure 4.3.1.14a) ^1H NMR spectrum of 2-naphthaldehyde selenosemicarbazone(H^{14}L)

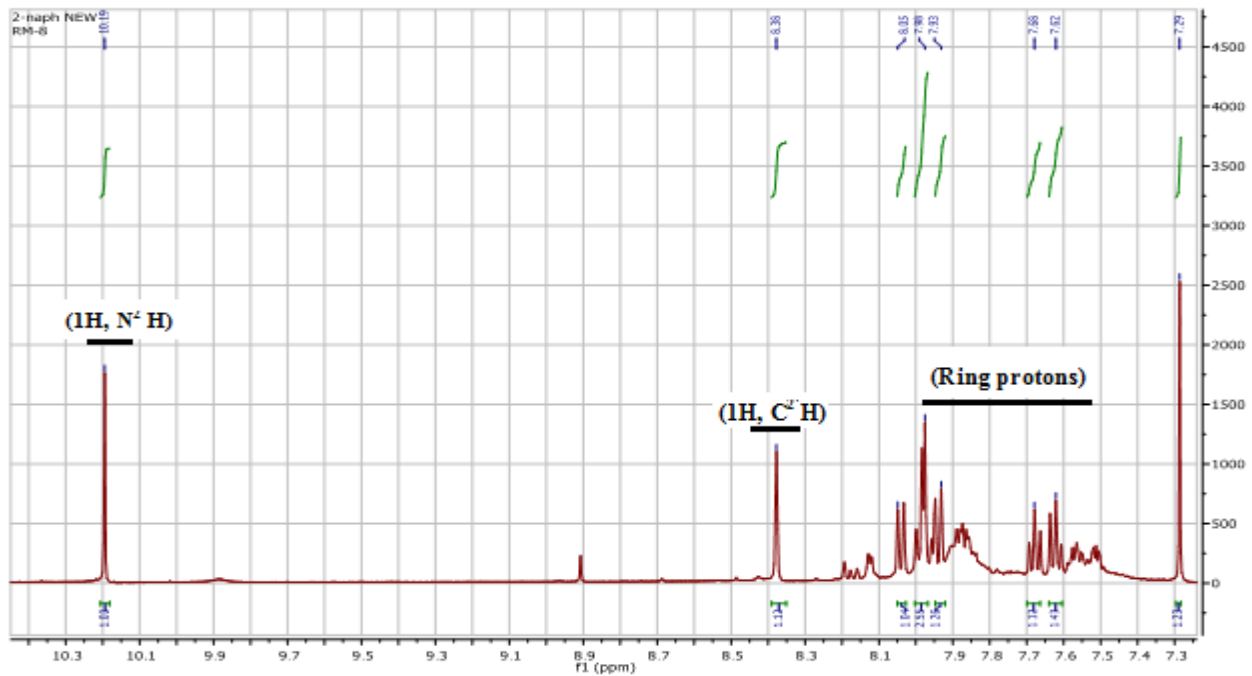


Figure 4.3.1.14b) ^1H NMR spectrum of 2-naphthaldehyde selenosemicarbazone(H^{14}L)(expanded form)

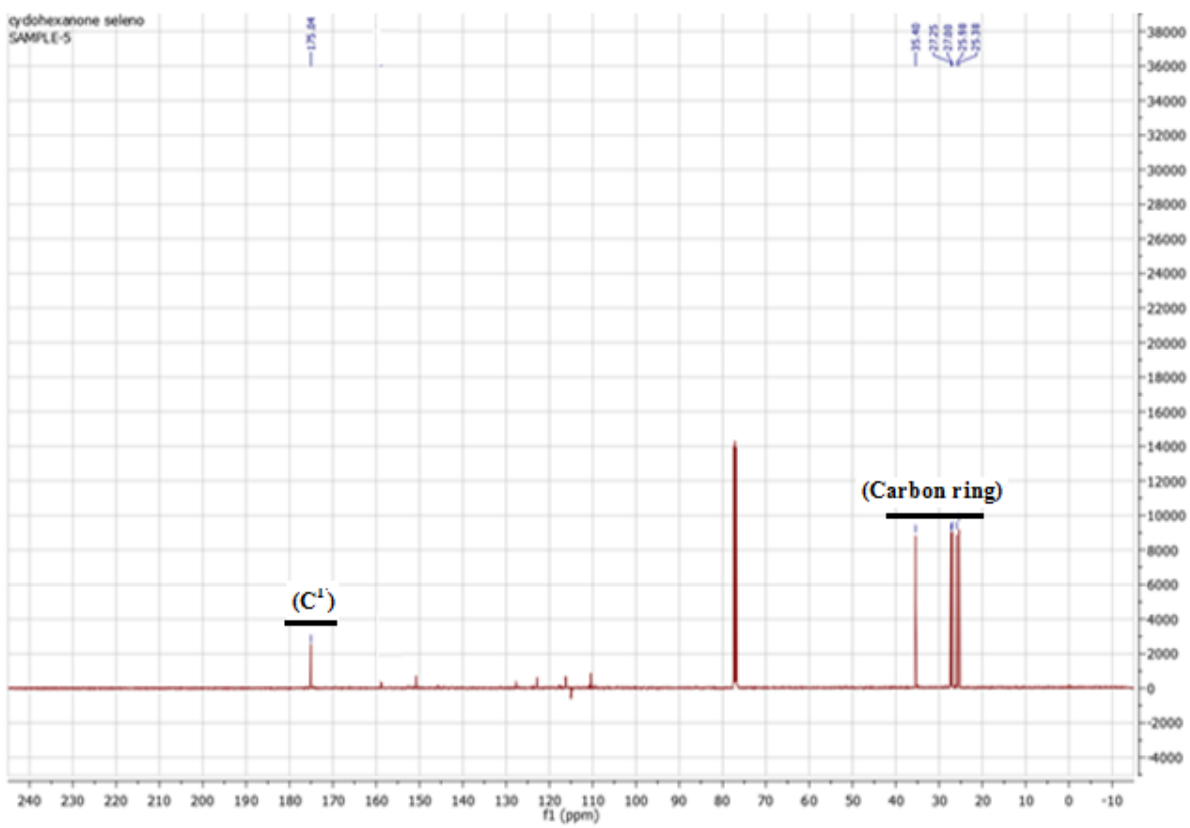


Figure 4.3.2.1 ^{13}C NMR spectrum of cyclohexanoneselenosemicarbazone(H^1L)

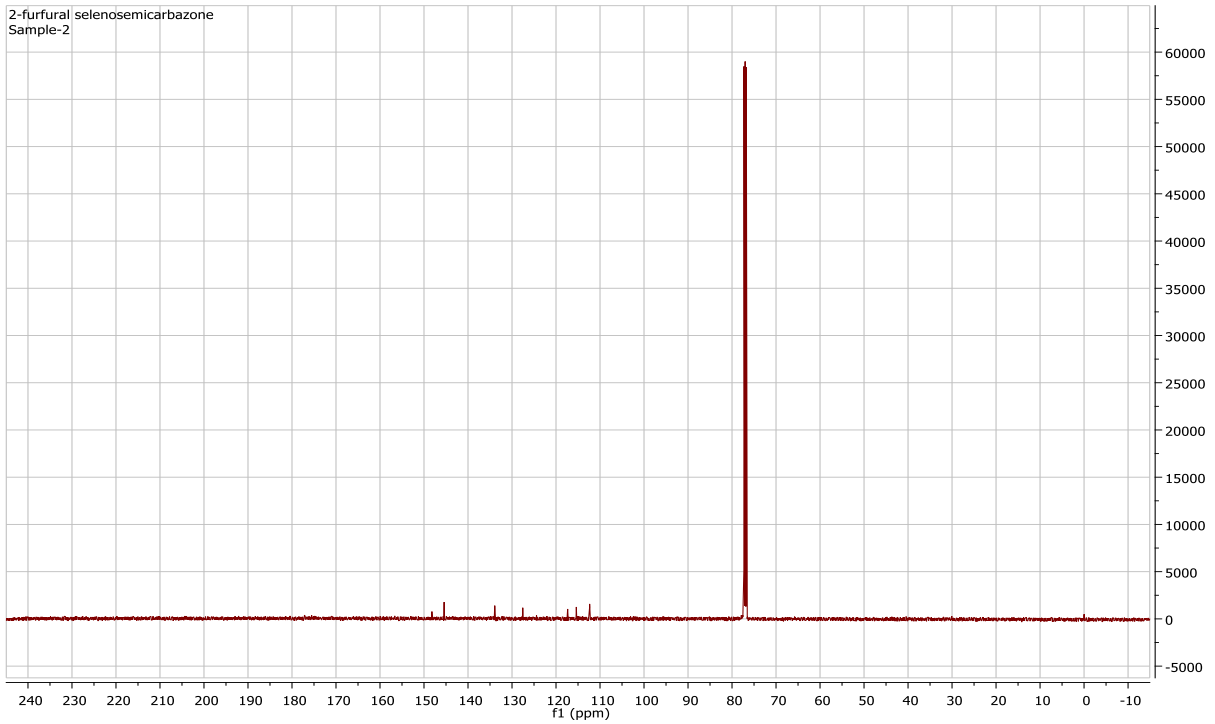


Figure 4.3.2.2a) ^{13}C NMR spectrum of 2-furfural selenosemicarbazone(H^2L)

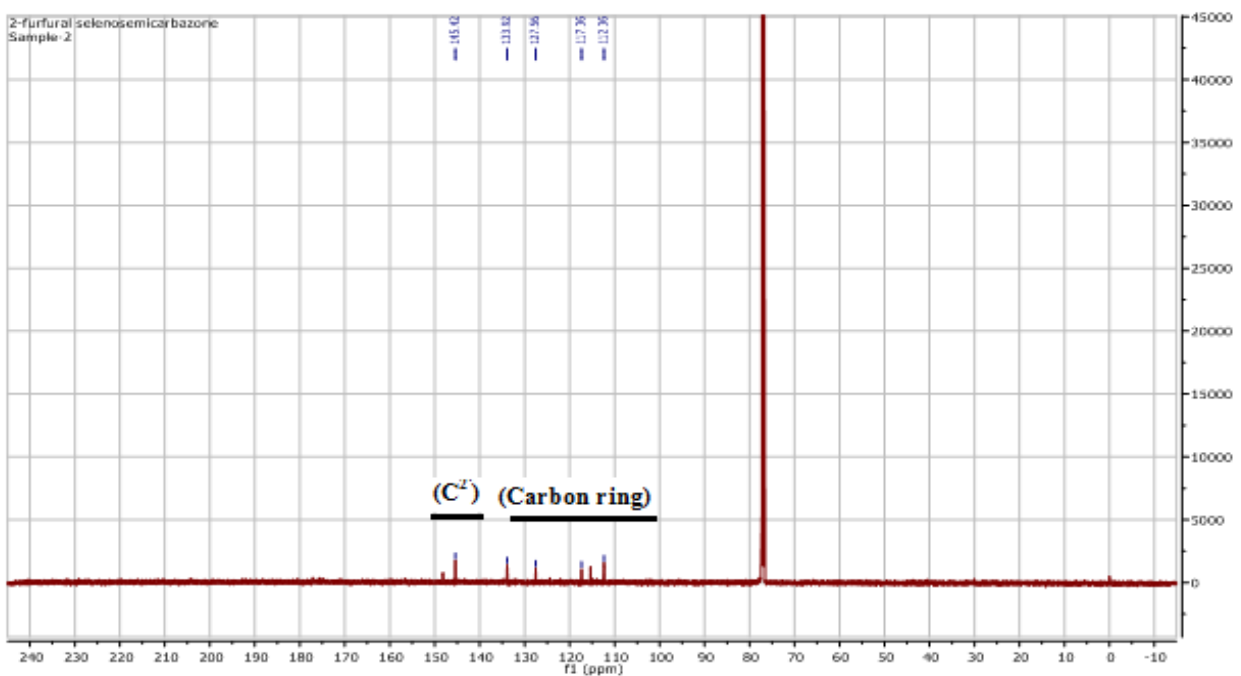


Figure 4.3.2.2b) ^{13}C NMR spectrum of 2-furfural selenosemicarbazone(H^2L)(expanded form)

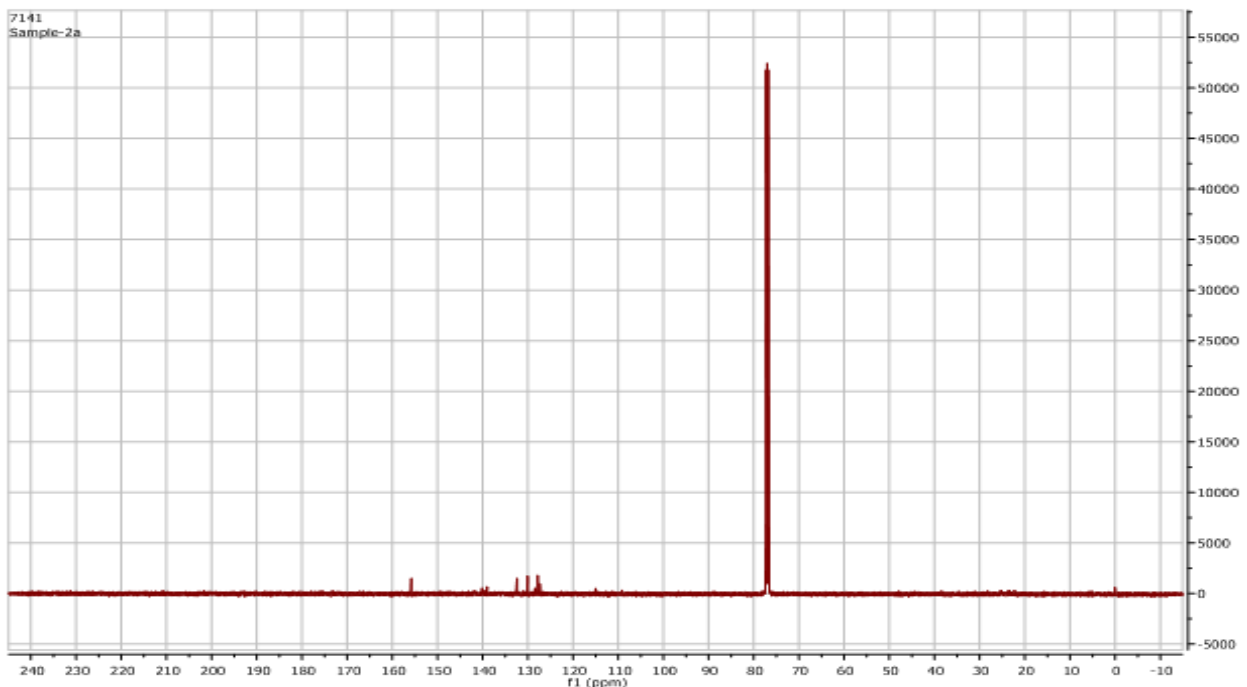


Figure 4.3.2.3a) ^{13}C NMR spectrum of 2-thiophene selenosemicarbazone(H^3L)

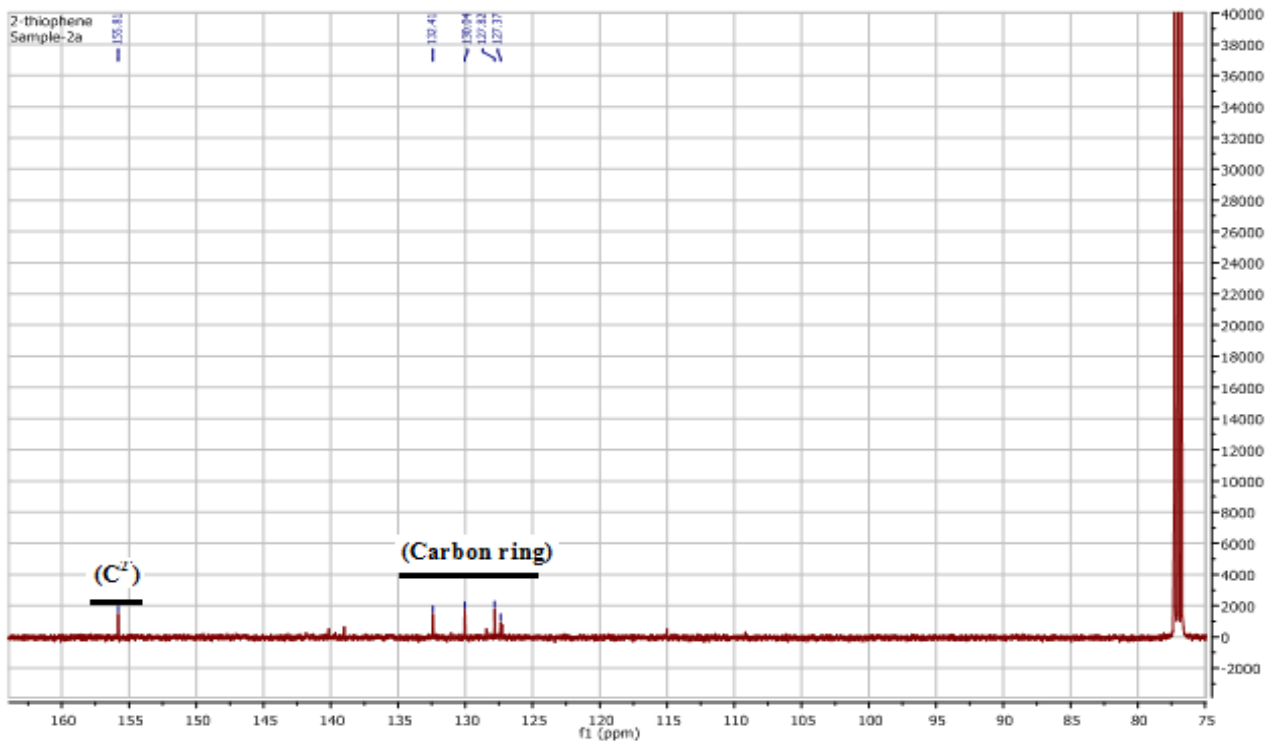


Figure 4.3.2.3b) ^{13}C NMR spectrum of 2-thiophene selenosemicarbazone(H^3L)(expanded form)

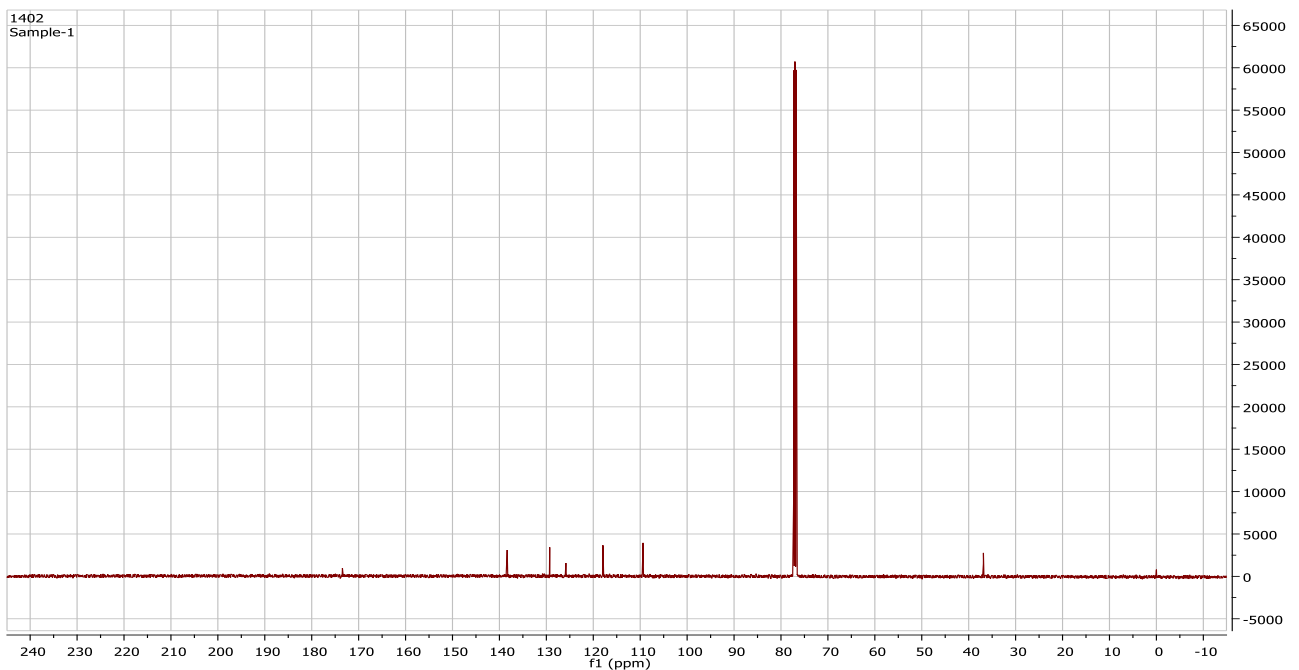


Figure 4.3.2.4a) ^{13}C NMR spectrum of N-methyl-2-pyrrole selenosemicarbazone(H^4L)

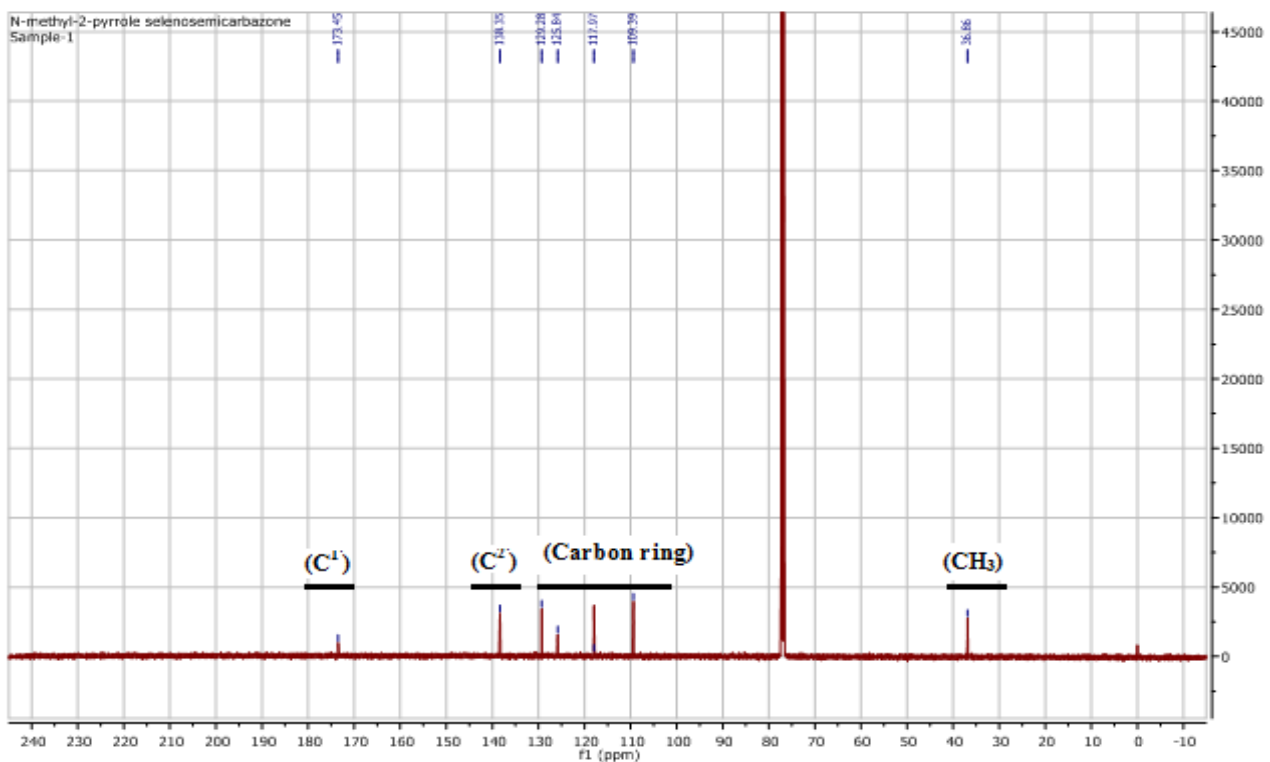


Figure 4.3.2.4b) ^{13}C NMR spectrum of N-methyl-2-pyrrole selenosemicarbazone (H^4L) (expanded form)

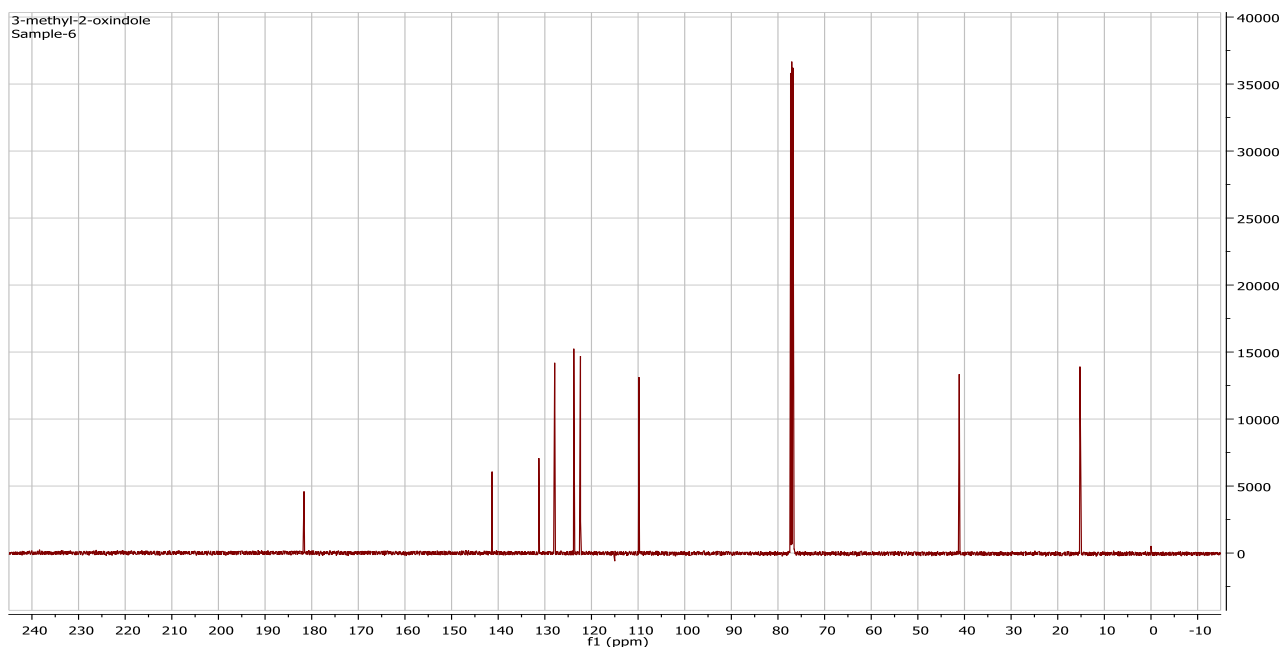


Figure 4.3.2.5a) ^{13}C NMR spectrum of 3-methyl-2-oxindole selenosemicarbazone (H^5L)

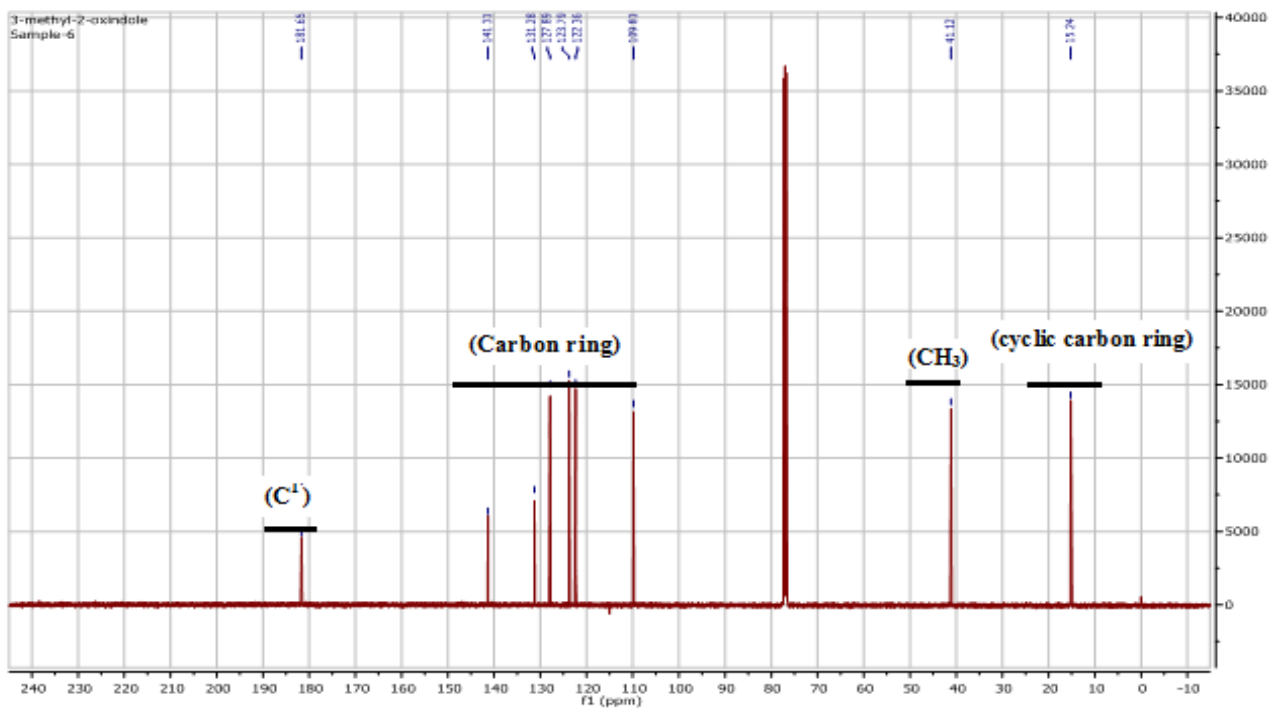


Figure 4.3.2.5b) ^{13}C NMR spectrum of 3-methyl-2-oxindole selenosemicarbazone (H^5L) (expanded form)

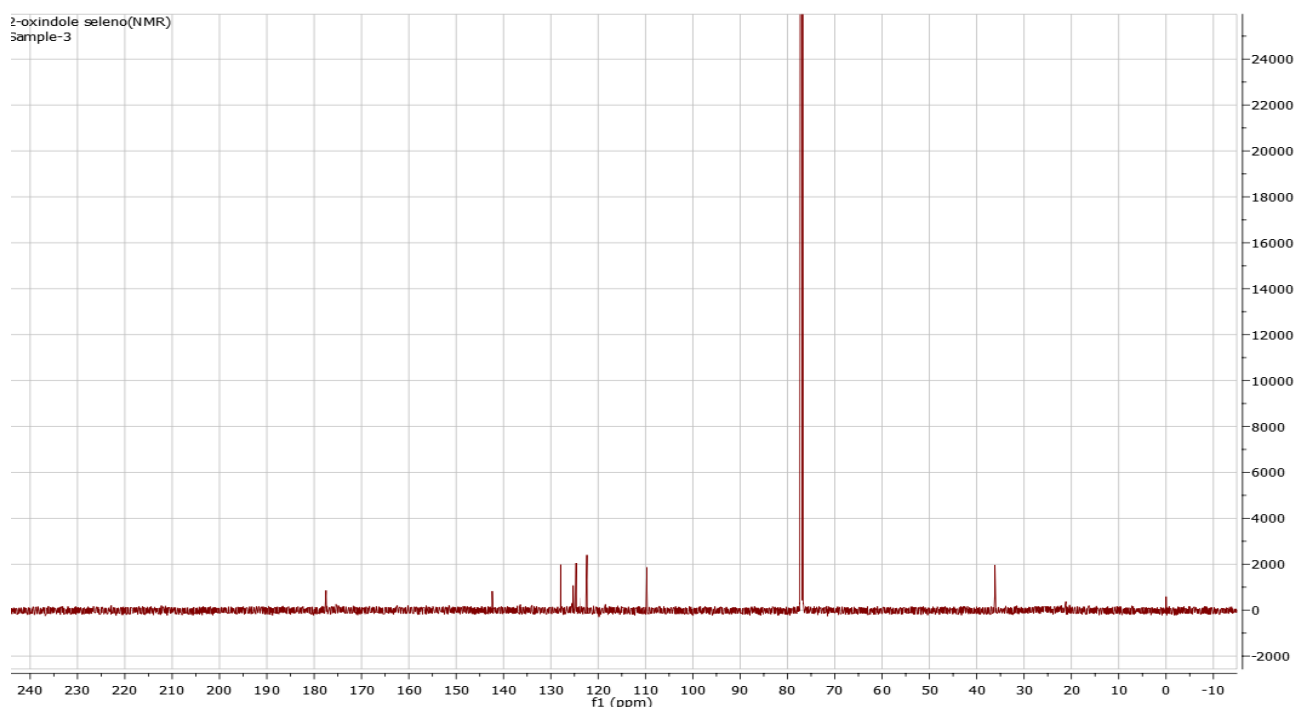


Figure 4.3.2.6a) ^{13}C NMR spectrum of 2-oxindole selenosemicarbazone (H^6L)

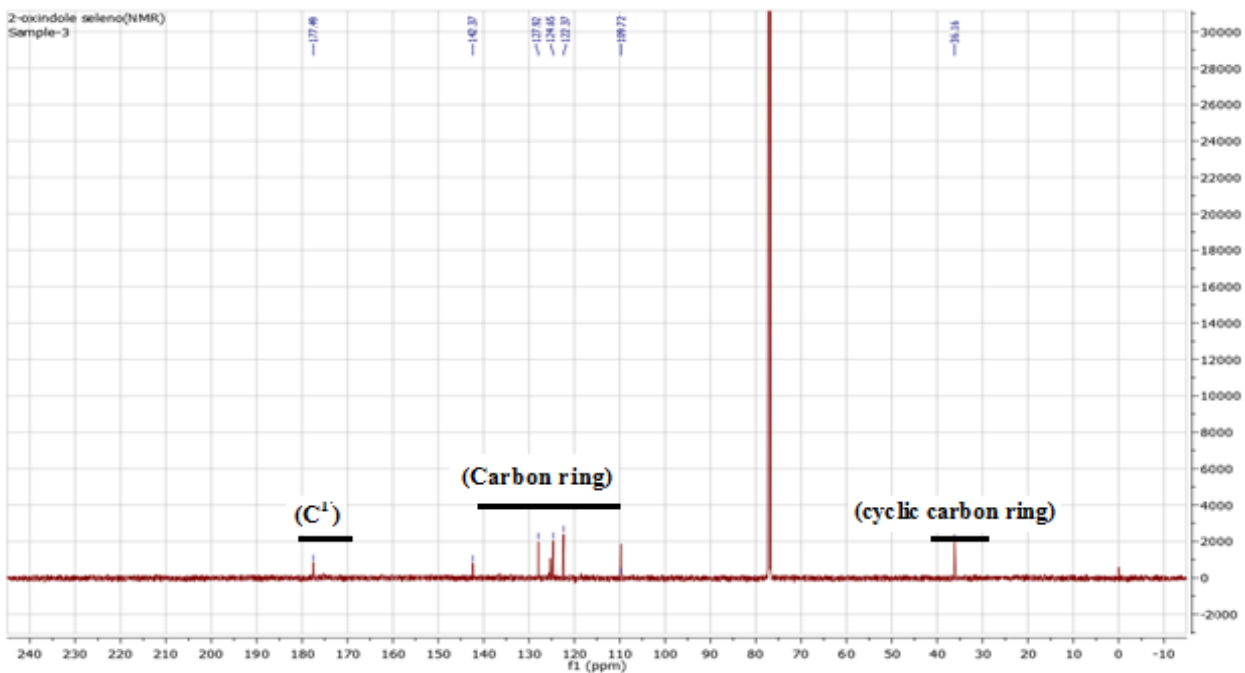


Figure 4.3.2.6b) ¹³C NMR spectrum of 2-oxindole selenosemicarbazone(H^6L)(expanded form)

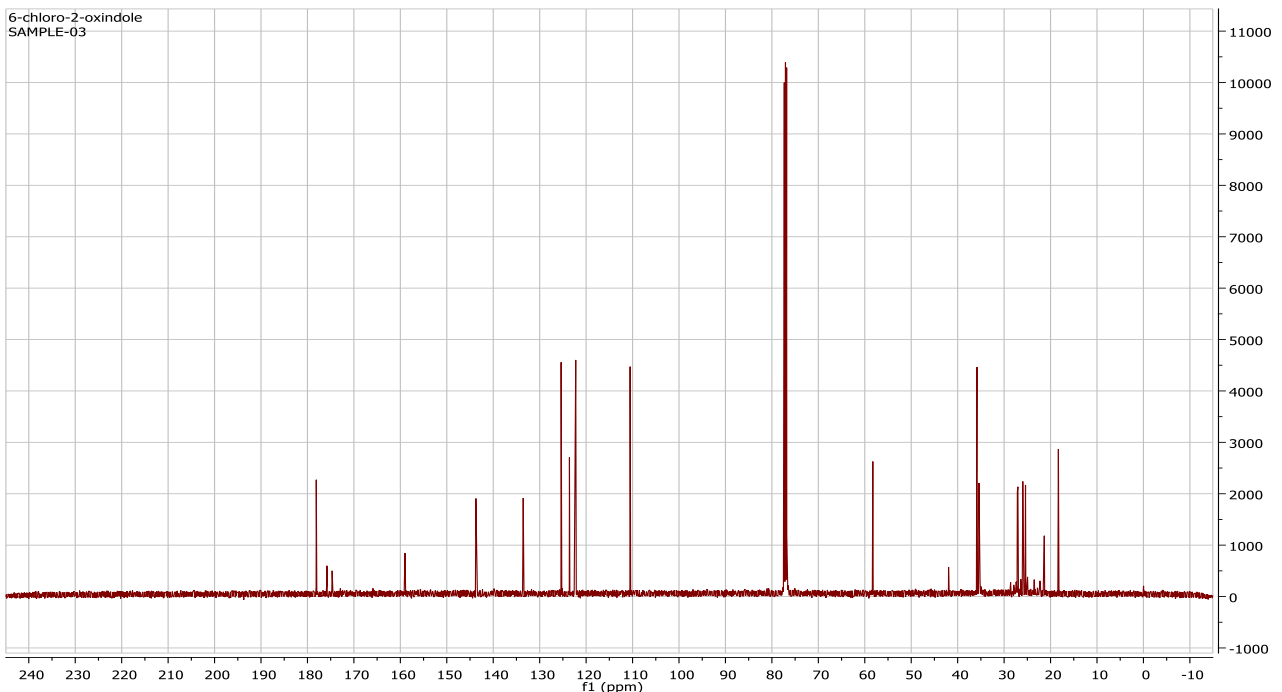


Figure 4.3.2.7a) ¹³C NMR spectrum of 6- chloro-2-oxindole selenosemicarbazone(H^7L)

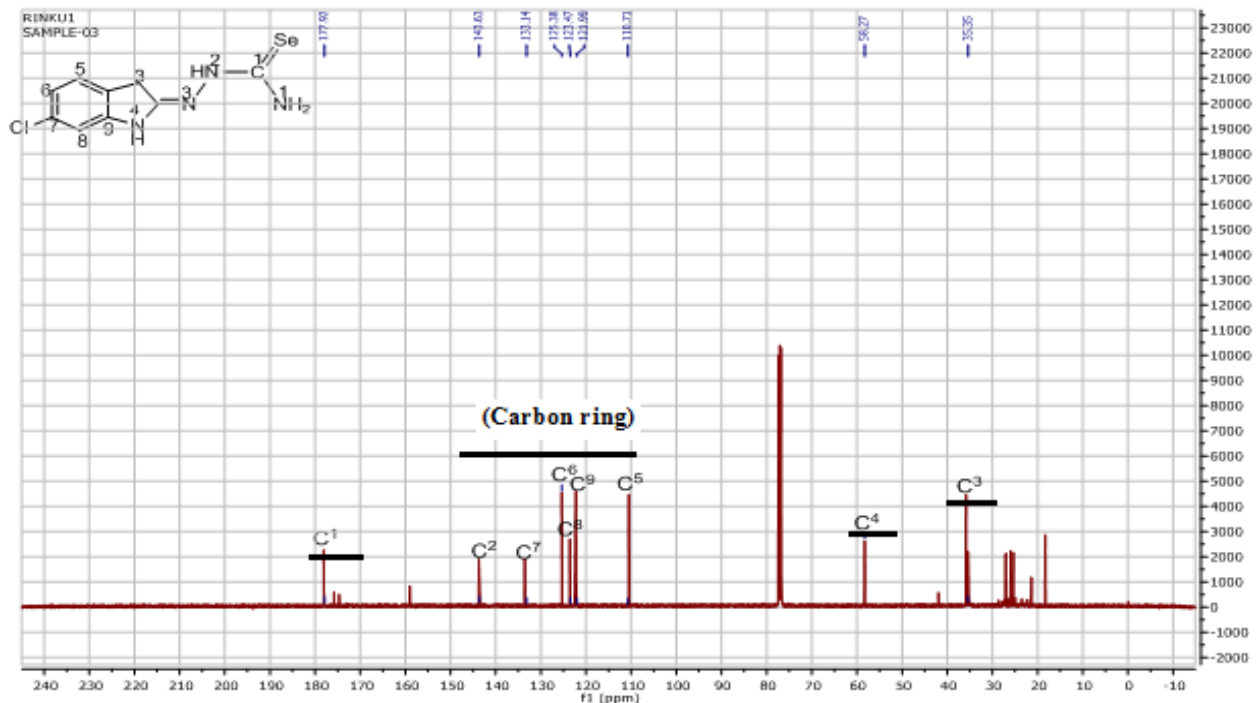


Figure 4.3.2.7b) ^{13}C NMR spectrum of 6-chloro-2-oxindoleselenosemicarbazone (H^6L) (expanded form)

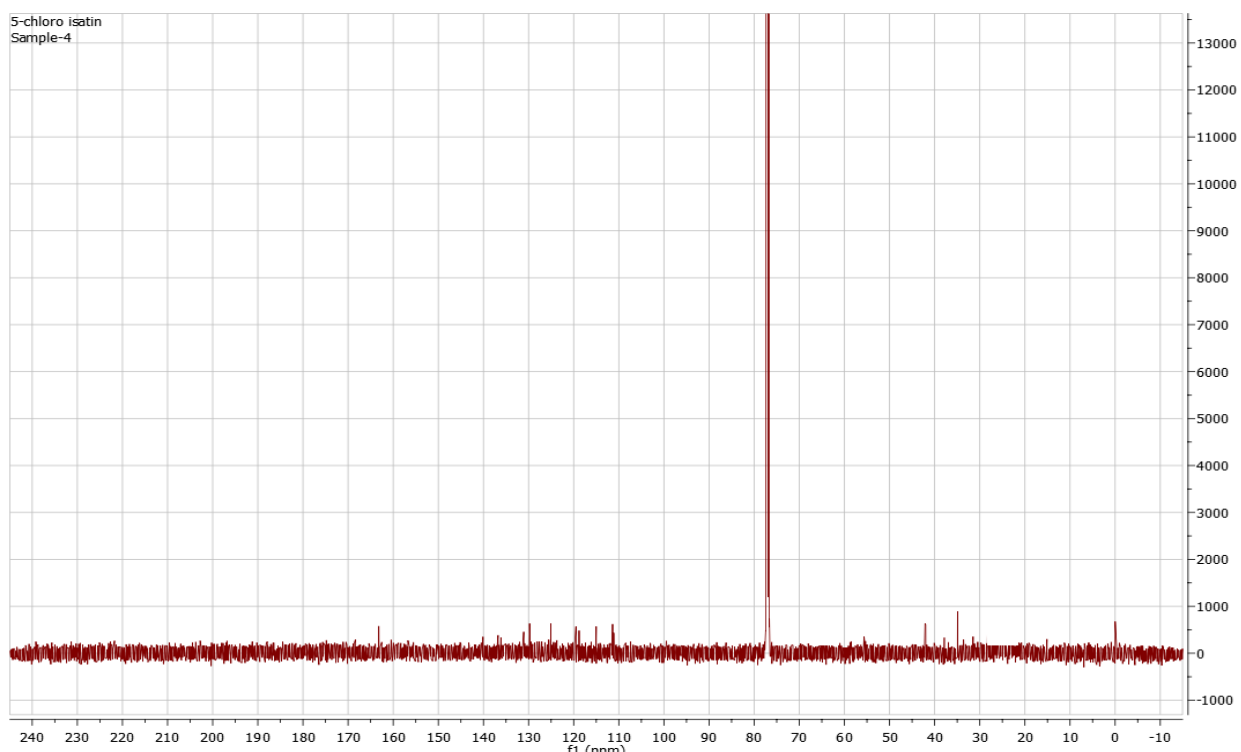


Figure 4.3.2.8a) ^{13}C NMR spectrum of 5-chloro isatin selenosemicarbazone (H^8L)

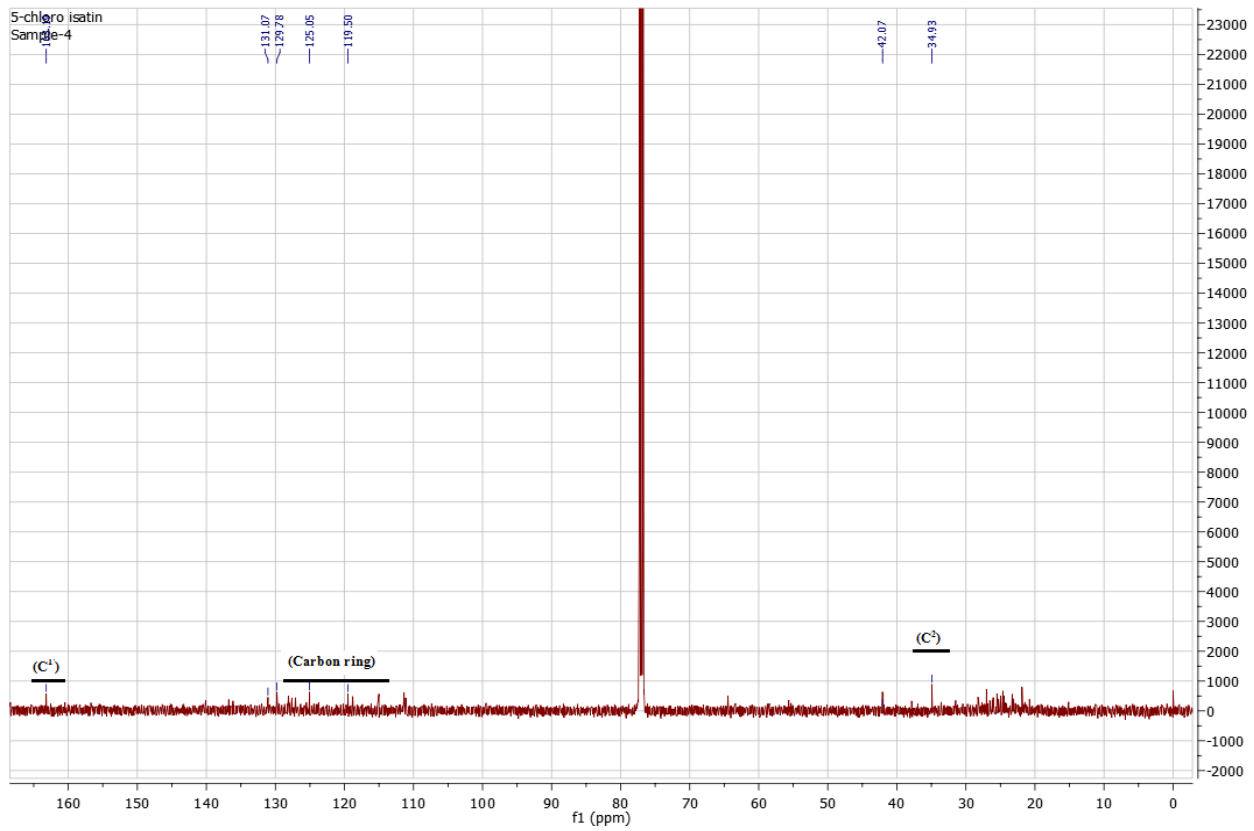


Figure 4.3.2.8b) ^{13}C NMR spectrum of 5- chloro isatin selenosemicarbazone(H^8L)(expanded form)

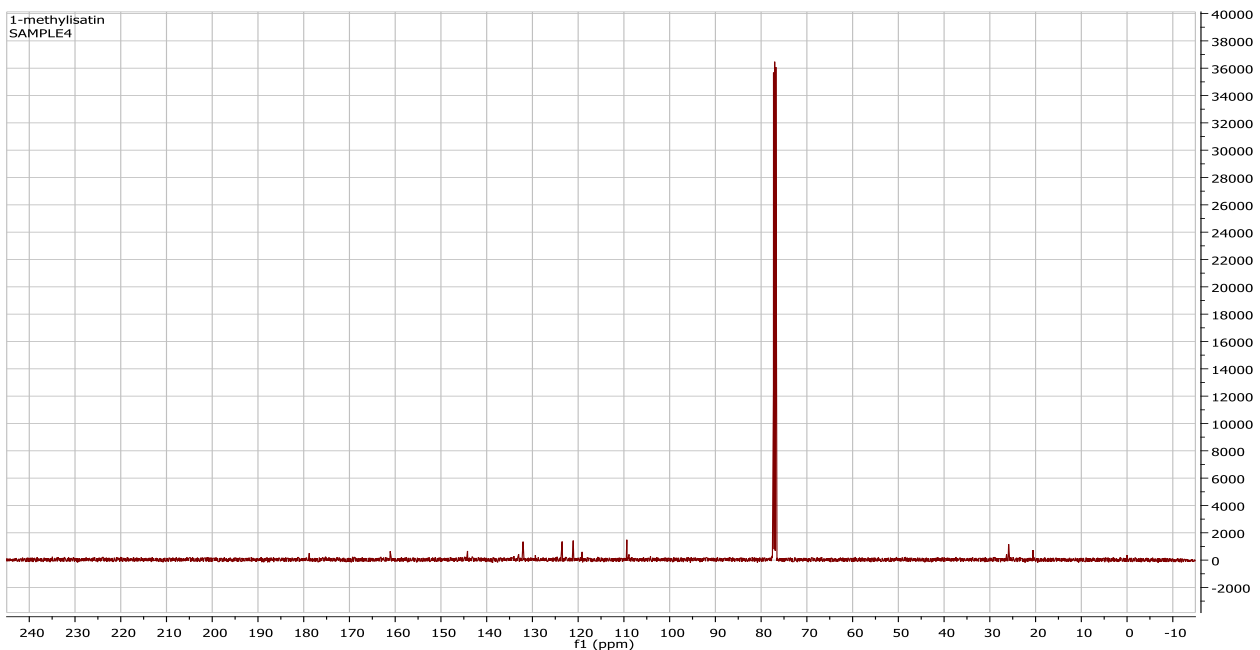


Figure 4.3.2.9a) ^{13}C NMR spectrum of 1-methyl isatin selenosemicarbazone(H^9L)

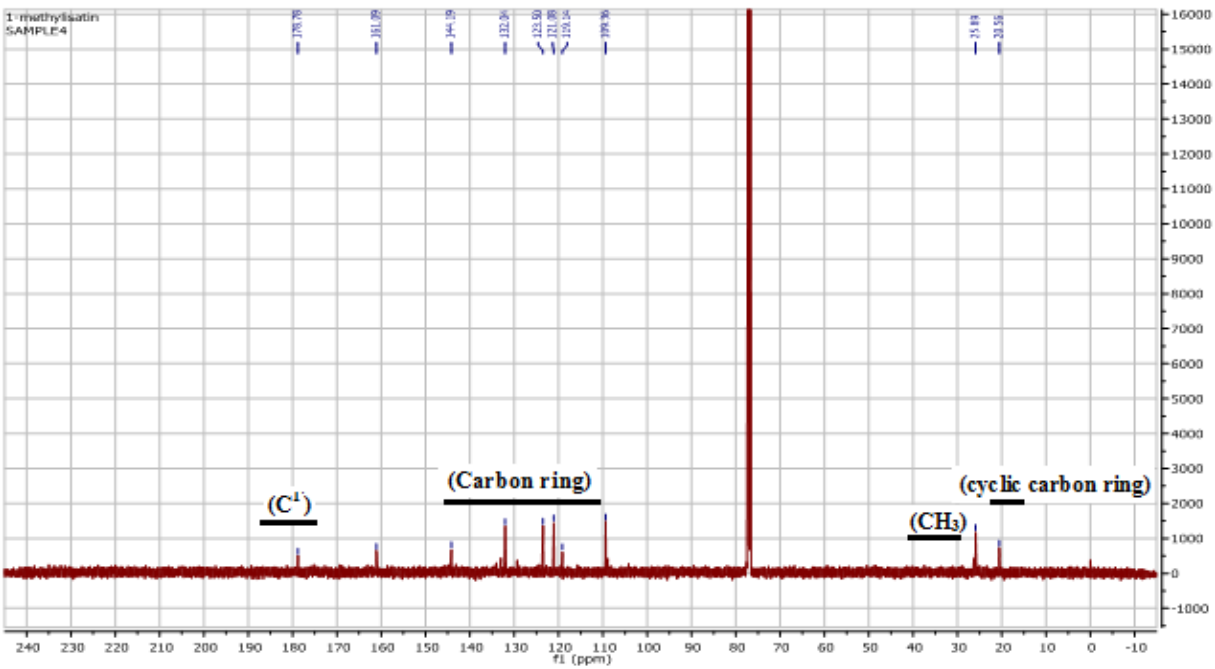


Figure 4.3.2.9b) ^{13}C NMR spectrum of 1-methylisatinselenosemicarbazone(H^9L)(expanded form)

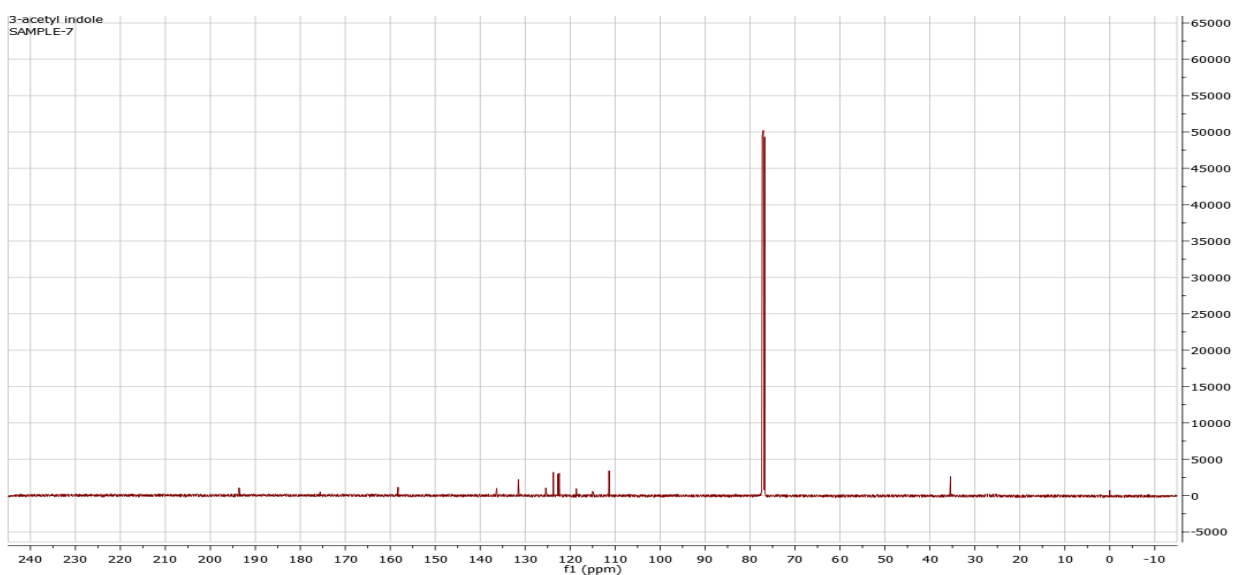


Figure 4.3.2.11a) ^{13}C NMR spectrum of 3-acetyl indole selenosemicarbazone(H^{11}L)

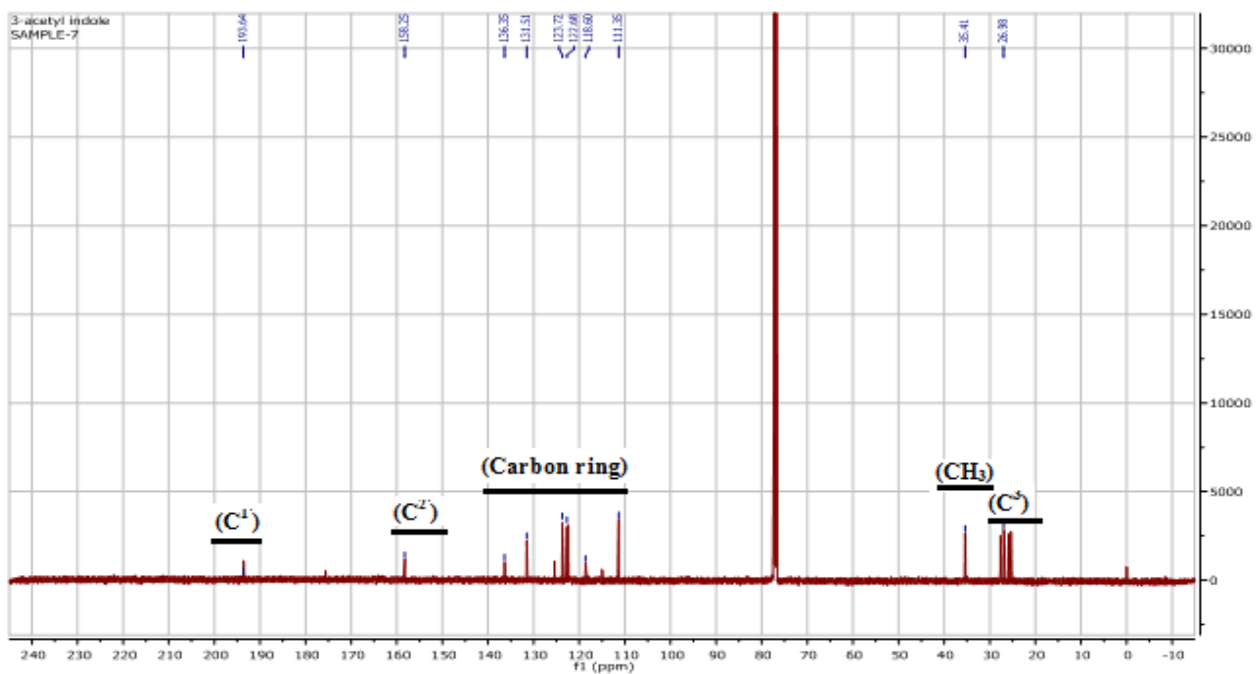


Figure 4.3.2.11b) ^{13}C NMR spectrum of 3-acetyl indoleselenosemicarbazone(H^{11}L)(expanded form)

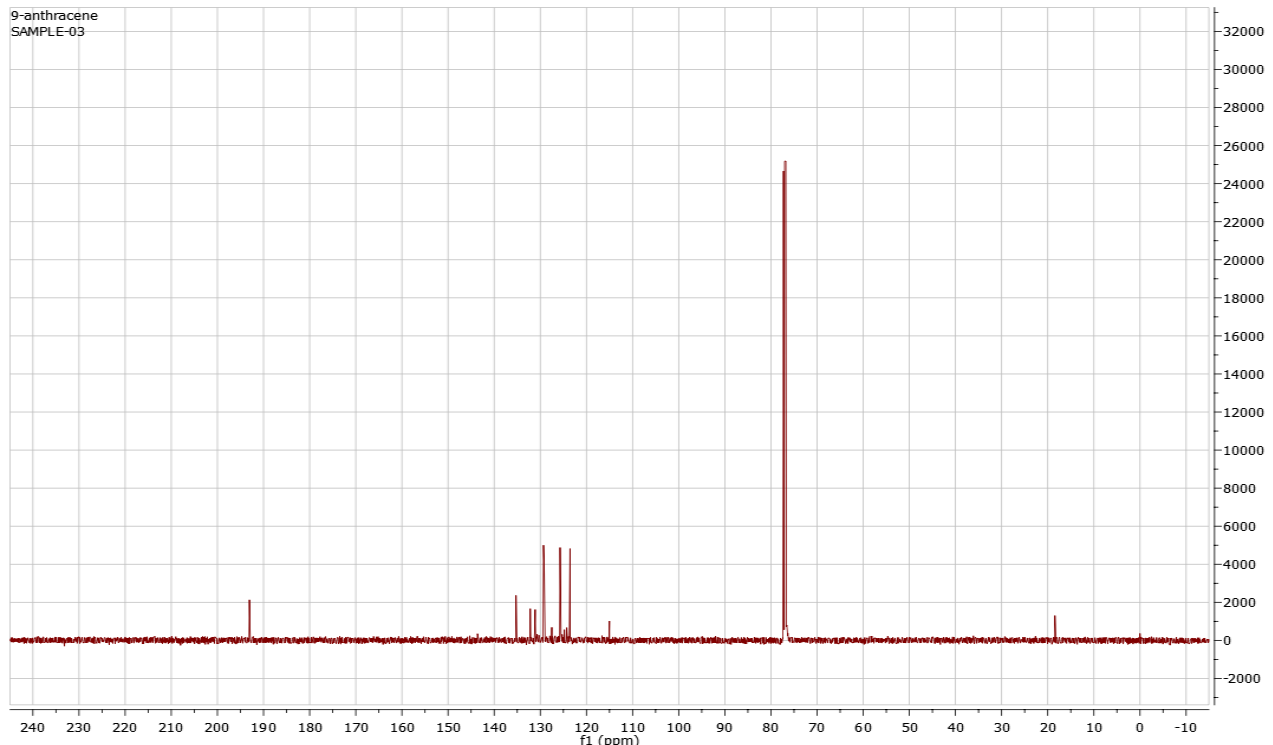


Figure 4.3.2.12a) ^{13}C NMR spectrum of 9-anthracene selenosemicarbazone(H^{12}L)

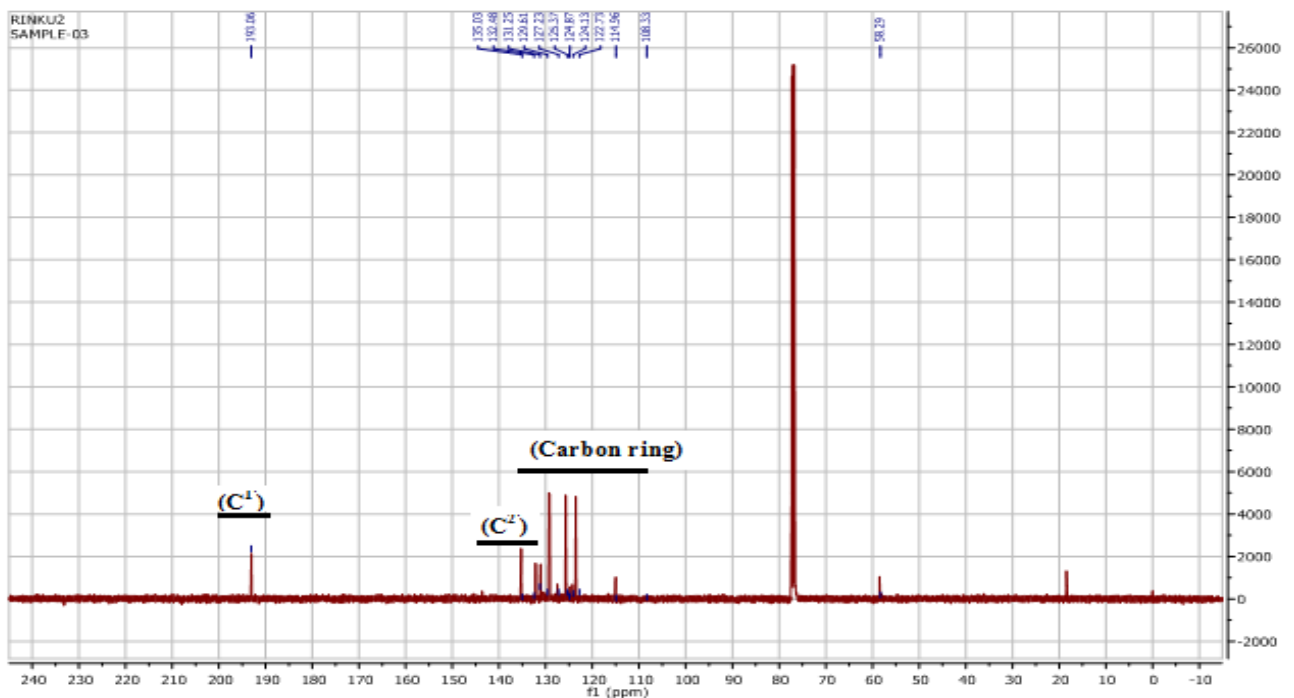


Figure 4.3.2.12b) ^{13}C NMR spectrum of 9-anthraceneselenosemicarbazone(H^{12}L)(expanded form)

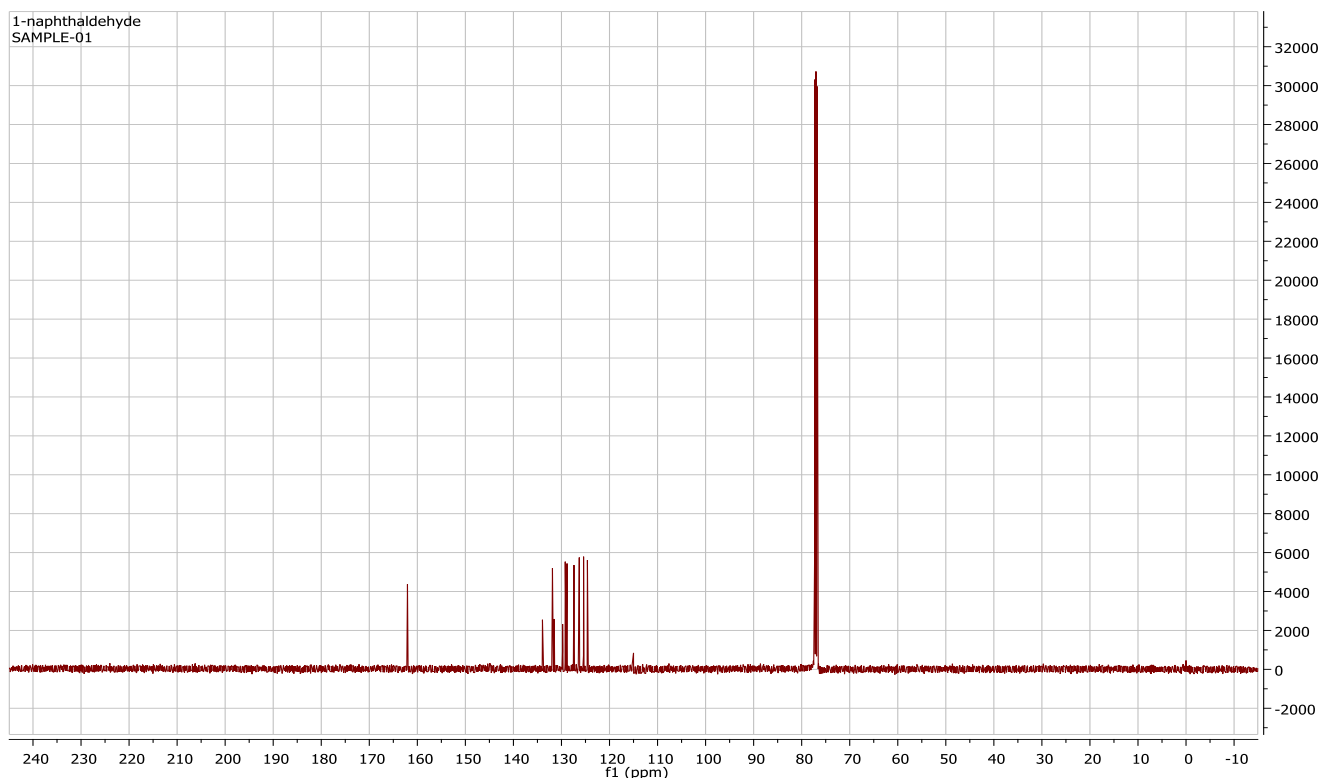


Figure 4.3.2.13a) ^{13}C NMR spectrum of 1-naphthaldehyde selenosemicarbazone(H^{13}L)

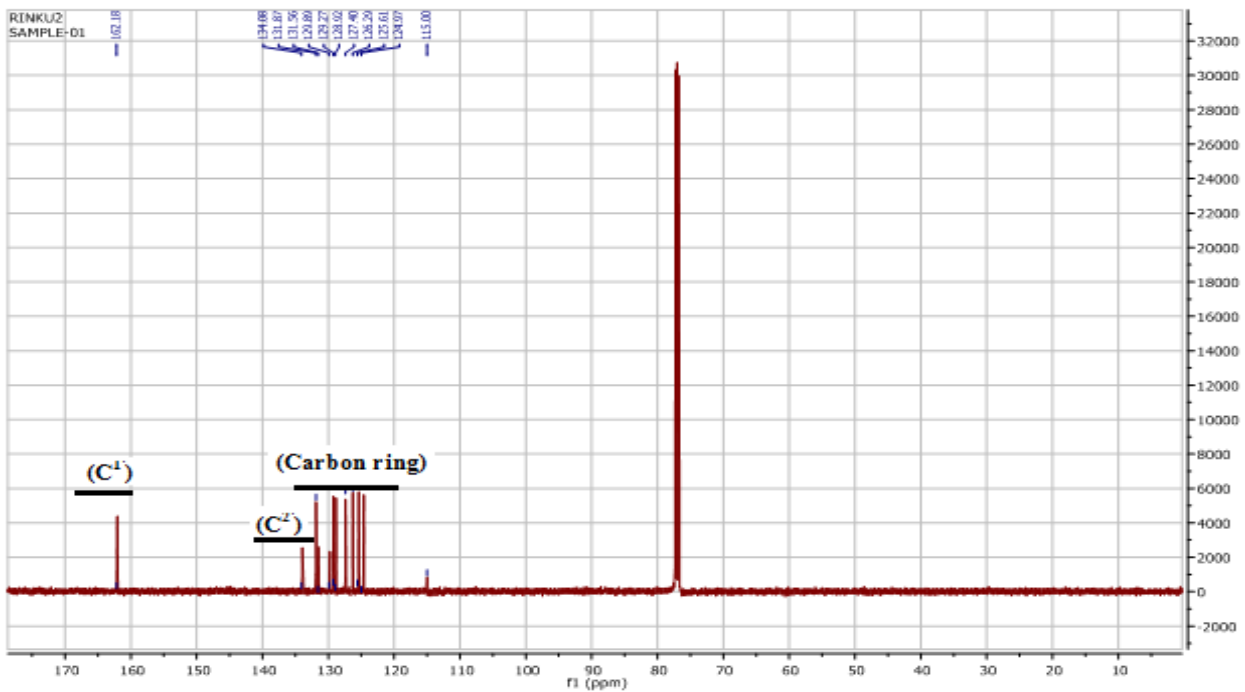


Figure 4.3.2.13b) ^{13}C NMR spectrum of 1-naphthaldehydeselenosemicarbazone (H^{13}L) (expanded form)

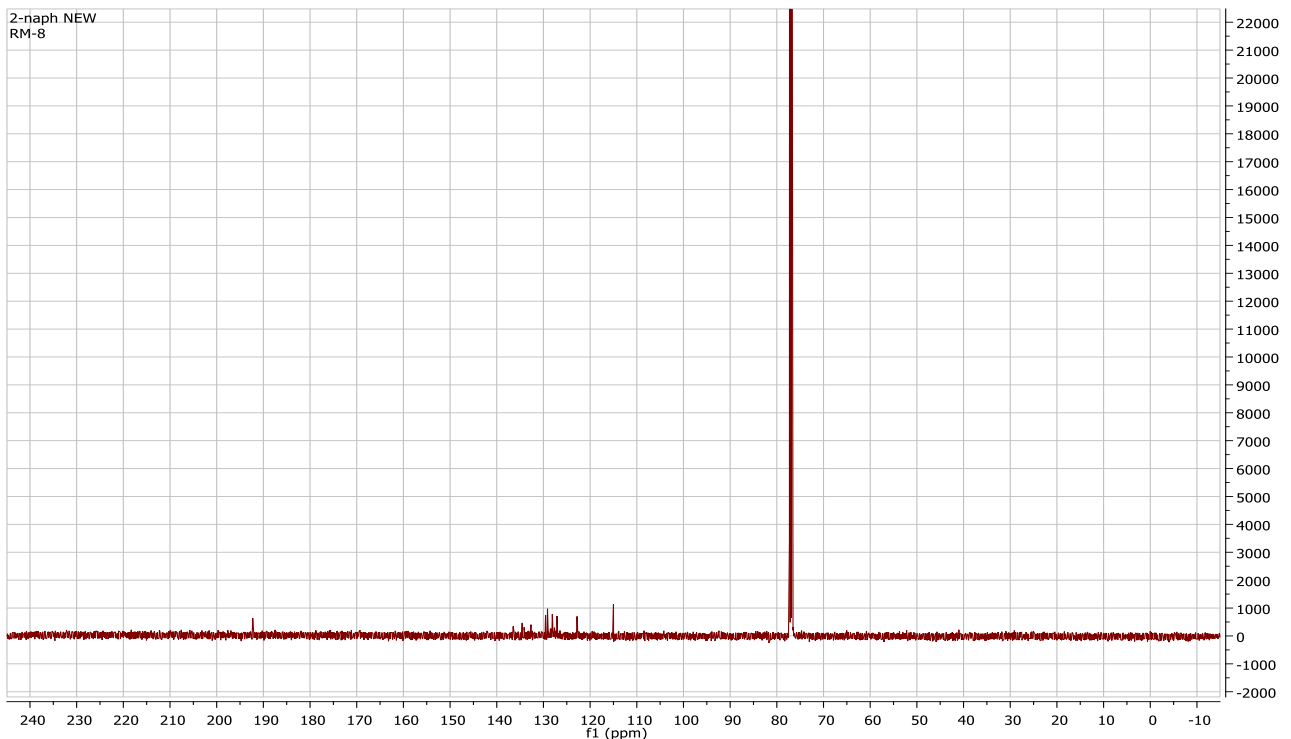


Figure 4.3.2.14a) ^{13}C NMR spectrum of 2-naphthaldehydeselenosemicarbazone (H^{14}L)

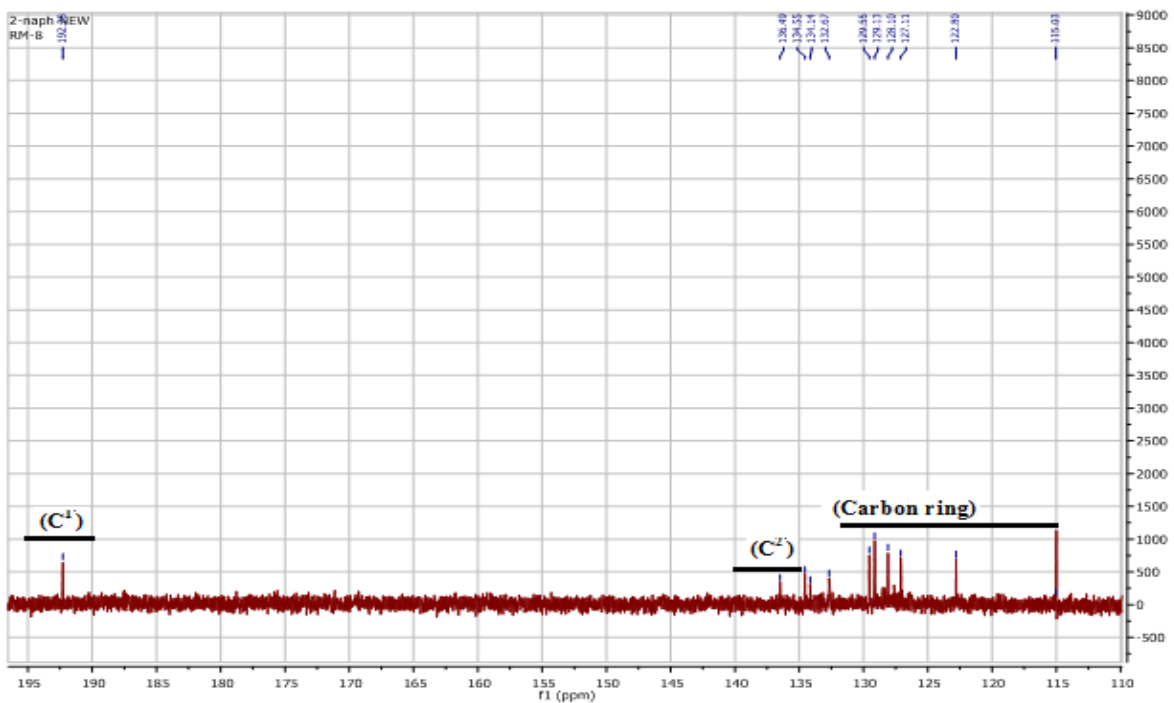


Figure 4.3.2.14b) ^{13}C NMR spectrum of 2-naphthaldehyde selenosemicarbazone(H^{14}L) (expanded form)

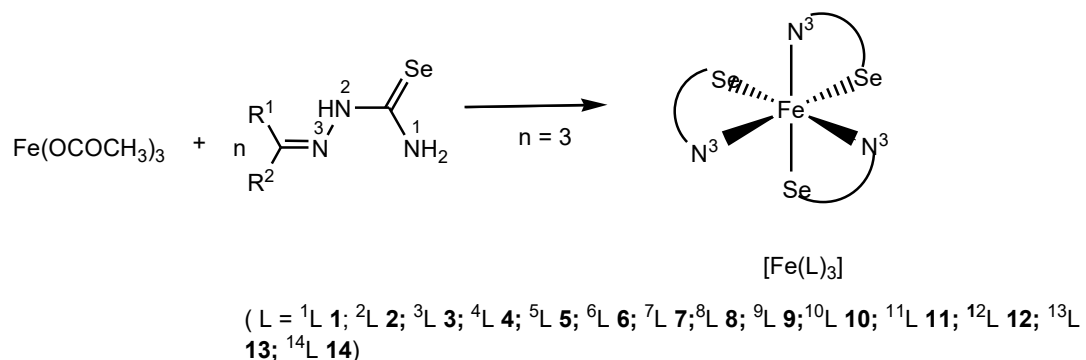
CHAPTER 5

IRON(III) COMPLEXES

5. Complexes of Iron(III)

5.1 Discussion on Synthesis of Iron metal complexes

Reaction of synthesized selenosemicarbazones ligands ($H^1L-H^{14}L$) with iron acetate in 3: 1(L : M) molar ratio has formed complexes of stoichiometry, $[Fe(L)_3]$ ($L = ^1L \text{ 1}; ^2L \text{ 2}; ^3L \text{ 3}; ^4L \text{ 4}; ^5L \text{ 5}; ^6L \text{ 6}; ^7L \text{ 7}; ^8L \text{ 8}; ^9L \text{ 9}; ^{10}L \text{ 10}; ^{11}L \text{ 11}; ^{12}L \text{ 12}; ^{13}L \text{ 13}; ^{14}L \text{ 14}$) (Scheme 5.1)



Scheme 5.1

All the synthesized complexes alongwith the structure of their respective selenosemicarbazones are given in Table 5.1

Table 5.1 list of selenosemicarbazone complexes of iron(III) **1-14**

Sr. No.	Selenosemicarbazone Ligands	Structure of Selenosemicarbazone Ligands	Complexes Formed
1.	Cyclohexanone selenosemicarbazone (Hcysesc, H¹L)		$[Fe(cysesc)_3]\text{1}$

2.	2-furfural selenosemicarbazone (2-Hfursesc, H²L)		[Fe(2-fursesc) ₃]2
3.	2-thiophene selenosemicarbazone (2-Hthiosesc, H³L)		[Fe(2-thiosesc) ₃]3
4.	N-methyl-2-pyrrole selenosemicarbazone (N-MeHPysesc, H⁴L)		[Fe(N-mepysesc) ₃]4
5.	3-methyl-2-oxindole selenosemicarbazone (3-MeHOxsesc, H⁵L)		[Fe(3-meoxsesc) ₃]5
6.	2-oxindole selenosemicarbazone (2-HOxsesc, H⁶L)		[Fe(2-oxsesc) ₃]6
7.	6-chloro-2-oxindole selenosemicarbazone (6-ClHOxsesc, H⁷L)		[Fe(6-cloxsesc) ₃]7
8.	5-chloro isatin selenosemicarbazone (5-ClHIstsesc, H⁸L)		[Fe(5-clistsesc) ₃]8

9.	1-methyl isatin selenosemicarbazone (1-MeHIsesc, H⁹L)		[Fe(1-meistsesc) ₃]9
10.	indole-3-selenosemicarbazone (3-HIndsesc, H¹⁰L)		[Fe(3-insesc) ₃]10
11.	3-acetyl indole selenosemicarbazone (3-AcHIndsesc, H¹¹L)		[Fe(3-acinsesc) ₃]11
12.	9-anthrinaldehyde selenosemicarbazone (9-HAnsesc, H¹²L)		[Fe(9-ansesc) ₃]12
13.	1-Naphthaldehyde selenosemicarbazone (1-HNapsesc, H¹³L)		[Fe(1-naphsesc) ₃]13
14.	2-Naphthaldehyde selenosemicarbazone (2-HNapsesc, H¹⁴L)		[Fe(2-naphsesc) ₃]14

5.2 IR Spectroscopy:

Important IR peaks of selenosemicarbazones and their iron(III) complexes are given in Table 5.2 and IR spectra of complexes **1-14** are given in Figures 5.2.1-5.2.14. The $\nu(\text{NH})$ band due to amino group in free ligands appeared in the range 3417-3223 cm^{-1} (H^1L - H^{14}L), which get slightly shifted to lower energy and appear in the range, 3399-3217 cm^{-1} .

Disappearance of amide band $\nu(-\text{NH}-)$ vis-a vis free ligands (appeared in the range 3157-3110 cm^{-1}) in complexes **1-14** indicates deprotonation and co-ordination of ligand to metal in anionic form. In some of the complexes a weak peak may appear in the range 3192-3147 cm^{-1} due to the NH group of heterocyclic ring which makes it difficult to determine the binding of ligand in neutral or anionic form.

The C=Se band in the ligands appeared in the range 898-854 cm^{-1} . On complexation with Fe(III), this band shifted to low energy and appeared in the range 780-715 cm^{-1} . The lower energy shift indicates the change of C=Se to C-Se⁻ thus suggests binding of ligand in selenate form [75]. Other IR peaks like $\nu(\text{C}=\text{N})$, $\nu(\text{C}=\text{C})$ and $\delta(\text{NH}_2)$ appeared in the range 1671-1411 cm^{-1} in complexes and showed no significant change vis-à-vis free ligands.

Table 5.2 Important IR peaks of selenosemicarbazones (H^1L - H^{14}L) and iron(III) complexes (**1-14**)

Synthesised Ligands and Metal Complexes	$\nu(\text{NH}_2)$	$\nu(-\text{NH}-)$	$\nu(\text{C}=\text{N})$, $\nu(\text{C}=\text{C})$, δ (NH_2)	$\nu(\text{C}=\text{Se})$	$\nu(-\text{NH}-)$ heterocyclic ring
Cyclohexanone Selenosemicarbazone (Hcysesc, H^1L)	3362m, 3225m	3157w	1591s, 1489m, 1454s	856s	-
[Fe(cysesc) ₃] 1	3354m	-	1635s, 1504m, 1438s	748s	-
2-furfural selenosemicarbazone (2-Hfursesc, H^2L)	3379m, 3340m	3142w	1600s, 1579m, 1464s	812s	-
[Fe(2-fursesc) ₃] 2	3366m	-	1617s, 1537m, 1439s	738s	-
2-thiophene selenosemicarbazone (2-Hthiosesc, H^3L)	3389m, 3221m	3095w	1599s, 1527m, 1415s	844s	-
[Fe(2-thiosesc) ₃] 3	3219m	-	1671s, 1605m, 1419s	715s	-

N-methyl-2-pyrrole selenosemicarbazone (N-MeHPysesc, H⁴L)	3412m, 3223m	3110w	1633s, 1562m, 1496s	854s	-
[Fe(N-mepysesc) ₃]4	3399m, 3244m	-	1599s, 1504m, 1465s	767s	-
3-methyl-2-oxindole selenosemicarbazone (3-MeHOxsesc, H⁵L)	3358m, 3248m	3157w	1591s, 1489m, 1425s	854s	-
[Fe(3-meoxsesc) ₃]5	3226m	-	1695s, 1617s, 1559m, 1447s	747s	-
2-oxindole selenosemicarbazone (2-HOxsesc, H⁶L)	3362m, 3225m	3157w	1591s, 1489m, 1454s	856s	-
[Fe(2-oxsesc) ₃]6	3267m	-	1656s, 1570m, 1411s	740s	3147w
6-chloro-2-oxindole selenosemicarbazone (6-ClHOxsesc, H⁷L)	3417m, 3255m	3142w	1589s, 1512m, 1499s	879s	-
[Fe(6-cloxsesc) ₃]7	3267m	-	1646s, 1517m, 1427s	739s	3192w
5-chloroisatin selenosemicarbazone (5-ClHIstsesc, H⁸L)	3219m	3110w	1694s, 1618s, 1559m, 1447s	885s	-
[Fe(5-clistsesc) ₃]8	3217m	-	1614s, 1511m, 1460s	747s	-
1-methylisatin selenosemicarbazone (1-MeHIstsesc, H⁹L)	3408m, 3228m	3128w	1676s, 1604s, 1492m, 1415s	889s	-
[Fe(1-meistsesc) ₃]9	3219m	-	1607m, 1466s	750s	-
3-indole selenosemicarbazone (3-HIndsesc, H¹⁰L)	3356m, 3246m	3153w	1591s, 1487m, 1450s	898s	-
[Fe(3-indsesc) ₃]10	3394m, 3240m	-	1643s, 1576m, 1464s	764s	3146w
3-acetylindole selenosemicarbazone (3-AcHIndsesc, H¹¹L)	3290m	3142w	1624s, 1502m, 1406s	877s	-

[Fe(3-acindsesc) ₃] 11	-	-	1613s, 1572m, 1432s	744s	3172w
9-anthracene selenosemicarbazone (9-HAnsesc, H¹²L)	3385m, 3248m	3151w	1639s, 1518m, 1402s	887s	-
[Fe(9-antrasesc) ₃] 12	3257m	-	1665s, 1552m, 1437s	780s	-
1-naphthaldehyde selenosemicarbazone (1-HNapsesc, H¹³L)	3400m	3147w	1599s, 1516m, 1452s	871s	-
[Fe(1-naphthsesc) ₃] 13	3358m	-	1631s, 1597s, 1446s	744s	-
2-naphthaldehyde selenosemicarbazone (2-HNapsesc, H¹⁴L)	3352m	3124w	1597s, 1533m, 1446s	856s	-
[Fe(2-naphthsesc) ₃] 14	3219m	-	1618s, 1539m, 1442s	745s	-

5.3 Vibrating Sample Magnetometer Spectroscopy:

VSM analysis was performed to measure the magnetic properties of the synthesized complexes. Complexes **1-14** were taken for VSM analysis. Magnetic hysteresis loops obtained experimentally and hysteresis loop after linear correction are given in figures 5.3.1-5.3.14.

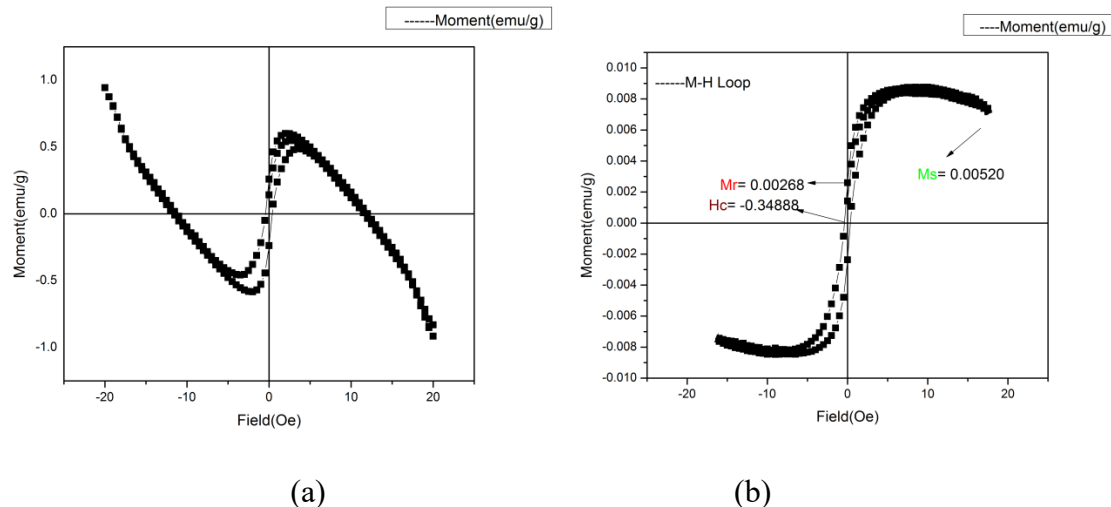


Figure 5.3.1 a) VSM hysteresis loop of complex**1**; b) linearly corrected mass normalized results

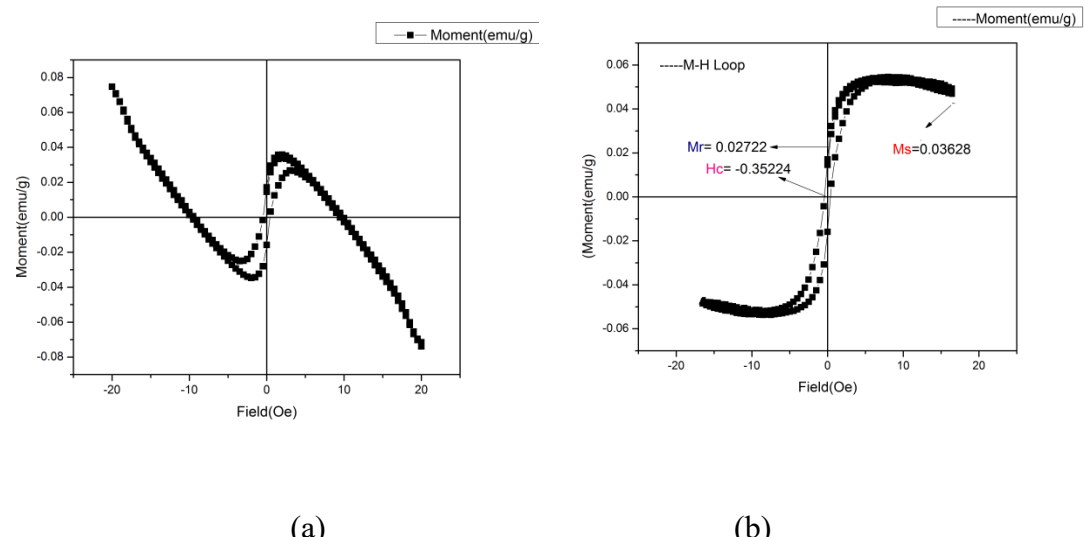


Figure 5.3.2 a) VSM hysteresis loop of complex**2**; b) linearly corrected mass normalized results

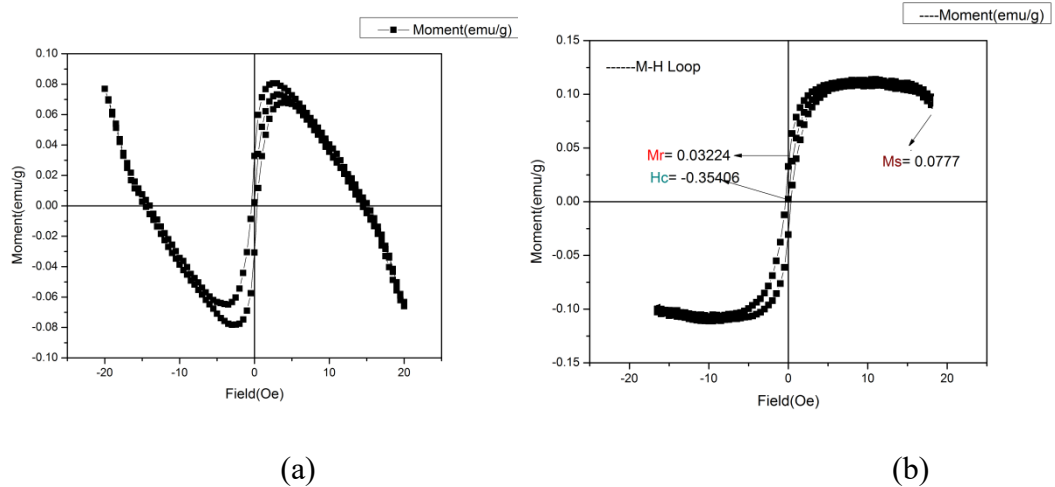


Figure 5.3.3 a) VSM hysteresis loop of complex3; b) linearly corrected mass normalized results

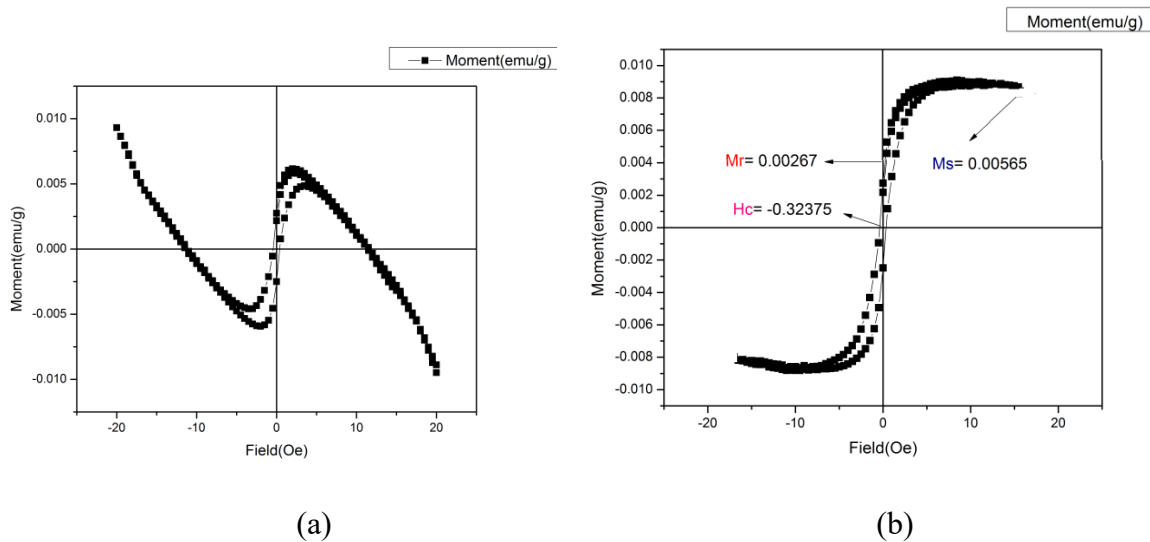


Figure 5.3.4 a) VSM hysteresis loop of complex4; b) linearly corrected mass normalized results

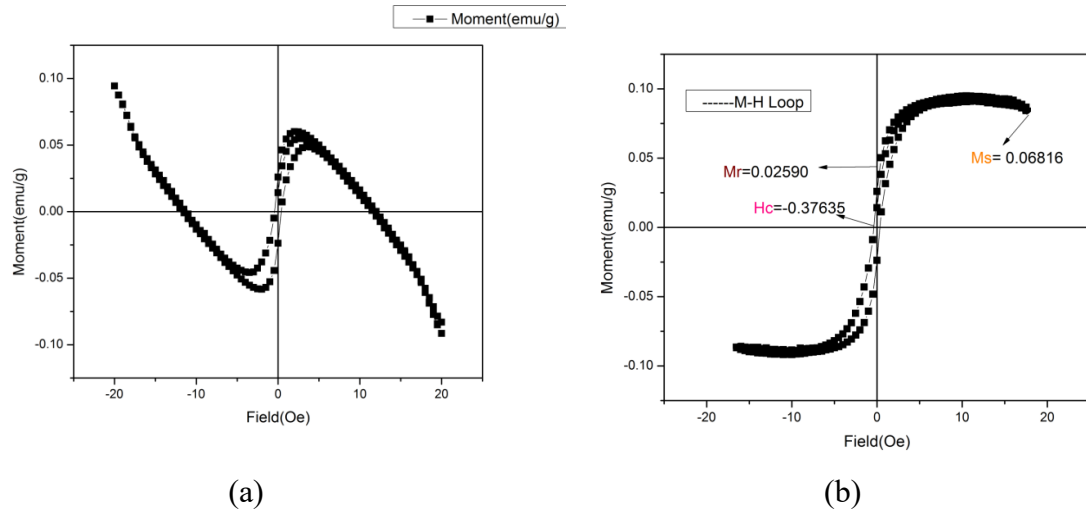


Figure 5.3.5 a) VSM hysteresis loop of complex 5; b) linearly corrected mass normalized results

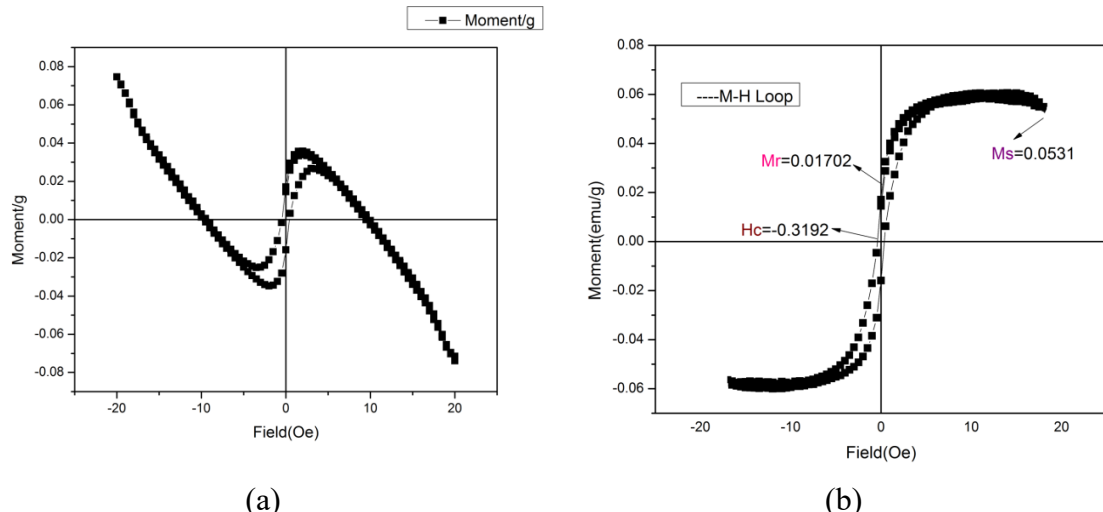


Figure 5.3.6 a) VSM hysteresis loop of complex 6; b) linearly corrected mass normalized results

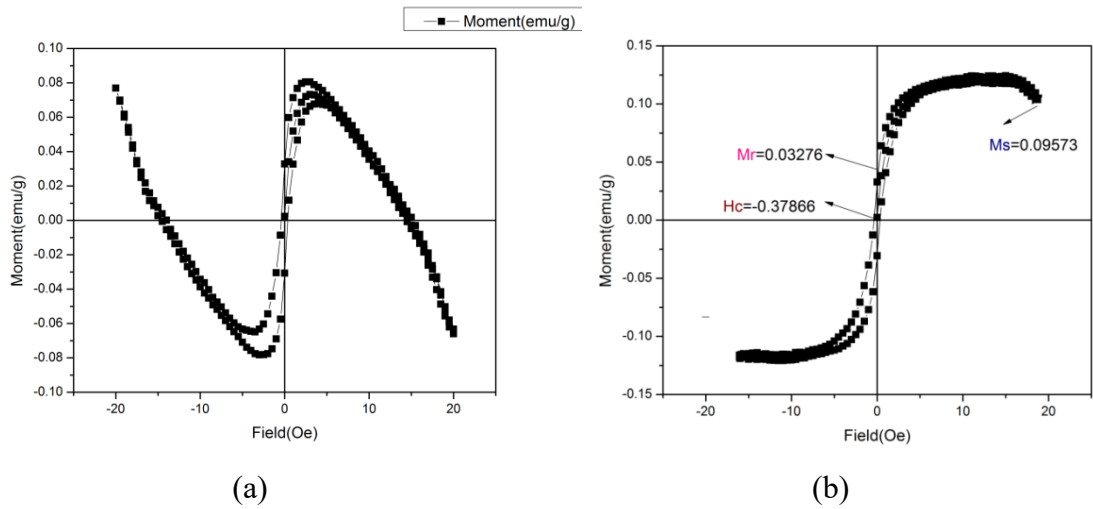


Figure 5.3.7 a) VSM hysteresis loop of complex7; b) linearly corrected mass normalized results

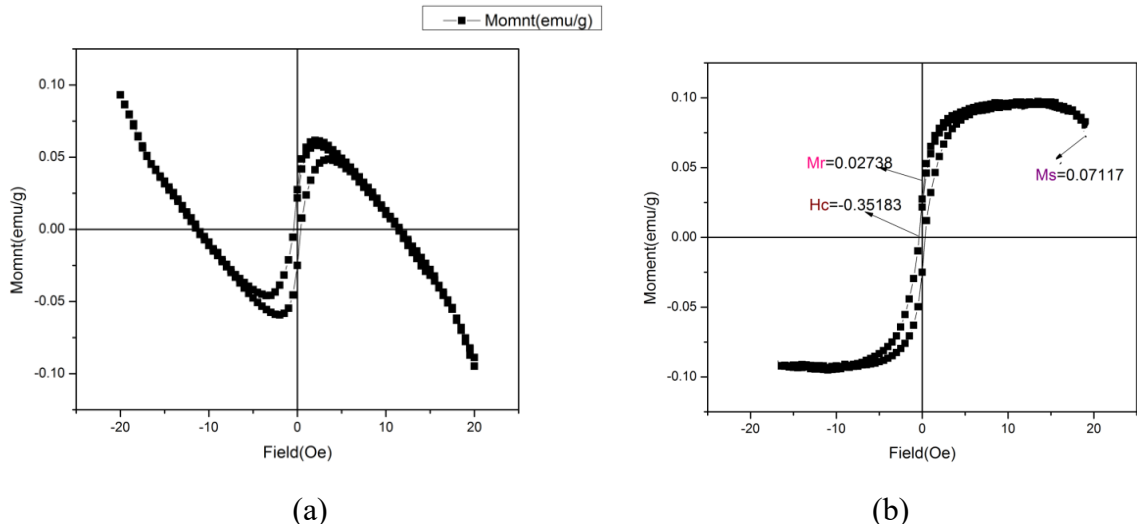


Figure 5.3.8 a) VSM hysteresis loop of complex8; b) linearly corrected mass normalized results

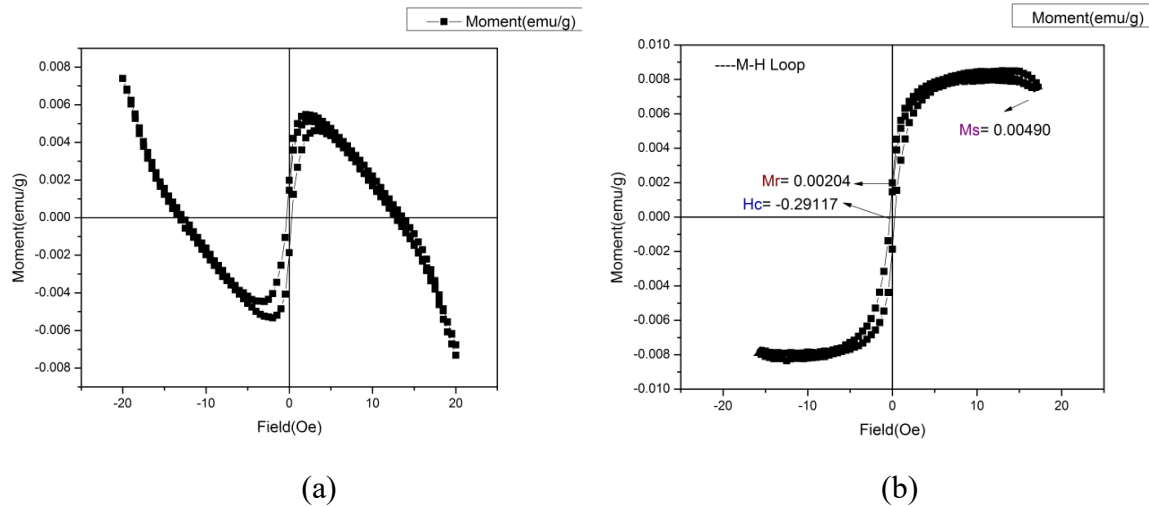


Figure 5.3.9 a) VSM hysteresis loop of complex 9; b) linearly corrected mass normalized results

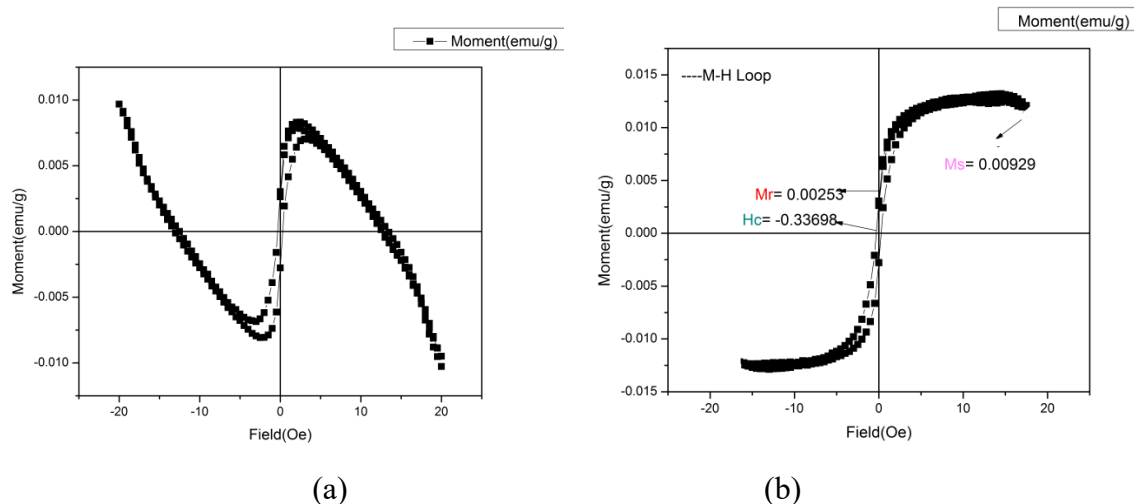


Figure 5.3.10 a) VSM hysteresis loop of complex 10; b) linearly corrected mass normalized results

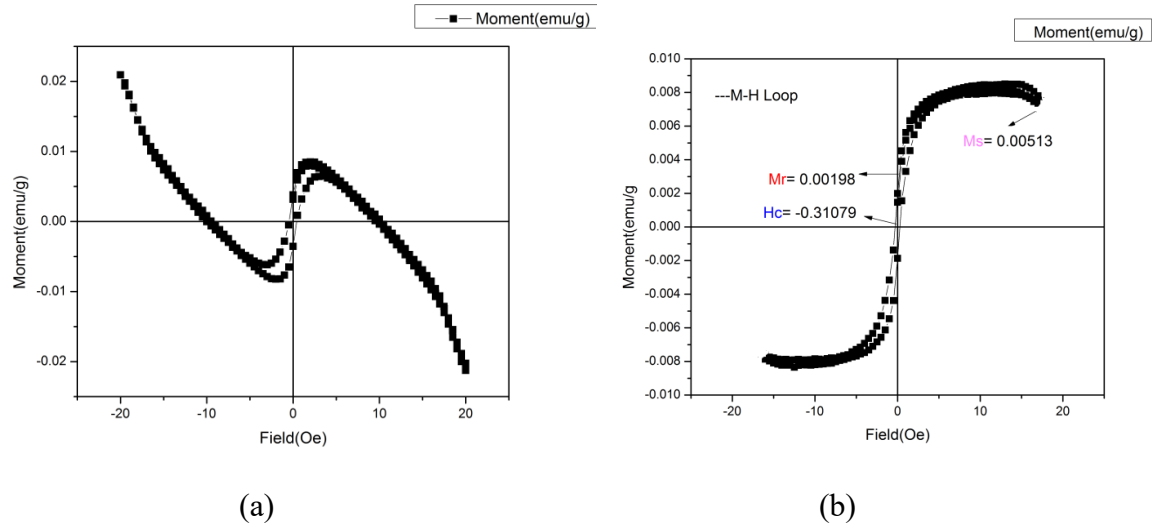


Figure 5.3.11 a) VSM hysteresis loop of complex 11; b) linearly corrected mass normalized results

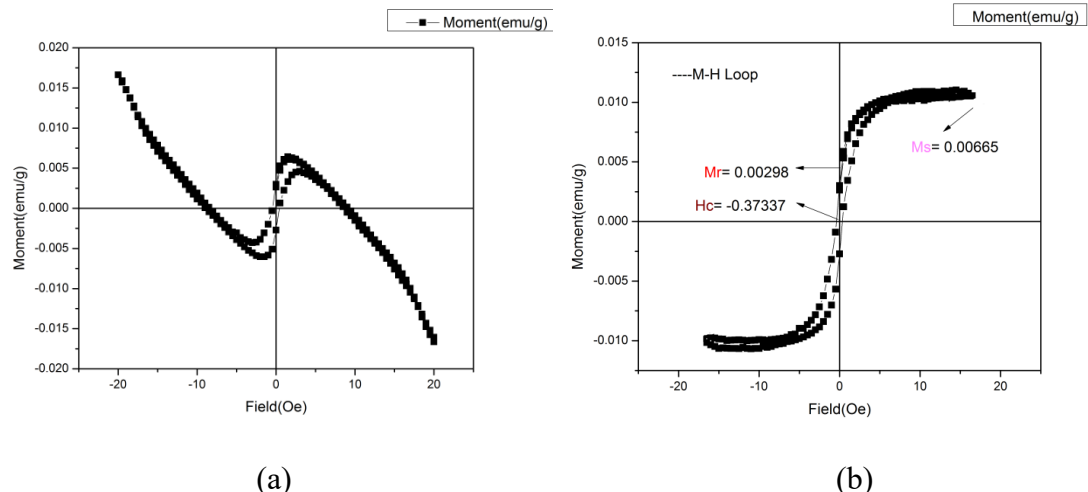


Figure 5.3.12 a) VSM hysteresis loop of complex 12; b) linearly corrected mass normalized results

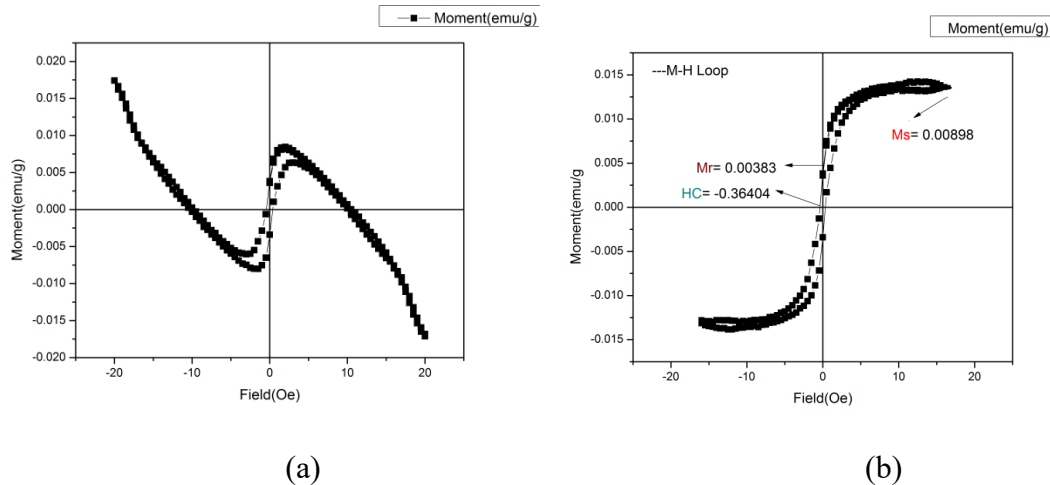


Figure 5.3.13 a) VSM hysteresis loop of complex 13; b) linearly corrected mass normalized results

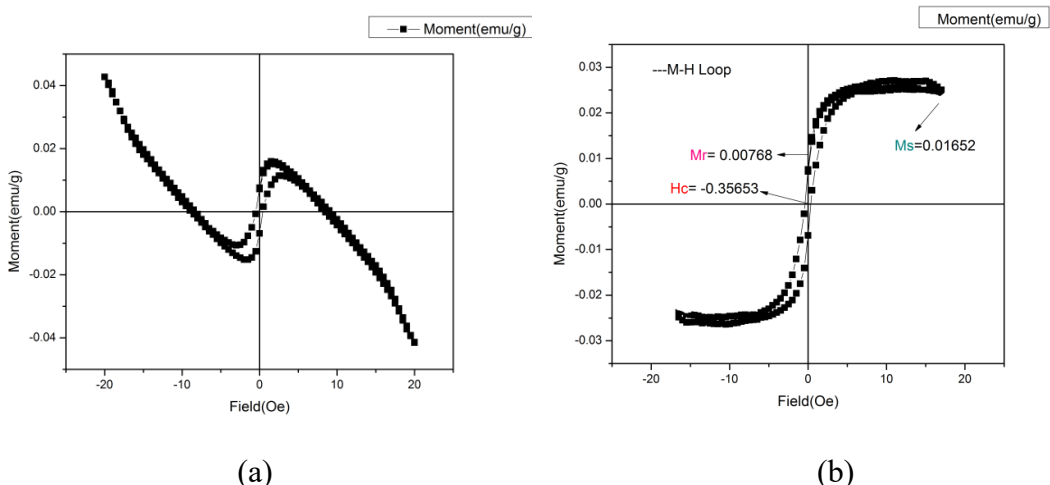


Figure 5.3.14 a) VSM hysteresis loop of complex 14; b) linearly corrected mass normalized results

From the VSM graphs, three parameters can be calculated: i) Saturation magnetization (M_s): A point when no further increase in magnetization is possible with increase in external magnetic field; ii) remanence (M_r): magnetization left behind after removal of external magnetic field; iii) coercivity (H_c): it is the measure of reverse field required to bring the magnetization to zero after saturation. The area within the loop indicates the amount of energy absorbed by the material during each cycle of the hysteresis loop [140-142]. These parameters calculated from hysteresis loop of complexes 1-14 are given in Table 5.3.

Table 5.3 Saturation magnetization, coercivity and remanence values of complexes **1-14**

Synthesized Iron Metal Complexes	Saturation magnetization(emu/g)	Coercivity magnetization (emu/g)	Remanence magnetization (emu/g)
[Fe(cysesc) ₃] 1	0.00520	0.00268	-0.34888
[Fe(2-fursesc) ₃] 2	0.03628	0.02722	-0.35224
[Fe(2-thiosesc) ₃] 3	0.07771	0.03224	-0.35406
[Fe(N-mepysesc) ₃] 4	0.00565	0.00267	-0.32375
[Fe(3-meoxsesc) ₃] 5	0.06816	0.02590	-0.37635
[Fe(2-oxsesc) ₃] 6	0.05313	0.01702	-0.31422
[Fe(6-cloxsesc) ₃] 7	0.09573	0.03276	-0.37866
[Fe(5-clistsesc) ₃] 8	0.07117	0.02738	-0.35183
[Fe(1-meistsesc) ₃] 9	0.00490	0.00204	-0.29117
[Fe(3-indsesc) ₃] 10	0.00929	0.00253	-0.33698
[Fe(3-acindsesc) ₃] 11	0.00513	0.00198	-0.31079
[Fe(9-anthrasesc) ₃] 12	0.00665	0.00298	-0.37337
[Fe(1-naphthsesc) ₃] 13	0.00898	0.00383	-0.36404
[Fe(2-naphthsesc) ₃] 14	0.01652	0.00768	-0.35653

From the table it is clear that saturation magnetization is high in case of complexes **3, 5, 6, 7** and **8** (0.05313-0.09573 emu/g) as compare to other complexes **1, 2, 4, 9-14** (0.00490-0.01652 emu/g). The remanence magnetization of complexes **1-14** falls in the range -0.37866 to -0.29117emu/g. The low ramanence magnetization values indicate that the iron metal in these complexes is magnetically soft.

5.4 Mössbauer spectroscopy:

To find out the geometry of complexes, a representative complex (**complex 2**) was studied for Mossbauer spectroscopy. Complex **2** was also studied for Mössbauer spectroscopy. Information regarding chemical state of and environment around iron can be obtained from Mössbauer spectroscopy. In ^{57}Fe , ground state has I value of $\frac{1}{2}$ and its first excited state has I value $\frac{3}{2}$. In the absence of any field gradient, the excited levels are degenerate thus give only one peak, but in the presence of field gradient degeneracy of excited levels (ground as well as excited) removed and the level gets split up (split up into doublets) thus giving a quadrupole splitting QS (Figure 5.4.1)

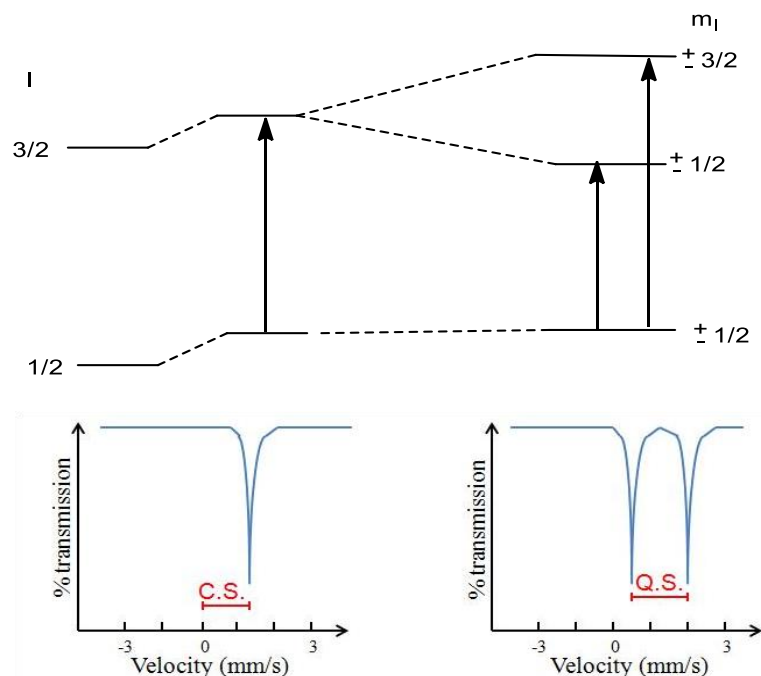


Figure 5.4.1 Splitting of Mossbauer peak in the presence of field gradient

Mössbauer spectrum of complex **2** was taken at two different temperatures i.e 300K and 15K. Spectrum is given in Figure 5.4.2 and various parameters like isomer shift, quadrupole splitting etc. are given in Table 5.4. Isomer shift (δ) is obtained as distance of center of quadrupolar distance from zero velocity, whereas quadrupolar splitting (Δ) give difference between velocities of two peaks obtained due to the interaction of quadrupolar moment of the

nucleus and electric field gradient. The formula to obtain δ and Δ is given in equation 1 and 2 respectively.

$$\delta \text{ (isomer shift)} = K(\rho_{\text{ex}}^2 - \rho_g^2)[R_{\text{ex}} - R_g / R_g] \quad \dots \dots \dots \text{Eq. 1}$$

Where K = constant, ρ_{ex} = s- electron density in excited state, ρ_g = s- electron density in ground state, R_{ex} = radii of nucleus in excited state, R_g = radii of nucleus in ground state

$$\Delta \text{ (quadrupolar splitting)} = \frac{1}{2} e_g^2 Q (1 + 1/3 \eta^2)^{1/2} \quad \dots \dots \dots \text{Eq. 2}$$

e_g = electric field, Q = ^{57}Fe nuclear quadrupole moment, η = symmetry parameter

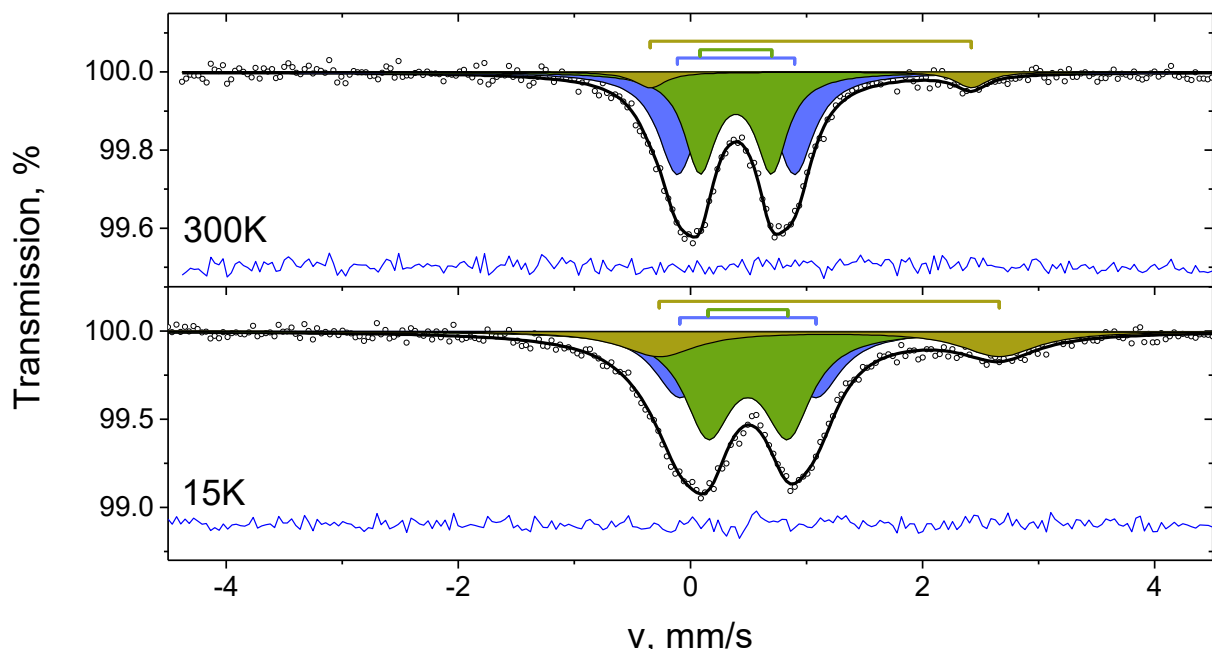


Figure 5.4.2 Mössbauer spectra of $[\text{Fe}(2\text{-fursesc})_3]\text{2}$

Table 5.4 Parameters of $[\text{Fe}(2\text{-fursesc})_3]\text{2}$ complex

T, K	Component	$\delta \pm 0.002$, mm/s	$\Delta \pm 0.002$, mm/s	$\Gamma \pm 0.002$, mm/s	A ± 1 , %	Fe state	χ^2
300	D1	0.393	1.012	0.399	52	Fe^{3+} HS	0.931
	D2	0.391	0.618	0.328	41	Fe^{3+} HS	

	D3	1.037	2.766	0.326	7	Fe ²⁺ HS	
15	D1	0.496	1.172	0.522	33	Fe ³⁺ HS	
	D2	0.496	0.688	0.495	47	Fe ³⁺ HS	1.049
	D3	1.196	2.928	0.792	20	Fe ²⁺ HS	

δ - isomer shift, Δ -quadrupole splitting for paramagnetic component, Γ - linewidth, A - component area, χ^2 - Pirson's criterion

For high spin iron(III) octahedral complexes, isomer shift (δ) generally obtained in the range of ,0.4 mm/s-0.9mm/s [143]. In complex **2** the isomer shift value of 0.393 mm/s indicates the formation of iron(III) high spin octahedral complex. Quadrupolar splitting indicates the asymmetric charge distribution around the iron(III) nuclei.

5.5 ESR spectroscopy:

Electron Spin Resonance spectroscopy has been used as a powerful technique to determine the spin state of iron(III) complexes [144-150]. To determine the oxidation and spin state of synthesized complexes, ESR spectrum of representative complex **12** was recorded and spectrum is give in Figure 5.5.1.

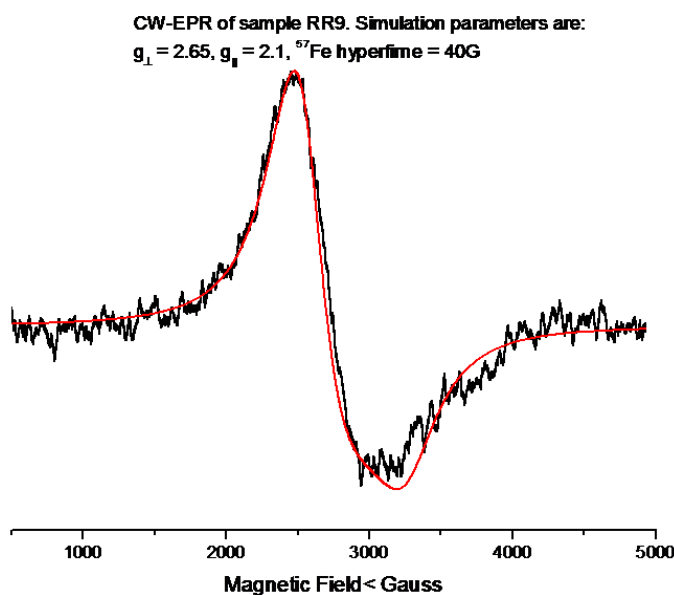


Figure 5.5.1 Experimental (black) and simulated (red) best fit EPR spectrum of [Fe(9-antrasesc)₃]**12** complex

Complex **12** give a broad signal with g value approximately equal to 2 supports formation of Fe(III) high spin complex with $S = 5/2$ in an octahedral environment [151,152].

5.6 Mass spectrometry:

Mass spectra of complexes **1-14** have been recorded and given in Figures 5.6.1-5.6.14. The observed molecular ion peaks $[M]^+$ are given in Table 5.6 and it is clear from the table that m/z value for complexes **1-14** are close to their proposed stoichiometry, $[Fe(L)_3]$ and thus confirmed the coordination of iron(III) with selenosemicarbazones.

Table 5.6 m/z value (amu) of complexes **1-14** obtained from mass spectra

Complex No.	Parent peak obtained from Mass spectra	Expected formula for parent ion (m/z) ⁺
1	709	$[Fe(C_7H_{14}N_3Se)_3]$
2	675	$Na-[Fe(C_6H_6N_3OSe)_3]$
3	751	$[Fe(C_6H_8N_3SSe)_3]$
4	731	$[Fe(C_7H_{13}N_4Se)_3]$
5	851	$[Fe(C_{10}H_{11}N_4Se)_3]$
6	809	$[Fe(C_9H_9N_4Se)_3]$
7	905	$[Fe(C_8H_6N_4ClSe)_3]$
8	950	$[Fe(C_9H_5N_4ClOSe)_3]$
9	881	$[Fe(C_{10}H_5N_4OSe)_3]$
10	850	$[Fe(C_{10}H_{13}N_4Se)_3]$
11	930	$[Fe(C_{11}H_{11}N_4Se)_3]$
12	1076	$Na_2-[Fe(C_{17}H_{16}N_3Se)_3]$
13	884	$[Fe(C_{12}H_{12}N_3Se)_3]$
14	875	$[Fe(C_{12}H_9N_3Se)_3]$

5.7 XRD studies:

In order to get more information about the crystalline structure of the metal-ligand complexes X-ray diffraction analysis was employed, and the results are presented in Figure 5.7.1.

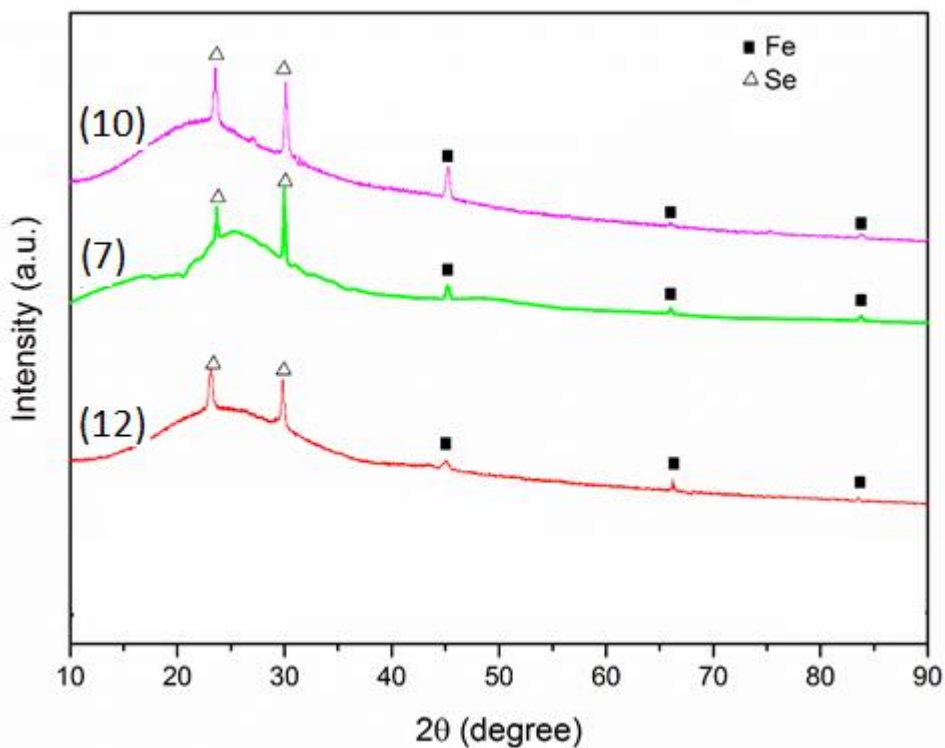


Figure 5.7.1 XRD patterns of iron-based (**7**, **10**, and **12**) metal-ligand complexes

As shown in Figure 5.7.1, all complexes showed a broad peak in the 2θ range of 15° - 35° . Furthermore, in the XRD patterns of all complexes, the peaks of selenium (JCPDS No. 00-006-0362 with hexagonal crystalline structure) can be seen at $2\theta = 23.5^\circ$ and 29.7° , attributed to the diffraction from the (1 0 0) and (1 1 0) crystalline planes. For complexes **7**, **10** and **12**, three diffraction peaks can be seen at around $2\theta = 45.3^\circ$, 66.0° and 83.8° which are ascribed to the diffraction from the (0 1 1), (0 0 2) and (1 1 2), crystalline planes of face-centered cubic (f c c) iron structure, respectively, with JCPDS No. 96-900-6601. The lattice parameter values obtained for complexes **7**, **10** and **12** was 2.827, 2.826 and 2.828 Å, respectively. No peaks from iron oxides species can be observed, indicating the formation of pure phases.

Crystallite size of the crystalline phases was assessed by Scherrer's equation (Eq. (1)) [153-156]

$$D = \lambda / \beta \cos(\theta) \quad (1)$$

Where D is the crystal size, λ is the X-ray wavelength (0.15418 nm), β is the corrected integral width, and θ is the Bragg angle for the (0 1 1) reflection for complexes **7**, **10** and **12**. According to the equation, the crystallite size of complexes **7**, **10** and **12** was equal to 20.1, 22.5 and 18.0 nm, respectively. For the selenium phase in the complexes, the Scherrer's formula was used for the (1 1 0) reflection and the obtained crystalline sizes were equal to

33.8, 33.9 and 34.1 nm for complexes **7**, **10**, and **12** respectively. Crystalline size and lattice parameters are represented in table 5.7.

Table 5.7 Crystallite size and lattice parameters of crystalline structures

Complex No.	Crystalline phase	Crystallite size (nm)	Lattice parameter (a) (Å)	Lattice parameter (b) (Å)	Lattice parameter (c) (Å)
7	Se (Hexagonal)	33.8	4.366	4.366	4.954
	Fe (FCC)	20.1	2.827	2.827	2.827
10	Se (Hexagonal)	33.9	4.366	4.366	4.954
	Fe (FCC)	22.5	2.826	2.826	2.826
12	Se (Hexagonal)	34.1	4.366	4.366	4.954
	Fe (FCC)	18.0	2.828	2.828	2.828

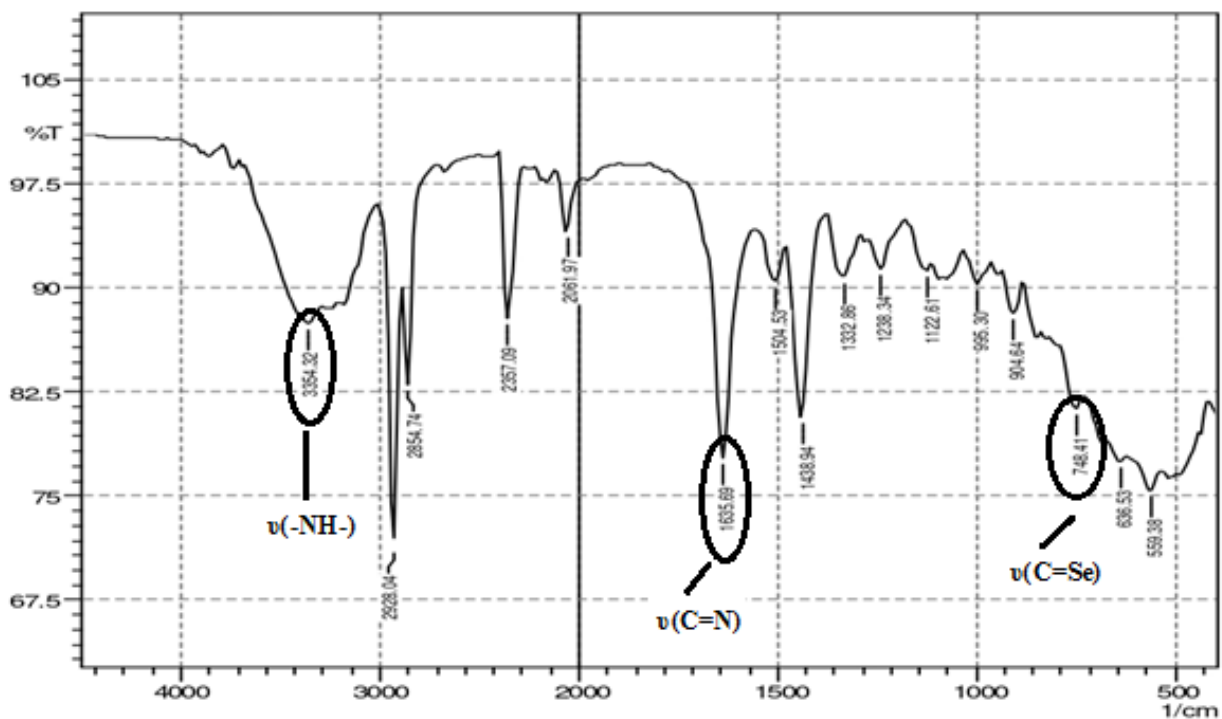


Figure 5.2.1 IR spectrum of $[\text{Fe}(\text{cysesc})_3]\mathbf{1}$

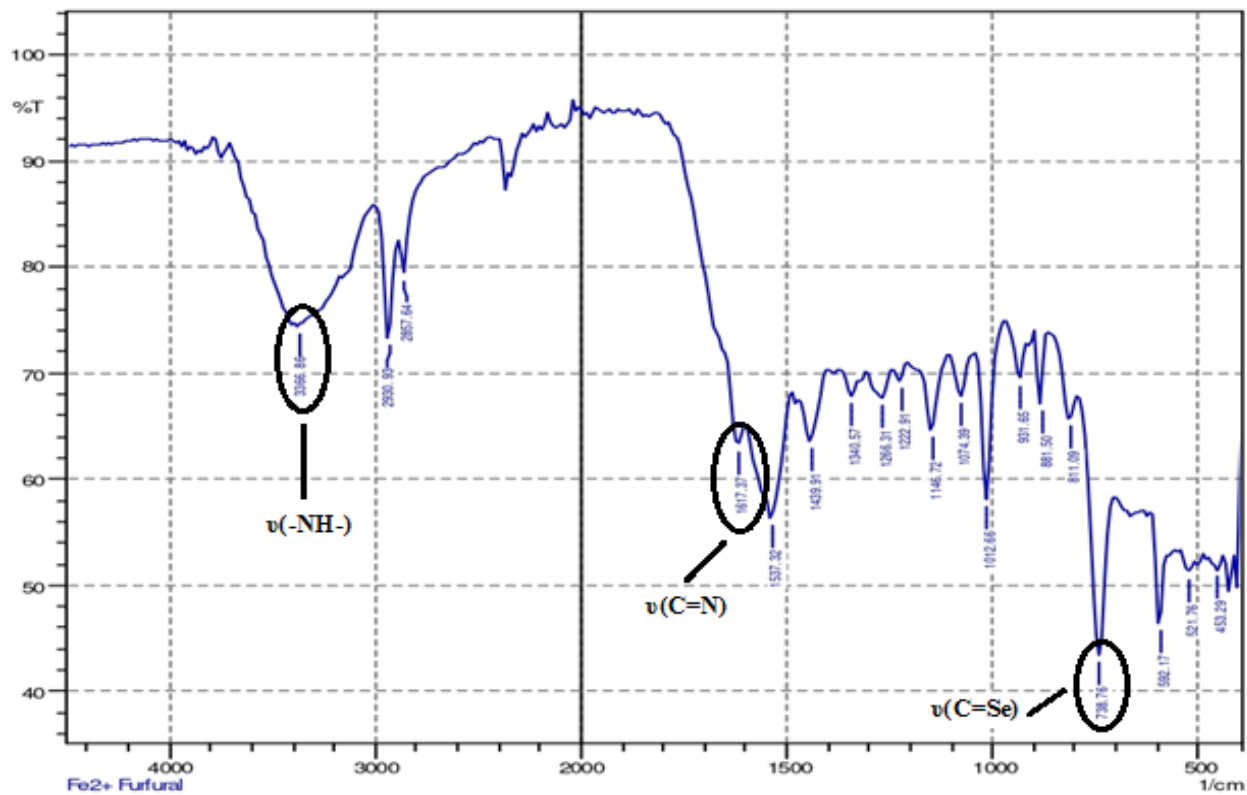


Figure 5.2.2 IR spectrum of $[\text{Fe}(2\text{-fursesc})_3]\mathbf{2}$

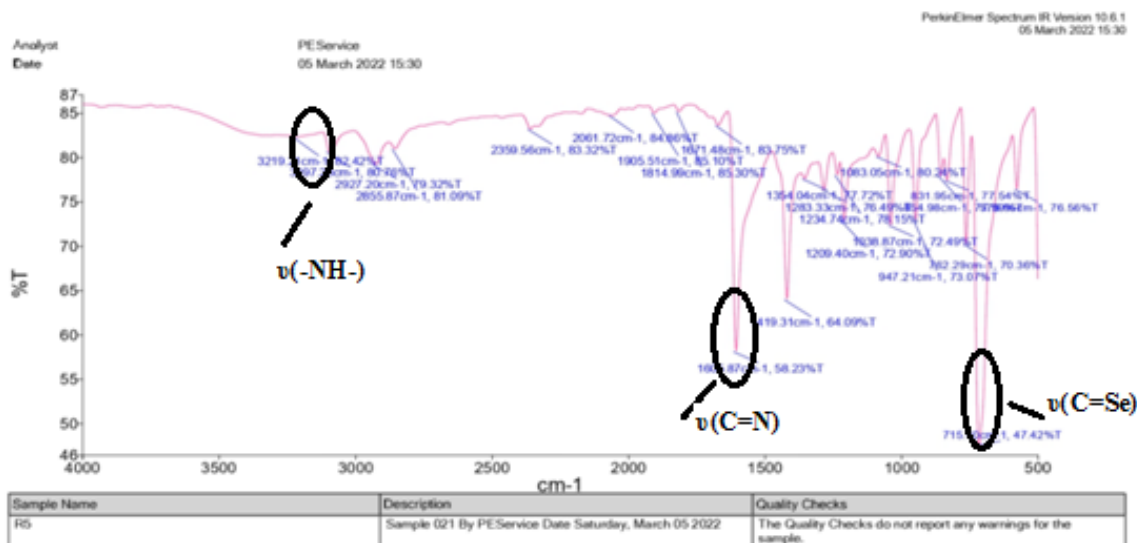


Figure 5.2.3 IR spectrum of $[\text{Fe}(2\text{-thiosesc})_3]3$

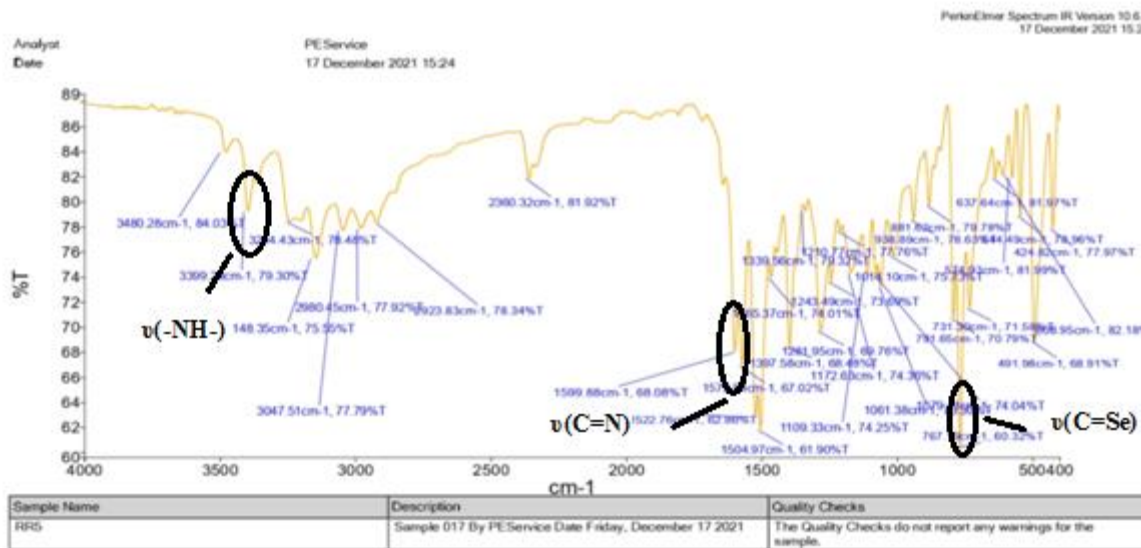


Figure 5.2.4 IR spectrum of $[\text{Fe}(\text{N-mepysesc})_3]4$

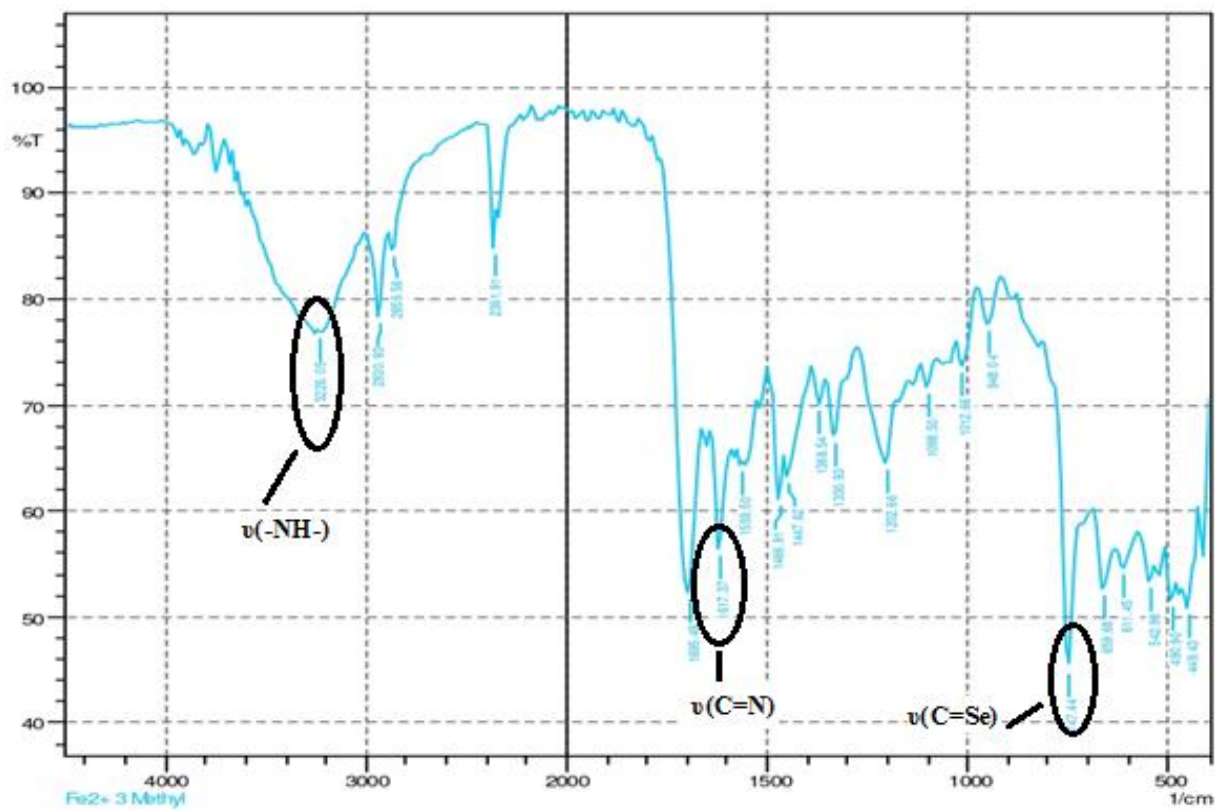


Figure 5.2.5 IR spectrum of $[\text{Fe}(3\text{-meoxsesc})_3]5$

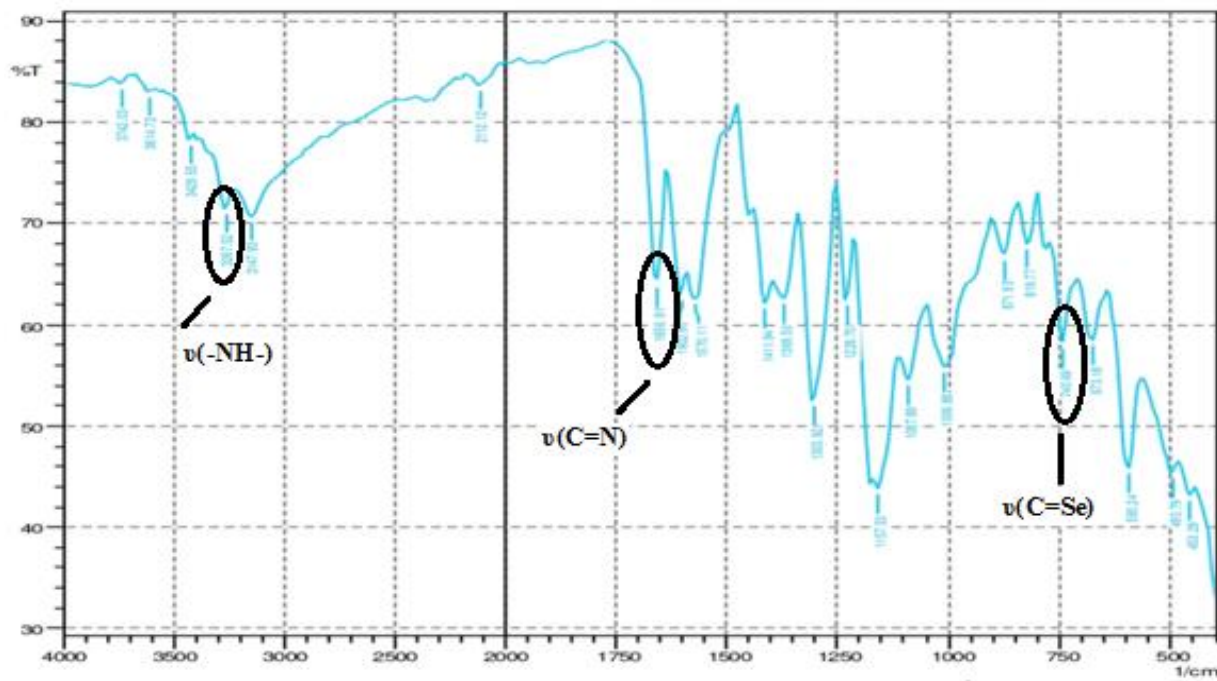


Figure 5.2.6 IR spectrum of $[\text{Fe}(2\text{-oxsesc})_3]6$

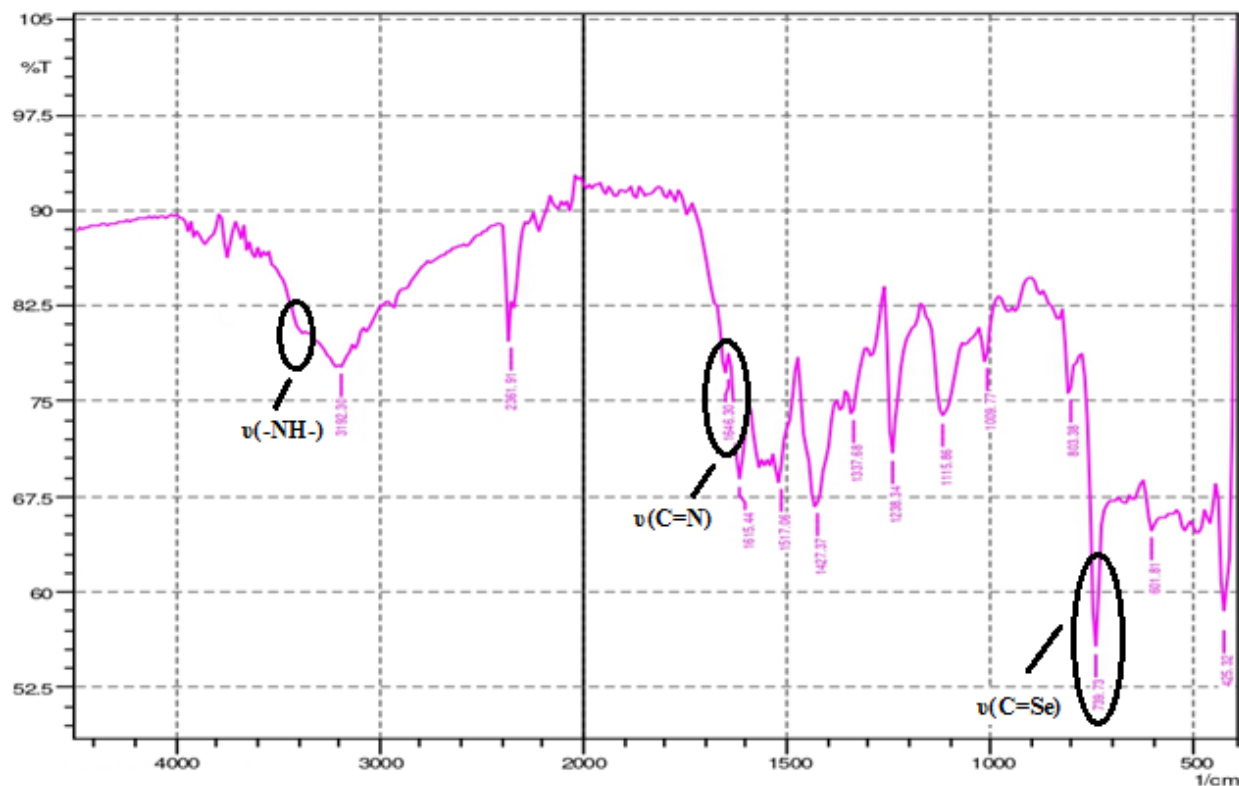


Figure 5.2.7 IR spectrum of $[\text{Fe}(6\text{-cloxsesc})_3]7$

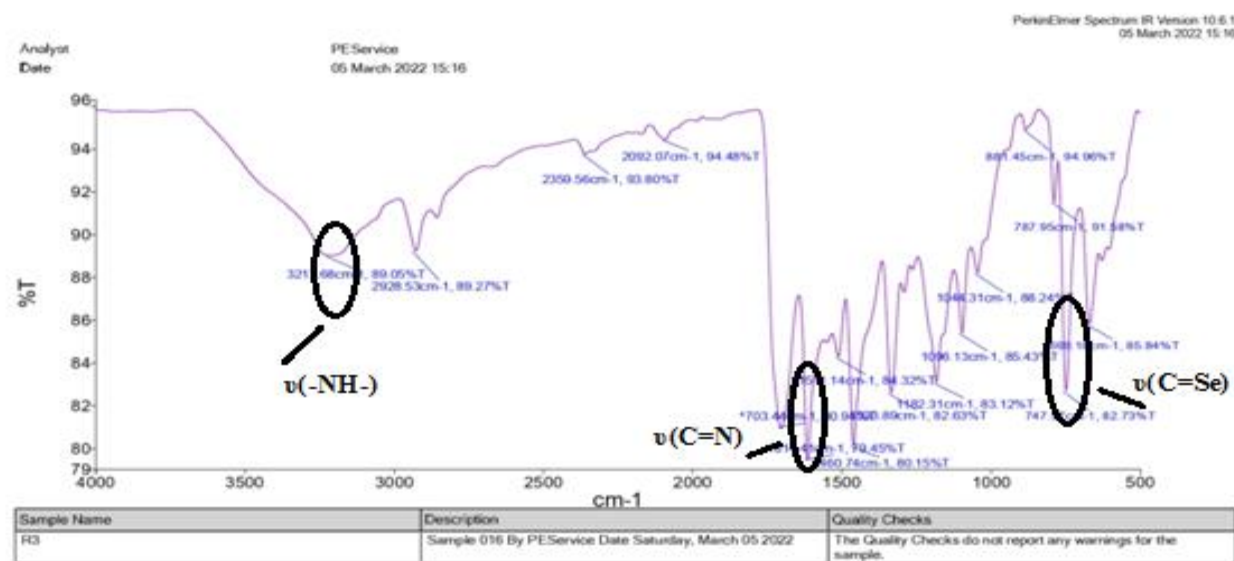


Figure 5.2.8 IR spectrum of $[\text{Fe}(5\text{-clistsesc})_3]8$



Figure 5.2.9 IR spectrum of $[\text{Fe}(1\text{-meistsesc})_3]9$

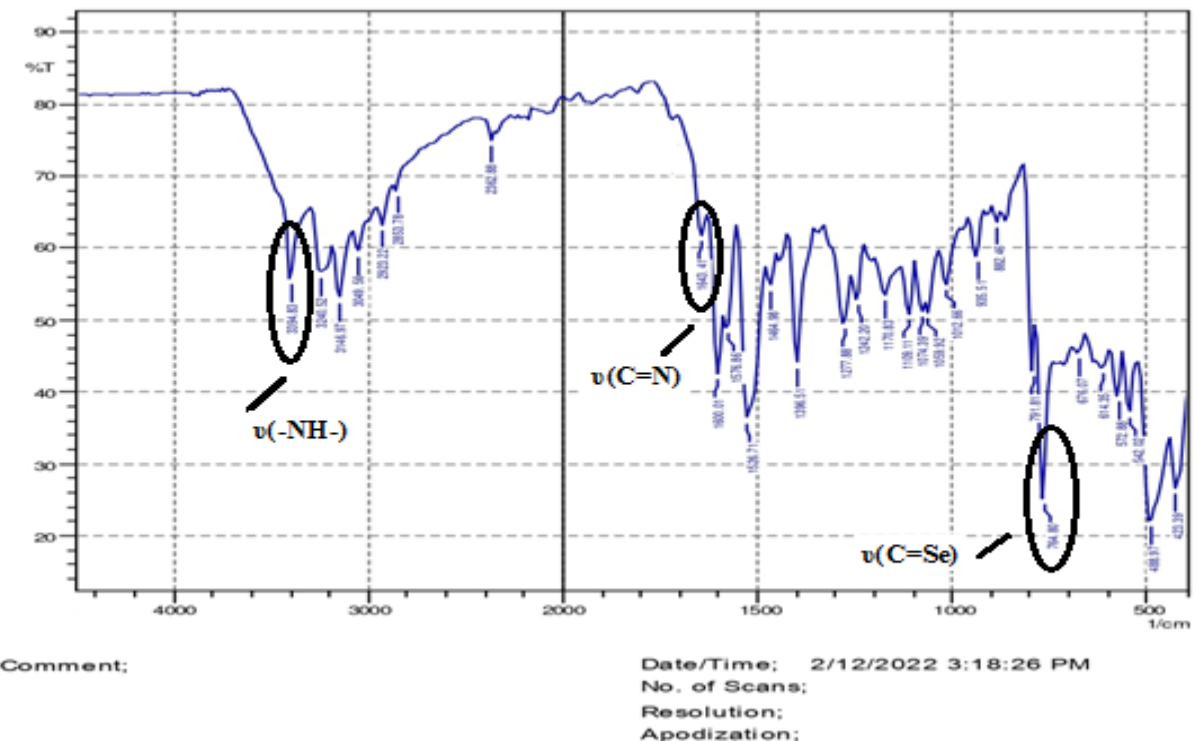


Figure 5.2.10 IR spectrum of $[\text{Fe}(3\text{-indsesc})_3]10$

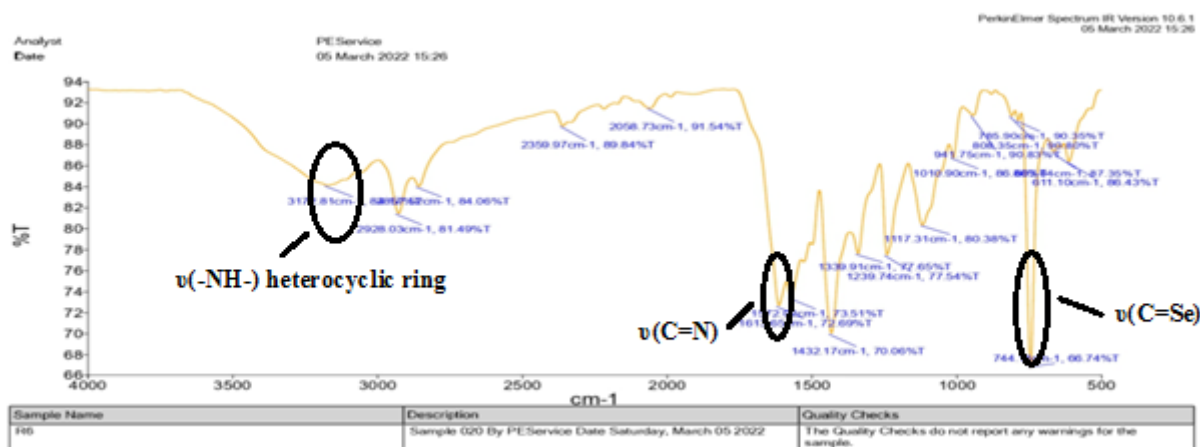


Figure 5.2.11 IR spectrum of $[\text{Fe}(3\text{-acindsesc})_3]11$

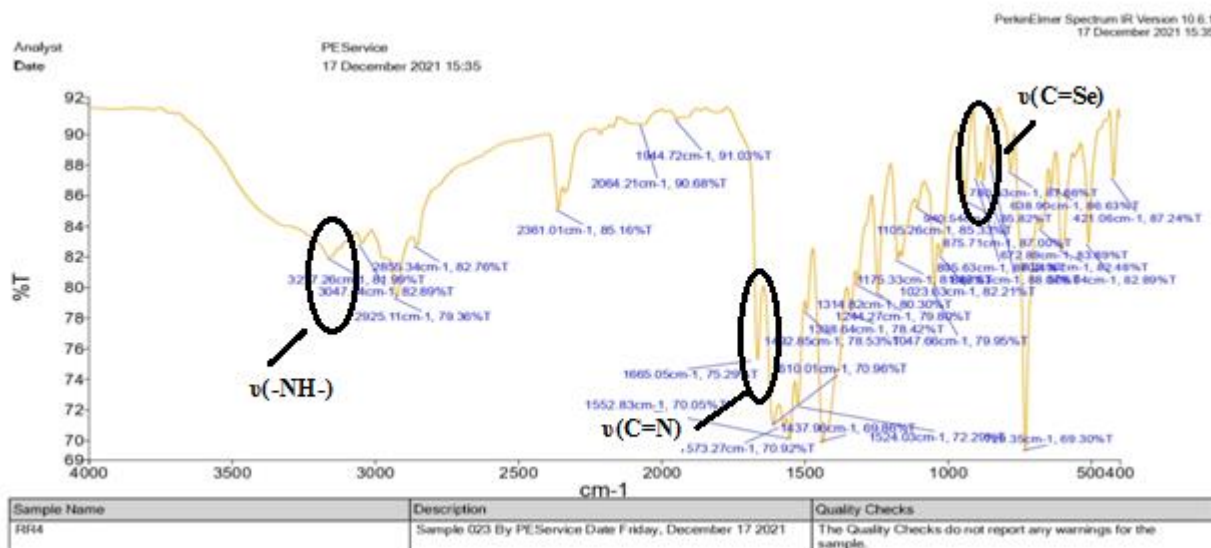


Figure 5.2.12 IR spectrum of $[\text{Fe}(9\text{-anthrasesc})_3]12$

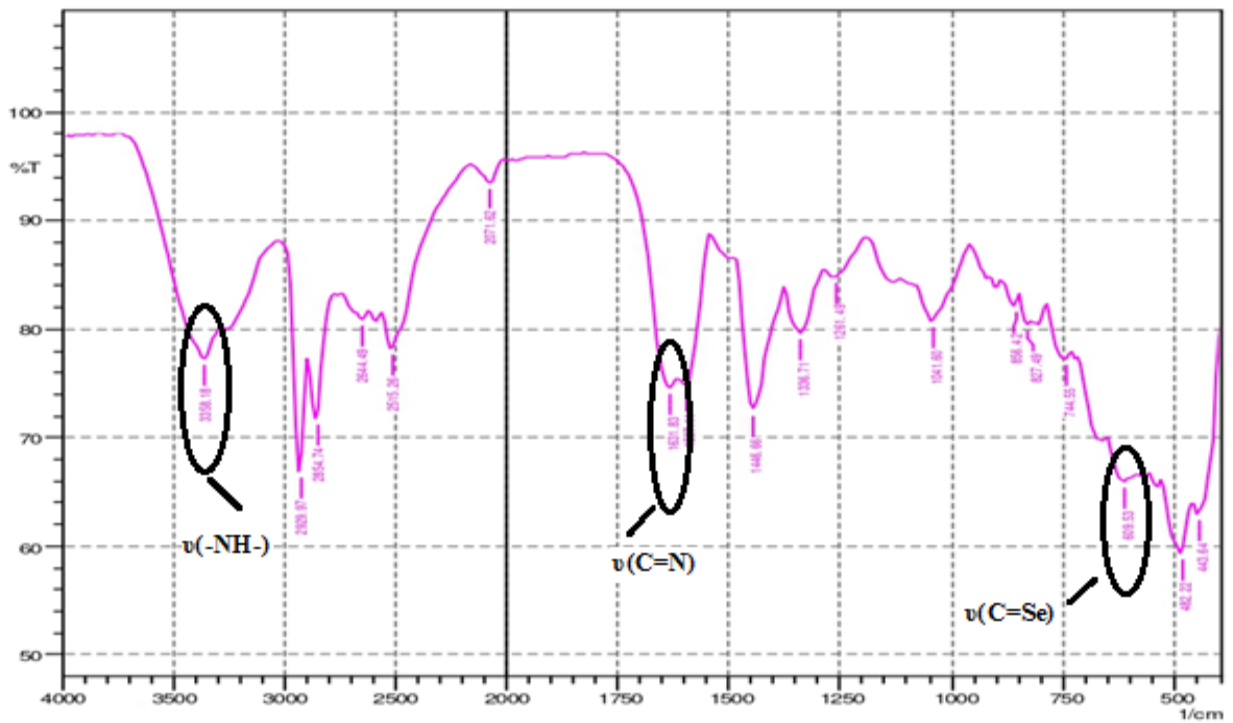


Figure 5.2.13 IR spectrum of $[\text{Fe}(1\text{-naphthsesc})_3]13$



Figure 5.2.14 IR spectrum of $[\text{Fe}(2\text{-naphthsesc})_2]14$

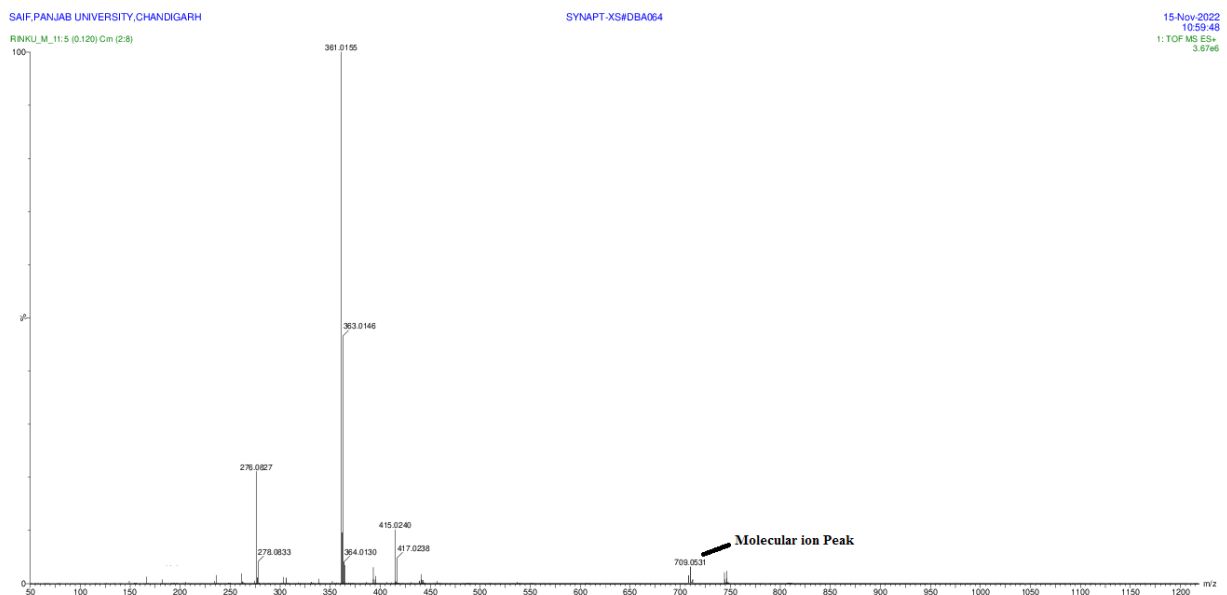


Figure 5.4.1 Mass Spectrum of $[\text{Fe}(\text{cysesc})_3]\mathbf{1}$

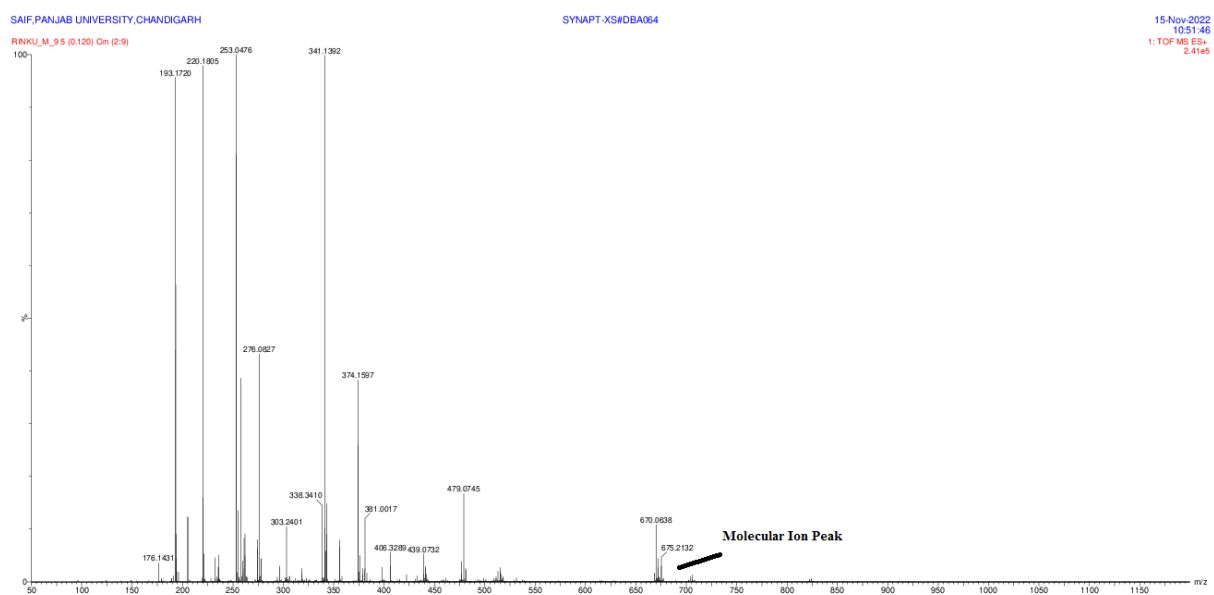


Figure 5.4.2 Mass Spectrum of $[\text{Fe}(2\text{-fursesc})_3]\mathbf{2}$

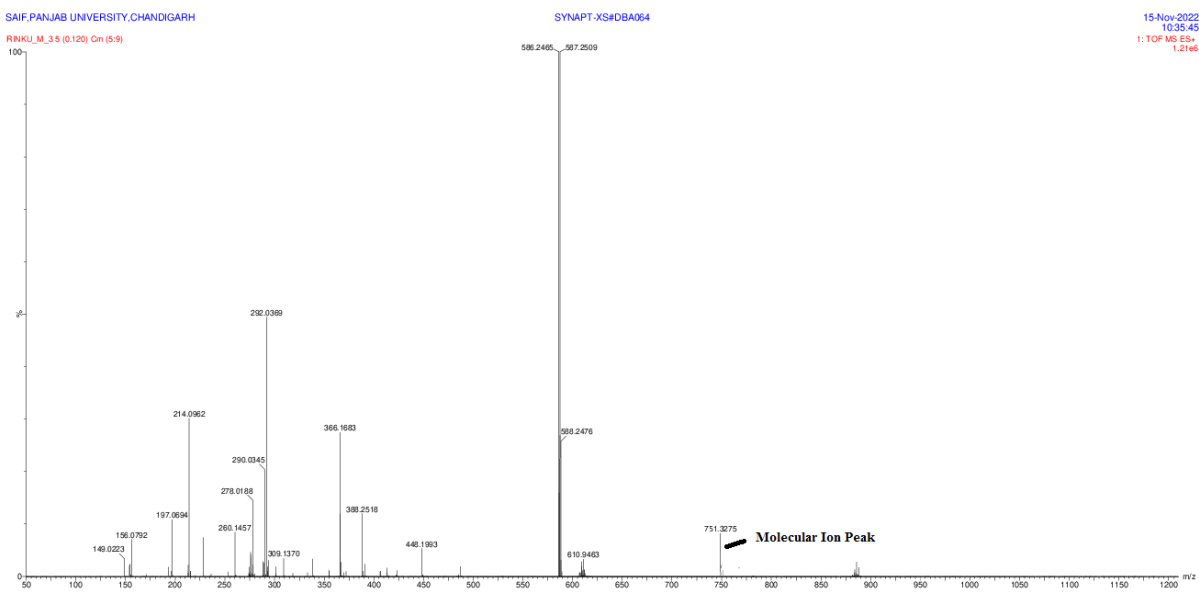


Figure 5.4.3 Mass Spectrum of $[\text{Fe}(2\text{-thiosesc})_3]3$

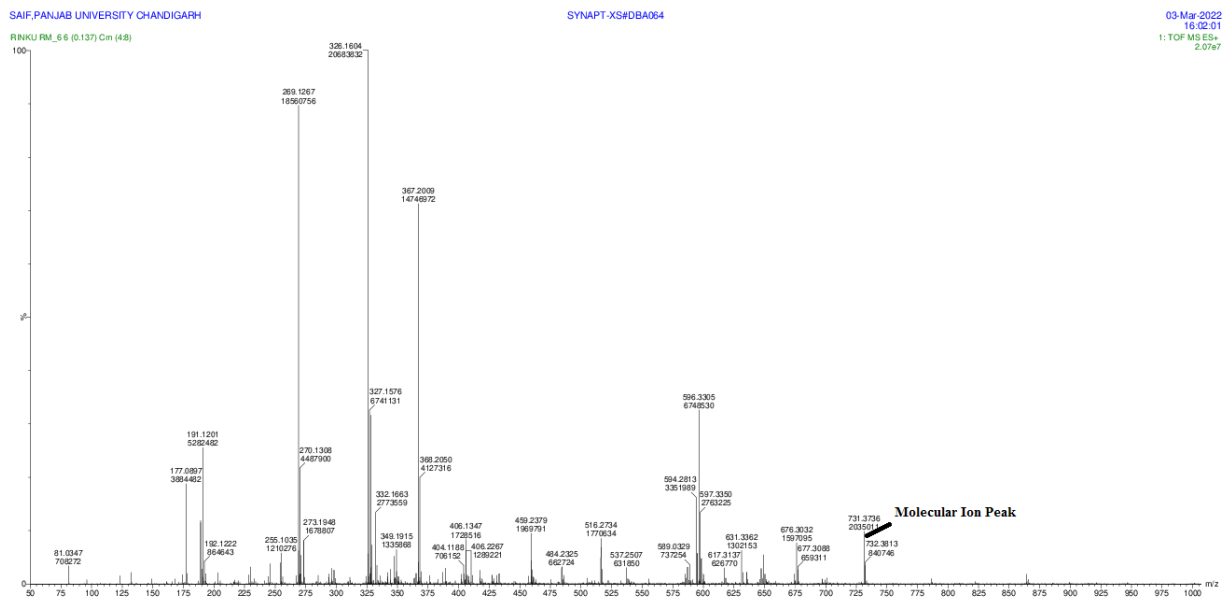


Figure 5.4.4 Mass Spectrum of $[\text{Fe}(\text{N-mepysesc})_3]4$

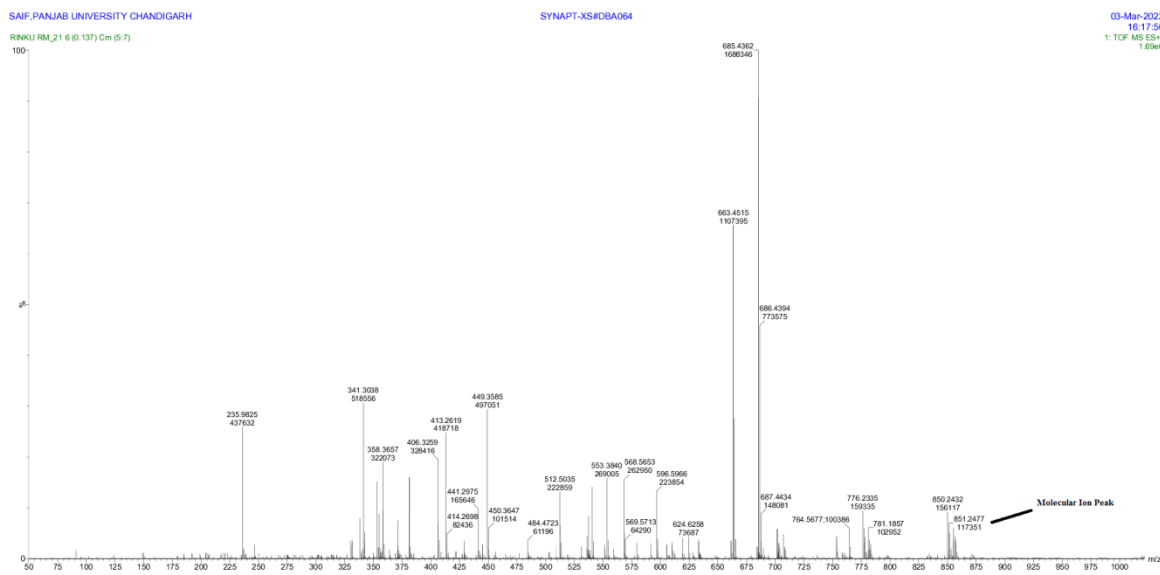


Figure 5.4.5 Mass Spectrum of $[\text{Fe}(3\text{-meoxsesc})_3]5$

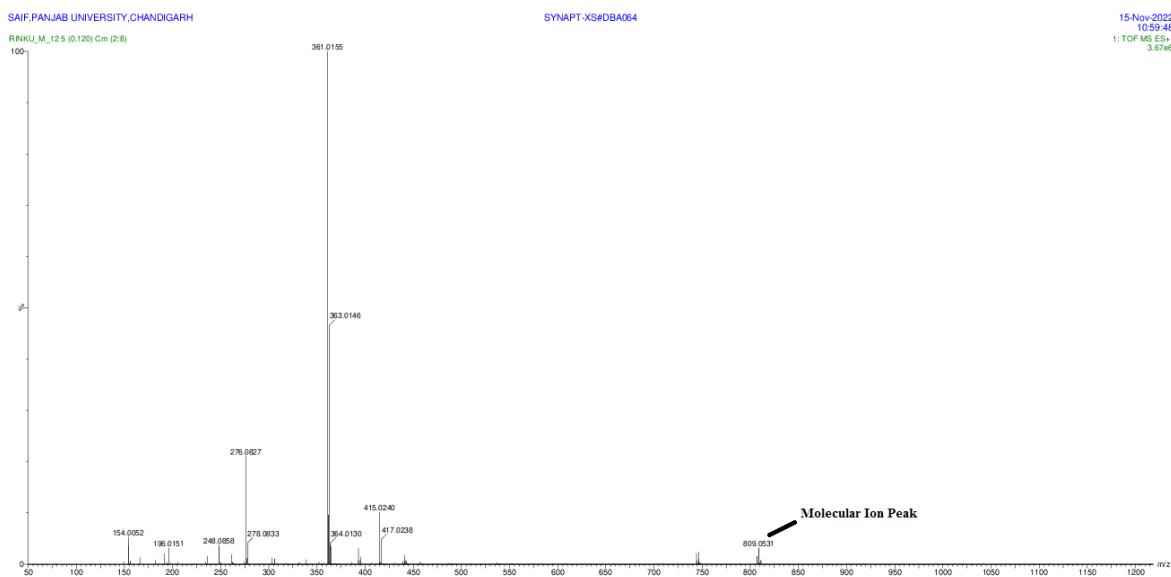


Figure 5.4.6 Mass Spectrum of $[\text{Fe}(2\text{-oxsesc})_3]6$

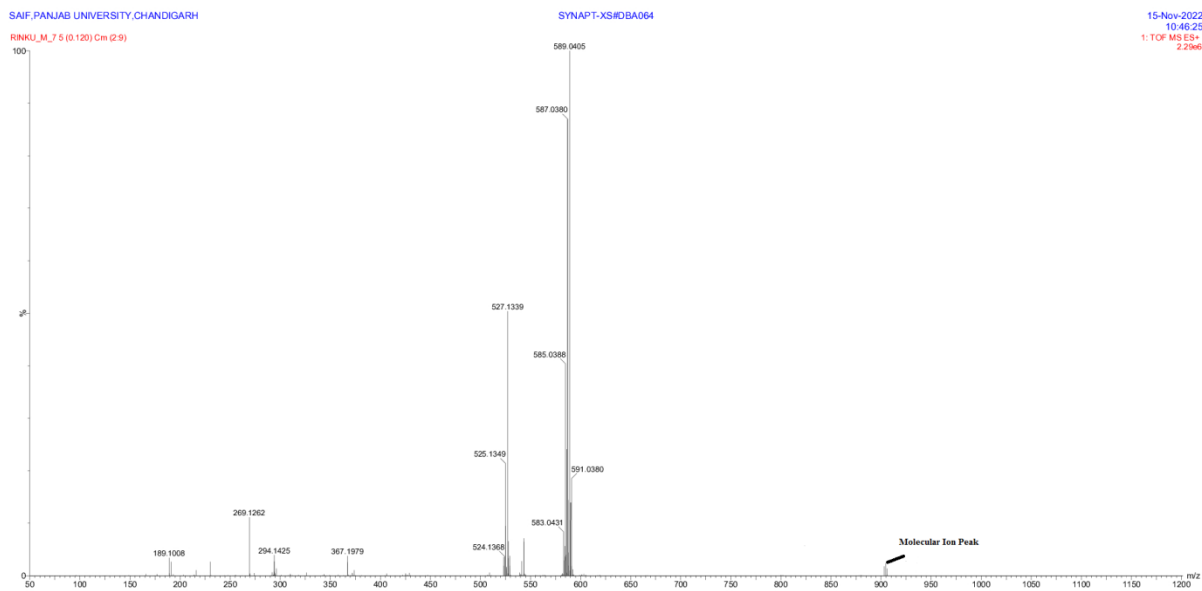


Figure 5.4.7 Mass Spectrum of $[\text{Fe}(6\text{-cloxsesc})_3]7$

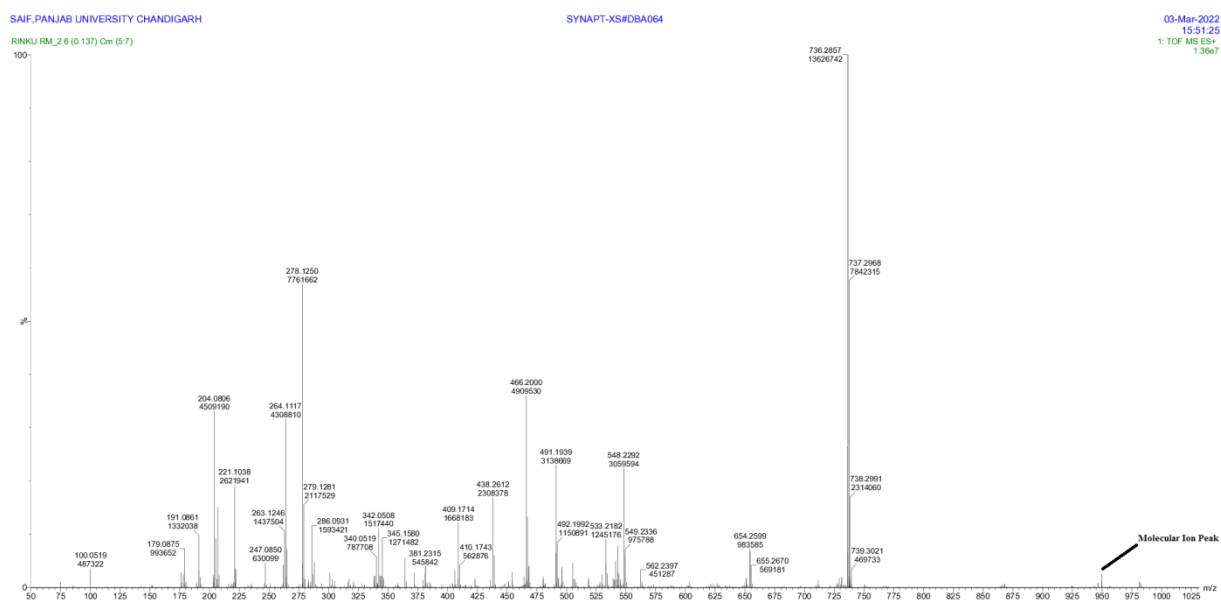


Figure 5.4.8 Mass Spectrum of $[\text{Fe}(5\text{-clistsesc})_3]8$

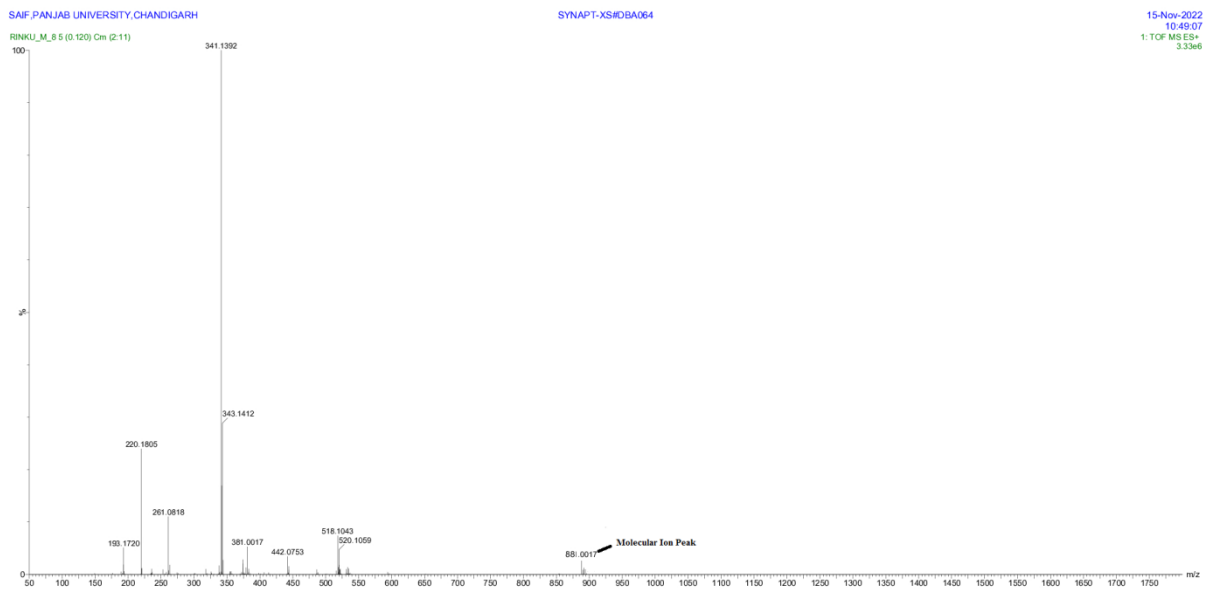


Figure 5.4.9 Mass Spectrum of $[\text{Fe}(1\text{-meistsesc})_3]\mathbf{9}$

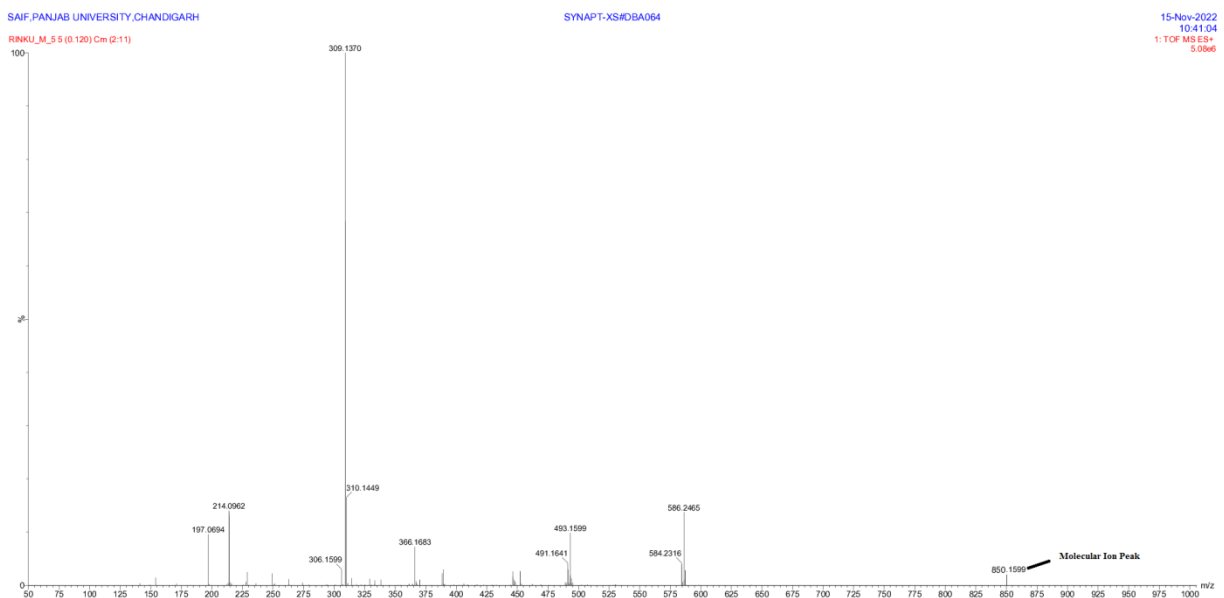


Figure 5.4.10 Mass Spectrum of $[\text{Fe}(3\text{-indsesc})_3]\mathbf{10}$

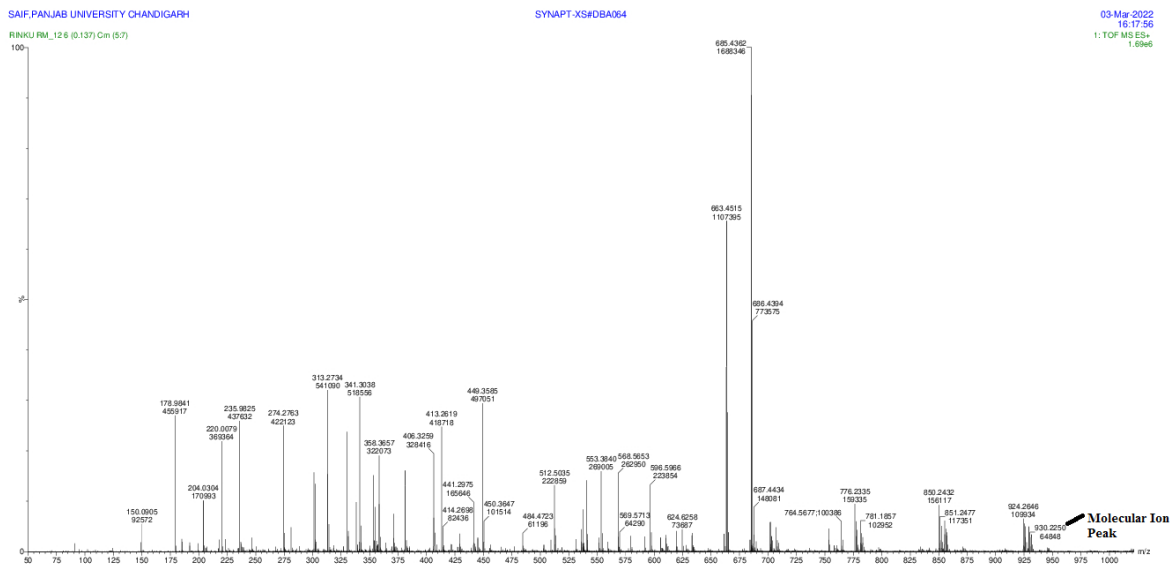


Figure 5.4.11 Mass Spectrum of $[\text{Fe}(3\text{-acindsesc})_3]11$

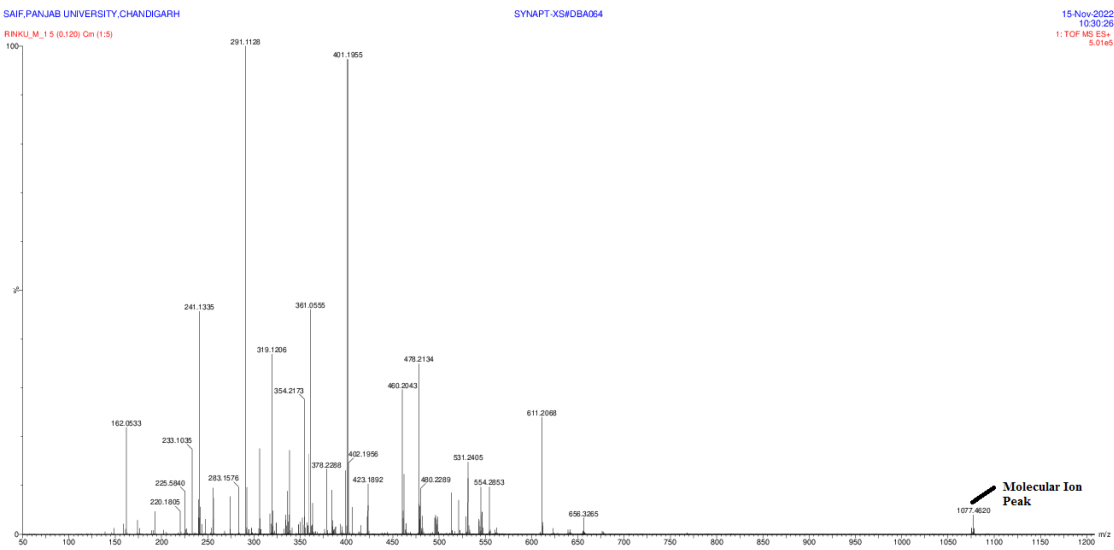


Figure 5.4.12 Mass Spectrum of $[\text{Fe}(9\text{-anthrasesc})_3]12$

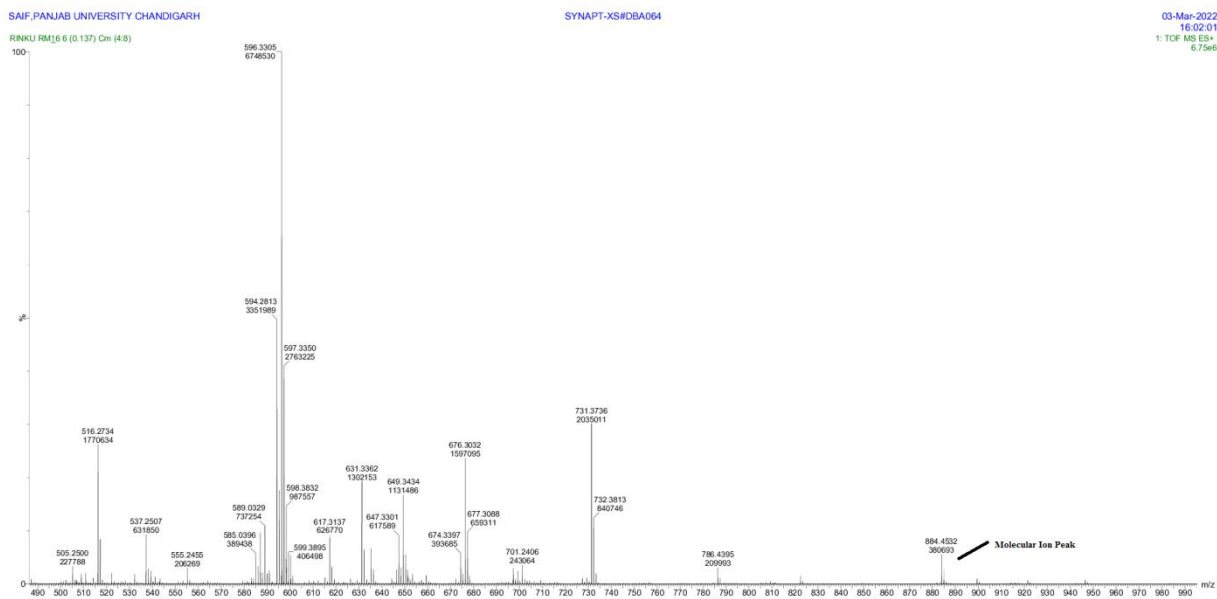


Figure 5.4.13 Mass Spectrum of $[\text{Fe}(1\text{-naphthsesc})_3]13$

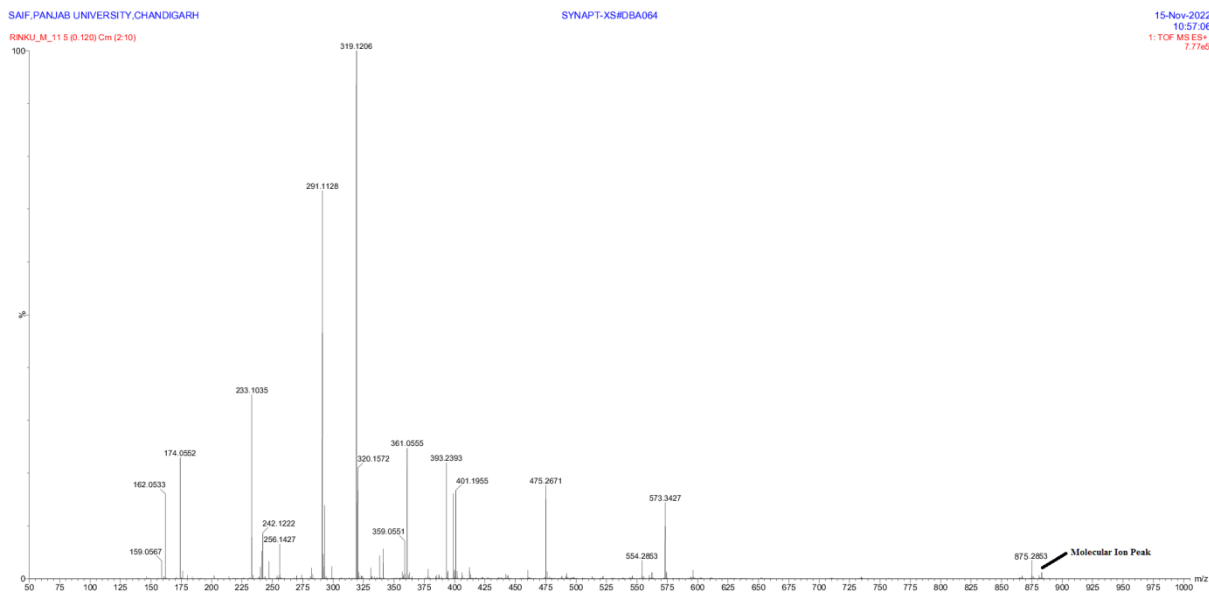


Figure 5.4.14 Mass Spectrum of $[\text{Fe}(2\text{-naphthsesc})_3]14$

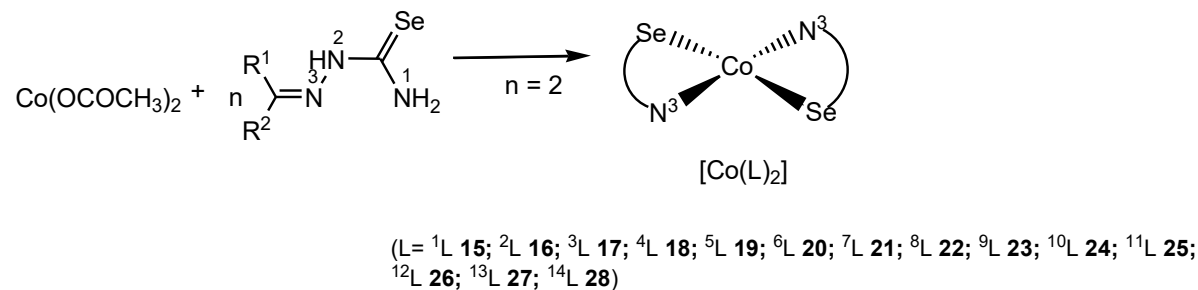
CHAPTER 6

COBALT(II) COMPLEXES

6 Complexes of Cobalt(II)

6.1 Discussion on Synthesis of cobalt metal complexes

Reaction of synthesized selenosemicarbazones ligands ($H^1L-H^{14}L$) with cobalt acetate in 2:1 may form complexes of stoichiometry, $[Co(L)_2]$ ($L = ^1L \text{ 15}; ^2L \text{ 16}; ^3L \text{ 17}; ^4L \text{ 18}; ^5L \text{ 19}; ^6L \text{ 20}; ^7L \text{ 21}; ^8L \text{ 22}; ^9L \text{ 23}; ^{10}L \text{ 24}; ^{11}L \text{ 25}; ^{12}L \text{ 26}; ^{13}L \text{ 27}; ^{14}L \text{ 28}$) (Scheme 6.1)



Scheme 6.1

All the synthesized complexes along with the structure of their respective selenosemicarbazones are given in table 6.1

Table 6.1 List of selenosemicarbazone complexes of cobalt(II) 15-28

Sr. No.	Selenosemicarbazone Ligands	Structure of Selenosemicarbazone Ligands	Complexes Formed
1.	Cyclohexanone selenosemicarbazone(Hcysesc, H^1L)		$[Co(cysesc)_2]15$
2.	2-furfural selenosemicarbazone (2-Hfursesc, H^2L)		$[Co(2-fursesc)_2]16$

3.	2-thiophene selenosemicarbazone (2-Hthiosesc, H³L)		[Co(2-thiosesc) ₂]17
4.	N-methyl-2-pyrrole selenosemicarbazone (N-MeHPysesc, H⁴L)		[Co(N-mepysesc) ₂]18
5.	3-methyl-2-oxindole selenosemicarbazone (3-MeHOxsesc, H⁵L)		[Co(3-meoxsesc) ₂]19
6.	2-oxindole selenosemicarbazone (2-HOxsesc, H⁶L)		[Co(2-oxsesc) ₂]20
7.	6-chloro-2-oxindole selenosemicarbazone (6-ClHOxsesc, H⁷L)		[Co(6-cloxsesc) ₂]21
8.	5-chloro isatin selenosemicarbazone (5-ClHIstsesc, H⁸L)		[Co(5-clistsesc) ₂]22
9.	1-methyl isatin selenosemicarbazone (1-MeHIstsesc, H⁹L)		[Co(1-meistsesc) ₂]23

10.	indole-3-selenosemicarbazone (3-HIndsesc, H¹⁰L)		[Co(3-insesc) ₂]24
11.	3-acetyl indoleselenosemicarba zone (3-AcHIndsesc, H¹¹L)		[Co(3-acinsesc) ₂]25
12.	9-anthrinaldehyde selenosemicarbazone (9-HAnsesc, H¹²L)		[Co(9-ansesc) ₂]26
13.	1-Naphthaldehyde selenosemicarbazone (1-HNapsesc, H¹³L)		[Co(1-naphsesc) ₂]27
14.	2-Naphthaldehyde selenosemicarbazone (2-HNapsesc, H¹⁴L)		[Co(2-naphsesc) ₂]28

6.2 IR Spectroscopy:

Important IR peaks of selenosemicarbazones are given in table 6.2 and IR spectra are given in figures 6.2.1-6.2.14. The $\nu(\text{NH})$ band due to amino group in free ligands appeared in the range 3417-3223 cm^{-1} (**H¹L-H¹⁴L**). On complexation with Cobalt(II) these bands showed slight shift to lower energy and appear in the range 3361-3208 cm^{-1} . The amide band $\nu(-$

NH-) in free ligands appeared in the range 3157-3110 cm⁻¹(**H¹L-H¹⁴L**). In ligands **H⁵L-H¹¹L**, amide band gets observed by stretching of -NH- group present in heterocyclic rings. In complexes **15-24, 26-28** absence of this band indicates deprotonation and coordination of ligand to metal in anionic form. In complex **25**, the presence of band in the range 3153 cm⁻¹ is due to the NH group of heterocyclic ring which makes it difficult to determine the binding of ligand in neutral or anionic form.

The C=Se band in the ligands appeared in the range 898-854 cm⁻¹. On complexation this band shifted to low energy and appeared in the range 792-703 cm⁻¹. The lower energy shift indicates the change of C=Se to C-Se⁻ thus suggests binding of ligand in selenate form.

Other IR peaks like $\nu(C=N)$, $\nu(C=C)$ and $\delta(NH_2)$ appeared in the range 1627-1418 cm⁻¹ in complexes and showed no significant change vis-à-vis free ligands.

Table 6.2 Important IR peaks of selenosemicarbazones (**H¹L-H¹⁴L**) and cobalt(II) complexes (**15-28**)

Synthesised Ligands and Metal Complexes	$\nu(NH_2)$	$\nu(-NH-)$	$\nu(C=N)$, $\nu(C=C)$, $\delta(NH_2)$	$\nu(C=Se)$	$\nu(-NH-)$ heterocyclic ring
Cyclohexanoneselenosemicarbazone (Hcysesc)H¹L	3362m, 3225m	3157w	1591s, 1489m, 1454s	856s	-
[Co(cysesc)₂]15	3301m	-	1627s, 1556m, 1422s	752s	-
2-furfural selenosemicarbazone (2-Hfursesc) H²L	3379m, 3340m	3142w	1600s, 1579m, 1464s	812s	-
[Co(2-fursesc)₂]16	3303m	-	1582s, 1499m, 1466s	744s	-
2-thiophene selenosemicarbazone (2-thiosesc) H³L	3389m, 3221m	3095w	1599s, 1527m, 1415s	844s	-
[Co(2-thiosesc)₂]17	3304m	-	1605s, 1564m, 1416s	703s	-

N-methyl-2-pyrrole selenosemicarbazone (N-Hmepysesc) H⁴L	3412m, 3223m	3110w	1633s, 1562m, 1496s	854s	-
[Co(N-mepysesc)₂]18	3344m	-	1598s, 1567m, 1417s	728s	-
3-methyl-2-oxindole selenosemicarbazone (3-Hmeoxsesc) H⁵L	3358m, 3248m	3157w	1591s, 1489m, 1425s	854s	-
[Co(3-meoxsesc)₂]19	3208m	-	1613s, 1572m, 1427s	742s	-
2-oxindole selenosemicarbazone (2-Hoxsesc) H⁶L	3362m, 3225m	3157w	1591s, 1489m, 1454s	856s	-
[Co(2-oxsesc)₂]20	3249m	-	1616s, 1554m, 1436s	792s	-
6-chloro-2-oxindole selenosemicarbazone (6-Hcloxsesc) H⁷L	3417m, 3255m	3142w	1589s, 1512m, 1499s	879s	-
[Co(6-cloxsesc)₂]21	3339m	-	1608s, 1598m, 1418s	717s	-
5-chloroisatin selenosemicarbazone (5-Hclistsesc) H⁸L	3219m	3110w	1694s, 1618s, 1559m, 1447s	885s	-
[Co(5-clistsesc)₂]22	3256m	-	1697s, 1610s, 1481m, 1446s	767s	-
1-methylisatin selenosemicarbazone (1-Hmeistsesc) H⁹L	3408m, 3228m	3128w	1676s, 1602s, 1492m, 1415s	889s	-
[Co(1-meistsesc)₂]23	3248m	-	1693s, 1604s, 1505m, 1464s	749s	-

3-indole selenosemicarbazone (3-Hindsesc) H¹⁰L	3356m, 3246m	3153w	1591s, 1487m, 1450s	898s	-
[Co(3-indsesc) ₂] 24	3361m	-	1615s, 1567s, 1500s	784s	-
3-acetylindole selenosemicarbazone (3-Hacindsesc) H¹¹L	3290m	3142w	1624s, 1502m, 1406s	877s	-
[Co(3-acindsesc) ₂] 25	-	-	1610s, 1573m, 1426s	749s	3156w
9-anthracene selenosemicarbazone (9-Hantrasesc) H¹²L	3385m, 3248m	3151w	1639s, 1518m, 1402s	887s	-
[Co(9-antrasesc) ₂] 26	3243m	-	1635s, 1547m, 1419s	752s	-
1-naphthaldehyde selenosemicarbazone (1-Hnaphthsesc) H¹³L	3400m	3147w	1599s, 1516m, 1452s	871s	-
[Co(1-naphthsesc) ₂] 27	3358m	-	1604s, 1545m, 1456s	765s	-
2-naphthaldehyde selenosemicarbazone (2-Hnaphthsesc) H¹⁴L	3352m	3124w	1597s, 1533m, 1446s	856s	-
[Co(2-naphthsesc) ₂] 28	3331m	-	1614s, 1543m, 1460s	765s	-

6.3 Mass Spectrometry:

Mass spectra of complexes **15-28**, has been recorded and given in figures 6.3.1-6.3.14. The observed molecular ion peak [M]⁺ are given in table 6.3. From the table it is clear that m/z values for complexes **15-28** are close to their proposed stoichiometry [Co(L)₂] and thus confirmed the co-ordination of Cobalt(II) with selenosemicarbazones.

Table 6.3 m/z values (amu) of complexes **15-28** obtained from Mass Spectra

Complex No.	Parent peak obtained from mass spectra	Expected formula for parent ion (m/z)⁺
15	492	[Co(C ₇ H ₁₂ N ₃ Se) ₂]
16	484	[Co(C ₆ H ₅ N ₃ OSe) ₂]
17	513	[Co(C ₆ H ₃ N ₃ SSe) ₂]
18	511	[Co(C ₇ H ₈ N ₄ Se) ₂]
19	593	[Co(C ₁₀ H ₁₃ N ₄ Se) ₂]
20	563	[Co(C ₉ H ₁₀ N ₄ Se) ₂]
21	631	[Co(C ₉ H ₉ N ₄ ClSe) ₂]
22	658	[Co(C ₉ H ₇ N ₄ OClSe) ₂]
23	614	[Co(C ₁₀ H ₈ N ₄ OSe) ₂]
24	587	[Co(C ₁₀ H ₉ N ₄ Se) ₂]
25	615	[Co(C ₁₁ H ₁₂ N ₄ Se) ₂]
26	709	[Co(C ₁₆ H ₁₃ N ₃ Se) ₂]
27	608	[Co(C ₁₂ H ₁₀ N ₃ Se) ₂]
28	610	[Co(C ₁₂ H ₁₂ N ₃ Se) ₂]

6.4 CHN Spectroscopy:

The percentage carbon, hydrogen and nitrogen in complexes **15-28** has been determined by elemental analysis and the result are given in Table 7.4. From the table, it is clear that the experimental values are in close proximity with the calculated value for the molecular formula [Co(L)₂] of complexes **15-28**.

Table 6.4 Carbon, hydrogen and nitrogen (%age) present in complexes **15-28**

S. No	Carbon		Hydrogen		Nitrogen		Expected formula for parent ion
	Calculated	Found	Calculated	Found	Calculated	Found	
1.	33.9	33.2	5.2	5.0	16.9	16.4	[Co(C ₇ H ₁₃ N ₃ Se) ₂] 15
2.	25.7	25.4	2.9	2.0	17.9	17.1	[Co(C ₆ H ₇ N ₃ OSe) ₂] 16
3.	24.0	23.8	2.8	2.3	16.9	16.4	[Co(C ₆ H ₇ N ₃ SSe) ₂] 17
4.	34.3	34.0	4.0	3.8	17.1	16.8	[Co(C ₇ H ₁₀ N ₄ Se) ₂] 18
5.	40.4	40.1	4.0	3.8	18.8	18.0	[Co(C ₁₀ H ₁₂ N ₄ Se) ₂] 19
6.	33.9	33.2	5.2	5.0	16.9	16.4	[Co(C ₉ H ₁₀ N ₄ Se) ₂] 20
7.	33.9	33.2	5.2	5.0	16.9	16.4	[Co(C ₉ H ₉ N ₄ ClSe) ₂] 21
8.	33.9	33.2	5.2	5.0	16.9	16.4	[Co(C ₉ H ₇ N ₄ ClOSe) ₂] 22
9.	33.9	33.2	5.2	5.0	16.9	16.4	[Co(C ₁₀ H ₁₀ N ₄ OSe) ₂] 23
10.	40.8	40.3	3.4	3.0	19.0	18.8	[Co(C ₁₀ H ₁₀ N ₄ Se) ₂] 24
11.	42.8	42.2	3.8	3.2	18.1	18.0	[Co(C ₁₁ H ₁₂ N ₄ Se) ₂] 25
12.	54.0	53.8	3.6	3.2	11.8	11.6	[Co(C ₁₆ H ₁₅ N ₃ Se) ₂] 26
13.	47.1	46.9	3.6	3.4	13.7	13.3	[Co(C ₁₂ H ₁₁ N ₃ Se) ₂] 27
14.	47.1	46.9	3.6	3.3	13.7	13.5	[Co(C ₁₂ H ₁₁ N ₃ Se) ₂] 28

6.5 ESR Spectroscopy:

Electron Spin Resonance spectroscopy has been used as a powerful technique to determine the spin state of Cobalt(II) complexes. To determine the oxidation and spin state of synthesized complexes, ESR spectrum of representative complex **28** was recorded and spectrum is give in Figure 6.5.1.

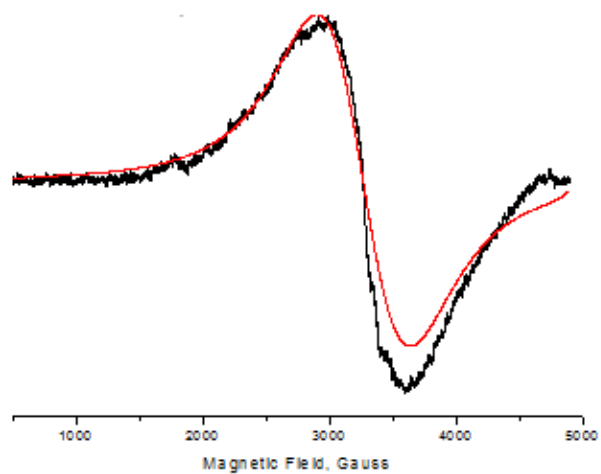


Figure 6.5.1 Experimental (black) and simulated (red) best fit EPR spectrum of $[\text{Co}(2\text{-naphthsesc})_2]\mathbf{28}$ complex

From ESR spectra, the structure of complex **28** is found to be square planar as measured with respect to given g values ($g_{||}=2.0$ and $g_{\perp}=2.2$) [157-170].

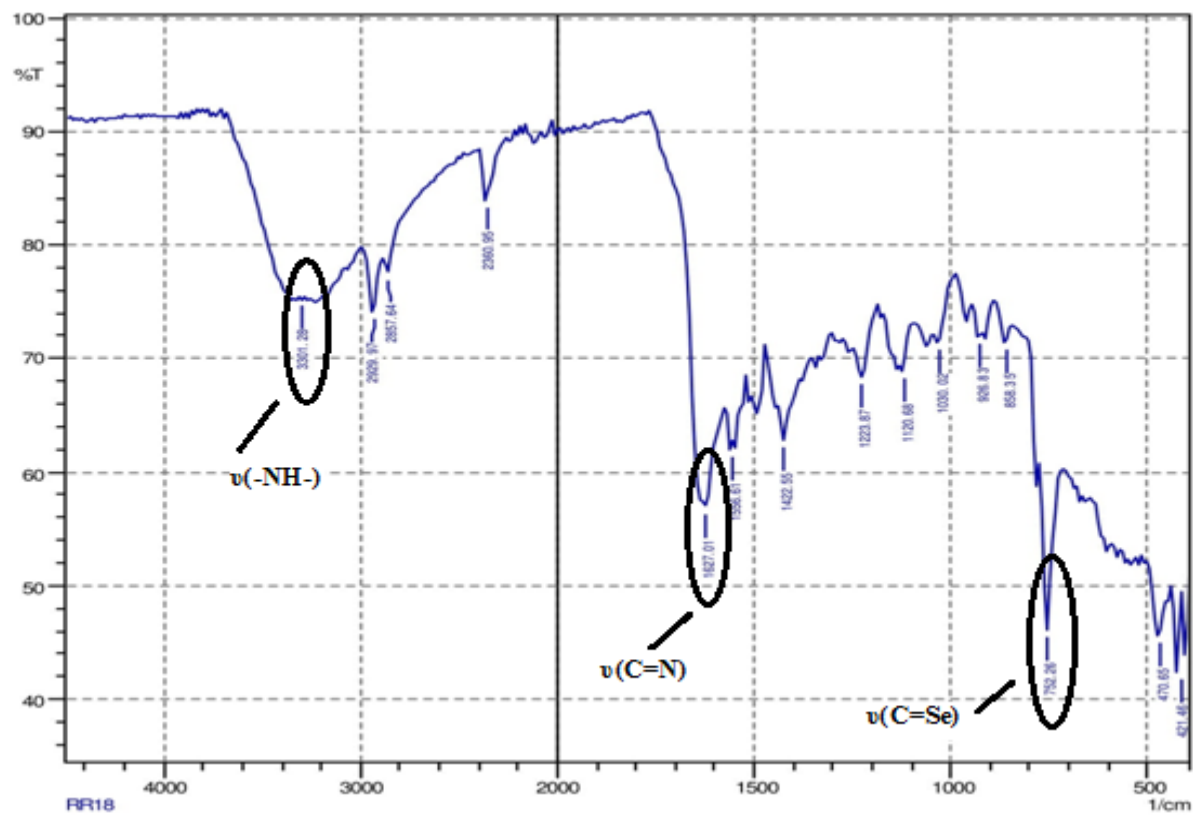


Figure 6.2.1 IR spectrum of $[\text{Co}(\text{cysesc})_2]\mathbf{15}$

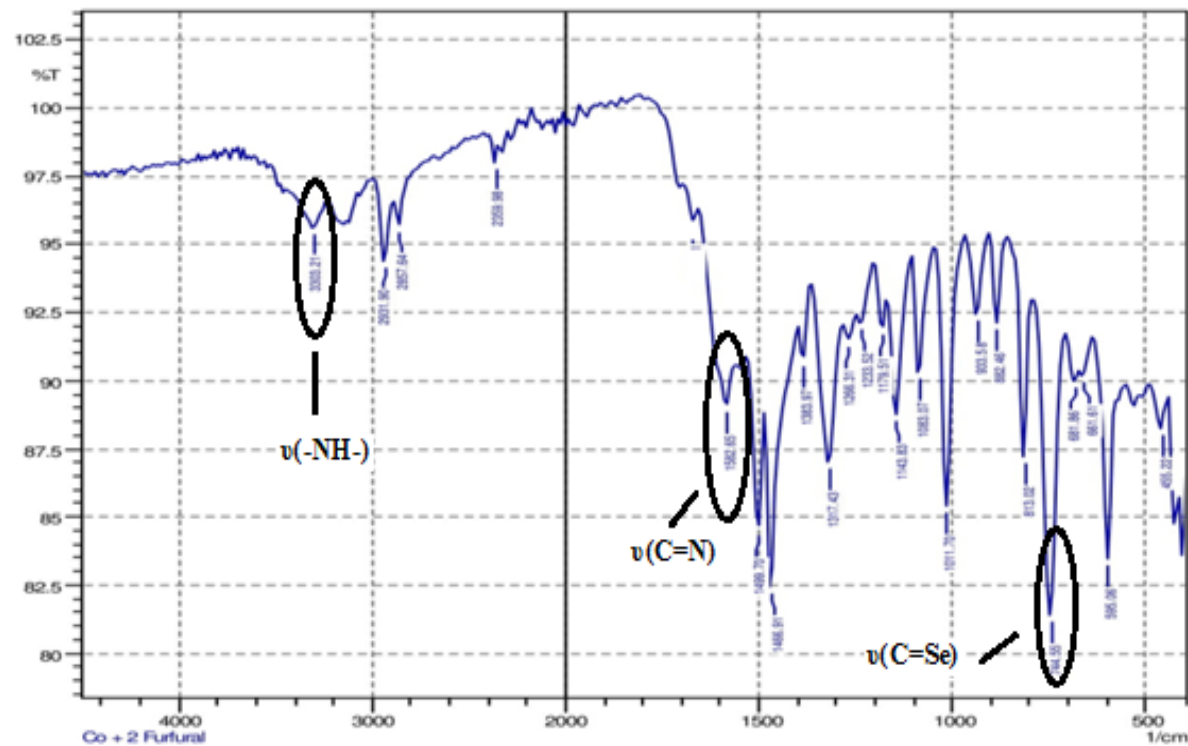


Figure 6.2.2 IR spectrum of $[\text{Co}(2\text{-fursesc})_2]\mathbf{16}$

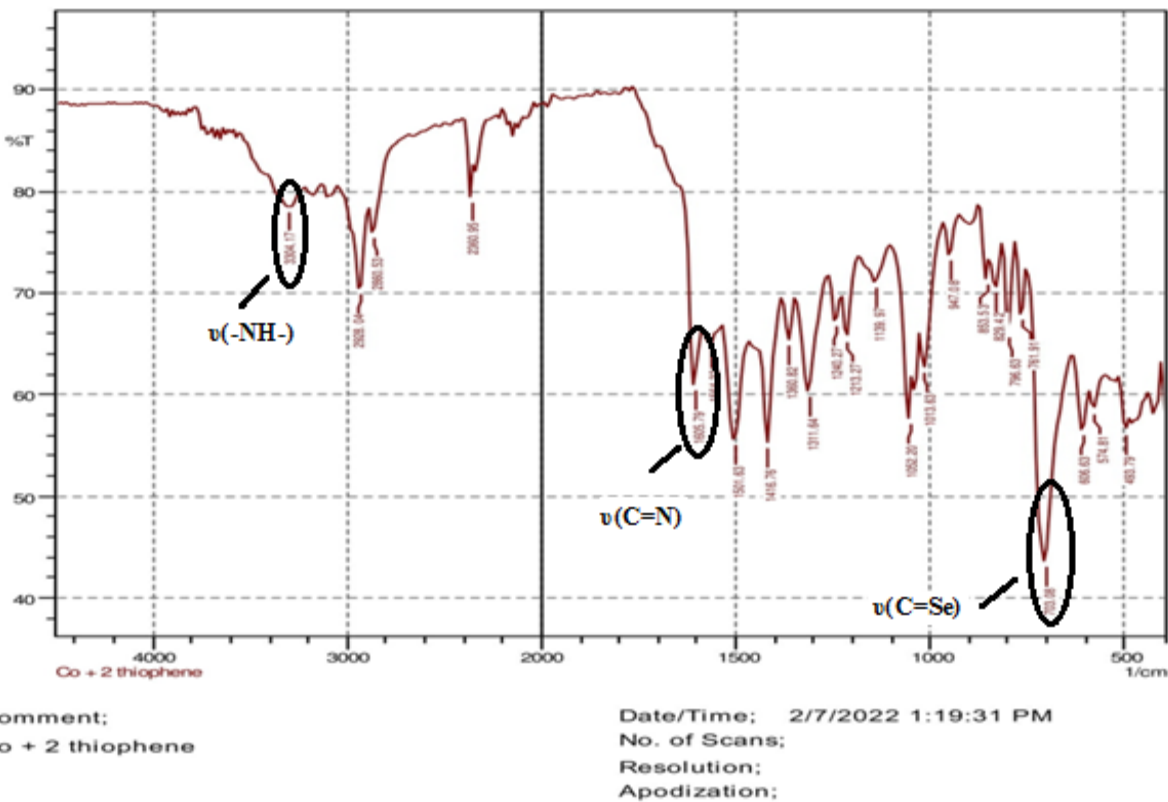


Figure 6.2.3 IR spectrum of $[\text{Co}(\text{2-thiosesc})_2]$ 17

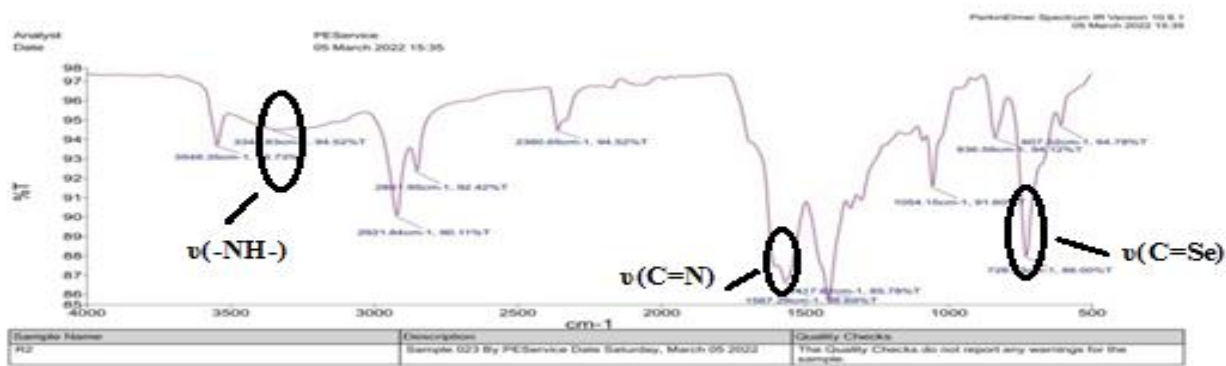


Figure 6.2.4 IR spectrum of $[\text{Co}(\text{N-mepysesc})_2]$ 18

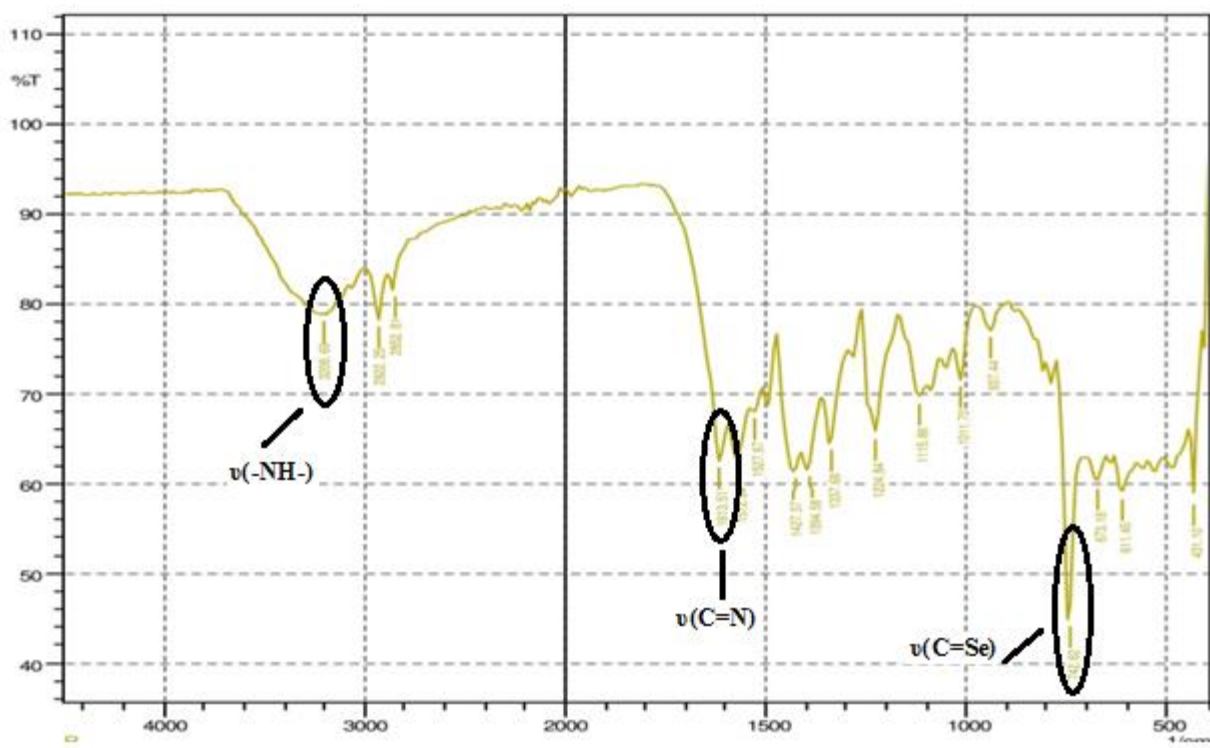


Figure 6.2.5 IR spectrum of $[\text{Co}(3\text{-meoxsesc})_2]$ 19

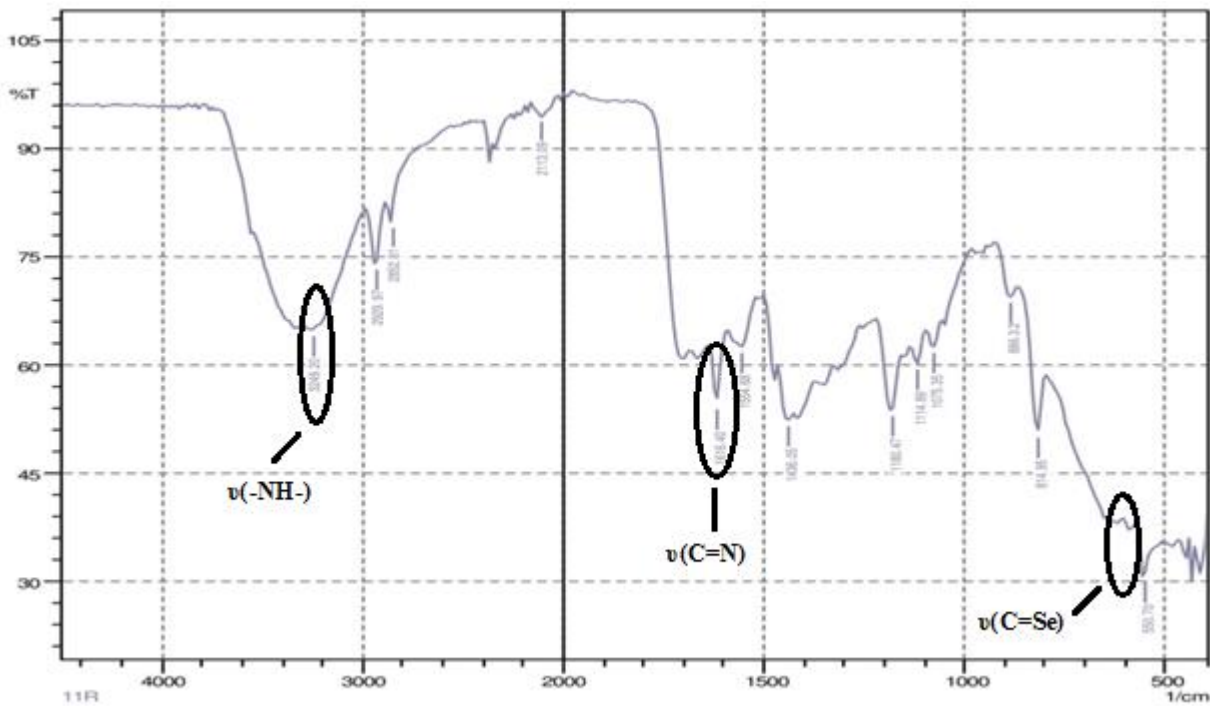


Figure 6.2.6 IR spectrum of $[\text{Co}(2\text{-oxsesc})_2]$ 20

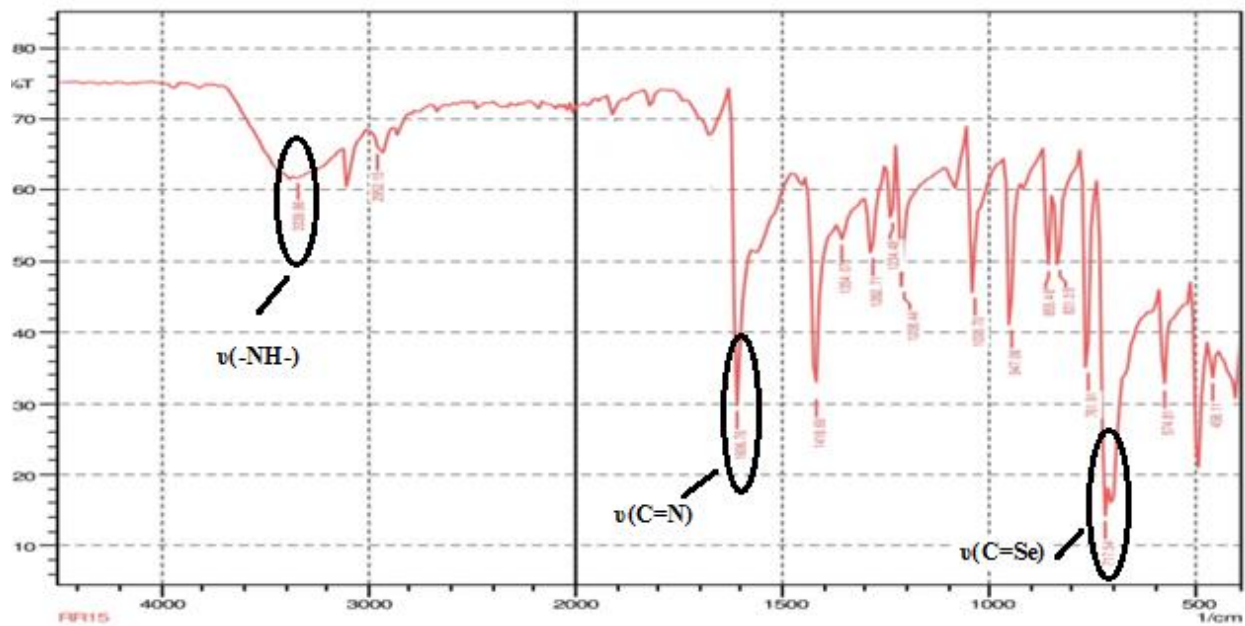


Figure 6.2.7 IR spectrum of $[\text{Co}(6\text{-cloxsesc})_2]21$

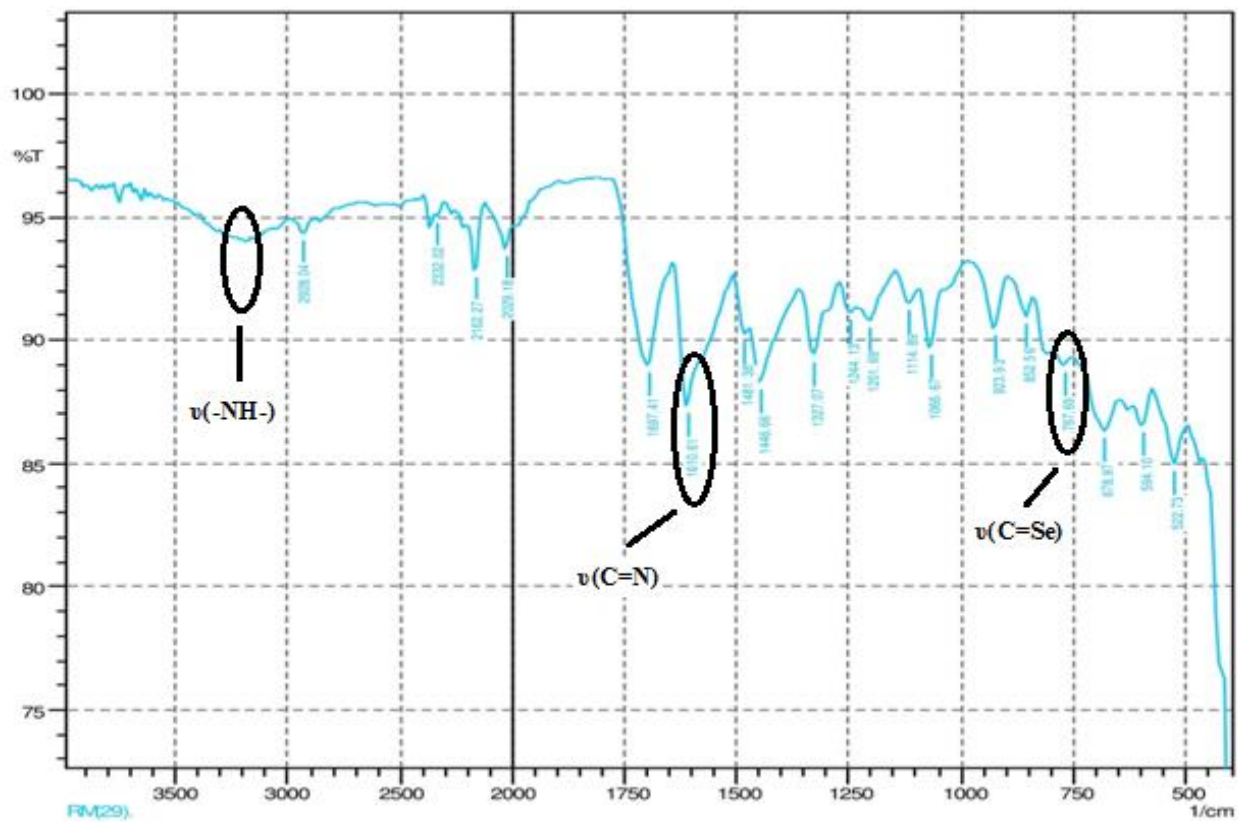


Figure 6.2.8 IR spectrum of $[\text{Co}(5\text{-clistsesc})_2]22$

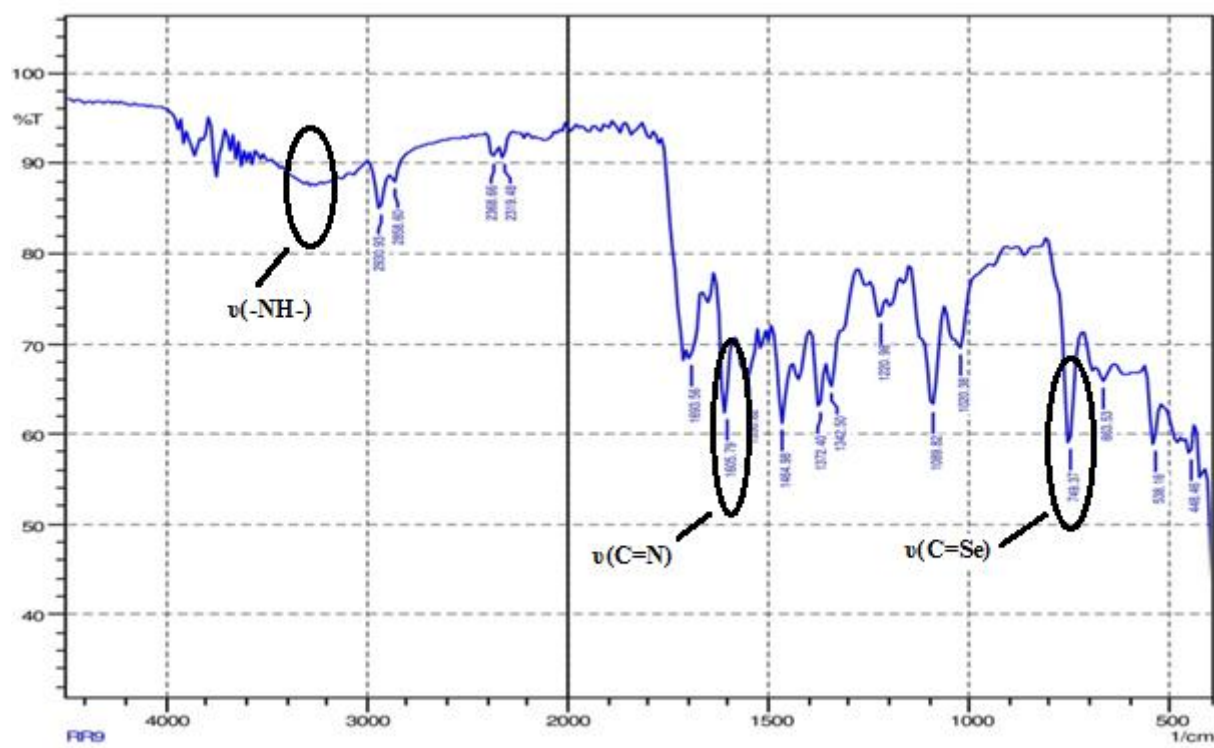


Figure 6.2.9 IR spectrum of $[\text{Co}(1\text{-meistsesc})_2]23$

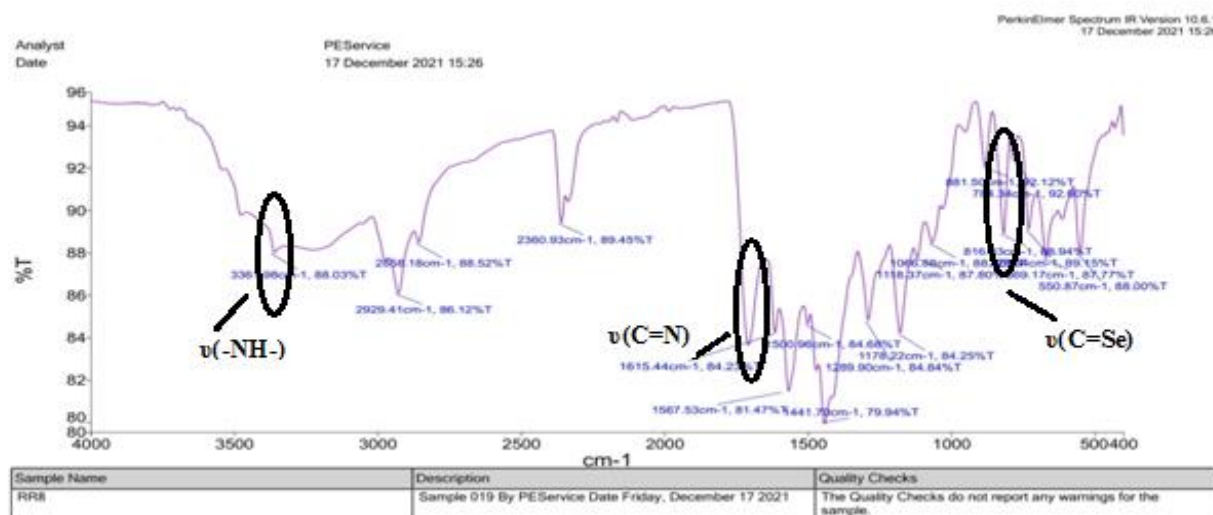


Figure 6.2.10 IR spectrum of $[\text{Co}(3\text{-indsesc})_2]24$

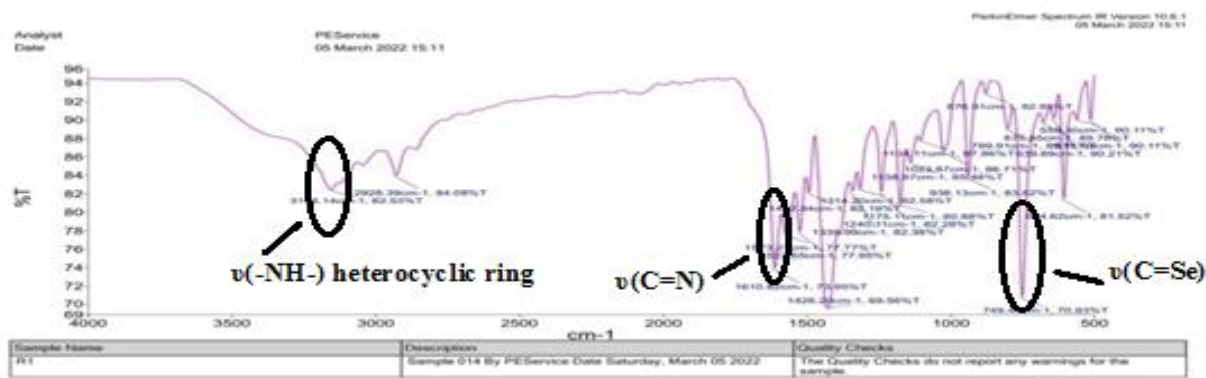


Figure 6.2.11 IR spectrum of $[\text{Co}(3\text{-acindsesc})_2]25$

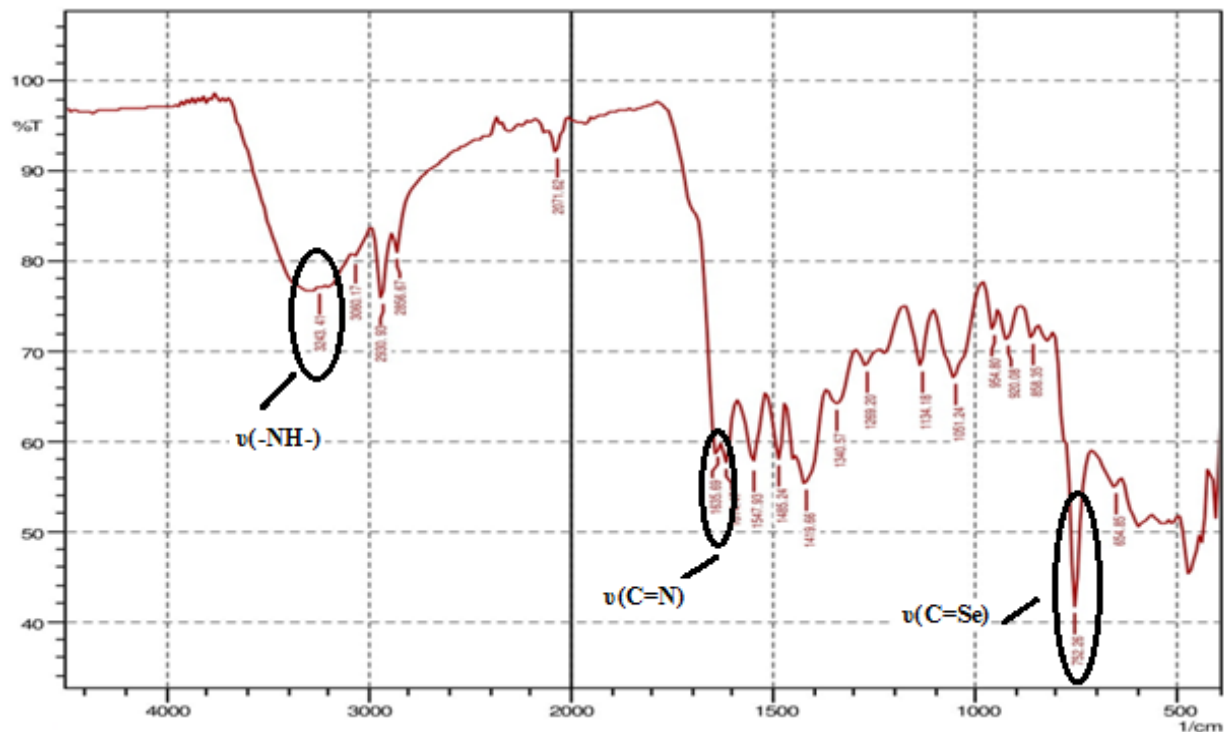


Figure 6.2.12 IR spectrum of $[\text{Co}(9\text{-anthrasesc})_2]26$

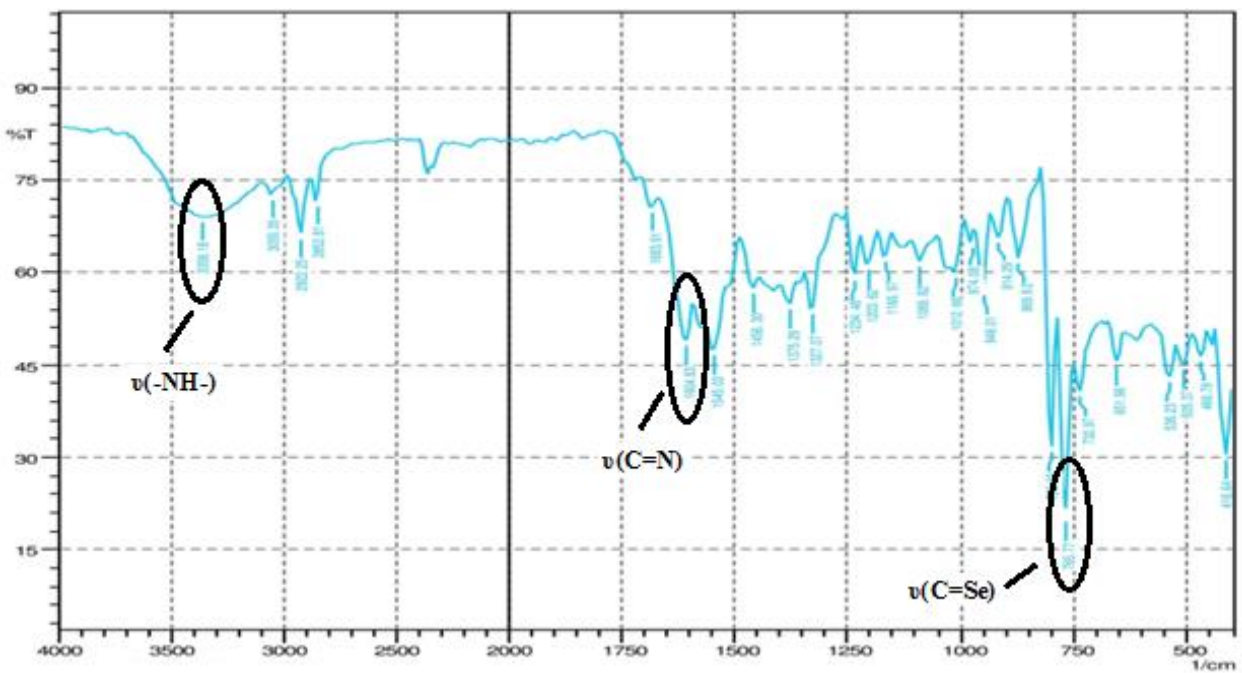


Figure 6.2.13 IR spectrum of $[\text{Co}(1\text{-naphthsesc})_2]27$

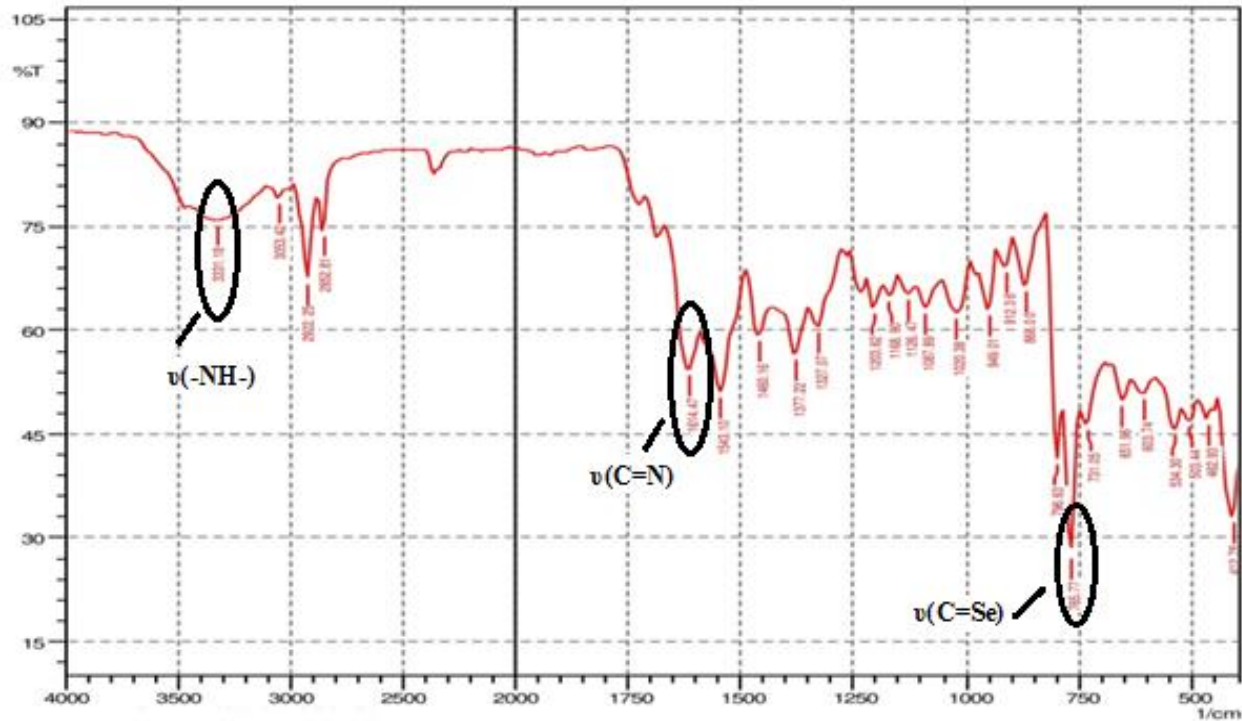


Figure 6.2.14 IR spectrum of $[\text{Co}(2\text{-naphthsesc})_2]28$



Figure 6.3.1a) Mass Spectrum of $[\text{Co}(\text{cysesc})_2]\mathbf{15}$

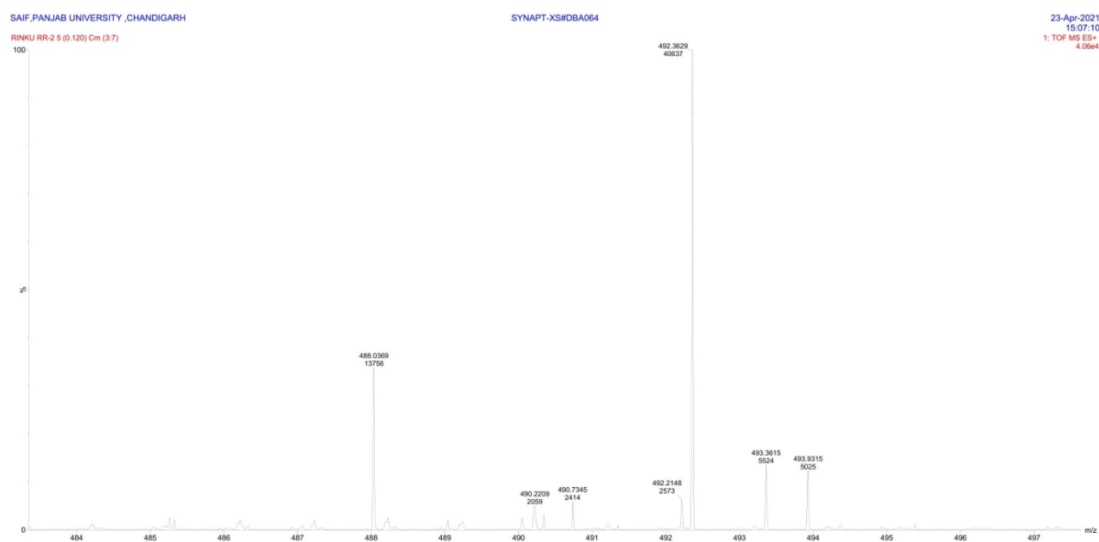


Figure 6.3.1b) Mass Spectrum of $[\text{Co}(\text{cysesc})_2]\mathbf{15}$

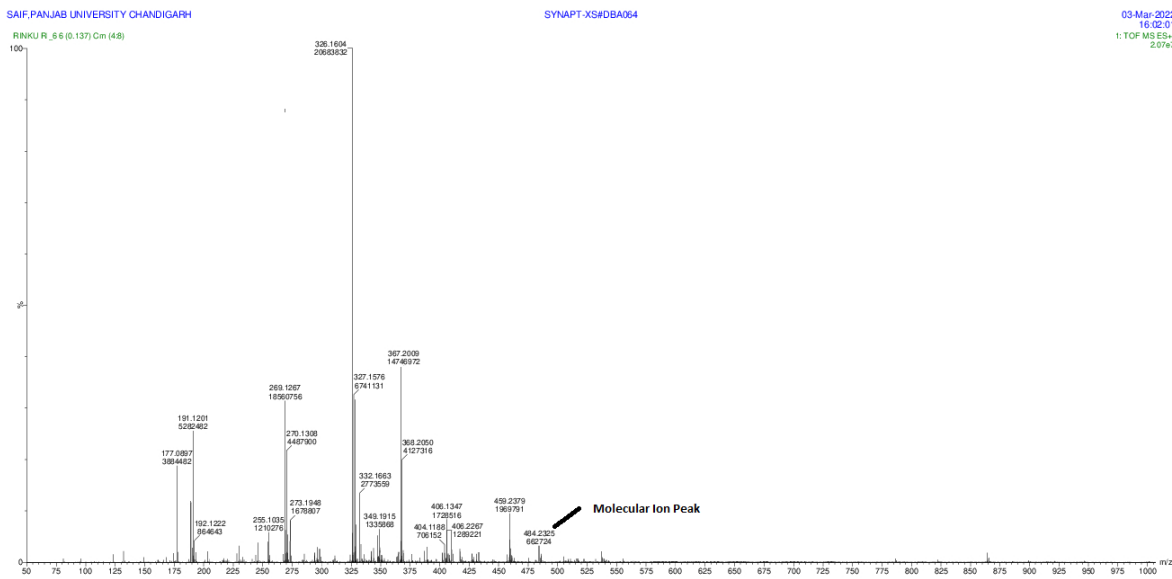


Figure 6.3.2 Mass Spectrum of $[\text{Co}(2\text{-fursesc})_2]\mathbf{16}$

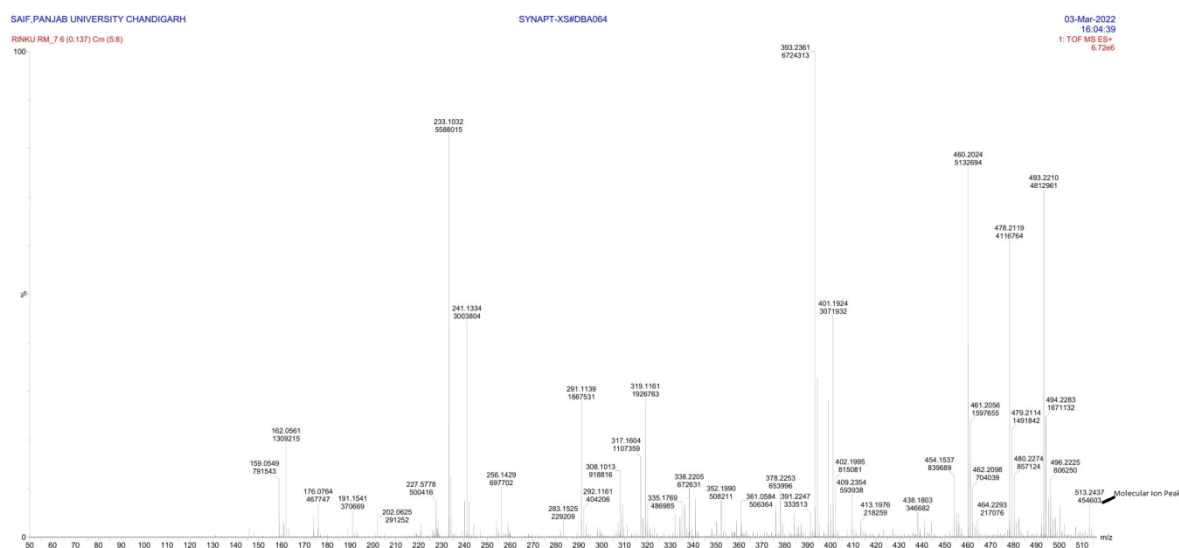


Figure 6.3.3 Mass Spectrum of $[\text{Co}(2\text{-thiosesc})_2]\mathbf{17}$

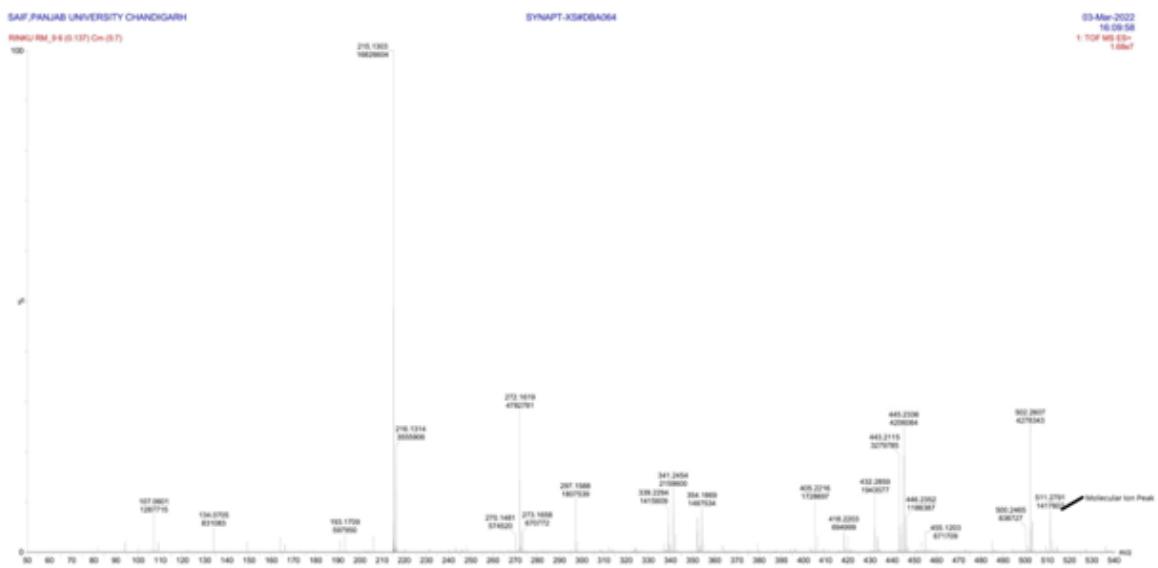


Figure 6.3.4 Mass Spectrum of $[\text{Co}(\text{N-mepysesc})_2]\mathbf{18}$

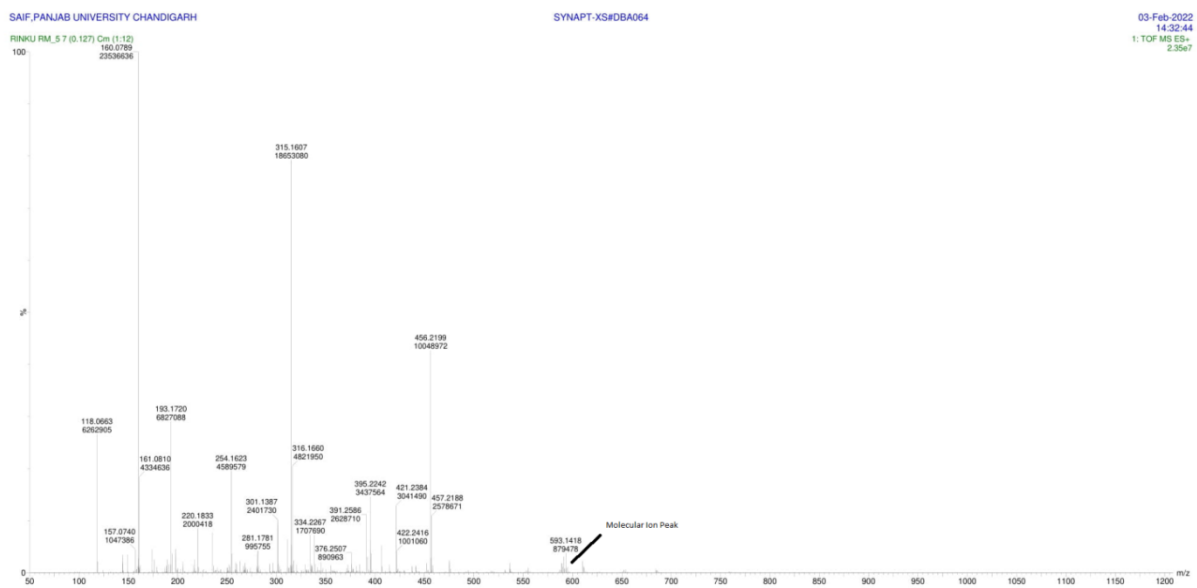


Figure 6.3.5 Mass Spectrum of $[\text{Co}(3\text{-meoxsesc})_2]\mathbf{19}$

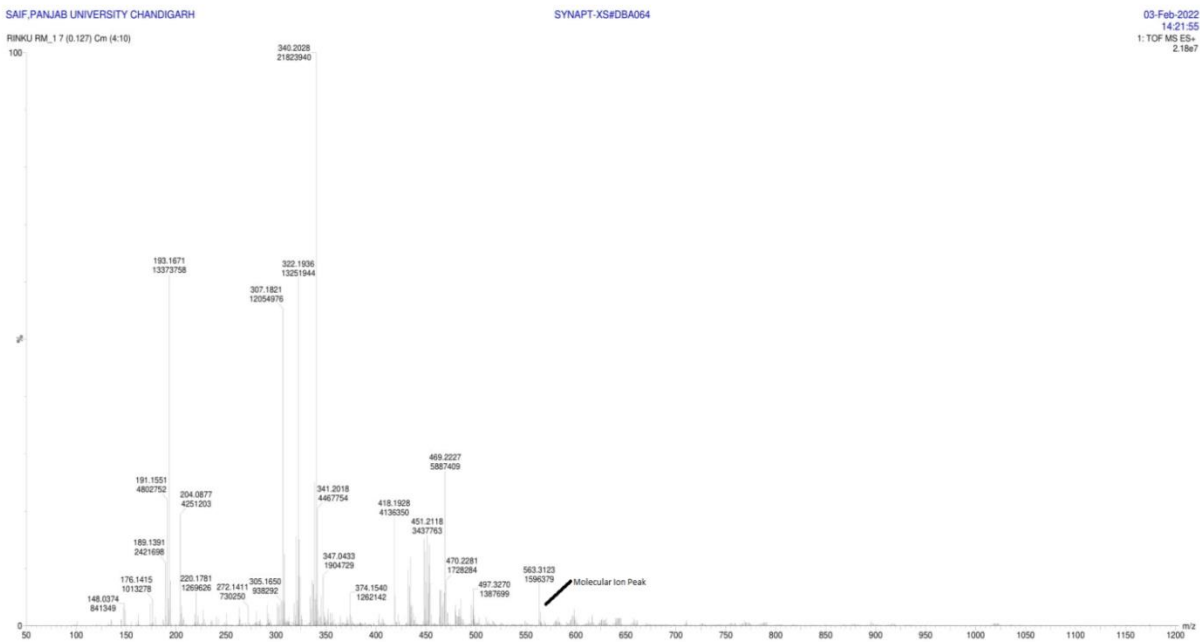


Figure 6.3.6 Mass Spectrum of $[\text{Co}(\text{oxsesc})_2]20$

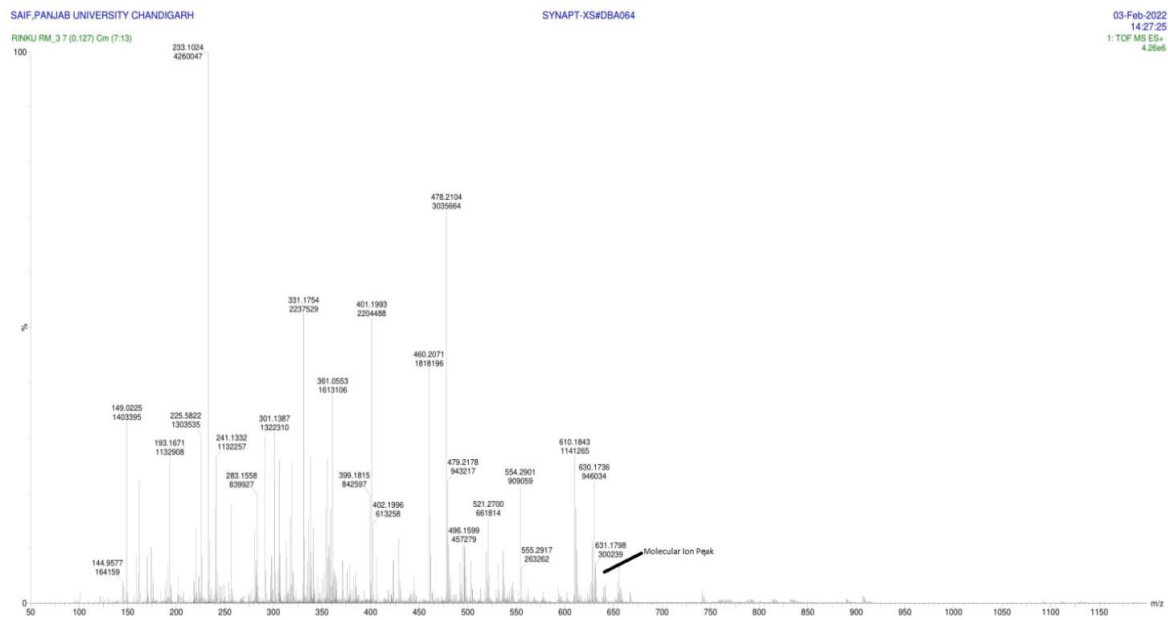


Figure 6.3.7 Mass Spectrum of $[\text{Co}(6\text{-cloxsesc})_2]21$

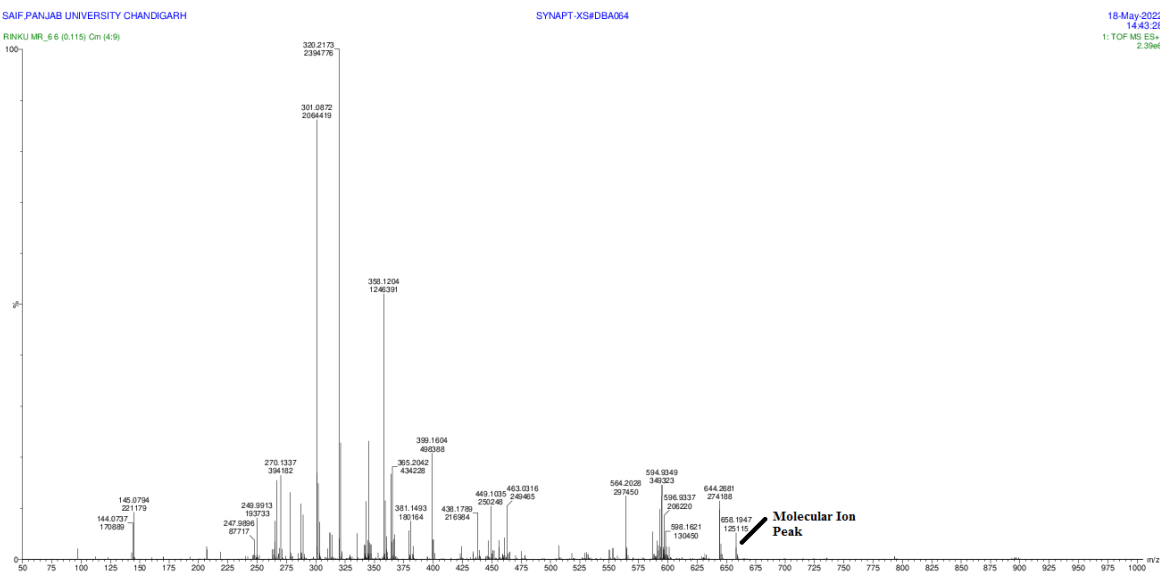


Figure 6.3.8 Mass Spectrum of $[\text{Co}(5\text{-clistsesc})_2]22$

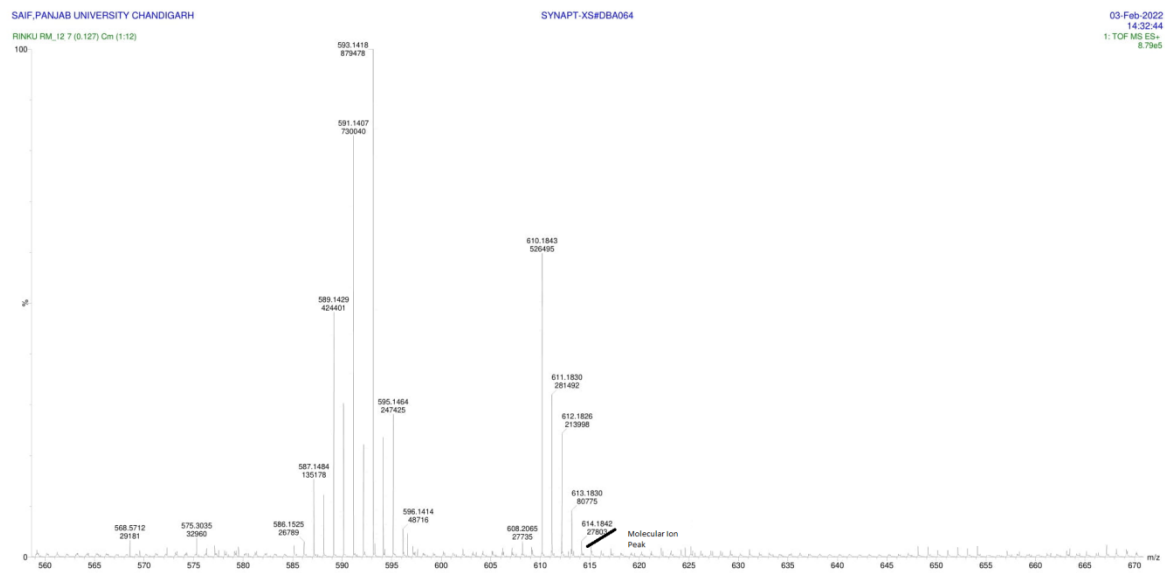


Figure 6.3.9 Mass Spectrum of $[\text{Co}(1\text{-meistsesc})_2]23$

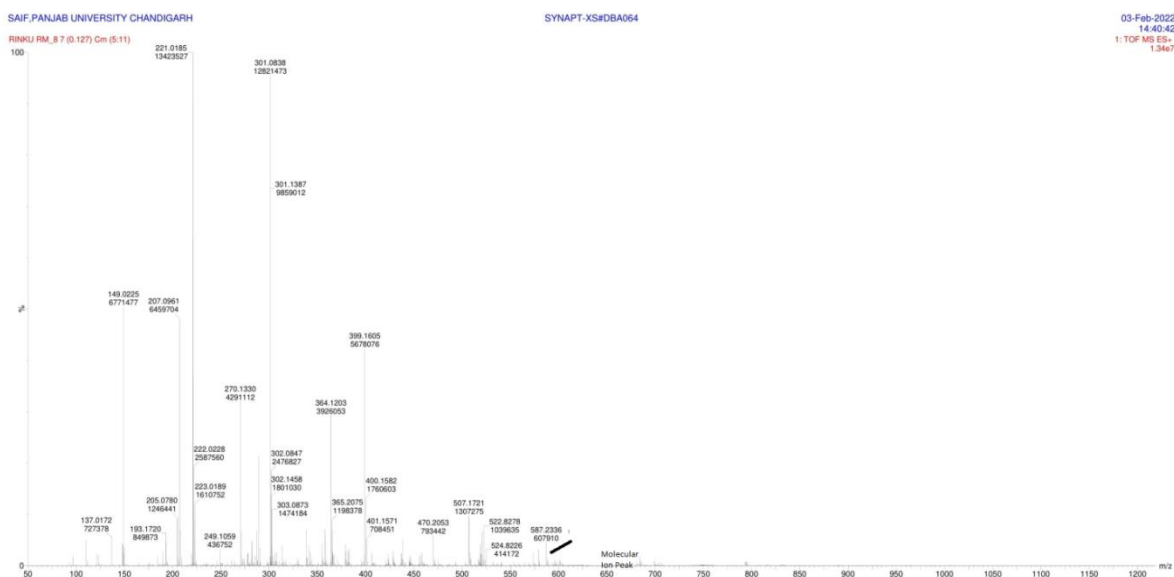


Figure 6.3.10 Mass Spectrum of $[\text{Co}(3\text{-indsesc})_2]24$

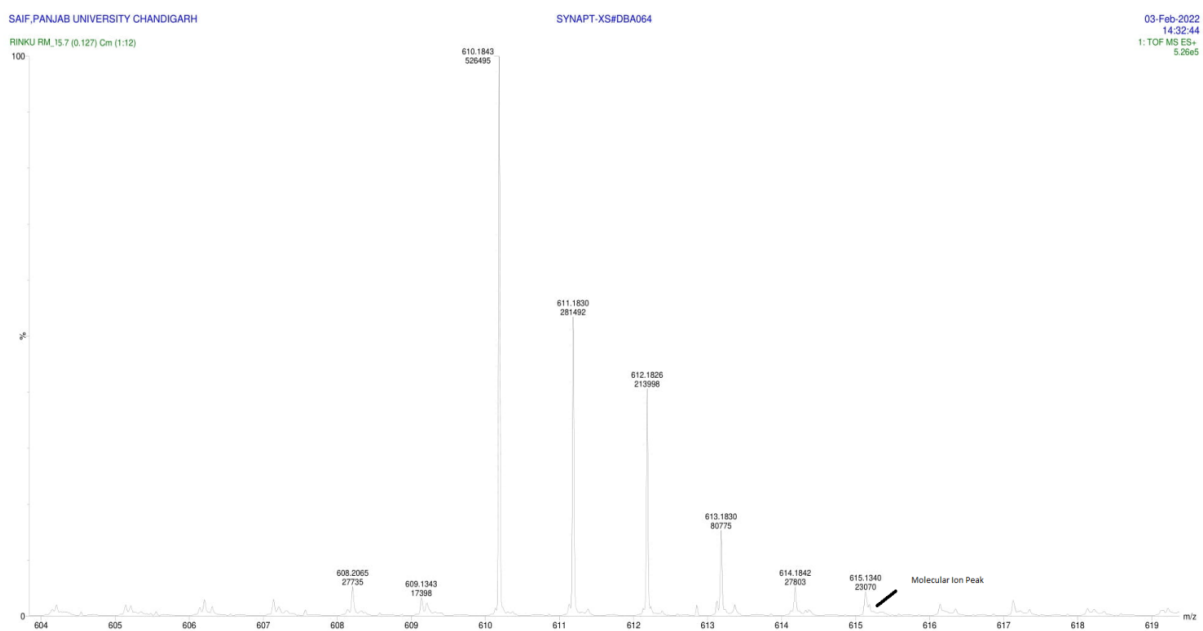


Figure 6.3.11 Mass Spectrum of $[\text{Co}(3\text{-acindsesc})_2]25$

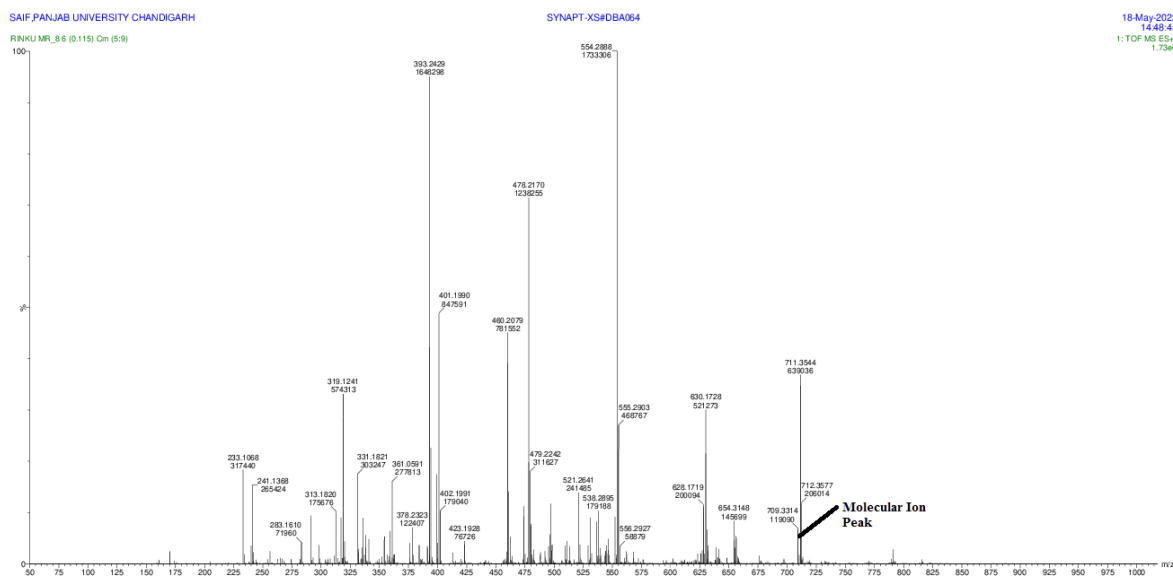


Figure 6.3.12 Mass Spectrum of $[\text{Co}(9\text{-anthracesc})_2]26$

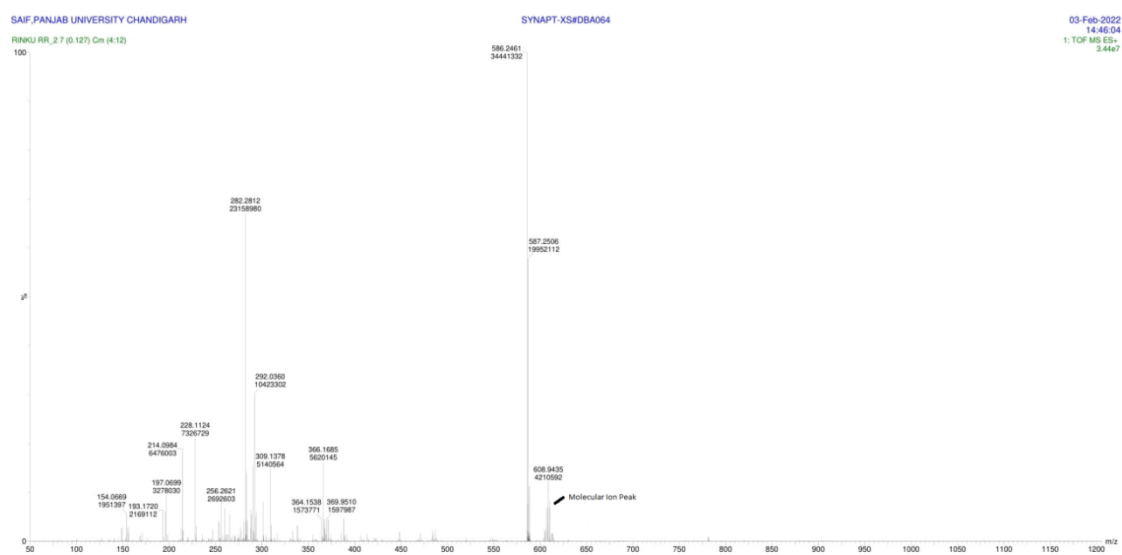


Figure 6.3.13 Mass Spectrum of $[\text{Co}(1\text{-naphthsesc})_2]27$

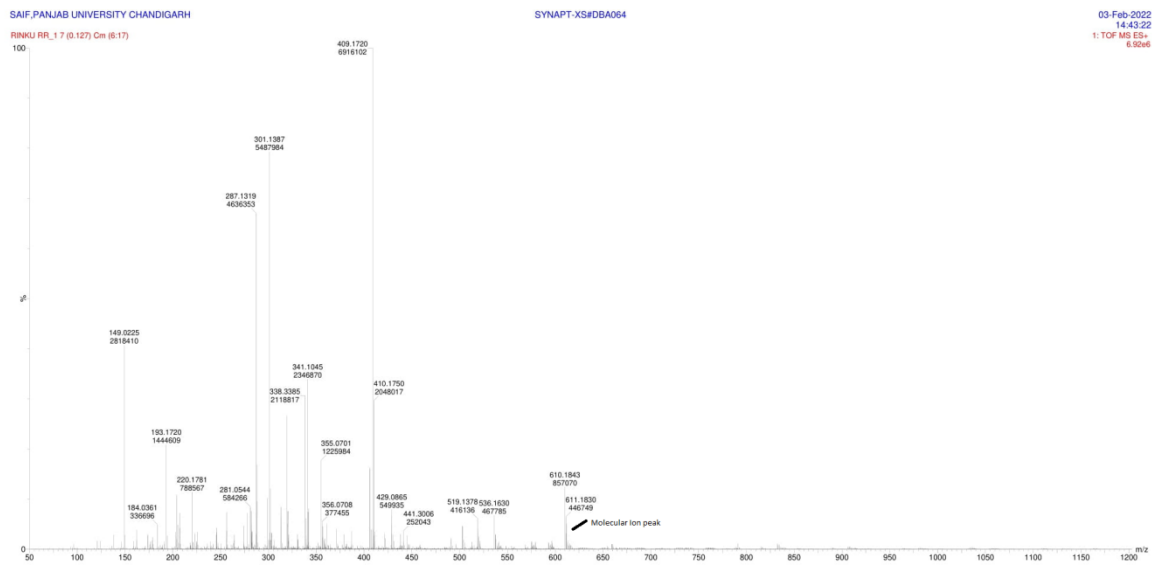


Figure 6.3.14 Mass Spectrum of $[\text{Co}(2\text{-naphthsesc})_2]28$

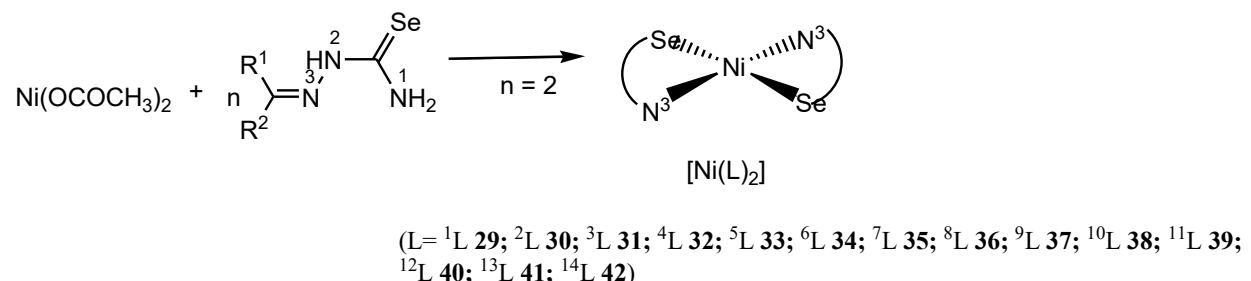
CHAPTER 7

NICKEL(II) COMPLEXES

7 Complexes of Nickel(II)

7.1 Discussion on Synthesis of nickel metal complexes

Reaction of synthesized selenosemicarbazones ligands ($H^1L-H^{14}L$) with nickel acetate in 2:1 may form complexes of stoichiometry, $[Ni(L)_2]$ ($L = ^1L \text{ 29}; ^2L \text{ 30}; ^3L \text{ 31}; ^4L \text{ 32}; ^5L \text{ 33}; ^6L \text{ 34}; ^7L \text{ 35}; ^8L \text{ 36}; ^9L \text{ 37}; ^{10}L \text{ 38}; ^{11}L \text{ 39}; ^{12}L \text{ 40}; ^{13}L \text{ 41}; ^{14}L \text{ 42}$) (Scheme 7.1)



Scheme 7.1

All the synthesized complexes along with the structure of their respective selenosemicarbazones are given in Table 7.1

Table 7.1 List of selenosemicarbazone complexes of nickel(II) 29-42

Sr. No.	Selenosemicarbazone Ligands	Structure of Selenosemicarbazone Ligands	Complexes Formed
1.	Cyclohexanone selenosemicarbazone (Hcysesc, H¹L)		$[Ni(\text{cysesc})_2] \text{ 29}$
2.	2-furfural selenosemicarbazone (2-Hfursesc, H²L)		$[Ni(2\text{-fursesc})_2] \text{ 30}$

3.	2-thiophene selenosemicarbazone (2-Hthiosesc, H³L)		[Ni(2-thiosesc) ₂]31
4.	N-methyl-2-pyrrole selenosemicarbazone (N-MeHPysesc, H⁴L)		[Ni(N-mepysesc) ₂]32
5.	3-methyl-2-oxindole selenosemicarbazone (3-MeHOxsesc, H⁵L)		[Ni(3-meoxsesc) ₂]33
6.	2-oxindole selenosemicarbazone (2-HOxsesc, H⁶L)		[Ni(2-oxsesc) ₂]34
7.	6-chloro-2-oxindole selenosemicarbazone (6-ClHOxsesc, H⁷L)		[Ni(6-cloxsesc) ₂]35
8.	5-chloro isatin selenosemicarbazone (5-ClHIstsesc, H⁸L)		[Ni(5-clistsesc) ₂]36
9.	1-methyl isatin selenosemicarbazone (1-MeHIstsesc, H⁹L)		[Ni(1-meistsesc) ₂]37
10.	indole-3-selenosemicarbazone (3-HIndsesc, H¹⁰L)		[Ni(3-insesc) ₂]38

11.	3-acetyl indole selenosemicarbazone (3-AcHIndsesc, H¹¹L)		[Ni(3-acinsesc) ₂]39
12.	9-anthrinaldehyde selenosemicarbazone (9-HAnsesc, H¹²L)		[Ni(9-ansesc) ₂]40
13.	1-Naphthaldehyde selenosemicarbazone (1-HNapsesc, H¹³L)		[Ni(1-naphsesc) ₂]41
14.	2-Naphthaldehyde selenosemicarbazone (2-HNapsesc, H¹⁴L)		[Ni(2-naphsesc) ₂]42

7.2 IR Spectroscopy:

Important IR peaks of selenosemicarbazones are given in table 7.2 and IR spectra are given in figures 7.2.1-7.2.14. The $\nu(\text{NH})$ band due to amino group in free ligands appeared in the range 3417-3223 cm^{-1} ($\text{H}^1\text{L}-\text{H}^{14}\text{L}$). On complexation with nickel(II) these bands showed slight shift to higher energy and appear in the range 3492-3273 cm^{-1} .

The amide band $\nu(-\text{NH}-)$ in free ligands appeared in the range 3157-3110 cm^{-1} ($\text{H}^1\text{L}-\text{H}^{14}\text{L}$). In ligands $\text{H}^5\text{L}-\text{H}^{11}\text{L}$, amide band gets observed by stretching of -NH- group present in heterocyclic rings. In complexes **29-32**, **37**, **40-42** absence of this band indicates deprotonation and co-ordination of ligand to metal in anionic form. In complexes **33-36**, **38**, **39**, the presence of band in the range 3147-3050 cm^{-1} is due to the NH group of heterocyclic ring which makes it difficult to determine the binding of ligand in neutral or anionic form.

The C=Se band in the ligands appeared in the range 898-854 cm^{-1} . On complexation this band shifted to low energy and appeared in the range 798-728 cm^{-1} . The lower energy shift indicates the appearance of C=Se to C-Se⁻ thus suggests binding of ligand in selenate form.

Other IR peaks like $\nu(\text{C}=\text{N})$, $\nu(\text{C}=\text{C})$ and $\delta(\text{NH}_2)$ appeared in the range 1649-1410 cm^{-1} in complexes and showed no significant change vis-à-vis free ligands.

Table 7.2 Important IR peaks of selenosemicarbazones ($\text{H}^1\text{L}-\text{H}^{14}\text{L}$) and nickel(II) complexes (**29-42**)

Synthesised Ligands and Metal Complexes	$\nu(\text{NH}_2)$	$\nu(-\text{NH}-)$	$\nu(\text{C}=\text{N})$, $\nu(\text{C}=\text{C})$, δ (NH_2)	$\nu(\text{C=Se})$	$\nu(-\text{NH}-)$ heterocyclic ring
Cyclohexanone Selenosemicarbazone	3362m, 3225m	3157w	1591s, 1489m, 1454s	856s	-
[Ni(cysesc) ₂] 29	3492m, 3371m, 3320m	-	1630s, 1584m, 1423s	781s	-
2-furfural selenosemicarbazone	3379m, 3340m	3142w	1600s, 1579m, 1464s	812s	-
[Ni(2-fursesc) ₂] 30	3410m, 3300m	-	1649s, 1597s, 1454s	738s	-
2-thiophene selenosemicarbazone	3389m, 3221m	3095w	1599s, 1527m, 1415s	844s	-

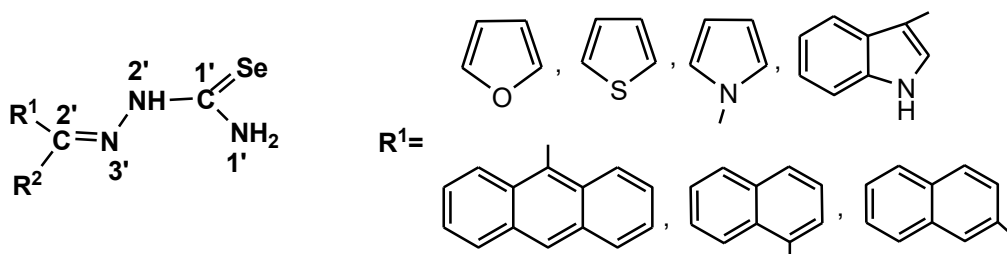
[Ni(2-thiosesc) ₂] 31	3291m	-	1607s, 1563m, 1417s	798s	-
N-methyl-2-pyrrole selenosemicarbazone	3412m, 3223m	3110w	1633s, 1562m, 1496s	854s	-
[Ni(N-mepysesc) ₂] 32	3443m, 3390m, 3242m	-	1548s, 1467m, 1410s	731s	-
3-methyl-2-oxindole selenosemicarbazone	3358m, 3248m	3157w	1591s, 1489m, 1425s	854s	-
[Ni(3-meoxsesc) ₂] 33	3377m, 3327m, 3273m	-	1626s, 1595m, 1473s	792s	3123w
2-oxindole selenosemicarbazone	3362m, 3225m	3157w	1591s, 1489m, 1454s	856s	-
[Ni(2-oxsesc) ₂] 34	3269m	-	1643s, 1602m, 1448s	742s	3134w
6-chloro-2-oxindole selenosemicarbazone	3417m, 3255m	3142w	1589s, 1512m, 1499s	879s	-
[Ni(6-cloxsesc) ₂] 35	3429m, 3267m	-	1656s, 1507m, 1411s	740s	3147w
5-chloroisatin selenosemicarbazone	3219m	3110w	1694s, 1618s, 1559m, 1447s	885s	-
[Ni(5-clistsesc) ₂] 36	3464m, 3257m	-	1681s, 1612s, 1575m, 1448s	779s	3147w
1-methylisatin selenosemicarbazone	3408m, 3228m	3128w	1676s, 1604s, 1492m, 1415s	889s	-
[Ni(1-meistsesc) ₂] 37	3410m, 3300m	-	1649s, 1597m, 1454s	738s	-
3-indole selenosemicarbazone	3356m, 3246m	3153w	1591s, 1487m, 1450s	898s	-
[Ni(3-indsesc) ₂] 38	3461m	-	1533s, 1495s, 1413s	739s	3050w
3-acetylindole selenosemicarbazone	3290m	3142w	1624s, 1502m, 1406s	877s	-
[Ni(3-acindsesc) ₂] 39	-	-	1608s, 1564m, 1421s	798s	3153w

9-anthracene selenosemicarbazone	3385m, 3248m	3151w	1639s, 1518m, 1402s	887s	-
[Ni(9-anthrasesc) ₂]40	3458m, 3262m	-	1616s, 1523m, 1440s	728s	-
1-naphthaldehyde selenosemicarbazone	3400m	3147w	1599s, 1516m, 1452s	871s	-
[Ni(1-naphthsesc) ₂]41	3396m	-	1602s, 1519m, 1465s	759s	-
2-naphthaldehyde selenosemicarbazone	3352m	3124w	1597s, 1533m, 1446s	856s	-
[Ni(2-naphthsesc) ₂]42	3269m	-	1662s, 1593m, 1448s	744s	-

7.3 NMR Spectroscopy:

7.3.1 ^1H NMR Spectroscopy:

Important ^1H NMR signals of metal complexes are given in Table 7.3.1a) and 7.3.1b) and ^1H NMR spectra of synthesized metal complexes are given in figures 7.3.1.1-7.3.1.11. For discussion of ^1H NMR signals of complexes of nickel(II) selenosemicarbazones, the complexes need to be divided in **Type 1** and **Type 2** depending upon the type of ligand attached to them.



Type 1

Scheme 7.3.1

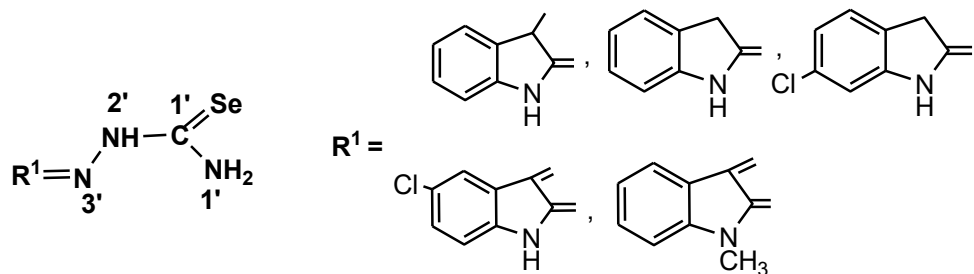
In ligands H^2L - H^4L and H^{11}L - H^{14}L the N^2H signal appeared in the range δ 11.6- δ 9.51 ppm and δ 10.95- δ 10.05 ppm. Disappearance of N^2H signal in complexes **Type 1** (scheme

7.3.1) ensure the deprotonation of ligand and is binding to metal atom in anionic form. The C²H proton signal appeared at the range δ 9.50-δ 7.88 ppm. The amino protons (N¹H₂) gave two or one broad singlet in the range δ 8.89- δ 7.29 ppm. Ring protons signal appeared in the range δ 9.04-δ 6.20 ppm. The methyl (CH₃) proton signal appeared at the range δ 3.87 ppm and δ 2.58 ppm respectively (Table 7.3.1a).

Table 7.3.1a) ¹H NMR Signals of Selenosemicarbazones (**Type 1**) with nickel(II) complexes

Ligands and Complexes	(1H, N ² H)	(1H, C ² H)	(1H, N ¹ H ₂)	(Ring protons)
2-Hfursesc, (H²L)	10.00 s 10.95 s	6.60 s, 6.54 s	10.00 s 8.80 s	7.87 d (1H, C ⁵ H), 7.74 d (1H, C ³ H), 7.58 t (1H, C ⁴ H) 7.51 d (1H, C ⁵ H), 7.14 t (1H, C ⁴ H), 7.45 d (1H, C ³ H)
[Ni(2-fursesc) ₂] 30	-	8.80 s	7.29 s	7.47 m (1H, C ⁴ H), 7.37 d (1H, C ³ H), 7.12 d (1H, C ⁵ H)
2-Hthiosesc, (H³L)	9.64 s	8.10 s	7.58 s, 6.71 s	7.51 d (1H, C ⁵ H), 7.14 t (1H, C ⁴ H), 7.45 d (1H, C ³ H)
[Ni(2-thiosesc) ₂] 31	-	8.80 s	7.29 s	7.98 d (1H, C ⁵ H), 6.82 t (1H, C ⁴ H), 6.62 d (1H, C ³ H), 3.87 (CH ₃)
N-MeHPysesc, (H⁴L)	10.05 s	-	6.21 s, 6.20 s	7.32 d (1H, C ⁵ H), 6.61 d (1H, C ³ H), 6.20 m (1H, C ⁴ H), 3.87 s (3H, CH ₃)
[Ni(N-mepysesc) ₂] 32	-	7.94 s	-	8.42 d (1H, C ⁷ H), 7.90 d (1H, C ⁶ H), 7.46-7.32 m (2H, C ^{5,8} H), 7.29 s (1H, C ² H), 2.58 s (3H, CH ₃)
3-AcHIndsesc, (H¹¹L)	-	-	7.65 s, 6.63 s	8.43 d (1H, C ⁵ H), 7.45 d (1H, C ⁸ H), 7.32 m (2H, C ^{6,7} H), 2.58 (CH ₃)
[Ni(3-acindsesc) ₂] 39	-	7.89 s	8.81 s	8.73 d (2H, C ^{3,11} H), 8.08 d (2H, C ^{6,8} H), 7.73 t (2H, C ^{5,9} H), 7.60 t (2H, C ^{4,10} H), 7.29 s (1H, C ⁷ H)
9-HAnsesc, (H¹²L)	11.5 s	9.02 s	-	9.00 d (1H, C ³ H), 8.18 d (1H, C ⁸ H), 8.01 d (1H, C ¹¹ H), 7.96 d (1H, C ⁶ H), 7.70-7.62 m (4H, C ^{4,5,9,10} H)
[Ni(9-anthrasesc) ₂] 40	-	9.50 s	8.56 s	8.17 d (1H, C ⁹ H), 8.02 d (1H, C ⁴ H),
1-HNapsesc,	9.51s	9.00 s	7.97 s	

(H¹³L)				7.95 d (1H, C ⁶ H), 7.62 m (2H, C ^{3,7} H), 7.29 s (1H, C ⁸ H)
[Ni(1-naphthsesc) ₂] 41	-	-	8.75 s	9.04 d (2H, C ^{6,9} H), 8.12 d (2H, C ^{4,2} H), 7.71 -7.59 m (4H, C ^{3,7} H)
2-HNapsesc, (H¹⁴L)	10.1 s	8.38 s	7.70 s	8.05-7.29 m (ring proton)
[Ni(2-naphthsesc) ₂] 42	-	-	8.89 s	7.16 d (1H, C ⁵ H), 7.01 d (1H, C ³ H), 5.12 s (1H, C ⁷ H), 2.97-2.38 m (4H, C ^{2,6} H)



Type 2

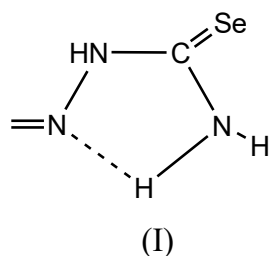
Scheme 7.3.1.1

In ligands **H⁵L**- **H⁸L**, the N^{2'}H signal appeared in the range δ 13.1- δ 9.03 ppm. Disappearance of N^{2'}H signal in complexes **Type 2** (scheme 7.3.1.1) ensure the deprotonation of ligand and its binding to metal atom in anionic form. The amino protons (N^{1'}H₂) gave two or one broad singlet in the range δ 8.71- δ 8.50 ppm. Ring protons signal appeared in the range δ 7.29- δ 6.92 ppm. The methyl (CH₃) proton signal appeared at the range δ 3.57 ppm and δ 3.49 ppm respectively (Table 7.3.1b).

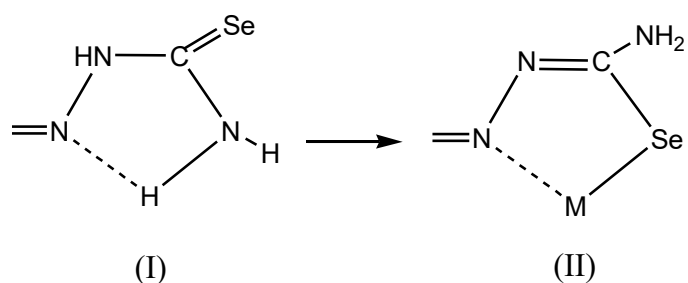
Table 7.3.1b) ^1H NMR Signals of Selenosemicarbazones (**Type 2**) with nickel(II) complexes

Ligands and Complexes	(1H, N ² H)	(1H, C ² H)	(1H, N ¹ 'H ₂)	(Ring protons)	Heterocyclic (1H, N ¹ H)
3-MeHOxsesc, (H⁵L)	9.16 s	-	-	7.24-6.95 m (4 H, C ^{5,6,7,8} H), 3.51 (3H, CH ₃), 1.54 s (cyclic proton ring)	-
[Ni(3-meoxsesc) ₂] 33	-	-	8.50 s	7.29 m (2H, C ^{6,7} H), 7.04 d (1H, C ⁵ H), 6.92 d (1H, C ⁸ H), 3.57 (CH ₃)	1.69s
2-HOxsesc, (H⁶L)	9.03 s	-	5.54 s, 5.46 s	8.34-6.90 m (4H, C ^{5,6,7,8} H), 3.56 (cyclic proton ring)	-
[Ni(2-oxsesc) ₂] 34	-	-	8.50 s	7.25 m (2H, C ^{6,7} H), 7.04 d (1H, C ⁵ H), 6.92 d (1H, C ⁸ H), 3.56 (cyclic proton ring)	1.68s
6-ClHOxsesc, (H⁷L)	9.51 s	-	4.89 s, 4.26 s	7.13 d (1H, C ⁷ H), 6.99 d (1H, C ⁴ H), 6.92s (1H, C ⁵ H)	-
[Ni(6-cloxsesc) ₂] 35	-	-	8.64 s	7.28 d (1H, C ⁷ H), 7.01 d (1H, C ⁴ H), 6.93 s (1H, C ⁵ H), 3.45 (cyclic ring)	-
1-MeHIstsesc, (H⁹L)	13.1 s	-	8.01 s 7.60 s	7.61-6.90 m (4H, C ^{5,6,7,8} H), 3.29 (CH ₃)	-
[Ni(1-meistsesc) ₂] 37	-	-	8.71 s	7.24 m (2H, C ^{5,8} H), 7.06 d (1H, C ⁶ H), 6.93 d (1H, C ⁷ H), 3.49 (CH ₃)	-

The amino protons (N¹'H₂) gave two broad singlet in the selenosemicarbazones ligands of **Type 1** and **Type 2** indicating that two protons are non-equivalent probably due to the H-bonding between one at the amino hydrogen and azomethine nitrogen (I).



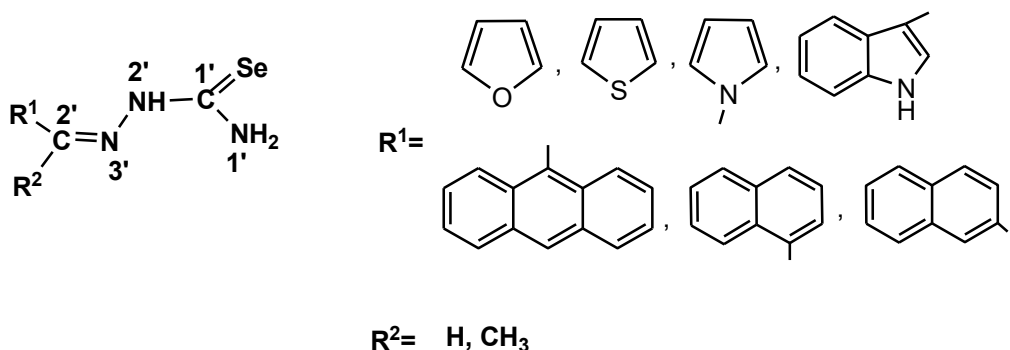
The amino protons (N^1H_2) gave one singlet in the complexes of **Type 1** and **Type 2** indicating that the two protons are equivalent probably during chelation (II) and also confirming that two protons are present in same environment.



The amino protons (N^1H_2) in the selenosemicarbazones ligands of **Type 1** and **Type 2** indicating that presence of one proton or no proton probably due to the low solubility of two protons of amino protons. The amino protons (N^1H_2) in the complexes of **Type 1** and **Type 2** indicating the presence of no proton is probably due to the low solubility of two protons of amino protons.

7.3.2. ^{13}C NMR Spectroscopy:

Important ^{13}C NMR signals of metal complexes are given in Table 7.3.2a) and 7.3.2b). ^{13}C NMR spectra of synthesized metal complexes are given in figures 7.3.2.1-7.3.2.10. For discussion of ^{13}C NMR signals of complexes of nickel(II) selenosemicarbazones, the complexes need to be divided in **Type 1** and **Type 2** categories depending upon the type of ligand attached to them.



Type 1

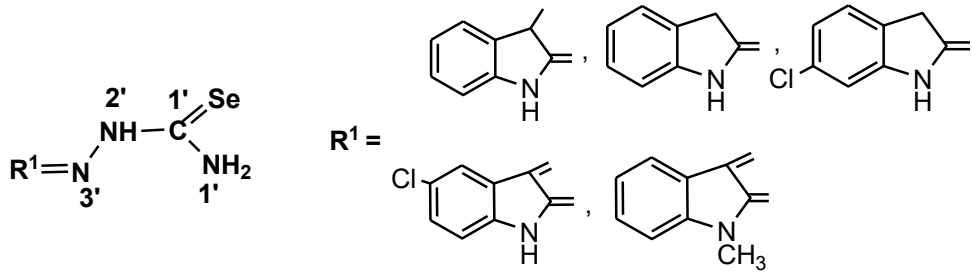
Scheme 7.3.2

In **Type 1** (scheme 7.3.2) complexes, C^{1'} signal appeared at the range between δ 193.0- δ 162.0 ppm and C^{2'} signal appeared at the range between δ 155.8- δ 131.8 ppm respectively and ring carbons showed the signal in between the range of δ 139.0- δ 109.4 ppm and whereas methyl group (CH₃) presented the signal at δ 36.8 ppm and δ 27.6 ppm in complexes of **Type 1** respectively (Table 7.3.2a).

Table 7.3.2 a) ¹³C NMR Signals of Selenosemicarbazones (**Type 1**) with nickel(II) complexes

Ligands and Complexes	(C ^{1'})	(C ^{2'})	(Ring carbons)
2-Hfursesc, (H²L)	-	145.2	133.9 (C ⁵), 127.5 (C ⁴), 117.3 (C ³), 112.3 (C ²)
[Ni(2-fursesc) ₂] 30	-	155.8	127.9 (C ²) 139.3 (C ⁴), 130.0 (C ⁵), 132.3 (C ³)
2-Hthiosesc, (H³L)	-	155.8	132.4 (C ⁵), 130.0 (C ⁴), 127.8 (C ³), 127.3 (C ²)
[Ni(2-thiosesc) ₂] 31	-	155.7	127.7 (C ²) 139.0 (C ⁴), 129.9 (C ⁵), 132.3 (C ³)
N-MeHPysesc, (H⁴L)	173.4	138.3	129.2 (C ⁴), 125.8 (C ⁵), 117.9 (C ³), 109.3 (C ²), 36.8 (CH ₃)
[Ni(N-mepysesc) ₂] 32	-.	138.2	129.3 (C ⁴) 125.8 (C ⁵), 118.0 (C ³), 109.4 (C ²), 36.8 (CH ₃)
3-AcHIndsesc, (H¹¹L)	193.6	158.2	131.5 (C ⁶), 123.7 (C ⁵), 122.6 (C ⁷), 118.6 (C ⁸), 111.3 (C ⁴), 35.4 (CH ₃), 26.9 (C ³)
[Ni(3-acindsesc) ₂] 39	-	136.3	131.4 (C ⁶) 125.4 (C ⁵), 122.4 (C ⁷), 118.6(C ⁸),

			111.3 (C ⁴), 27.6 (CH ₃)
9-HAnsesc, (H¹²L)	193.0	135.0	132.4-122.7 (ring carbon), 114.0 (C ⁸)
[Ni(9-anthrasesc) ₂]40	162.0	131.8	131.5-124.6 (aromatic carbon ring)
1-HNapsesc, (H¹³L)	162.1	134.1	131.8-124.9 (ring carbon), 115.0 (C ⁵)
[Ni(1-naphthsesc) ₂]41	193.0	135.2	132.1(C ⁷), 131.1(C ⁶), 129.3(C ⁸), 129.1(C ⁴), 125.7(C ³) and 123.5(C ²)



Type 2

Scheme 7.3.2.1

In **Type 2** (scheme 7.3.2.1) complexes, C^{1'} signal appeared at the range δ 181.4 ppm. Ring carbons showed the signal in between the range of δ 143.4-δ 109.6 ppm and whereas methyl group (CH₃) presented the signal at the range δ 41.0 ppm (Table 7.3.2b).

Table 7.3.2 b) ¹³C NMR Signals of Selenosemicarbazones (**Type 2**) with nickel(II) complexes

Ligands and Complexes	(C ^{1'})	(C ^{2'})	(Ring carbons)
3-MeHOxsesc, (H⁵L)	181.6	-	141.3 (C ⁵), 131.2 (C ⁶), 127.8 (C ⁷), 123.7 (C ⁸), 109.8 (C ⁹), 41.1 (CH ₃), 15.2 (cyclic carbon ring).
[Ni(3-meoxsesc) ₂]33	-	-	141.1(C ⁵), 131.2 (C ⁶), 127.8 (C ⁷), 123.7 (C ⁸), 122.4 (C ⁴), 109.6 (C ³) and 41.0 (CH ₃)
2-HOxsesc, (H⁶L)	177.4	-	142.3 (C ⁵), 127.9 (C ⁶), 124.6 (C ⁷), 122.3 (C ⁸), 109.7 (C ⁹), 36.1 (cyclic carbon ring).
[Ni(2-oxsesc) ₂]34	-.	-	142.4(C ⁵)127.9 (C ⁶), 124.6 (C ⁷), 122.3 (C ⁸), 109.6 (C ⁴) and 36.2 (C ³)

6-ClHOxsesc, (H⁷L)	177.9	-	143.6 (C ⁵), 133.1 (C ⁶), 125.3 (C ⁷), 110.7 (C ⁸), 58.2 (C ⁴), 35.3 (C ³)
[Ni(6-cloxsesc) ₂] 35	-.	-	143.4(C ⁵), 133.6 (C ⁶), 125.5(C ⁷), 123.3 (C ⁸) 110.3 (C ⁹), 35.7 (C ³)
1-MeHIstsesc, (H⁹L)	178.7	-	161.0 (C ⁵), 144.1 (C ⁶), 132.0 (C ⁸), 129.2 (C ⁷), 123.6 (C ⁹), 121.1 (C ³), 119.1 (C ²), 109.3 (C ⁴), 25.8(CH ₃), 20.4(cyclic ring).
[Ni(1-meistsesc) ₂] 37	-	-	141.1(C ⁶), 131.2 (C ⁸), 127.8 (C ⁷), 123.8 (C ⁹), 122.4(C ³), 109.6 (C ⁴), 41.0 (CH ₃)

7.4 Mass Spectrometry:

Mass spectra of complexes **29**, **33**, **36-38** and **42**, has been recorded and given in figures 7.4.1- 7.4.5. The observed molecular ion peak [M]⁺ are given in table 7.4. From the table it is clear that m/z values for complexes **29**, **33**, **36-38** and **42**, are close to their proposed stoichiometry [Ni(L)₂] and thus confirmed the co-ordination of nickel(II) with selenosemicarbazones.

Table 7.4 m/z values (amu) of complexes **29**, **33**, **36-38** and **42** obtained from Mass Spectra

Complex No.	Parent peak obtained from mass spectra	Expected formula for parent ion (m/z) ⁺
29	492amu	[Ni(C ₇ H ₁₃ N ₃ Se) ₂]
33	594 amu	[Ni(C ₁₀ H ₁₄ N ₄ Se) ₂]
36	649 amu	[Ni(C ₉ H ₄ N ₄ OClSe) ₂]
37	619 amu	[Ni(C ₁₀ H ₁₀ N ₄ OSe) ₂]
38	591 amu	[Ni(C ₁₀ H ₁₂ N ₄ Se) ₂]
42	606 amu	[Ni(C ₁₂ H ₁₀ N ₃ Se) ₂]

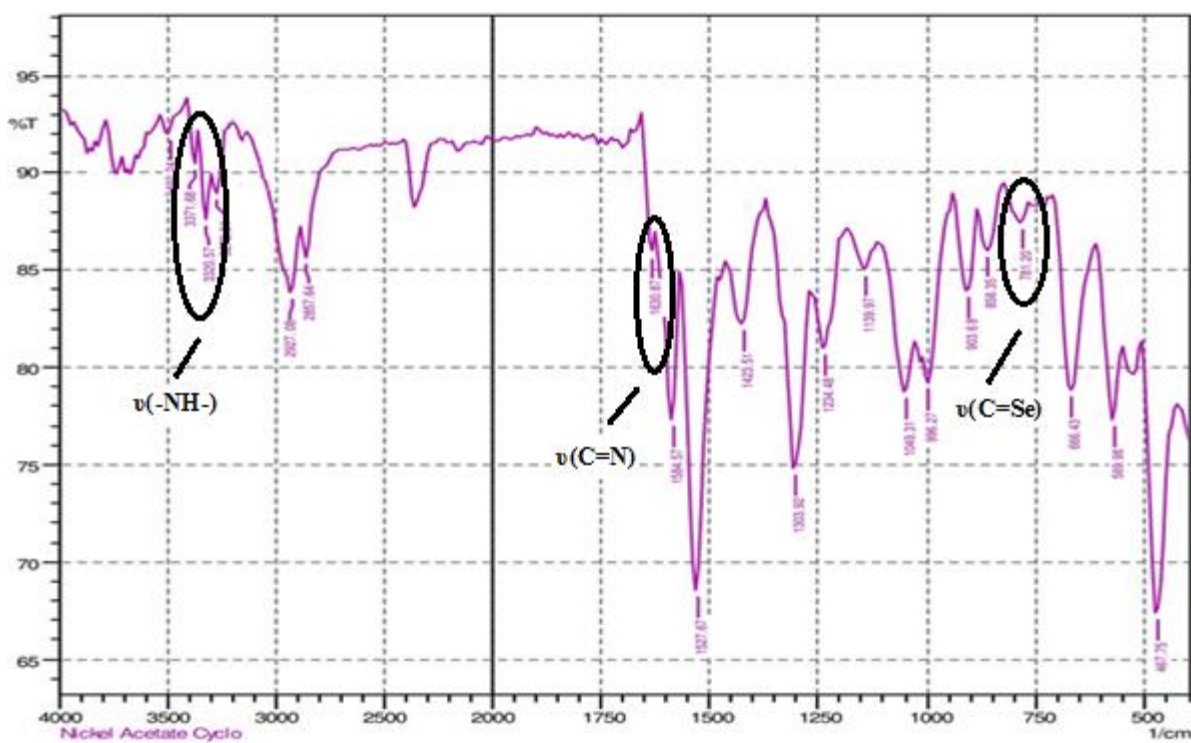


Figure 7.2.1 IR spectrum of $[\text{Ni}(\text{cysesc})_2]$ 29

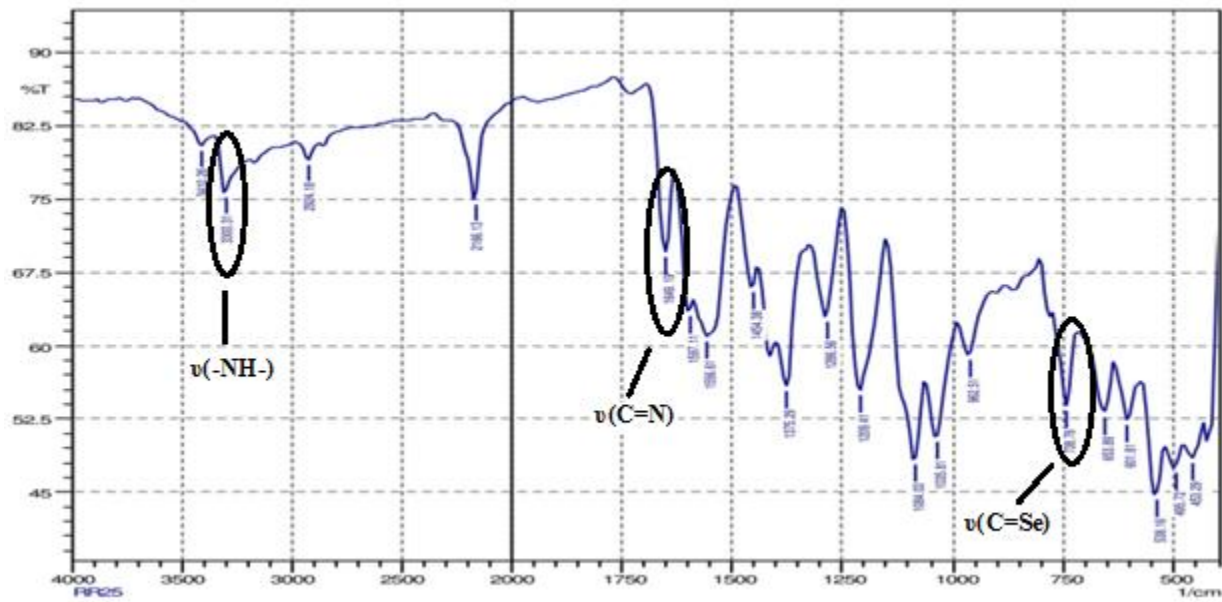


Figure 7.2.2 IR spectrum of $[\text{Ni}(2\text{-fursesc})_2]$ 30

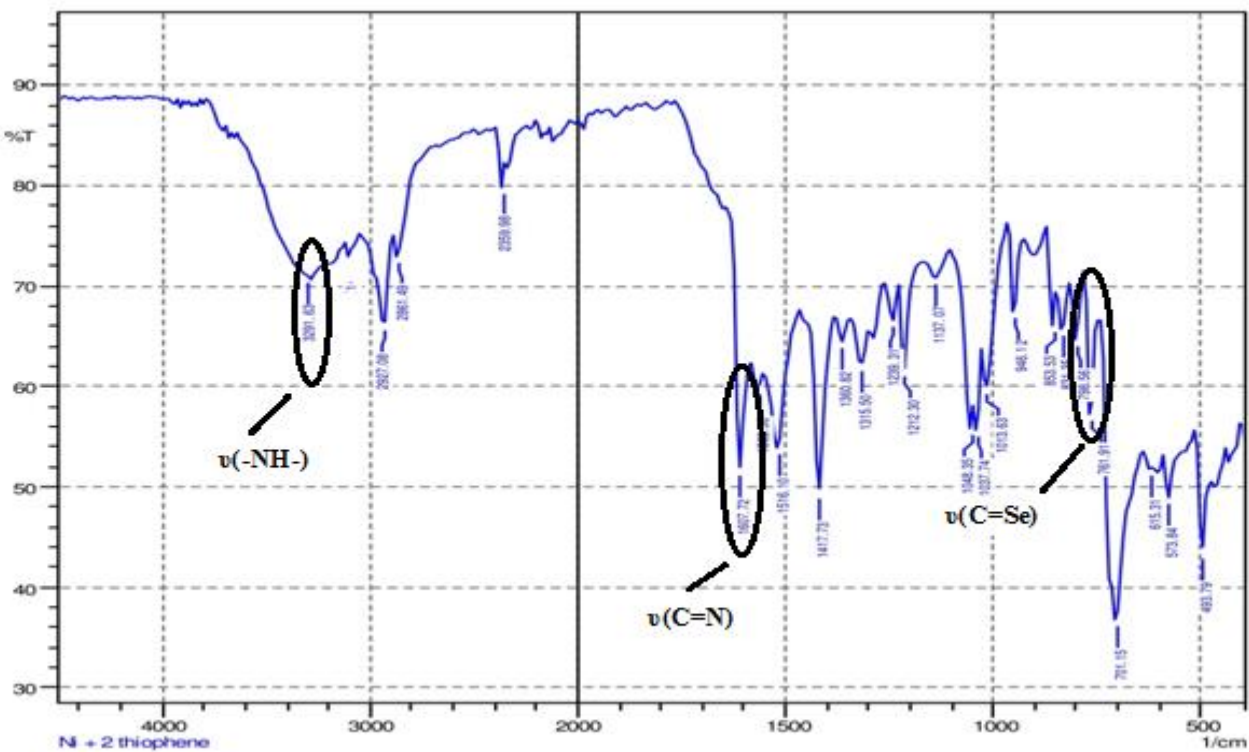


Figure 7.2.3 IR spectrum of $[\text{Ni}(2\text{-thiosesc})_2]31$

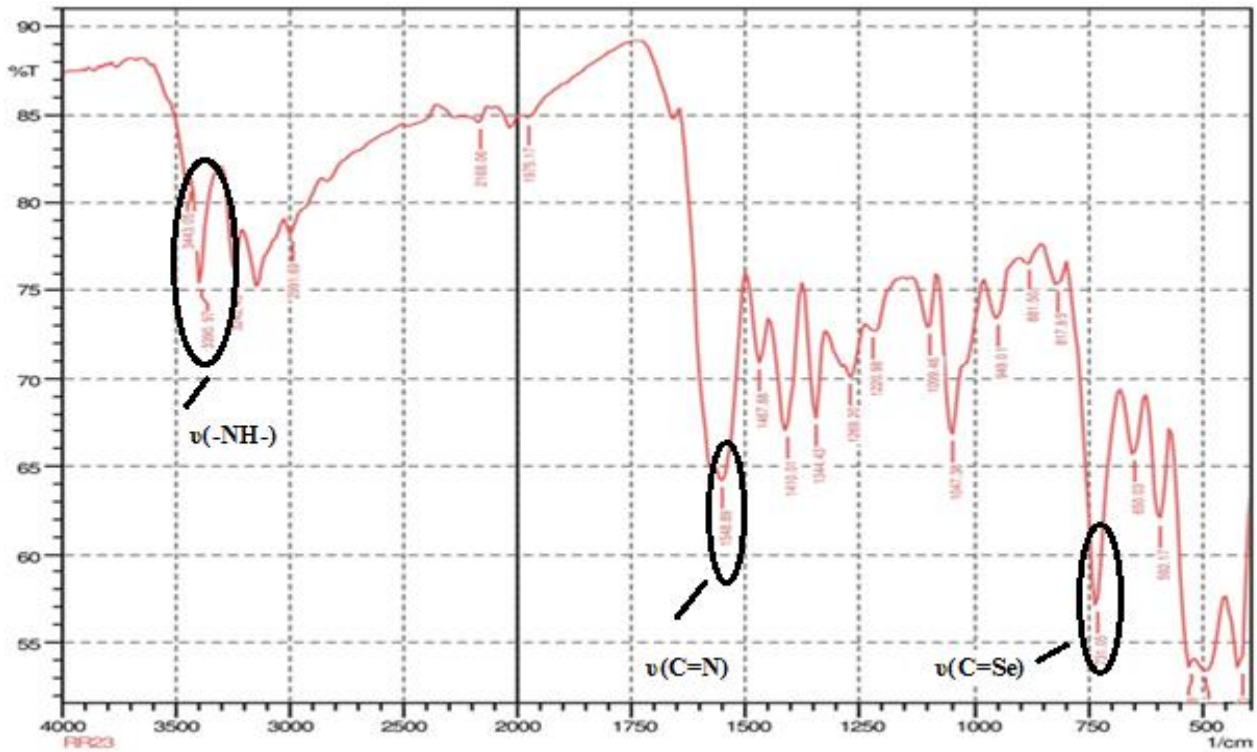


Figure 7.2.4 IR spectrum of $[\text{Ni}(\text{N-mepysesc})_2]32$

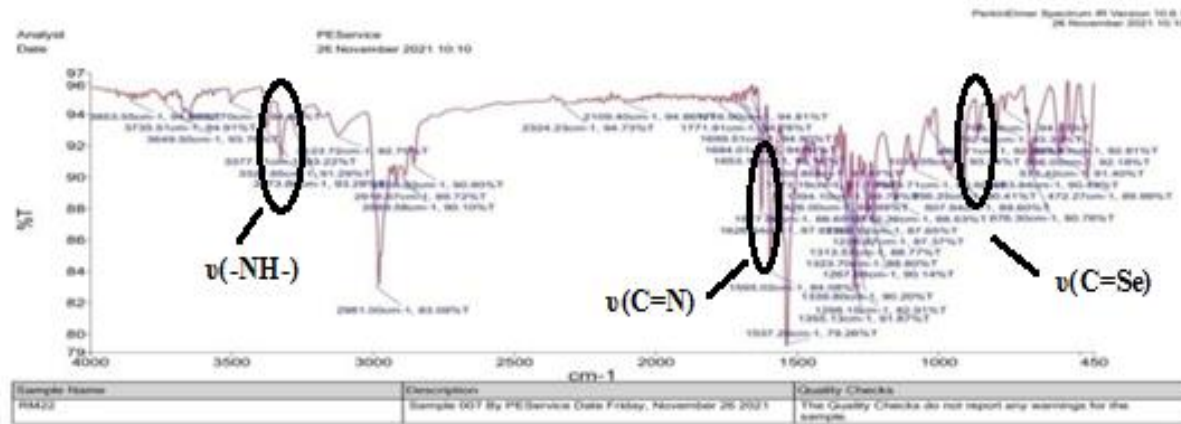


Figure 7.2.5 IR spectrum of $[\text{Ni}(3\text{-meoxsesc})_2]33$

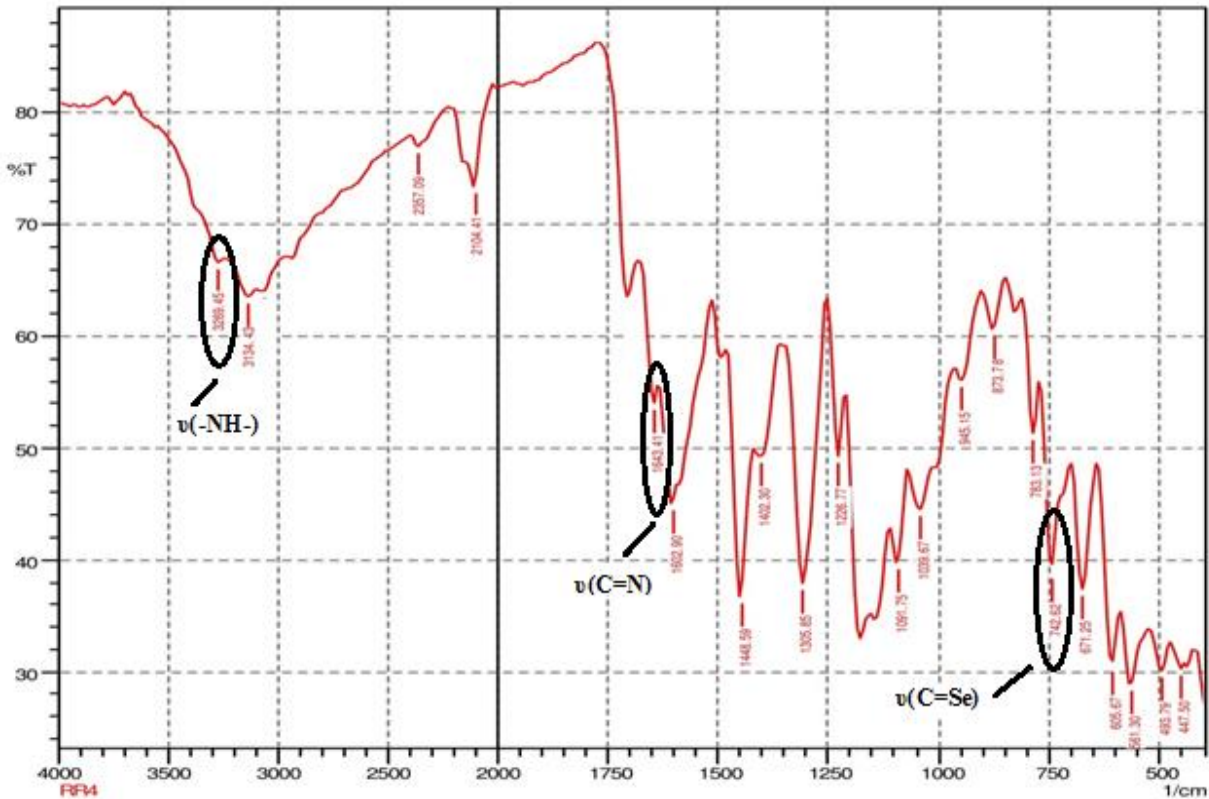


Figure 7.2.6 IR spectrum of $[\text{Ni}(2\text{-oxsesc})_2]34$

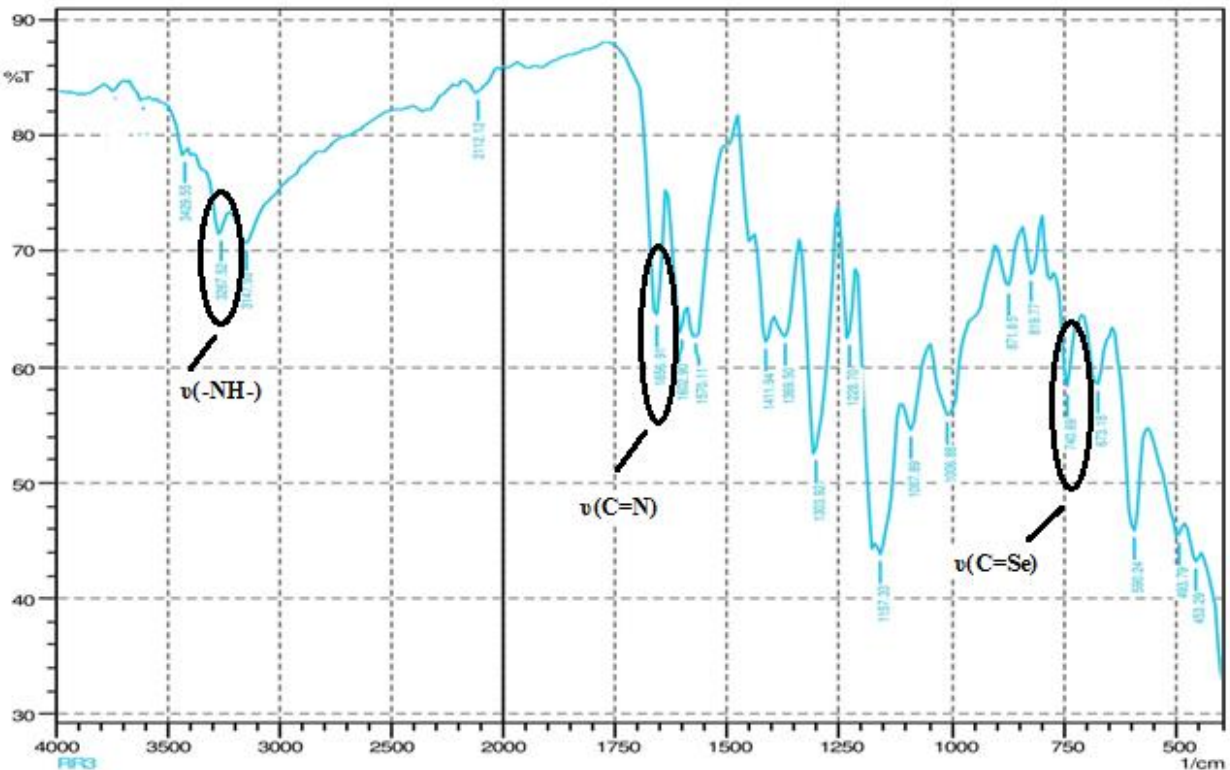


Figure 7.2.7 IR spectrum of $[\text{Ni}(6\text{-cloxsesc})_2]35$

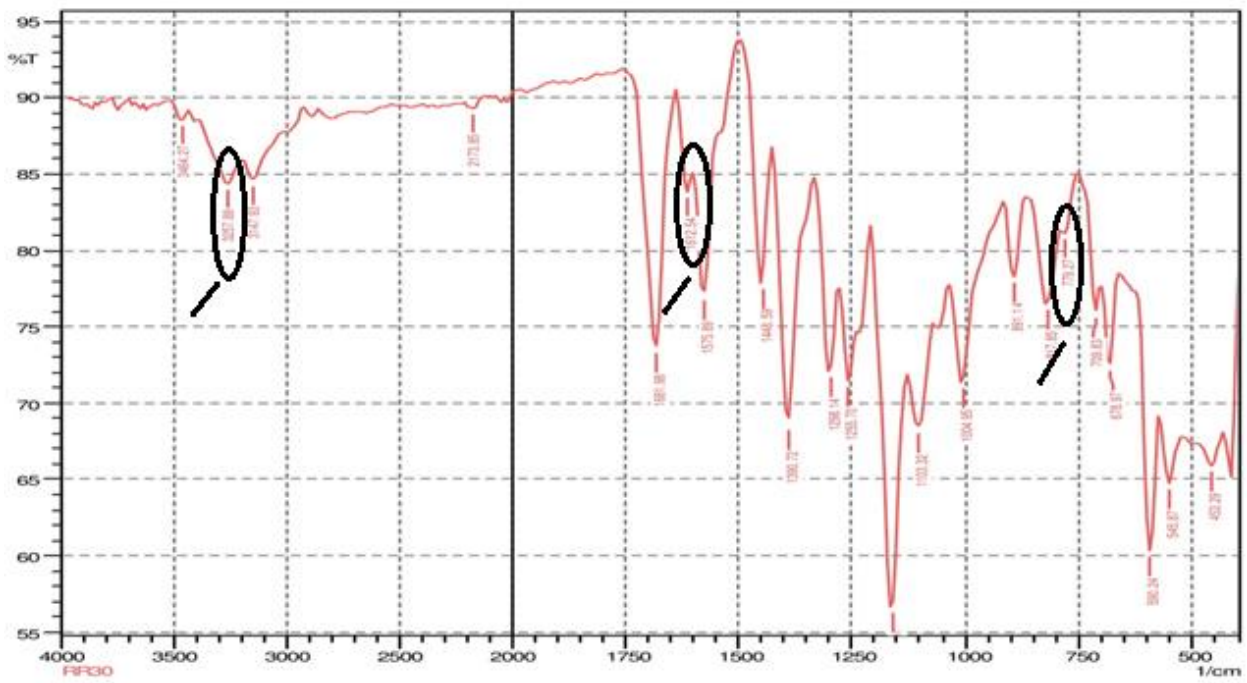


Figure 7.2.8 IR spectrum of $[\text{Ni}(5\text{-elistsesc})_2]36$

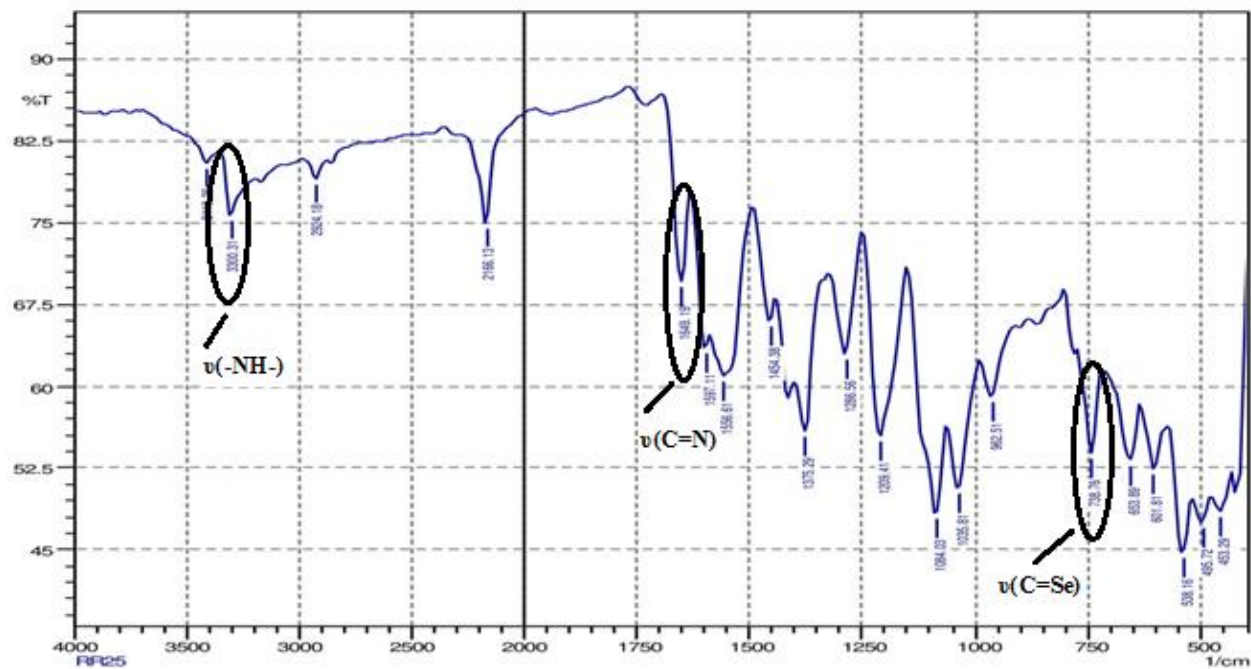
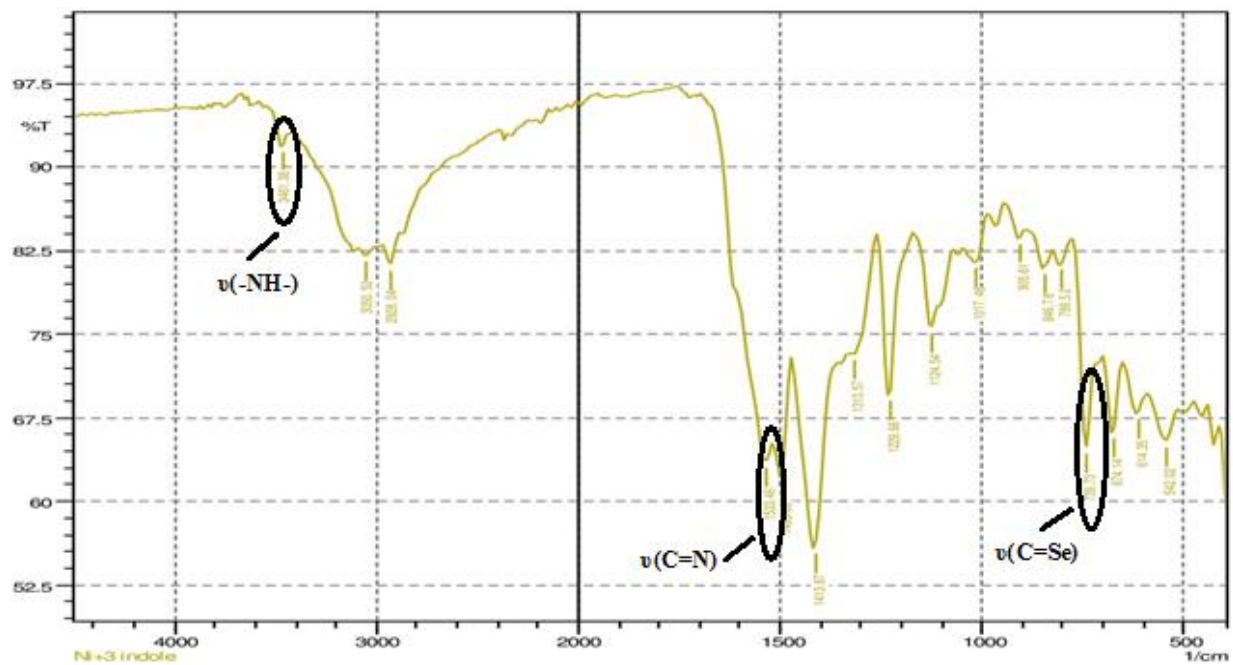


Figure 7.2.9 IR spectrum of $[\text{Ni}(1\text{-meistsesc})_2]37$



Comment:
 $\text{Ni}+3$ indole

Date/Time: 2/7/2022 3:25:17 PM
 No. of Scans:
 Resolution:
 Apodization:

Figure 7.2.10 IR spectrum of $[\text{Ni}(3\text{-indsesc})_2]38$

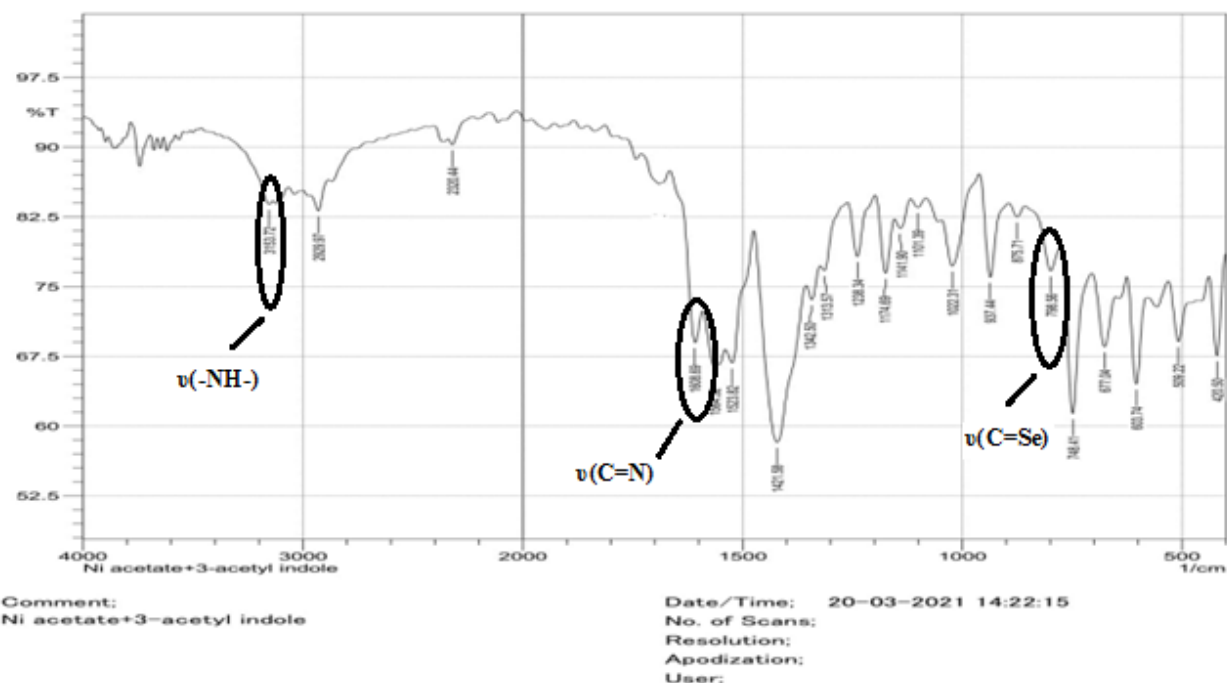


Figure 7.2.11 IR spectrum of $[\text{Ni}(3\text{-acindsesc})_2]39$

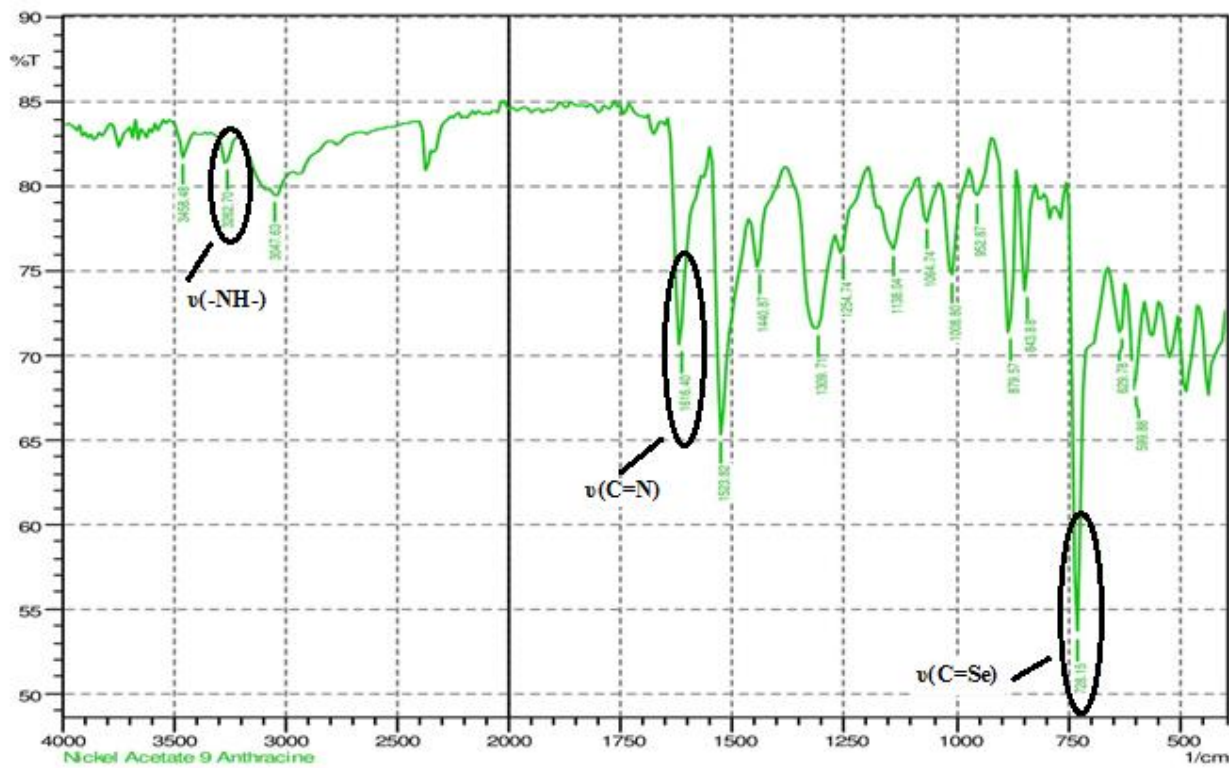


Figure 7.2.12 IR spectrum of $[\text{Ni}(9\text{-anthrasesc})_2]40$

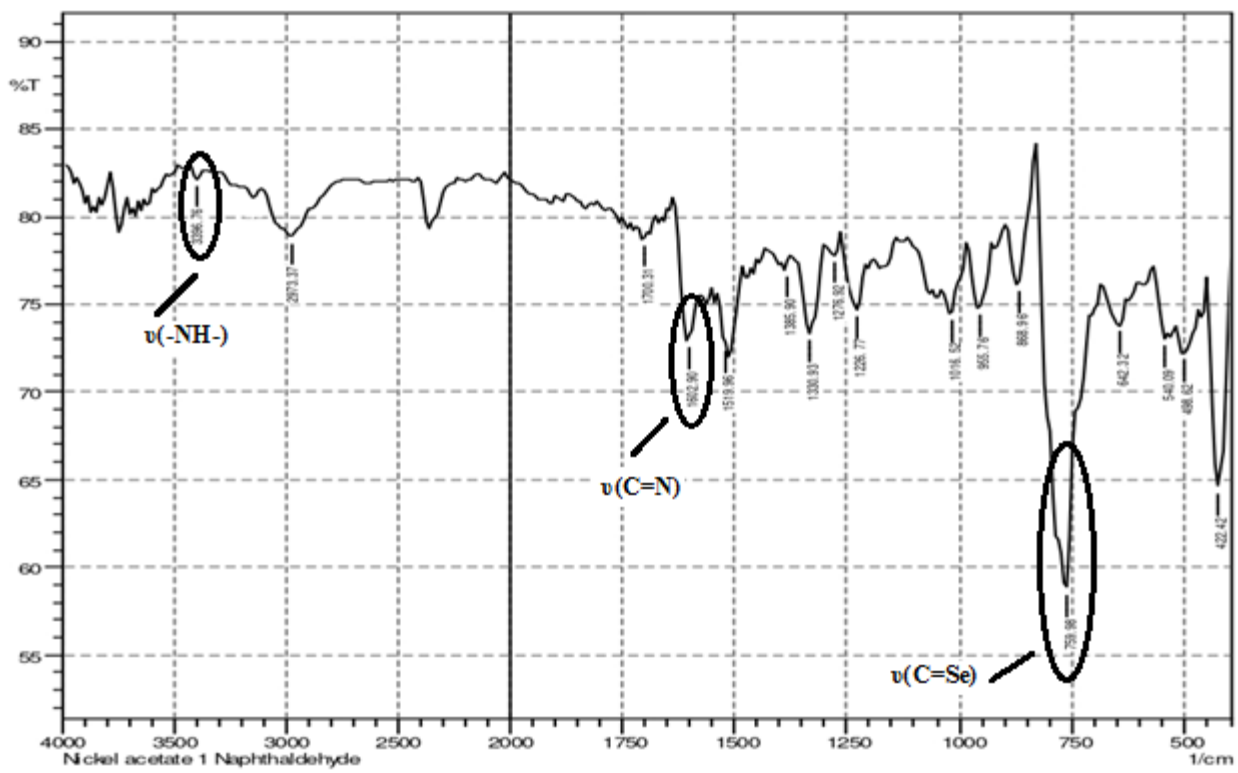


Figure 7.2.13 IR spectrum of $[\text{Ni}(1\text{-naphthsesc})_2]41$

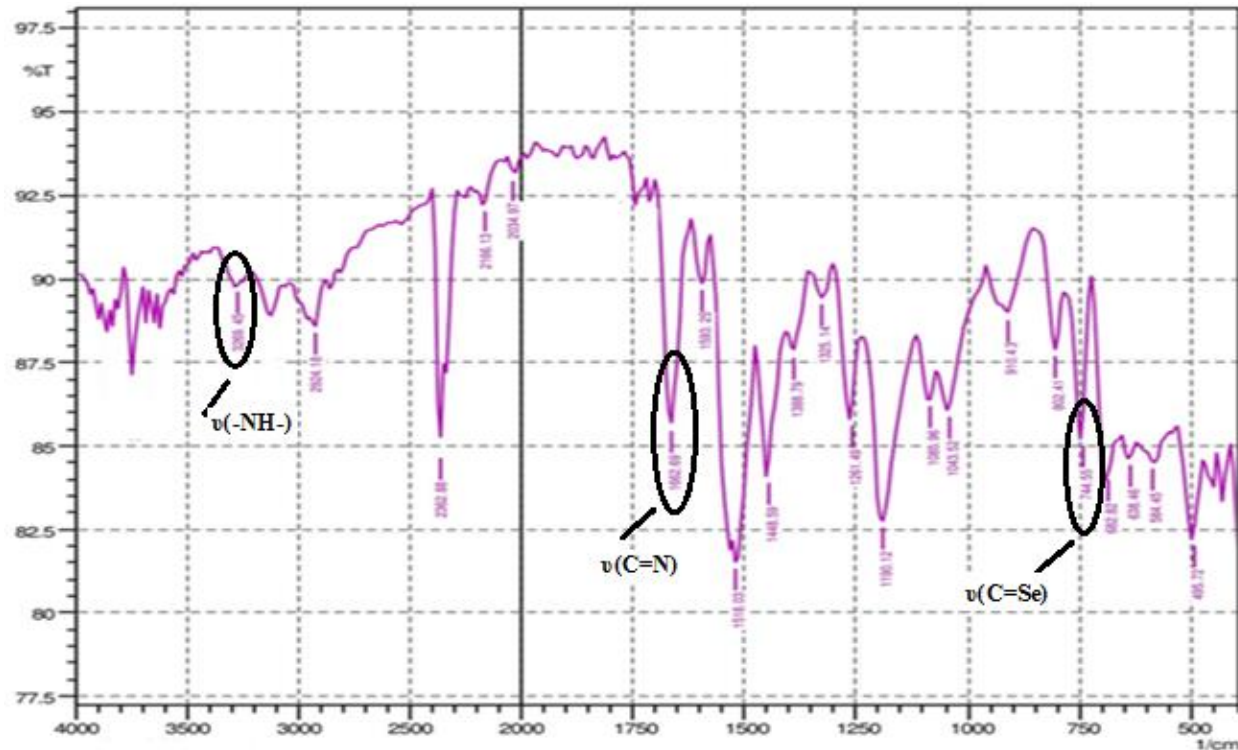


Figure 7.2.14 IR spectrum of $[\text{Ni}(2\text{-naphthsesc})_2]42$

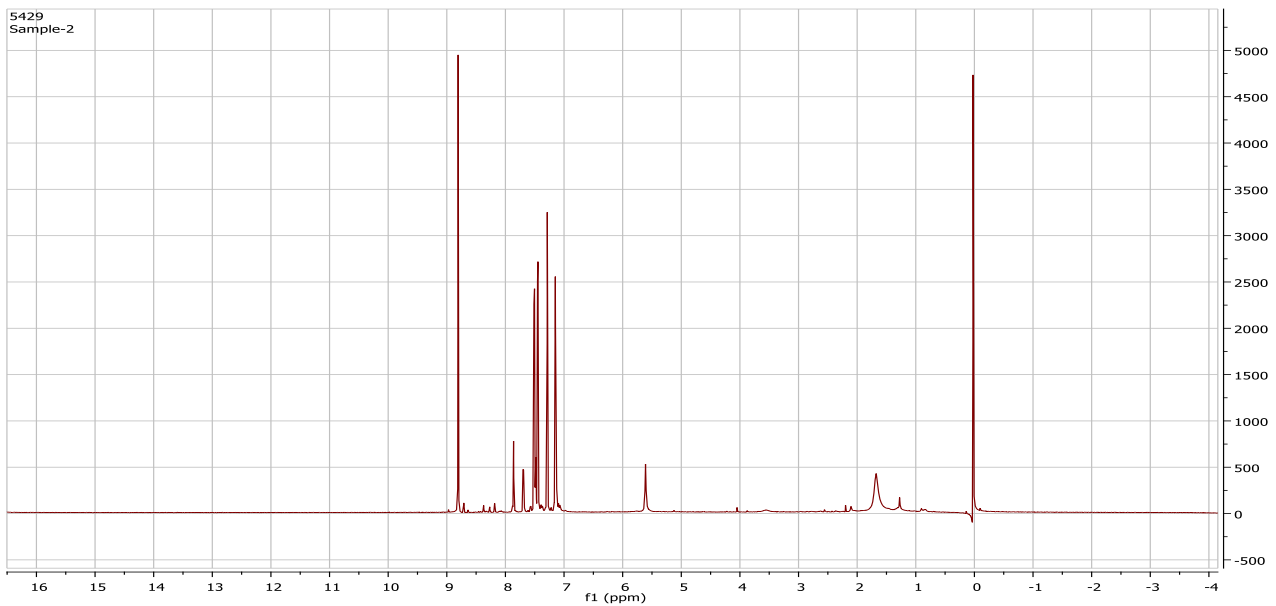


Figure 7.3.1.1a) ¹H NMR spectrum of complex 30

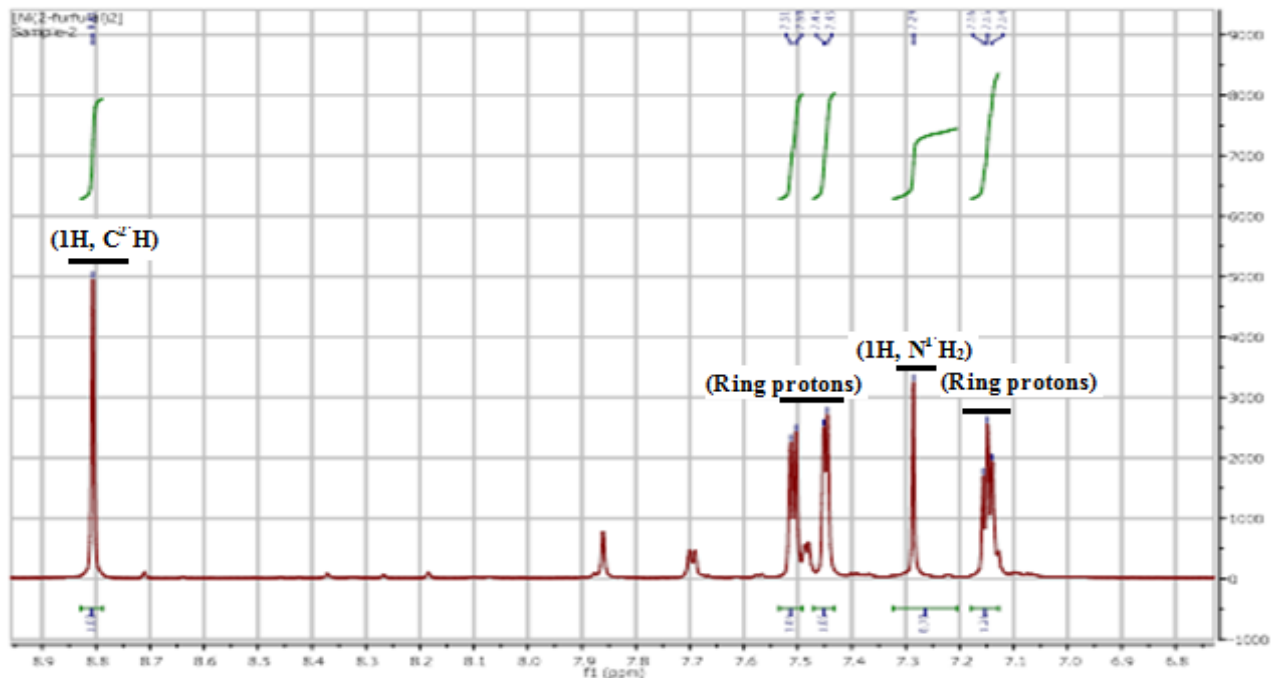


Figure 7.3.1.1b) ¹H NMR spectrum of complex 30(expansion form)

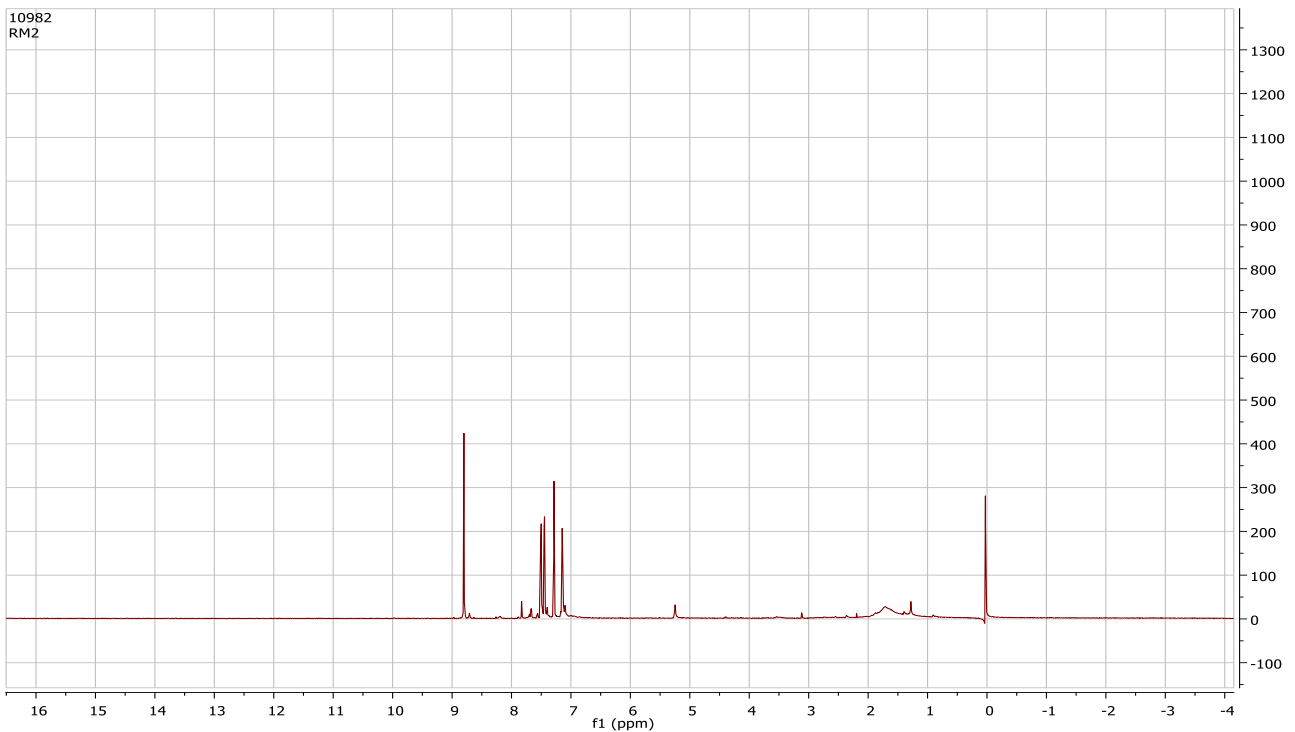


Figure 7.3.1.2a) ^1H NMR spectrum of complex **31**

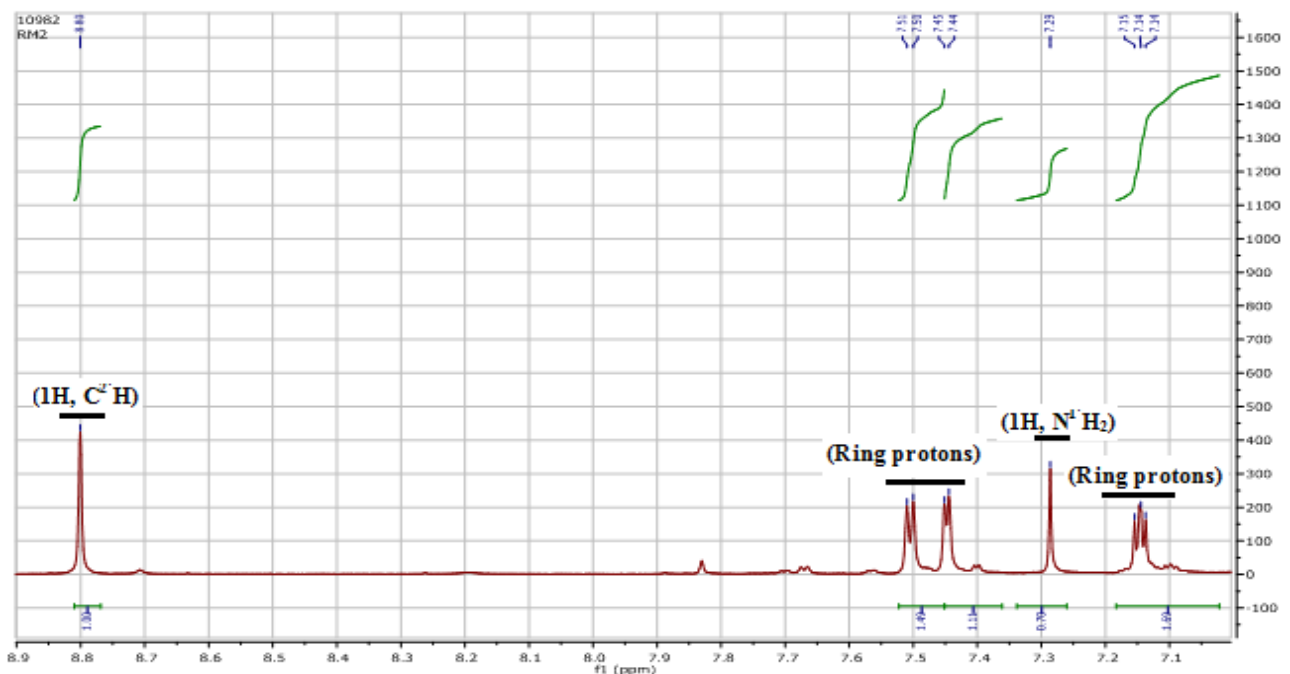


Figure 7.3.1.2b) ^1H NMR spectrum of complex **31**(expansion form)

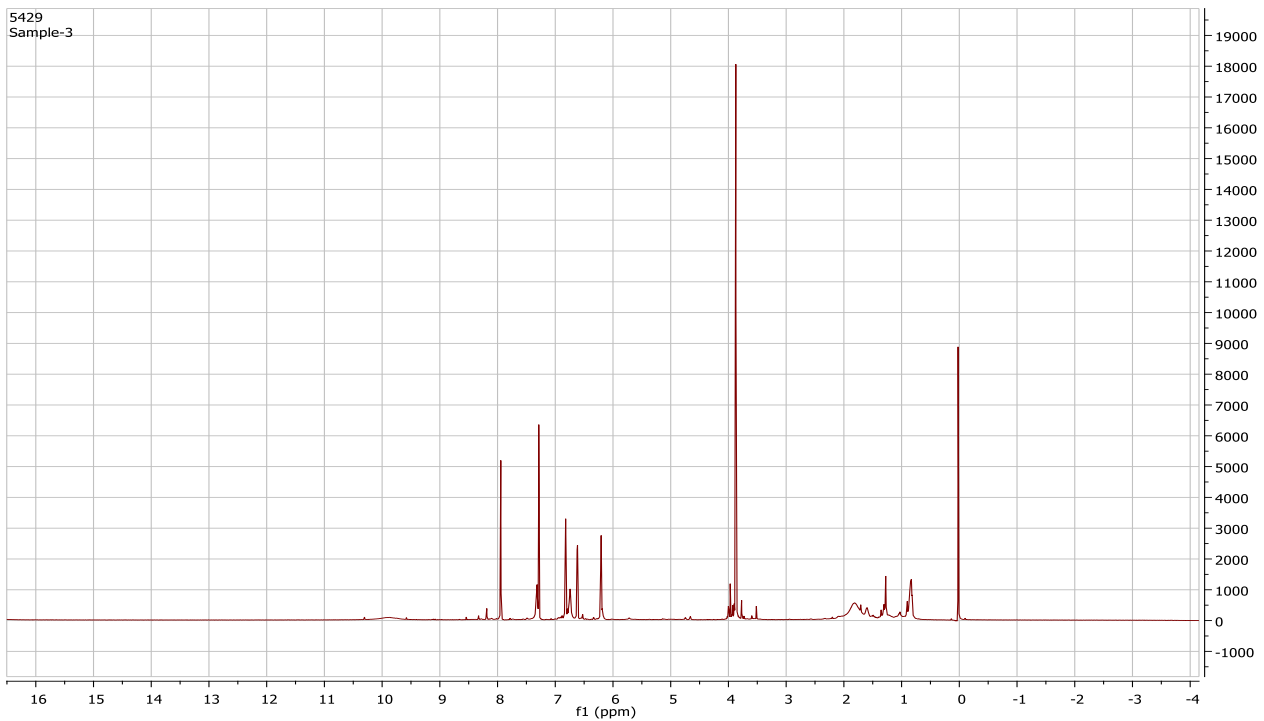


Figure 7.3.1.3a) ^1H NMR spectrum of complex **32**

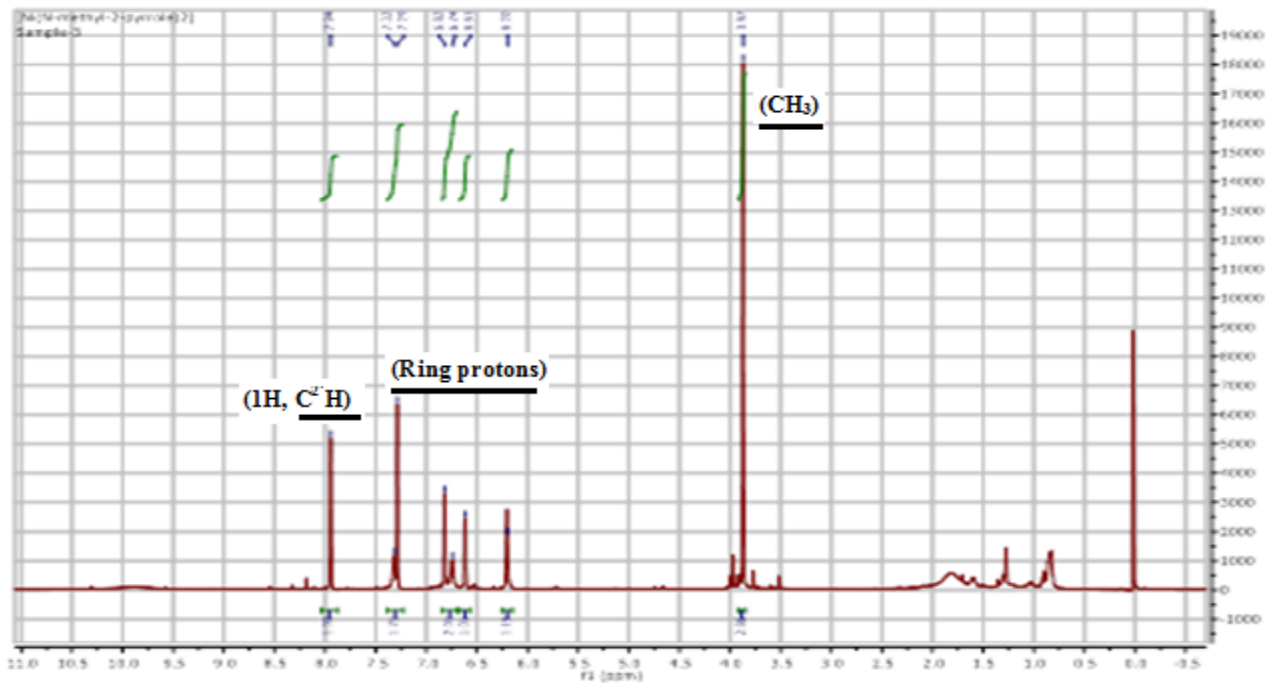


Figure 7.3.1.3b) ^1H NMR spectrum of complex **32**(expansion form)

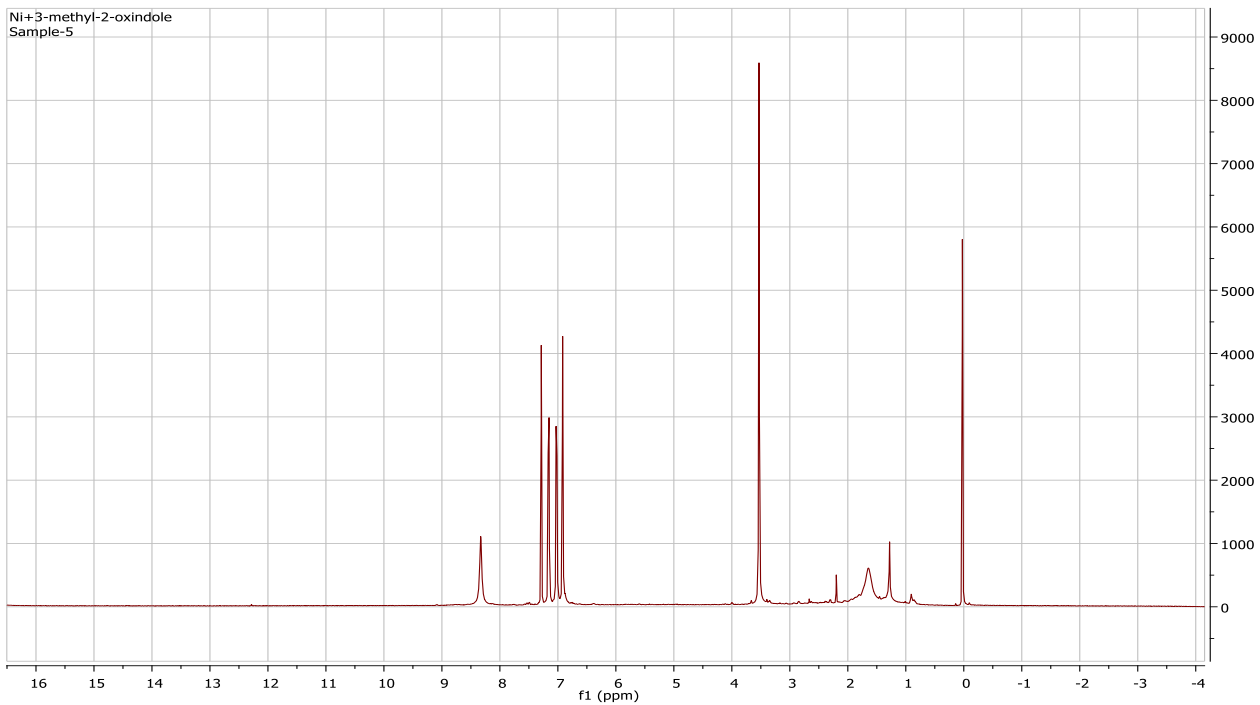


Figure 7.3.1.4a) ¹H NMR spectrum of complex 33

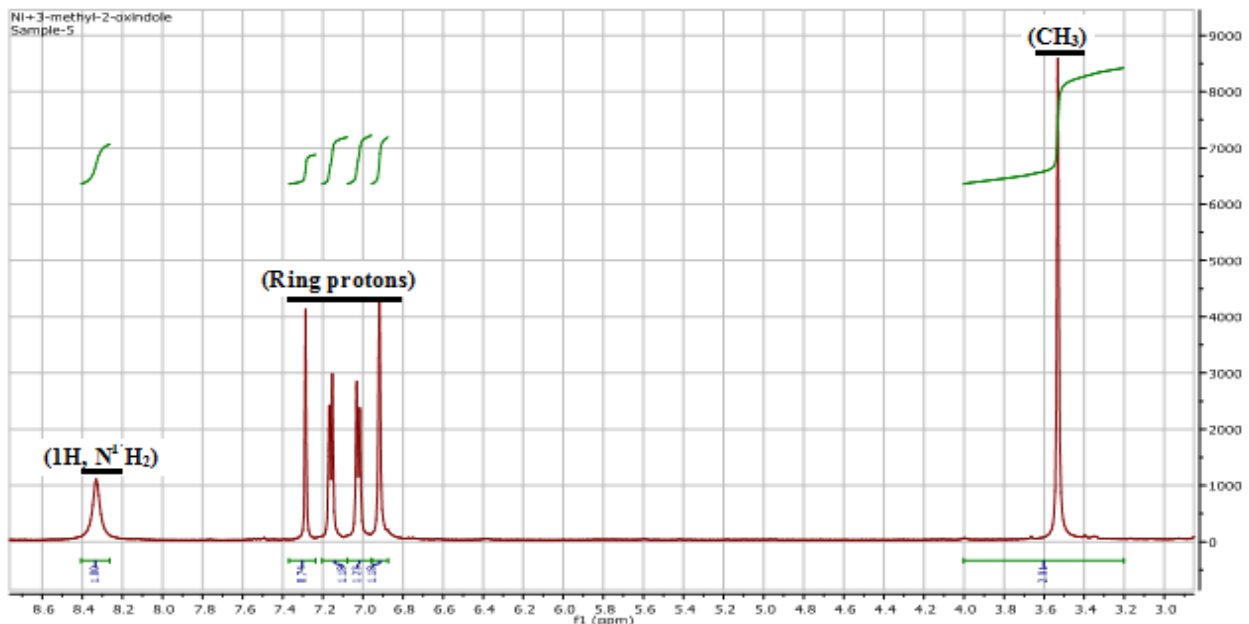


Figure 7.3.1.4b) ¹H NMR spectrum of complex 33(expansion form)

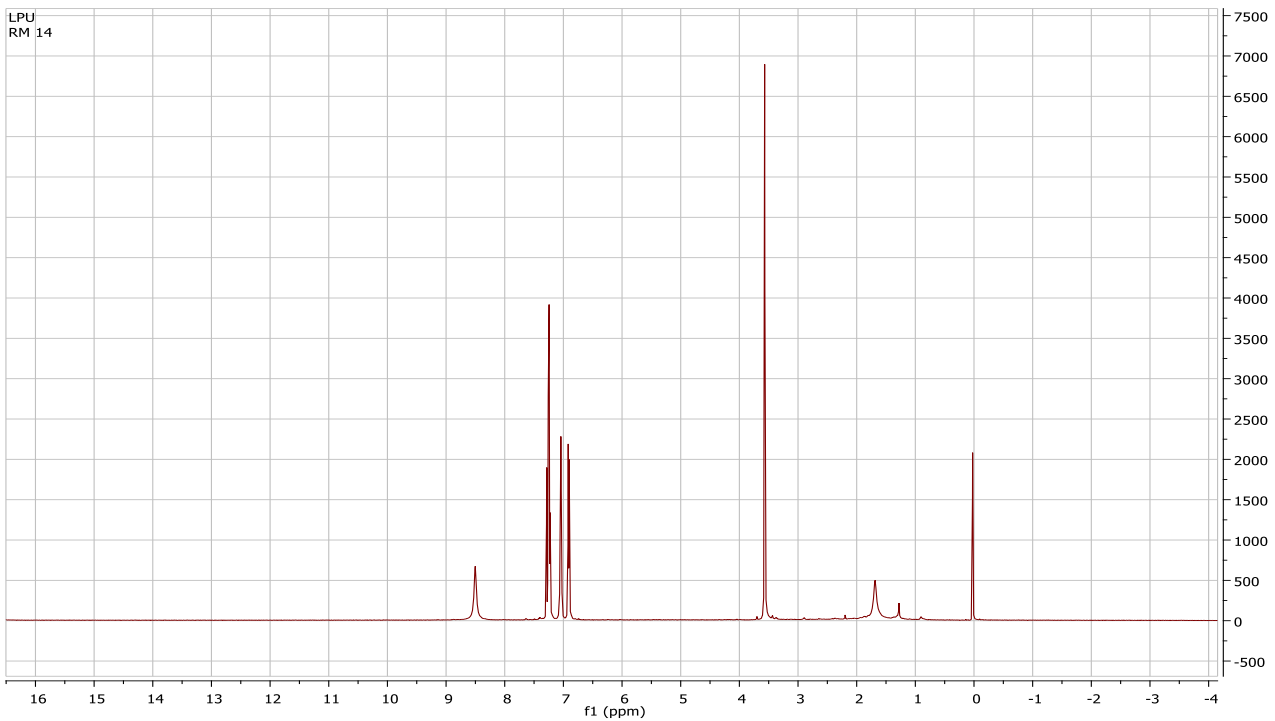


Figure 7.3.1.5a) ^1H NMR spectrum of complex **34**

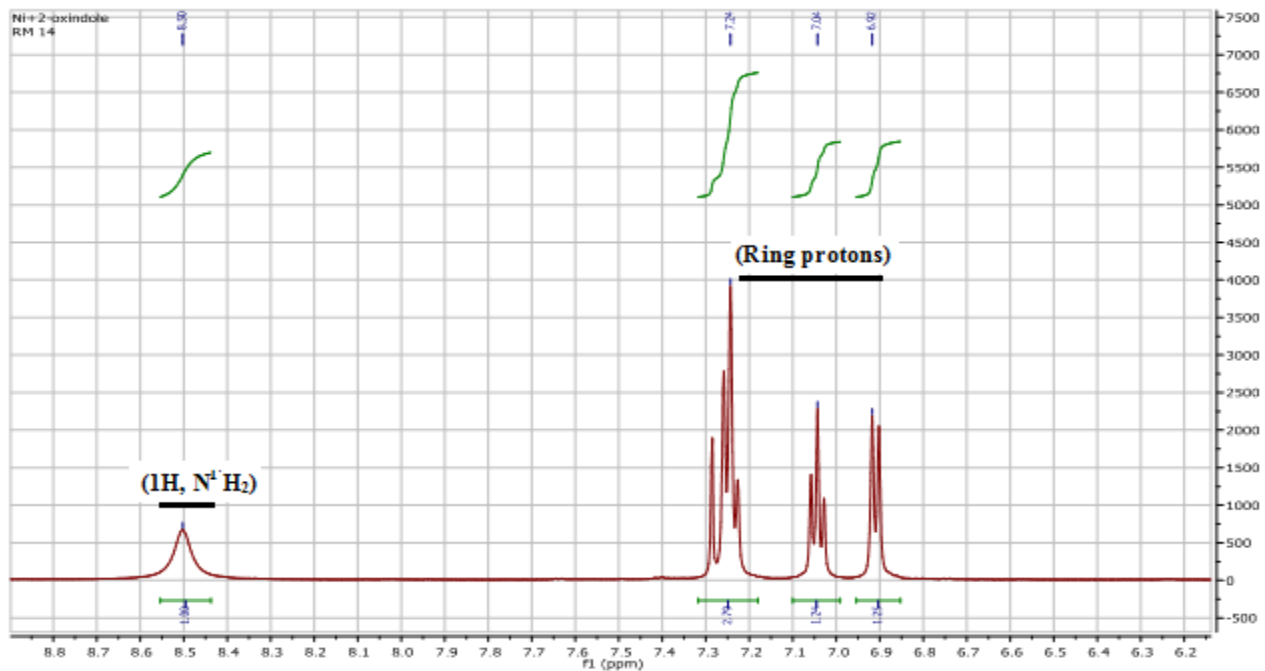


Figure 7.3.1.5b) ^1H NMR spectrum of complex **34**(expansion form)

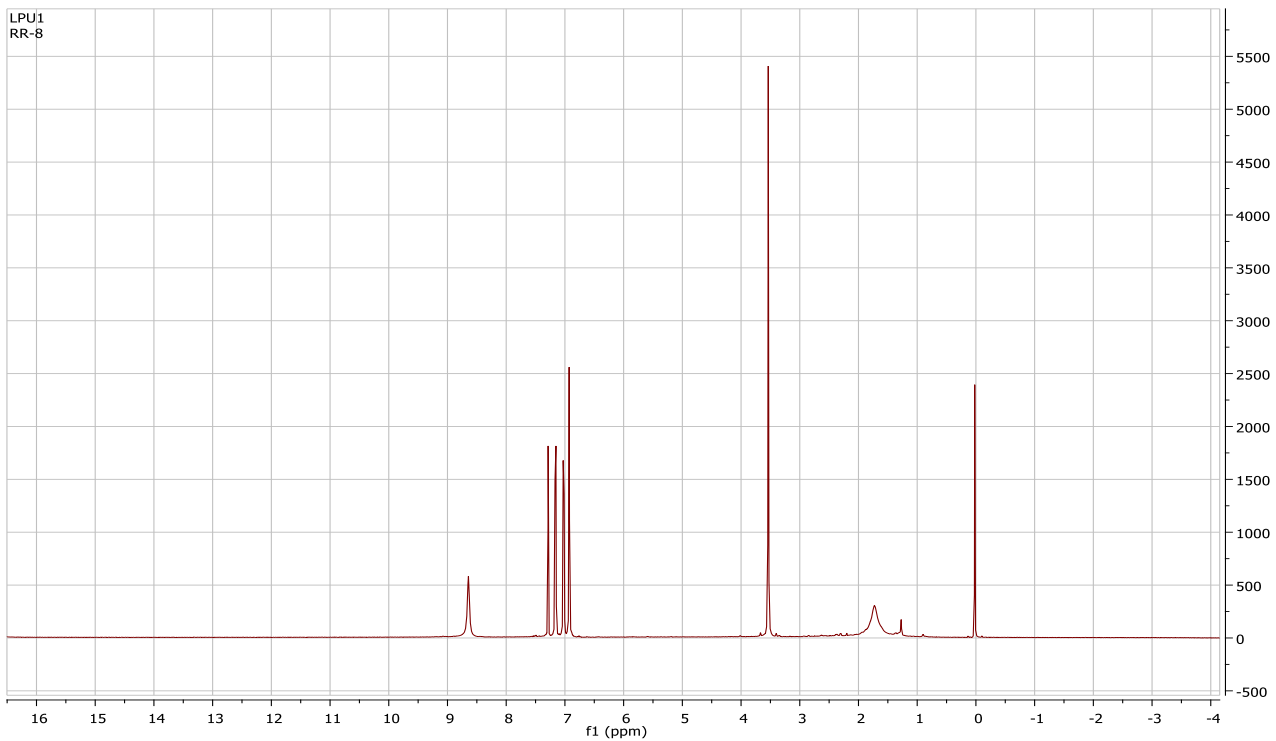


Figure 7.3.1.6a) ¹H NMR spectrum of complex **35**

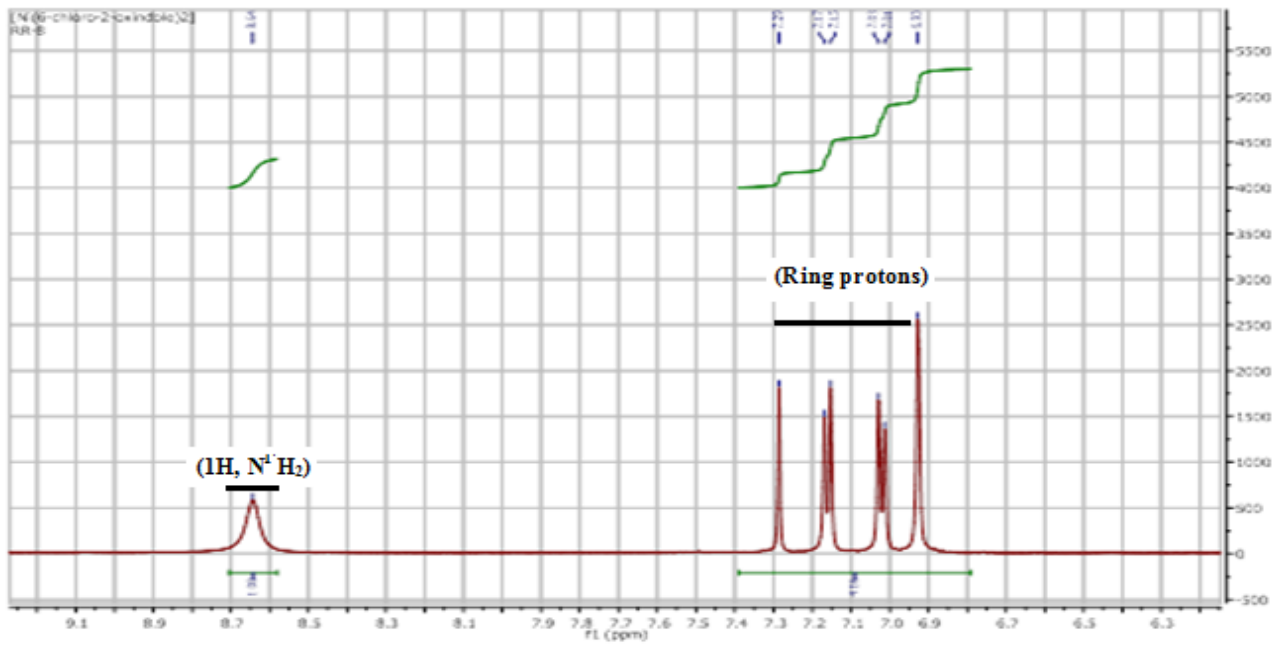


Figure 7.3.1.6b) ¹H NMR spectrum of complex **35**(expansion form)

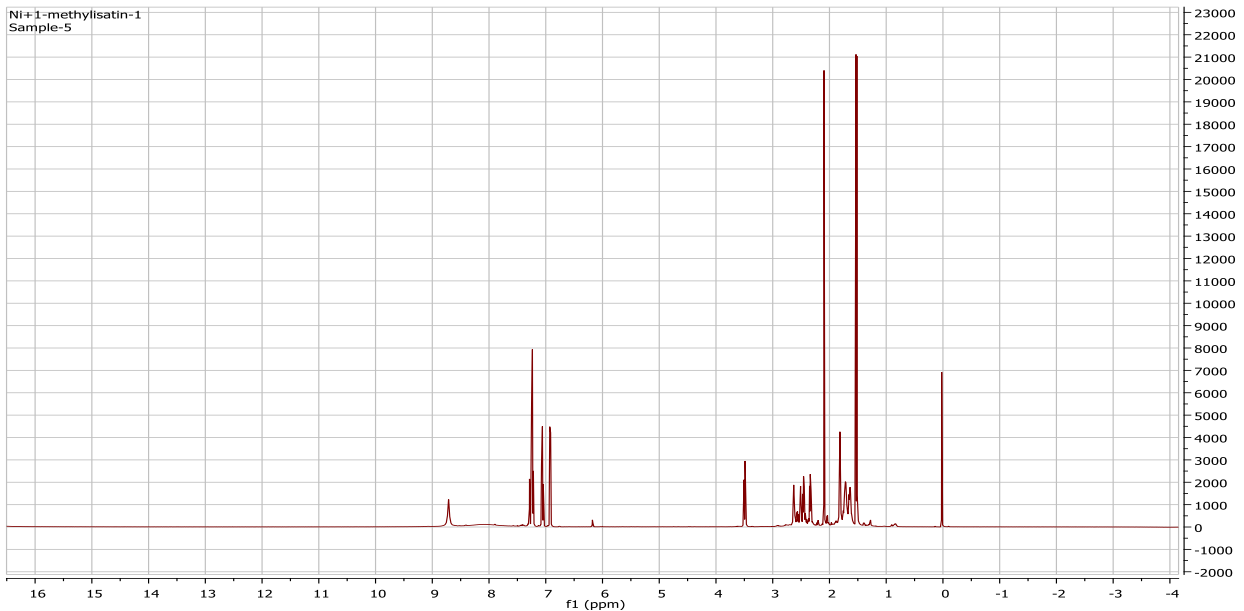


Figure 7.3.1.7a) ¹H NMR spectrum of complex 37

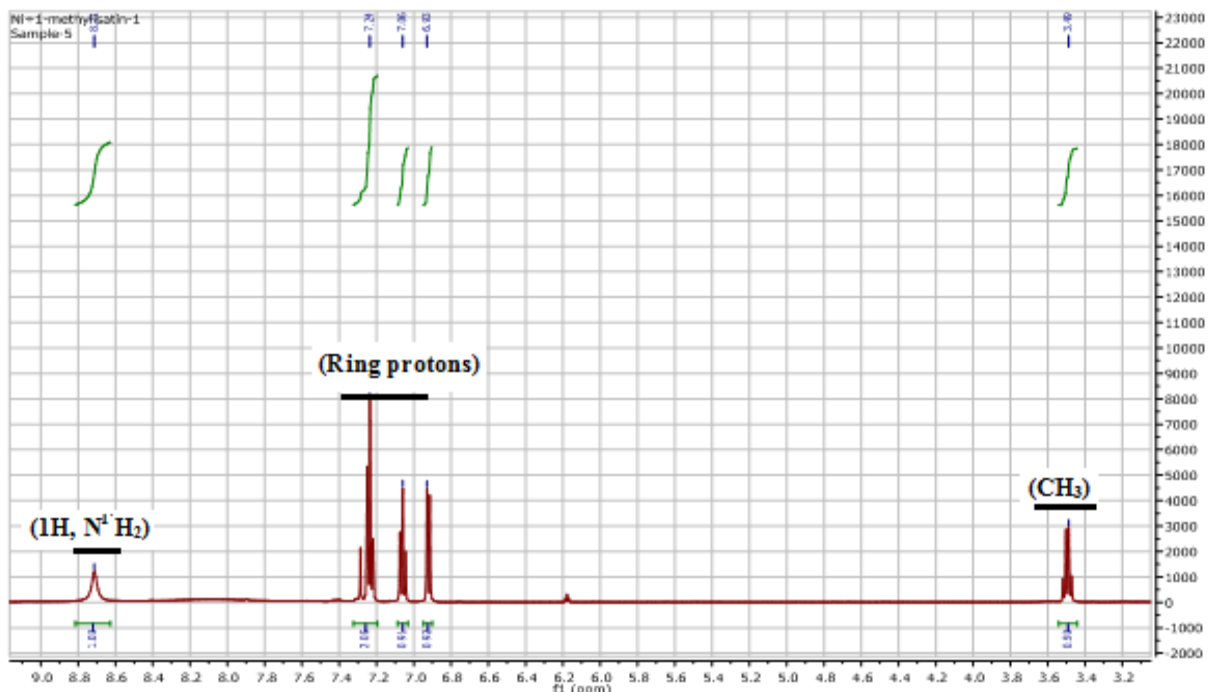


Figure 7.3.1.7b) ¹H NMR spectrum of complex 37(expansion form)

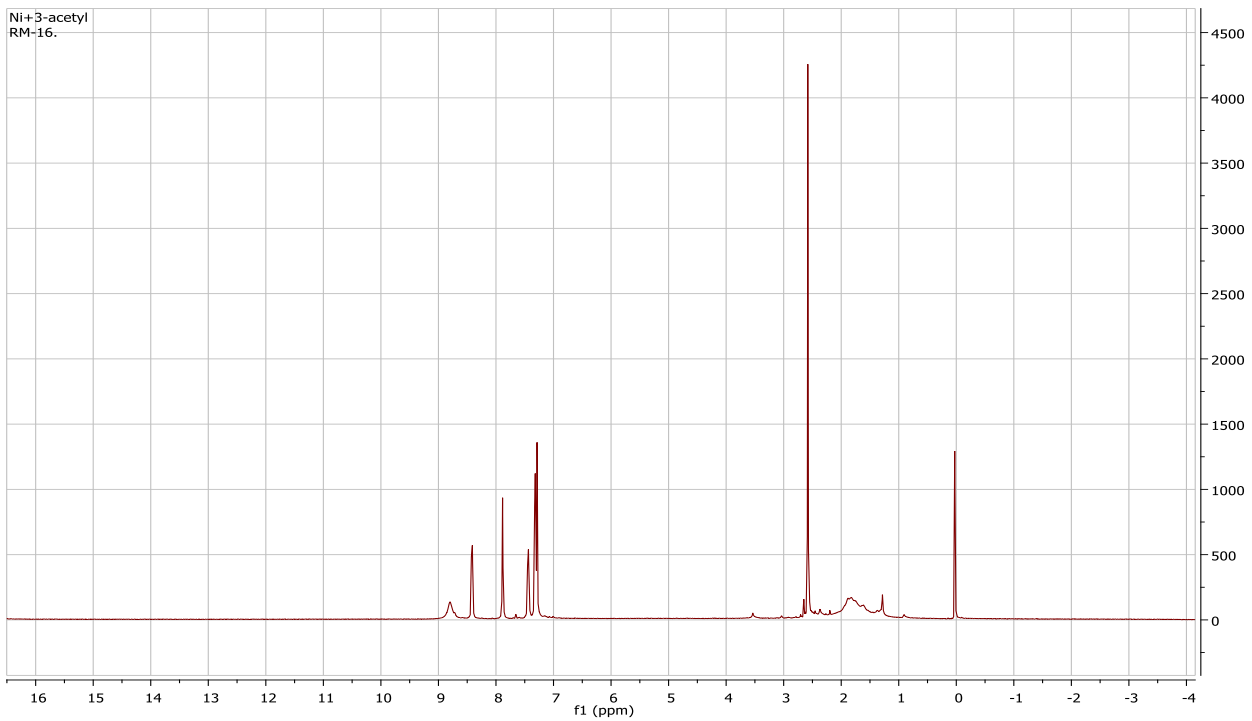


Figure 7.3.1.8a) ¹H NMR spectrum of complex 39

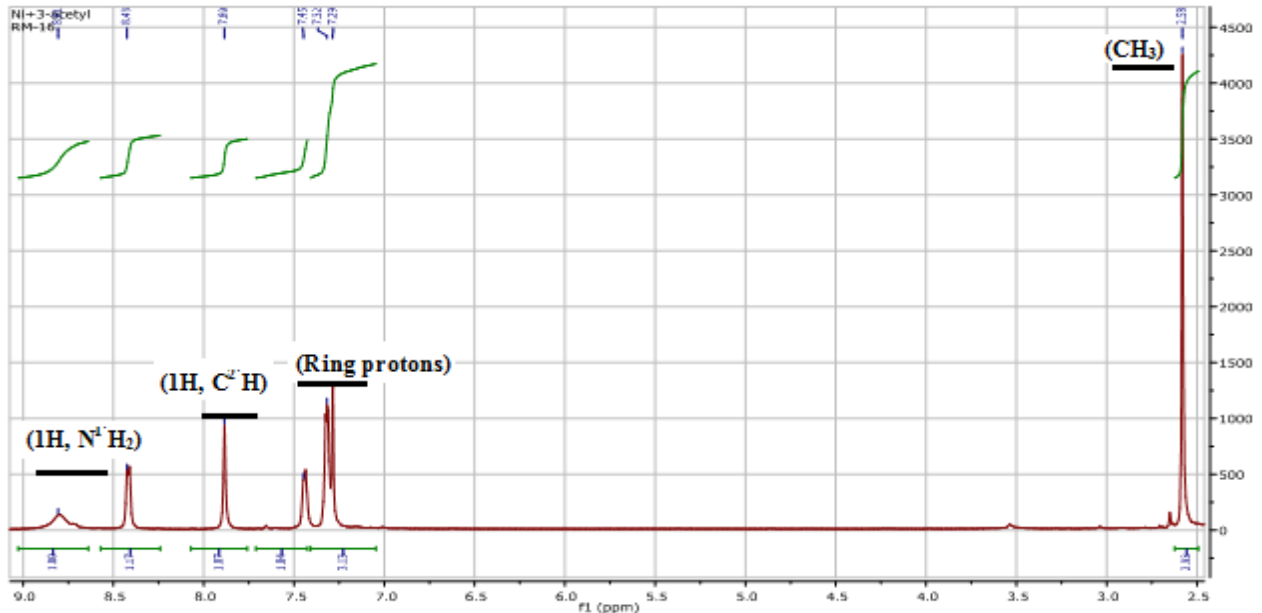


Figure 7.3.1.8b) ¹H NMR spectrum of complex 39(expansion form)

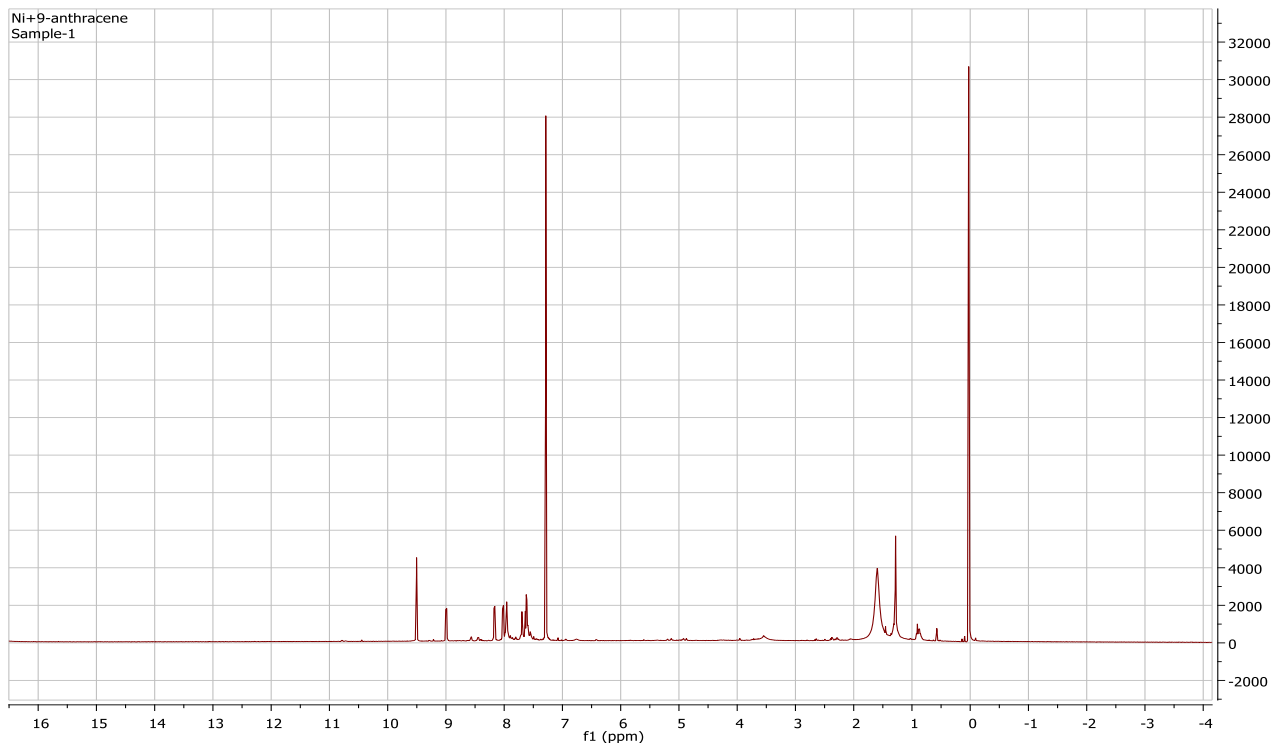


Figure 7.3.1.9a) ¹H NMR spectrum of complex **40**

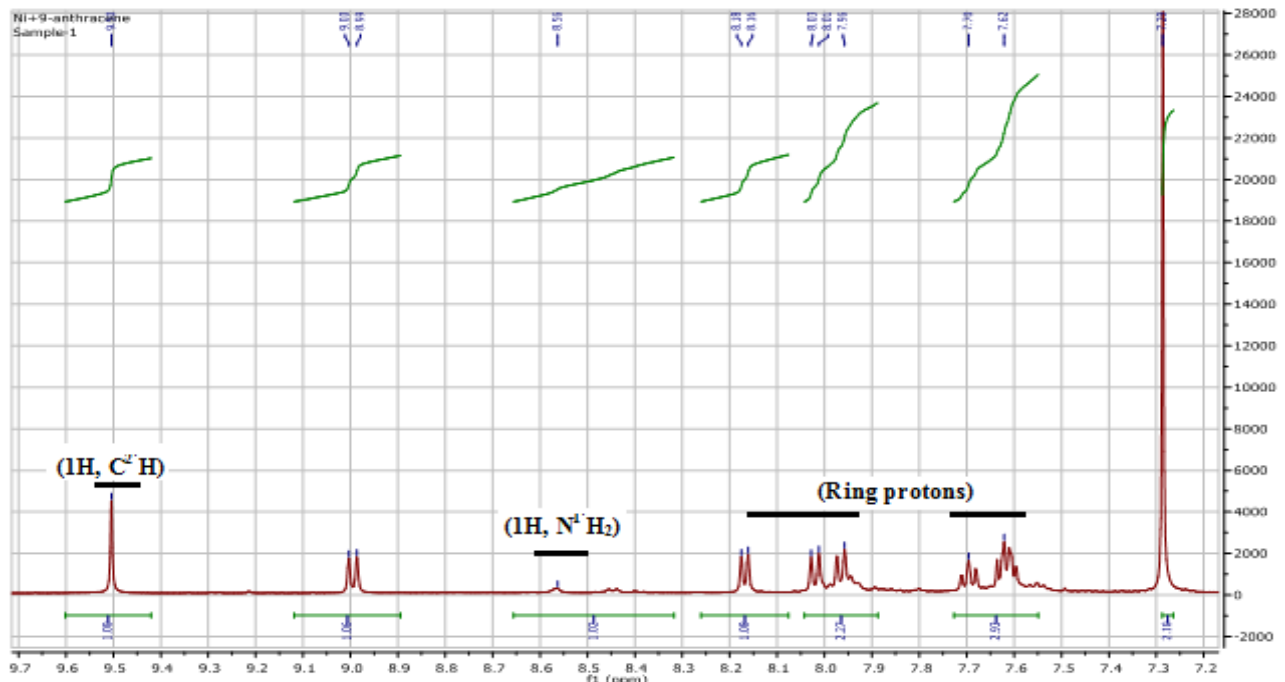


Figure 7.3.1.9b) ¹H NMR spectrum of complex **40**(expansion form)

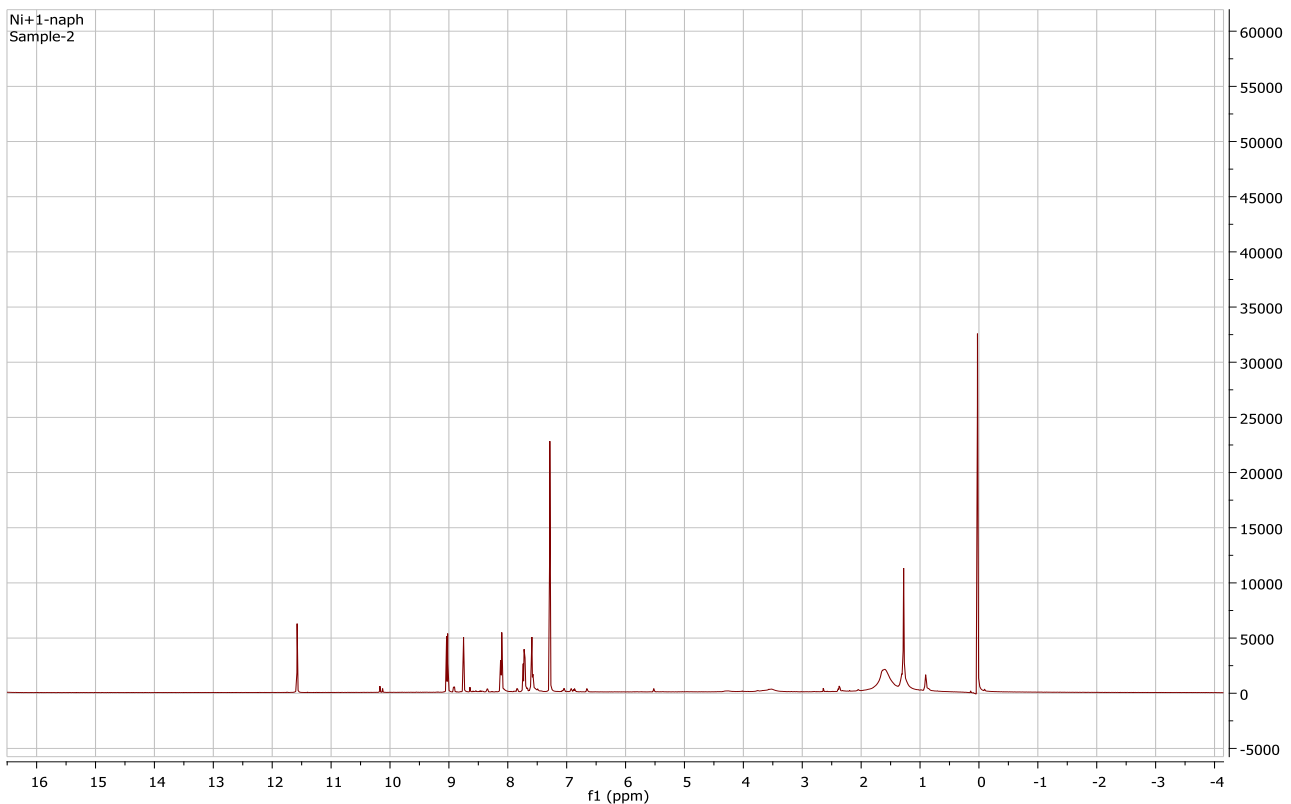


Figure 7.3.1.10a) ¹H NMR spectrum of complex 41

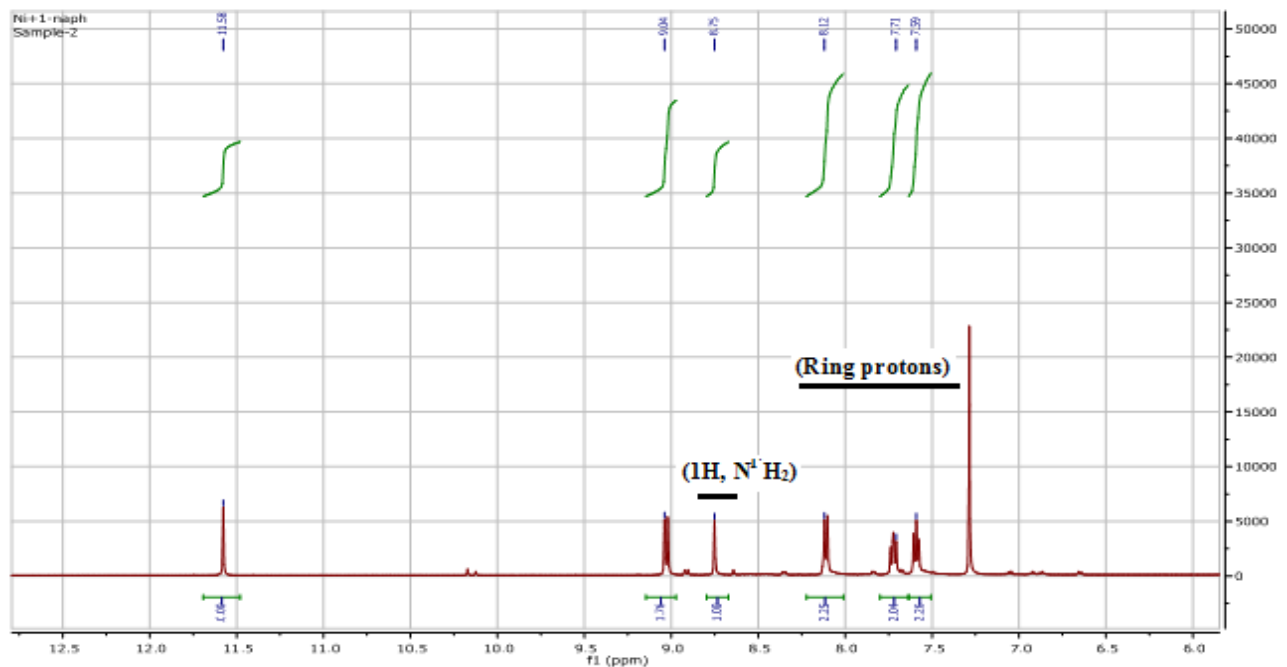


Figure 7.3.1.10b) ¹H NMR spectrum of complex 41(expansion form)

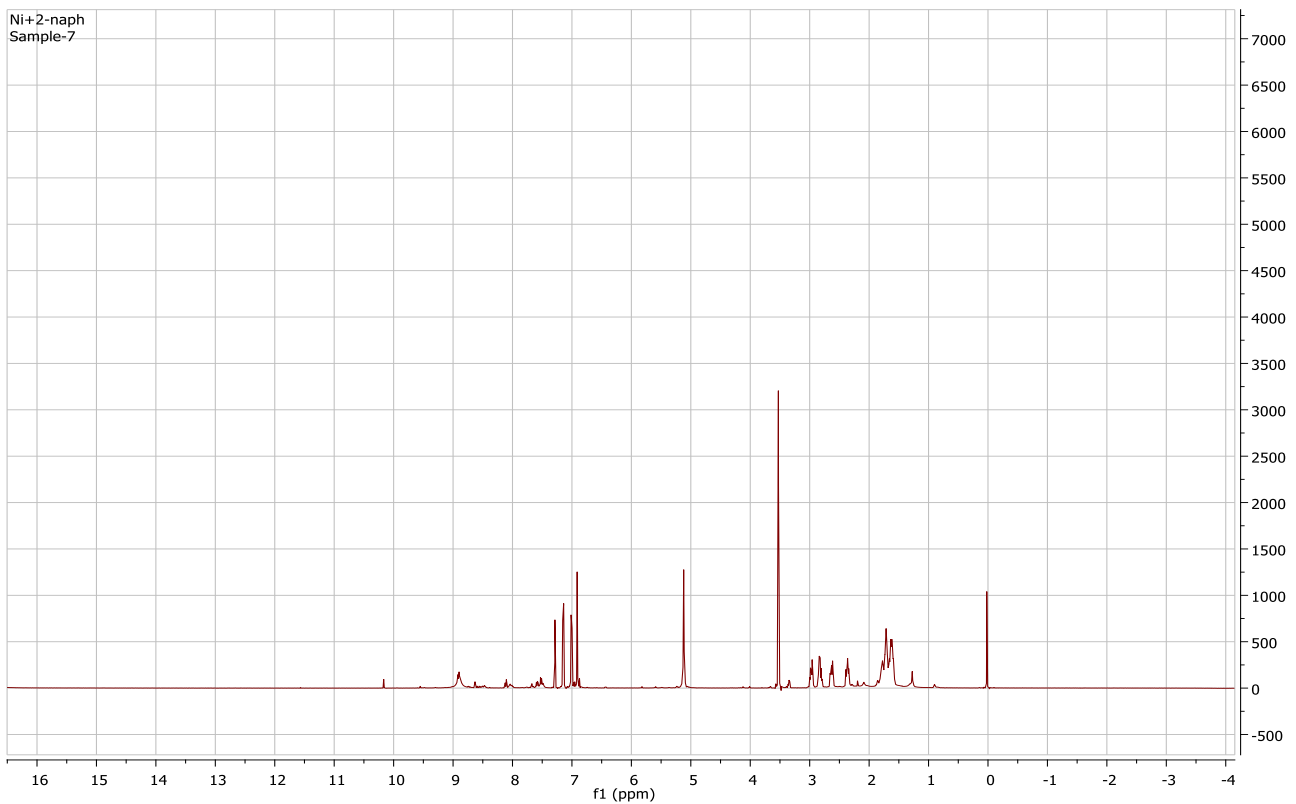


Figure 7.3.1.11a) ^1H NMR spectrum of complex **42**

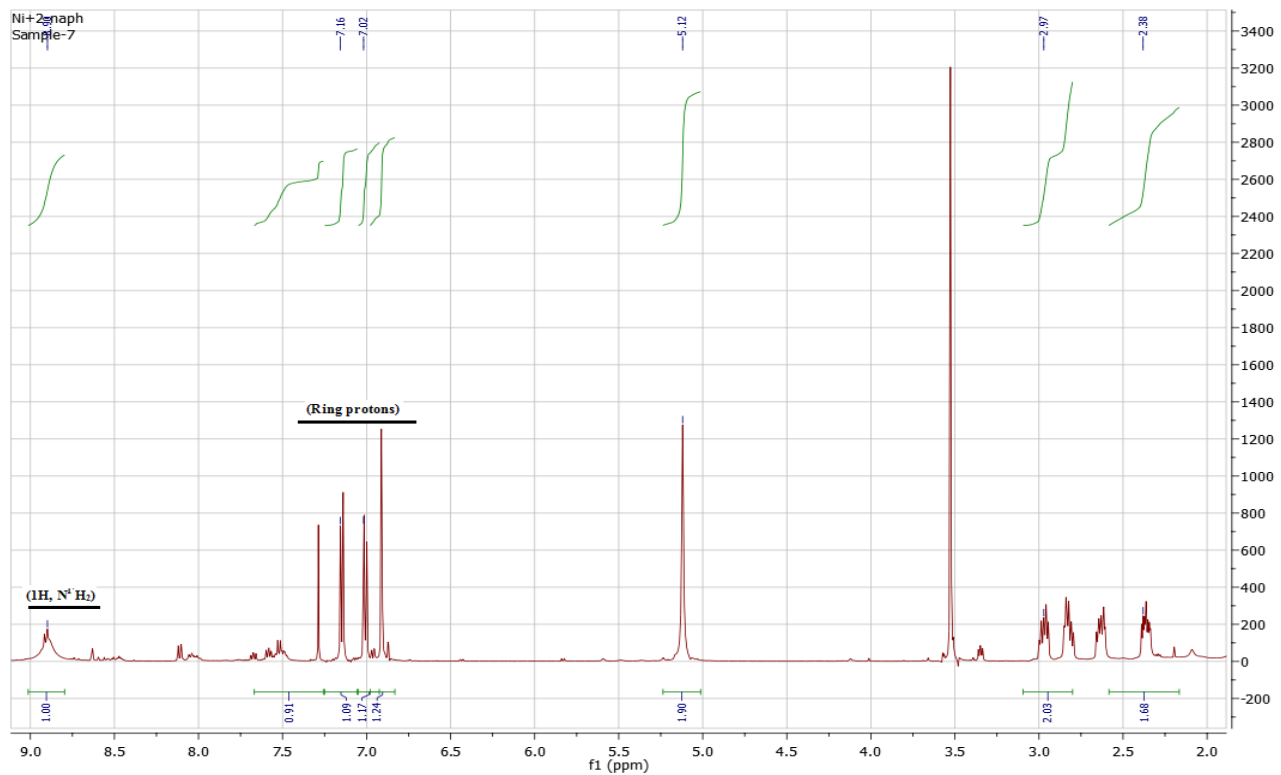


Figure 7.3.1.11b) ^1H NMR spectrum of complex **42**(expansion form)

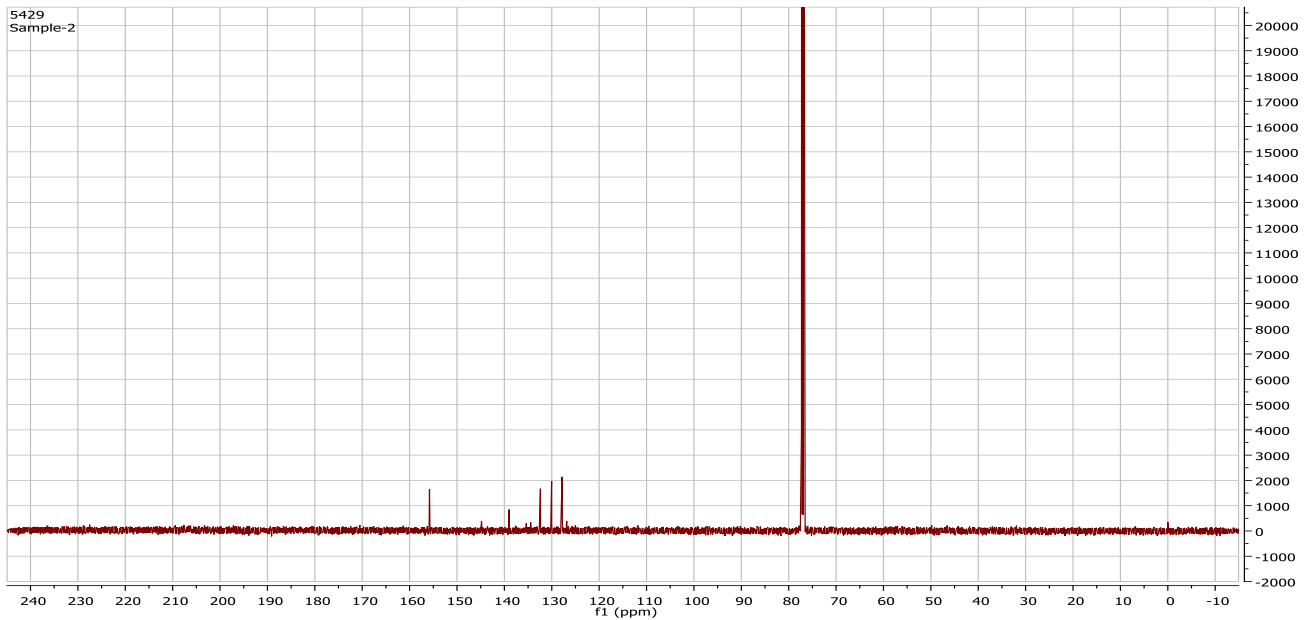


Figure 7.3.2.1a) ^{13}C NMR spectrum of complex **30**

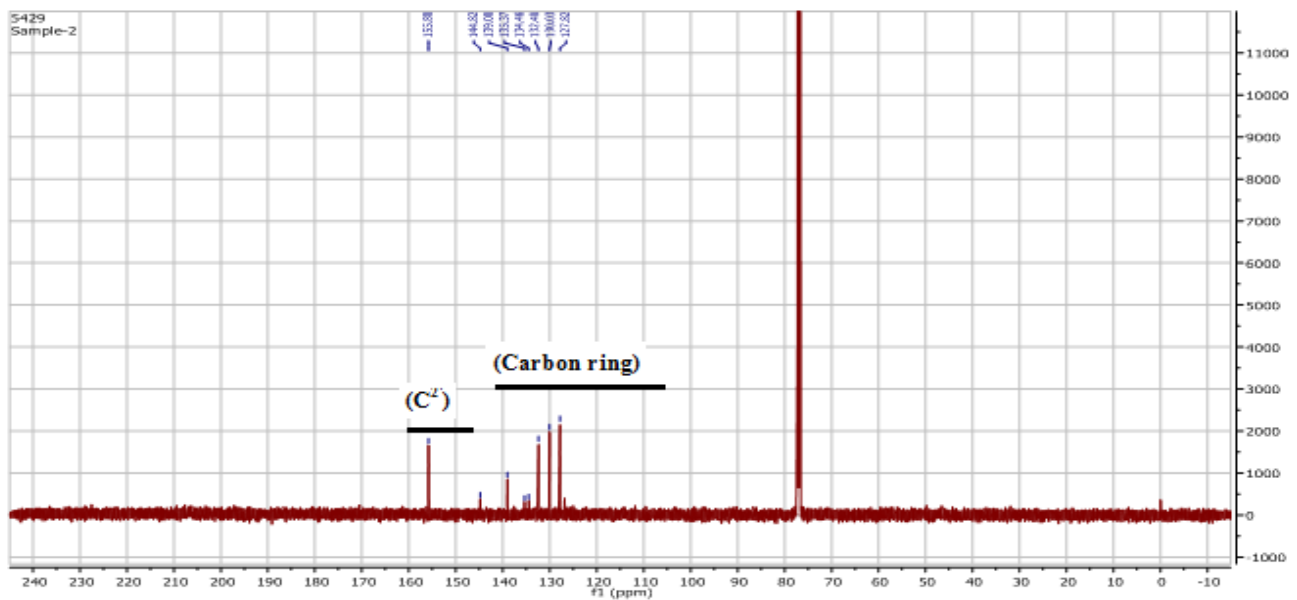


Figure 7.3.2.1b) ^{13}C NMR spectrum with full view of complex **30**

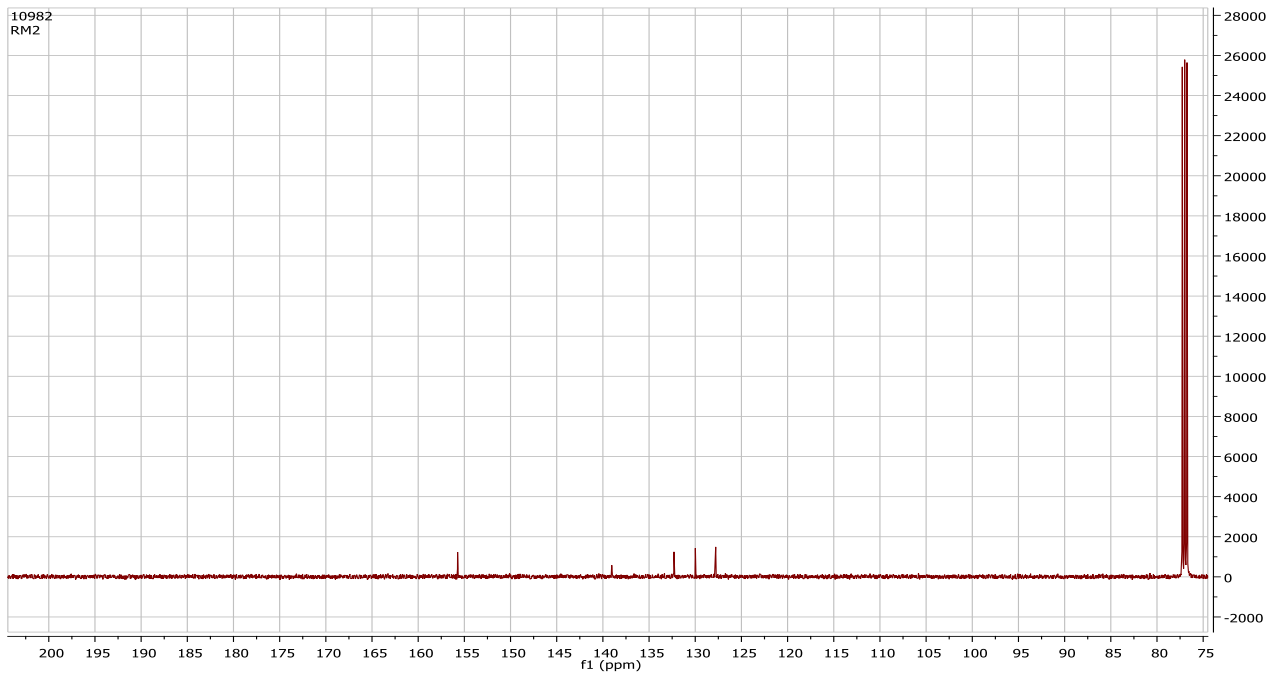


Figure 7.3.2.2a) ^{13}C NMR spectrum of complex **31**

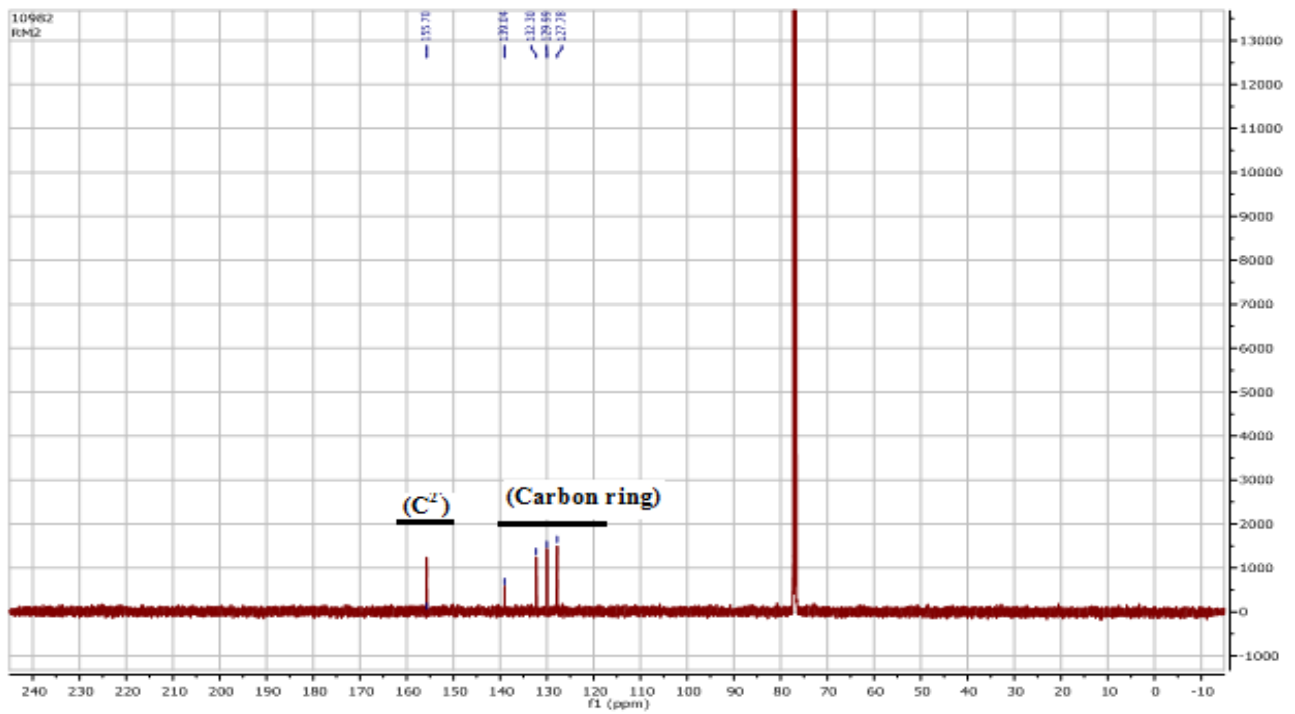


Figure 7.3.2.2b) ^{13}C NMR spectrum with full view of complex **31**

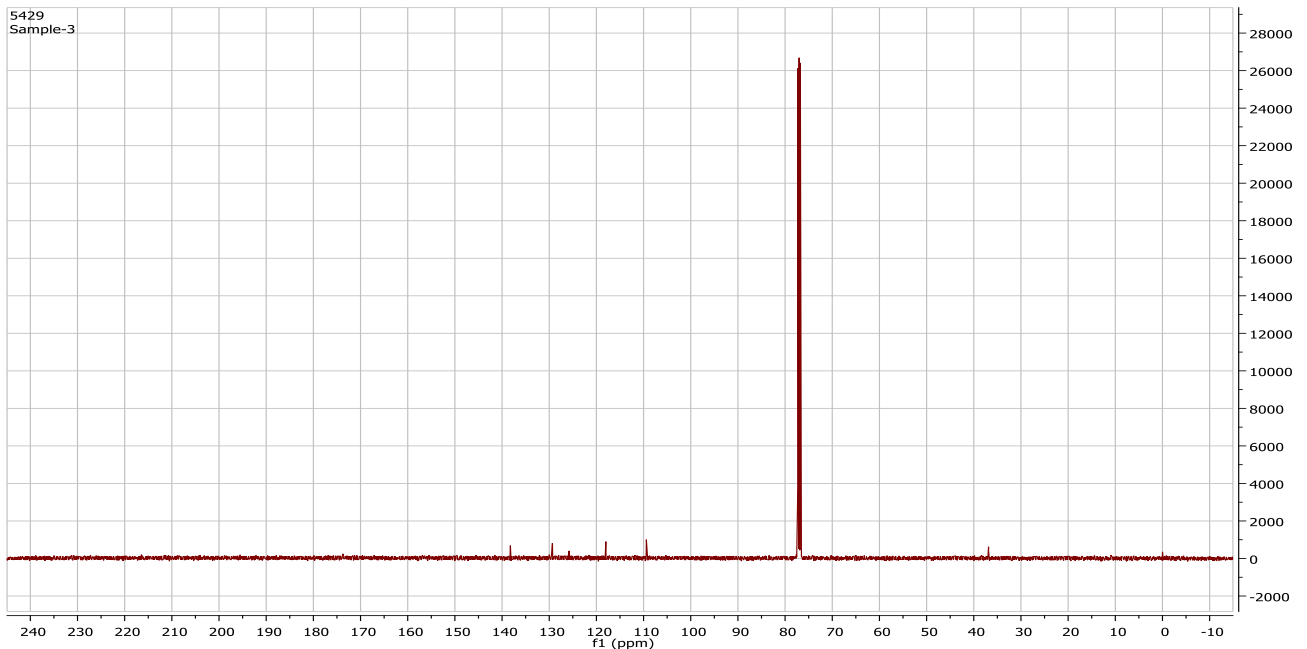


Figure 7.3.2.3a) ¹³C NMR spectrum of complex 32

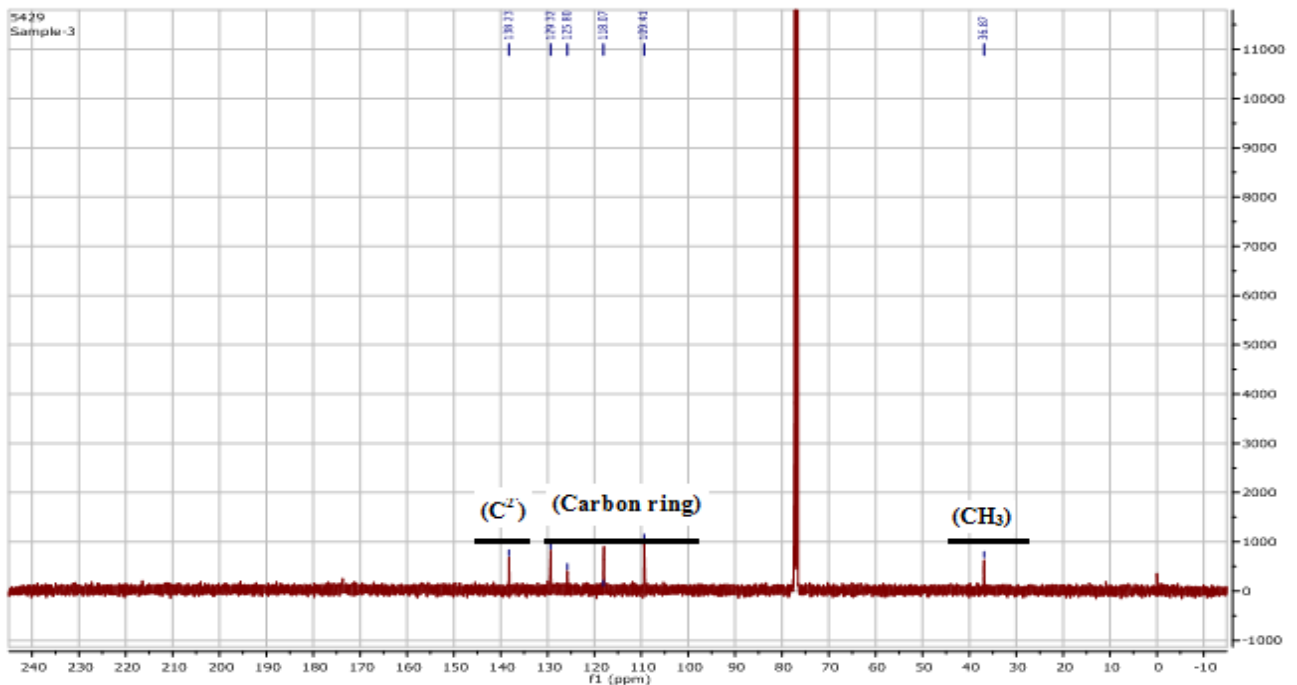


Figure 7.3.2.3b) ¹³C NMR spectrum with full view of complex 32

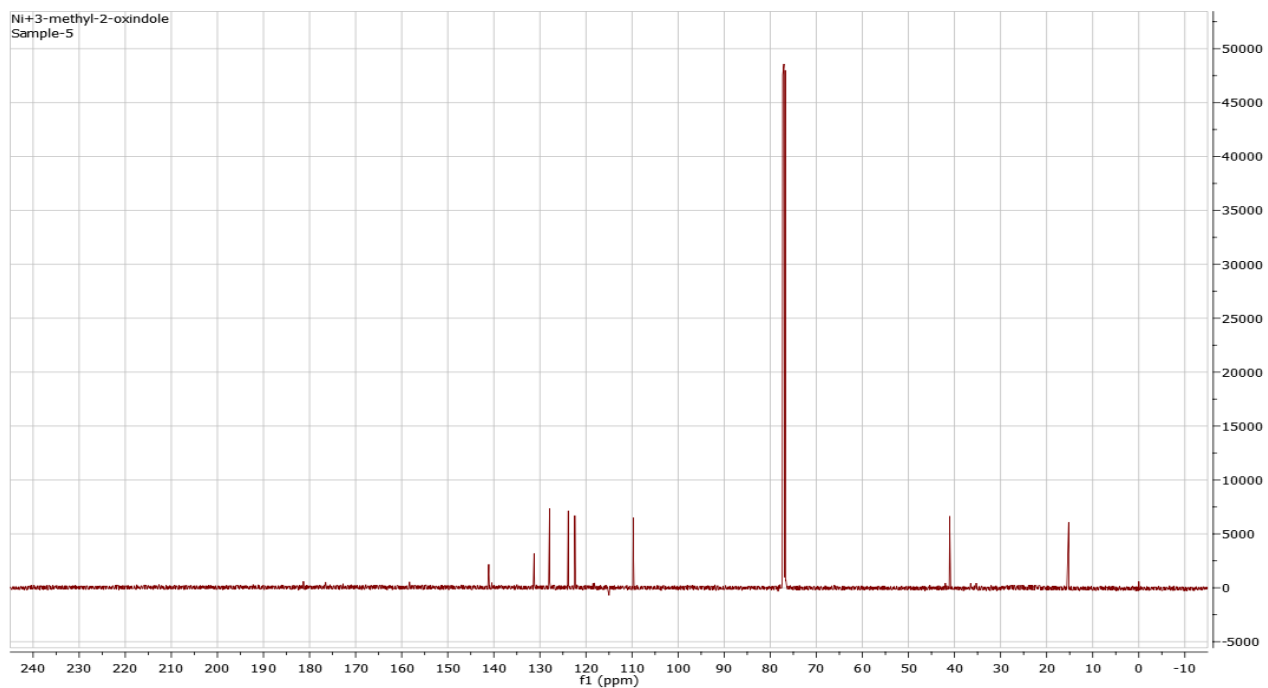


Figure 7.3.2.4a) ¹³C NMR spectrum of complex 33

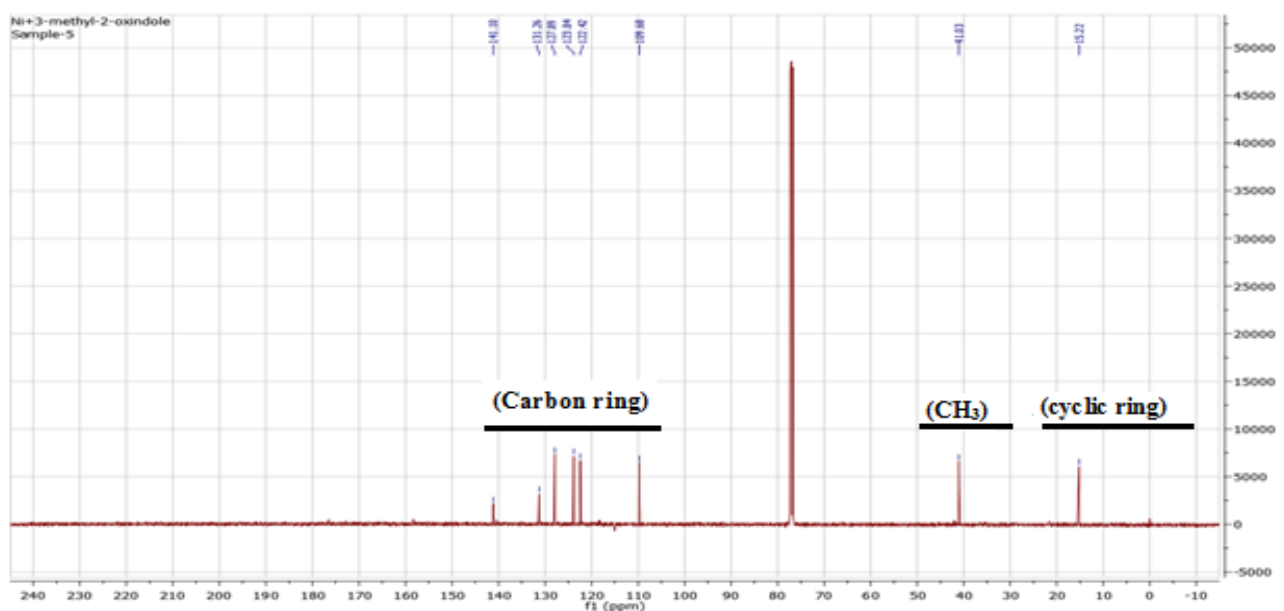


Figure 7.3.2.4b) ¹³C NMR spectrum with full view of complex 33

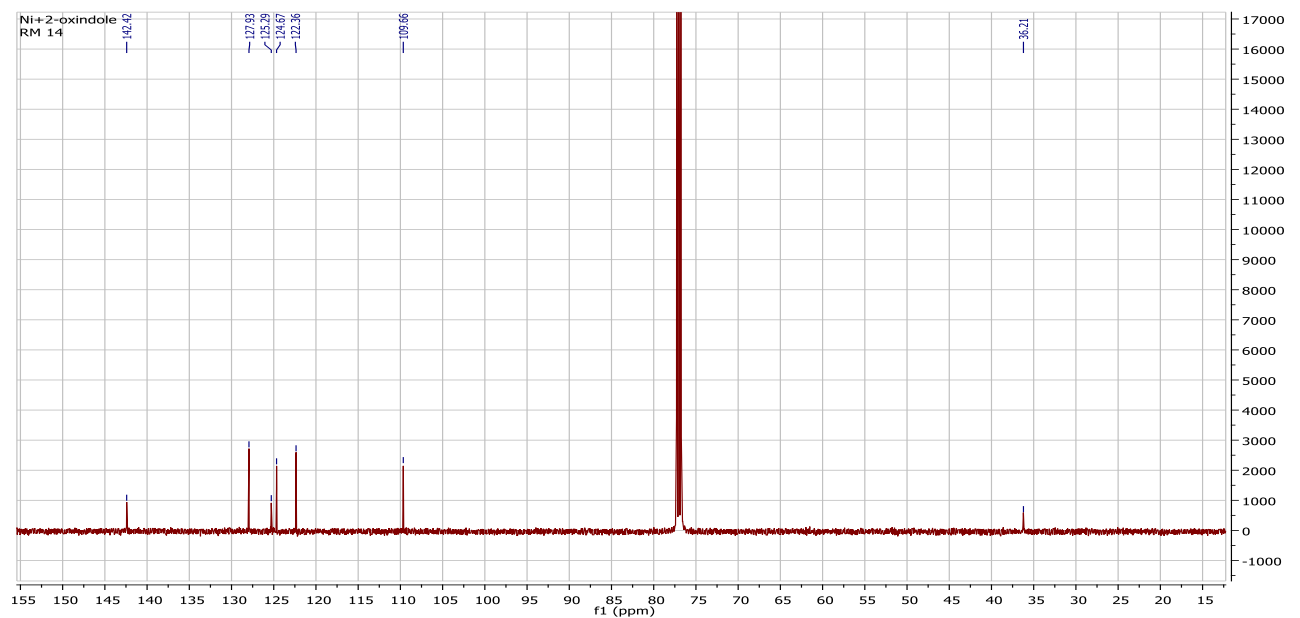


Figure 7.3.2.5a) ^{13}C NMR spectrum of complex 34

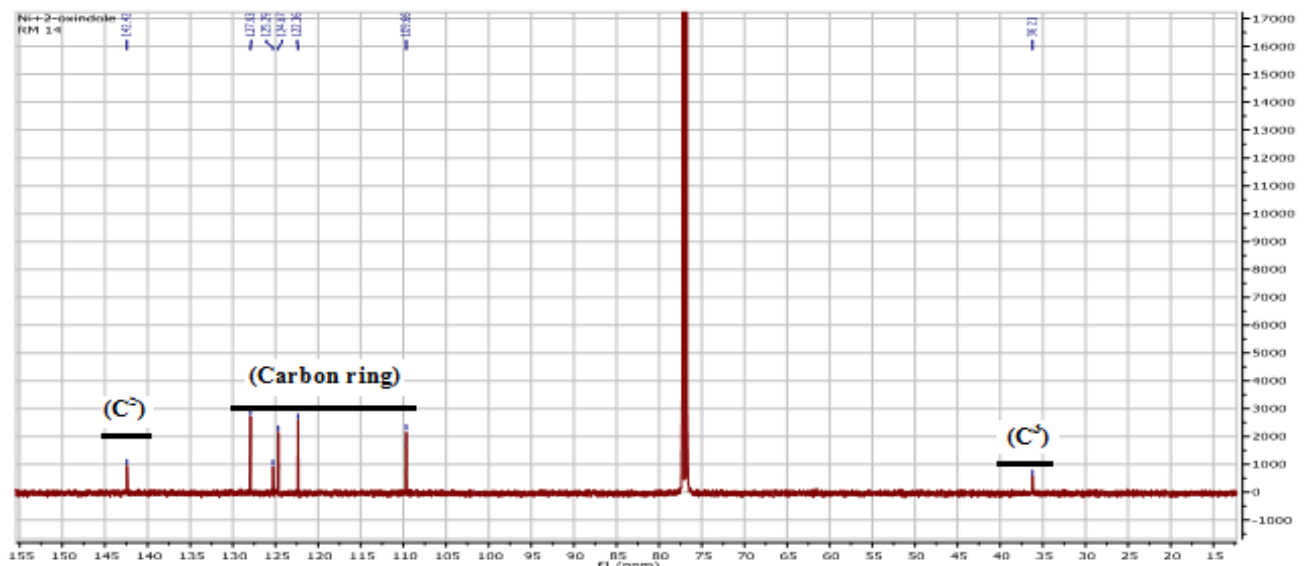


Figure 7.3.2.5b) ^{13}C NMR spectrum of complex 34(expansion form)

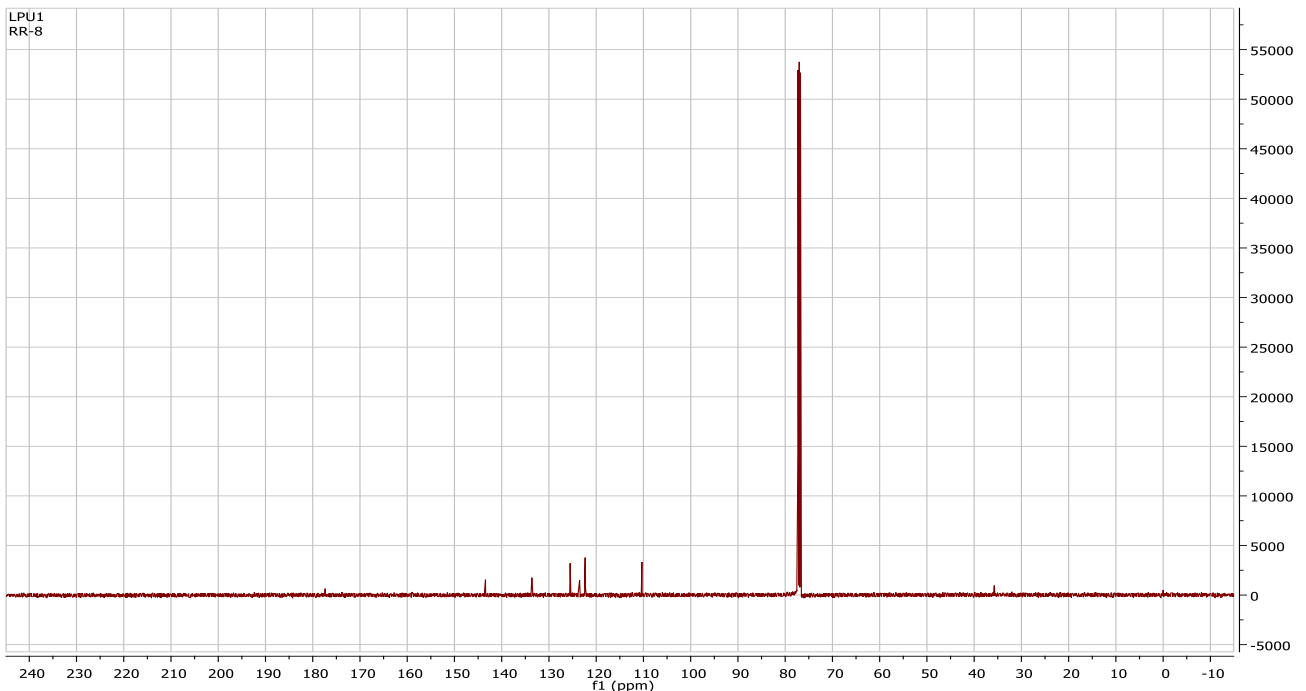


Figure 7.3.2.6a) ¹³C NMR spectrum of complex **35**

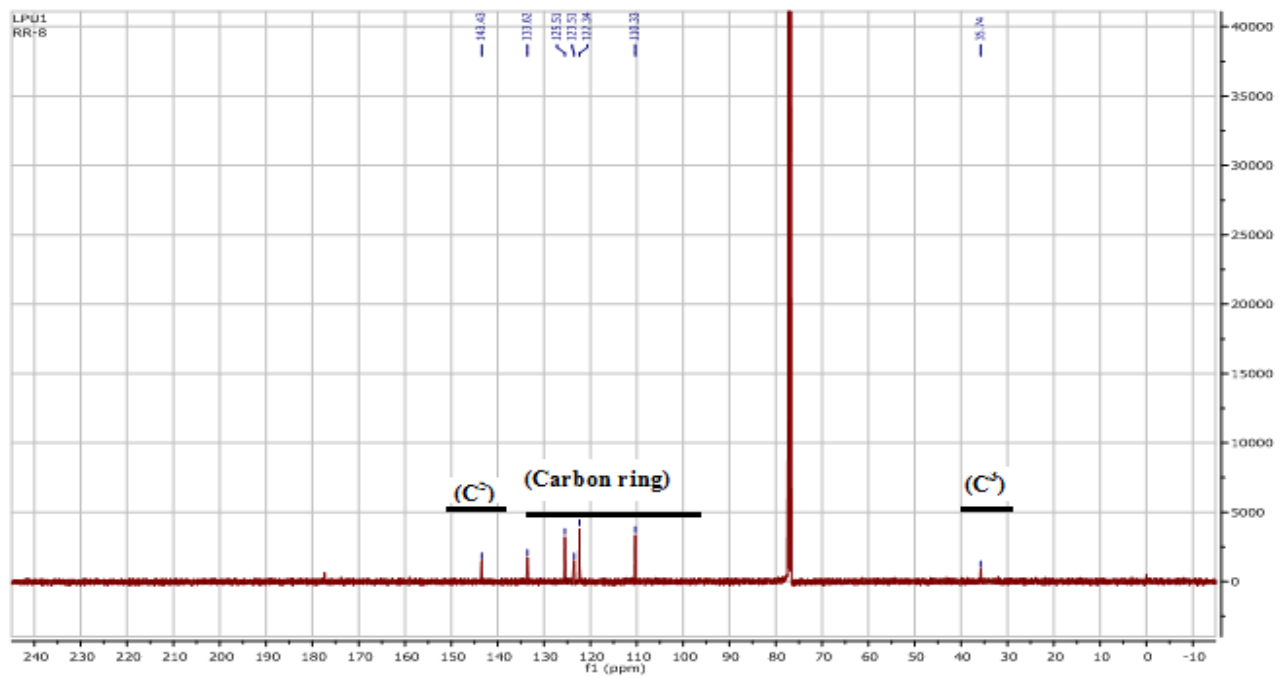


Figure 7.3.2.6b) ¹³C NMR spectrum with full view of complex **35**

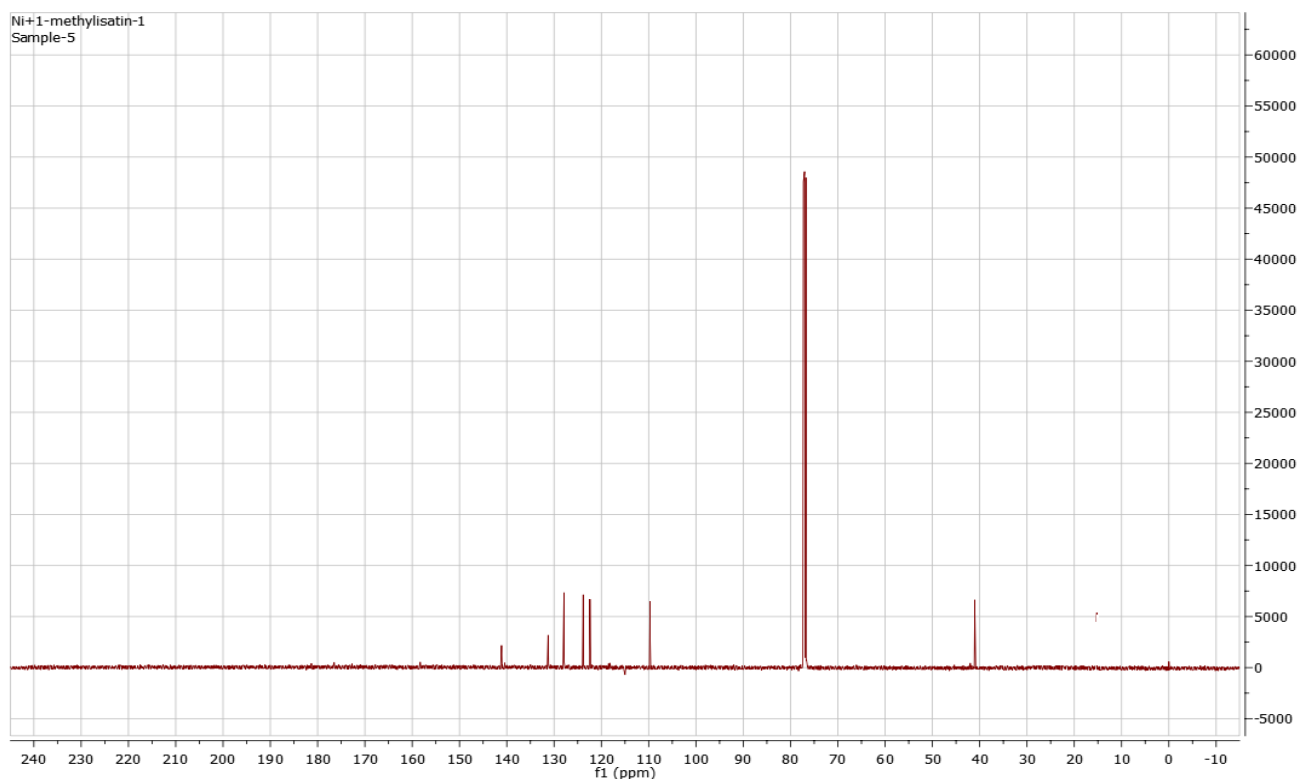


Figure 7.3.2.7a) ^{13}C NMR spectrum of complex **37**

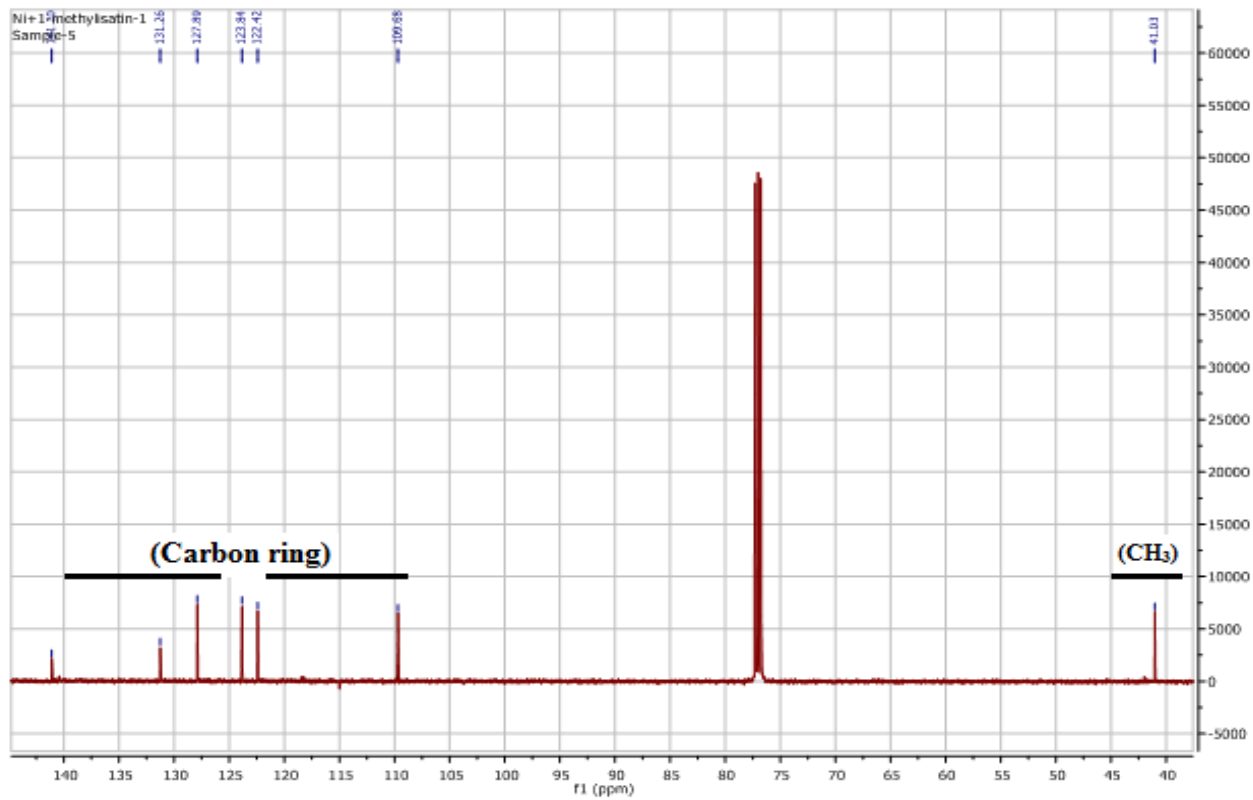


Figure 7.3.2.7b) ^{13}C NMR spectrum with full view of complex **37**

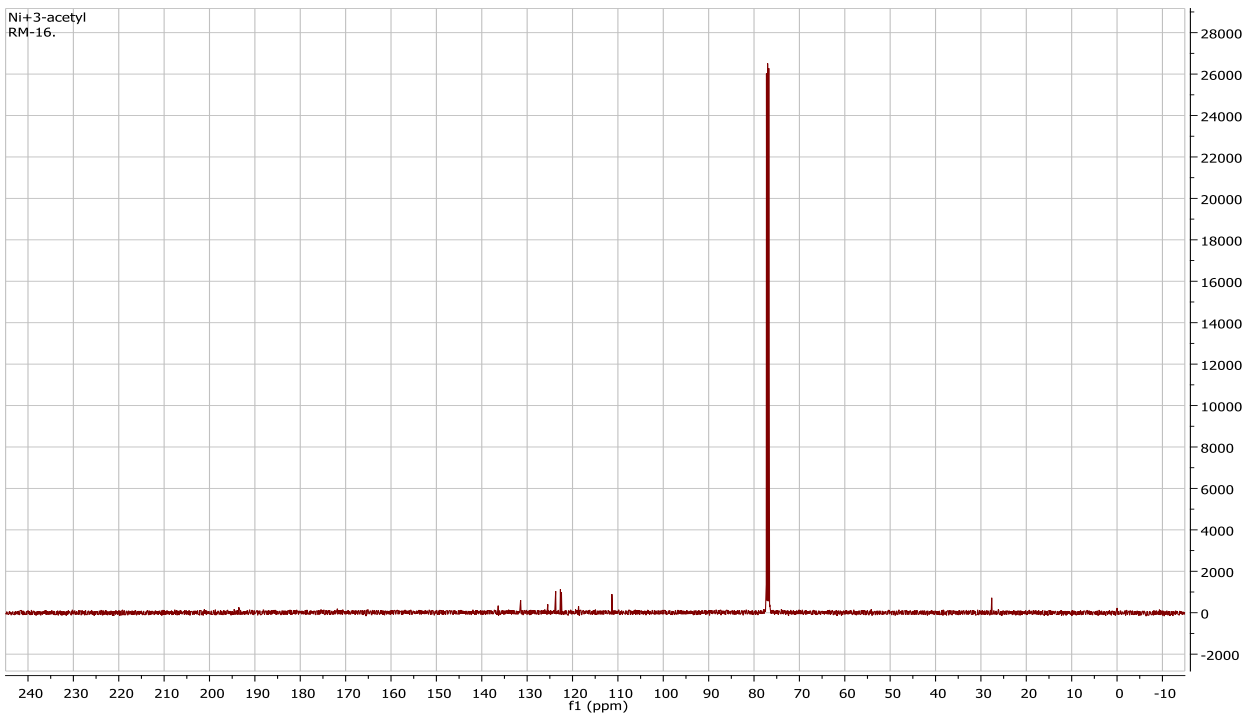


Figure 7.3.2.8a) ¹³C NMR spectrum of complex 39

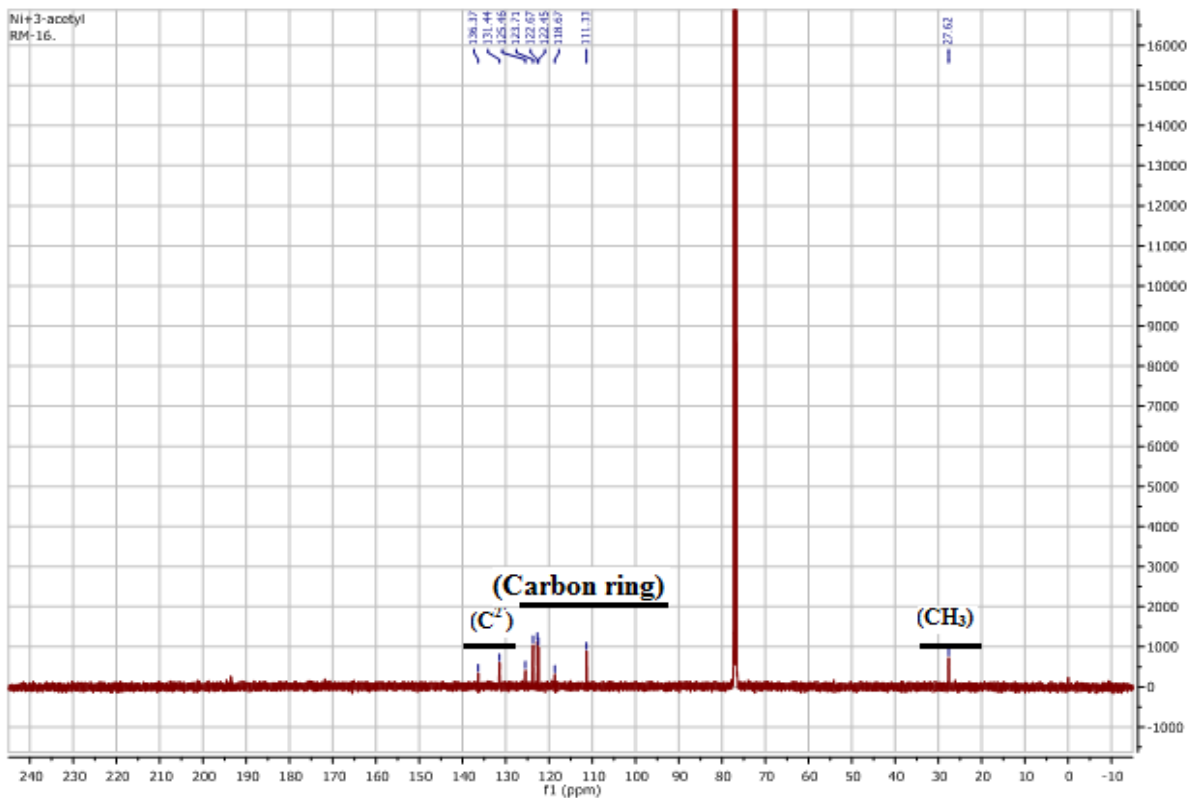


Figure 7.3.2.8b) ¹³C NMR spectrum with full view of complex 39

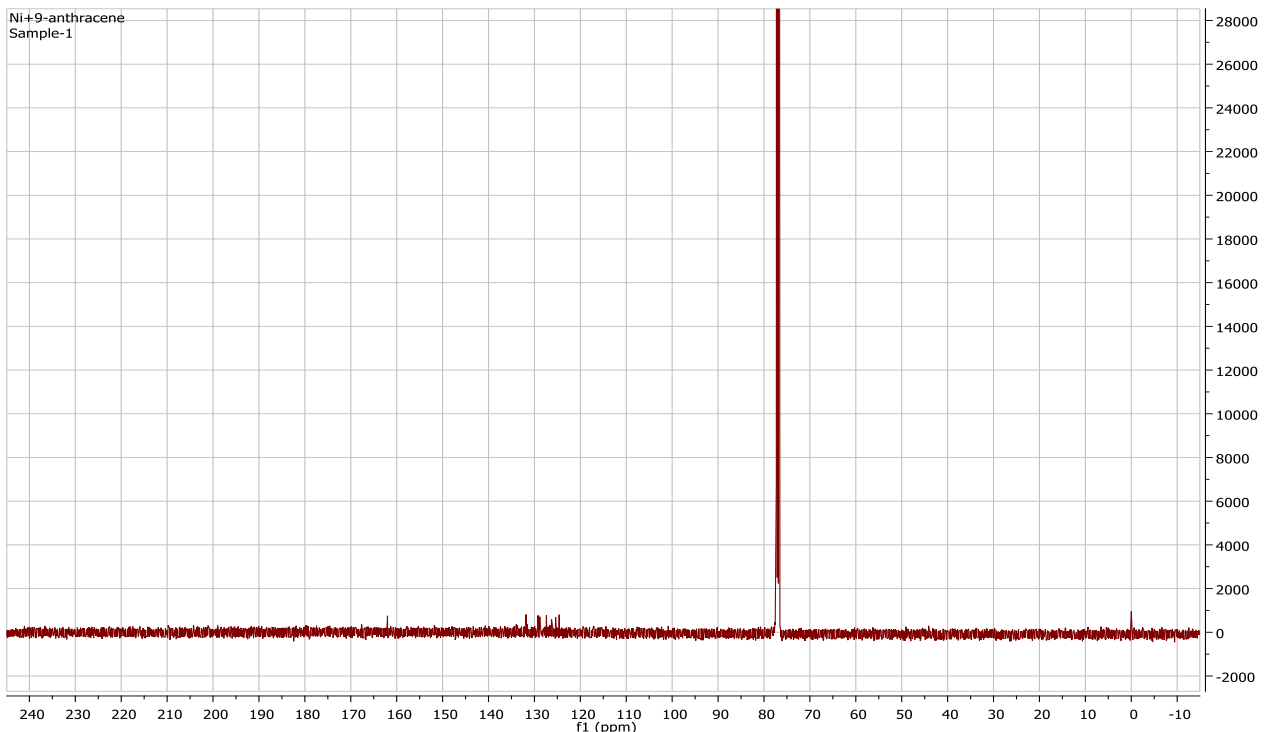


Figure 7.3.2.9a) ¹³C NMR spectrum of complex **40**

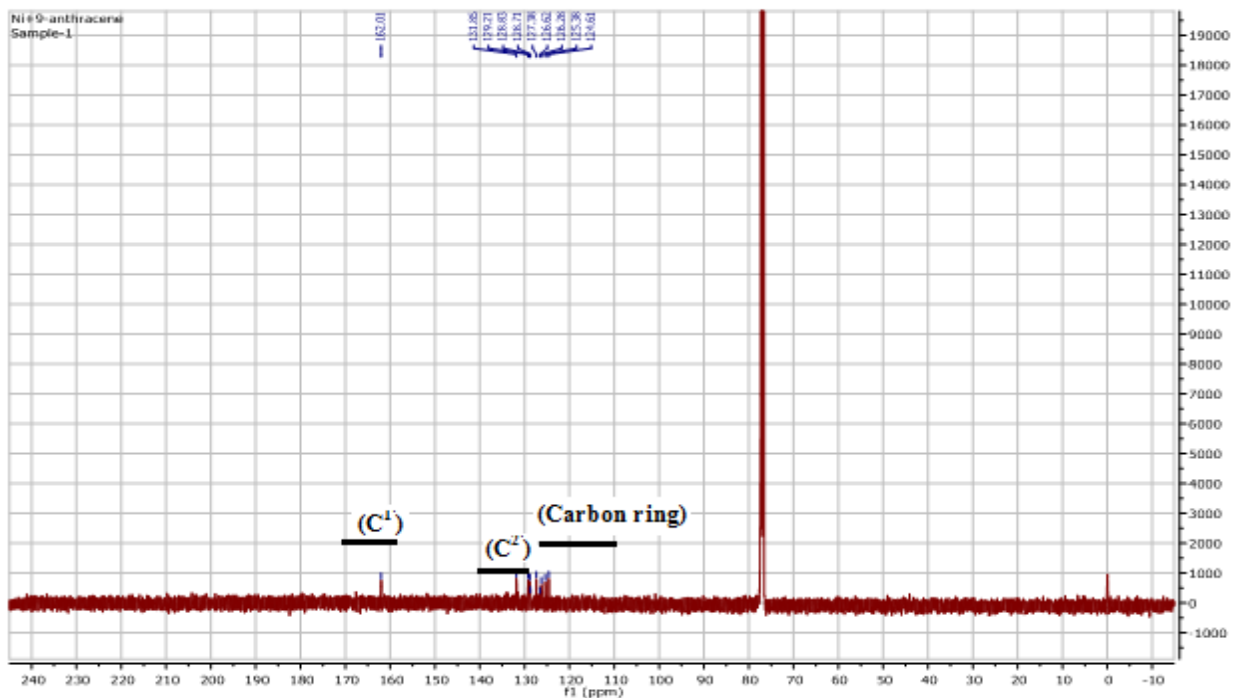


Figure 7.3.2.9b) ¹³C NMR spectrum with full view of complex **40**

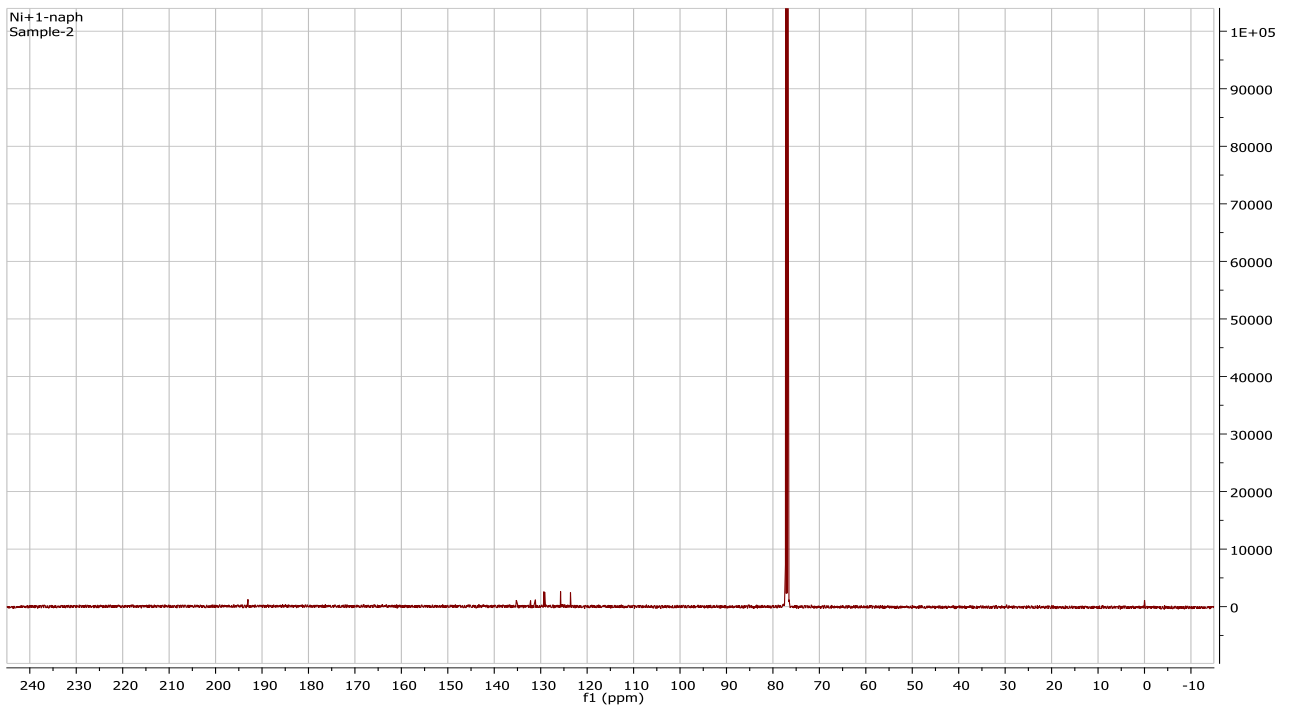


Figure 7.3.2.10a) ¹³C NMR spectrum of complex **41**

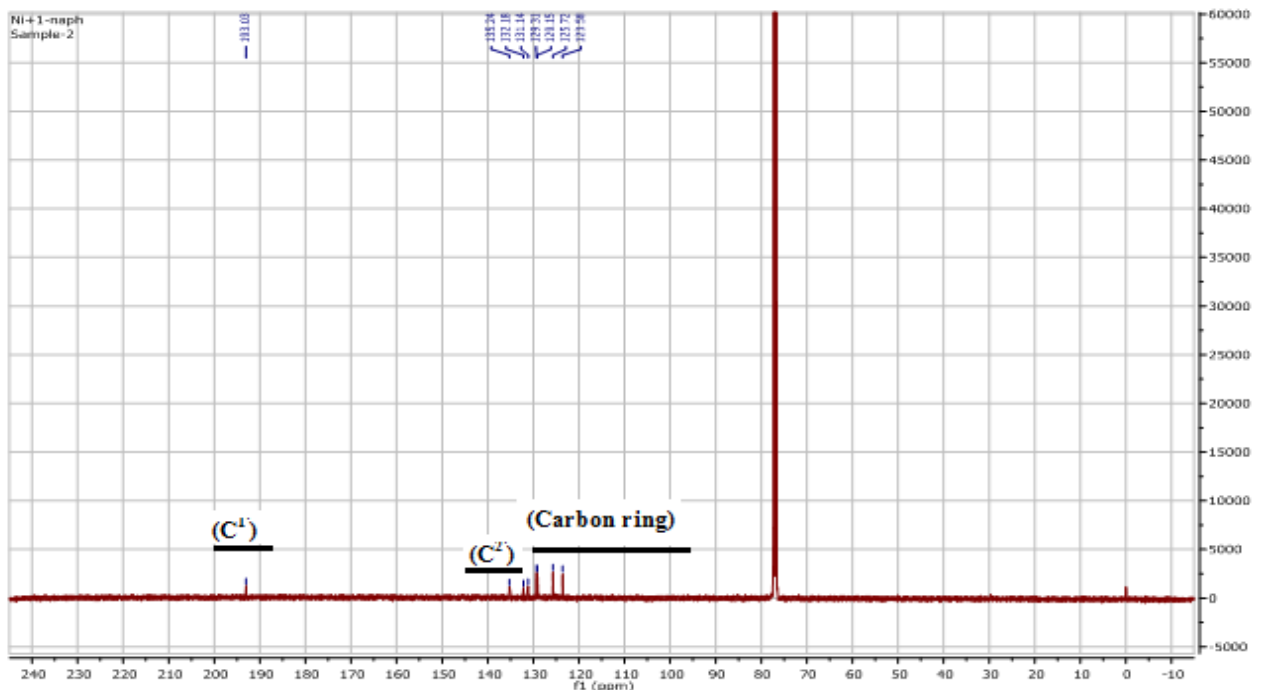


Figure 7.3.2.10b) ¹³C NMR spectrum with full view of complex **41**

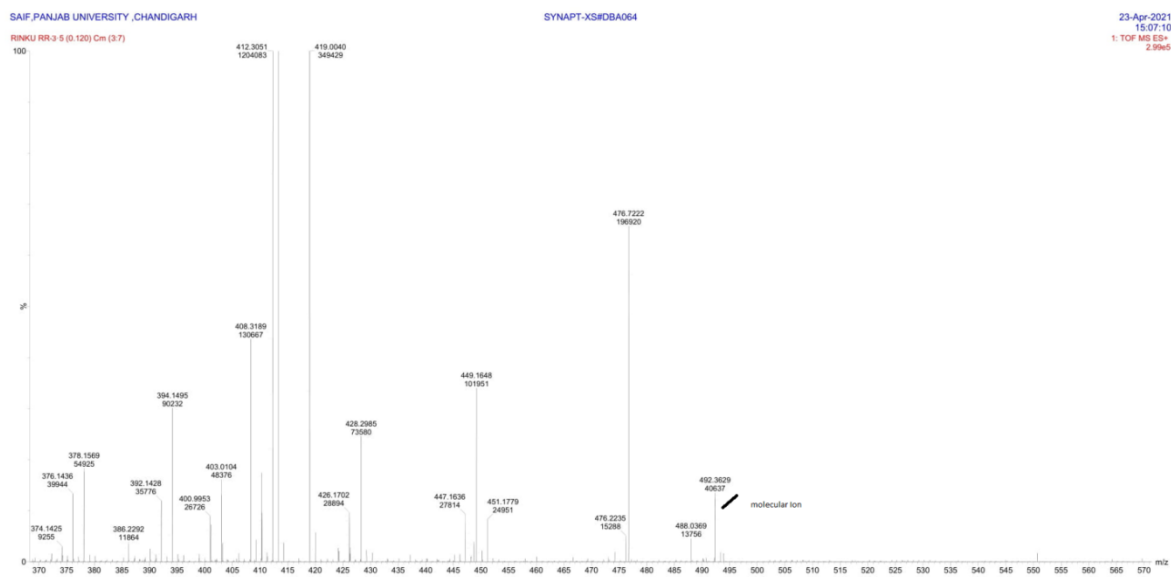


Figure 7.4.1 Mass Spectrum of $[\text{Ni}(\text{cysesc})_2]29$

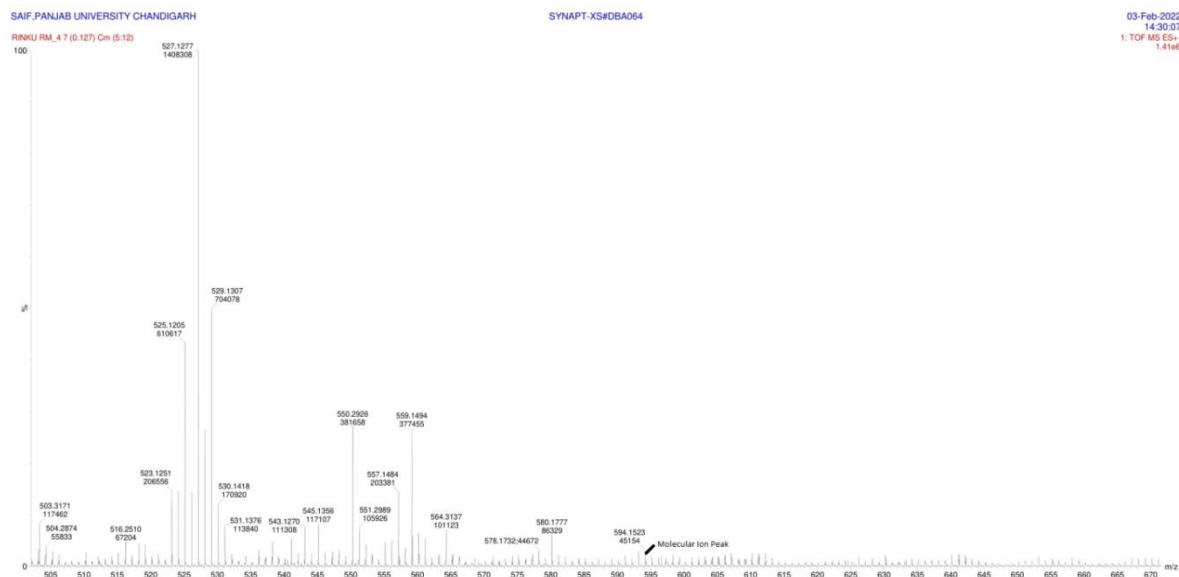


Figure 7.4.2 Mass Spectrum of $[\text{Ni}(3\text{-meoxsesc})_2]33$

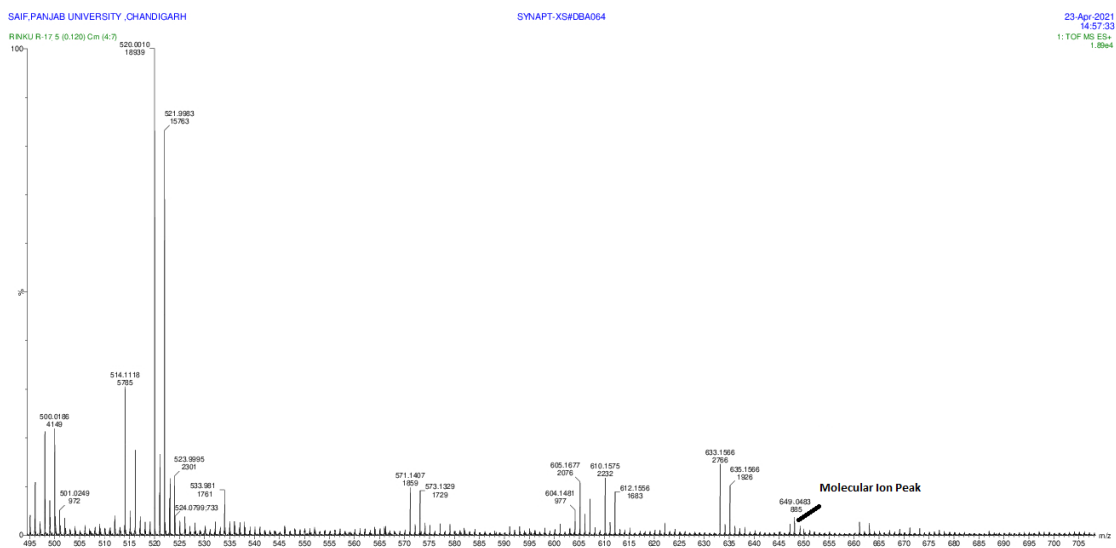


Figure 7.4.3 Mass Spectrum of $[\text{Ni}(5\text{-clistsesc})_2]36$

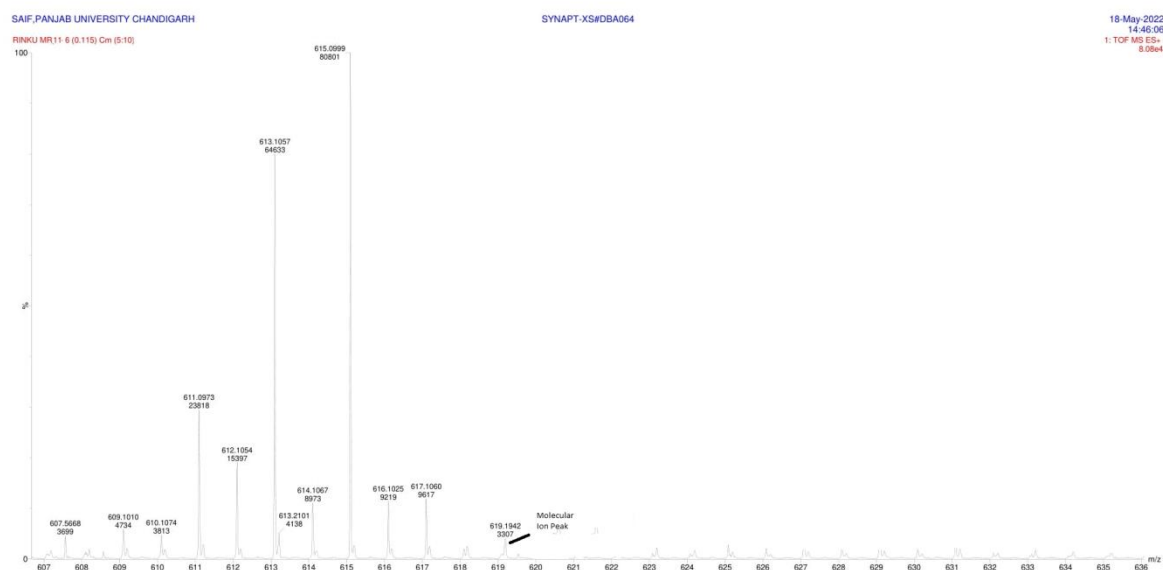


Figure 7.4.4 Mass Spectrum of $[\text{Ni}(1\text{-meistsesc})_2]37$

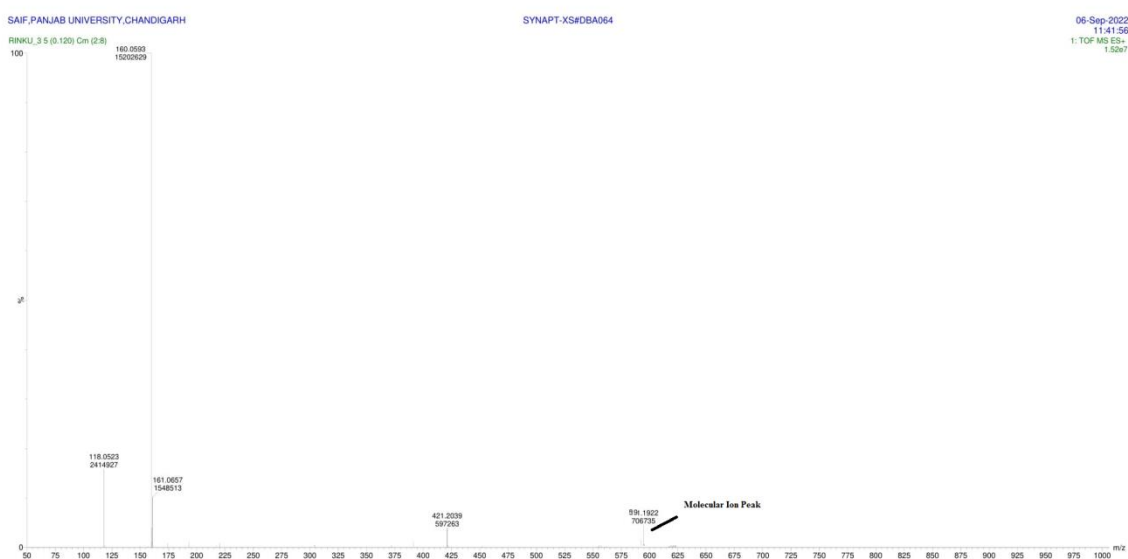


Figure 7.4.5 Mass Spectrum of $[\text{Ni}(3\text{-indsesc})_2]38$

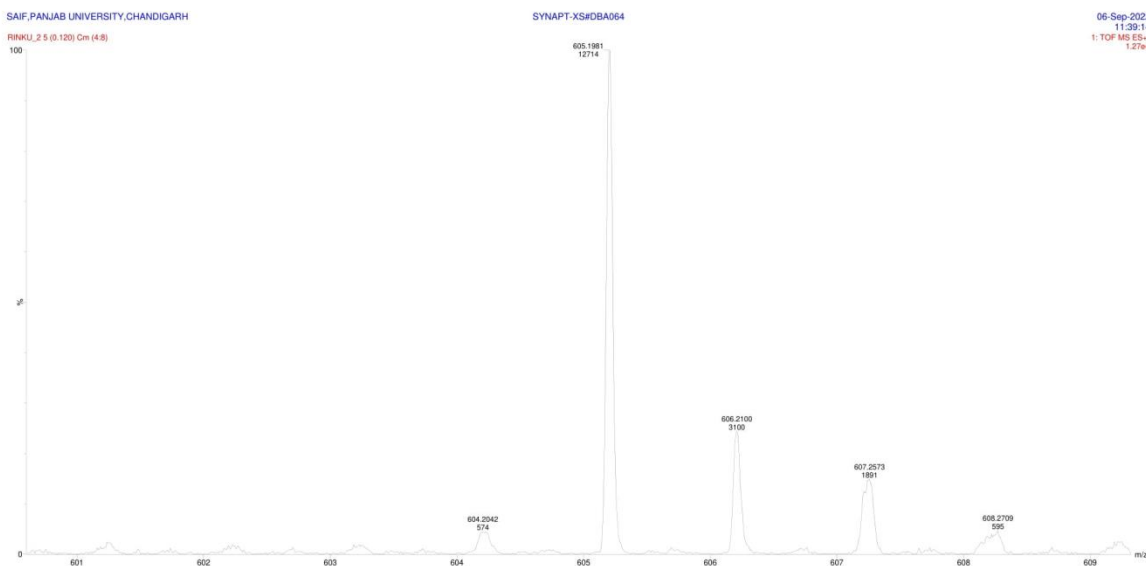


Figure 7.4.6 a) Mass Spectrum of $[\text{Ni}(2\text{-naphthsesc})_2]42$

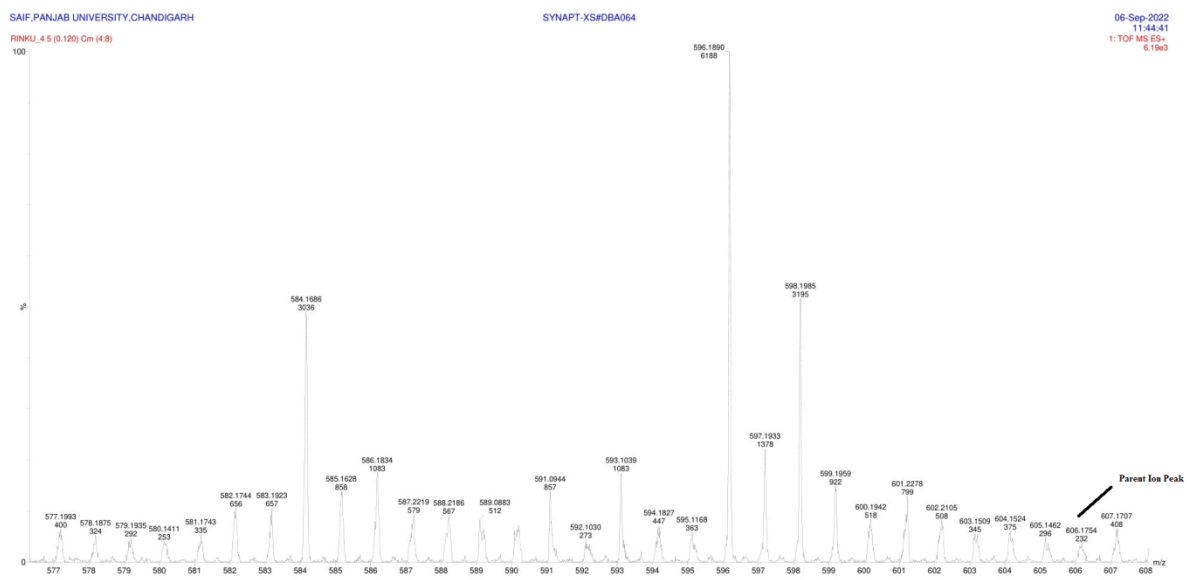


Figure 7.4.6 b) Mass Spectrum of $[\text{Ni}(2\text{-naphthsesc})_2]42$

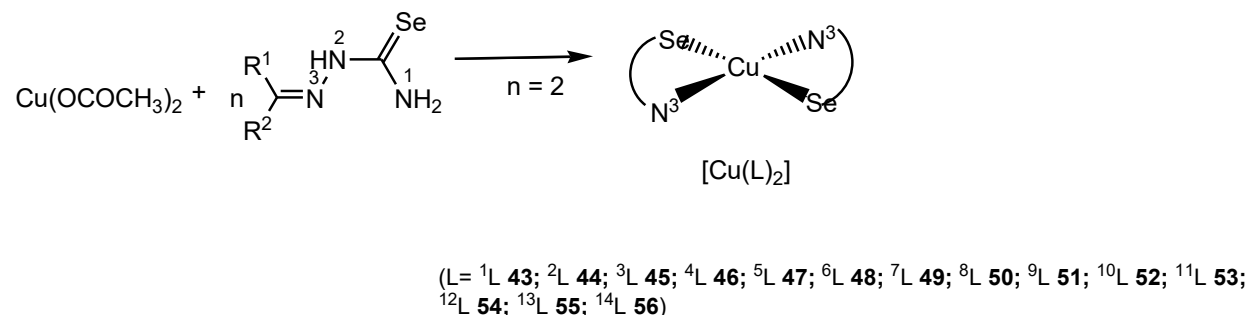
CHAPTER 8

COPPER(II) COMPLEXES

8 Complexes of Copper(II)

8.1 Discussion on Synthesis of copper metal complexes

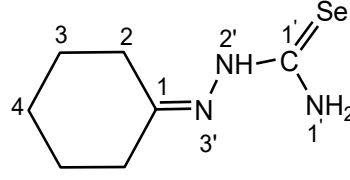
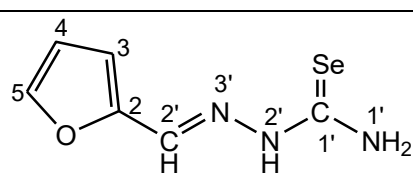
Reaction of synthesized selenosemicarbazones ligands ($H^1L-H^{14}L$) with copper acetate in 2:1 may form complexes of stoichiometry, $[Cu(L)_2]$ ($L = ^1L$ **43**; 2L **44**; 3L **45**; 4L **46**; 5L **47**; 6L **48**; 7L **49**; 8L **50**; 9L **51**; ^{10}L **52**; ^{11}L **53**; ^{12}L **54**; ^{13}L **55**; ^{14}L **56**) (Scheme 8.1)



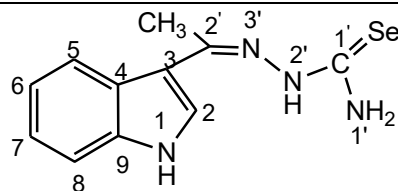
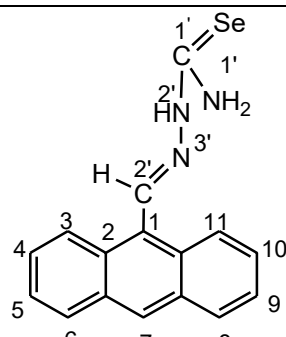
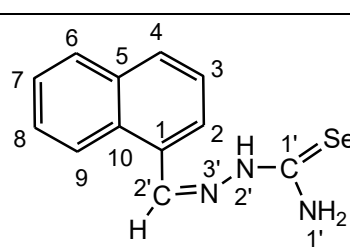
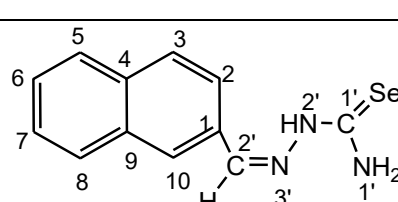
Scheme 8.1

All the synthesized complexes along with the structure of their respective selenosemicarbazones are given in Table 8.1

Table 8.1 List of selenosemicarbazone complexes of copper(II) **43-56**

Sr. No.	Selenosemicarbazone Ligands	Structure of Selenosemicarbazone Ligands	Complexes Formed
1.	Cyclohexanone Selenosemicarbazone (Hcysesc, H¹L)		$[\text{Cu}(\text{cysesc})_2]43$
2.	2-furfural selenosemicarbazone (2-Hfursesc, H²L)		$[\text{Cu}(2\text{-fursesc})_2]44$

3.	2-thiophene selenosemicarbazone (2-Hthiosesc, H³L)		[Cu(2-thiosesc) ₂]45
4.	N-methyl-2-pyrrole selenosemicarbazone (N-MeHPyesc, H⁴L)		[Cu(N-mepysesesc) ₂]46
5.	3-methyl-2-oxindole selenosemicarbazone (3-MeHOxsesc, H⁵L)		[Cu(3-meoxsesc) ₂]47
6.	2-oxindole selenosemicarbazone (2-HOxsesc, H⁶L)		[Cu(2-oxsesc) ₂]48
7.	6-chloro-2-oxindole selenosemicarbazone (6-ClHOxsesc, H⁷L)		[Cu(6-cloxsesc) ₂]49
8.	5-chloro isatin selenosemicarbazone (5-ClHIsesc, H⁸L)		[Cu(5-clistsesc) ₂]50
9.	1-methyl isatin selenosemicarbazone (1-MeHIsesc, H⁹L)		[Cu(1-meistsesc) ₂]51
10.	indole-3-selenosemicarbazone (3-HIndsesc, H¹⁰L)		[Cu(3-insesc) ₂]52

11.	3-acetyl indole selenosemicarbazone (3-AcHIndsesc, H¹¹L)		[Cu(3-acinsesc) ₂]53
12.	9-anthrinaldehyde selenosemicarbazone (9-HAnsesc, H¹²L)		[Cu(9-ansesc) ₂]54
13.	1-Naphthaldehyde selenosemicarbazone (1-HNapsesc, H¹³L)		[Cu(1-naphsesc) ₂]55
14.	2-Naphthaldehyde selenosemicarbazone (2-HNapsesc, H¹⁴L)		[Cu(2-naphsesc) ₂]56

8.2 IR Spectroscopy:

Important IR peaks of selenosemicarbazones are given in table 8.2 and IR spectra are given in figures 8.2.1- 8.2.14. The $\nu(\text{NH})$ band due to amino group in free ligands appeared in the range 3417-3223 cm^{-1} (**H¹L-H¹⁴L**). On complexation with copper(II) these bands showed slight shift to higher energy and appear in the range 3481-3204 cm^{-1} .

The amide band $\nu(-\text{NH}-)$ in free ligands appeared in the range 3157-3110 cm^{-1} (**H¹L-H¹⁴L**). In ligands **H⁵L-H¹¹L**, amide band gets observed by stretching of -NH- group present in heterocyclic rings. In complexes, absence of this band indicates deprotonation and co-ordination of ligand to metal in anionic form. The C=Se band in the ligands appeared in the range 898-854 cm^{-1} . On complexation this band shifted to low energy and

appeared in the range 765-717 cm⁻¹. The lower energy shift indicates the appearance of C=Se to C-Se⁻ thus suggests binding of ligand in selenate form.

Other IR peaks like $\nu(C=N)$, $\nu(C=C)$ and $\delta(NH_2)$ appeared in the range 1647-1406 cm⁻¹ in complexes and showed no significant change vis-à-vis free ligands.

Table 8.2 Important IR peaks of selenosemicarbazones ($H^1L-H^{14}L$) and copper(II) complexes (43-56)

Synthesised Ligands and Metal Complexes	$\nu(NH_2)$	$\nu(-NH-)$	$\nu(C=N), \nu(C=C), \delta(NH_2)$	$\nu(C=Se)$
Cyclohexanone Selenosemicarbazone	3362m, 3225m	3157w	1591s, 1489m, 1454s	856s
[Cu(cysesc) ₂]43	3274m	-	1647s, 1547m, 1413s	717s
2-furfural selenosemicarbazone	3379m, 3340m	3142w	1600s, 1579m, 1464s	812s
[Cu(2-fursesc) ₂]44	3333m	-	1648s, 1546m, 1461s	736s
2-thiophene selenosemicarbazone	3389m, 3221m	3095w	1599s, 1527m, 1415s	844s
[Cu(2-thiosesc) ₂]45	3361m	-	1606s, 1548m, 1418s	717s
N-methyl-2-pyrrole selenosemicarbazone	3412m, 3223m	3110w	1633s, 1562m, 1496s	854s
[Cu(N-mepysesc) ₂]46	3215m	-	1619s, 1542m, 1464s	721s
3-methyl-2-oxindole selenosemicarbazone	3358m, 3248m	3157w	1591s, 1489m, 1425s	854s
[Cu(3-meoxsesc) ₂]47	3373m	-	1608s, 1527m, 1421s	754s
2-oxindole selenosemicarbazone	3362m, 3225m	3157w	1591s, 1489m, 1454s	856s
[Cu(2-oxsesc) ₂]48	3342m	-	1547s, 1489m, 1413s	730s

6-chloro-2-oxindole selenosemicarbazone	3417m, 3255m	3142w	1589s, 1512m, 1499s	879s
[Cu(6-cloxsesc) ₂] 49	3453m	-	1610s, 1483m, 1435s	723s
5-chloroisatin selenosemicarbazone	3219m	3110w	1694s, 1618s, 1559m, 1447s	885s
[Cu(5-clistsesc) ₂] 50	3249m	-	1694s, 1617s, 1470m, 1443s	742s
1-methylisatin selenosemicarbazone	3408m, 3228m	3128w	1676s, 1604s, 1492m, 1415s	889s
[Cu(1-meistsesc) ₂] 51	3440m	-	1695s, 1607m, 1465s	749s
3-indole selenosemicarbazone	3356m, 3246m	3153w	1591s, 1487m, 1450s	898s
[Cu(3-indsesc) ₂] 52	3452m	-	1602s, 1546s, 1417s	759s
3-acetylindole selenosemicarbazone	3290m	3142w	1624s, 1502m, 1406s	877s
[Cu(3-acindsesc) ₂] 53	3204m	-	1609s, 1572m, 1430s	748s
9-anthracene selenosemicarbazone	3385m, 3248m	3151w	1639s, 1518m, 1402s	887s
[Cu(9-anthrasesc) ₂] 54	3481m, 3362m	-	1569s, 1499m, 1406s	732s
1-naphthaldehyde selenosemicarbazone	3400m	3147w	1599s, 1516m, 1452s	871s
[Cu(1-naphthsesc) ₂] 55	3331m	-	1614s, 1543m, 1406s	765s
2-naphthaldehyde selenosemicarbazone	3352m	3124w	1597s, 1533m, 1446s	856s
[Cu(2-naphthsesc) ₂] 56	3218m	-	1607s, 1546m, 1406s	758s

8.3 ESR Spectroscopy:

ESR spectroscopy is widely used to determine the electronic structure of paramagnetic metals like copper(II) (one unpaired electron). Magnetic energy of unpaired electrons in copper(II) depend upon two factors: 1) The Zeeman effect: energy changes due to unpaired electron spin with the applied magnetic field B_0 . 2) Hyperfine coupling (hfc): resulted from interaction between electron spin and nuclear spin. The energy changes can be collectively expressed by spin Hamiltonian, H :

$$H = \beta e S \cdot g \cdot B_0 + h S \cdot A \cdot I \quad (1)$$

Where g = the electronic g -tensor

βe = electron Bohr magneton

S = electron spin operator

A = hfc tensor

h = Planck's constant

I = nuclear spin operator (3/2 for ^{63}Cu)

A powder Patten ESR spectra is obtained for solid samples such as polycrystalline samples, powder or frozen solution, molecular motions are restricted, and the complexes are oriented in random directions with respect to the applied magnetic field

Symmetry of the ligand field reflects from the shape of spectra. The g value is generally written as g_x , g_y and g_z according to the direction of the direction of the g tensor. In case of symmetric ligand field (isotropic), a single line is obtained where, $g_x = g_y = g_z$ indicating a cubic symmetry coordination environment. In case of axial symmetry, $g_x = g_y \neq g_z$ indicates a tetragonal field and possible geometries can be elongated octahedral, square pyramidal or square planar. In case of asymmetric field, $g_x \neq g_y \neq g_z$ indicates rhombic. The various parameters like crystal-field splitting, covalency, and electron delocalization can be determined through g value.

The ESR spectra of copper(II) complexes **43-56** in polycrystalline state was taken at RT. The ESR parameters are given in table 8.3.1 and 8.3.2. The ESR spectra of complexes **43-56** are given in Figures 8.3.1- 8.3.14. The two well-defined g values i.e. g_{\parallel} and g_{\perp} in these complexes (except 53), represents axially symmetrical system. In these complexes g value follows the trend, $g_{\parallel} > g_{\perp} > g_e$ suggesting the $d_{x^2-y^2}$ ground term in square planar geometry [171]. The ESR spectrum of complex **53** gave three g values (g_1 , 2.095; g_2 , 2.15; g_3 , 2.26) indicate rhombic distortion in its geometry. In a polycrystalline material, exchange interaction

between copper centers can be measured in terms of geometric parameter, G . The geometric parameter for axial spectra and rhombic spectra can be calculated by using equation 2 and 3 respectively.

$$G_{(\text{axial})} = g_{\parallel} - 2.0023 / g_{\perp} - 2.0023 \quad (2)$$

$$G_{(\text{rhombic})} = g_3 - 2.0023 / g_{\perp} - 2.0023, \quad \text{where } g_{\perp} = g_1 + g_2 / 2 \quad (3)$$

According to Hathaway and Tomlinson, G value greater than 4 indicates parallel alignment of tetragonal axes with very less misalignment. In this condition, the exchange interactions will be negligible. If the G value is less than 4, significant exchange interactions are present with considerable misalignment [172, 173]. In complexes **43, 45, 46, 49, 51, 52, 53** and **54, 55** the value of geometric parameters is less than 4 hence a significant exchange interaction, whereas no exchange interactions are observed in complexes **44, 47, 48, 50** and **56** ($G > 4$). The empirical factor $f = g_{\parallel}/A_{\parallel}$ (cm^{-1}) can be used to identify the geometry of complexes and extend of distortion [174-176]. In square planar complexes, reported range of empirical factor is 105-135 cm. For tetrahedral complexes the range is 150-250 cm. The value of f for complexes **43, 45-47, 49-54** and **56** lies in the range, 102-135 cm indicating a square planar geometry with small distortion, whereas as in complex **44, 53** and **55** value ($f = 182 \text{ cm}, 146 \text{ cm}$ and 153 cm) is close to tetrahedral geometry with larger distortion. The isotropic value of g factor and hyperfine coupling constant can be calculated using equation 3 and 4 respectively [177]. The isotropic value of g factor and hyperfine coupling constant can be calculated using equation 3 and 4 respectively.

$$g_{\text{iso}} = g_{\parallel} + 2g_{\perp}/3 \quad (3)$$

$$A_{\text{iso}} = A_{\parallel} + 2A_{\perp}/3 \quad (4)$$

Equation 5 indicates relationship of isotropic g factor and isotropic hyperfine coupling constant with σ -bonding parameter [178].

$$\alpha^2 = \frac{A_{\text{iso}}}{PK} + \frac{g_{\text{iso}} - 2.0023}{K} \quad (5)$$

Where P is free ion dipole term ($P = 0.036 \text{ cm}^{-1}$) and K is Fermi contact ($K = 0.43$) [171]. The value of $\alpha^2 = 1$ supports pure ionic bonding and that of 0.5 to pure covalent bonding. The values of α^2 in complexes **43-46, 48, 50-56** ranges from 0.500-0.787 indicating a mixed ionic-covalent bonding.

Table 8.3.1 ESR parameters of complexes **43-56** at RT

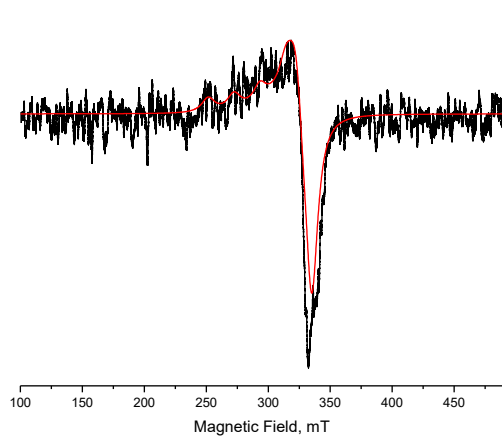
Compound	Polycrystalline state (at RT)	g_{\perp}	g_{\parallel}	g_{iso}	${}^*A_{\parallel}$	${}^*A_{\perp}$	${}^*A_{iso}$
[Cu(cysesc) ₂] 43	2.24 / 2.07 ($g_{\parallel} / g_{\perp}$)	2.07	2.24	2.126	180	20	73.3
[Cu(2-fursesc) ₂] 44	2.28 / 2.07 ($g_{\parallel} / g_{\perp}$)	2.07	2.28	2.14	125	15	88.3
[Cu(2-thiosesc) ₂] 45	2.19 / 2.07 ($g_{\parallel} / g_{\perp}$)	2.07	2.19	2.11	210	20	147
[Cu(N-mepysesc) ₂] 46	2.30 / 2.07 ($g_{\parallel} / g_{\perp}$)	2.08	2.30	2.15	110	20	80
[Cu(3-meoxsesc) ₂] 47	2.25 / 2.02 ($g_{\parallel} / g_{\perp}$)	2.02	2.25	2.08	160	20	113
[Cu(2-oxsesc) ₂] 48	2.31 / 2.05 ($g_{\parallel} / g_{\perp}$)	2.05	2.31	2.13	150	30	110
[Cu(6-cloxsesc) ₂] 49	2.21 / 2.0 ($g_{\parallel} / g_{\perp}$)	2.0	2.21	2.07	210	20	147
[Cu(5-clistsesc) ₂] 50	2.24 / 2.05 ($g_{\parallel} / g_{\perp}$)	2.05	2.24	2.113	165	20	68.3
[Cu(1-meistsesc) ₂] 51	2.19 / 2.075 ($g_{\parallel} / g_{\perp}$)	2.075	2.19	2.113	202	20	80.6
[Cu(3-insesc) ₂] 52	2.24 / 2.13 ($g_{\parallel} / g_{\perp}$)	2.13	2.24	2.166	220	35	96.6
[Cu(3-acinsesc) ₂] 53	2.26 / 2.15 / 2.04 ($g_3/g_2/g_1$)	2.095	2.26	2.15	155	35	75.0
[Cu(9-ansesc) ₂] 54	2.24 / 2.07 ($g_{\parallel} / g_{\perp}$)	2.07	2.24	2.12	250	20	175
[Cu(1-naphsesc) ₂] 55	2.24 / 2.07 ($g_{\parallel} / g_{\perp}$)	2.08	2.3	2.15	145	15	102
[Cu(2-naphsesc) ₂] 56	2.23 / 2.04 ($g_{\parallel} / g_{\perp}$)	2.04	2.23	2.103	170	20	70.0

* Expressed in units of cm^{-1} multiplied by a factor of 10^{-4}

Table 8.3.2 ESR bonding parameters for complexes **43-56**

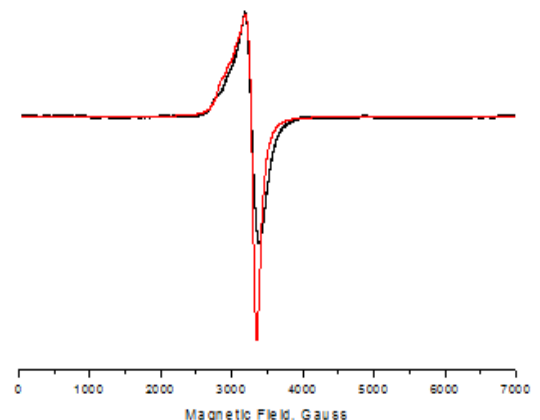
Compound	G (at RT)	α^2	f ^a
[Cu(cysesc) ₂]43	3.51	0.761	124
[Cu(2-fursesesc) ₂]44	4.08	0.468≈0.5	182
[Cu(2-thiosesc) ₂]45	2.58	0.487≈0.5	109
[Cu(N-mepysesc) ₂]46	3.83	0.487≈0.5	115
[Cu(3-meoxsesc) ₂]47	8.94	0.369≈0.4	112
[Cu(2-oxsesc) ₂]48	6.45	0.496≈0.5	77
[Cu(6-cloxsesc) ₂]49	1.7	0.394≈0.4	110
[Cu(5-clistsesc) ₂]50	4.98	0.698	135
[Cu(1-meistsesc) ₂]51	2.58	0.776	108
[Cu(3-insesc) ₂]52	1.86	0.787	102
[Cu(3-acinsesc) ₂]53	2.78	0.634	146
[Cu(9-anseesc) ₂]54	3.51	0.547	112
[Cu(1-naphsesc) ₂]55	3.83	0.510	153
[Cu(2-naphsesc) ₂]56	6.04	0.555	131

^a Expressed in units of (cm)



(43)

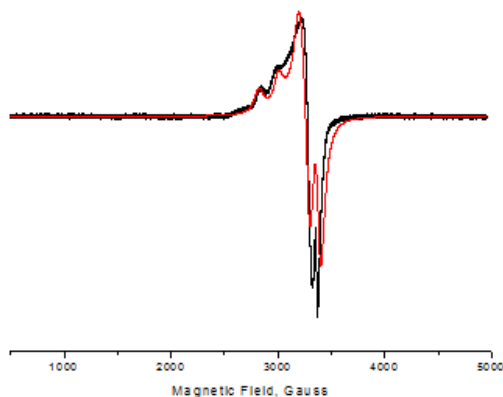
Experimental (black) and simulated (red) best fit ESR spectrum of complex 43



(44)

Figure 8.3.2

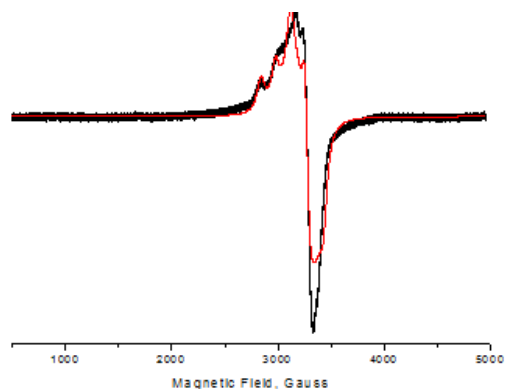
Experimental (black) and simulated (red) best fit ESR spectrum of complex 44



(45)

Figure 8.3.3

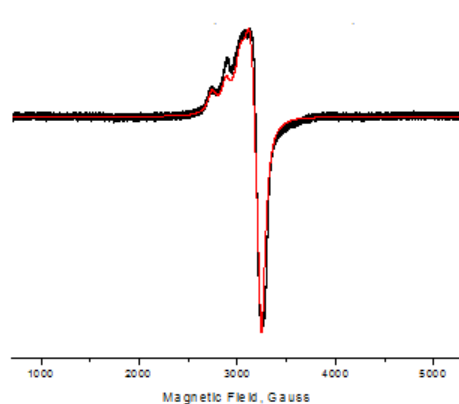
Experimental (black) and simulated (red) best fit ESR spectrum of complex 45



(46)

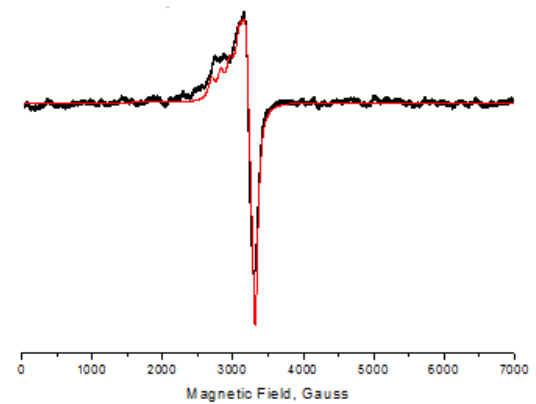
Figure 8.3.4

Experimental (black) and simulated (red) best fit ESR spectrum of complex 46



(47)

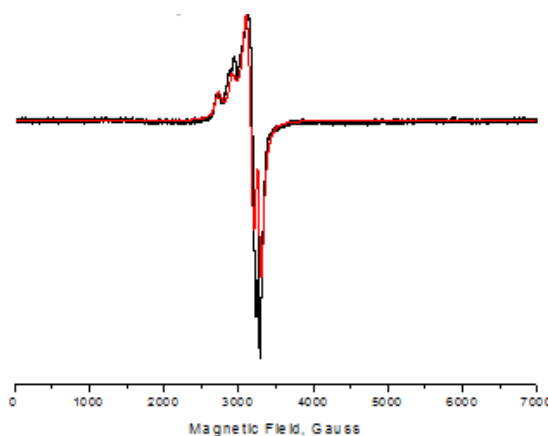
Figure 8.3.5
Experimental (black) and simulated (red)
spectrume of complex 47



(48)

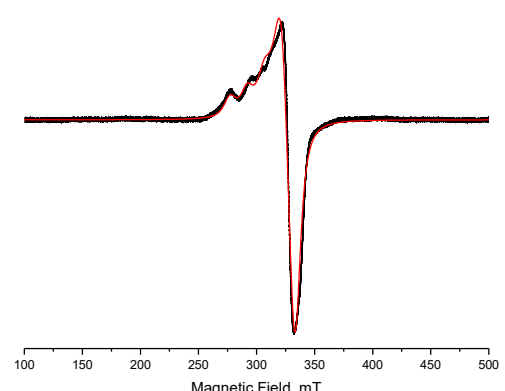
Figure 8.3.6

Experimental (black) and simulated (red)
best fit ESR spectrum of complex 48



(49)

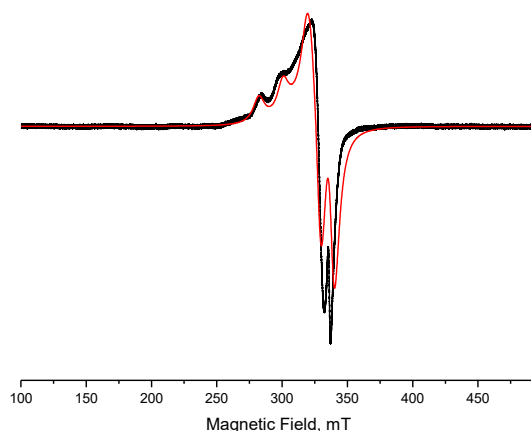
Figure 8.3.7
Experimental (black) and simulated (red)
spectrume of complex 49



(50)

Figure 8.3.8

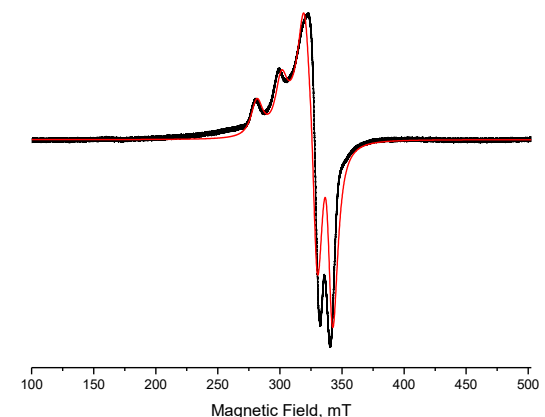
Experimental (black) and simulated (red)
best fit ESR spectrum of complex 50



(51)

Figure 8.3.9

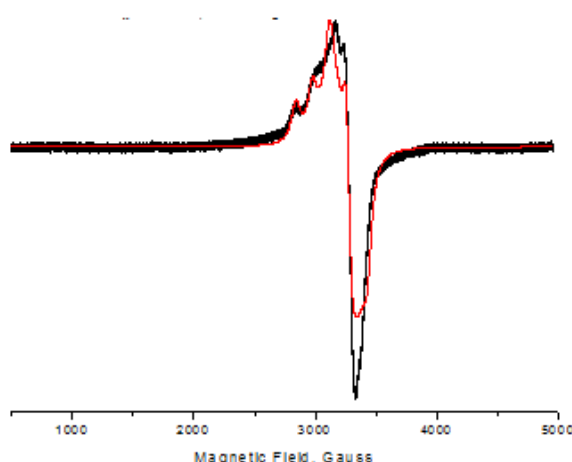
Experimental (black) and simulated (red) best fit ESR spectrum of complex **51**



(52)

Figure 8.3.10

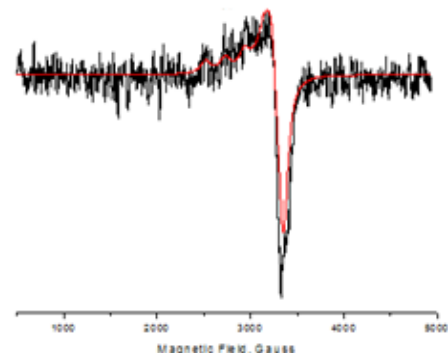
Experimental (black) and simulated (red) best fit ESR spectrum of complex **52**



(53)

Figure 8.3.11

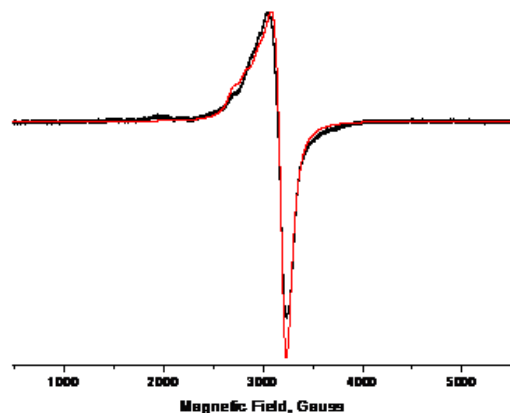
Experimental (black) and simulated (red) best fit ESR spectrum of complex **53**



(54)

Figure 8.3.12

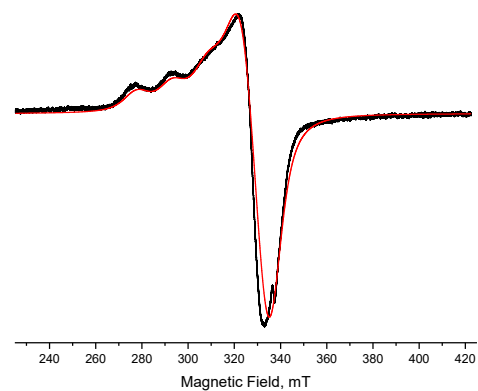
Experimental (black) and simulated (red) best fit ESR spectrum of complex **54**



(55)

Figure 8.3.13

Experimental (black) and simulated (red) best fit ESR spectrum of complex **55**



(56)

Figure 8.3.14

Experimental (black) and simulated (red) best fit ESR spectrum of complex **56**

8.4 Mass Spectrometry:

Mass spectra of few complexes **43, 50-53 and 56**, has also been recorded and are given in figures 8.4.1- 8.4.6. The observed molecular ion peak $[M]^+$ are given in table 8.4. From the table it is clear that m/z values for complexes **43, 50-53 and 41**, are close to their proposed stoichiometry $[Cu(L)_2]$ and thus confirmed the co-ordination of copper(II) with selenosemicarbazones.

Table 8.4 m/z values (amu) of complexes **29-42** obtained from Mass Spectra

Complex No.	Parent peak obtained from mass spectra	Expected formula for parent ion (m/z) ⁺
43	496 amu	$[Cu(C_7H_{11}N_3Se)_2]$
50	666 amu	$[Cu(C_9H_8N_4OClSe)_2]$
51	624 amu	$[Cu(C_{10}H_{10}N_4OSe)_2]$
52	594 amu	$[Cu(C_{10}H_{11}N_4Se)_2]$
53	617 amu	$[Cu(C_{11}H_{11}N_4Se)_2]$
56	612 amu	$[Cu(C_{12}H_{10}N_3Se)_2]$

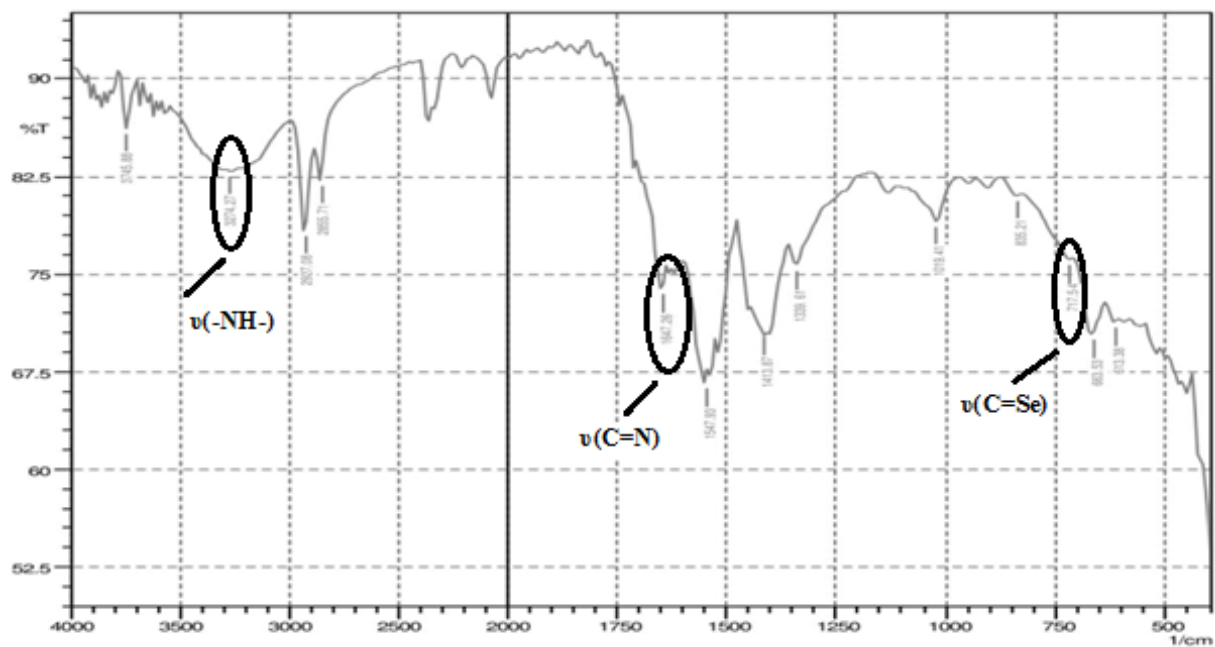


Figure 8.2.1 IR spectrum of $[\text{Cu}(\text{cysesc})_2]43$

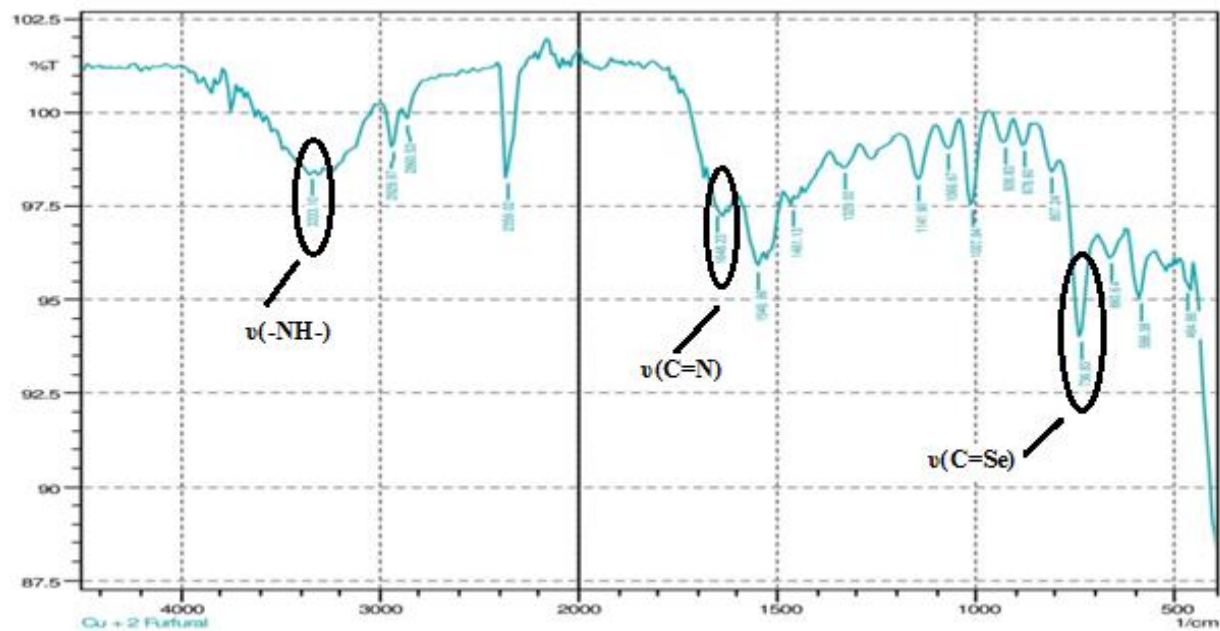


Figure 8.2.2 IR spectrum of $[\text{Cu}(2\text{-fursesc})_2]44$

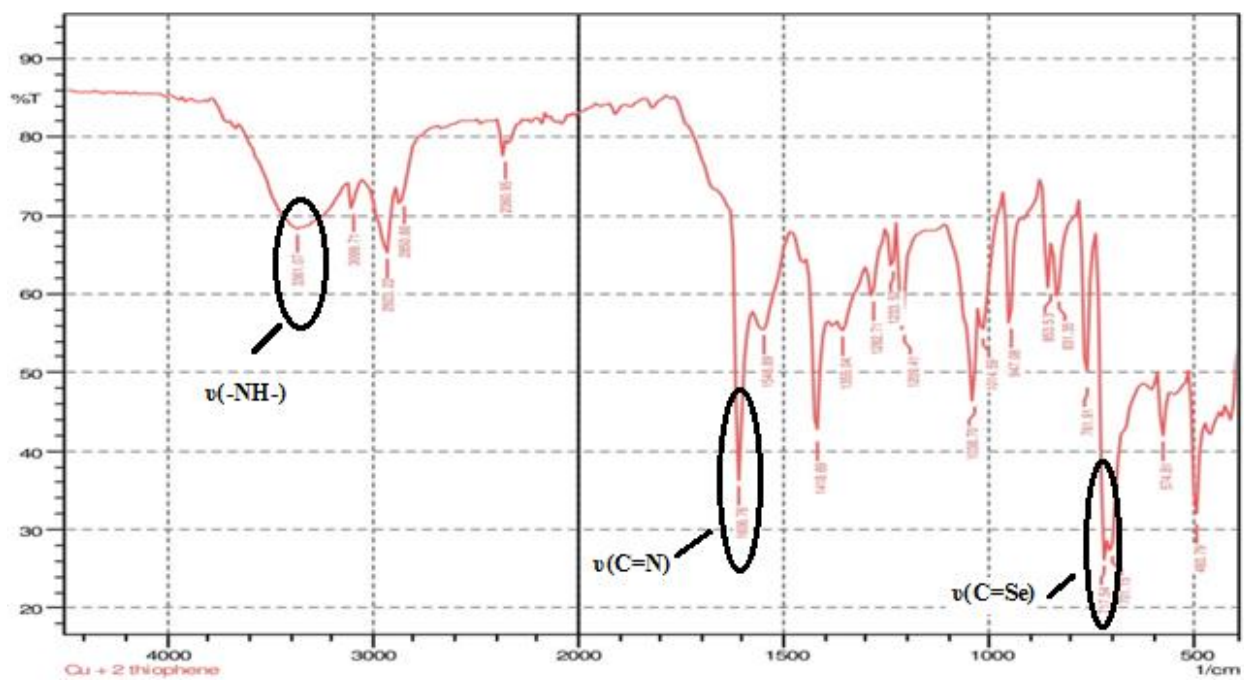


Figure 8.2.3 IR spectrum of $[\text{Cu}(2\text{-thiosesc})_2]45$

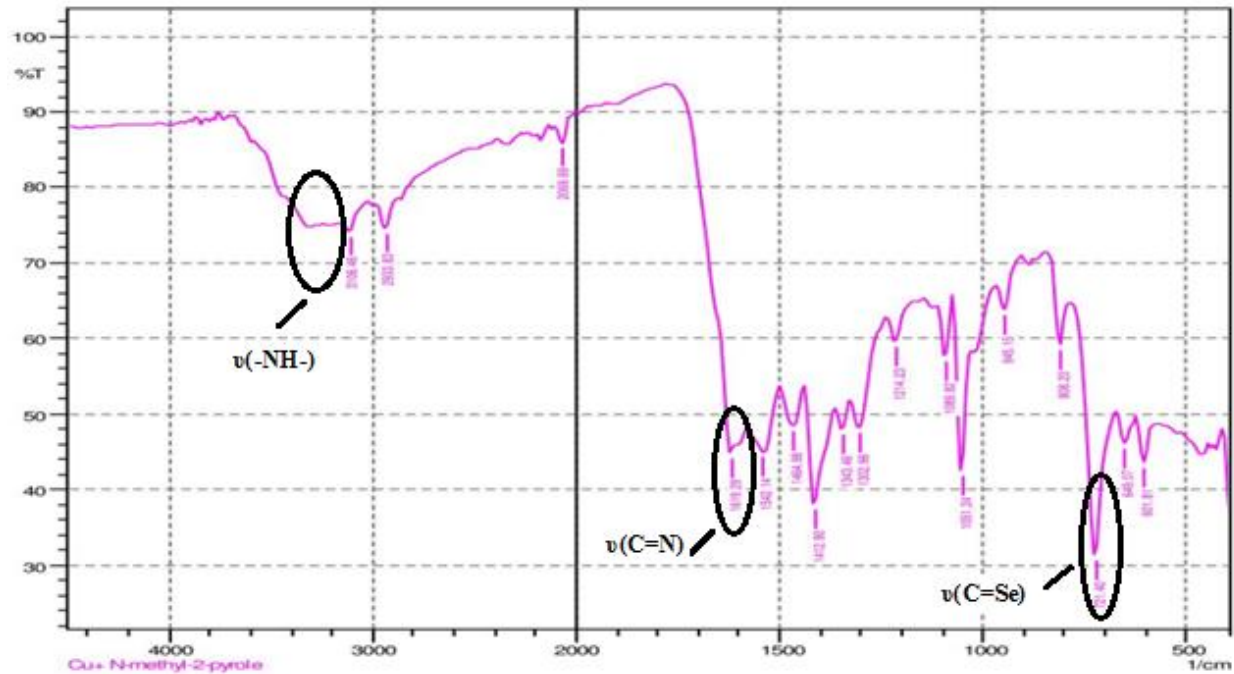


Figure 8.2.4 IR spectrum of $[\text{Cu}(\text{N-mepysesc})_2]46$

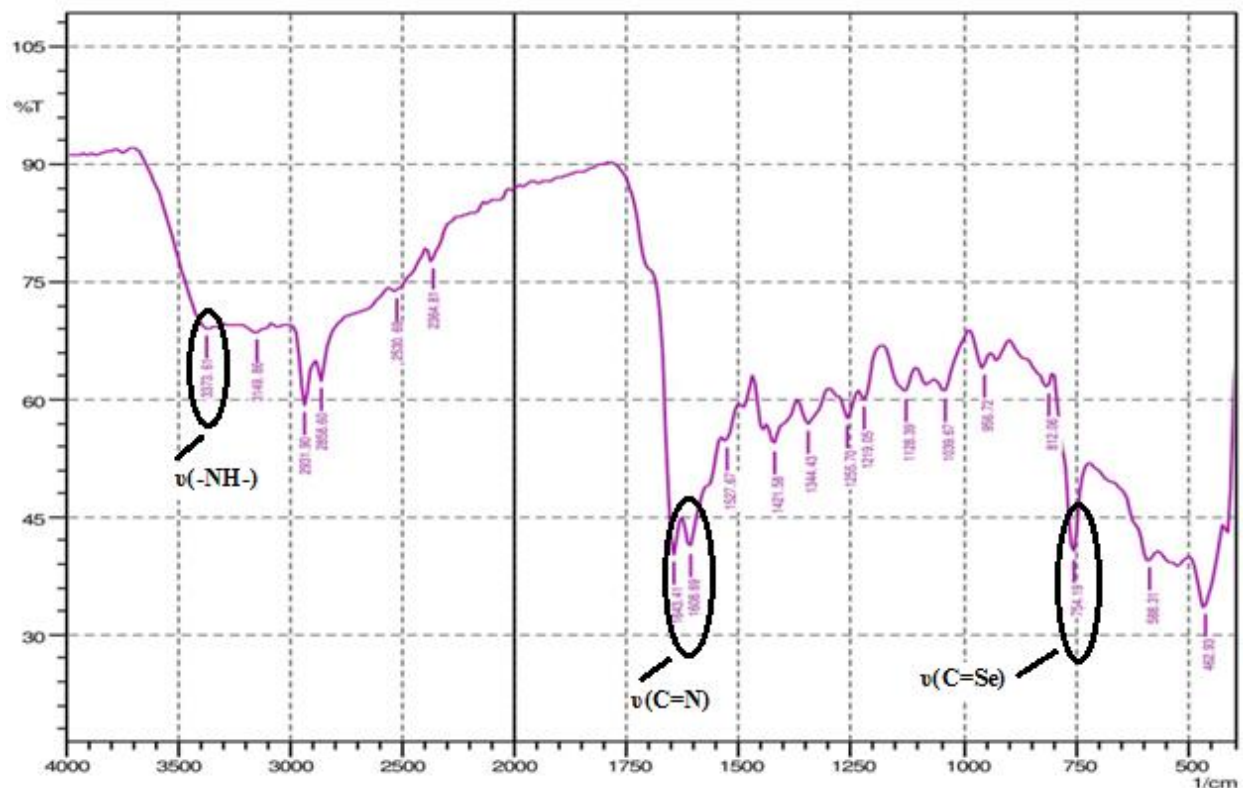


Figure 8.2.5 IR spectrum of $[\text{Cu}(3\text{-meoxsesc})_2]47$

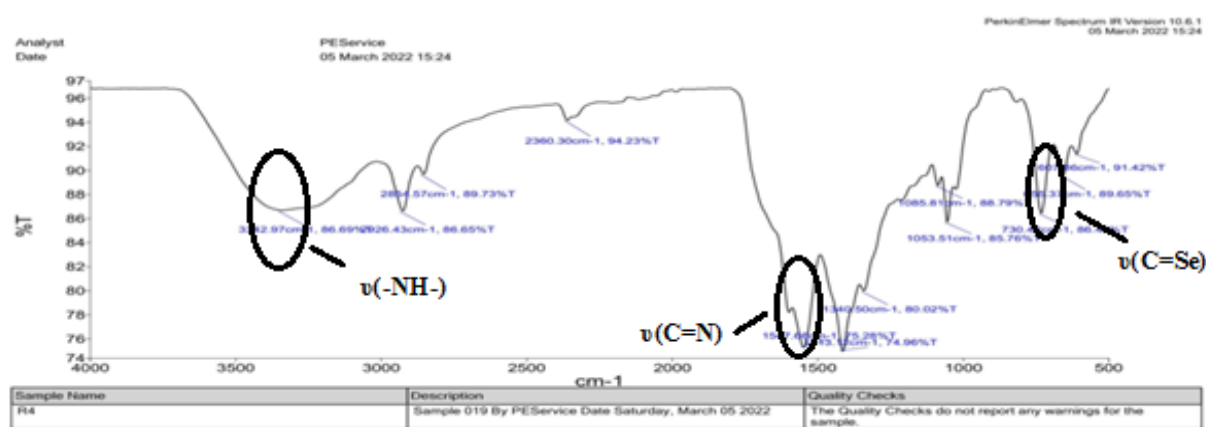


Figure 8.2.6 IR spectrum of $[\text{Cu}(2\text{-oxsesc})_2]48$

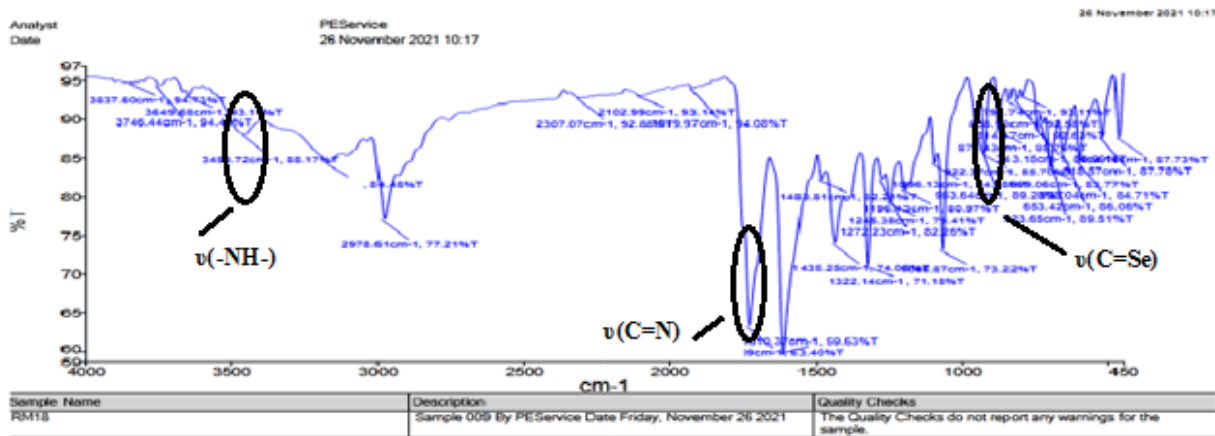


Figure 8.2.7 IR spectrum of $[\text{Cu}(6\text{-cloxsesc})_2]49$

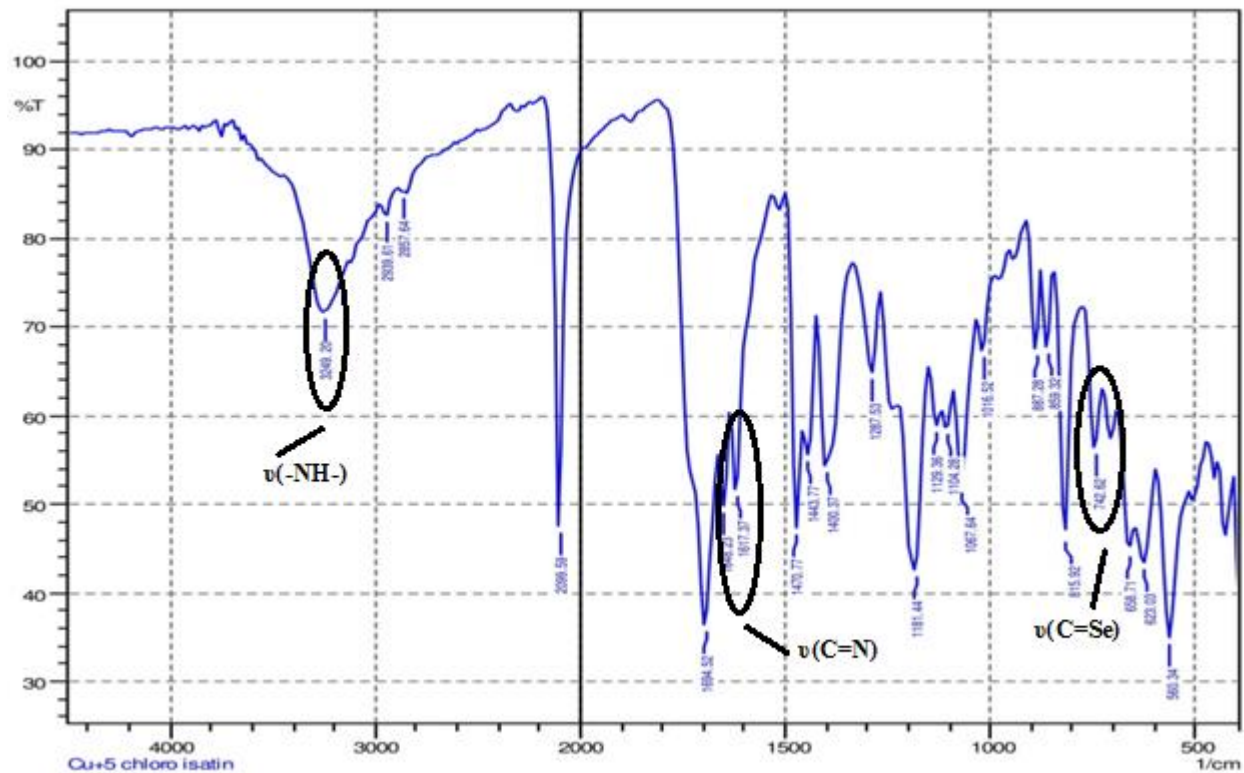


Figure 8.2.8 IR spectrum of $[\text{Cu}(5\text{-clistsesc})_2]50$

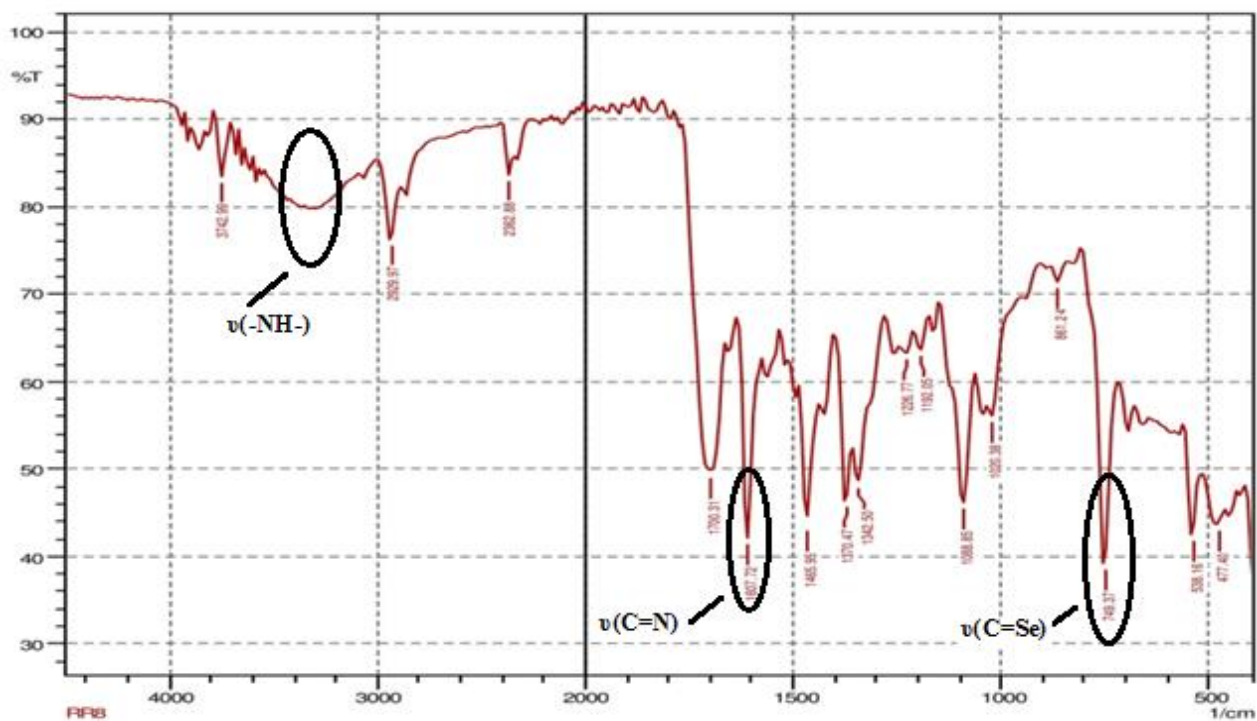


Figure 8.2.9 IR spectrum of $[\text{Cu}(1\text{-meistsesc})_2]\mathbf{51}$

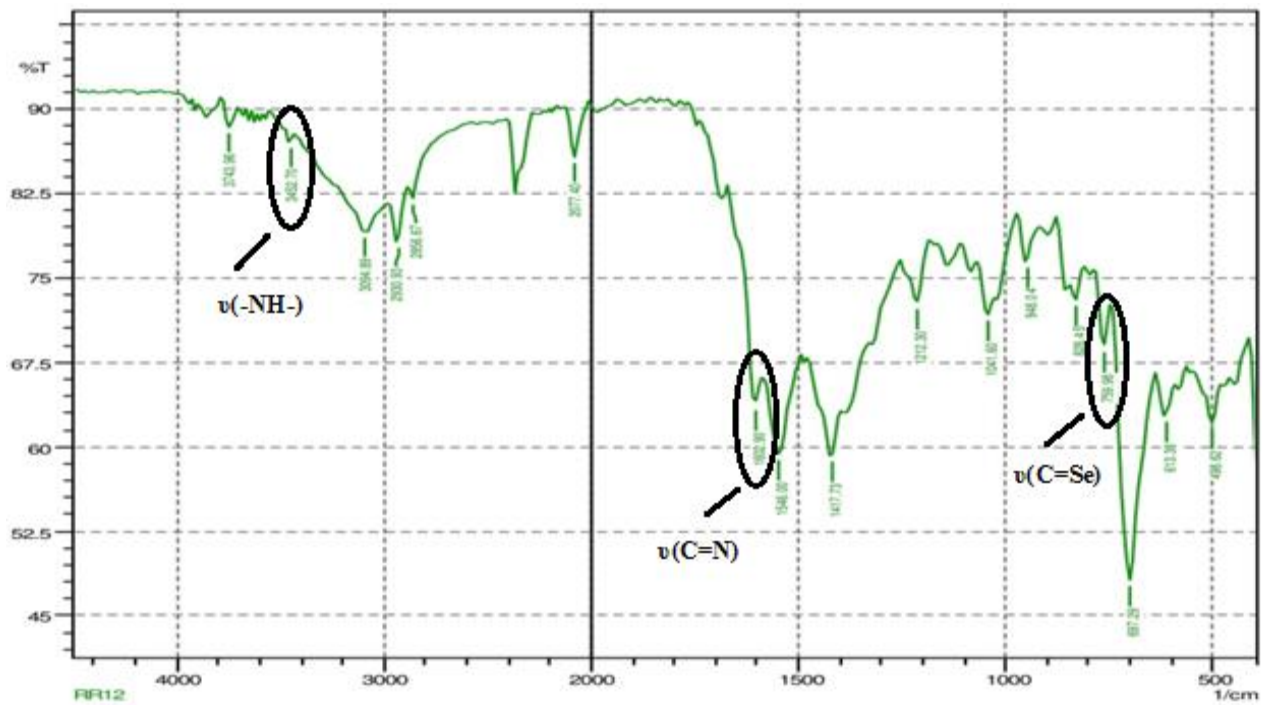


Figure 8.2.10 IR spectrum of $[\text{Cu}(3\text{-indsesc})_2]\mathbf{52}$

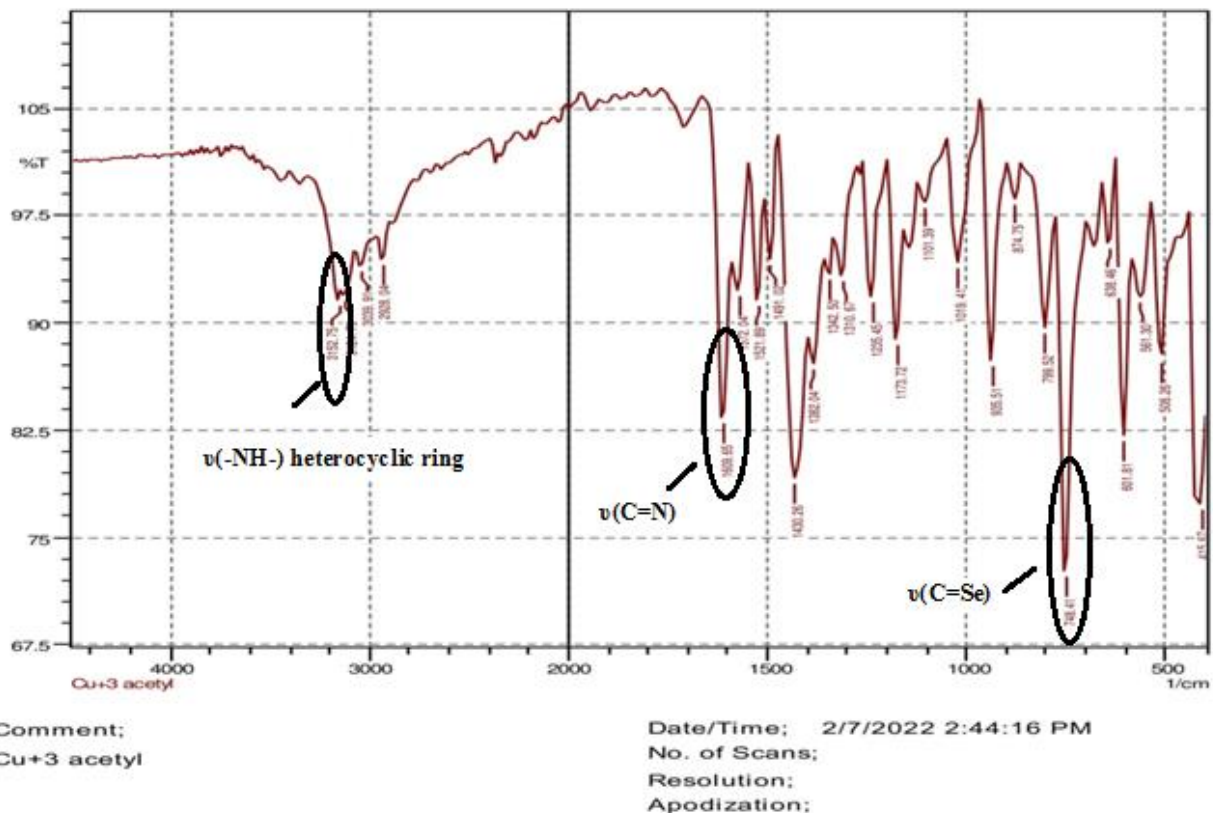


Figure 8.2.11 IR spectrum of $[\text{Cu}(3\text{-acindsesc})_2]53$

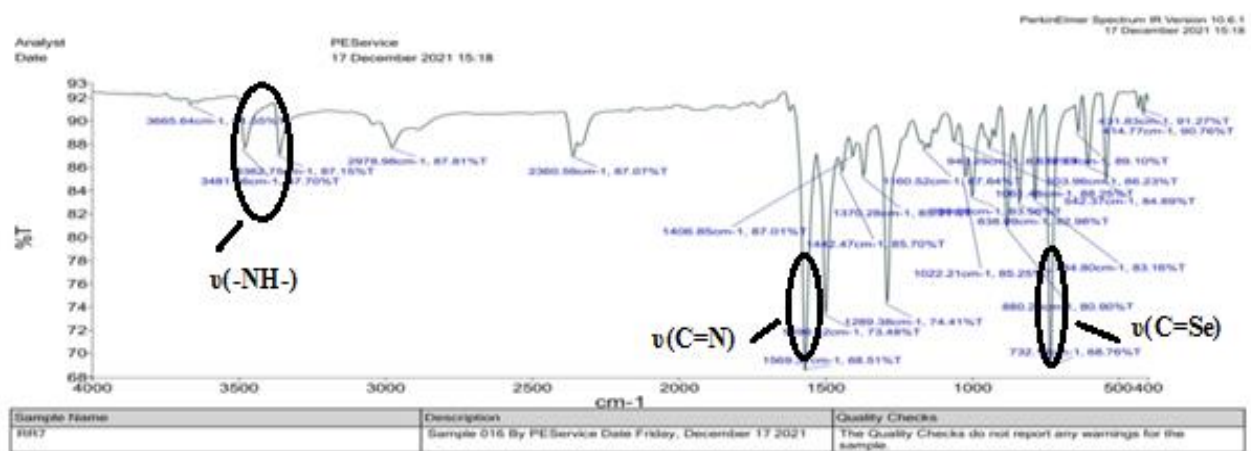


Figure 8.2.12 IR spectrum of $[\text{Cu}(9\text{-anthrasesc})_2]54$

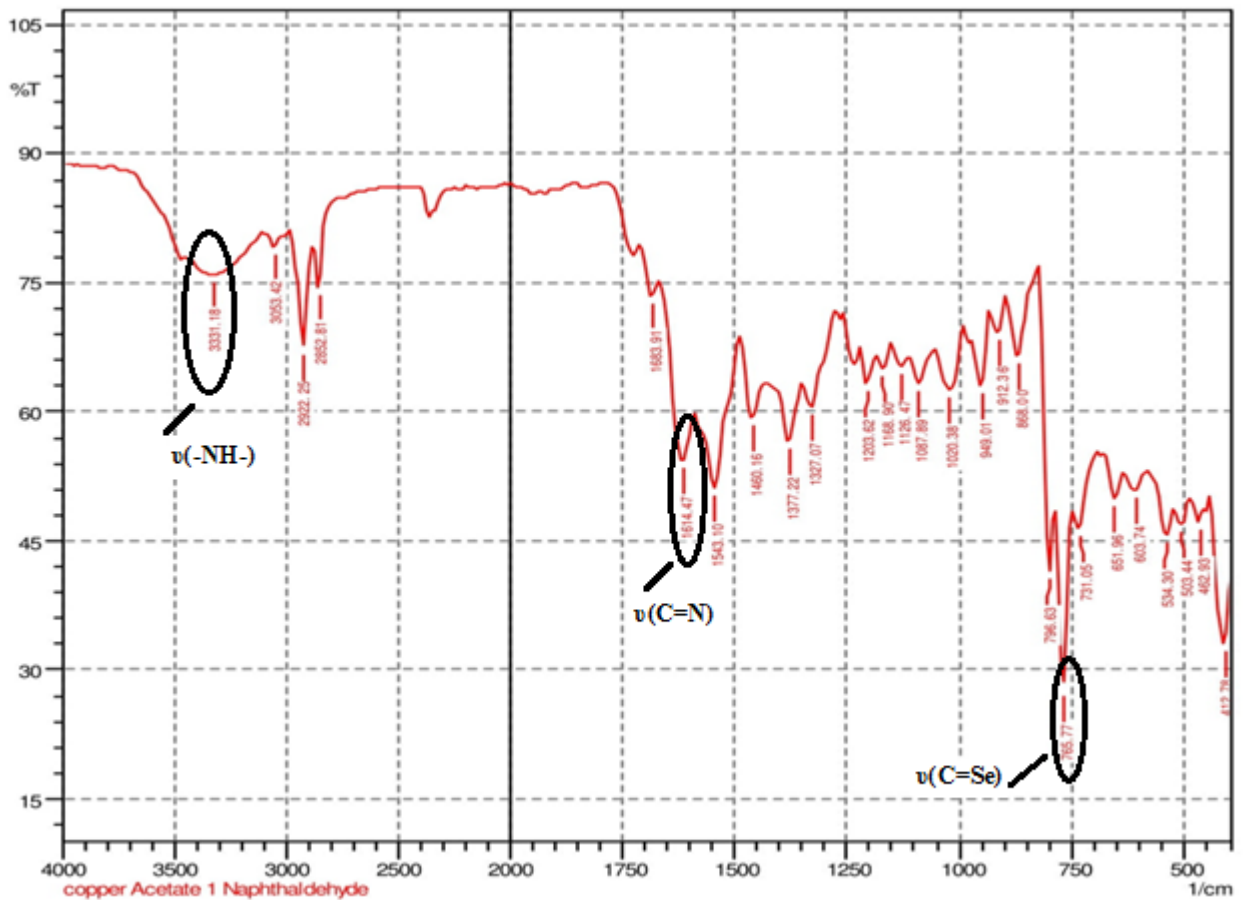


Figure 8.2.13 IR spectrum of $[\text{Cu}(1\text{-naphthsesc})_2]55$

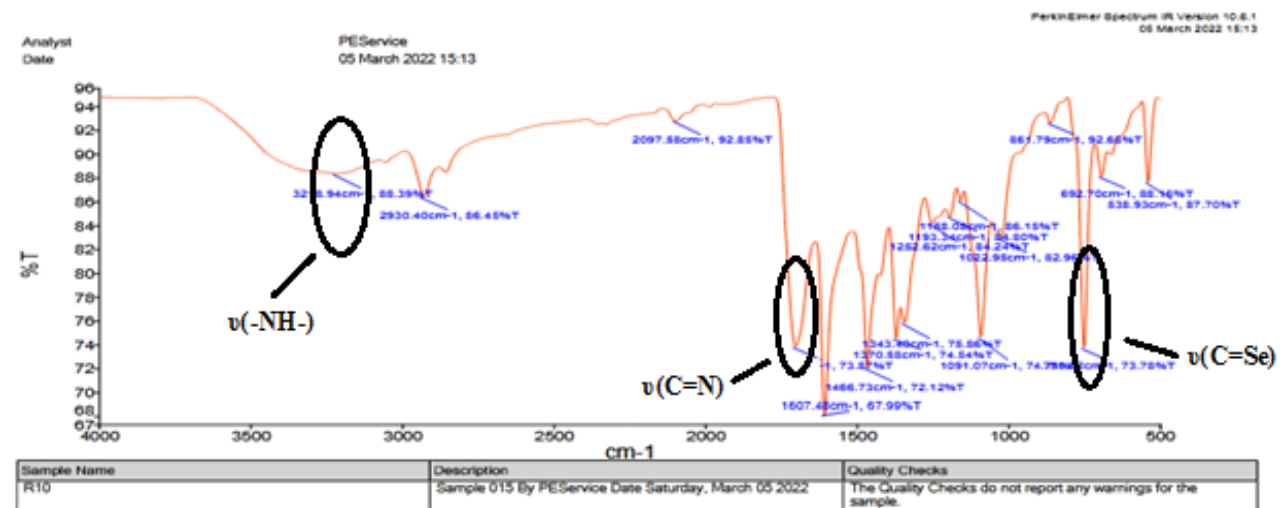


Figure 8.2.14 IR spectrum of $[\text{Cu}(2\text{-naphthsesc})_2]56$

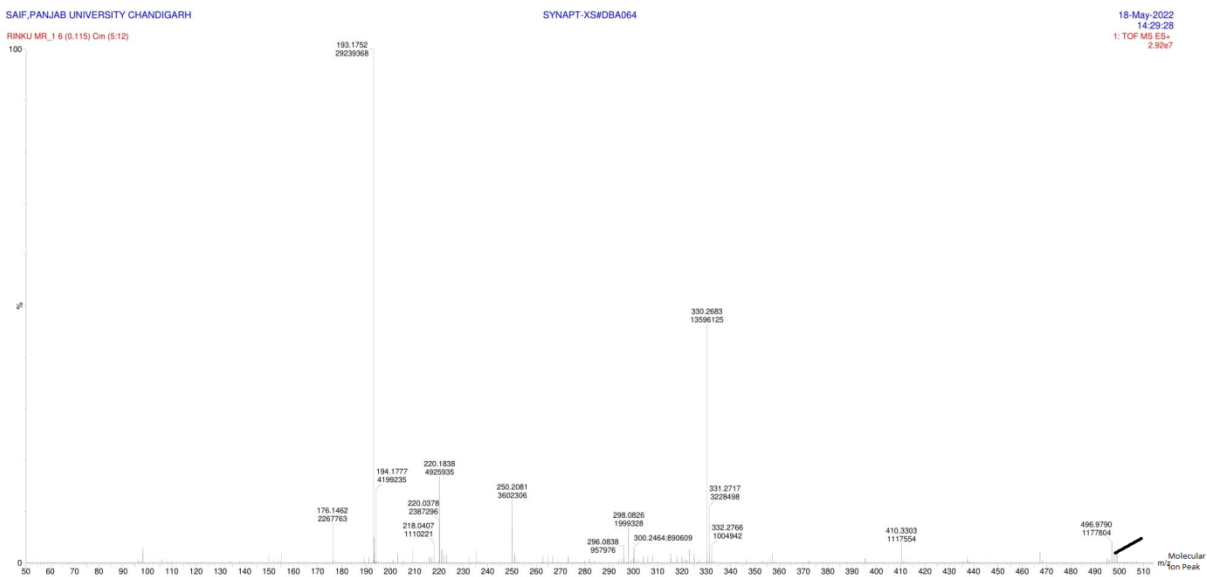


Figure 8.4.1 Mass Spectrum of $[\text{Cu}(\text{cysesc})_2]43$

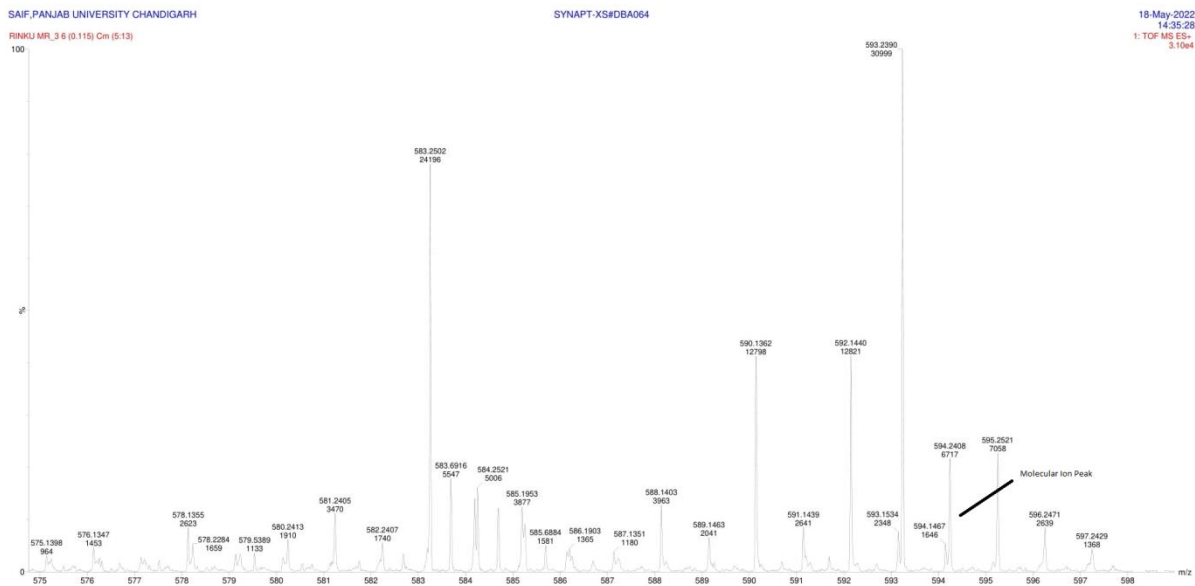


Figure 8.4.2 Mass Spectrum of $[\text{Cu}(5\text{-clistsesc})_2]50$

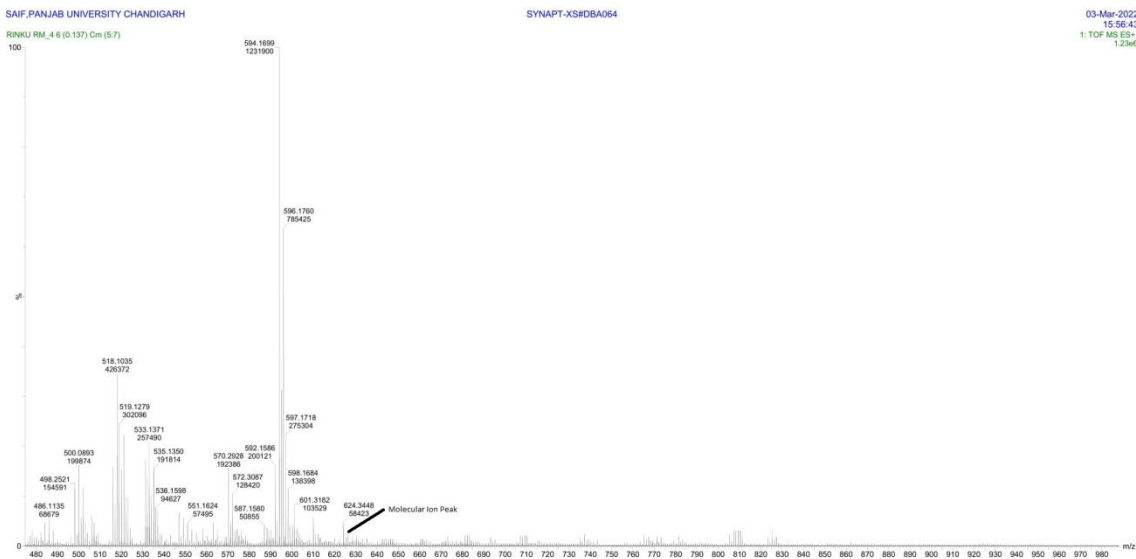


Figure 8.4.3 Mass Spectrum of $[\text{Cu}(1\text{-meistsesc})_2]51$

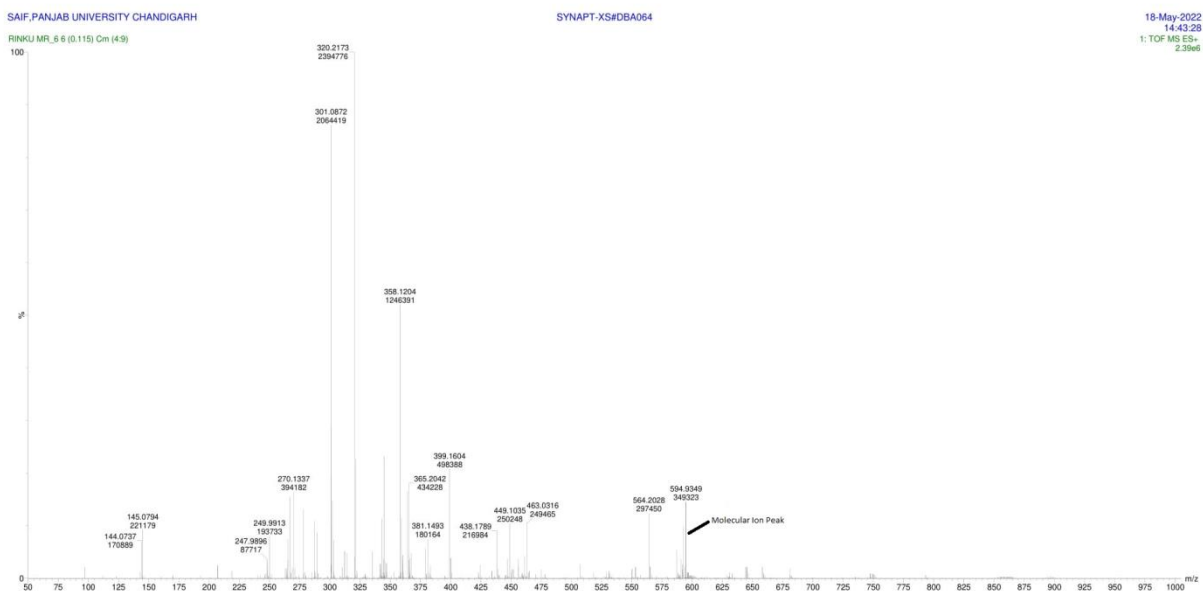


Figure 8.4.4 Mass Spectrum of $[\text{Cu}(3\text{indsesc})_2]52$

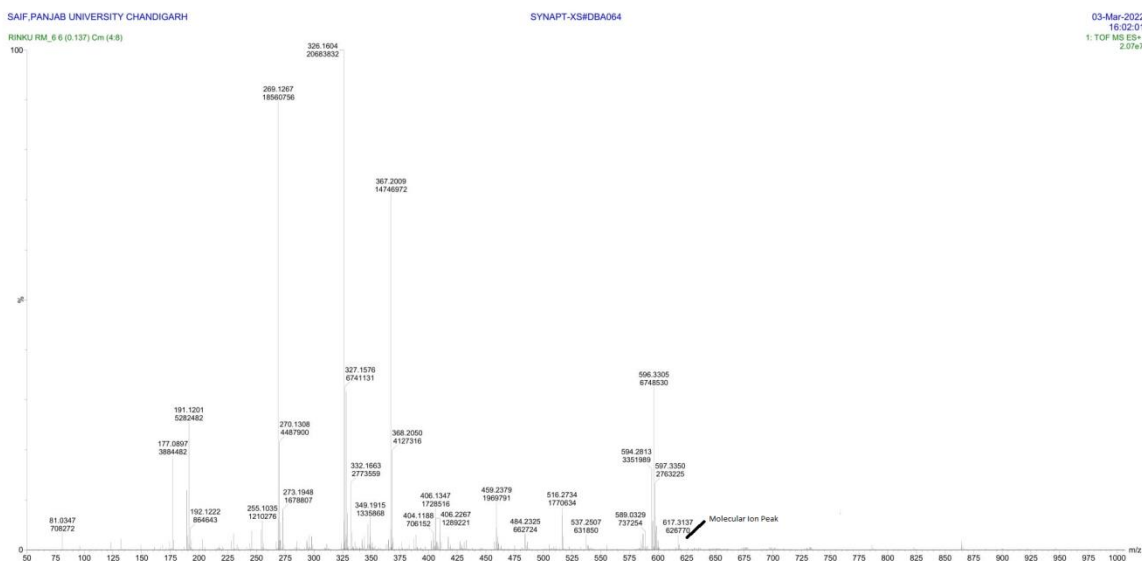


Figure 8.4.5 Mass Spectrum of $[\text{Cu}(3\text{-acindsesc})_2]53$

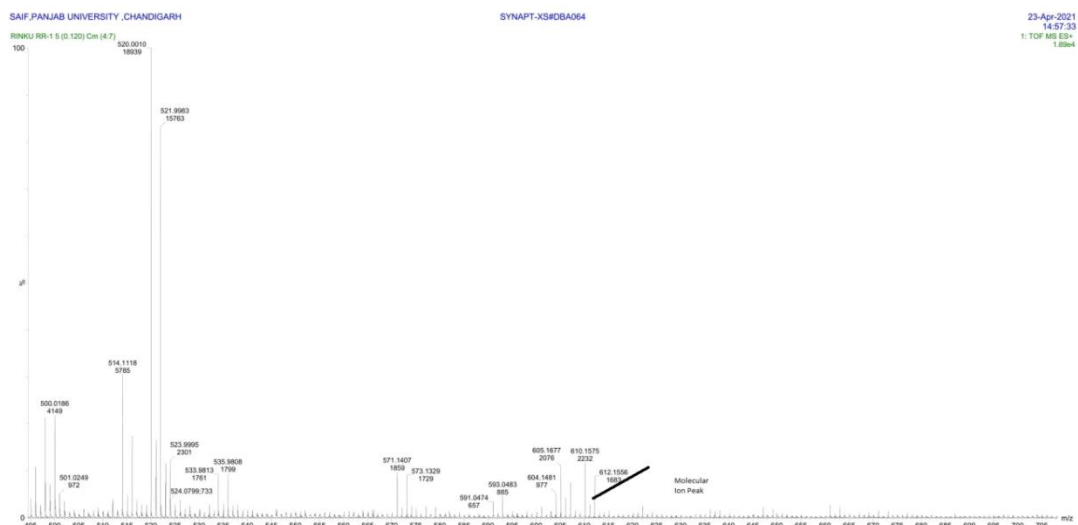


Figure 8.4.6 Mass Spectrum of $[\text{Cu}(2\text{-naphthsesc})_2]56$

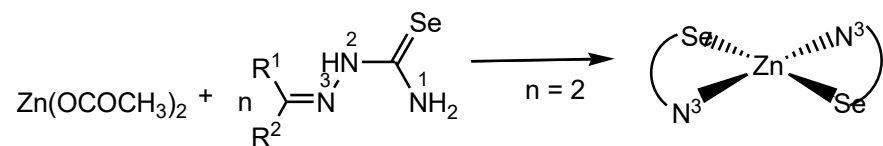
CHAPTER 9

ZINC(II) COMPLEXES

9. Complexes of Zinc(II)

9.1 Discussion on Synthesis of zinc metal complexes

Reaction of synthesized selenosemicarbazones ligands ($H^1L-H^{14}L$) with zinc acetate in 2: 1(L : M) molar ratio has formed complexes of stoichiometry, $[Zn(L)_2]$ ($L = ^1L \text{ } 57; ^2L \text{ } 58; ^3L \text{ } 59; ^4L \text{ } 60; ^5L \text{ } 61; ^6L \text{ } 62; ^7L \text{ } 63; ^8L \text{ } 64; ^9L \text{ } 65; ^{10}L \text{ } 66; ^{11}L \text{ } 67; ^{12}L \text{ } 68; ^{13}L \text{ } 69; ^{14}L \text{ } 70$) (Scheme 9.1)



Scheme 9.1

$[Zn(L)_2]$

$(L = ^1L \text{ } 57; ^2L \text{ } 58; ^3L \text{ } 59; ^4L \text{ } 60; ^5L \text{ } 61; ^6L \text{ } 62; ^7L \text{ } 63; ^8L \text{ } 64; ^9L \text{ } 65; ^{10}L \text{ } 66; ^{11}L \text{ } 67; ^{12}L \text{ } 68; ^{13}L \text{ } 69; ^{14}L \text{ } 70)$

All the synthesized complexes along with the structure of their respective selenosemicarbazones are given in Table 9.1

Table 9.1 list of selenosemicarbazone complexes of zinc(II) **57-70**

Sr. No.	Selenosemicarbazone Ligands	Structure of Selenosemicarbazone Ligands	Complexes Formed
1.	Cyclohexanone Selenosemicarbazone (Hcysesc, H¹L)		$[Zn(cysesc)_2] \text{ } 57$
2.	2-furfural selenosemicarbazone (2-Hfursesc, H²L)		$[Zn(2-fursesc)_2] \text{ } 58$
3.	2-thiophene selenosemicarbazone (2-Hthiosesc, H³L)		$[Zn(2-thiosesc)_2] \text{ } 59$

4.	N-methyl-2-pyrrole selenosemicarbazone (N-MeHPysesc, H⁴L)		[Zn(N-mepysesc) ₂]60
5.	3-methyl-2-oxindole selenosemicarbazone (3-MeHOxsesc, H⁵L)		[Zn(3-meoxsesc) ₂]61
6.	2-oxindole selenosemicarbazone (2-HOxsesc, H⁶L)		[Zn(2-oxsesc) ₂]62
7.	6-chloro-2-oxindole selenosemicarbazone (6-ClHOxsesc, H⁷L)		[Zn(6-cloxsesc) ₂]63
8.	5-chloro isatin selenosemicarbazone (5-ClHIstsesc, H⁸L)		[Zn(5-clistsesc) ₂]64
9.	1-methyl isatin selenosemicarbazone (1-MeHIstsesc, H⁹L)		[Zn(1-meistsesc) ₂]65
10.	indole-3-selenosemicarbazone (3-HIndsesc, H¹⁰L)		[Zn(3-insesc) ₂]66
11.	3-acetyl indole selenosemicarbazone (3-AcHIndsesc, H¹¹L)		[Zn(3-acinsesc) ₂]67

12.	9-anthrinaldehyde selenosemicarbazone (9-HAnsesc, H¹²L)		[Zn(9-ansesc) ₂]68
13.	1-Naphthaldehyde selenosemicarbazone (1-HNapsesc, H¹³L)		[Zn(1-naphsesc) ₂]69
14.	2-Naphthaldehyde selenosemicarbazone (2-HNapsesc, H¹⁴L)		[Zn(2-naphsesc) ₂]70

9.2 IR Spectroscopy:

Important IR peaks of selenosemicarbazones are given in table 9.2 and IR spectra are given in figures 9.2.1- 9.2.14. The $\nu(\text{NH})$ band due to amino group in free ligands appeared in the range 3417-3223 cm^{-1} (H^1L - H^{14}L). On complexation with zinc(II) these bands showed shift to lower energy and appear in the range 3398-3228 cm^{-1} .

The amide band $\nu(-\text{NH}-)$ in free ligands appeared in the range 3157-3110 cm^{-1} (H^1L - H^{14}L). In ligands H^5L - H^{11}L , amide band gets observed by stretching of -NH- group present in heterocyclic rings. In complexes **57-60**, **68-70** absence of this band indicates deprotonation and co-ordination of ligand to metal in anionic form. In complexes **61-67** the presence of band in the range 3161-3126 cm^{-1} is due to the NH group of heterocyclic ring which makes it difficult to determine the binding of ligand in neutral or anionic form.

The C=Se band in the ligands appeared in the range 898-854 cm^{-1} . On complexation this band shifted to low energy and appeared in the range 796-710 cm^{-1} . The lower energy shift indicates the change of C=Se to C-Se⁻ thus suggests binding of ligand in selenate form.

Other IR peaks like $\nu(\text{C}=\text{N})$, $\nu(\text{C}=\text{C})$ and $\delta(\text{NH}_2)$ appeared in the range 1683-1400 cm^{-1} in

complexes and showed no significant change vis-à-vis free ligands.

Table 9.2 Important IR peaks of selenosemicarbazones (H^1L - H^{14}L) and zinc(II) complexes (**57-70**)

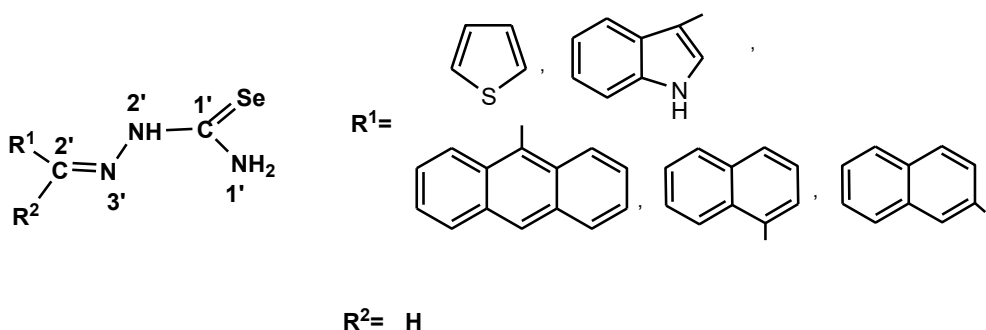
Synthesised Ligands and Metal Complexes	$\nu(\text{NH}_2)$	$\nu(-\text{NH}-)$	$\nu(\text{C}=\text{N})$, $\nu(\text{C}=\text{C})$, $\delta(\text{NH}_2)$	$\nu(\text{C}=\text{Se})$	$\nu(-\text{NH}-)$ heterocyclic ring
Cyclohexanone Selenosemicarbazone	3362m, 3225m	3157w	1591s, 1489m, 1454s	856s	-
[Zn(cysesc) ₂] 57	3364m, 3293m	-	1606s, 1580m, 1432s	710s	-
2-furfural selenosemicarbazone	3379m, 3340m	3142w	1600s, 1579m, 1464s	812s	-
[Zn(2-fursesc) ₂] 58	3350m, 3230m	-	1595s, 1531m, 1479s	744s	-
2-thiophene selenosemicarbazone	3389m, 3221m	3095w	1599s, 1527m, 1415s	844s	-
[Zn(2-thiosesc) ₂] 59	3451m	-	1645s, 1542m, 1420s	702s	-
N-methyl-2-pyrrole selenosemicarbazone	3412m, 3223m	3110w	1633s, 1562m, 1496s	854s	-
[Zn(N-mepysesc) ₂] 60	3397m, 3248m	-	1586s, 1560m, 1477s	734s	-
3-methyl-2-oxindole selenosemicarbazone	3358m, 3248m	3157w	1591s, 1489m, 1425s	854s	-
[Zn(3-meoxsesc) ₂] 61	3362m	-	1677s, 1585m, 1446s	771s	3142w
2-oxindole selenosemicarbazone	3362m, 3225m	3157w	1591s, 1489m, 1454s	856s	-
[Zn(2-oxsesc) ₂] 62	3398m, 3242m	-	1599s, 1516m, 1452s	761s	3147w
6-chloro-2-oxindole selenosemicarbazone	3417m, 3255m	3142w	1589s, 1512m, 1499s	879s	-
[Zn(6-cloxsesc) ₂] 63	3396m	-	1599s, 1514m, 1498s	763s	3146w

5-chloroisatin selenosemicarbazone	3219m	3110w	1694s, 1618s, 1559m, 1447s	885s	-
[Zn(5-clistsesc) ₂] 64	3417m, 3254m	-	1668s, 1589s, 1516m, 1448s	725s	3144w
1-methylisatin selenosemicarbazone	3408m, 3228m	3128w	1676s, 1604s, 1492m, 1415s	889s	-
[Zn(1-meistsesc) ₂] 65	3281m	-	1683s, 1566m, 1404s	740s	3161w
3-indole selenosemicarbazone	3356m, 3246m	3153w	1591s, 1487m, 1450s	898s	-
[Zn(3-indsesc) ₂] 66	3352m, 3234m	-	1595s, 1533s, 1498s	742s	3126w
3-acetylindole selenosemicarbazone	3290m	3142w	1624s, 1502m, 1406s	877s	-
[Zn(3-acindsesc) ₂] 67	-	-	1608s, 1572m, 1418s	750s	3155w
9-anthracene selenosemicarbazone	3385m, 3248m	3151w	1639s, 1518m, 1402s	887s	-
[Zn(9-antrasesc) ₂] 68	3317m	-	1566s, 1496m, 1400s	796s	-
1-naphthaldehyde selenosemicarbazone	3400m	3147w	1599s, 1516m, 1452s	871s	-
[Zn(1-naphthsesc) ₂] 69	3346m, 3228m	-	1593s, 1527m, 1440s	736s	-
2-naphthaldehyde selenosemicarbazone	3352m	3124w	1597s, 1533m, 1446s	856s	-
[Zn(2-naphthsesc) ₂] 70	3348m, 3230m	3128w	1568s, 1535m, 1400s	742s	-

9.3 NMR Spectroscopy:

9.3.1 ^1H NMR Spectroscopy:

Important NMR signals of metal complexes are given in Table 9.3.1a) and 9.3.1b). ^1H NMR spectra of synthesized metal complexes are given in figures 9.3.1.1-9.3.1.7. For discussion of ^1H NMR and ^{13}C NMR signals of complexes of zinc(II) selenosemiarbazones, the complexes need to be divided in **Type 1** and **Type 2** depending upon the type of ligand attached to them.



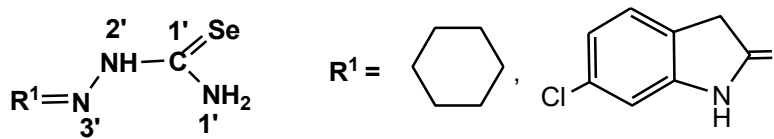
Type 1

Scheme 9.3.1

In ligands H^3L , H^{10}L , H^{12}L – H^{14}L , the $\text{N}^{2'}\text{H}$ signal appeared in the range δ 11.5– δ 9.51 ppm. Disappearance of $\text{N}^{2'}\text{H}$ signal in complexes of **Type 1** (scheme 9.3.1) ensured the deprotonation of ligand and its binding to metal atom in anionic form. The $\text{C}^{2'}\text{H}$ proton signal appeared in the range δ 9.51– δ 8.80 ppm and the amino protons ($\text{N}^{1'}\text{H}_2$) gave one or two broad singlet in the range δ 9.84– δ 7.22 ppm. Ring protons signal showed the range in between δ 8.98– δ 7.15 ppm (Table 9.3.1a).

Table 9.3.1a) Important ^1H NMR signals of selenosemicarbazones (**Type 1**) with zinc(II) complexes

Ligands and Complexes	(1H, N ^{2'} H)	(1H, C ^{2'} H)	(1H, N ^{1'} H ₂)	(Ring protons)
2-Hthiosesc, (H³L)	9.64 s	8.10 s	7.58 s, 6.71 s	7.47 m (1H, C ⁴ H), 7.37 d (1H, C ³ H), 7.12 d (1H, C ⁵ H)
[Zn(2-thiosesc) ₂] 59	-	8.80 s	7.37 s, 7.22 s	7.50 d (1H, C ⁴ H), 7.44 d (1H, C ³ H), 7.15 t (1H, C ⁵ H)
3-HIndsesc, (H¹⁰L)	10.0 s	7.85 s	7.76 s, 7.56 s	8.30-7.28 (5H, cyclic ring proton).
[Zn(3-indsesc) ₂] 66	-	8.86 s	7.86 s	8.51 d (1H, C ⁵ H), 8.35 d (1H, C ⁸ H), 7.45-7.36 m (2H, C ^{6,7} H),
9-HAnsesc, (H¹²L)	11.5 s	9.02 s	-	8.73 d (2H, C ^{3,11} H), 8.08 d (2H, C ^{6,8} H), 7.73 t (2H, C ^{5,9} H), 7.60 t (t, 2H, C ^{4,10} H), 7.29 s (1H, C ⁷ H)
[Zn(9-anthrasesc) ₂] 68	-	9.10 s	9.84 s, 9.26 s	8.10 m (2H, C ^{3,11} H), 8.01 m (2H, C ^{6,8} H), 7.86 t (2H, C ^{5,9} H), 7.67 t (2H, C ^{4,10} H)
1-HNapsesc, (H¹³L)	9.51 s	9.00 s	7.97 s	8.17 d (1H, C ⁹ H), 8.02 d (1H, C ⁴ H), 7.95 d (1H, C ⁶ H), 7.62 m (2H, C ^{3,7} H), 7.29 s (1H, C ⁸ H)
[Zn(1-naphthsesc) ₂] 69	-	9.51 s	-	8.98 d (1H, C ⁴ H), 8.16 d (1H, C ⁹ H), 8.01 d (1H, C ⁴ H), 7.97 d (1H, C ⁶ H), 7.70 m (1H, C ³ H), 7.62 m (1H, C ⁸ H)
2-HNapsesc, (H¹⁴L)	10.1 s	8.38 s	7.70 s	8.05-7.29 (aromatic ring proton)
[Zn(2-naphthsesc) ₂] 70	-	8.91 s	-	8.18-7.29 (aromatic ring proton)



Type 2

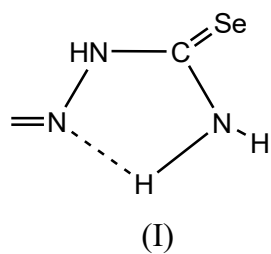
Scheme 9.3.1.1

In ligands **H¹L** and **H⁷L**, the N^2H signal appeared at the range δ 9.23 ppm and δ 9.51 ppm respectively, disappearance of N^2H proton signal in complexes of **Type 2** (scheme 9.3.1.1) confirmed deprotonation and is binding of ligand to metal in anionic form and the amino protons (N^1H_2) gave one broad singlet in the range δ 5.08 ppm and δ 8.48 ppm respectively. Ring protons signal showed the range at δ 7.16- δ 6.92 ppm and cyclic ring protons showed the signal range at δ 3.31- δ 1.65 ppm respectively (Table 9.3.1b).

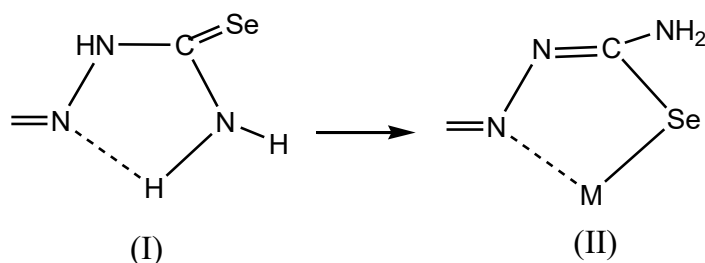
Table 9.3.1b) Important ^1H NMR signals of selenosemicarbazones (**Type 2**) with Zn(II) complexes

Ligands and Complexes	(1H, N^2H)	(1H, C^2H)	(1H, N^1H_2)	(Ring protons)
Hcysesc, H¹L	9.23 s	-	7.65 s, 7.15 s	2.32-1.54 m (10H, cyclic ring proton)
[Zn(cysesc) ₂] 57	-	-	5.08 s	3.52-1.73 m (10H, cyclic ring proton).
6-ClHOxsesc, (H⁷L)	9.51 s	-	4.89 s, 4.26 s	7.13 d (1H, C^7H), 6.99 d (1H, C^4H), 6.92s (1H, C^5H)
[Zn(6-cloxsesc) ₂] 63	-	-	8.48 s	7.15 d (1H, C^7H), 7.03 d (1H, C^4H), 6.92 s (1H, C^5H), 3.54 (cyclic proton ring)

The amino protons (N^1H_2) gave two broad singlet in the selenosemicarbazones ligands of **Type 1** and **Type 2** indicating that two protons are non-equivalent probably due to the H-bonding between one at the amino hydrogen and azomethine nitrogen (I).



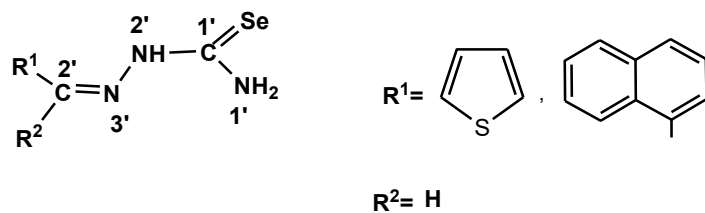
Similarly in some cases the amino protons ($N^{1'}H_2$) gave one singlet in the complexes of **Type 1** and **Type 2** indicating that the two protons are equivalent probably during chelation (II) and also confirming that two protons are present in same environment.



The amino protons ($N^{1'}H_2$) in the selenosemicarbazones ligands of **Type 1** and **Type 2** indicating that presence of one proton or no proton probably due to the low solubility of two protons of amino protons. The amino protons ($N^{1'}H_2$) in the complexes of **Type 1** and **Type 2** indicating that presence of no proton probably due to the low solubility of two protons of amino protons.

9.3.2 ^{13}C NMR Spectroscopy:

Important ^{13}C NMR signals of metal complexes are given in Table 9.3.2a) and 9.3.2b), ^{13}C NMR spectra of synthesized metal complexes are given in figures 9.3.2.1-9.3.2.4.

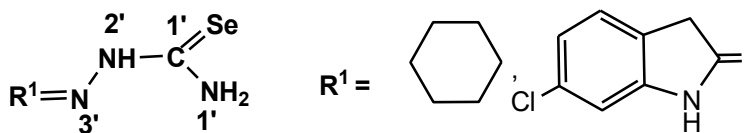


Scheme 9.3.2

In case of complexes of **Type 1** (scheme 9.3.2), C^{1'} signal appeared at the range δ 162.0 ppm and disappearance of C^{1'} signal in some cases showed the low solubility of complexes of **Type 1**. C^{2'} signal appeared at the range δ 155.7 ppm and δ 133.9 ppm respectively. Ring carbons showed the signal in between the range of δ 132.3 ppm and δ 115.0 ppm respectively. These signals gave the assurance that there is the formation of metal complexes (Table 9.3.2a).

Table 9.3.2a) Important¹³C NMR signals of selenosemicarbazones (**Type 1**) with zinc(II) complexes

Ligands and Complexes	(C ^{1'})	(C ^{2'})	(Ring carbons)
2-Hthiosesc, (H³L)	-	155.8	132.4 (C ⁵), 130.0 (C ⁴), 127.8 (C ³), 127.3 (C ²)
[Zn(2-thiosesc) ₂] 59	-	155.7	132.3 (C ⁵), 130.0 (C ⁴), 127.8 (C ³), 115.0 (C ²)
1-HNapsesc, (H¹³L)	162.1	134.1	131.8-124.9 (aromatic ring carbon), 115.0 (C ⁵)
[Zn(1-naphthsesc) ₂] 69	162.0	133.9	131.6-124.2 (aromatic ring carbon)



Type 2

Scheme 9.3.2.1

In case of complexes of **Type 2** (scheme 9.3.2.1), C^{1'} signal appeared at the range δ 177.1 ppm and δ 172.6 ppm respectively. Ring Carbons and cyclic ring carbons showed the signal in between the range of δ 143.4-δ 110.2 ppm and δ 36.1-δ 25.3 ppm respectively. The signals gave the assurance that there is the formation of metal complexes (Table 9.3.2b).

Table 9.3.2b) Important¹³C NMR signals of selenosemicarbazones (**H¹L**, **H⁷L**) with zinc(II) complexes (**Type 2**)

Ligands and Complexes	(C ^{1'})	(C ^{2'})	(Ring carbons)
Hcysesc, H¹L	175.6	-	35.4-25.3
[Zn(cysesc) ₂] 57	172.6	-	36.1-25.5 (cyclic carbon ring)

6-ClHOxsesc, (H^7L)	177.9	-	143.6 (C ⁵), 133.1 (C ⁶), 125.3 (C ⁷), 110.7 (C ⁸), 58.2 (C ⁴), 35.3 (C ³)
[Zn(6-cloxsesc) ₂] 63	177.1	-	143.4 (C ⁵), 133.6 (C ⁶), 125.5 (C ⁷), 110.2 (C ⁸), 35.3 (C ³)

9.4 Mass Spectrometry:

Mass spectra of complexes **57-70** have been recorded and given in Figures 9.4.1-9.4.14. The observed molecular ion peaks $[M]^+$ are given in Table 9.4. From the table it is clear that m/z value for complexes **57-70** are close to their proposed stoichiometry, $[Zn(L)_2]$ and thus confirmed the coordination of zinc(II) with selenosemicarbazones.

Table 9.4 m/z value (amu) of complexes **57-70** obtained from mass spectra

Complex No.	Parent peak obtained from mass spectra	Expected formula for parent ion (m/z)⁺
57	497 amu	$[Zn(C_7H_{12}N_3Se)_2]$
58	494 amu	$[Zn(C_6H_6N_3OSe)_2]$
59	528 amu	$[Zn(C_6H_7N_3SSe)_2]$
60	514 amu	$[Zn(C_7H_7N_4Se)_2]$
61	596 amu	$[Zn(C_{10}H_{11}N_4Se)_2]$
62	574 amu	$[Zn(C_9H_9N_4Se)_2]$
64	662 amu	$[Zn(C_9H_5N_4ClOSe)_2]$
65	624 amu	$[Zn(C_{10}H_9N_4OSe)_2]$
66	591 amu	$[Zn(C_{10}H_9N_4Se)_2]$
67	621 amu	$[Zn(C_{11}H_{12}N_4Se)_2]$
68	707 amu	$[Zn(C_{16}H_9N_3Se)_2]$
69	610 amu	$[Zn(C_{12}H_8N_3Se)_2]$
70	611 amu	$[Zn(C_{12}H_9N_3Se)_2]$

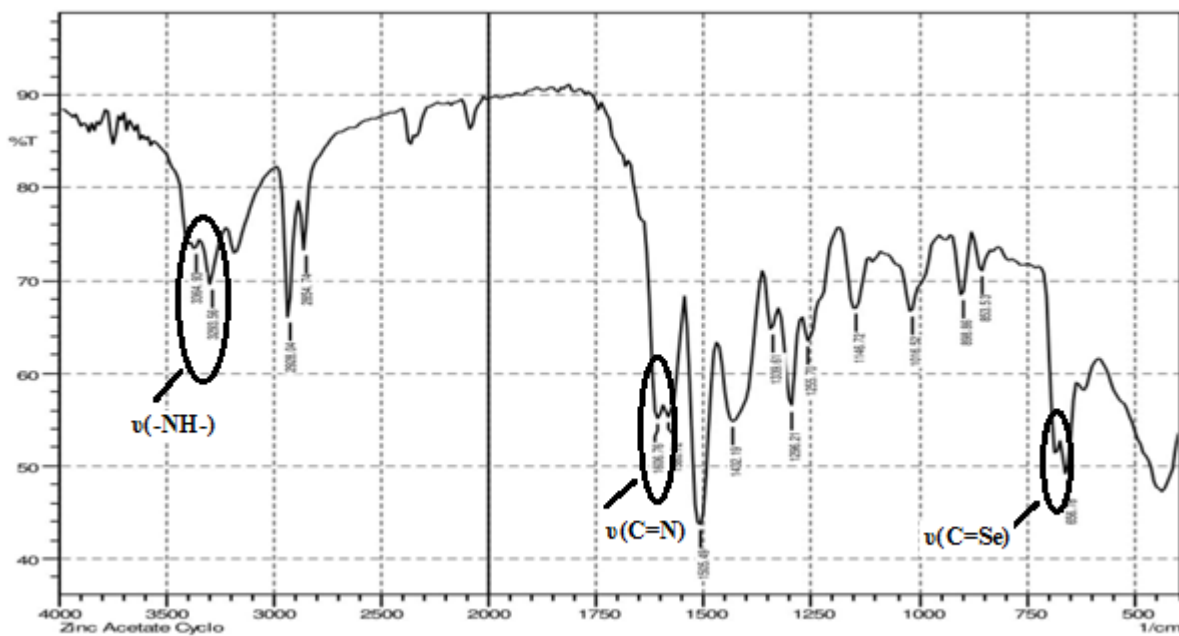


Figure 9.2.1 IR spectrum of $[Zn(\text{cysesc})_2]57$

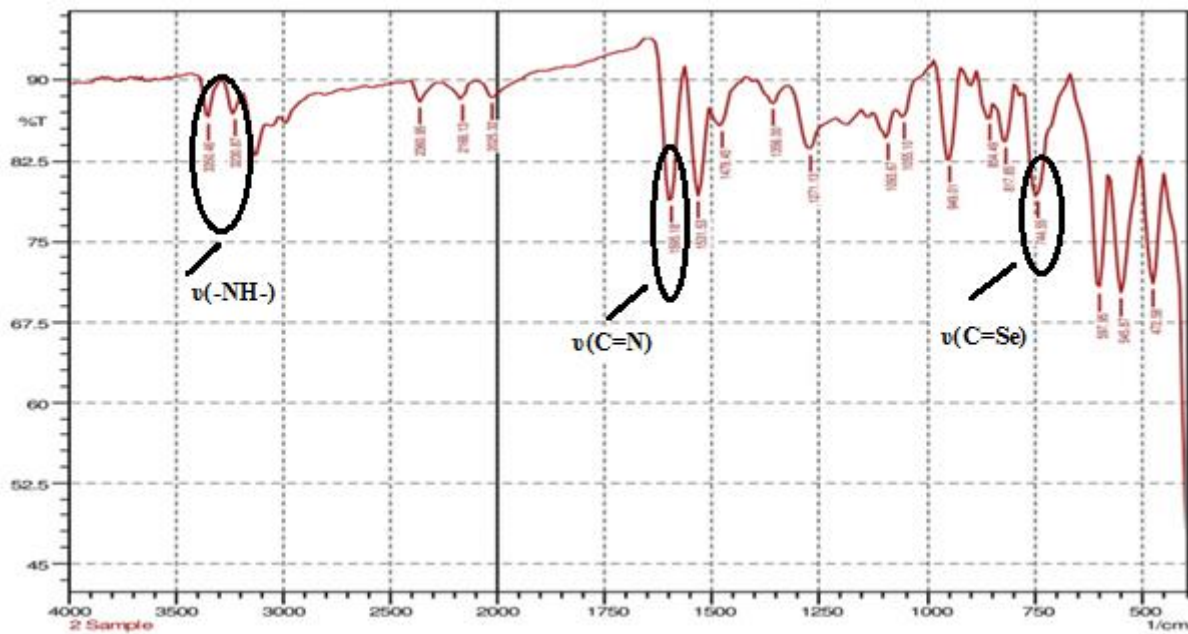


Figure 9.2.2 IR spectrum of $[Zn(2\text{-fursesc})_2]58$

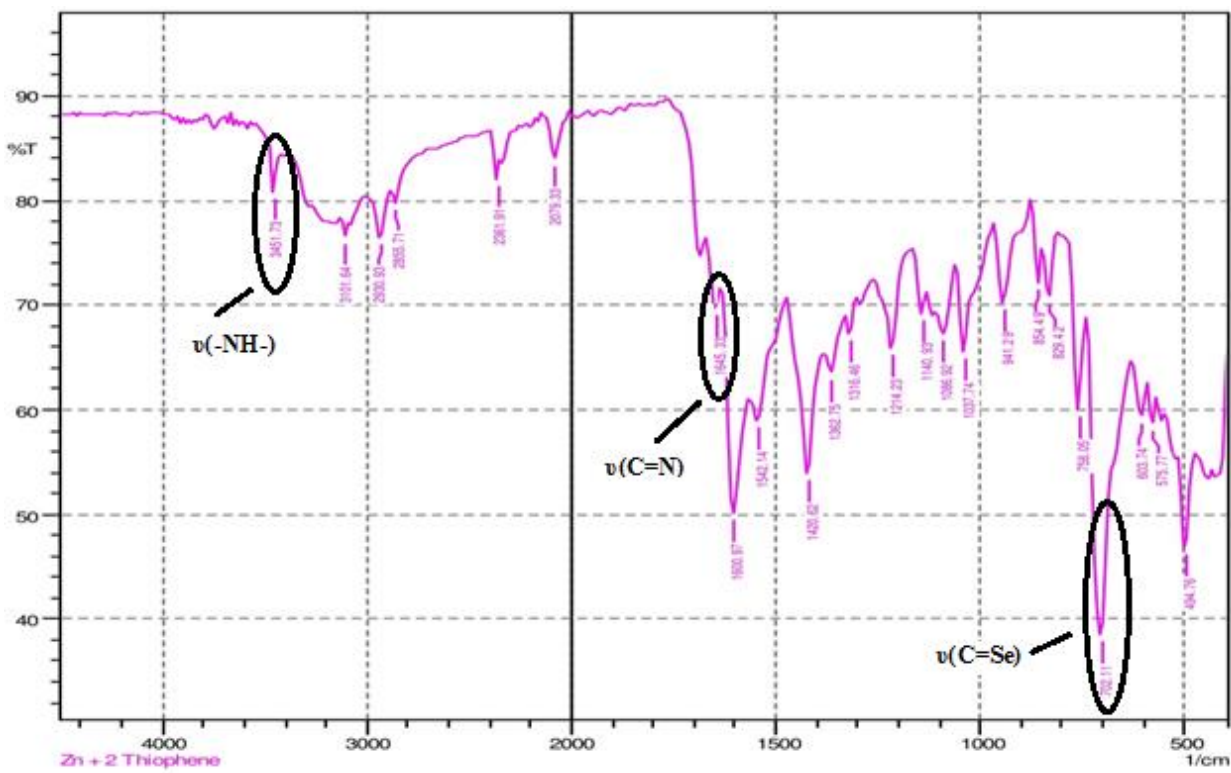


Figure 9.2.3 IR spectrum of $[\text{Zn}(2\text{-thiosesc})_2]59$

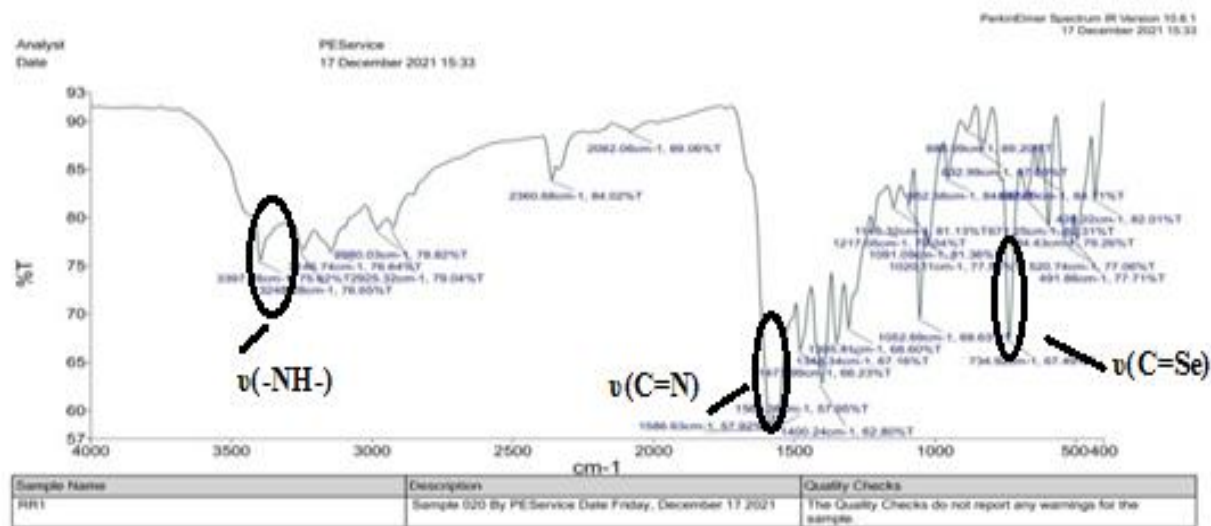


Figure 9.2.4 IR spectrum of $[\text{Zn}(\text{N-mepysesc})_2]60$

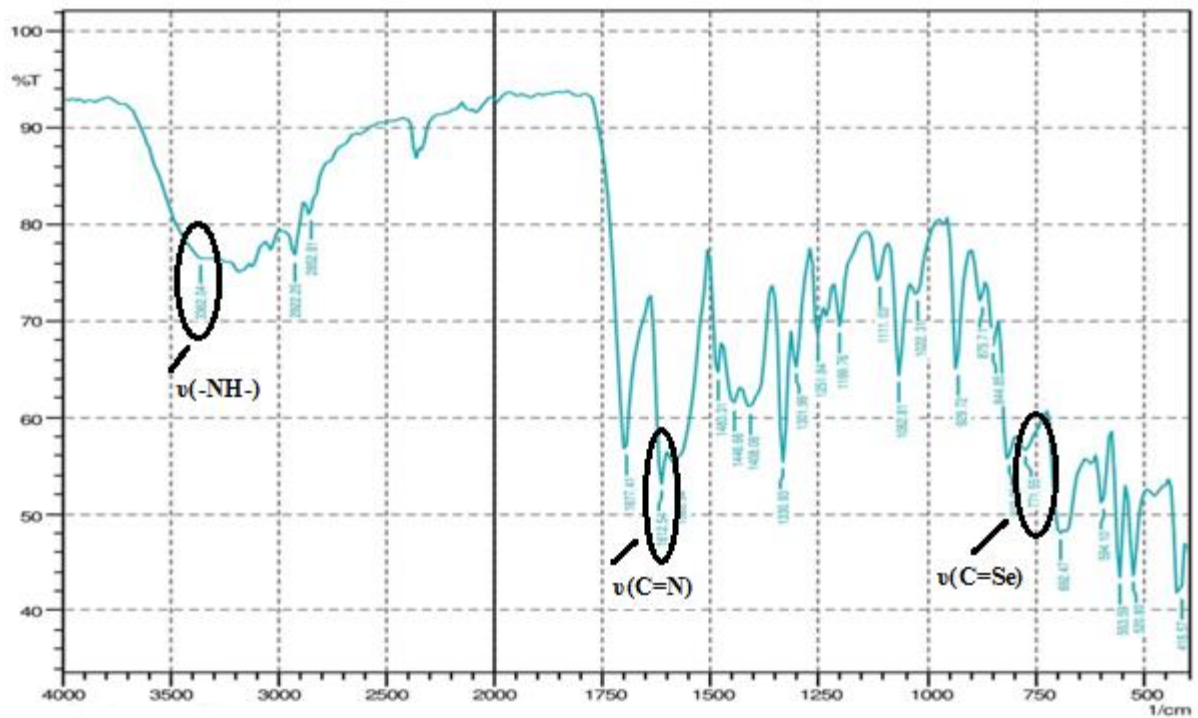


Figure 9.2.5 IR spectrum of $[Zn(3\text{-meoxsesc})_2]$ 61

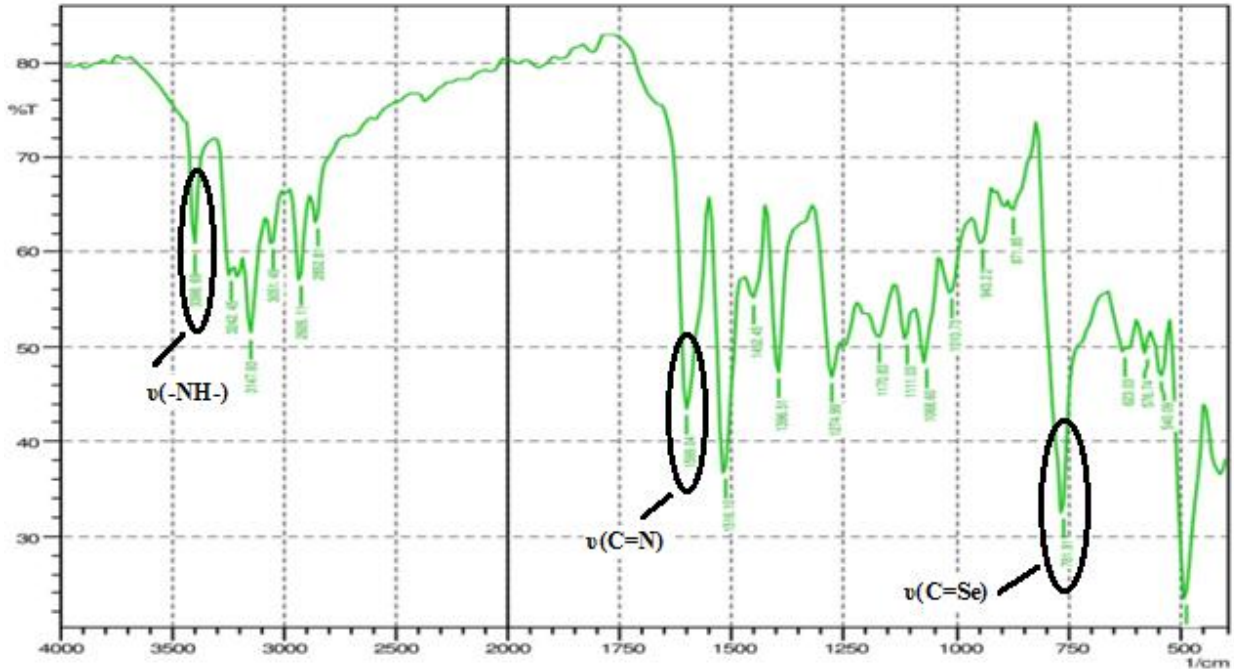


Figure 9.2.6 IR spectrum of $[Zn(2\text{-oxsesc})_2]$ 62

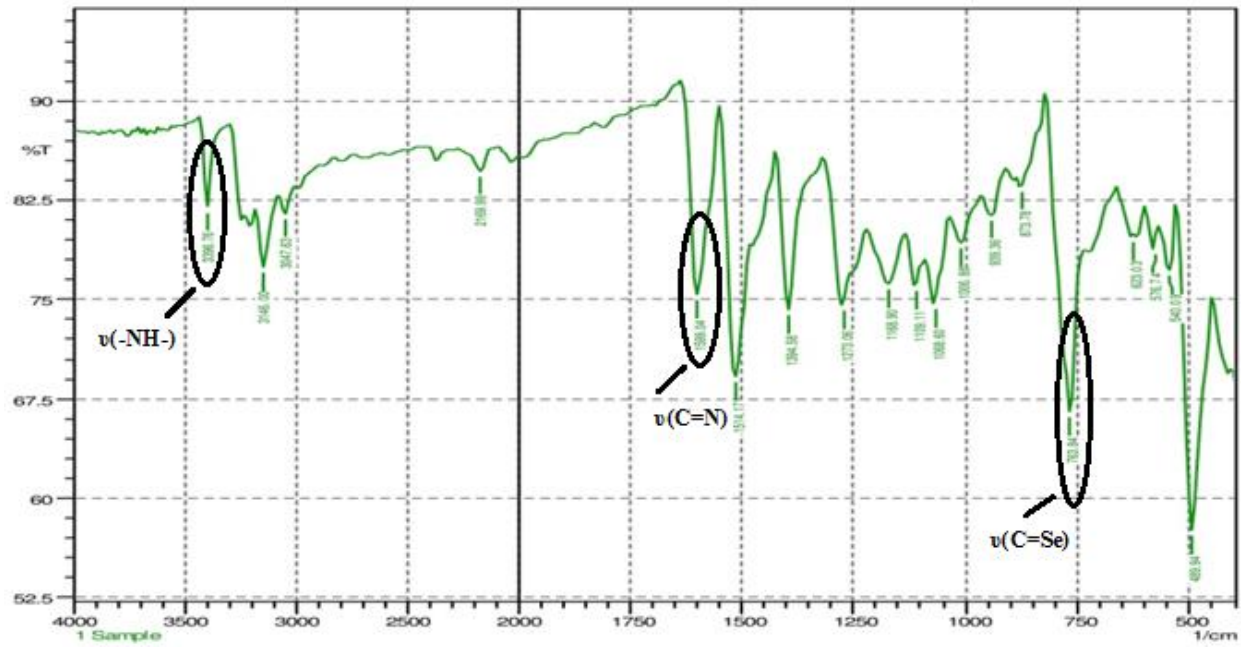


Figure 9.2.7 IR spectrum of $[\text{Zn}(6\text{-cloxsesc})_2]63$

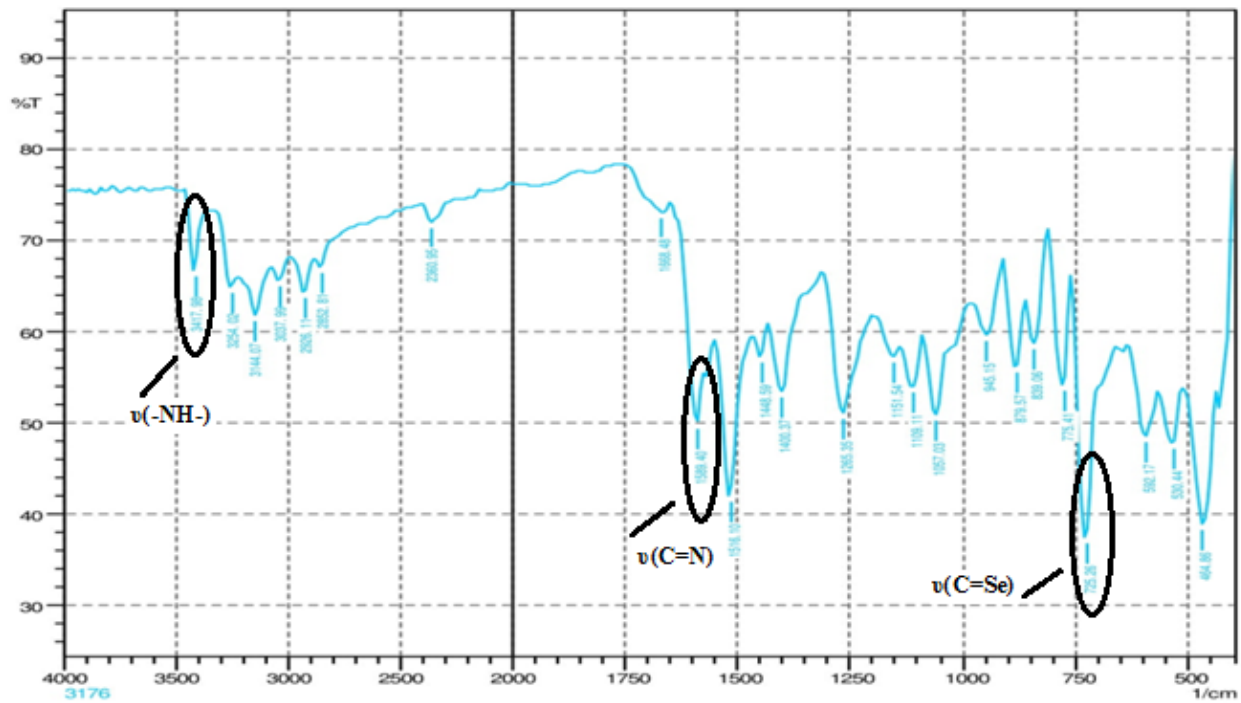
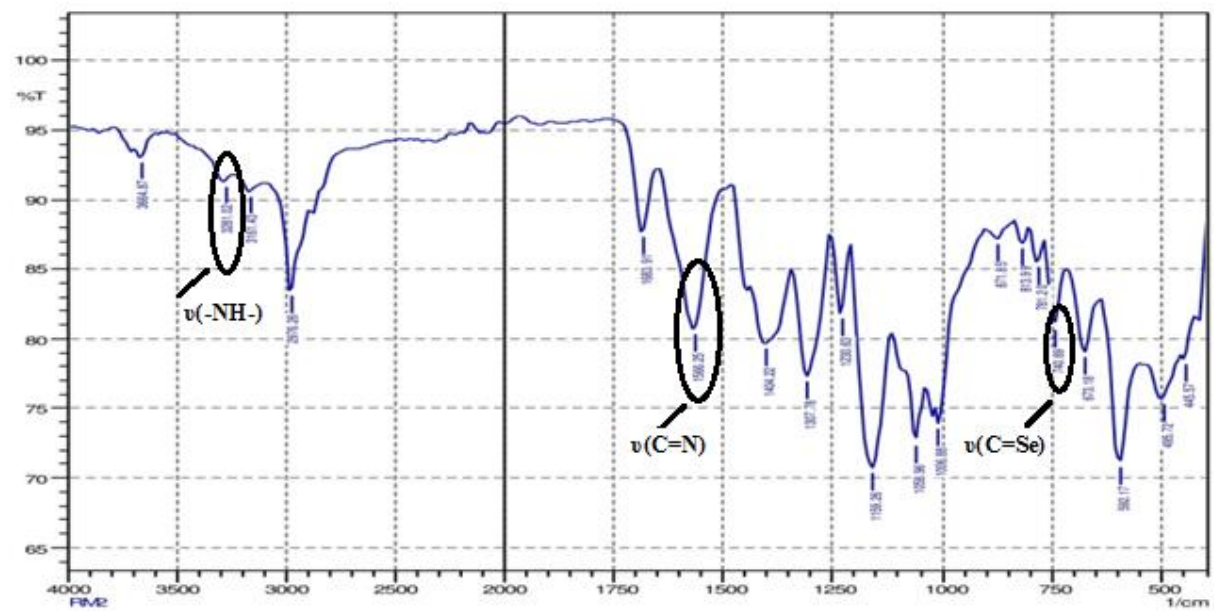


Figure 9.2.8 IR spectrum of $[\text{Zn}(5\text{-clistsesc})_2]64$



Comment:
RM2

Date/Time: 4/19/2021 12:12:43 PM
No. of Scans:
Resolution:
Apodization:

Figure 9.2.9 IR spectrum of [Zn(1-meistsesc)₂]65

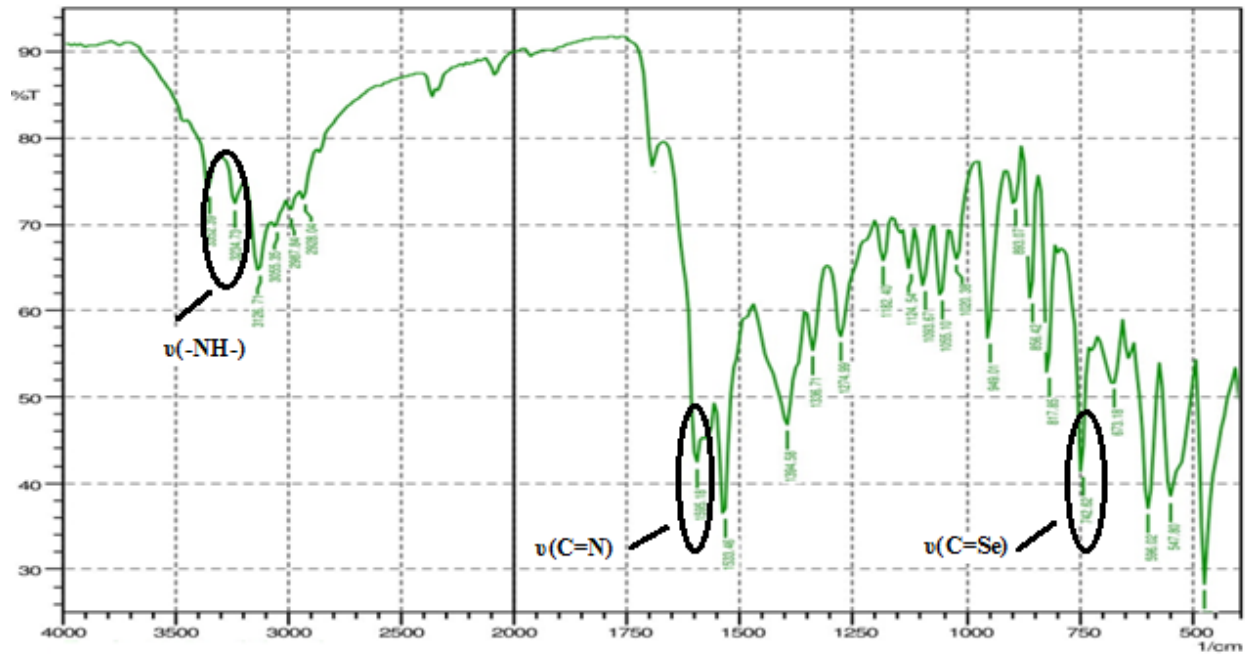


Figure 9.2.10 IR spectrum of [Zn(3-indsesc)₂]66

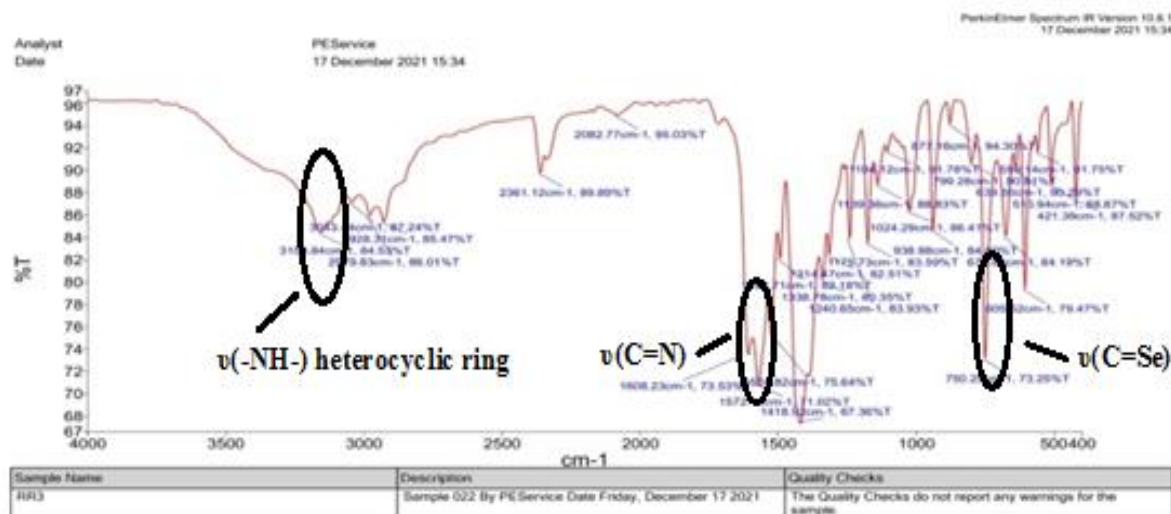


Figure 9.2.11 IR spectrum of $[\text{Zn}(3\text{-acindsesc})_2]$ **67**

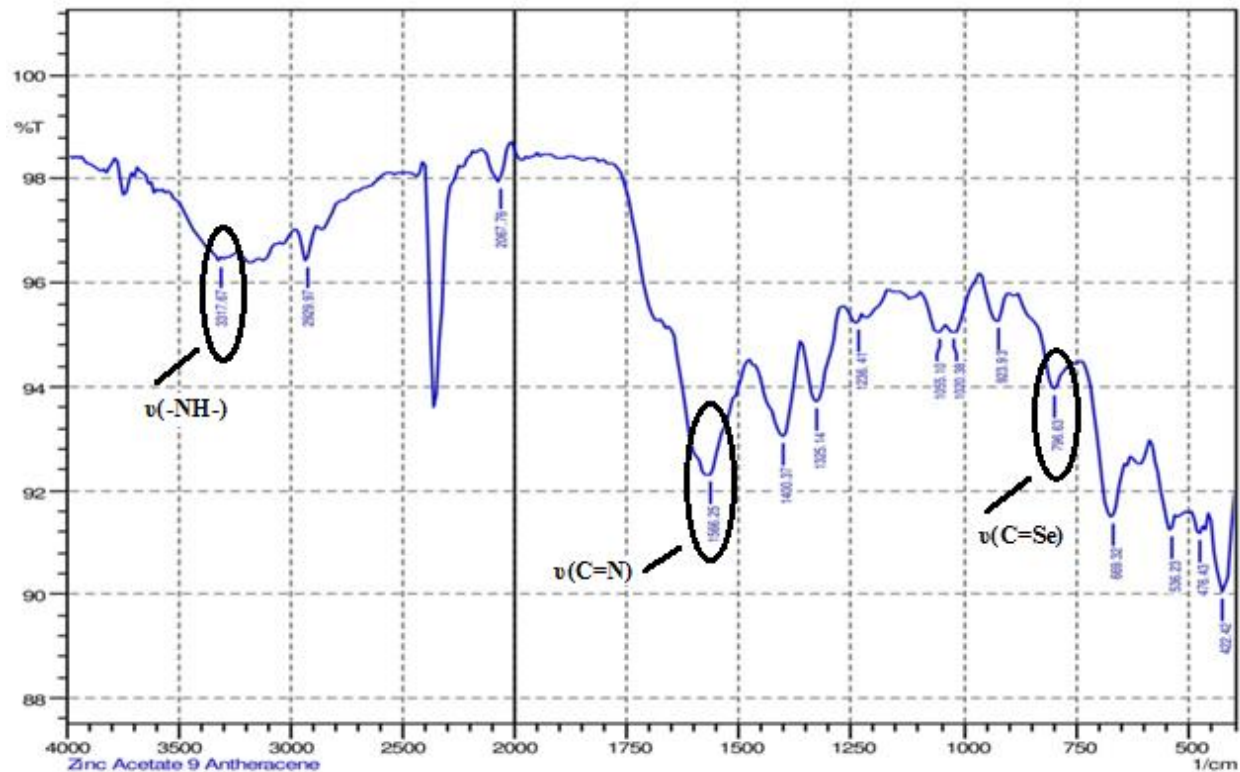


Figure 9.2.12 IR spectrum of $[\text{Zn}(9\text{-anthracene})_2]$ **68**

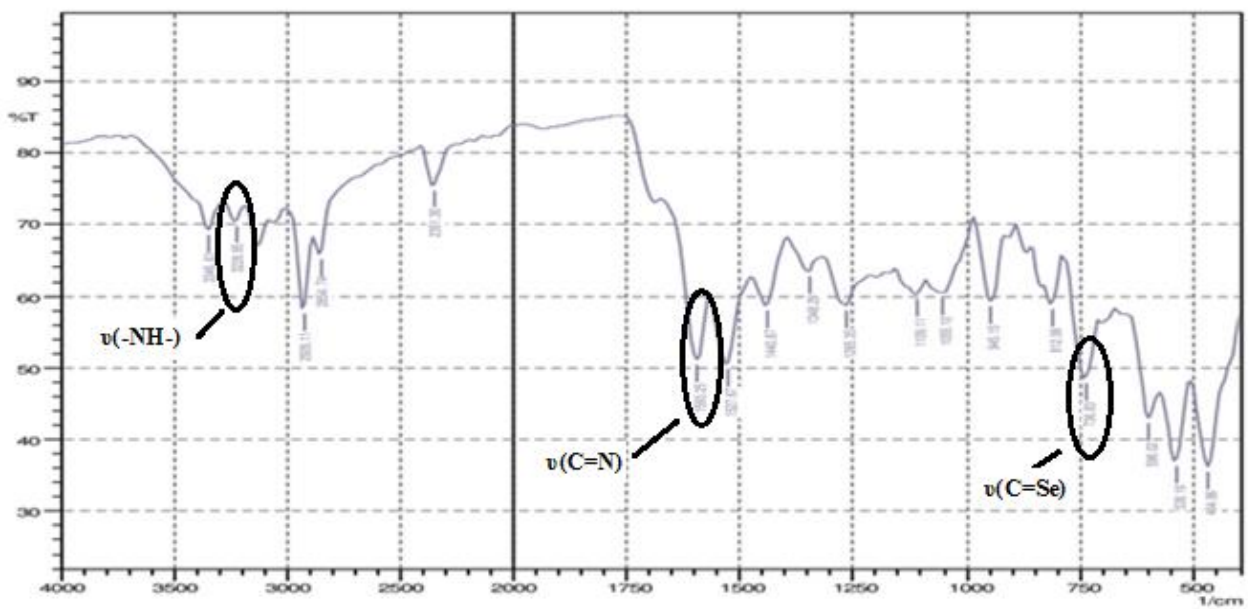


Figure 9.2.13 IR spectrum of $[\text{Zn}(1\text{-naphthsesc})_2]69$

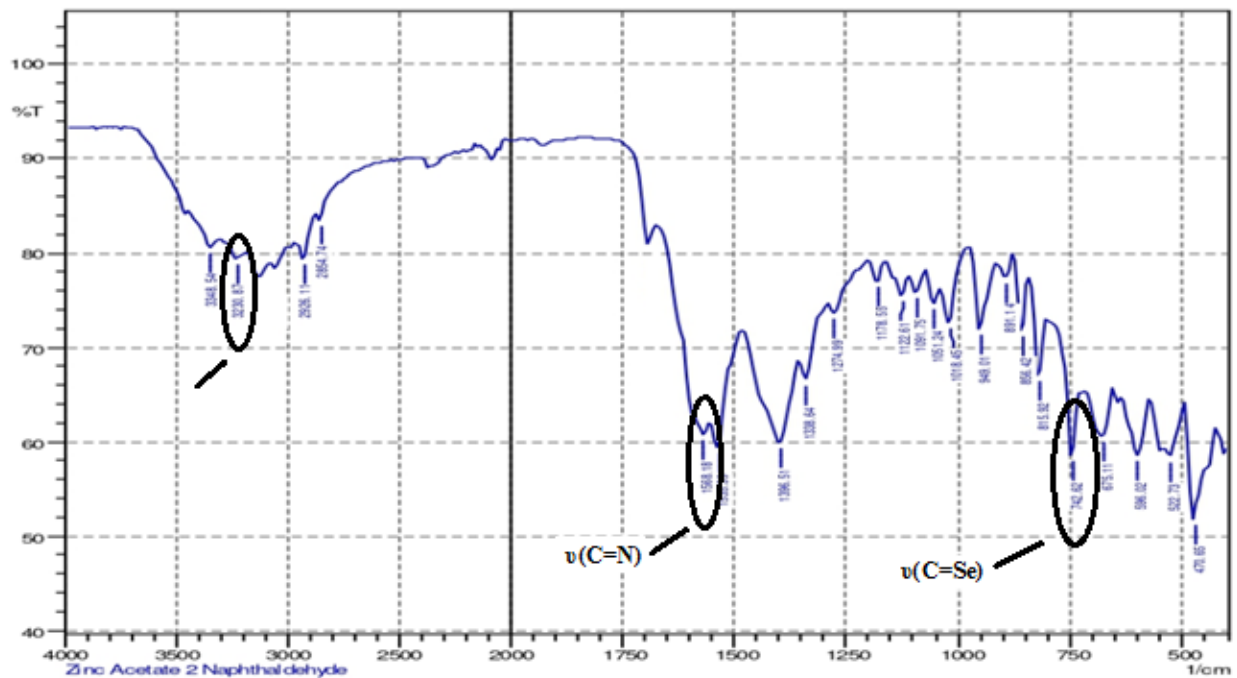


Figure 9.2.14 IR spectrum of $[\text{Zn}(2\text{-naphthsesc})_2]70$

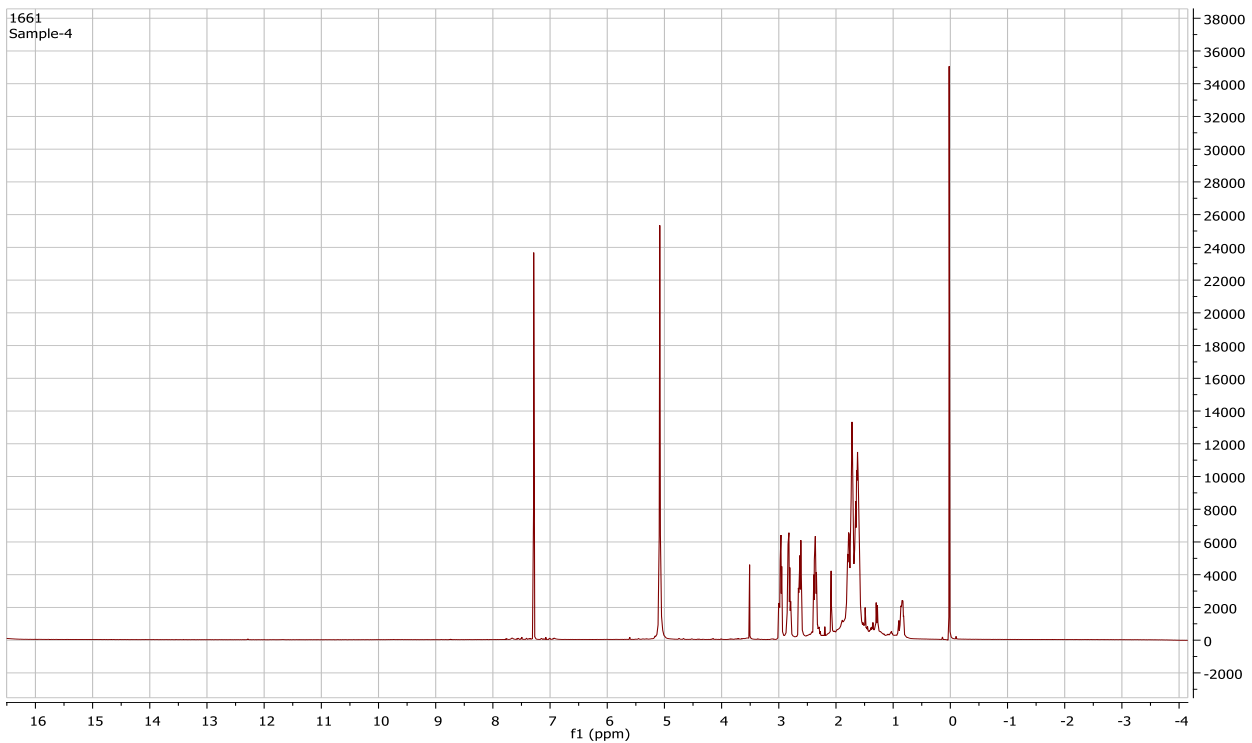


Figure 9.3.1.1a) ¹H NMR spectrum of complex **57**

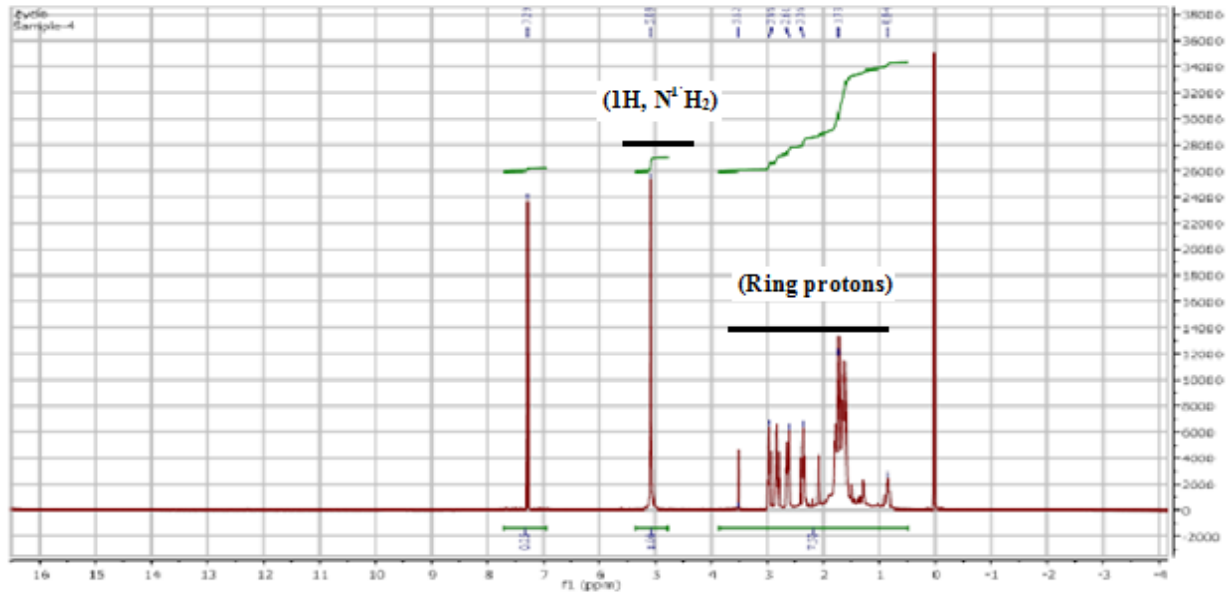


Figure 9.3.1.1b) ¹H NMR spectrum of complex **57**(expansion form)

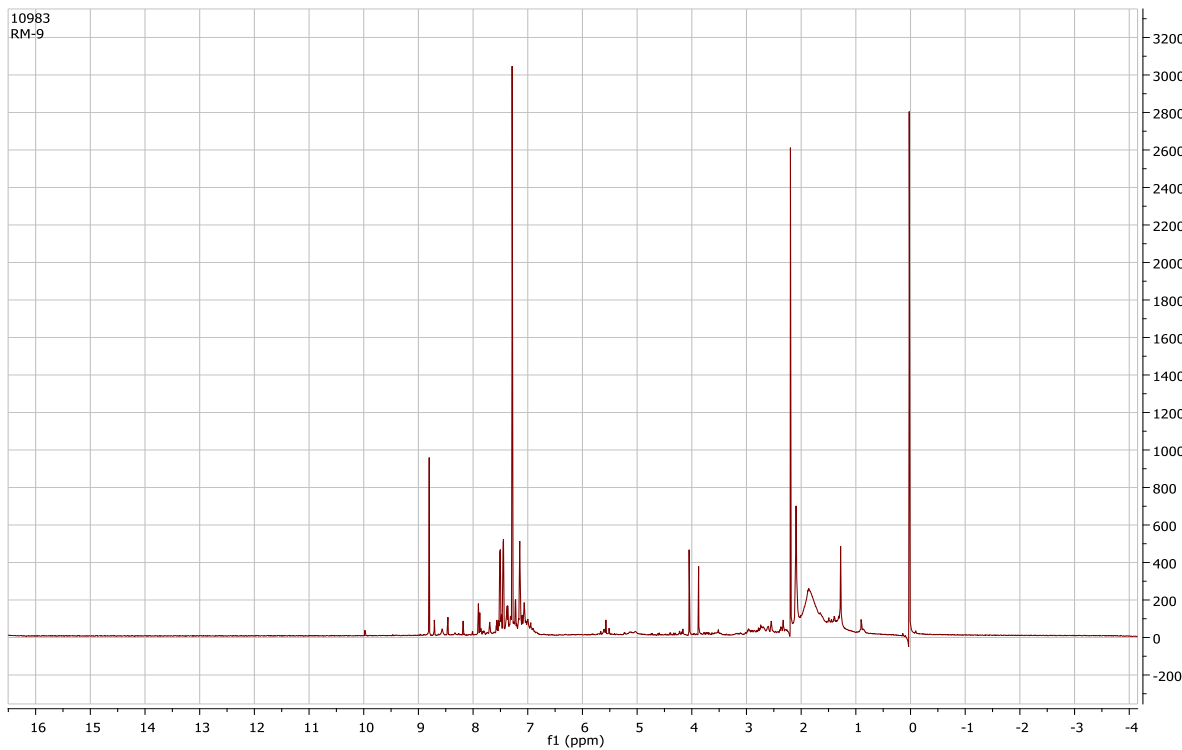


Figure 9.3.1.2a) ^1H NMR spectrum of complex **59**

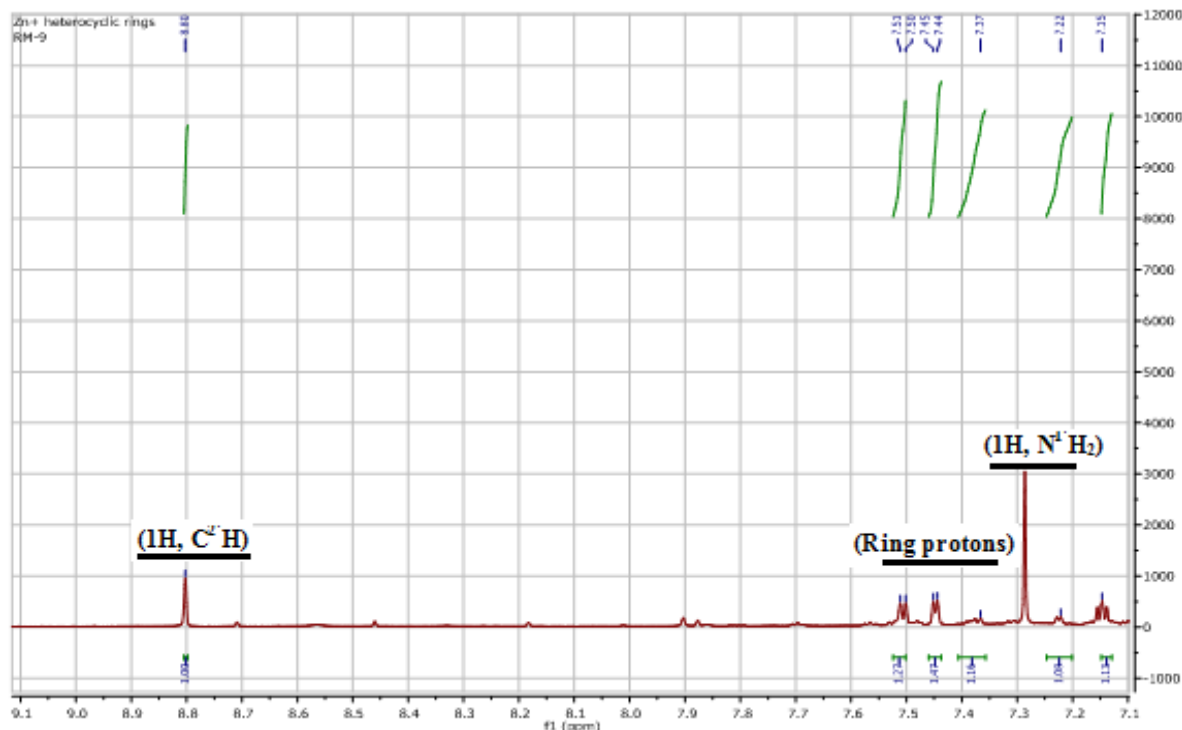


Figure 9.3.1.2b) ^1H NMR spectrum of complex **59**(expansion form)

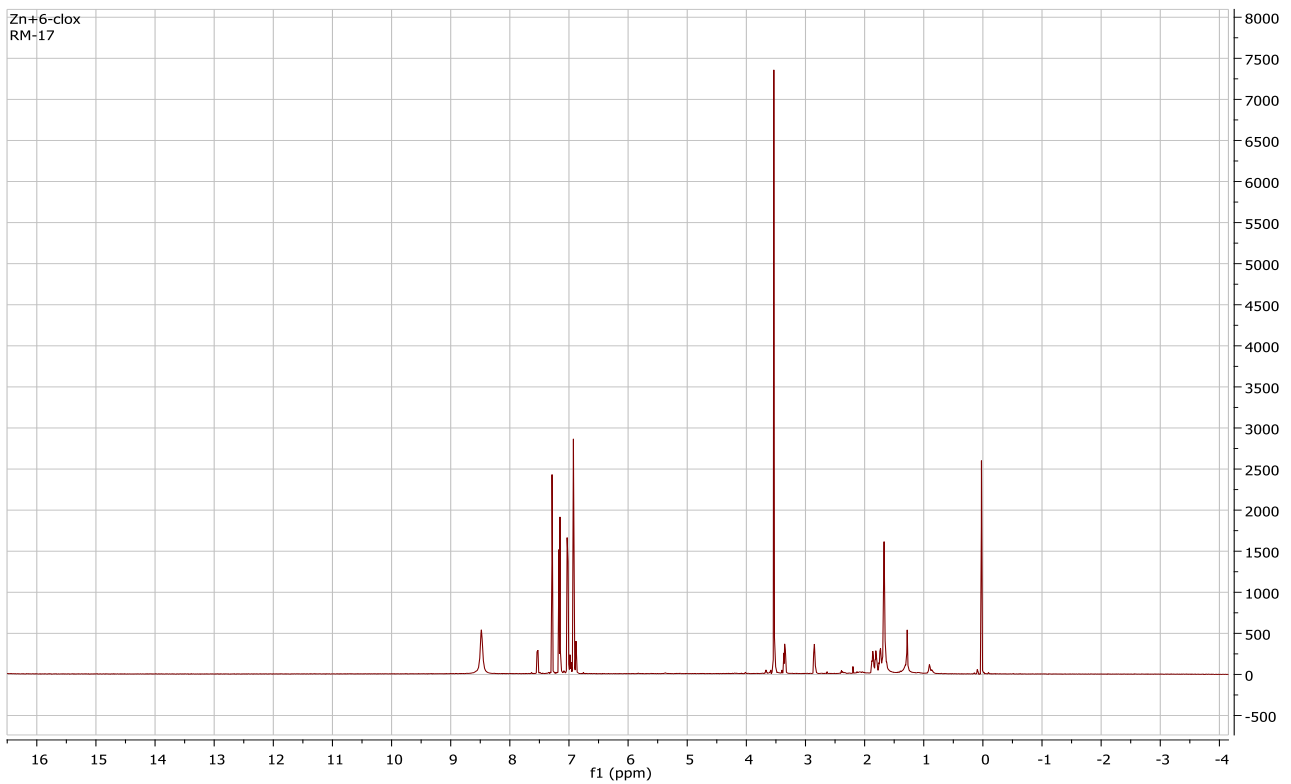


Figure 9.3.1.3a) ¹H NMR spectrum of complex **63**

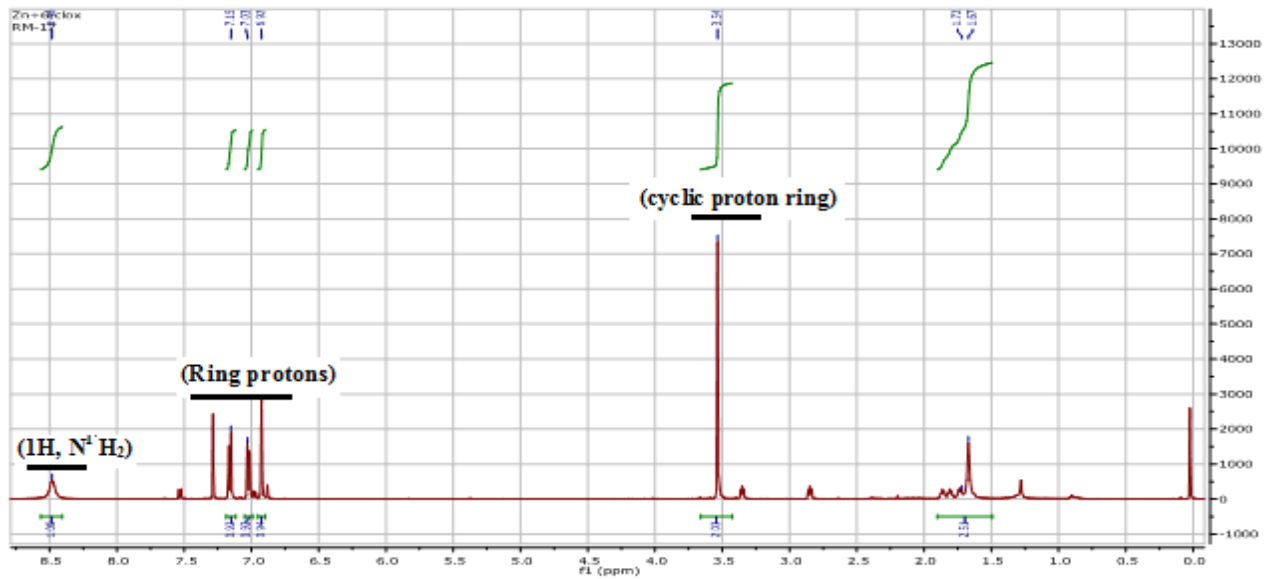


Figure 9.3.1.3b) ¹H NMR spectrum of complex **63**(expansion form)

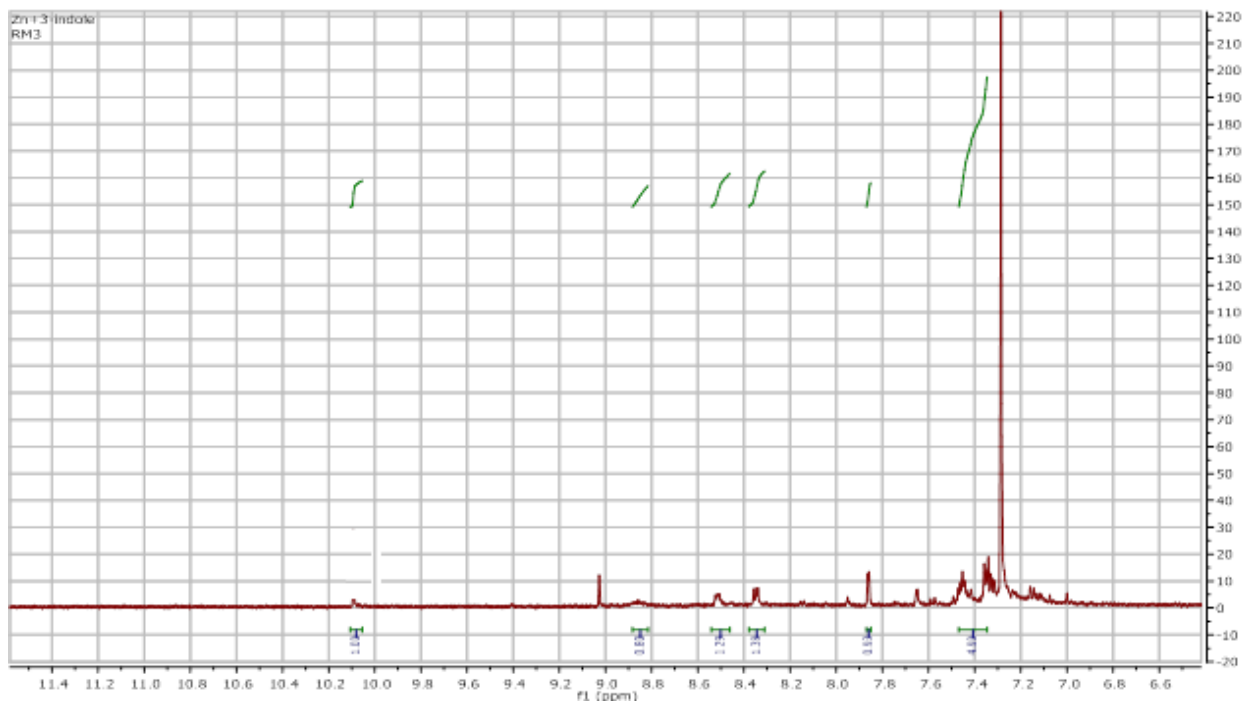


Figure 9.3.1.4a) ^1H NMR spectrum of complex **66**

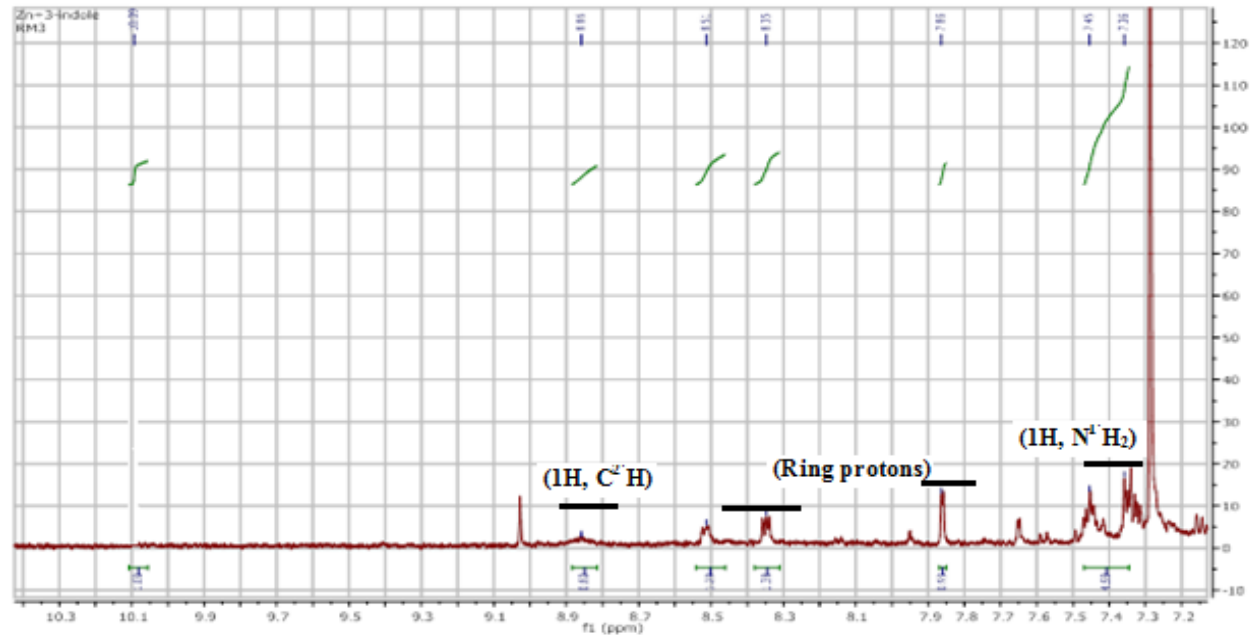


Figure 9.3.1.4b) ^1H NMR spectrum of complex **66**(expansion form)

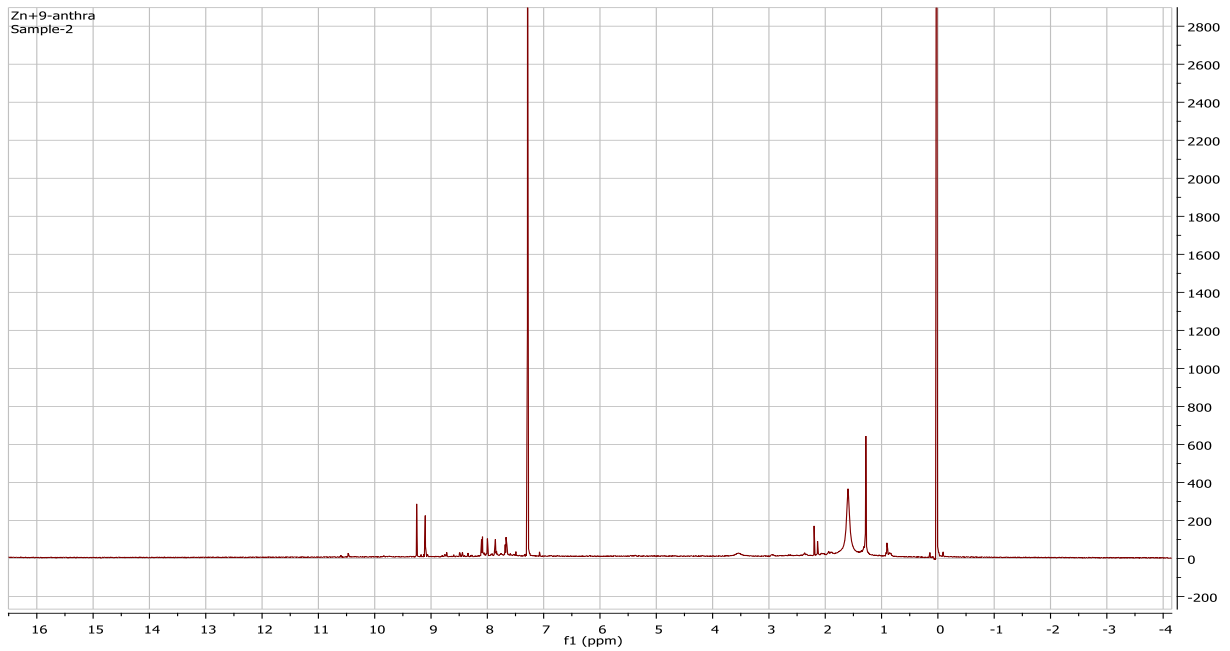


Figure 9.3.1.5a) ¹H NMR spectrum of complex **68**

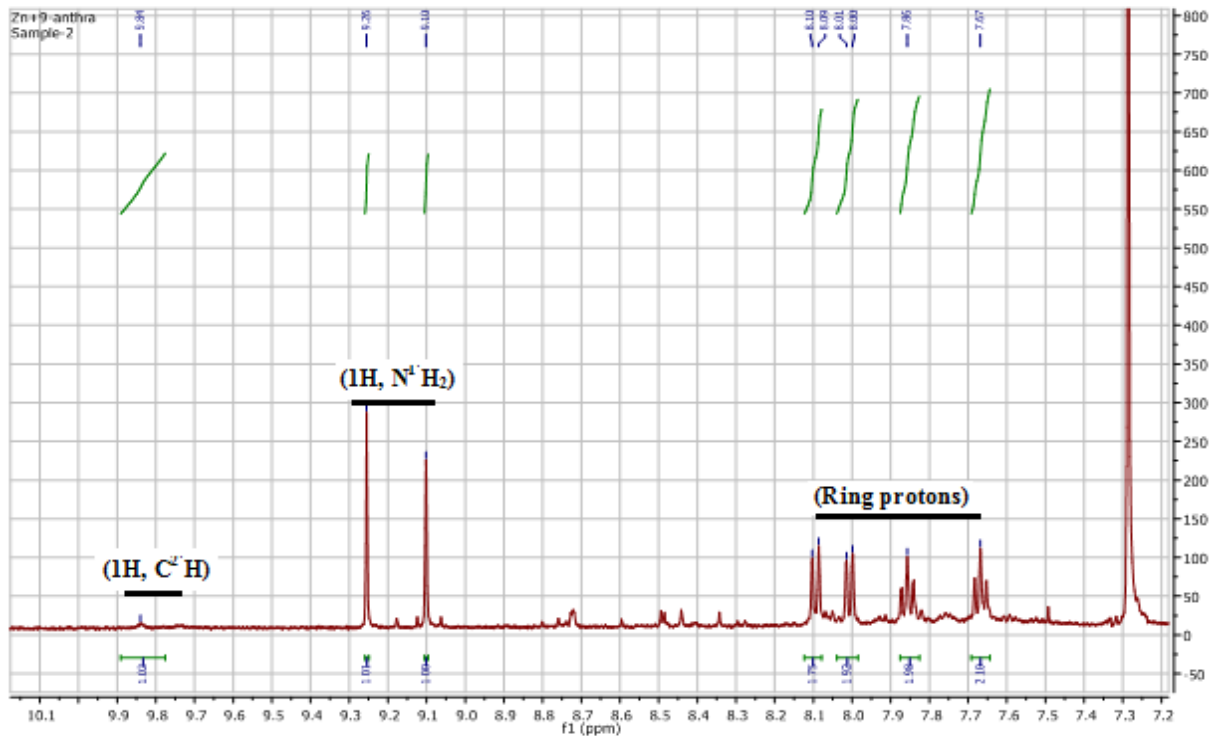


Figure 9.3.1.5b) ¹H NMR spectrum of complex **68**(expansion form)

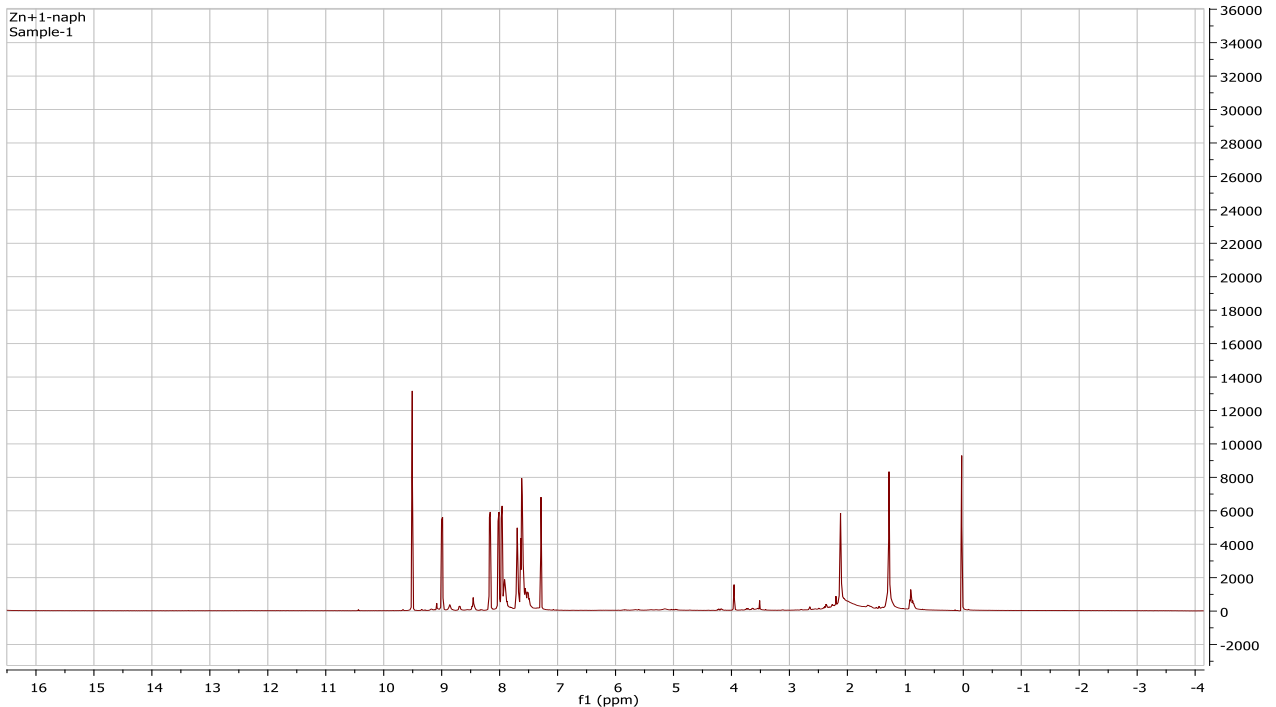


Figure 9.3.1.6a) ¹H NMR spectrum of complex 69

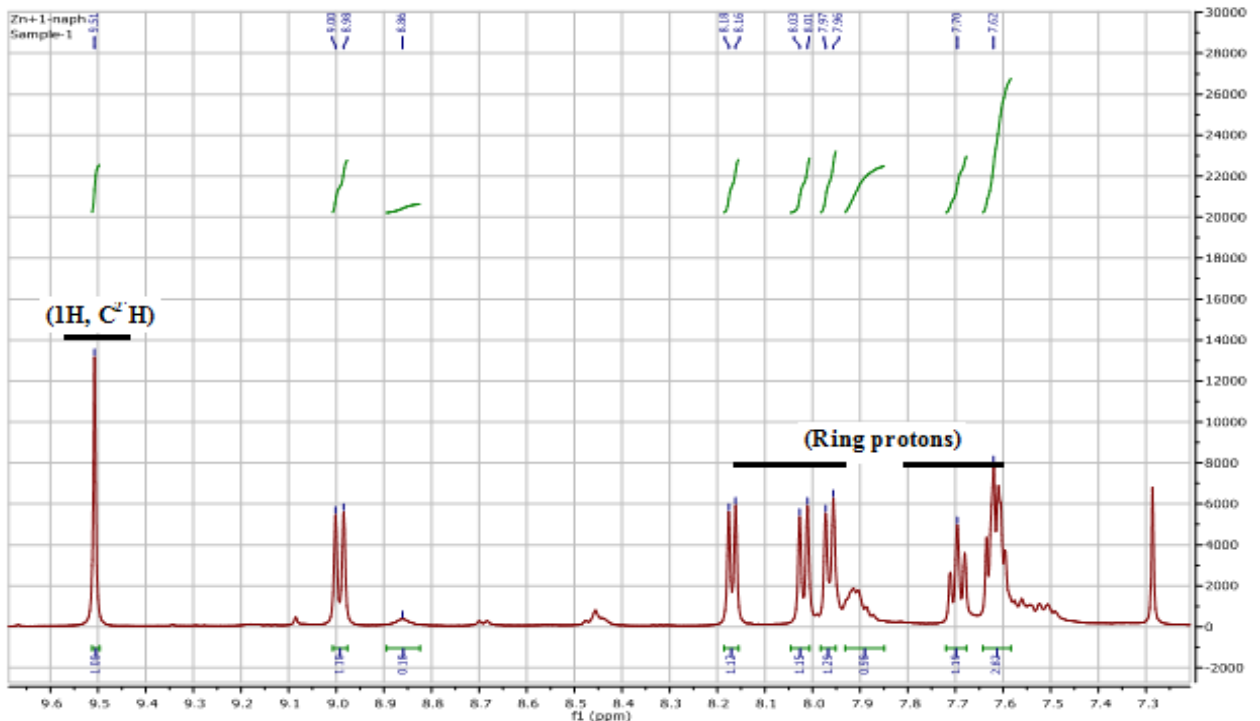


Figure 9.3.1.6b) ¹H NMR spectrum of complex 69(expansion form)

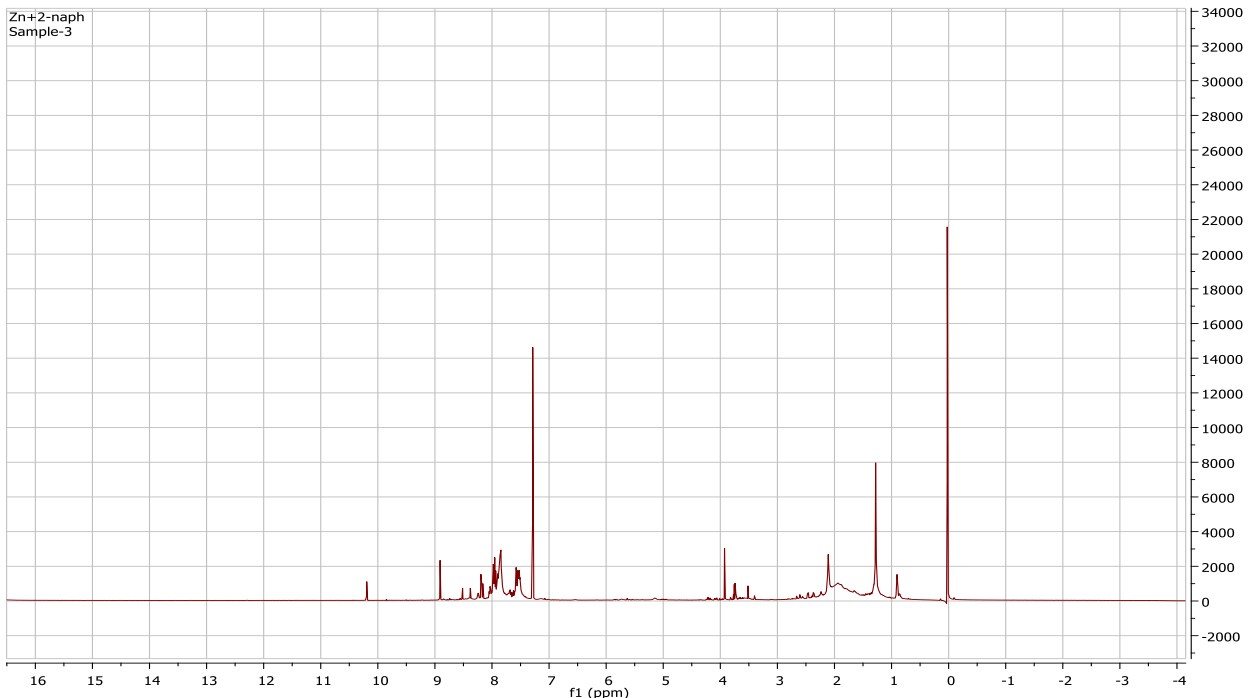


Figure 9.3.1.7a) ¹H NMR spectrum of complex 70

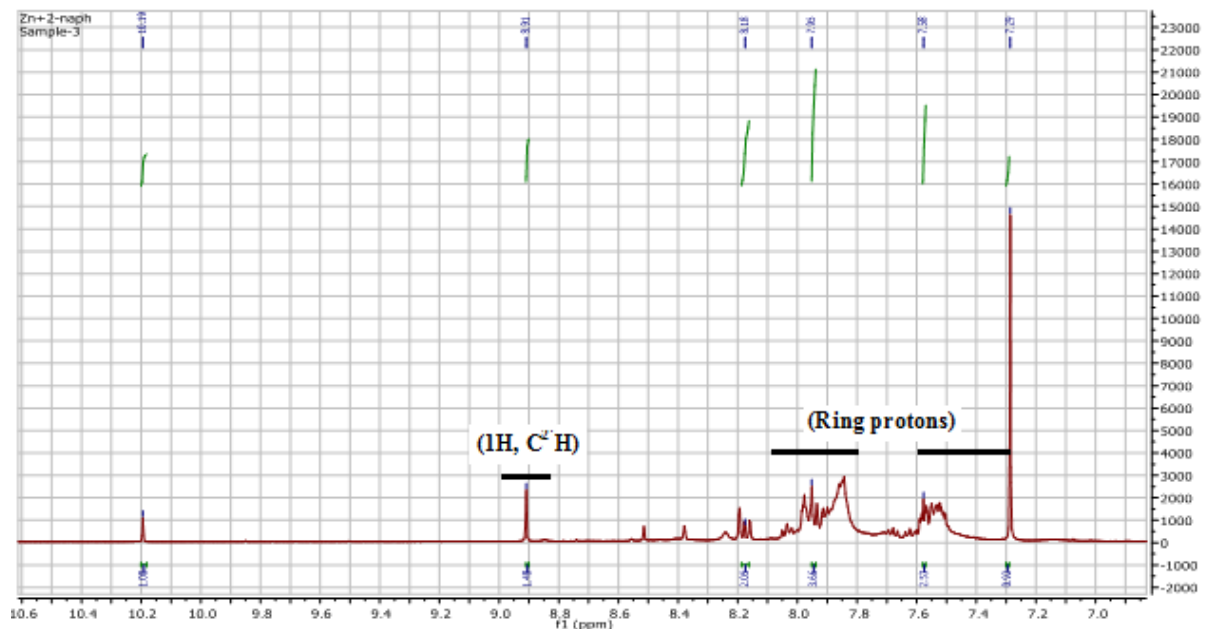


Figure 9.3.1.7 b) ¹H NMR spectrum of complex 70(expansion form)

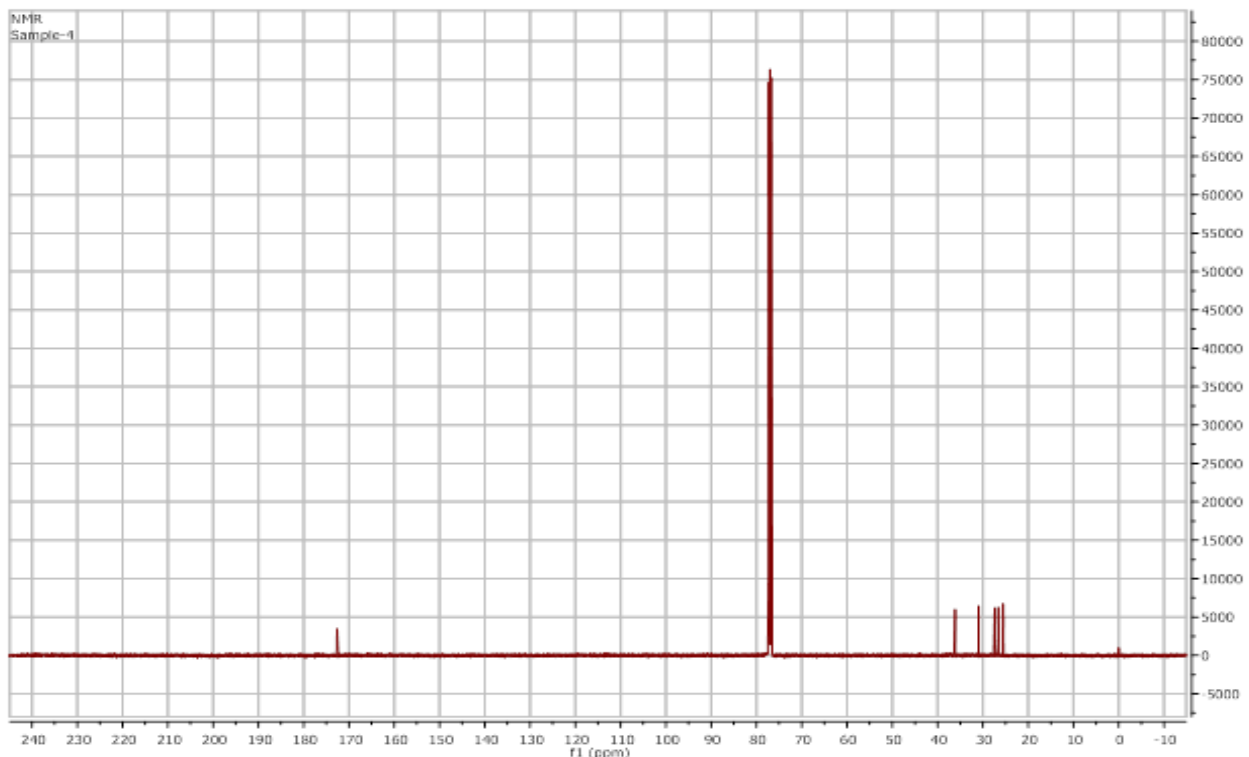


Figure 9.3.2.1a) ^{13}C NMR spectrum of complex **57**

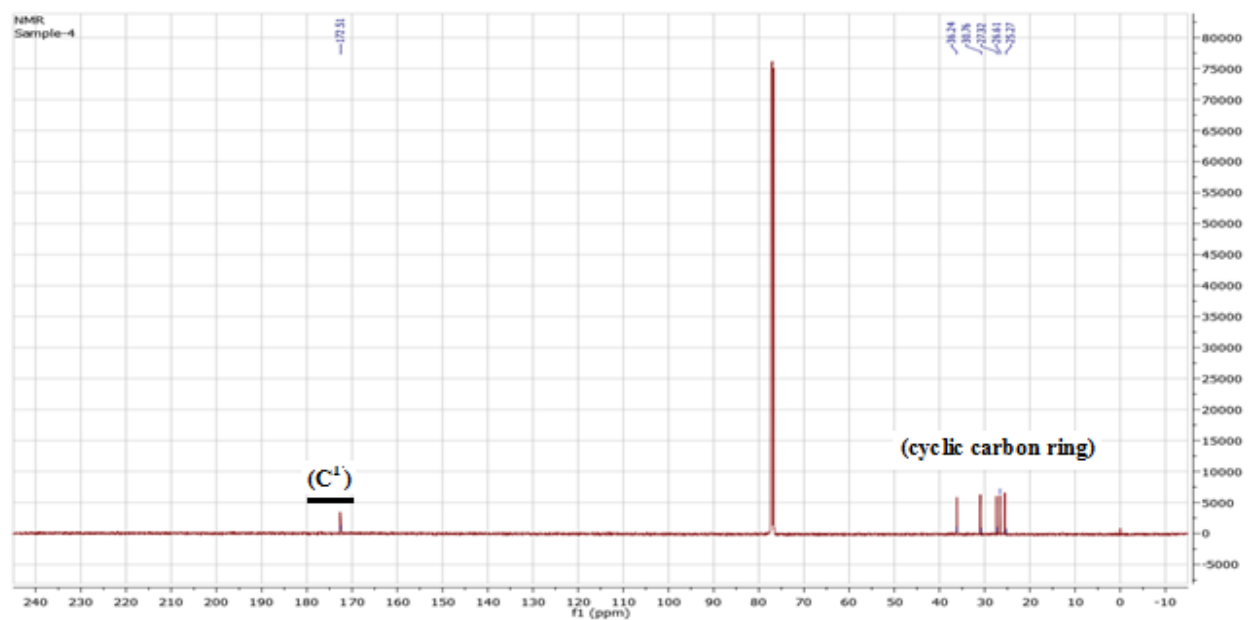


Figure 9.3.2.1b) ^{13}C NMR spectrum with full view of complex **57**

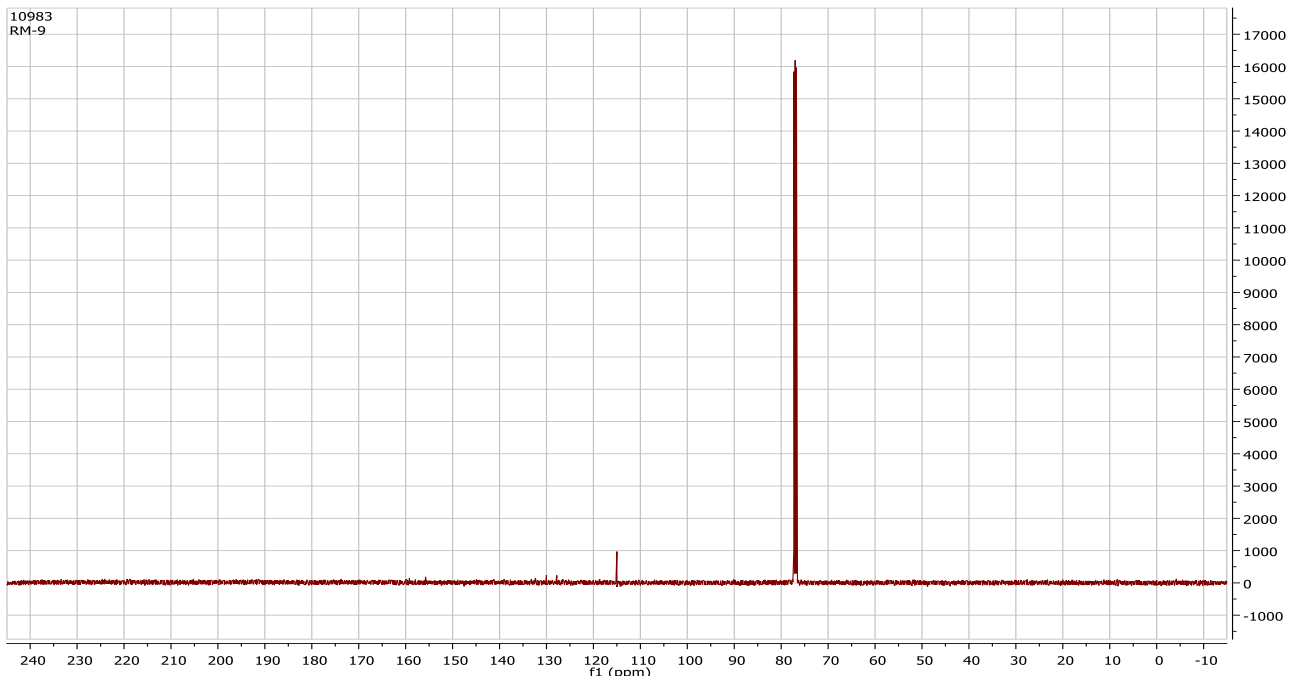


Figure 9.3.2.2a) ¹³C NMR spectrum of complex **59**

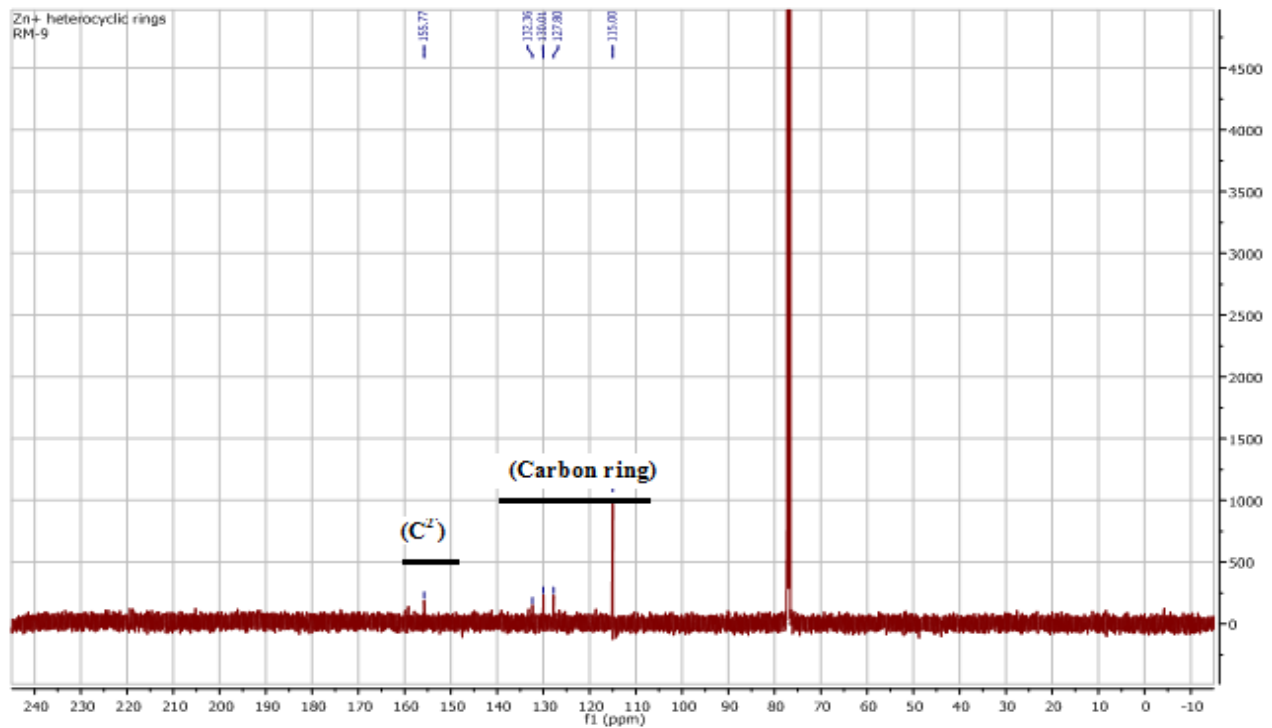


Figure 9.3.2.2b) ¹³C NMR spectrum with full view of complex **59**

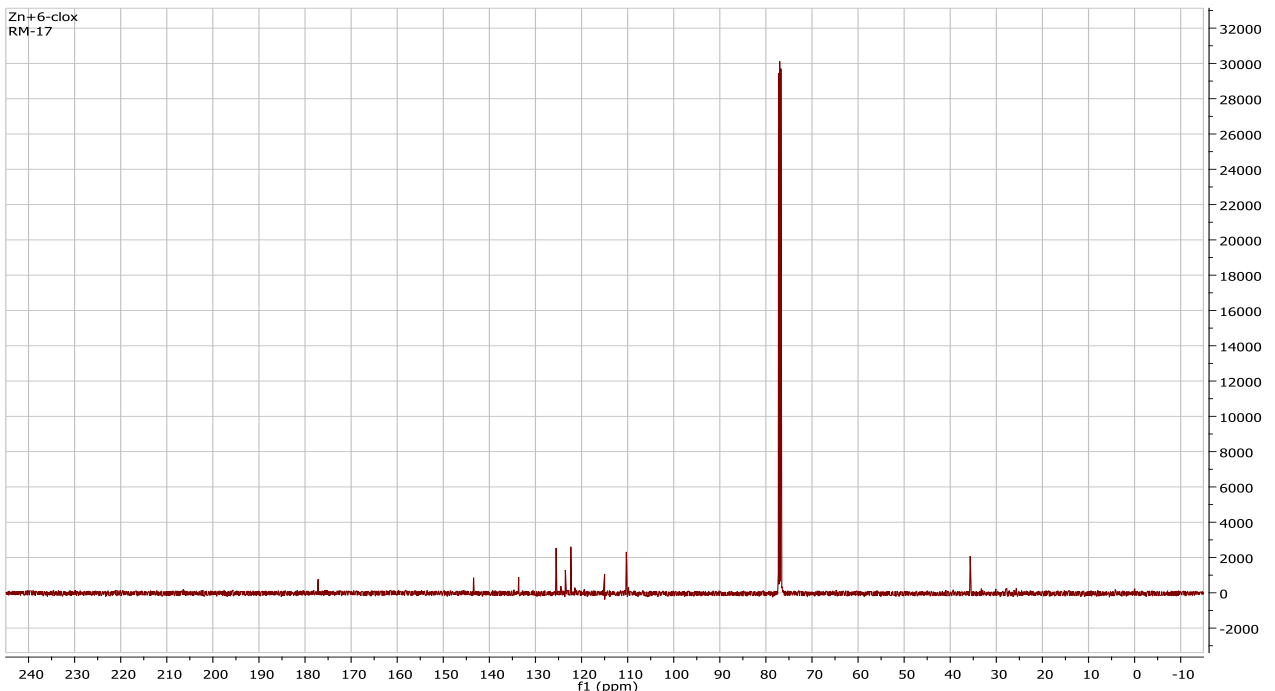


Figure 9.3.2.3a) ¹³C NMR spectrum of complex **63**

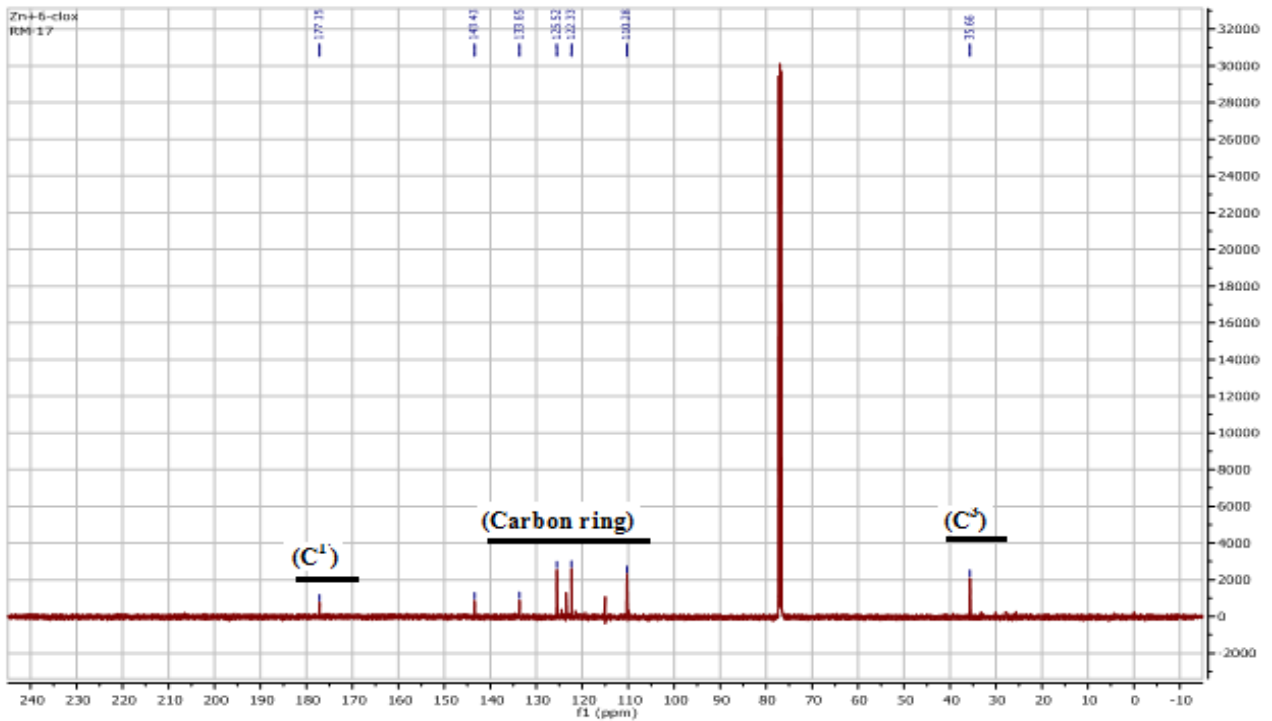


Figure 9.3.2.3b) ¹³C NMR spectrum with full view of complex **63**

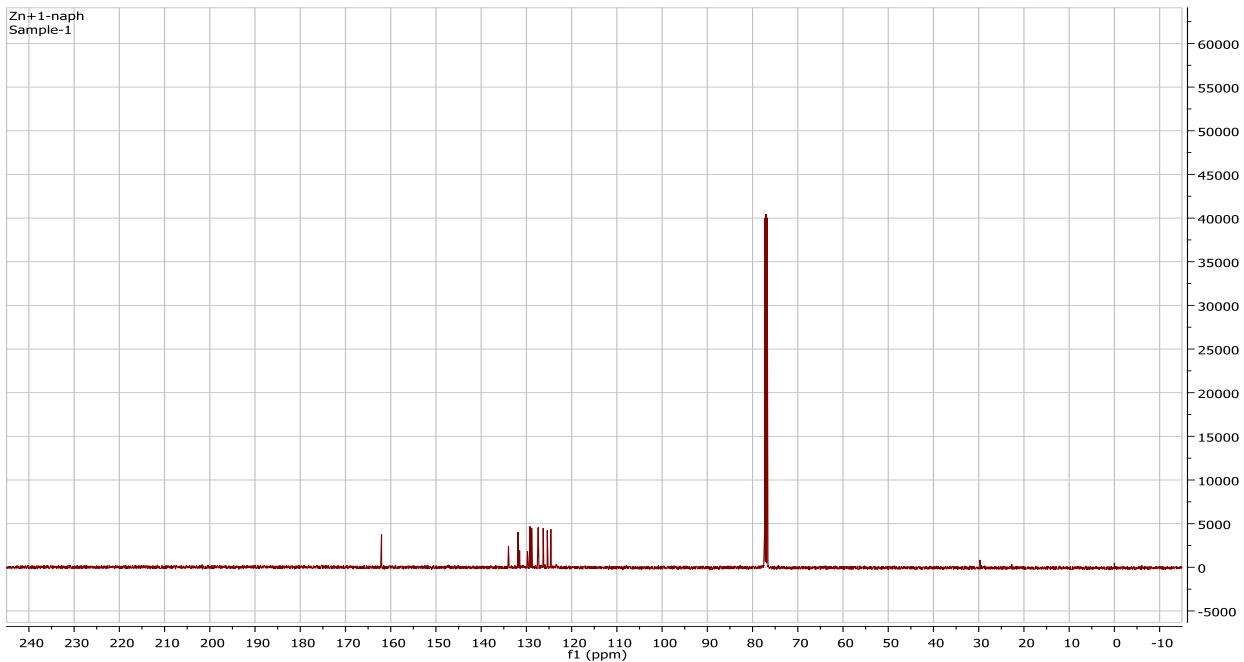


Figure 9.3.2.4 a) ^{13}C NMR spectrum of complex **69**

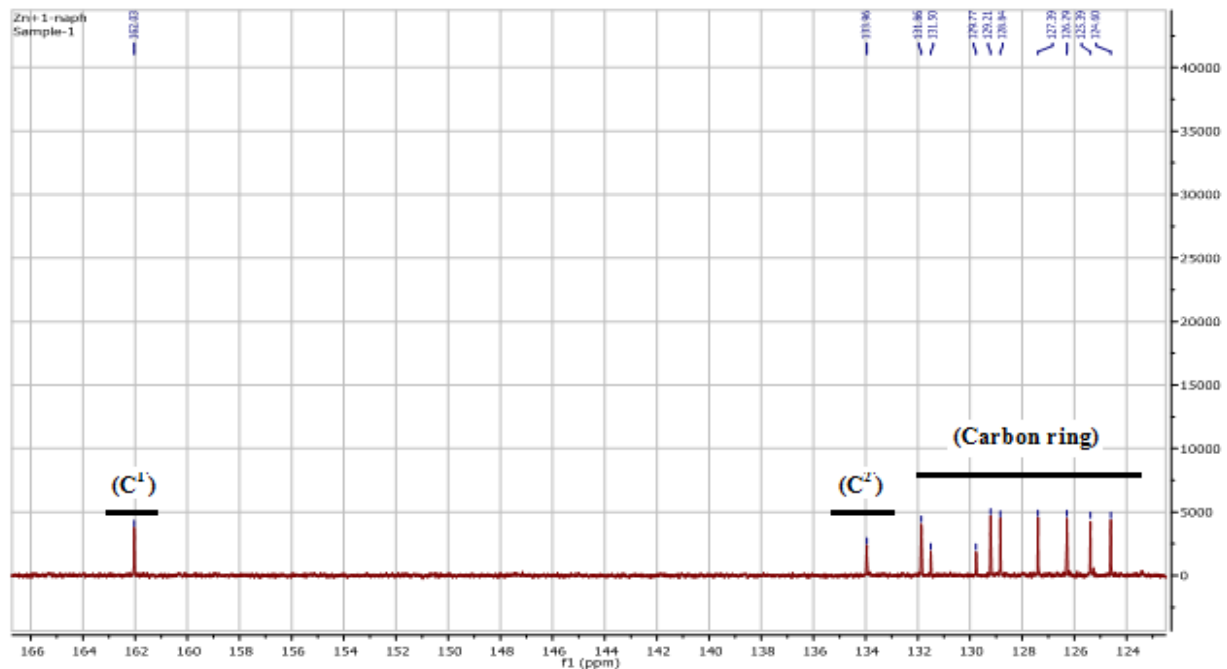


Figure 9.3.2.4b) ^{13}C NMR spectrum of complex **69**(expansion form)

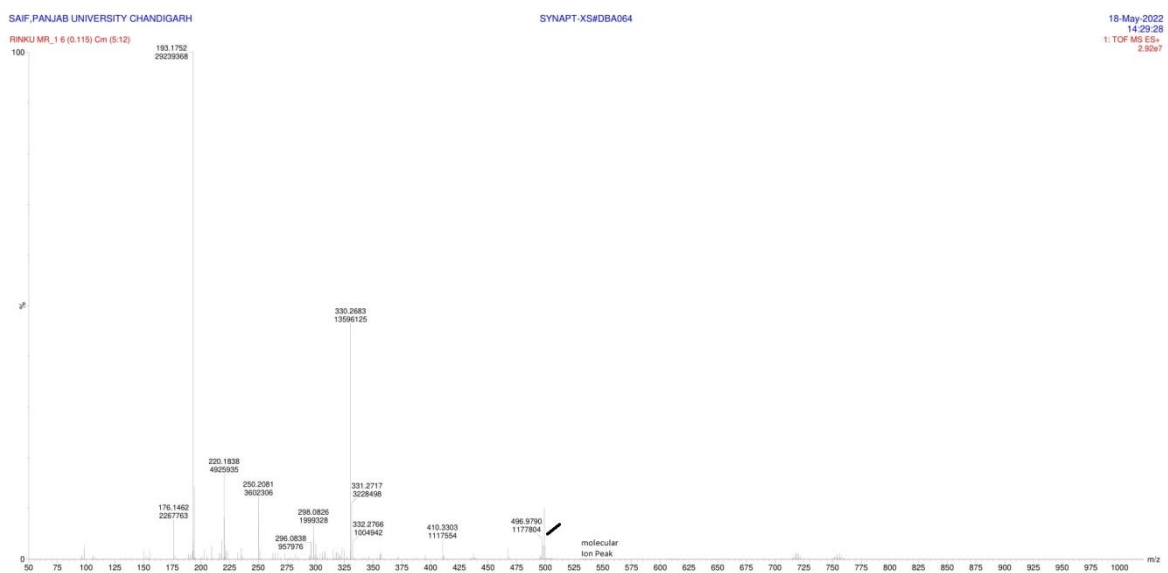


Figure 9.4.1 a) Mass Spectrum of $[Zn(\text{cysesc})_2]57$

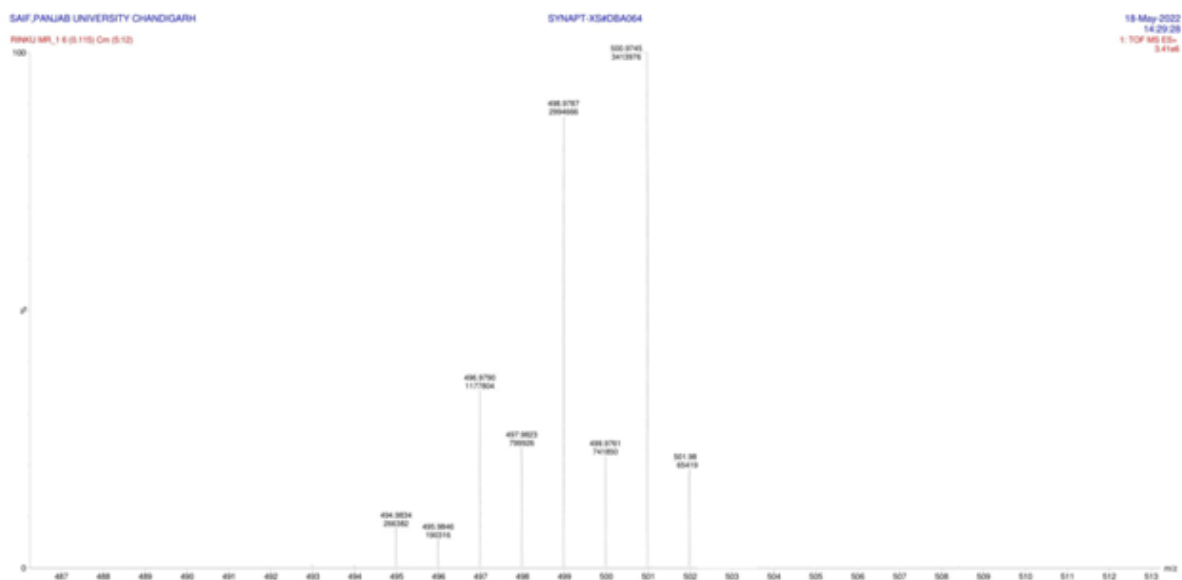


Figure 9.4.1 b) Mass Spectrum of $[Zn(\text{cysesc})_2]57$



Figure 9.4.2 Mass Spectrum of $[\text{Zn}(2\text{-fursesc})_2]58$

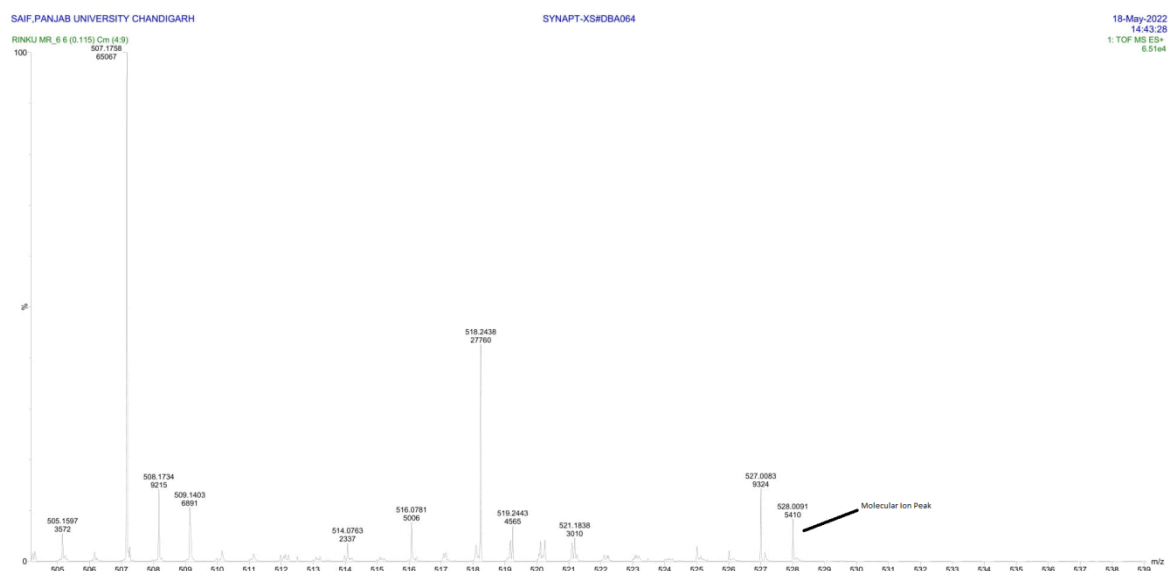


Figure 9.4.3 Mass Spectrum of $[\text{Zn}(2\text{-thiosesc})_2]59$

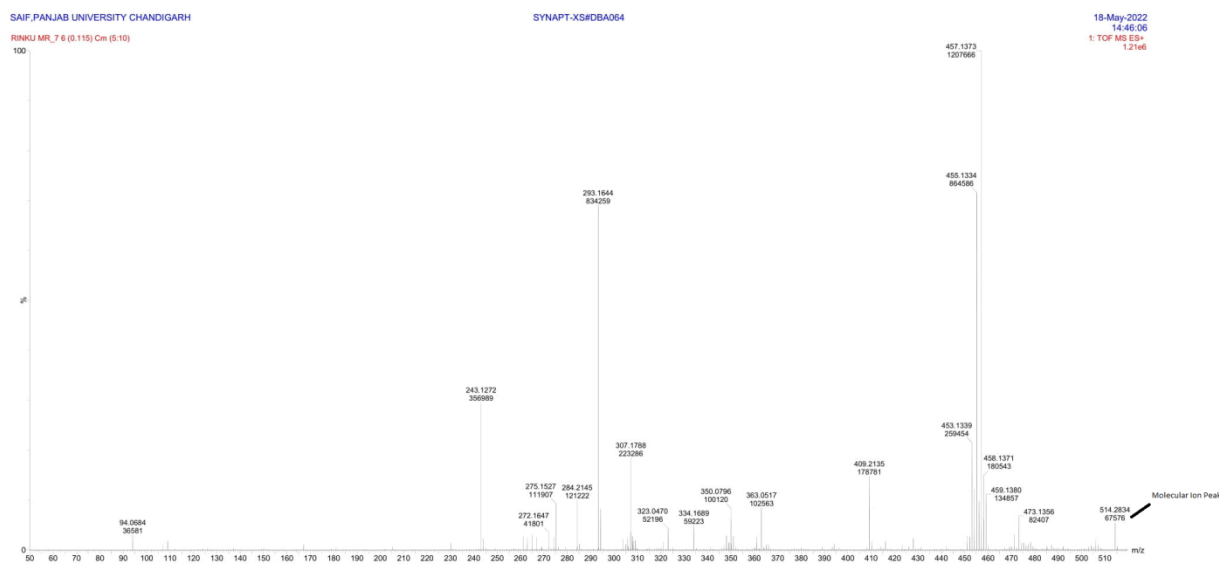


Figure 9.4.4 Mass Spectrum of $[Zn(N\text{-}mepysesc)_2]60$

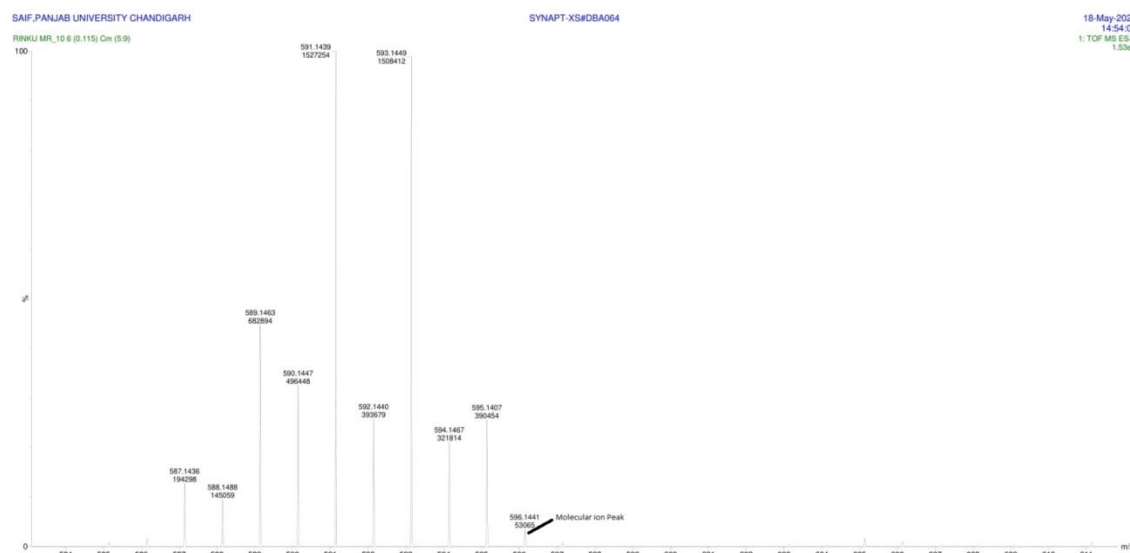


Figure 9.4.5 Mass Spectrum of $[Zn(3\text{-}meoxsesc)_2]61$

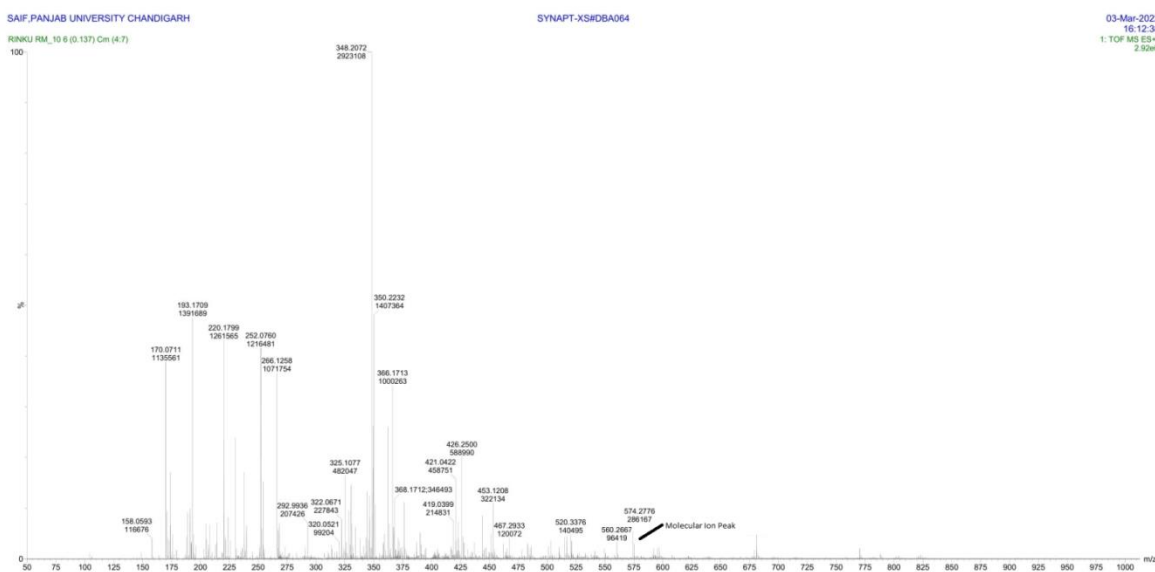


Figure 9.4.6 Mass Spectrum of $[Zn(2\text{-oxsesc})_2]62$

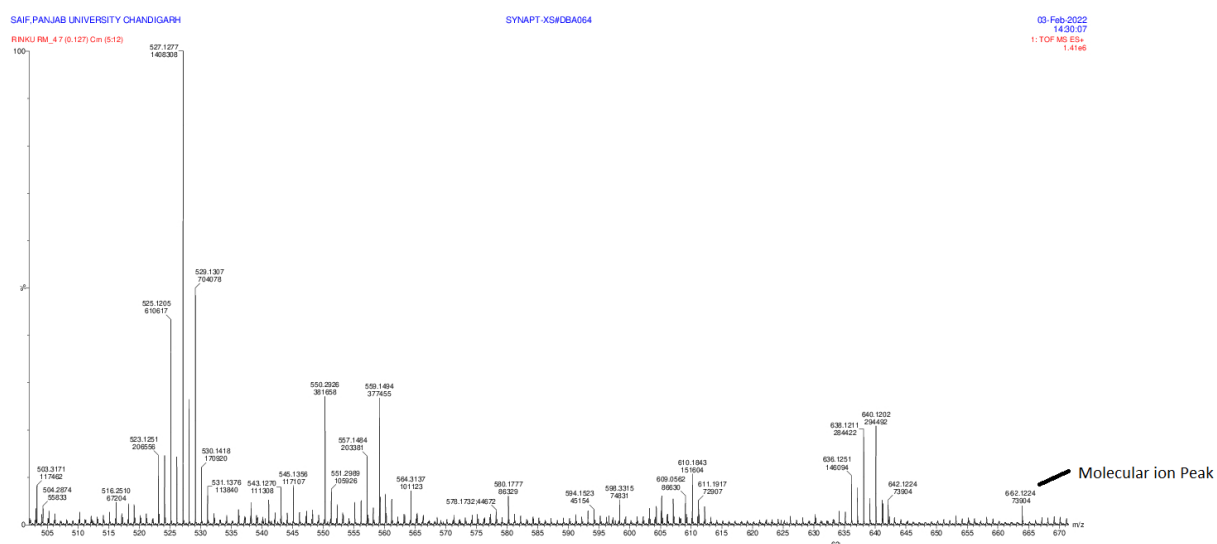


Figure 9.4.7 Mass Spectrum of $[Zn(5\text{-clistsesc})_2]64$

SAIF,PANJAB UNIVERSITY CHANDIGARH
RINKU_M.R_8.6 (0.110) Cm (5.9)
100 556.2927
58879

SYNAPT-XS#DBA064

18-May-2022
10:46:45
1: TOF MS ES+
5.89e4

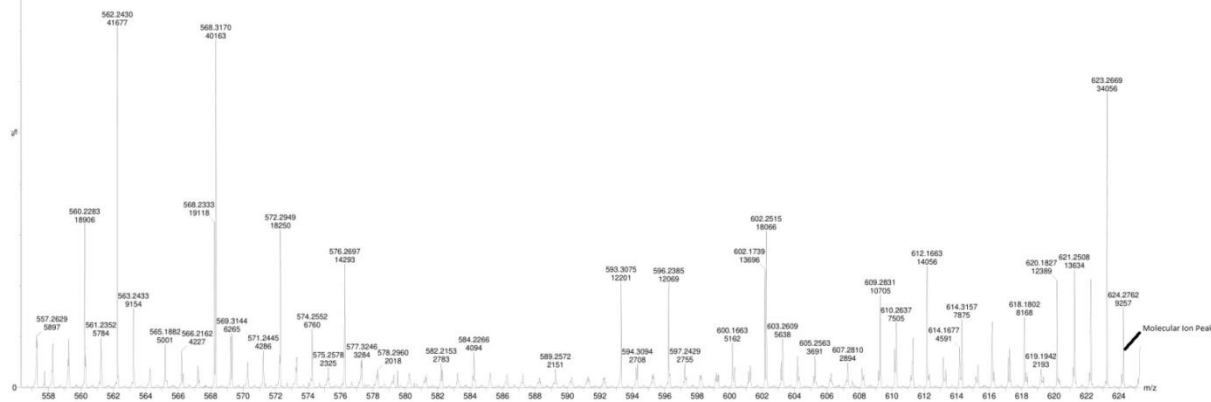


Figure 9.4.8 Mass Spectrum of $[Zn(1\text{-meistsesc})_2]65$

SAIF,PANJAB UNIVERSITY,CHANDIGARH
RINKU_M_7.5 (0.120) Cm (2.9)

SYNAPT-XS#DBA064

15-Nov-2022
10:46:25
1: TOF MS ES+
2.29e5

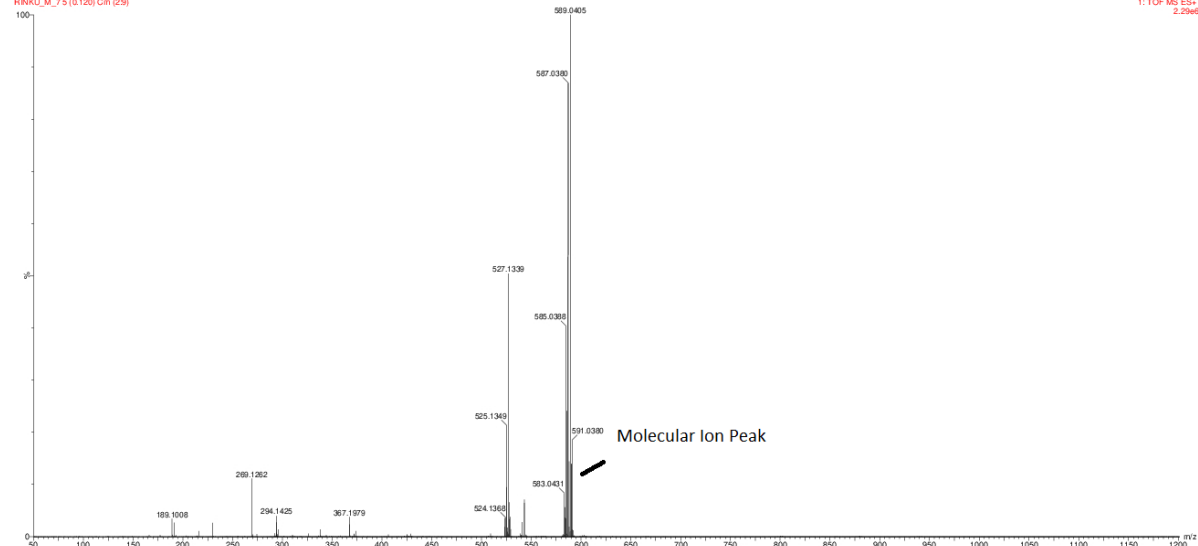


Figure 9.4.9 Mass Spectrum of $[Zn(3\text{-indsesc})_2]66$

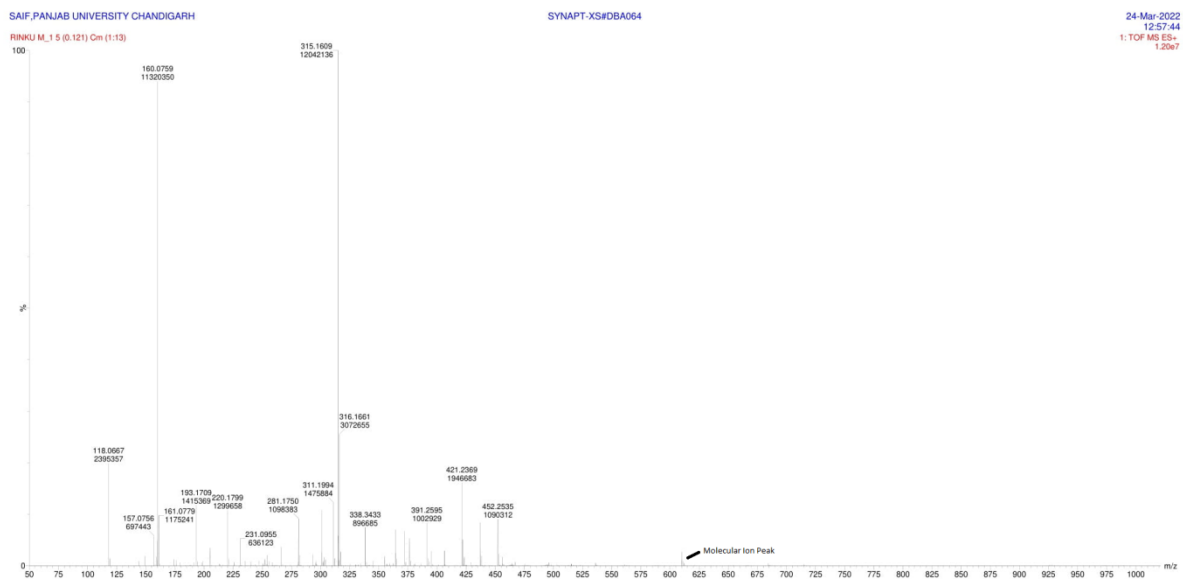


Figure 9.4.10 a) Mass Spectrum of $[Zn(3\text{-acindsesc})_2]67$

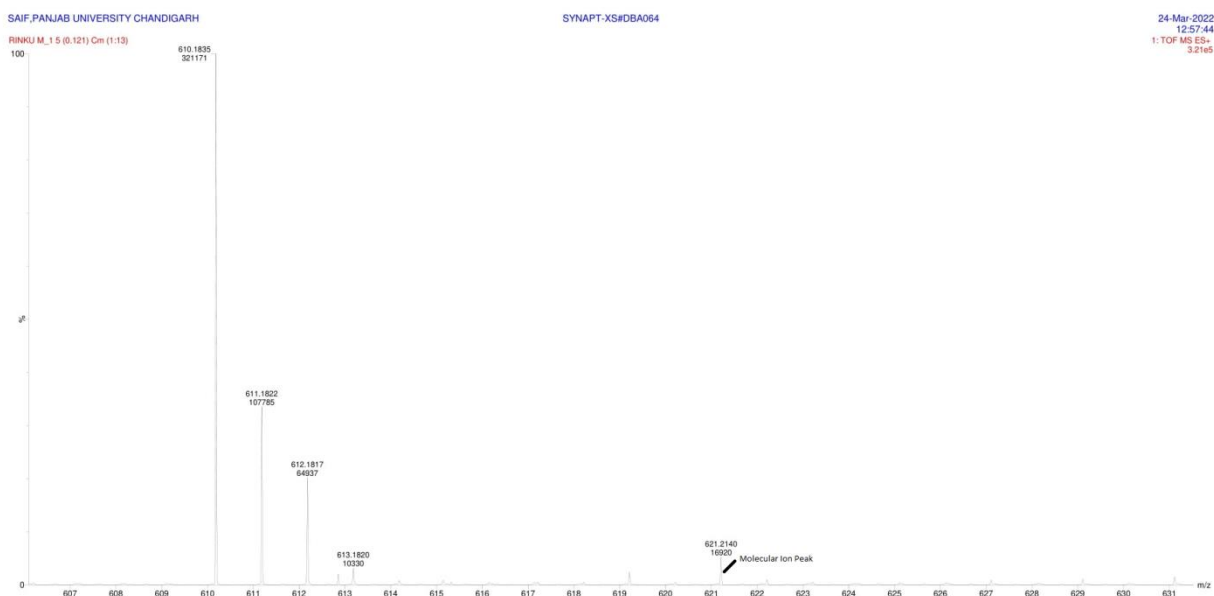


Figure 9.4.10 b) Mass Spectrum of $[Zn(3\text{-acindsesc})_2]67$

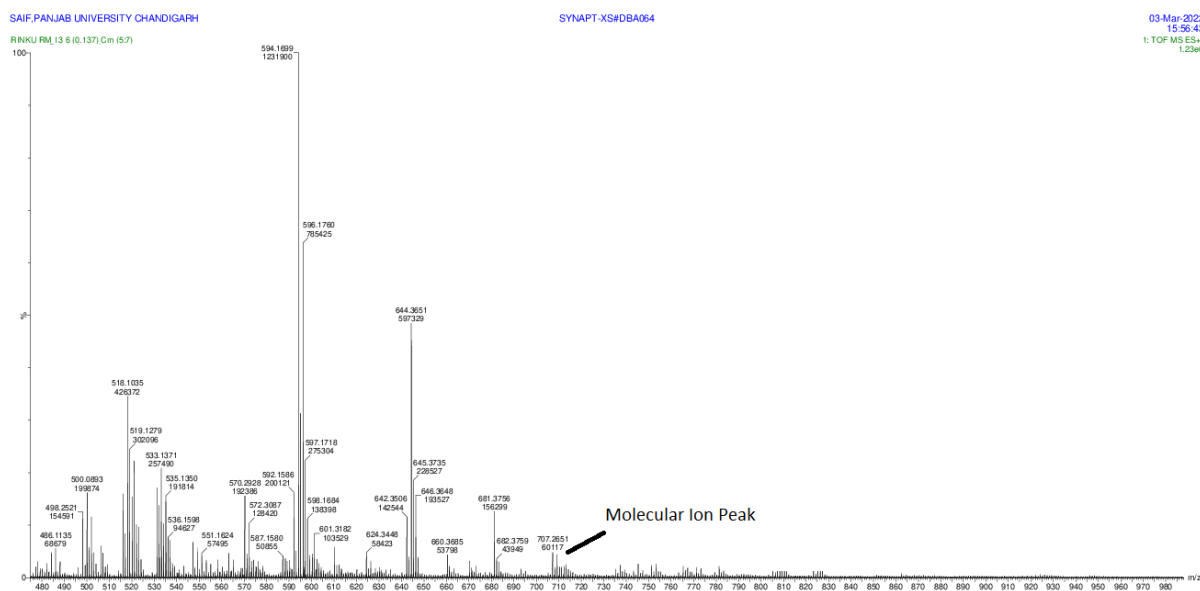


Figure 9.4.11 Mass Spectrum of $[Zn(9\text{-anthracesc})_2]68$

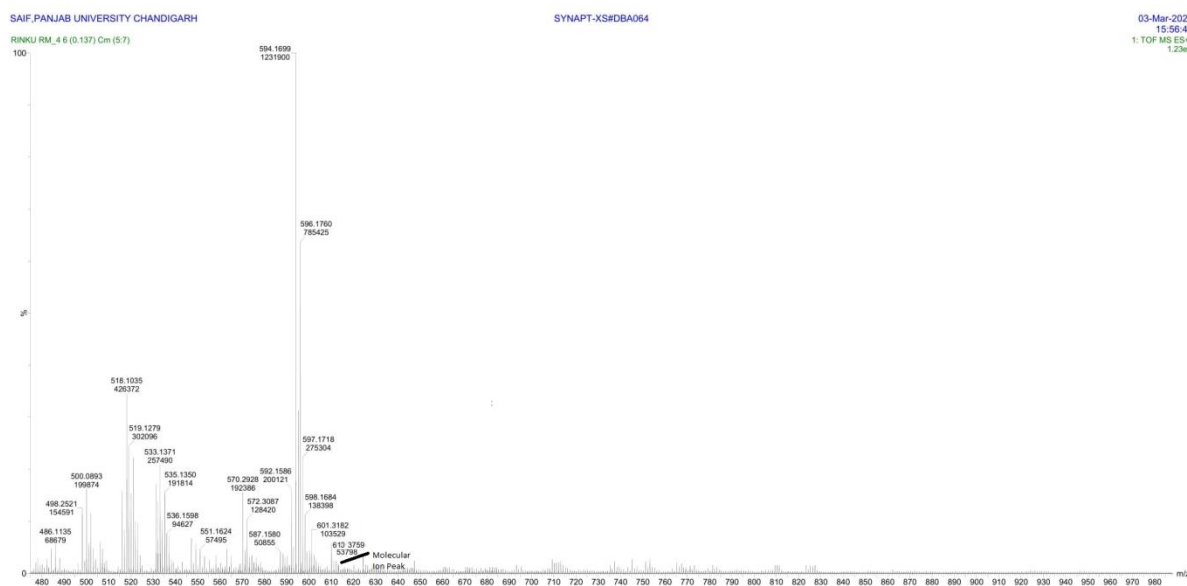


Figure 9.4.12 Mass Spectrum of $[Zn(1\text{-naphthesc})_2]69$

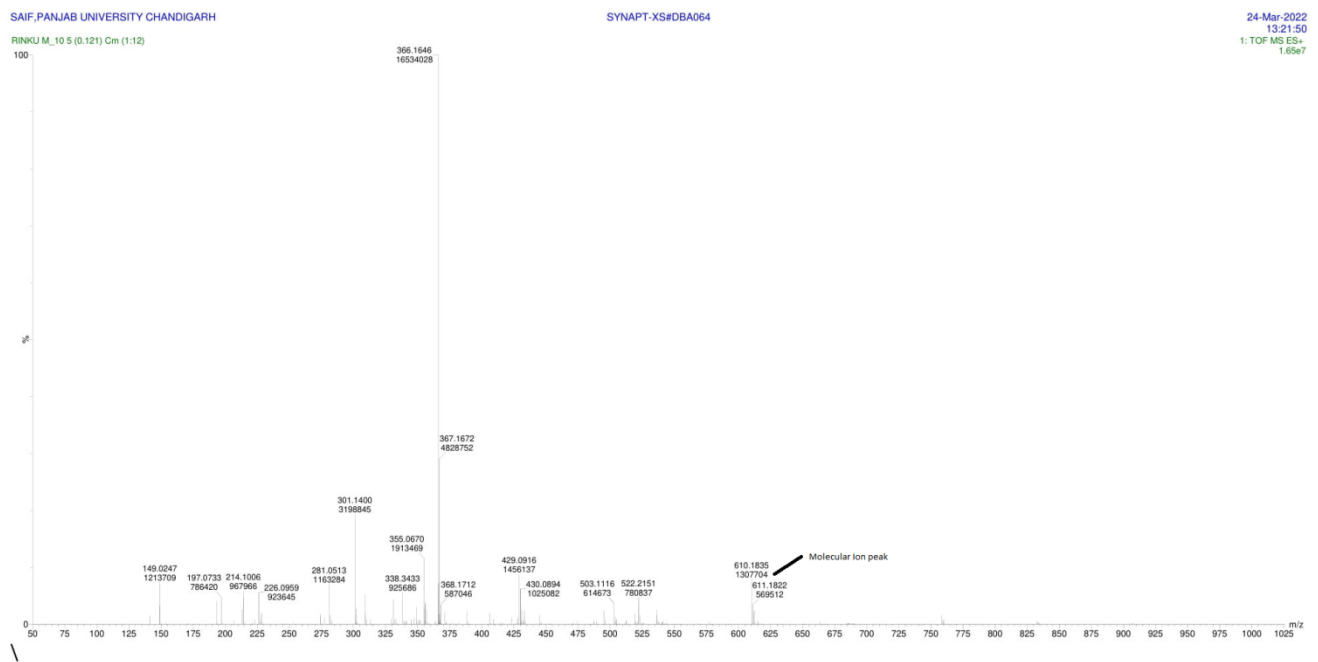


Figure 9.4.13 Mass Spectrum of $[Zn(2\text{-naphthsesc})_2]70$

CHAPTER 10

BIOLOGICAL ACTIVITIES

10.1 Anti M. Tuberculosis Activity:

Synthesized selenosemicarbazones and their metal complexes were tested for their anti-M Tuberculosis activity. Table 10.1.1 and 10.1.2 contains the list of ligands and complexes along with their numbering.

Table 10.1.1 List of selenosemicarbazones and their iron(III) and cobalt(II) complexes

Selenosemicarbazones	Iron(III)-complexes	Cobalt(II)-complexes
Hcysesc, H¹L	[Fe(cysesc) ₃] 1	[Co(cysesc) ₃] 15
2-Hfursesc, H²L	[Fe(2-fursesc) ₃] 2	[Co(2-fursesc) ₃] 16
2-Hthiosesc, H³L	[Fe(2-thiosesc) ₃] 3	[Co(2-thiosesc) ₃] 17
N-MeHpyesc, H⁴L	[Fe(N-mepysesesc) ₃] 4	[Co(N-mepysesesc) ₃] 18
3-MeHOxsesc, H⁵L	[Fe(3-meoxsesc) ₃] 5	[Co(3-meoxsesc) ₃] 19
2-HOxsesc, H⁶L	[Fe(2-oxsesc) ₃] 6	[Co(2-oxsesc) ₃] 20
6-ClHOxsesc, H⁷L	[Fe(6-cloxsesc) ₃] 7	[Co(6-cloxsesc) ₃] 21
5-ClHIstsesc, H⁸L	[Fe(5-clistsesc) ₃] 8	[Co(5-clistsesc) ₃] 22
1-MeHIstsesc, H⁹L	[Fe(1-meistsesc) ₃] 9	[Co(1-meistsesc) ₃] 23
3-HIndsesc, H¹⁰L	[Fe(3-insesc) ₃] 10	[Co(3-insesc) ₃] 24
3-AcHIndsesc, H¹¹L	[Fe(3-acinsesc) ₃] 11	[Co(3-acinsesc) ₃] 25
9-HAnsesc, H¹²L	[Fe(9-ansesc) ₃] 12	[Co(9-ansesc) ₃] 26
1-HNapsesc, H¹³L	[Fe(1-naphsesc) ₃] 13	[Co(1-naphsesc) ₃] 27
2-HNapsesc, H¹⁴L	[Fe(2-naphsesc) ₃] 14	[Co(2-naphsesc) ₃] 28

Table 10.1.2 List of nickel(II), copper(II) and zinc(II) complexes

Nickel(II)-complexes	Copper(II)-complexes	Zinc(II)-complexes
[Ni(cysesc) ₂] 29	[Cu(cysesc) ₂] 43	[Zn(cysesc) ₂] 57
[Ni(2-fursesc) ₂] 30	[Cu(2-fursesc) ₂] 44	[Zn(2-fursesc) ₂] 58
[Ni(2-thiosesc) ₂] 31	[Cu(2-thiosesc) ₂] 45	[Zn(2-thiosesc) ₂] 59
[Ni(N-mepysesc) ₂] 32	[Cu(N-mepysesc) ₂] 46	[Zn(N-mepysesc) ₂] 60
[Ni(3-meoxsesc) ₂] 33	[Cu(3-meoxsesc) ₂] 47	[Zn(3-meoxsesc) ₂] 61
[Ni(2-oxsesc) ₂] 34	[Cu(2-oxsesc) ₂] 48	[Zn(2-oxsesc) ₂] 62
[Ni(6-cloxsesc) ₂] 35	[Cu(6-cloxsesc) ₂] 49	[Zn(6-cloxsesc) ₂] 63
[Ni(5-clistsesc) ₂] 36	[Cu(5-clistsesc) ₂] 50	[Zn(5-clistsesc) ₂] 64
[Ni(1-meistsesc) ₂] 37	[Cu(1-meistsesc) ₂] 51	[Zn(1-meistsesc) ₂] 65
[Ni(3-insesc) ₂] 38	[Cu(3-insesc) ₂] 52	[Zn(3-insesc) ₂] 66
[Ni(3-acinsesc) ₂] 39	[Cu(3-acinsesc) ₂] 53	[Zn(3-acinsesc) ₂] 67
[Ni(9-ansesc) ₂] 40	[Cu(9-ansesc) ₂] 54	[Zn(9-ansesc) ₂] 68
[Ni(1-naphsesc) ₂] 41	[Cu(1-naphsesc) ₂] 55	[Zn(1-naphsesc) ₂] 69
[Ni(2-naphsesc) ₂] 42	[Cu(2-naphsesc) ₂] 56	[Zn(2-naphsesc) ₂] 70

The antimycobacterial activity of compounds (**H¹L-H¹⁴L**) and complexes **1-70** were assessed against *M. tuberculosis* using a microplate Alamar Blue assay (MABA) [34]. This methodology is non-toxic and uses a thermally stable reagent and shows good correlation with proportional and BACTEC radiometric methods. Briefly, 200 µl of sterile de-ionized water was added to all outer perimeter wells of a sterile 96 wells-plate to minimize evaporation of the medium in the test-wells during incubation. The 96 wells-plate received 100 µl of the Middlebrooks 7H9 broth and a serial dilution of the compounds was carried out directly on the plate. The final drug concentrations were tested at 100 to 0.2µg/ml. Each test was carried out in triplicate. Plates were covered and sealed with para film and incubated at 37°C for five days in sealed plastic bags with 5% CO₂ atmosphere. After this time, 25 µl of a freshly prepared 1:1 mixture of Almar Blue reagent and 10% tween 80 was added to the plate and incubated for 24 h. A blue color in the well was interpreted as no bacterial growth, and a pink color was scored as growth. Pyrazinamide, ciprofloxacin and streptomycin were included as markers for standard drugs [179,180]. The acceptable range (MIC) of the standard drugs used 3.125µg/ml, 3.125µg/ml and 6.25µg/ml, respectively.

10.1.1 Anti M. Tuberculosis activity of selenosemicarbazones (H^1L - H^{14}L)

The MIC values of selenosemicarbazones (H^1L - H^{14}L) are given in Table 10.1.3. Hcysesc (H^1L), 2-Hthiosesc (H^3L), 1-MeHlstsesc (H^9L), 9-HAnsesc (H^{12}L), 1-HNapsesc (H^{13}L) and 2-HNapsesc (H^{14}L) are found to be most active (MIC = 1.6 μg /mL). Presence of fused benzene rings in H^{12}L , H^{13}L and H^{14}L may have enhanced the lipophilicity of the ligands, which thus facilitated the permeability of these ligands through the lipid rich bacterial wall and increased anti-microbial activity. Lipophilicity of H^9L is also more than its chloro-substituent due to the presence of methyl group at N-atom atom of isatin ring, thus increasing the permeability of H^9L through lipid rich wall of bacteria. Sulfur atom at thiophene ring of H^3L have tendency for intermolecular interactions with amino acids of bacterial cell wall thus capable of inhibiting bacterial growth. The small size of H^1L as compare to other selenosemicarbazones has an advantage for its movement inside the bacterial cell wall and responsible for its high antiM.tuberculosis activity. Their anti-TB activities are similar to standard drugs Isoniazid, Ethambutol (MIC = 1.6 $\mu\text{g}/\text{ml}$) and more than Pyrazinamide (MIC = 3.125 $\mu\text{g}/\text{mL}$).

Table 10.1.3 Anti-tubercular activity of selenosemicarbazones (H^1L - H^{14}L)

S.No	Compound	Mycobacterium tuberculosis H37RV strain							
		100	50	25	12.5	6.25	3.12	1.6	0.8
1.	H^1L	S	S	S	S	S	S	S	R
2.	H^2L	S	R	R	R	R	R	R	R
3.	H^3L	S	S	S	S	S	S	S	R
4.	H^4L	S	S	R	R	R	R	R	R
5.	H^5L	S	S	S	S	S	S	R	R
6.	H^6L	S	S	S	S	S	R	R	R
7.	H^7L	S	S	S	S	S	S	R	R
8.	H^8L	S	S	S	R	R	R	R	R
9.	H^9L	S	S	S	S	S	S	S	R
10.	H^{10}L	S	S	S	R	R	R	R	R
11.	H^{11}L	S	S	S	R	R	R	R	R
12.	H^{12}L	S	S	S	S	S	S	S	R
13.	H^{13}L	S	S	S	S	S	S	S	R
14.	H^{14}L	S	S	S	S	S	S	S	R
15.	Isoniazid*	S	S	S	S	S	S	S	R
16.	Ethambutol*	S	S	S	S	S	S	S	R
17.	Pyrazinamide*	S	S	S	S	S	S	R	R

* = Control

S= Sensitive, R = Resistant

Complexes of selenosemicarbazones (**H¹L-H¹⁴L**) with iron(III), cobalt(II), nickel(II), copper(II) and zinc(II) were also tested for their antiTB activity and MIC value obtained is given in Table 10.1.4. The antiTB activity of **H²L**, **H⁴L**, **H⁸L**, **H¹⁰L** and **H¹¹L** get enhanced on complexation. Enhancement in antiTB activity is more in case of **H¹¹L** (MIC = 25 µg/mL) and its nickel(II) complex (**39**) is found to be most active (MIC = 0.8 µg/mL). Its activity is even better than the standard drugs used Pyrazinamide (MIC = 3.125 µg/mL), Ethambutol (MIC = 1.6 µg/mL) and Isoniazid (MIC = 1.6 µg/mL). Amongst the various metals, copper(II) and nickel(II) complexes have shown better result.

Table 10.1.4 Anti-TB activity of selenosemicarbazones (**H¹L-H¹⁴L**) and their complexes (**1-70**)

Mycobacterium tuberculosis H37RV strain						
MIC (µg /mL)	HL	[Fe(L) ₃]	[Co(L) ₂]	[Ni(L) ₂]	[Cu(L) ₂]	[Zn(L) ₂]
Hcysesc, H¹L	1.6	12.5	12.5	3.12	12.5	100
2-Hfursesc, H²L	100	25	25	50	12.5	100
2-Httsesc, H³L	1.6	6.25	25	12.5	25	12.5
N-MeHPysesc, H⁴L	50	3.12	3.12	50	25	0.8
3-MeHOxsesc, H⁵L	1.6	3.12	25	1.6	25	3.12
2-HOxsesc, H⁶L	6.25	25	12.5	12.5	6.25	25
6-ClHOxsesc, H⁷L	3.12	12.5	12.5	3.12	12.5	100
5-ClHIsesc, H⁸L	25	12.5	12.5	1.6	12.5	1.6
1-MeHIsesc, H⁹L	1.6	3.12	12.5	1.6	12.5	6.25
3-HIndses, H¹⁰L	25	3.12	12.5	50	25	6.25
3-AcHIndses, H¹¹L	25	6.25	12.5	0.8	12.5	1.6
9-HAnsesc, H¹²L	1.6	1.6	12.5	12.5	12.5	100
1-HNapsesc, H¹³L	1.6	25	25	12.5	100	50
2-HNapsesc, H¹⁴L	1.6	100	100	1.6	1.6	100

10.2 Anticancer activity:

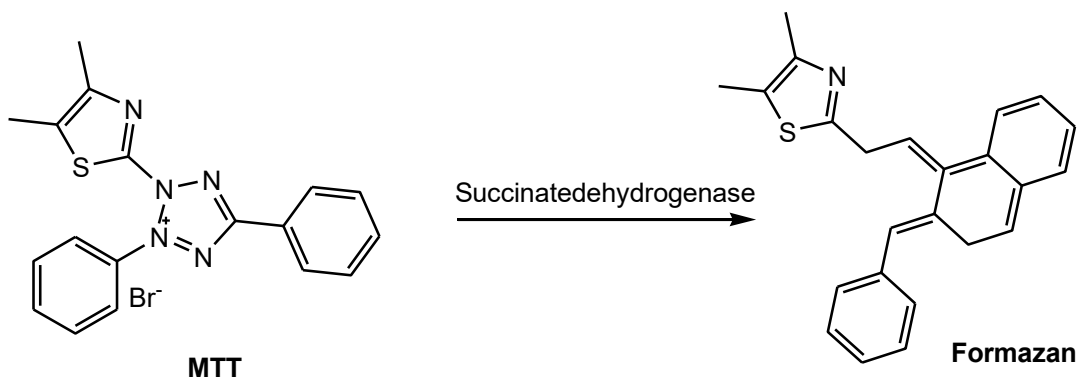
It has been observed from literature survey that selenosemicarbazone with fused ring and their complexes of nickel(II) and zinc(II) have shown good anticancer activities against various cell lines, thus in current research work, only fused ring selenosemicarbazones (H^5L - $H^{14}L$), cyclohexanone selenosemicarbazone (H^1L)and their complexes with nickel(II) and zinc(II) has been considered for testing their anti-cancer activities activity against PA-1 (human ovarian cancer) and DU145 (human prostate cancer) cell lines. Doxorubicin was taken as control.

10.2.1 Cell culture

PA-1 (human ovarian cancer) and DU145 (human prostate cancer) cell lines were used to study the anticancer activity of selenosemicarbazone and their nickel(II) and zinc(II) complexes. Cell lines were maintained in Dulbecco's Modified Eagle Media (DMEM) with low glucose. To the medium 10% fetal bovine serum (Gibco, Invitrogen) and 1% antibiotics (Antimycotic 100X, ThermoFisher Scientific) was added.

10.2.2 MTT assay

This is a colorimetric assay that measures the reduction of yellow 3-(4, 5-dimethylthiazol-2-yl)-2,5-diphenyl tetrazolium bromide (MTT) by mitochondrial succinate dehydrogenase. The MTT enters the cells and passes into the mitochondria where it is reduced to an insoluble, coloured (dark purple) formazan product (Scheme I). The cells are then solubilized with an organic solvent (eg. DMSO, Isopropanol), and the released, solubilized formazan reagent, (E, Z) -5- (4, 5- dimethylthiazol- 2- yl) - 1, 3- diphenylformazan is measured spectrophotometrically. Since reductions of MTT can only occur in metabolically active cells the level of activity is a measure of the viability of the cell.



Scheme 1

The cells were seeded in a 96-well flat-bottom microplate and maintained at 37°C in 95% humidity and 5% CO₂ overnight. Different concentration (100, 50, 25, 12.5, 6.25, 3.125 µg/ml) of samples were treated. The cells were incubated for another 48 hours. The wells were washed twice with PBS and 20 µL of the MTT staining solution was added to each well and the plate was incubated at 37°C. After 4h, 100 µL of DMSO was added to each well to dissolve the formazan crystals, and absorbance was recorded with a 570 nm using microplate reader [181-200]. The percentage survival cells were calculated using formula given below:

$$\text{Surviving cells (\%)} = \frac{\text{Mean OD of test compound}}{\text{Mean OD of Negative control}} \times 100$$

Sample codes used for selected selenosemicarbazones and their complexes are mentioned in the table 10.2.1.

Table 10.2.1 Sample codes of selenosemicarbazones and their complexes for anticancer activity

S. No	Compound	Sample Code
1.	Cyclohexanone selenosemicarbazone, Hcysesc (H¹L)	C1
2.	3-methyl-2-oxindole selenosemicarbazone, 3-MeHOxsesc(H⁵L)	C2
3.	2-oxindole selenosemicarbazone, 2-HOxsesc(H⁶L)	C3
4.	6-chloro-2-oxindole selenosemicarbazone, 6-ClHOxsesc (H⁷L)	C4
5.	5-chloro isatin selenosemicarbazone, 5-ClHIstsesesc(H⁸L)	C5
6.	1-methyl isatin selenosemicarbazone, 1-MeHIstsesesc(H⁹L)	C6
7.	indole-3-selenosemicarbazone, 3-HIndsesesc (H¹⁰L)	C7
8.	3-acetyl indoleselenosemicarbazone, 3-AcHIndsesesc(H¹¹L)	C8
9.	9-anthraldehyde selenosemicarbazone, 9-HAnsesc(H¹²L)	C9
10.	1-Naphthaldehyde selenosemicarbazone, 1-HNapsesc(H¹³L)	C10
11.	2-Naphthaldehyde selenosemicarbazone, 2-HNapsesc(H¹⁴L)	C11
12.	[Ni(3-MeOxsesc) ₂] 33	RC1
13.	[Zn(3-MeOxsesc) ₂] 61	RC2
14.	[Ni(2-Oxsesc) ₂] 34	RC3
15.	[Zn(2-Oxsesc) ₂] 62	RC4

16.	[Ni(6-ClOxsesc) ₂] 35	RC5
17.	[Zn(6-ClOxsesc) ₂] 63	RC6
18.	[Ni(1-MeIstsesc) ₂] 37	RC7
19.	[Zn(1-MeIstsesc) ₂] 65	RC8
20.	[Ni(3-Indsesc) ₂] 38	RC9
21.	[Zn(3-Indsesc) ₂] 66	RC10
22.	[Ni(9-HAnsesc) ₂] 40	RC11
23.	[Zn(9-HAnsesc) ₂] 68	RC12
24.	[Ni(1-Napsesc) ₂] 41	RC13
25.	[Zn(1-Napsesc) ₂] 69	RC14
26.	[Ni(cysesc) ₂] 29	RC15
27.	[Zn(cysesc) ₂] 57	RC16
28.	[Ni(3-AcIndsesc) ₂] 39	RC1*
29.	[Ni(5-ClIstsesc) ₂] 36	RC2*
30.	[Zn(5-ClIstsesc) ₂] 64	RC3*
31.	[Ni(2-Napsesc) ₂] 42	RC4*
32.	[Zn(2-Napsesc) ₂] 70	RC5*

* Samples sent in second slot

The anticancer activity of all the compounds was tested in triplicates (Annexure 1). IC₅₀ value of compounds was calculated using graph Pad Prism Version 5.1. IC₅₀ value of free ligands and their nickel(II) and zinc(II) complexes against PA-1 and DU145 is given in Table 10.2.2 and 10.2.3 respectively.

Table 10.2.2 IC₅₀ value of free ligands and their nickel(II) and zinc(II) complexes against PA-1

IC ₅₀ values (μg/ml)				IC ₅₀ values (μg/ml)			
Compound	Sample code	Mean	SD	Compound	Sample code	Mean	SD
H ¹ L	C1	12.70	0.22	[Ni(¹ L) ₂] 29	RC15	2.48	0.25
H ⁵ L	C2	8.42	0.30	[Ni(⁵ L) ₂] 33	RC1	8.29	0.25
H ⁶ L	C3	1.76	0.04	[Ni(⁶ L) ₂] 34	RC3	1.41	0.05
H ⁷ L	C4	6.80	0.10	[Ni(⁷ L) ₂] 35	RC5	4.14	0.20
H ⁸ L	C5	5.57	0.06	[Ni(⁸ L) ₂] 36	RC5*	5.94	0.25
H ⁹ L	C6	7.91	0.11	[Ni(⁹ L) ₂] 37	RC7	4.23	0.09
H ¹⁰ L	C7	5.34	0.09	[Ni(¹⁰ L) ₂] 38	RC9	2.93	0.10
H ¹¹ L	C8	1.63	0.01	[Ni(¹¹ L) ₂] 39	RC1*	1.99	0.05
H ¹² L	C9	3.72	0.07	[Ni(¹² L) ₂] 40	RC11	2.57	0.05
H ¹³ L	C10	6.51	0.11	[Ni(¹³ L) ₂] 41	RC13	1.28	0.04
H ¹⁴ L	C11	3.22	0.02	[Ni(¹⁴ L) ₂] 42	RC4*	7.73	0.77
[Zn(¹ L) ₂] 57	RC16	3.12	0.04	[Zn(¹⁰ L) ₂] 66	RC10	4.91	0.15
[Zn(⁵ L) ₂] 61	RC2	5.94	0.05	[Zn(¹¹ L) ₂] 67	-	-	-
[Zn(⁶ L) ₂] 62	RC4	3.22	0.10	[Zn(¹² L) ₂] 68	RC12	2.32	0.08
[Zn(⁷ L) ₂] 63	RC6	6.10	0.21	[Zn(¹³ L) ₂] 69	RC14	1.26	0.01
[Zn(⁸ L) ₂] 64	RC3*	3.51	0.04	[Zn(¹⁴ L) ₂] 70	RC5*	5.94	0.25
[Zn(⁹ L) ₂] 65	RC8	1.30	0.03	Doxorubicin		1.60	0.06

Table 10.2.3 IC₅₀ value of free ligands and their nickel(II) and zinc(II) complexes against DU145

IC ₅₀ values (μg/ml)				IC ₅₀ values (μg/ml)			
Compound	Sample code	Mean	SD	Compound	Sample code	Mean	SD
H ¹ L	C1	22.107	0.368	[Ni(¹ L) ₂] 29	RC15	6.25	1.35
H ⁵ L	C2	3.179	0.021	[Ni(⁵ L) ₂] 33	RC1	7.48	0.56
H ⁶ L	C3	13.747	0.318	[Ni(⁶ L) ₂] 34	RC3	8.32	0.38
H ⁷ L	C4	9.565	0.178	[Ni(⁷ L) ₂] 35	RC5	3.83	0.78
H ⁸ L	C5	24.987	0.856	[Ni(⁸ L) ₂] 36	RC5*	22.71	0.29
H ⁹ L	C6	34.790	1.170	[Ni(⁹ L) ₂] 37	RC7	11.80	4.35
H ¹⁰ L	C7	6.094	0.182	[Ni(¹⁰ L) ₂] 38	RC9	6.97	0.18
H ¹¹ L	C8	72.053	0.972	[Ni(¹¹ L) ₂] 39	RC1*	4.63	0.08
H ¹² L	C9	4.463	0.004	[Ni(¹² L) ₂] 40	RC11	12.79	0.11
H ¹³ L	C10	10.427	0.204	[Ni(¹³ L) ₂] 41	RC13	8.67	0.04
H ¹⁴ L	C11	81.873	1.407	[Ni(¹⁴ L) ₂] 42	RC4*	23.63	0.51
[Zn(¹ L) ₂] 57	RC16	13.37	0.31	[Zn(¹⁰ L) ₂] 66	RC10	6.38	0.15
[Zn(⁵ L) ₂] 61	RC2	10.60	0.07	[Zn(¹¹ L) ₂] 67	-	-	-
[Zn(⁶ L) ₂] 62	RC4	7.69	3.05	[Zn(¹² L) ₂] 68	RC12	7.00	0.02
[Zn(⁷ L) ₂] 63	RC6	4.05	0.15	[Zn(¹³ L) ₂] 69	RC14	13.31	0.06
[Zn(⁸ L) ₂] 64	RC3*	4.43	0.30	[Zn(¹⁴ L) ₂] 70	RC5*	22.71	0.29
[Zn(⁹ L) ₂] 65	RC8	3.29	0.07	Doxorubicin		3.60	0.16

All the ligands exhibit very good anti-cancer activity against PA-1 as compare to DU145. In case of anticancer activity against PA-1, amongst the various selenosemicarbazones, 2-oxindole selenosemicarbazone (H⁶L, IC₅₀, 1.76 μg/ml) and 3-acetyl indoleselenosemicarbazoe (H¹¹L, IC₅₀ 1.63 μg/ml) are most active compounds. Their activity is almost similar or close to the Doxorubicin (control, IC₅₀, 1.60 μg/ml). On complexation with zinc(II) or nickel(II) metals, anticancer activity of most of the selenosemicarbazones get enhanced against both the cell lines PA-1 and DU145. Selenosemicarbazone complexes of zinc(II) metal have shown better results than nickel(II). Complexes [Zn(⁹L)₂] **65** and [Zn(¹³L)₂] **69** have shown highest anticancer activity against PA-1 with IC₅₀ value of 1.30

$\mu\text{g}/\text{ml}$ and $1.26 \mu\text{g}/\text{ml}$ respectively. The anticancer activity of these complexes is even better than standard drug doxorubicin (IC_{50} , $1.60 \mu\text{g}/\text{ml}$).

A comparative studies of IC_{50} value of free ligands and their nickel(II) and zinc(II) complexes against PA-1 and DU145 is given in Table 10.2.4 and 10.2.5 respectively.

Table 10.2.4 Comparative studies of IC_{50} value of free ligands and their nickel(II) and zinc(II) complexes against PA-1

H^1L	12.70	$[\text{Ni}(\text{L})_2] \mathbf{29}$	2.48	$[\text{Zn}(\text{L})_2] \mathbf{57}$	3.12
H^5L	8.42	$[\text{Ni}(\text{L})_2] \mathbf{33}$	8.29	$[\text{Zn}(\text{L})_2] \mathbf{61}$	5.94
H^6L	1.76	$[\text{Ni}(\text{L})_2] \mathbf{34}$	1.41	$[\text{Zn}(\text{L})_2] \mathbf{62}$	3.22
H^7L	6.80	$[\text{Ni}(\text{L})_2] \mathbf{35}$	4.14	$[\text{Zn}(\text{L})_2] \mathbf{63}$	6.10
H^8L	5.57	$[\text{Ni}(\text{L})_2] \mathbf{36}$	5.94	$[\text{Zn}(\text{L})_2] \mathbf{64}$	3.51
H^9L	7.91	$[\text{Ni}(\text{L})_2] \mathbf{37}$	4.23	$[\text{Zn}(\text{L})_2] \mathbf{65}$	1.30
H^{10}L	5.34	$[\text{Ni}(\text{L})_2] \mathbf{38}$	2.93	$[\text{Zn}(\text{L})_2] \mathbf{66}$	4.91
H^{11}L	1.63	$[\text{Ni}(\text{L})_2] \mathbf{39}$	1.99	$[\text{Zn}(\text{L})_2] \mathbf{67}$	-
H^{12}L	3.72	$[\text{Ni}(\text{L})_2] \mathbf{40}$	2.57	$[\text{Zn}(\text{L})_2] \mathbf{68}$	2.32
H^{13}L	6.51	$[\text{Ni}(\text{L})_2] \mathbf{41}$	1.28	$[\text{Zn}(\text{L})_2] \mathbf{69}$	1.26
H^{14}L	3.22	$[\text{Ni}(\text{L})_2] \mathbf{42}$	7.73	$[\text{Zn}(\text{L})_2] \mathbf{70}$	5.94

All the ligands, nickel(II) and zinc(II) metal complexes exhibit very good anticancer activity against PA-1. In case of anticancer activity against PA-1, amongst the various selenosemicarbazones, 2-oxindole selenosemicarbazone (H^6L , IC_{50} , $1.76 \mu\text{g}/\text{ml}$) and 3-acetyl indoleselenosemicarbazoe (H^{11}L , IC_{50} , $1.63 \mu\text{g}/\text{ml}$) are most active compounds. Their activity is almost similar or close to the Doxorubicin (control, IC_{50} , $1.60 \mu\text{g}/\text{ml}$). On complexation with zinc(II) or nickel(II) metals, anticancer activity of most of the selenosemicarbazones get enhanced against the cell lines PA-1. Selenosemicarbazone complexes of zinc(II) metal have shown better results than nickel(II) metal. Complexes $[\text{Zn}(\text{L})_2] \mathbf{65}$ and $[\text{Zn}(\text{L})_2] \mathbf{69}$ have shown highest anticancer activity against PA-1 with IC_{50} value of $1.30 \mu\text{g}/\text{ml}$ and $1.26 \mu\text{g}/\text{ml}$ respectively. The anticancer activity of zinc(II) metal complexes is even better than standard drug doxorubicin (IC_{50} , $1.60 \mu\text{g}/\text{ml}$) and also better than selenosemicarbazone ligands and nickel(II) metal complexes.

Table 10.2.5 Comparative studies of IC₅₀ value of free ligands and their nickel(II) and zinc(II) complexes against DU-145

H ¹ L	22.107	[Ni(¹ L) ₂] 29	6.25	[Zn(¹ L) ₂] 57	13.37
H ⁵ L	3.179	[Ni(⁵ L) ₂] 33	7.48	[Zn(⁵ L) ₂] 61	10.60
H ⁶ L	13.747	[Ni(⁶ L) ₂] 34	8.32	[Zn(⁶ L) ₂] 62	7.69
H ⁷ L	9.565	[Ni(⁷ L) ₂] 35	3.83	[Zn(⁷ L) ₂] 63	4.05
H ⁸ L	24.987	[Ni(⁸ L) ₂] 36	22.71	[Zn(⁸ L) ₂] 64	4.43
H ⁹ L	34.790	[Ni(⁹ L) ₂] 37	11.80	[Zn(⁹ L) ₂] 65	3.29
H ¹⁰ L	6.094	[Ni(¹⁰ L) ₂] 38	6.97	[Zn(¹⁰ L) ₂] 66	6.38
H ¹¹ L	72.053	[Ni(¹¹ L) ₂] 39	4.63	[Zn(¹¹ L) ₂] 67	-
H ¹² L	4.463	[Ni(¹² L) ₂] 40	12.79	[Zn(¹² L) ₂] 68	7.00
H ¹³ L	10.427	[Ni(¹³ L) ₂] 41	8.67	[Zn(¹³ L) ₂] 69	13.31
H ¹⁴ L	81.873	[Ni(¹⁴ L) ₂] 42	23.63	[Zn(¹⁴ L) ₂] 70	22.71

All the ligands, nickel(II) and zinc(II) metal complexes exhibit very good anticancer activity against DU145. In case of anticancer activity against DU 145, amongst the various selenosemicarbazones, 3-methyl-2-oxindole selenosemicarbazone (H⁵L, IC₅₀, 3.17 µg/ml) is most active compound. The activity is almost similar or close to the Doxorubicin (control, IC₅₀, 3.60 µg/ml). On complexation with zinc(II) or nickel(II) metals, anticancer activity of most of the selenosemicarbazones get enhanced against the cell lines DU145. Selenosemicarbazone complexes of zinc(II) metal have shown better results than nickel(II). Complexes [Zn(⁹L)₂] **65** has shown highest anticancer activity against DU145 with IC₅₀ value of 3.29 µg/ml and ligand shows(H⁵L, IC₅₀, 3.17 µg/ml) better anticancer activity as compare with nickel(II) and zinc(II) metal complexes. The anticancer activity of zinc(II) metal complex and ligand is even better than standard drug doxorubicin (IC₅₀, 3.60µg/ml) and also better than nickel(II) metal complexes.

ANNEXURE I

Results

The IC₅₀ value of compounds (µg/ml) against PA-1

IC50 valuesTable		
Sample Code	Mean	SD
C1	12.70	0.22
C2	8.42	0.30
C3	1.76	0.04
C4	6.80	0.10
C5	5.57	0.06
C6	7.91	0.11
C7	5.34	0.09
C8	1.63	0.01
C9	3.72	0.07
C10	6.51	0.11
C11	3.22	0.02
C12	3.13	0.07
Dox	1.60	0.06

Concentration µg/ml	C1			C2			C3			C4		
100	15.64	14.69	14.38	17.69	18.01	17.54	16.75	15.96	16.11	16.59	16.9	16.27
50	19.12	19.75	17.85	18.17	18.33	18.64	18.8	18.33	18.64	16.59	16.9	16.9
25	37.6	36.49	36.97	19.59	19.91	21.17	19.59	19.43	20.06	18.8	19.12	19.75
12.5	55.92	57.66	57.66	34.76	34.6	34.44	20.22	20.38	20.54	24.17	23.38	23.54
6.25	75.99	76.94	76.62	65.09	66.03	65.72	21.17	20.85	21.33	31.75	32.39	32.7
3.12	49.92	51.66	51.03	73.93	66.03	65.09	26.38	25.59	26.54	99.21	100.16	100.95
5												
Negative Control	100											

Concentration µg/ml	C5			C6			C7			C8		
100	19.75	18.8	17.54	17.69	16.11	16.27	16.59	16.9	17.85	15.8	17.06	17.38
50	20.22	19.75	19.59	18.96	19.59	20.22	21.01	21.01	21.64	18.01	18.48	17.69
25	20.85	21.64	22.59	28.75	27.49	27.01	22.27	22.43	23.54	18.96	19.12	19.43
12.5	28.91	29.86	29.54	38.23	37.6	36.18	24.49	24.33	25.12	20.06	19.27	20.06
6.25	37.28	35.7	34.44	51.5	51.66	51.97	36.81	35.7	35.86	20.7	20.38	20.54
3.125	67.14	69.19	69.19	68.25	68.09	68.88	67.46	68.88	69.04	24.01	24.8	24.01
Negative Control	100											

Concentration µg/ml	C9			C10			C11		
100	18.8	17.69	18.33	30.65	30.96	30.17	15.17	15.48	14.53
50	22.27	20.7	21.01	31.12	32.23	31.91	15.64	15.96	16.11
25	24.17	24.49	24.64	34.12	33.97	33.81	18.64	18.33	18.64
12.5	30.96	31.75	32.39	36.18	35.39	34.28	26.38	25.12	24.8
6.25	34.12	33.49	33.97	42.02	40.92	39.97	35.39	36.49	37.44
3.125	41.07	39.81	40.28	50.71	52.61	53.24	39.02	38.7	38.7
Negative Control	100								

Concentration µg/ml	C12			Doxorubicin		
100	12.01	11.85	10.58	12.8	13.9	13.11
50	16.32	16.01	17.482	13.59	14.22	14.53
25	20.9	21.75	21.06	16.27	15.96	16.27
12.5	27.7	28.49	26.64	16.43	17.06	16.9
6.25	33.18	33.65	33.49	20.7	20.38	20.7
3.125	39.02	37.28	36.97	25.59	27.96	25.59
Negative Control	100					

The IC₅₀ value of compounds (µg/ml) against DU-145

IC ₅₀ values		
Sample Code	Mean	SD
C1	22.107	0.368
C2	3.179	0.021
C3	13.747	0.318
C4	9.565	0.178
C5	24.987	0.856
C6	34.790	1.170
C7	6.094	0.182
C8	72.053	0.972
C9	4.463	0.004
C10	10.427	0.204
C11	81.873	1.407
C12	10.710	0.106
Dox	6.206	0.286



MarathaMandhal's CentralResearchLaboratory

MarathaMandal's NGH Institute of Dental Sciences and Research Centre,
R. S. No. 57B/2, Bauxhite Road, Belgaum-590010

Ph.No.0831-2477681E-mail:mmnghidsc@gmail.com/mmcrlo1@gmail.co



Cell Viability of DU 145													
Concentration $\mu\text{g/ml}$	C1			C2			C3			C4			
100	14.51	13.72	12.92	5.39	5.27	5.63	15.55	15.13	14.27	6.06	6.67	6.18	
50	26.94	25.23	25.60	6.31	6.49	6.18	17.27	17.58	18.19	7.29	7.29	6.98	
25	42.56	43.42	42.93	11.51	11.82	12.06	25.96	24.00	24.19	7.72	8.27	8.14	
12.5	76.91	76.00	75.57	12.49	12.80	12.43	63.81	63.56	64.24	54.01	53.70	53.09	
6.25	80.34	80.71	80.59	24.25	24.00	23.58	72.14	71.95	71.46	73.12	70.79	70.91	
3.125	82.30	81.32	81.57	63.99	63.20	63.56	78.63	75.57	75.87	76.79	75.81	75.81	
Negative Control	100												

Cell Viability of DU145													
Concentration $\mu\text{g/ml}$	C5			C6			C7			C8			
100	20.27	19.72	17.94	29.88	27.37	28.41	4.47	4.78	4.96	43.91	45.38	45.68	
50	36.68	35.76	32.95	45.68	43.66	43.91	5.51	5.94	5.63	68.46	68.71	68.89	
25	53.64	53.52	53.34	61.79	61.36	61.79	21.86	19.66	19.78	70.42	69.87	69.99	
12.5	68.03	68.46	68.52	72.93	72.50	72.20	31.17	30.74	31.05	76.67	76.85	76.30	
6.25	77.59	75.14	75.26	74.53	74.65	75.14	51.87	48.93	48.38	79.79	79.67	79.91	
3.125	79.06	79.67	79.98	83.53	81.81	81.87	69.01	69.63	69.32	88.00	87.69	87.88	
Negative Control	100												

Concentration µg/ml	C9			C10			C11		
100	6.06	5.88	5.57	15.98	13.35	12.98	57.99	58.48	57.99
50	6.80	6.98	6.86	33.80	31.90	31.97	65.09	64.61	64.79
25	8.45	8.27	8.82	39.01	38.33	37.84	68.28	68.34	68.46
12.5	12.06	12.49	13.29	45.07	45.25	45.13	78.63	76.85	75.08
6.25	37.11	37.29	36.93	50.70	50.89	50.64	80.47	80.40	80.53
3.125	78.51	77.95	77.59	67.61	67.67	68.28	83.83	83.04	82.91
Negative Control	100								

Concentration µg/ml	C12			Dox		
100	4.72	5.39	5.08	12.80	12.31	12.61
50	5.82	5.51	5.63	12.86	12.98	13.78
25	8.70	8.02	8.14	28.05	28.23	28.35
12.5	66.81	65.03	64.73	38.21	38.27	39.56
6.25	72.20	72.87	72.93	45.13	44.76	48.07
3.125	75.44	75.75	75.44	55.85	57.07	57.26
Negative Control						

Reference

- 1.Kumbar VM, Muddapur UM, BhatKG, ShwethaHR, Kugaji MS, Peram MR, Dindawar S.Cancer stem cell trait sintumor spheres derived from primary laryngeal carcinoma celllines. Contemporary Clinical Dentistry.2021Jul;12(3):247.

Place: Belagavi
Date:02.09.2022

Dr.KishoreJ.Bhat
MD,(Microbiology)

MARATHA
MANDAL'S
CRL

MARATHA MANDAL BELAGAVI



MarathaMandhal's CentralResearchLaboratory

MarathaMandal's NGH Institute of Dental Sciences and Research Centre, R.S.No. 57B/2, Bauxhite Road, Belgaum-590010

Ph.No.0831-2477681 E-mail:mmnghidsc@gmail.com/mmcr101@gmail.co



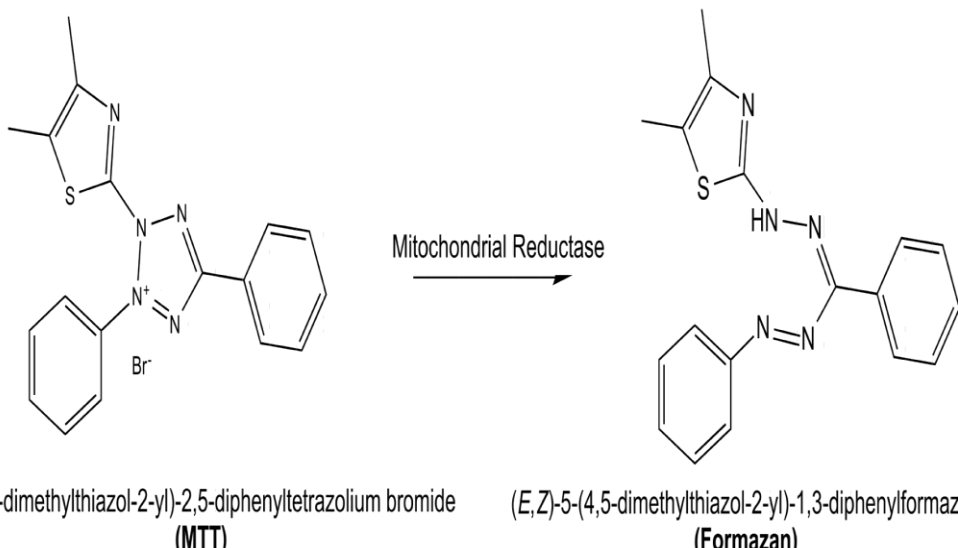
Cytotoxic activity

Cytotoxic activity carried by MTT assay

MTT

Principle of assay:

This is a colorimetric assay that measures the reduction of yellow 3-(4,5-dimethylthiazol-2-yl)-2,5-diphenyl tetrazolium bromide (MTT) by mitochondrial succinate dehydrogenase. The MTT enters the cells and passes into the mitochondria where it is reduced to an insoluble, coloured (dark purple) formazan product. The cells are then solubilized with an organic solvent (eg. DMSO, Isopropanol), and the released, solubilized formazan reagent is measured spectrophotometrically. Since reductions of MTT can only occur in metabolically active cells the level of activity is a measure of the viability of the cells.





MarathaMandhal's CentralResearchLaboratory

MarathaMandal's NGH Institute of Dental Sciences and Research Centre, R.S.No. 57B/2, Bauxhite Road, Belgaum-590010

Ph.No.0831-2477681 E-mail:mmnghidsc@gmail.com/mmcr101@gmail.co



Results

The IC₅₀ value of compounds (μg/ml) against PA-1

IC ₅₀ values (μg/ml)		
Sample Code	Mean	SD
RC1	8.29	0.25
RC2	5.94	0.05
RC3	1.41	0.05
RC4	3.22	0.10
RC5	4.14	0.20
RC6	6.10	0.21
RC7	4.23	0.09
RC8	1.30	0.03
RC9	2.93	0.10
RC10	4.91	0.15
RC11	2.57	0.05
RC12	2.32	0.08
RC13	1.28	0.04
RC14	1.26	0.01
RC15	2.48	0.25
RC16	3.12	0.04
RC17	1.60	0.06

Cell Viability of PA-1

Concentration μg/ml	RC1			RC2			RC3			RC4		
100	13.45	12.04	11.64	15.37	15.13	14.59	14.48	13.22	13.26	14.34	14.1	13.41
50	16.7	16.76	14.89	15.81	15.43	15.62	16.4	15.43	15.62	14.34	14.1	14
25	33.95	32.39	32.73	17.14	16.9	17.98	17.14	16.46	16.95	16.4	16.17	16.66
12.5	42.46	43.55	41.86	31.3	30.62	30.37	17.73	17.35	17.39	21.42	20.15	20.2
6.25	51.06	52.15	52.05	49.62	51.97	53.58	18.61	17.79	18.13	28.5	28.56	28.75
3.125	65.79	66.15	63.75	62.88	59.97	58.99	23.48	22.21	23	51.48	50.83	48.47
Negative Control	100											



MarathaMandhal's CentralResearchLaboratory

MarathaMandal'sNGHInstituteofDentalSciencesandResearchCentre,R.S.No. 57B/2, Bauxhite Road, Belgaum-
590010

Ph.No.0831-2477681E-mail:mmnghidsc@gmail.com/mmcr101@gmail.co



Cell Viability of PA-1													
Concentration μg/ml	RC5			RC6			RC7			RC8			
100	17.29	15.87	14.59	15.37	13.36	13.41	14.34	14.1	14.89	13.6	14.25	14.44	
50	17.73	16.76	16.51	16.55	16.61	17.1	18.47	17.94	18.43	15.66	15.58	14.74	
25	18.32	18.53	19.31	25.69	23.98	23.44	19.65	19.26	20.2	16.55	16.17	16.36	
12.5	25.84	26.2	25.8	34.54	33.42	32	21.71	21.03	21.67	17.58	16.31	16.95	
6.25	33.66	31.65	30.37	46.93	46.55	46.75	33.22	31.65	31.7	18.17	17.35	17.39	
3.125	58.53	56.92	55.82	60.57	61.89	59.53	58.83	61.63	62.67	21.27	21.48	20.64	
Negative Control	100												



MarathaMandhal's CentralResearchLaboratory

MarathaMandal's NGH Institute of Dental Science sand Research Centre,
R. S. No. 57B/2, Bauxhite Road, Belgaum-590010



Ph.No.0831-2477681E-mail:mmnghidsc@gmail.com/mmcr01@gmail.co

Cell Viability of PA-1												
Concentration $\mu\text{g}/\text{ml}$	RC9			RC10			RC11			RC12		
100	16.4	14.84	15.33	27.46	27.23	26.39	13.01	12.77	11.79	10.06	9.38	8.1
50	19.65	17.64	17.84	27.91	28.41	28.01	13.45	13.22	13.26	13.16	12.33	12.67
25	21.42	21.18	21.23	30.71	30.03	29.78	16.25	15.43	15.62	14.63	13.95	14.15
12.5	27.76	27.97	28.46	32.63	31.36	30.23	23.48	21.77	21.38	20.97	21.18	21.23
6.25	30.71	29.59	29.93	38.08	36.52	35.54	31.89	32.39	33.18	29.82	29.74	29.49
3.125	37.2	35.49	35.83	46.2	47.44	47.93	35.28	34.46	34.36	35.28	33.13	32.73
Negative Control	100											

Cell Viability of PA-1									
Concentration $\mu\text{g}/\text{ml}$	RC13			RC14			RC15		
100	10.8	11.3	10.46	11.09	10.27	10.9	23.04	22.21	21.82
50	11.53	11.59	11.79	11.24	11.89	10.76	25.25	24.57	23.74
25	14.04	13.22	13.41	13.3	13.22	13.41	27.02	26.34	26.54
12.5	14.19	14.25	14	18.02	16.76	16.8	27.76	13.22	13.41
6.25	18.17	17.35	17.54	18.91	19.12	18.13	29.23	29	27.87
3.125	22.74	24.43	22.11	20.38	20.74	21.08	30.27	32.1	32.29
Negative Control	100								

Concentration $\mu\text{g}/\text{ml}$	RC16			Dox		
100	14.04	14.1	13.26	12.8	13.9	13.11
50	14.19	13.81	13.85	13.59	14.22	14.53
25	16.4	16.31	16.66	16.27	15.96	16.27
12.5	17.88	17.64	17.84	16.43	17.06	16.9
6.25	28.35	27.08	27.13	20.7	20.38	20.7
3.125	51.09	51.89	50.9	25.59	27.96	25.59
Negative Control	100					



MarathaMandhal's CentralResearchLaboratory

MarathaMandal's NGH Institute of Dental Sciences and
Research Centre, R. S. No. 57B/2, Bauxhite
Road, Belgaum-590010

Ph.No.0831-2477681E-mail:mmnghidsc@gmail.com/mmcr101@gmail.co



The IC50 value of compounds ($\mu\text{g/ml}$) against DU-145

IC50 values		
Sample Code	Mean	SD
RC1	7.48	0.56
RC2	10.60	0.07
RC3	8.32	0.38
RC4	7.69	3.05
RC5	3.83	0.78
RC6	4.05	0.15
RC7	11.80	4.35
RC8	3.29	0.07
RC9	6.97	0.18
RC10	6.38	0.15
RC11	12.79	0.11
RC12	7.00	0.02
RC13	8.67	0.04
RC14	13.31	0.06
RC15	6.23	1.35
RC16	13.37	0.31
Doxo	3.60	0.16

MarathaMandhal's CentralResearchLaboratory

MarathaMandal's NGH Institute of Dental Sciences and Research
Centre, R. S. No. 57B/2, Bauxhite Road, Belgaum-590010

Ph.No.0831-2477681E-mail:mmnghidsc@gmail.com/mmcr101@gmail.co



Cell Viability of DU145												
Concentration µg/ml	RC1			RC2			RC3			RC4		
100	3.47	3.78	3.41	15.83	15.73	16.09	5.43	5.48	5.28	11.85	11.23	11.54
50	27	28.19	7.4	25.92	26.49	26.28	22.71	22.56	22.3	26.69	26.23	26.75
25	41.02	41.65	41.59	37.97	37.71	37.3	31.87	31.71	31.4	37.92	37.71	38.02
12.5	42.37	42.68	43.2	43.61	43.51	43.15	42.01	41.33	36.37	44.28	43.35	42.89
6.25	47.13	47.44	47.85	56.96	57.84	57.73	49.25	48.73	48.89	52.2	0.26	52.1
3.125	54.01	54.16	52.92	68.75	68.18	67.87	72.53	72.01	71.81	64.87	63.84	64.1
Negative Control	100											



Maratha Mandhal's Central Research Laboratory

MarathaMandal's NGH Institute of Dental Sciences and Research

Centre, R. S. No. 57B/2, Bauxhite Road, Belgaum-590010

Ph.No.0831-2477681E-mail:mmnghidsc@gmail.com/mmcr101@gmail.co



Cell Viability of DU 145

Concentration µg/ml	RC5			RC6			RC7			RC8		
100	5.48	5.64	5.23	9.31	9.93	9.98	33.63	33.47	33.11	8.59	8.17	7.81
50	6.88	6.67	6.93	12.21	12.11	12.31	36.78	36.89	37.09	15.47	15.88	16.14
25	9	60.79	8.43	19.24	19.35	8.85	43.66	43.04	42.89	18.11	16.61	16.71
12.5	11.07	11.23	11.23	21.06	21.62	21.68	51.16	50.91	50.65	24.57	21.83	22.09
6.25	19.5	18.42	18.52	37.56	37.61	37.71	55.87	54.84	53.13	30.21	30.99	30.52
3.125	74.19	74.39	74.39	57.32	56.96	57.22	64.56	12.21	63.99	48.58	48.47	48.22
Negative Control	100											

Cell Viability of DU 145

Concentration µg/ml	RC9			RC10			RC11			RC12		
100	10.76	9.88	9.98	11.48	11.85	11.54	28.09	27.88	27.78	13.86	13.19	11.69
50	17.69	17.18	17.33	19.71	19.3	18.99	37.87	36.63	36.83	19.09	18.42	18.31
25	30.99	31.09	31.3	26.13	26.07	26.75	42.42	42.47	42.52	21.62	21.52	21.62
12.5	38.9	39.06	38.59	40.71	41.18	40.92	49.41	49.72	50.03	26.75	26.13	26.23
6.25	49.15	48.68	48.94	43.61	43.15	43.04	52.2	52.04	52.15	57.63	58.2	57.84
3.125	60.99	58.04	58.2	60.53	57.68	57.63	62.96	62.34	62.86	68.39	68.8	69.06
Negative Control	100											

Cell Viability of DU 145									
Concentration µg/ml	RC13			RC14			RC15		
100	10.29	10.4	10.5	24.42	23.85	23.95	20.12	16.76	16.61
50	25.09	25.35	25.4	28.45	28.71	28.25	21.68	19.87	19.5
25	34.4	34.25	33.99	32.95	33.16	33.42	28.04	21.37	21.57
12.5	43.3	42.83	42.99	51.94	51.84	51.99	43.25	28.19	27.63
6.25	46.77	46.92	46.66	65.7	66.27	66.48	48.16	42.73	42.47
3.125	69.01	69.17	68.91	69.37	68.91	69.06	61.87	61.61	61.72
Negative Control	100								

Cell Viability of DU 145						
Concentration µg/ml	RC16			Dox		
100	21.62	21.99	21.31	12.8	13.9	13.11
50	32.33	32.13	32.18	13.59	14.22	14.53
25	43.04	42.73	42.83	20.7	20.38	20.7
12.5	48.99	48.37	47.34	25.59	27.96	25.59
6.25	59.08	58.51	58.3	36.43	37.06	36.9
3.125	70.1	69.27	69.17	43.59	44.22	45.53
Negative Control	100					

Reference

- Kumbar VM, Muddapur UM, Bhat KG, Shwetha HR, Kugaji MS, Peram MR, Dindawar S. Cancer stem cell traits in tumor spheres derived from primary laryngeal carcinoma cell lines. Contemporary Clinical Dentistry. 2021 Jul;12(3):247.

Place:Belagavi
Date:02.09.2022

Dr.Kishore J.Bhat
MD,(Microbiology)

MARATHA MANDAL BELAGAVI

Tukar

Results

IC50 value of compounds (µg/ml)

Sample Codes	PA-1		DU145	
	Mean	SD	Mean	SD
RC-1	1.99	0.05	3.54	0.02
RC-2	3.27	0.12	4.63	0.08
RC-3	3.51	0.04	4.43	0.30
RC-4	7.73	0.77	23.63	0.51
RC-5	5.94	0.25	22.71	0.29
Doxorubicin	2.72	0.13	4.63	0.08

Cell Viability of PA-1									
Concentration µg/ml	RC1			RC2			RC3		
100	20.73	20.36	19.27	21.82	21.09	20.73	20.73	20.73	20.36
50	21.09	20.73	21.09	23.27	22.55	22.91	22.18	21.82	21.82
25	21.45	21.45	21.82	23.64	24.36	24.73	22.55	22.91	23.27
12.5	22.18	23.27	22.55	25.45	26.18	26.55	23.64	24.00	24.36
6.25	24.00	22.91	23.64	27.27	28.36	28.73	27.64	26.91	27.27
3.125	27.64	26.18	26.55	41.09	42.18	42.55	48.73	49.82	48.00
Negative Control	100								

Cell Viability of PA-1									
Concentration µg/ml	RC4			RC5			Doxorubicin		
100	22.55	25.82	25.45	25.82	23.64	25.82	15.82	13.64	15.82
50	26.18	28.36	29.09	28.73	28.36	26.91	18.73	18.36	16.91
25	27.64	31.64	30.55	30.55	30.18	29.82	20.55	20.18	21.82
12.5	31.27	34.55	35.27	33.45	36.00	31.64	23.45	26.00	25.64
6.25	32.73	38.91	37.45	37.45	38.91	39.27	27.45	28.91	29.27
3.125	79.27	78.91	79.64	54.91	56.73	56.00	34.91	36.73	36.00
Negative Control	100								

Cell Viability of DU145									
Concentration µg/ml	RC1			RC2			RC3		
100	25.28	24.54	23.42	24.91	21.56	21.19	22.30	21.19	20.82
50	27.88	26.77	26.39	28.25	27.51	27.14	27.14	27.51	26.77
25	28.25	29.37	29.00	30.48	31.60	30.86	29.37	29.00	28.25
12.5	31.23	31.23	30.48	31.97	32.34	32.71	30.86	29.74	30.11
6.25	32.34	33.46	34.20	33.09	33.46	34.20	31.60	31.23	27.88
3.125	34.94	34.20	34.57	46.10	46.84	47.21	51.67	50.93	49.07
Negative Control	100								

Cell Viability of DU145									
Concentration µg/ml	RC4			RC5			Doxorubicin		
100	26.77	26.02	27.14	37.17	35.32	36.06	24.91	21.56	21.19
50	30.48	30.11	31.60	37.92	40.15	38.66	28.25	27.51	27.14
25	33.46	32.71	33.09	41.64	42.01	41.64	30.48	31.60	30.86
12.5	68.77	69.52	64.68	56.13	55.39	54.65	31.97	32.34	32.71
6.25	90.33	91.08	88.10	68.40	69.52	69.89	33.09	33.46	34.20
3.125	94.05	95.54	96.28	95.91	95.17	94.42	46.10	46.84	47.21
Negative Control	100								

Reference

- Kumbar VM, Peram MR, Kugaji MS, Shah T, Patil SP, Muddapur UM, Bhat KG. Effect of curcumonin growth, bio film formation and virulence fact or gene expression of Porphyromonas gingivalis. Odontology. 2021 Jan; 109(1):18-28.

Place:Belgaum
Date:15.05.2022

Dr.KishoreG. Bhat

Bhat



Conclusion

Reaction of cyclohexanone with KSeCN and hydrazine hydrate in acidic medium results in the formation of cyclohexanone selenosemicarbazone, which was then reacted to various aldehydes or ketones to form respective selenosemicarbazones. These selenosemicarbazones are: Cyclohexanone Selenosemicarbazone (**Hcysesc**, **H¹L**); 2-furfural selenosemicarbazone (**2-Hfursesc**, **H²L**); 2-thiophene selenosemicarbazone (**2-Hthiosesc**, **H³L**); N-methyl-2-pyrrole selenosemicarbazone (**N-MeHPysesc**, **H⁴L**); 3-methyl-2-oxindole selenosemicarbazone (**3-MeHOxsesc**, **H⁵L**); 2-oxindole selenosemicarbazone (**2-HOxsesc**, **H⁶L**); 6-chloro-2-oxindole selenosemicarbazone (**6-ClHOxsesc**, **H⁷L**); 5-chloro isatin selenosemicarbazone (**5-ClHIstsesc**, **H⁸L**); 1-methyl isatin selenosemicarbazone (**1-MeHIstsesc**, **H⁹L**); indole-3-selenosemicarbazone (**3-HIndsesc**, **H¹⁰L**); 3-acetyl indole selenosemicarbazone (**3-AcHIndsesc**, **H¹¹L**); 9-anthraldehyde selenosemicarbazone (**9-HAnsesc**, **H¹²L**); 1-Naphthaldehyde selenosemicarbazone (**1-HNapsesc**, **H¹³L**); 2-Naphthaldehyde selenosemicarbazone (**2-HNapsesc**, **H¹⁴L**). All these ligands are characterized using M.P., IR and NMR (¹H and ¹³C NMR).

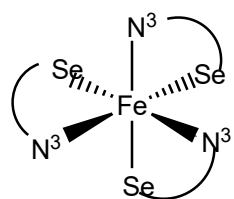
Reaction of iron acetate with selenosemicarbazones (HL) in 1: 3 (M : L) molar ratio in methanol has formed complexes of stoichiometry , [Fe(L)₃] (L = ¹L **1**; ²L **2**; ³L **3**; ⁴L **4**; ⁵L **5**; ⁶L **6**; ⁷L **7**; ⁸L **8**; ⁹L **9**; ¹⁰L **10**; ¹¹L **11**; ¹²L **12**; ¹³L **13**; ¹⁴L **14**). Complexes are characterized via IR and VSM studies. Representative complexes are also studied using ESR, Mossbauer spectroscopy and XRD studies to establish their geometry. From the VSM graphs, three parameters has been calculated: i) Saturation magnetization (M_s): A point when no further increase in magnetization is possible with increase in external magnetic field; ii) remanence (M_r): magnetization left behind after removal of external magnetic field; iii) coercivity (H_c): it is the measure of reverse field required to bring the magnetization to zero after saturation. The remanence magnetization of **1-14** lie in the range, -0.37866 to -0.29117emu/g, indicates that the iron metal in these complexes is magnetically very soft. To establish the oxidation state and spin state, complex **2** was studied for Mossbauer spectroscopy. Isomer shift value of 0.393 mm/s in complex **2** indicates the formation of iron(III) high spin octahedral complex. Quadrupolar splitting indicates the asymmetric charge distribution around the iron(III) nuclei. ESR spectrum of complex **12** give a broad signal with g value approximately equal to 2 supports formation X-ray diffraction analysis was employed for complex **7**, **10** and **12** respectively and peaks obtained confirmed the formation of complexes.

Reaction of synthesized selenosemicarbazones ligands (**H¹L-H¹⁴L**) with cobalt acetate in 2: 1 formed complexes of stoichiometry,[Co(L)₂] (L = ¹L **15**; ²L **16**; ³L **17**; ⁴L **18**; ⁵L **19**; ⁶L **20**; ⁷L **21**; ⁸L **22**; ⁹L **23**; ¹⁰L **24**; ¹¹L **25**; ¹²L **26**; ¹³L **27**; ¹⁴L **28**). Complexes are characterized by IR spectroscopy, Mass spectrometry and elemental analysis. Parent ion peak in mass spectrum and % age carbon, hydrogen and nitrogen in elemental

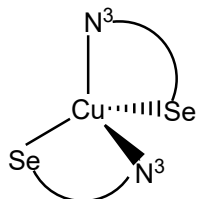
analysis are in well agreement with the proposed stoichiometry. Electron Spin Resonance spectroscopy has been used as a powerful technique to determine the spin state of cobalt(II) complexes. From ESR spectra, the structure of complex **28** is found to be square planar as measured with respect to given g values ($g_{\parallel}=2.0$ and $g_{\perp}=2.2$).

Reaction of nickel acetate with selenosemicarbazones (**H¹L-H¹⁴L**) in 1 : 2 molar ratio has yielded complexes of stoichiometry, $[\text{Ni}(\text{L})_2]$ ($\text{L} = ^1\text{L}$ **29**; ^2L **30**; ^3L **31**; ^4L **32**; ^5L **33**; ^6L **34**; ^7L **35**; ^8L **36**; ^9L **37**; ^{10}L **38**; ^{11}L **39**; ^{12}L **40**; ^{13}L **41**; ^{14}L **42**). All the complexes are characterized using IR, NMR (^1H and ^{13}NMR) spectroscopy and Mass spectrometry. Similarly reaction of synthesized selenosemicarbazones ligands (**H¹L-H¹⁴L**) with copper acetate in 2: 1 may form complexes of stoichiometry, $[\text{Cu}(\text{L})_2]$ ($\text{L} = ^1\text{L}$ **43**; ^2L **44**; ^3L **45**; ^4L **46**; ^5L **47**; ^6L **48**; ^7L **49**; ^8L **50**; ^9L **51**; ^{10}L **52**; ^{11}L **53**; ^{12}L **54**; ^{13}L **55**; ^{14}L **56**). All the complexes are characterized using IR, Electron Spin Resonance spectroscopy and Mass spectrometry (few complexes). Parent ion peak obtained in the mass spectrum of complexes is in accordance to the proposed stoichiometry. The ESR spectra of copper(II) complexes **43-56** in polycrystalline state was taken at RT. In complexes **43**, **45**, **46**, **49**, **51**, **52**, **53** and **54**, **55** the value of geometric parameters (G) is less 4 hence a significant exchange interaction, whereas no exchange interactions are observed in complexes **44**, **47**, **48**, **50** and **56** ($G > 4$). The value of f for complexes **43**, **45-47**, **49-54** and **56** lies in the range, 102-135 cm indicating a square planar geometry with small distortion, where as in complex **44**, **53** and **55** value ($f=182$ cm, 146 cm and 153 cm) is close to tetrahedral geometry with larger distortion. The values of α^2 in complexes **43-46**, **48**, **50-56** ranges from 0.500-0.787 indicating a mixed ionic-covalent bonding. The observed molecular ion peak $[\text{M}]^+$ in mass spectra and m/z values for complexes **43**, **50-53** and **41**, are close to their proposed stoichiometry $[\text{Cu}(\text{L})_2]$ and confirmed the co-ordination of Cu(II) with selenosemicarbazones.

Reaction of synthesized selenosemicarbazones ligands (**H¹L-H¹⁴L**) with zinc acetate in 2: 1($\text{L} : \text{M}$) molar ratio has formed complexes of stoichiometry, $[\text{Zn}(\text{L})_3]$ ($\text{L} = ^1\text{L}$ **57**; ^2L **58**; ^3L **59**; ^4L **60**; ^5L **61**; ^6L **62**; ^7L **63**; ^8L **64**; ^9L **65**; ^{10}L **66**; ^{11}L **67**; ^{12}L **68**; ^{13}L **69**; ^{14}L **70**). The complexes are characterized using IR, NMR spectroscopy and mass spectrometry. Based on the various analytical and spectral characterizations the proposed geometry for the complexes 1-70 is given below:



1-14



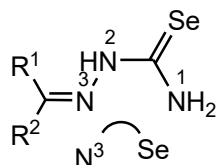
44, 53, 55



M= Cu (**43, 45-47, 49-53, 56**)

Ni (**29-42**)

Zn (**57-70**)



Expected geometry for complexes **1-70**

Selenosemicarbazones (**H¹L-H¹⁴L**) and their complexes **1-70** are tested for their antimycobacterial against *M. tuberculosis*. Hcysesc (**H¹L**), 2-Hthiosesc (**H³L**), 1-MeHstsesc (**H⁹L**), 9-HAnsesc (**H¹²L**), 1-HNapsesc (**H¹³L**) and 2-HNapsesc (**H¹⁴L**) are found to be most active (MIC = 1.6 µg /mL). The antiTB activity of **H²L**, **H⁴L**, **H⁸L**, **H¹⁰L** and **H¹¹L** get enhanced on complexation. Enhancement in anti-TB activity is more in case of **H¹¹L** (MIC = 25 µg/mL) and its nickel(II) complex (**39**) is found to be most active (MIC = 0.8 µg/mL). Its activity is even better than the standard drugs used Pyrazinamide (MIC = 3.125 µg/mL), Ethambutol (MIC = 1.6 µg/mL) and Isoniazid (MIC = 1.6 µg/mL). Amongst the various metals, copper(II) and nickel(II) complexes have shown better result. Fused ring selenosemicarbazones (**H⁵L-H¹⁴L**), cyclohexanone selenosemicarbazone (**H¹L**) and their complexes with nickel(II) and zinc(II) has been tested for their anticancer activity against PA-1 (human ovarian cancer) and DU145 (human prostate cancer) cell lines. All the ligands exhibit very good anticancer activity against PA-1 as compare to DU145. In case of anticancer activity against PA-1, amongst the various selenosemicarbazones, 2-oxindole selenosemicarbazone (**H⁶L**, IC₅₀, 1.76 µg/ml) and 3-acetyl indoleselenosemicarbazoe (**H¹¹L**, IC₅₀ 1.63 µg/ml) are most active compounds. Their activity is almost similar or close to the Doxorubicin (control, IC₅₀, 1.60 µg/ml). On complexation with zinc(II) or nickel(II) metals, anticancer activity of most of the selenosemicarbazones get enhanced against both the cell lines PA-1 and DU145. Selenosemicarbazone complexes of zinc(II) metal have shown better results than nickel(II). Complexes [Zn(⁹L)₂]**65** and [Zn(¹³L)₂]**69** have shown highest anticancer activity against PA-1 with IC₅₀ value of 1.30 µg/ml and 1.26 µg/ml respectively.

References

1. W. C. Butterman, R. D. Brown, Mineral Commodity Profiles Selenium (**2004**) 20.
2. M. Vahdati, T.T. Moghadam, Sci. Rep. 10 (**2020**) 510.
3. X.M. Liu, L.A. Silks, C.P. Liu, M. Ollivault-Shiflett, X. Huang, J. Li, G.M. Luo, Y. M. Hou, J. Q. Liu, J. C. Shen, Angew. Chem. Int.Ed. Engl. 48 (**2009**) 2023.
4. G. Audi, O. Bersillon, J. Blachot, A. H. Wapstra, Nuclear Physics A. 729 (**2003**) 128.
5. E. Dumont, F. Vanhaecke, R. Cornelis, Analytical and Bioanalytical Chemistry 385 (**2006**) 1323.
6. P. O. Amoako, P. C. Uden, J. F. Tyson, Anayttica Chimica Acta 652 (**2009**) 323.
7. G. Mugesh, W. W. Du Mont, H. Sies, Chemical Reviews 101 (**2001**) 2179.
8. M. Soriano-Garcia, Current Medicinal Chemistry 11 (**2004**) 1669.
9. A.C. Chen, S. Chatterjee, Chem. Soc. Rev. 42 (**2013**) 5438.
10. T. Maseko, D. L. Callahan, F. R. Doronila, S. D. Kolev, K. Ng, Food Chemistry 141 (**2013**) 3687.
11. A. C. Pappas, E. Zoidis, P. F. Surai, G. Zervas, Biochemistry & Molecular Biology 151 (**2008**) 372.
12. T. G. Back, Encyclopedia of Inorganic and Bioinorganic Chemistry (**2011**).
13. R. M. Rosa, D. J. Moura, A. C. Romano e Silva, J. Saffi, J. A. Pegas-Henriques, Mutation Research 63 (**2007**) 54.
14. T. W. Campbell, H. G. Walker, G. M. Coppinger, Chemical Reviews 50 (**1952**) 349.
15. R. K. Das, S. Banerjee, S. Bhattacharya, Experimental and Toxicologic Pathology 58 (**2007**) 360.
16. G. Jean-Claude, Current Organic Chemistry 15 (**2011**) 1687.
17. I. Molina-Villalba, M. Lacasaña, M. Rodríguez-Barranco, A.F. Hernández, B. Gonzalez-Alzaga, C. Aguilar-Garduño, F. Gil, Chemosphere 124 (**2015**) 91.
18. E. Muro, T. Pons, N. Lequeux, A. Fragola, N. Sanson, Z. Lenkei, B. Dubertret, J. Am. Chem. Soc. 132 (**2010**) 4557.
19. L. R. Puntel, D. S. Avila, D. H. Roos, S. Pinton, Curr. Org. Chem. 20 (**2016**) 210.
20. A. Valizadeh, H. Mikaeili, M. Samiei, S.M. Farkhani, N. Zarghami, M. Kouhi, A. Akbarzadeh, S. Davaran, Nanoscale Res. Lett. 7 (**2012**) 480.
21. S. B. Gusberg, P. Zamecnik, J. C. Aub, Journal Pharm Exp. Ther. 71 (**1941**) 245.
22. K. El- Bayoumy, Y. H. Chae, P. Upadhyaya, C. Meschter, L. A. Cohen, B. S. Reddy, Cancer Res. 52 (**1992**) 2407.
23. K. El-Bayoumy, R. Sinha, Mutat. Res. Fund. Mol. Mech. Mut. 551 (**2004**) 197.
24. D. L. Hatfield, V. N. Gladyshev, Mol. Cell. Biol. 22 (**2002**) 3576.
25. J. V. J. Comasseto Braz. Chem. Sac. 21 (**2010**) 2031.
26. R. Rakauskaite, G. Urbanaviciute, A. Ruksenaite, Z. Liutkeviciute, R. Juskenas, V. Masevicius, S. Klimasauskas, Chem. Commun. 51(**2015**) 8248
27. A. L. Moxon, R. Morrison, Physiol Rev. 23 (**1943**) 337.
28. K. E.Hill, H. S. Chittum, P. R. Lyons, M. E. Boeglin, R. F. Burk, Biochim. Biophys. Acta1313 (**1996**) 34.
29. C.L. Gan, Y.P. Zhang, D. Battaglia, X.G. Peng, M. Xiao, Appl. Phys. Lett. 92(**2008**) 241111.

30. L.A. Pham-Huy, H. He, C. Pham-Huy, Int. J. Biomed. Sci. 4 (2008) 96.
31. Y.P. Wei, X.P. Liu, C.J. Mao, H.L. Niu, J.M. Song, B. K. Jin, Biosens. Bioelectron. 103 (2018) 103.
32. F.M. Qiao, Q.Q. Qi, Z.Z. Wang, K. Xu, S. Y. Ai, Sens. Actuators B 229 (2016) 385.
33. J. E House, Inorganic Chemistry Academic (2008).
34. C.K. Abrams, S.M. Siram, C. Galsim, H. Johnson-Hamilton, F.L. Munford, H. Mezghebe, Nutr. Clin. Pract. 7 (1992) 175.
35. M. P. Longnecker, P. R. Taylor, O. A. Levander, M. Howe, C. Veillon, P. A. McAdam, K.Y. Patterson, J. M. Holden, M. J. Stamper, J. S. Morris, W. C. Willett, Am. J. Clin. Nutr. 53 (1991) 1294.
36. D. Behne, H. Hilmet, S. Scheid, H. Gessner, W. Elger, Biochim. Biophys. Acta 996 (1988) 21.
37. H. M. Saleh, M. N. Ershaidat, A. M. J. Ahmad, N. B. Bulos, M. M. A. G. Jafar, Optical Review 24 (2017) 277.
38. D. A. Minkov, G. M. Gavrilov, G. V. Angelov, J. M. D. Moreno, C. G. Vazquez, S. M. F. Ruano, E. Marquez, Thin Solid Films 654 (2018) 378.
39. B. Wang, Annu. Rev. Nutr. 29 (2009) 222.
40. P. Vera, Y. Echegoyen, E. Canellas, C. Nerín, M. Palomo, Y. Madrid, C. Cámara, Anal. Bioanal. Chem. 408 (2016) 6670.
41. M. P. Rayman, British Journal of Nutrition 100 (2008) 268.
42. J. A. Tan, W. Y. Zhu, W. Y. Wang, R. B. Li, S. F. Hou, D. C. Wang, L. S. Yang, Science of the Total Environment 284 (2002) 235.
43. N. Li, Z. D. Gao, D. G. Luo, X. Tang, D. F. Chen, Y. H. Hu, China. Science of the Total Environment 381 (2007) 111.
44. J. K. Wrobel, R. Power, M. Toborek: revisited, IUBMB Life 68 (2016) 105.
45. M. Spadoni, M. Voltaggio, M. Carcea, E. Coni, A. Raggi, F. Cubadda, Science of The Total Environment 376 (2007) 177.
46. F. J. Zhao, F. J. Lopez-Bellido, C. W. Gray, W. R. Whalley, L. J. Clark, S. P. McGrath, Science of The Total Environment 372 (2007) 439.
47. Y. G. Zhu, E. A. H. Pilon-Smits, F. J. Zhao, P. N. Williams, A. A. Meharg Trends in Plants Science 14 (2009) 442.
48. L. D. Temmerman, N. Waegeneers, C. Thiry, G. D. Laing, F. Tack, A. Ruttens, Science of The Total Environment 468 (2014) 82.
49. M. R. Broadley, P. J. White, R. J. Bryson Proceedings of the Nutrition Society 65 (2006) 181.
50. E. Dumont, F. Vanhaecke and R. Cornelis Analytical, Bioanalytical Chemistry 385 (2006) 1323.
51. A. Mehri, Int J. Prev. Med. 48 (2020) 19.
52. Z.R. Lou, P. Li, K. L. Han, Acc. Chem. Res. 48 (2015) 1368.
53. J. Clausen, G. E. Jensen, S. A. Nielsen, Biol. Trace Elem. Res. 15 (1988) 203.
54. C. Jeandel, M. B. Nicolas, F. Dubois, F. Nabet-Belleville, F. Penin, G. Cuny, Gerontology, 35 (1989) 282.
55. I. Ceballos-Picot, M. Merad-Boudia, A. Nicole, M. Thevenin, G. Hellier, S. Legrain, C. Berr, Free Rad. Biol. Med. 20 (1996) 587.
56. C. Syburra, S. Passi, Ukr. Biokhim. Zh. 71 (1999) 115.

57. J. Kalra, A. H. Rajput, S. V. Mantha and K. Prasad, Mol. Cell Biochem. 110 (1992) 165-168.
58. J. Poirier and A. Barbeau, Neurosci. Lett. 75 (1987) 348.
59. R. J. Marttila, H. Lorentz and U. K. Rinne, J. Neurol. Sci. 86 (1988) 331.
60. T. S. Lobana, R. Sharma, G. Bawa, S. Khanna, Coord. Chem. Rev. 253 (2009) 977.
61. Z. Al-Eisawi, C. Stefani, P. Jansson, A. Arvind, P. C. Sharpe, M. Basha, G. M. Iskander, N. Kumar, Z. Kovacevic, D. J. R. Lane, S. Sahni, P. V. Bernhardt, D. R. Richardson, D. S. Kalinowski, J. Med. Chem. 59 (2016) 294.
62. Y. K. Bhoon, J. P. Scovill, D. L. Klayman, Spectrochim. Acta 40A (1984) 691.
63. P. Bippus, A. Molter, D. Muller, F. Mohr, J. Organomet Chem. 695 (2010) 1657.
64. K. C. Agrawal, B. A. Booth, R. L. Michudi, E. C. Moore, A. C. Sartorelli, Biochem. Pharm. 23 (1974) 2421.
65. H. Shen, H. Zhu, M. Song, Y. Tian, Y. Huang, H. Zheng, R. Cao, J. Lin, Z. Bi ,W. Zhong, Shen et al. BMC Cancer 629 (2014) 1471.
66. C. Pizzo, P. Faral-Tello, G. Yaluff, E. Serna, S. Torres, N. Vera, C. Saiz, C. Robello, G. Mahler, Eur. J. Med. Chem. 109 (2016) 107.
67. H. G. Raubenheimer, G. J. Krager, L. Linford, C. F. Marais, R. Otte, J. T. Z. Hattingh, A. Lombard, J. Chem. Soc. Dalton Trans. (1989) 1565.
68. S. Fuchs, K. Angermaier, A. Bauer, H. Schmidoaur, Chem. Ber. 130 (1997) 105.
69. C.O. Kienitz, C. Thone, P. G. Jones, Inorg. Chem. 35 (1996) 342.
70. Y. Cheng, T. J. Emge, J. G. Brennan, Inorg. Chem. 35 (1996) 342.
71. Y. Cheng, T. J. Emge, J. G. Brennan, Inorg. Chem. 35 (1996) 7339.
72. H. G. Mautner, W. D. Kumler, Y. Okano, R. Pratt, Antibiot. Chemother. (Northfield) 6 (1956) 51.
73. L. M. Matrisian, Bio Essays 14 (1992) 445.
74. C. Pizzo, P. Faral-Tello, G. Salinas, M. Flo, C. Robello, P. Wipf, S. G. Mahler, Med. Chem. Comm. 3 (2012) 362.
75. T. R. Todorovic A. Bacchi, D. M. Sladic, N. M. Todorovic, T. T. Bozic , D. D. Radanovic, N. R. Filipovic, G. Pelizzi, K. K. Andelkovic, Inorg. Chim. Acta 362 (2009) 3813.
76. M. D. Revenko, V. I. Prisacari, A. V. Dizdari, E. F. Stratulat, I. D. Corja, L. M. Proca, Pharm. Chem. J. 45 (2011) 351.
77. K. Bednarz, Diss. Pharm. 10 (1958) 93.
78. A. Khurana, S. Tekula, M.A. Saifi, P. Venkatesh, C. Godugu, Biomed. Pharmacother. 111 (2019) 812.
79. D. L. Klayman, J. P. Scovill, J. F. Bartosevich, J. Bruce, J. Med. Chem. 26 (1983) 35.

80. D. L. Klayman, J. P. Scovill, J. F. Bartosevich, C. J. Mason, Eur. J. Med. Chem. 16 (**1981**) 317.
81. S. N. Pandeya, J. R. Dimmock, Pharmazine 48(**1993**) 659.
82. V. Zaharia, A. Ignat, B. Ngameni, V. Kuete, M. L. Moungang, C. N. Fokunang, M. Vasilescu, N. Palibroda, C. Cristea, L. Silaghi-Dumitrescu, B. T. Ngadjui, Med.Chem. Res. 22 (**2013**) 5670.
83. M. Liu, P. L. Xu, Z. J. Wang, Yao Xue Xue Bao, 27 (**1992**) 388.
84. V. Calcaterra, O. Lopez, J. G. Fernandez-Bolanos, G. B. Plata, J. M. Padron, Eur. J. Med. Chem. 94 (**2015**) 63.
85. D. L. Klayman, J. P. Scovill, C. J. Mason, J. F. Bartosevich, J. Bruce, A. J. Lin, Arzneimittelforschung, 33 (**1983**) 909.
86. M. Zec, T. Srdic-Rajic, A. Konic-Ristic, T. Todorovic, K. Andjelkovic, I. Filipovic- Ljeskovic, S. Radulovic, Med. Chem. 12 (**2012**) 1071.
87. T. Srdic-Rajic, M. Zec, T. Todorovic, K. Andelkovic and S. Radulovic, Eur. J. Med. Chem. 46 (**2011**) 3734.
88. M. Zec, T. Srdic-Rajic, A. Krivokuca, R. Jankovic, T. Todorovic, K. Andelkovic, S. Radulovic, Med. Chem. 10 (**2014**) 759.
89. S. Bjelogrlic, T. Todorovic, A. Bacchi, M. Zec, D. Sladic, T. Srdic-Rajic, D. Radanovic, S. Radulovic, G. Pelizzi, K. Andelkovic, J. Inorg. Biochem. 104 (**2010**) 673.
90. N. Gligorijevic, T. Todorovic, S. Radulovic, D. Sladic, N. Filipovic, D. Godevac, D. Jeremic, K. Andelkovic, Eur. J. Med. Chem. 44 (**2009**) 1623.
91. F. W. Bowman, J. Pharm Sci 58 (**1969**) 1301.
92. C. R. Kowol, R. Eichinger, M. A. Jakupc, M. Galanski, V. B. Arion, B. K. Keppler, J. Inorg. Biochem. 101 (**2007**) 1946.
93. H. Elshaflu, T. R. Todorovic, M. Nikolic, A. Lolic , A. Visnjevac , S. Hagenow , J. M. Padron , A. T. Garcia-Sosa , I. S. Djordjevic , S. Grubisic , H. Stark and N. R. Filipovic, Frontiers in Chemistry 6 (**2018**) 247.
94. R. Khandia, A. Dwivedi, A. Sahu, P. Vishwakarma, A. Kumar, K. Dhama, A. Munjal, Journal of Biological Sciences (**2017**) 42.
95. S. Zaman, Xin Yu, A. F. Bencivenga, A. R. Blanden, Yue Liu, T. Withers, Bing Na, A. J. Blayney, J. Gilleran, D. A. Boothman, S. N. Loh, S. D. Kimball, D. R. Carpizo, Molecular Cancer Therapeutics (**2019**).
96. Xin Yu, A. Blanden, A. T. Tsang, S. Zaman, Y. Liu, J. Gilleran, A. F. Bencivenga, S. D. Kimball, S. N. Loh, D. R. Carpizo, Mol Pharmacol 91(**2017**) 567.
97. S.R. Turk, C. Jr. Shipman, J. C. Drach, J. Gen. Virol. 67 (**1986**) 1625.

98. W. Brucker, H.G. Rohde, *Pharmazie* 23 (1968) 310.
99. I. D. Brcesk, V. M. Leovac, G. A. Bogdanovic, S. P. Sovilj, M. Revenco, *Inorg. Chem. Comm.* 7 (2004) 253.
100. C. Pizzo, P. Wipf, G. Mahler, *Setembro* 1 (2013).
101. A. Bhattacharjee, A. Basu, S. Bhattacharya, *Nucleus* 62 (2019) 268.
102. B.A. Gingrads, T. Suprunchuakn, C. H. Bayley, *Can. J. Chem.* 43 (1965) 1650.
103. N. R. Filipovic, S. K. Bjelogrlic, S. Pelliccia, V. B. Jovanovic, M. Kojic, M. Sencanski, G. La-Regina, R. Silvestri, C. D. Muller, T. R. Todorovic, *Arab. J. Chem.* (2017).
104. J.M. Cano Pavon, F. Pino, *Talanta* 19 (12) (1972) 1659.
105. A. Molter, G. N. KaluCerovi, H. Kommera, R. Paschke, T. L. R. Pottgen, F. Mohra, J. *Organomet. Chem.* 701 (2012) 80.
106. B. S. Garg, M. R. P. Kurup, *Trans. Met. Chem.* 13 (1998) 92.
107. T.R. Todorovic, A. Bacchi, N.O. Juranic, D.M. Sladic, G. Pelizzi, T.T. Bozic, N.R. Filipovic, K.K. AnCelkovic, *Polyhedron* (2007) 3428.
108. N. Filipovic, N. Polovic, B. Raskovic, S. Misirlic-Dencic, M. Dulovic, M. Savic, M. Niksic, D. Mitic, K. Andelkovic, T. Todorovic, *Mona. Chem.* 145 (2014) 1089.
109. I. S. Djordjevic, J. Vukasinovic, T. R. Todorovic, N. R. Filipovic, M. V. Rodic, A. Lolic, G. Portalone, M. Zlatovic, S. Grubisici, *J. Serb. Chem. Soc.* 8 (2017) 825.
110. N. R. Filipovic, S. Bjelogrlic, A. Marinkovic, T. Z. Verbic, I. N. Cvijetic, M. Sencanski, M. Rodic, M. Vujcic, D. Sladic, Z. Strikovic, T. R. Todorovic, C. D. Muller, *RSC Adv.* 5 (2015) 95191.
111. N. R. Filipovic, S. Bjelogrlic, G. Portalone, S. Pelliccia, R. Silvestri, O. Klisuric, M. Senćanski, D. Stankovic, T. R. Todorovic, C. D. Mulleri, *Med. Chem. Comm.* 7 (2016) 1604.
112. T. R. Todorovic, A. Bacchi, G. Pelizzi, N. O. Juranic, D. M. Sladic, I. D. Brceski, K. K. Andelkovic, *Inorg. Chem. Comm.* 9 (2006) 862.
113. D. Dekansk, T. Todorović, D. Mitic, N. Filipovic, N. Polovic, K. Andelkovic, *J. Ser. Chem. Soc.* 78 (2013) 1503.
114. T. C. Castle, R. I. Maurer, F. E. Sowrey, M. J. Went, C. A. Reynolds, E. J. L. McInnes, P. J. Blower, *J. Am. Chem. Soc.* 125 (2003) 10040.
115. P. McQuade, K. E. Martin, T. C. Castle, M. J. Went, P. J. Blower, M. J. Welch, J. S. Lewis, *Nucl. Med. Bio.* 32 (2005) 147.
116. T. S. Lobana, R. Sharma, S. Indoria, R. J. Butcher, *Polyhedron* 91 (2015) 89.
117. T. S. Lobana, R. Sharma, R. Sharma, R. Sultana, R. J. Butcher, Z. Anorg Allg Chem. 634

- (2008) 718.
118. R. Sharma, T. S. Lobana, M. Kaur, N. Thathai, G. Hundal, J. P. Jasinski, R. J. Butcher, *J. Chem. Sci.* 128 (2016) 1103
119. A. Khan, J. P. Jasinski, V. A. Smoleaski, K. Paul, G. Singh, R. Sharma, *Inorganica Chimica Acta* 449 (2016) 119.
120. T. S. Lobana, P. Kumari, R. Sharma, A. Castineiras, R. J. Butcher, T. Akitsu, Y. Aritake, *J. Chem. Soc. Dalton Trans.* 40 (2011) 3219.
121. T. S. Lobana, R. Sharma, R. J. Butcher, *Polyhedron* 28 (2009) 1103.
122. R. Sharma, T. S. Lobana, A. Castineiras, R. J. Butcher, T. Akitsud, *Polyhedron* 158 (2019) 449.
123. A. Khan, J. P. Jasinski, V. A. Smolenski, E. P. Hotchkiss, P. T. Kelley, Z. A. Shalit, M. Kaur, K. Paul, R. Sharma, *Bioorganic Chemistry* 80 (2018) 303.
124. A. Khan, P. Sharma, Rajnikant, V. K Gupta, N. Padha, R. Sharma, *J. Chem. Sci.* 128 (2016) 185.
125. A. Khan, J. P. Jasinski, V. A. Smoleaski, K. Paul, G. Singh, R. Sharma, *Inorganica Chimica Acta* 449 (2016) 119.
126. T. S. Lobana, R. Sharma, R. J. Butcher, T. W. Failes, P. Turner, *J. Coord. Chem.* 58 (2005) 1369.
127. T. S. Lobana, R. Sharma, A. Castineiras, *Inorg. Chem. Comm.* 8(12) (2005) 1094.
128. R. Sharma, T. S. Lobana, M. Kaur, N. Thathai, G. Hundal, J. P. Jasinski, R. J. Butcher, *J. Chem. Sci.* 128 (2016) 1103.
129. T. S. Lobana, R. Sharma, A. Castineiras, R. J. Butcher, *Z. Anorg. Allg. Chem.* 636 (2010) 2698.
130. T. S. Lobana, R. Sharma, *Z. Anorg. Allg. Chem.* 635 (2009) 2150.
131. A. Molter, E. Bill, F. Mohr, *Inorg. Chem. Comm.* (2012) 124.
132. A. Molter, F. Mohr, *Polyhedron* 120 (2016) 118.
133. A. Molter, J. Rust, C. W. Lehmann, G. Deepa, P. Chiba, F. Mohr, *Dalton Trans.* 40 (2011) 9810.
134. A. Molter, F. Mohr, *Dalton Transactions* 40 (2011) 3754.
135. T. H. Mawat, M. J. Al-Jeboori, *Journal of Molecular Structure* 1208 (2020) 127876.
136. B. P. Nandeshwarappa, S. Chandrashekharappa, R. Ningegowda, *Chemical Data Collections* (2020).
137. S. Rostan, G. Mahler, L. Otero, *Current Medicinal Chemistry* (2021).
138. A. Molter, J. Kuchar, F. Mohr, *Royal Society of Chemistry* 46 (2022) 4549.
139. A. S. Kshrisagar and P. K. Khanna, *Current Chemical Biology* 16 (2022) 34.
140. T. Thomson, *Met. Film. Electron. Opt. Magn. Appl.* (2014) 546.
141. A.O. Adeyeye, G. Shimon, *Handb. Surf. Sci.* 5 (2015) 41.

142. A. Nikzad, A. Ghasemi, M.K. Tehrani, G.R. Gordani, J. Supercond. Nov. Magn. 29 (**2016**) 1664.
143. V. Pathak, K.K. Bharadwaj, A. Agrawal, Asian J. of Chemistry 22 (**2010**) 7566.
144. A. J.Conti, R. K.Chadha, K. M. Sena, A. L. Rheinhold, D. N.Hendrickson, Inorg. Chem. 32 (**1993**) 2680.
145. H.Ohshio, Y. Maeda, Y. Takashima, Inorg. Chem. 22 (**1983**) 2689.
146. Y. Maeda, N. Tsutsumi, Y. Takashima, Inorg. Chem. 23 (**1984**) 2447.
147. M. D.Timken, C. E. Strouse, S. M. Soltis, S. A. Daverio, D. N.Hendrickson, A. M. Adbel-Mawgoud, S. R. Wilson, J. Am. Chem. Soc. 108 (**1986**) 402.
148. B. J.Kennedy, A. C.McGrath, K. S.Murray, B. W. Skelton, Inorg. Chem. 26 (**1987**) 495.
149. M. Mohan, N. S.Gupta, L. Chandra, N. K. Jha, R. S. Prasad, Inorg. Chim. Acta 141 (**1988**) 192.
150. M. M. Bhadbhade, D. Srinivas, Polyhedron 17 (**1998**) 2711.
151. N. E. Domracheva, A. V. Pyataev, V. E. Vorobeva, E. M. Zueva, J. Phys. Chem. B 117(**2013**) 7842.
152. S. Sundaresan, I. A. Kuhne, C. T. Kelly, A. Barker, D. Salley, H. Muller-Bunz, A. K. Powell, G. G. Morgan, Crystals 9 (**2019**) 19.
153. E. M. Abdalla, S. S. Hassan, H. H. Elganzory, S. A. Aly, H. Alshater, Molecules. 26 (**2021**) 5851.
154. K. Buldurun, N. Turan, A. Aras, A. Mantarcı, F. Turkan, E. Bursal, Chem. Biodivers. 16 (**2019**) 1900243.
155. Y. S. El-Sayed, M. Gaber, R. M. Fahmy, S. Fathallah, Appl. Organomet. Chem. 36 (**2022**) 6628.
156. A. Patterson, Phys. Rev. 56 (**1939**) 978 .
157. Y. Nishida, S. Kida, 45(**1972**) 465.
158. Y. Nishida, K. Ida, S. Kida, Inorganica Chimica Acta, 38(**1980**) 116.
159. Y. Nishida, S. Kida, Bulletin of The Chemical Society of Japan 48 (**1975**) 1046.
160. T. P. J.Garret, D. J.Glingeleffer, J. M. Guss, S. J. Rogers, H. C. Freeman, J. Biol. Chem. 259 (**1984**) 2825.
161. A. L.Raphael, H. B. Gray, J. Am. Chem. Soc. 113 (**1991**) 1040.
162. M. K. Geno, J. Halpern, J. Am. Chem. Soc. 109 (**1987**) 1240.
163. S.K. Lau, G.A. Chass, B. Penke, I.G. Csizmadia, J. Mol. Struct. (Theochem) 667 (**2003**) 437.
164. P.E. Smith, J.J. Tanner, J. Am. Chem. Soc. 121 (**1999**) 8644
165. G.R. Stockwell, J.M. Thornton, J. Mol. Biol. 356 (**2006**) 944.
166. J.P. Bidwell, J. Thomas, J. Stuehr, J. Am. Chem. Soc. 108 (**1986**) 825.

167. L.A. Herrero, J.C. Cerro-Garrido, M.C. Apella, A. Terron-Homar, *J. Biol. Inorg. Chem.* 7 (2002) 317.
168. G. Micera, D. Sanna, E. Kiss, E. Garribba, T. Kiss, *J. Inorg. Biochem.* 75 309 (1999) 75.
169. R. Parthasarathy, S.M. Fridey, *Science* 226 (1984) 971
170. Q. Cui, M. Karplus, *J. Phys. Chem. B.* 104 (2000) 3743.
171. R. S. Joseyphus, M. S. Nair, *Arabian J. Chem.* 3 (2010) 204.
172. I. M. Proctor, B. J. Hathaway, P. Nicholis, *J. Chem. Soc.* (1968) 1684.
173. B. J. Hathaway, D. E. Billing, *Coord. Chem. Rev.* 5 (1970) 207.
174. U. Sakaguchi, A. W. Addison, *J. Chem. Soc. Dalton Trans.* 4 (1979) 608.
175. D. E. Nickles, M. J. Power, F. L. Vrbach, *Inorg. Chem.* 22 (1983) 3217.
176. L. Latheef, M. R. Kurup, *Spectrochim. Acta A* 70 (2008) 93.
177. E. B. Seena, M. Sithambaresan, S. Vasudevan, M. R. P. Kurup, *J. Chem. Sci.* (2020) 49.
178. H. A. Kuska, M. T. Rogers, A. E. Martell (Editor) *Van Nostrand Reinhold Co. New York* (1971).
179. M. C. S. Lourenco, M. V. N deSouza, A. C Pinheiro, M. de L. Ferreira, R. S. B. Goncalves, T. C. M Nogueira, M. A. Peralta, *ARKIVOC*, 15 (2007) 191.
180. S. G. Franzblau, R. S. Witzig, J. C. McLaughlin, P. Torres, G. Madico, A. Hernandez, M. T. Degnan, M. B. Cook, V. K. Quenzer, R. M. Ferguson, R. H. Gilman, *J Clin Microbiol* 36 (1998) 366.
181. V. M. Kumbar, M. R. Peram, M. S. Kugaji, T. Shah, S. P. Patil, U. M. Muddapur, K. G. Bhat, *Odontology*. 109 (2021) 28.
182. S. T. Galatage, A. S. Hebalkar, R. V. Gote, O. R. Mali, S. G. Killedar, D. A. Bhagwat, V. M. Kumbhar, S. T. Galatage, A. S. Hebalkar, R. V. Gote, O. R. Mali, S. G. Killedar, D. A. Bhagwat, V. M. Kumbhar, *J. F. of Pharm. Sci.* 6 (2020).
183. S.G. Alegaon, P. Parchure, L. D. Araujo, P. S. Salve, K.R. Alagawadi, S. S.Jalalpure, V. M. Kumbar, *Bioorganic & Medicinal Chemistry Letters* (2017).
184. D. A. Bhagwat, P. A. Swami, S. J. Nadaf, P. B. Choudhari, V. M. Kumbar, H. N. More, S. G. Killedar, P. S. Kawtikwar, *J. Pharmaceutical Sciences* 110 (2021) 291.
185. D. Hegde, S. Dodamani, V. Kumbar, S. Jalalpure, K. B. Gudasi, *Appl. Organometal Chem.* (2017) 3851.
186. S. S. Bhat, N. Shivalingegowda, V. K. Revankar, N. K. Lokanath, M. S. Kugaji, V. Kumbar, K. Bhat, *J. Inorganic Biochemistry* 177 (2017) 137.
187. S. S. Bhat, V. K. Revankar, V. Kumbar, K. Bhat, V. A. Kawade, *Acta Cryst.* (2018).

188. S. S. Bhat, A. A. Kumbhar, H. Heptullah, A. A. Khan, V. V. Gobre, S. P. Gejji, V. G. Puranik, Inorg. Chem. 50 (2011) 558.
189. K. E. Erkkila, D. T. Odom, J. K. Barton, Chem. Rev. 99 (1999) 2796.
190. S. Ghosh, A. C. Barve, A. A. Kumbhar, A. S. Kumbhar, V. G. Puranik, P. A. Datar, U. B. Sonawane, R. R. Joshi, J. Inorg. Biochem. 100 (2006) 343.
191. S. S. Bhat, V. K. Revankar, N. Shivalingegowda, N. K. Lokanath, Acta Cryst. C73 (2017) 717.
192. M. A. Billadeau, H. Morrison, J. Inorg. Biochem. 57 (1995) 270.
193. P. Biswas, S. Dutta, M. Ghosh, Polyhedron 27 (2008) 2112.
194. N. Hall, M. Orio, M. Gennari, C. Wills, F. Molton, C. Philouze, G. B. Jameson, M. A. Halcrow, A. G. Blackman, C. Duboc, Inorg. Chem. 55 (2016) 1504.
195. L. J. Childs, J. Malina, B. E. Rolfsnes, M. Pascu, M. J. Prieto, M. J. Broome, P. M. Rodger, E. Sletten, V. Moreno, A. Rodger, M. J. Hannon, J. Chem. Eur. 12 (2006) 4927.
196. G. Conte, A. J. Bortoluzzi, H. Gallardo, Synthesis, pp. (2006) 3947.
197. O. V. Dolomanov, L. J. Bourhis, R. J. Gildea, J. A. K. Howard, H. Puschmann, J. Appl. Cryst. 42 (2009) 341.
198. A. R. Biju, M. V. Rajasekharan, S. S. Bhat, A. A. Khan, A. S. Kumbhar, Inorg. Chim. Acta, 423 (2014) 97.
199. A. Barve, A. Kumbhar, M. Bhat, B. Joshi, R. Butcher, U. Sonawane, R. Joshi, Inorg. Chem. 48 (2009) 9132.
200. J. K. Barton, E. Lolis, J. Am. Chem. Soc. 107 (1985) 709.

LIST OF PUBLICATIONS

1. “Synthesis, Characterization and Anti-Tubercular Activity of Selenosemicarbazones Containing Fused Aromatic Rings” Plant Archives 20 (**2020**) 3243.
2. “Synthesis, Characterization and Anti-Tubercular Activities of Heterocyclic Selenosemicarbazones”, Bioorganic Chemistry 126 (**2022**) 105907.
3. “Copper(II) complexes of fused ring selenosemicarbazones: Synthesis, structure elucidation, biological activity and molecular modeling”, Polyhedron 233 (**2023**) 116319.

LIST OF CONFERENCES

1. Poster Presentation entitled “**The Essentiality of Selenium Trace Element**” during 8th International Selenium Conference (**Se 2019**) held at Thapar Institute of Engineering and Technology, Patiala during November 20-23, 2019.
2. Oral Presentation entitled “**Synthesis, Characterization and Anti-tubercular activity of Heterocyclic Selenosemicarbazones**” during International Conference on “Recent Advances in Fundamental and Applied Sciences” (**RAFAS 2021**) held on June 25-26, 2021, organized by School of Chemical Engineering and Physical Sciences, Lovely Faculty of Technology and Sciences, Lovely Professional University, Punjab.
3. Oral Presentation entitled “**Synthesis, Characterization and Anti-tubercular activity of Aromatic Fused Selenosemicarbazones**” during International Conference on “Advances in Multi-Disciplinary Sciences and Engineering Research (**ICAMSER-2021**) held on July 2-3, 2021, Chitkara University, Himachal Pradesh.
4. Oral Presentation entitled “**A Study on Selenium and its Comparative Analogues**” during International Chemical Engineering Conference (**ICHEEC-2021**) held on September 16-19, 2021, organized by Department of Chemical Engineering, Dr. B. R. Ambedkar National Institute of Technology, Punjab.

LIST OF SHORT TERM COURSES AND WORKSHOPS

1. Short Term Course on “**Scientific Writing Using Type setting Software LaTex**” held during October 17, 2020 to November 01, 2020 organized by Lovely Professsioanl University.
2. Short Term Course on “**Material Characterization: Analysis and Interpretation**” held during 23rd to 28th August 2021 organized by PerkinElmer-LPU Centre of Excellence in Materials’ Characterization, Bruker-LPU Centre of Excellence for Microstructural Studies, JEOL-LPU Centre of Excellence for Advanced Microscopic Studies and Shimadzu-LPU Centre for Advanced Chromatography and Mass Spectrometry in association with Central Instrumentation Facility, Division of Research and development of Lovely Professional University, Punjab.
3. Workshop on “**Molecular Docking and Analysis Virtual Hands-on Workshop**” organized by Excel Education Services, Hyderabad on August 18-19, 2022.
4. Workshop on “Deep Dive into Python” from 24th -28th August 2021, organized by Department of Applied Sciences, Chitkara University, Himachal Pradesh.

ANNEUXURE II



SYNTHESIS, CHARACTERIZATION AND ANTI-TUBERCULAR ACTIVITY OF SELENOSEMICARBAZONES CONTAINING FUSED AROMATIC RINGS

Rinku Malhi^a and Rekha Sharma^{a*}

^aDepartment of Chemistry, Lovely Professional University, Phagwara, 144411, India.

Abstract

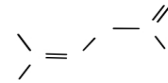
Reaction of cyclohexanone selenosemicarbazone with 9-anthrinaldehyde, N-methyl-2-pyrrole carbaldehyde, Indole-3-carbaldehyde, 1-naphthaldehyde and 2-naphthaldehyde in 1:1 molar ratio resulted into the formation of 9-anthrinaldehyde selenosemicarbazone (9-Hansesc, H¹L), N-methyl-2-pyrrole carbaldehyde selenosemicarbazone (N-MeHpsc, H²L), Indole-3-carbaldehyde selenosemicarbazone (HInesc, H³L), 1-naphthaldehyde selenosemicarbazone (1-Hnpsc, H⁴L) and 2-naphthaldehyde selenosemicarbazone (2-Hnpsc, H⁵L) respectively. All the synthesized compounds were characterized using elemental analysis, IR and ¹H NMR. These compounds were tested for anti-tubercular activity and selenosemicarbazone ligands with no heteroatom are found to be more active.

Keywords : cyclohexanone selenosemicarbazone, naphthaldehyde, elemental analysis, anti-tubercular activity.

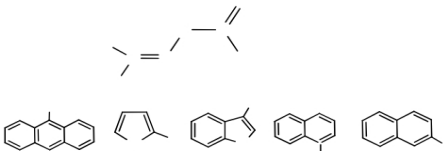
Introduction

Ligands containing chalcogen (O, S, Se) or nitrogen as donor atoms are prime focus of research for many researchers. Main reason for that is the number of biological activities exhibited by them for example, 1,2,3-triazole based ligands show antibacterial activity (Singh *et al.*, 2018), chromone based thiosemicarbazones exhibit antioxidant properties (Singh *et al.*, 2019; Singh *et al.*, 2018; Singh *et al.*, 2015) and chalcone based ligands exhibit anti-tubercular activities (Jaryal *et al.*, 2017; Rawat *et al.*, 2017; Talniya *et al.*, 2016). Many other such ligands known to be bioactive molecules (Arora *et al.*, 2016; Handa *et al.*, 2019) and also exhibit number of biological applications (Bashary *et al.*, 2019; Bhat *et al.*, 2019; Sharma *et al.*, 2017; Sharma *et al.*, 2017; Sharma *et al.*, 2016; Sharma *et al.*, 2016; Shiekh *et al.*, 2014; Mansoori *et al.*, 2018; Nirjanan *et al.*, 2019; Masta *et al.*, 2019; Divya *et al.*, 2019; Kumar *et al.*, 2018; Mansoori *et al.*, 2018; Bedi *et al.*, 2018; Datusalia *et al.*, 2018; Khatik *et al.*, 2018; Kumar *et al.*, 2018; Sarma *et al.*, 2017; Kumar *et al.*, 2017; Sharma *et al.*, 2016; Sharma *et al.*, 2017). Apart from biological activities, these ligands can be used as sensors (Singh *et al.*, 2019; Singh *et al.*, 2019; Kaur *et al.*, 2018; Kaur *et al.*, 2014), in photocells (Kumar *et al.*, 2018; Malik *et al.*, 2018), as corrosion inhibitors (Ansari *et al.*, 2014; Ansari *et al.*, 2015; Ansari *et al.*, 2015; Ambrish *et al.*, 2015; Bashir *et al.*, 2019) and sensors (Gupta *et al.*, 2012). Ligand of selenium donor are less common as earlier it was considered toxic. Importance of selenium in human body comes into existence after the discovery of selenocystein, the 21st amino acid (Sunde *et al.*, 1997). Selenoproteins with enzymatic activity have selenocystein in their active site, where selenium acts as redox centre (Sunde *et al.*, 1997; Allan *et al.*, 1999; Diplock *et al.*, 1994). Thus now a days, selenium compounds like selenosemicarbazones are not treated as toxic, rather they exhibit number of biological activities like antitumor, antimicrobial, antiviral etc. (Liu *et al.*, 1992; Turk *et al.*, 1986; Al-Eisawi *et al.*, 2016; Filipovic *et al.*, 2014). But the chemistry of selenosemicarbazone is still not explored much due to: i) elemental selenium get separated out during complexation (Castle *et al.*, 2003)], ii) ligands get changed, leaving hydrogen selenide as side product (Todorovic *et al.*, 2006), iii) undergo oxidation to form diselenide bridge (Andaloussi *et al.*, 2010).

Selenosemicarbazones, {R¹C²H=N-NH-C¹(=S)NHR²} (I) known till date can be categorized into: a) having unsubstituted and substituted aromatic ring at C² carbon (Bippus *et al.*, 2010; Pizzo *et al.*, 2016; Liu *et al.*, 1992; Calcaterra *et al.*, 2015; Gingrads *et al.*, 1965); b) with aliphatic chain at C² carbon (Bhooon *et al.*, 1984); c) with heterocyclic ring at C² carbon (Al-Eisawi *et al.*, 2016; Shen *et al.*, 2014; Ma Lourenco *et al.*, 2007).



In present paper, synthesis of new selenosemicarbazone namely, 9-anthrinaldehyde selenosemicarbazone (9-Hansesc), N-methyl-2-pyrrole carbaldehyde selenosemicarbazone (N-MeHpsc), Indole-3-carbaldehyde selenosemicarbazone (HInesc), 1-naphthaldehyde selenosemicarbazone (1-Hnpsc) and 2-naphthaldehyde selenosemicarbazone (2-Hnpsc) (Scheme 1) has been done. Characterization of synthesized molecules is done by elemental analysis, IR, ¹H NMR. All these compounds were also tested for their anti-tubercular activity.





View PDF



Access through your institution

Purchase PDF

Search ScienceDirect

Bioorganic Chemistry
Volume 126, September 2022, 105907

Recommended articles



No articles found.

Synthesis, characterization and antitubercular activities of heterocyclic selenosemicarbazones

Rinku Malhi ^a, Jerry P. Jasinski ^b, Manpreet Kaur ^b, Kamaldeep Paul ^c, Rekha Sharma ^a

Show more ▾

+ Add to Mendeley Share Cite

<https://doi.org/10.1016/j.bioorg.2022.105907>

Get rights and content

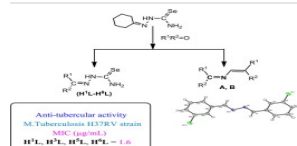
Highlights

- Presence of heterocyclic rings on aldehyde/ketone facilitates the formation of respective selenosemicarbazone.
- Geometry of ligands is confirmed by 2D NMR.
- Excellent anti-Tubercular activity shown by synthesized compounds (**H¹L**, **H³L**, **H⁵L**, **H⁶L**).

Abstract

Reaction of cyclohexanoneselenosemicarbazone with aldehydes and ketones containing heterocyclic rings (2-oxindole, 6-chloro-2-oxindole, 3-methyl-2-oxindole, isatin, 1-methyl isatin, furfural, pyrrole-2-carboxaldehyde) in ethanol yielded, respective, selenosemicarbazones [2-oxindoleselenosemicarbazone (2-HOxses, **H²L**), 6-chloro-2-oxindole selenosemicarbazone (6-ClHOxses, **H²L**), 3-methyl-2-oxindole selenosemicarbazone (3-MeHOxses, **H³L**), isatin selenosemicarbazone (**H¹L**, **H⁴L**), 1-methyl isatin selenosemicarbazone (1-MeH¹Istses, **H⁵L**), 2-thiopheneselenosemicarbazone (2-Hthioses, **H⁶L**), 2-furfuralselenosemicarbazone (2-Hfurases, **H⁷L**) and 2-pyrrole selenosemicarbazone (2-Hpyres, **H⁸L**)]. However the similar reaction with aldehyde containing single aromatic ring (3-chlorobenzaldehyde and 4-chlorobenzaldehyde) formed 1, 2-bis(3-chlorobenzylidene) hydrazine (**A**) and 1, 2-bis(4-chlorobenzylidene) hydrazine (**B**) rather than selenosemicarbazone. All the synthesized compounds were characterized using IR and NMR (¹H, ¹³C) spectroscopy. Structure of **A** and **B** were confirmed by single crystal X-ray crystallography. The synthesized selenosemicarbazones were tested for their anti-tubercular activities and **H¹L**, **H³L**, **H⁵L** and **H⁶L** are found to exhibit excellent anti-TB activity. The experimental data will give an opportunity to examine their anti-tubercular activities and identify the lead molecule.

Graphical abstract



Download : Download high-res image (82KB)
Download : Download full-size image

[Outline](#)[Abstract](#)[Graphical abstract](#)[Keywords](#)[1. Introduction](#)[2. Experimental](#)[3. Result and discussion](#)[4. Molecular docking](#)[5. Conclusion](#)[Declaration of competing interest](#)[Acknowledgement](#)[Appendix A. Supplementary data](#)[Data availability](#)[References](#)[Show full outline](#) [Figures \(9\)](#)

Copper(II) complexes of fused ring selenosemicarbazones: Synthesis, structure elucidation, biological activity and molecular modeling

Rinku Malhotra^a, Jyoti Singh^b, Renuka Chauhan^c, Abhishek Saini^d,
Riddhi Sharma^a, A. K.

[Show more](#) [+ Add to Mendeley](#) <https://doi.org/10.1016/j.poly.2023.114018>

© 2023 rights reserved

[FEEDBACK](#)

Abstract

Reaction of copper(II) acetate with cyclohexanone selenosemicarbazone (**1**); 5-chloro isatin selenosemicarbazone (**2**–**CBisesc**); 1-methyl isatin selenosemicarbazone (**1**–MeHIsesc), 3-indole selenosemicarbazone (**3**–HIsesc); 3-acetylindole selenosemicarbazone (**3**–AcHIsesc) and 2-naphthaldehyde selenosemicarbazone (**2**–Naapesc) in 1:2 (M:L) molar ratio yielded complexes of stoichiometry, $[\text{Cu}(\text{L})_2] \text{ 1–6}$ (L=cysesc **1**; **2**–**CBisesc** **2**; **1**–MeHIsesc **3**; **3**–HIsesc **4**; **3**–AcHIsesc **5**; **2**–Naapesc **6**). All the complexes are characterized by IR, Mass and ESR spectroscopy. Two well defined g values (g_{\parallel} and g_{\perp}) in ESR spectrum of complexes **1**–**4**, **6** indicate axial symmetry, whereas tetrahedral around copper(II) metal in complex **5** is

CERTIFICATE OF PARTICIPATION



This certificate is to appreciate **Rinku Malhi**
For actively attending the webinar on the topic "**COMPOSITE MATERIALS - METAL MATRIX COMPOSITE**" Organized by IFERP on 26th September 2020 from 11:00 AM to 12:30 PM for 1 hour 30 Minutes.



Dr. B. Radha Krishnan
Assistant Professor
Department of Mechanical Engineering
Nadar Saraswathi College of Engineering and Technology
India



Mr. Rudra Bhanu Satpathy
Chief Executive Officer
IFERP

CERTIFICATE PARTICIPATION

This is to Certify that
Rinku Malhi

For actively attending the Webinar on the topic "**ADVANCED EMERGING TECHNOLOGIES, RESEARCH AND PRACTICAL APPLICATION**" organized by Institute For Engineering Research and Publication on 18th May 2022.

SESSION SPECIFICS

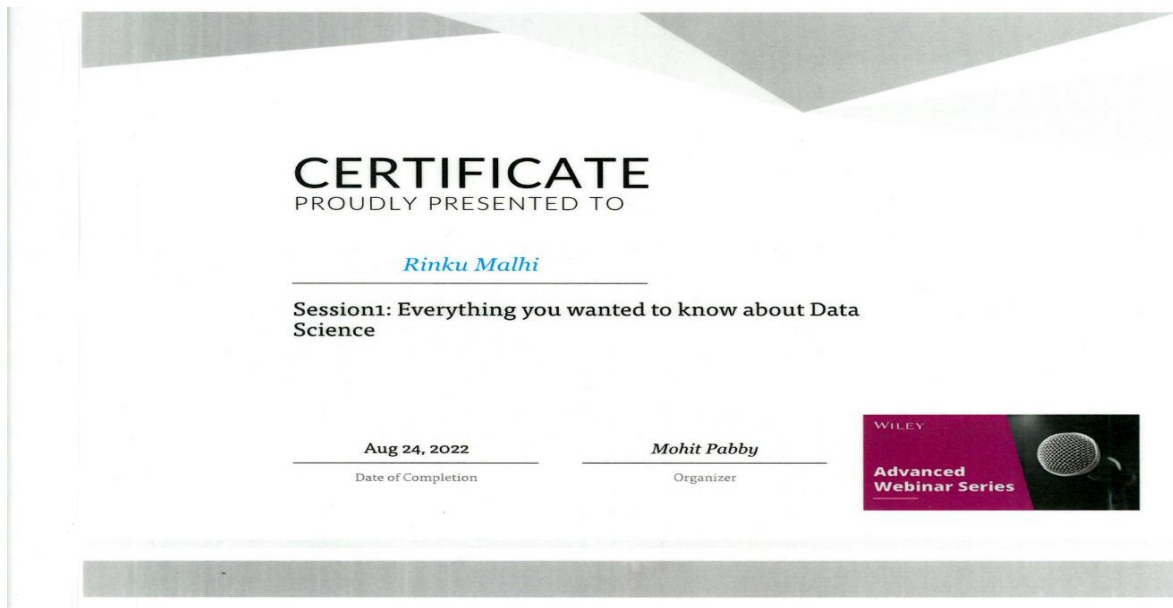
Date : 18-May-2022 | Time : 05:00 pm - 06:00 pm
Topic : ADVANCED EMERGING TECHNOLOGIES, RESEARCH AND PRACTICAL APPLICATION
Speaker : Mr. Aryan Chaudhary



Mr. Aryan Chaudhary
Research Head at Niji HealthCare,
Editor In Chief at Taylor & Francis Group.
Kolkata.



Mr. Rudra Bhanu Satpathy
Chief Executive Officer
Institute For Engineering Research
and Publication (IFERP)





THE INDIAN SCIENCE CONGRESS ASSOCIATION

(Professional Body under Department of Science & Technology,
Ministry of Science & Technology, Government of India)

14, Dr. Bires Guha Street, Kolkata – 700 017

Participation Certificate

This is to certify that Prof./Dr./Shri/Smt. RINKU MAHIL,.....
CHEMISTRY DEPARTMENT OF LOVELY PROFESSIONAL
UNIVERSITY,....PUNJAB.....

has participated in the 106th Indian Science Congress held at Lovely Professional University, Phagwara, Jalandhar from January 3 to 7, 2019.

His/Her Membership Number is L37402.....

Date 07.01.2019.....

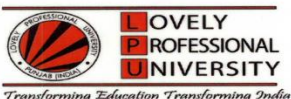
Prof. Gangadhar
General Secretary
(Membership Affairs)



Office Seal

Prof. P. P. Mathur
General Secretary
(Scientific Activities)

Certificate No. 225258



Certificate of Participation

This is to certify that Ms. Rinku Mahil
of Lovely Professional University
has given oral presentation on Synthesis, Characterization and Anti-tubercular activity of Heterocyclic
Selenosemicarbazones
in the International Conference on "Recent Advances in Fundamental and Applied Sciences" (RAFAS 2021) held on
June 25-26, 2021, organized by School of Chemical Engineering and Physical Sciences, Lovely Faculty of Technology
and Sciences, Lovely Professional University, Punjab.

Date of Issue : 15-07-2021
Place of Issue: Phagwara (India)

Prepared by
(Administrative Officer-Records)

Organizing Secretary
(RAFAS 2021)

Convener
(RAFAS 2021)





डा बी आर अम्बेडकर राष्ट्रीय प्रौद्योगिकी संस्थान जालंधर
Dr. B R AMBEDKAR NATIONAL INSTITUTE OF TECHNOLOGY, JALANDHAR
(PUNJAB), INDIA

2nd INTERNATIONAL CONFERENCE
ON
CHEMICAL, BIO & ENVIRONMENTAL ENGINEERING
(CHEMBIOEN-2021)
August 20-22, 2021
CERTIFICATE

This is to certify that Prof/Dr/Mr/Mrs/Ms **Rinku Malhi**
has presented a paper entitled "A Study- Synthesis, Characterization and Anti-tubercular activity of
selenosemicarbazone and Heterocyclic selenosemicarbazones".
Co-authored with Prof/Dr/Mr/Mrs/Ms **Rekha Sharma**
in 2nd International Conference on "CHEMICAL, BIO & ENVIRONMENTAL ENGINEERING (CHEMBIOEN-2021)"
held on virtual mode at Department of Chemical Engineering, Dr B R Ambedkar National Institute of Technology,
Jalandhar, Punjab (INDIA).


Organizing Secretary


Organizing Chairman



Dr B R Ambedkar National Institute of Technology
Jalandhar-144011 Punjab (INDIA)

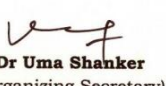
International Conference
On
Chemical Constellation Cheminar – 2019
(C³-2019)
October 12-13, 2019

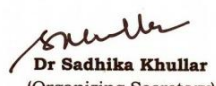
CERTIFICATE

This is to certify that Prof/Dr/Mr/Ms **Rinku Malhi** of
Department of Chemistry Lovely Professional University Phagwara
..... Jalandhar has delivered Oral/Poster presentation on the
Topic "Synthesis and Characterization of Selenosemicarbazones"
..... during the International Conference on "Chemical
Constellation Cheminar-2019 (C³-2019)" organized by Department of Chemistry, Dr B R Ambedkar
National Institute of Technology Jalandhar-144011, Punjab (INDIA) from October 12-13, 2019.


Professor B S Kaith
(Coordinator)


Professor N C Kothiyal
(Coordinator)


Dr Uma Shanker
(Organizing Secretary)


Dr Sadhika Khullar
(Organizing Secretary)



Certificate No. 182075



Certificate of Participation

This is to certify that Prof./Dr. Rinku Malhi of
Lovely Professional University, Phagwara has given poster / oral presentation
on Synthesis, Characterization and Anti-tubercular activity of Selenosemicarbazones
in the International Conference on "Recent Advances in Fundamental and Applied Sciences" (RAFAS 2019) held on November 5-6, 2019, organized by School of Chemical Engineering and Physical Sciences, Lovely Faculty of Technology and Sciences, Lovely Professional University, Punjab.

Date of Issue : 05-11-2019
Place of Issue: Phagwara (India)

Prepared by
(Administrative Officer-Records)

Organizing Secretary
(RAFAS 2019)

Convener
(RAFAS 2019)

Se2019 8TH INTERNATIONAL
SELENIUM CONFERENCE
November 20-23, 2019, TIET, Patiala, India

Certificate of Presentation

This certificate has been awarded to Rinku Malhi for presenting a poster entitled "**The Essentiality of Selenium Trace Element**" at 8th International Selenium Conference held at Thapar Institute of Engineering and Technology, Patiala, India during November 20-23, 2019.

Dr N. Tejo Prakash
Organizing Secretary

Prof. Ajay Batish
Patron

Prof. P. Gopalan
Chief Patron









**Two Days International e-Conference on
Recent Advancements in Chemical Sciences: Health, Environment and Society
(ICRACS - 2022)
8th - 9th April 2022**

Certificate of Participation

Proudly presented to

Rinku Malhi, Lovely professional University, Jalandhar

for active participation in the International e-Conference ICRACS - 2022, organized by
Department of Chemistry, Deshbandhu College, University of Delhi

Dr Umesh Kumar
(Convener)

Prof. Sushila Singhal
(Convener)

Prof. Rajiv Aggarwal
(Principal)



Certificate No. 245203



Certificate of Participation

Presented to Ms. Rinku Malhi of Lovely Professional University in recognition of his/her participation in "International Conference on Innovation and Intellectual Property Rights" held on 18-19th April, 2022 organized by Division of Research and Development, Lovely Professional University, Punjab.

Date of Issue: 13-05-2022
Place: Phagwara (Punjab), India

Prepared by
(Administrative Officer-Records)

Convenor
Dr. Ranjith Tondon
IIAIPR 2022

Dr. Chander Prakash
CD, Division of Research
and Development

**International Conference on
'Science, Engineering & Technological Innovations'**



Date: 13 - 14 August, 2022. Bangkok, Thailand

Jointly organized by
Scientific Research Association
Chreso University (CU), Zambia, Southern Africa
Research Culture Society

&
Institute of Science and Technology, Eurasian University



Certificate of Participation and Presentation

This is to Certify that

RINKU MALHI

has participated and presented a Paper / Article / Poster / Project titled

Selenium Biochemistry

in the 'International Conference on Science, Engineering & Technological Innovations' dated 13 - 14 August, 2022.
at Bangkok, Thailand.

Certificate Ref.No: ICSETI-22/CPP/015

Jessica
Dr. Jessica C.

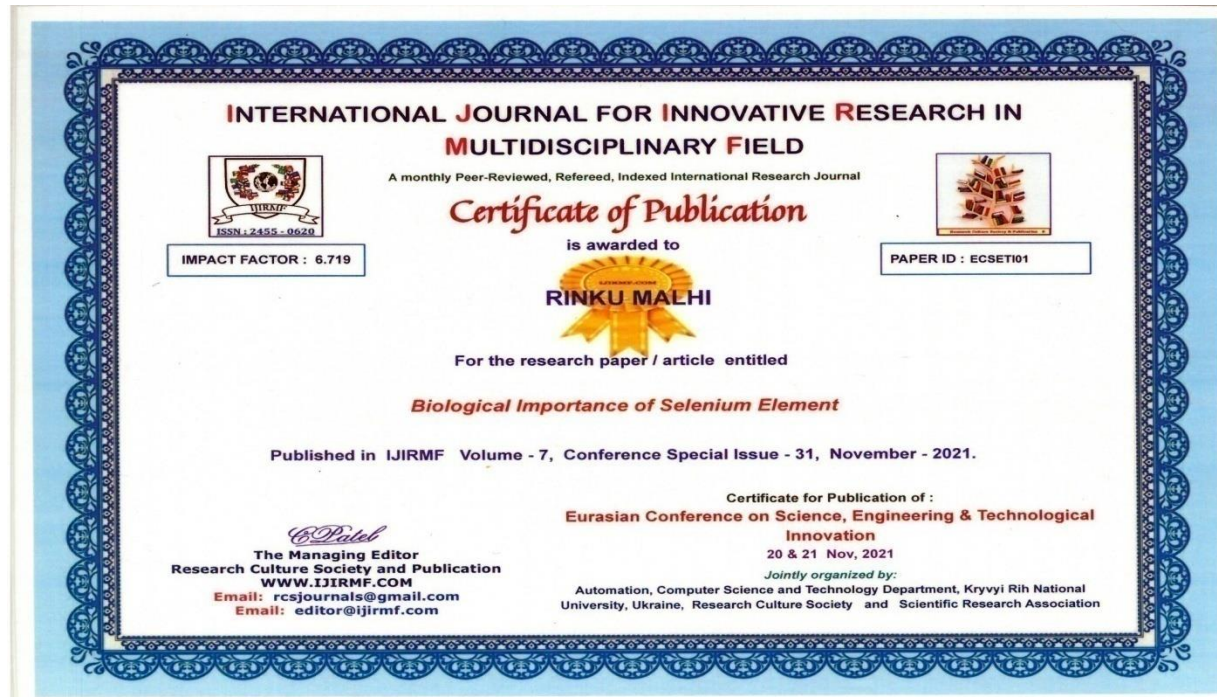
ICSETI - 2022 Conference Chair
Head, Scientific Research Association
Institute of Science and Technology, EU

Christopher Simoonga
Prof. Christopher Simoonga

ICSETI - 2022 Conference Chair
Vice Chancellor, Chreso University, Zambia
<https://chresouniversity.edu.zm/>

Bhavin Patel
Dr. C. M. Patel

Director, Research Culture Society.
President, Scientific Research Organization.
<http://www.researchculturesociety.org>



**INTERNATIONAL JOURNAL FOR INNOVATIVE RESEARCH IN
MULTIDISCIPLINARY FIELD**



ISSN : 2455 - 0620
IMPACT FACTOR : 6.719

A monthly Peer-Reviewed, Refereed, Indexed International Research Journal

Certificate of Publication

is awarded to



For the research paper / article entitled

Synthesis, Characterization and Biological Activity of Aromatic Ring Selenosemicarbazone

Published in IJIRMF Volume - 8, Conference Special Issue - 37, August - 2022.



PAPER ID : ICSETI-2022/008

Certificate for Publication of:
**International Conference on Science, Engineering &
Technological Innovations**

13 – 14 August, 2022 Bangkok, Thailand

Jointly organized by:

Scientific Research Association ; Chreso University (CU), Zambia ; Institute of Science
and Technology, Eurasian University; & 'Research Culture Society'

C Patel

The Managing Editor
Research Culture Society and Publication
WWW.IJIRMF.COM
Email: rcsjournals@gmail.com
Email: editor@ijirmf.com

HUMAN RESOURCE DEVELOPMENT CENTER

[Under the Aegis of Lovely Professional University, Jalandhar-Delhi G.T Road, Phagwara (Punjab)]

Certificate No. 211999

Certificate of Participation

This is to certify that **Ms. Rinku Malhi** D/o Sh. Surinder Malhi participated in **Short Term Course on Scientific Writing Using Typesetting Software LaTeX** organized by Lovely Professional University w.e.f. **October 17, 2020 to November 01, 2020 (6 Days)**.

Date of Issue : 01-11-2020
Place : Phagwara (Punjab), India

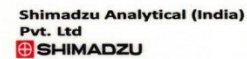


Prepared by
(Administrative Officer-Records)




Checked By
Program Coordinator


Head
Human Resource Development Center



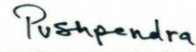
Certificate No.235504

Certificate of Participation

This is to certify that **Dr./Mr./Ms. Rinku Malhi** has presented his/her poster successfully during the conduct of the online **Short Term Course on Material Characterization: Analysis and Interpretation** held during **23rd to 28th August 2021** organized by PerkinElmer-LPU Centre of Excellence in Materials' Characterization, Bruker-LPU Centre of Excellence for Microstructural Studies, JEOL -LPU Centre of Excellence for Advanced Microscopic Studies and Shimadzu-LPU Centre for Advanced Chromatography and Mass Spectrometry in association with Central Instrumentation Facility, Division of Research and Development at Lovely Professional University, Punjab.

Date of Issue : 30-10-2021
Place : Phagwara (Punjab), India


Prepared by
(Administrative Officer-Records)


Pushpendra
Central Instrumentation Facility, LPU


DBudheri
Head
Division of Research and development, LPU



CERTIFICATE OF PARTICIPATION

This is to certify that

Mr/Ms/Dr _____

RINKU MALHI

has participated in a Five days International Short Term Training Programme On
"Advanced Approaches for Sustainable Environmental Management (AASEM-2021)"

Organised by:

DEPARTMENT OF ENVIRONMENTAL SCIENCE & ENGINEERING, MARWADI UNIVERSITY

Co-Sponsored by:

GUJARAT COUNCIL ON SCIENCE AND TECHNOLOGY, GOVERNMENT OF GUJARAT

On 20th - 24th September, 2021

DR NITIN KUMAR SINGH
COORDINATOR

MR ABHISHEK GUPTA
HoD & COORDINATOR

PROF.(DR) RAJENDRA SINGH JADEJA
DEAN, MU

PROF.(DR) SANDEEP SANCHETI
PROVOST, MU

Serial No.25.....

One Week Multi-disciplinary **FACULTY DEVELOPMENT PROGRAM (FDP)**

on
Environmental Security : Approaches & Issues
(November 5 - 11, 2021)

Organized by : Faculty of Sciences



BARING UNION CHRISTIAN COLLEGE

BATALA-143505 (Punjab)

This is to certify that Dr./Mr./Ms. Rinku Malhi, Asst. Prof., Chemistry Dept.....
of Baring Union Christian College, Batala.....
attended as /acted as.... participant /by... presented paper... on.... "Biological Importance
of Selenium"
in one week multi-disciplinary Faculty Development Program (FDP) from November 5 - 11, 2021.

The Most Rev. (Dr.) P.K. Samantary
Chief Patron (Chairman)

Prof. (Dr.) Edward Masih
Patron (Principal)

Prof. Mandeep Bedi
Co-Patron

Dr. Amita
Co-Patron

Prof. (Dr.) Derick Engles
Secretary



CERTIFICATE

— PARTICIPATION —

This is to Certify that

Rinku Malhi

For actively attending the Faculty Development Programme on the topic
"Teaching and Learning in Higher and Professional Education-the challenges and opportunities" organized by Institute For Engineering Research and Publication on 18th April 2022.

SESSION SPECIFICS

Date : 18-April-2022 | Time : 12:30 pm - 01:30 pm

Topic : Teaching and Learning in Higher and Professional Education-the challenges and opportunities

Speaker : Dr. Indranil Bose

Dr. Indranil Bose
Dean, School of Business
University of Bolton, UAE



Mr. Rudra Bhanu Satpathy
CEO & Founder
Institute For Engineering Research
and Publication (IFERP)



Certificate of Participation

This certificate is presented to

Rinku Malhi

of

Lovely Professional University, Jalandhar

for successful participation in One Week National Workshop on
"Deep Dive Into Python" from 24th August to 28th August, 2021
organized by Department of Applied Sciences ,
Chitkara University, Himachal Pradesh.

Dr Shefali Batra

Convener

Dr Sita Ram Sharma

Dy. Dean(Applied Sciences)

MOLECULAR DOCKING & ANALYSIS

VIRTUAL HANDS-ON WORKSHOP

18th and 19th August 2022

Organized by

EXCEL Education Services, Hyderabad.

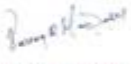
PARTICIPATION CERTIFICATE

This is to certify that

RINKU MALHI

have attended "**MOLECULAR DOCKING AND ANALYSIS VIRTUAL HANDS-ON WORKSHOP**" organized by **EXCEL Education Services**, Hyderabad on 18th & 19th August, 2022.




Pavan K Madasu M.Sc., (Ph.D)
Director, EXCEL ES.

EXCEL Education Services
PIONEERING EDUCATIONAL STANDARDS